Center for Medical Physics and Biomedical Engineering
Medical University of Vienna

Austrian Society for Biomedical Engineering (ÖGBMT)
International FES Society (IFESS)

10th VIENNA INTERNATIONAL WORKSHOP ON FUNCTIONAL ELECTRICAL STIMULATION

15th ANNUAL CONFERENCE OF THE INTERNATIONAL FES SOCIETY

NEUROMODULATION 2010: THE WAY AHEAD



Imperial Riding School, Vienna

Vienna, Austria, September 8th – 12th, 2010

PROCEEDINGS

ISBN 978-3-900928-09-4

Proceedings

of the

10th Vienna International Workshop on Functional Electrical Stimulation

and

15th IFESS Annual Conference, 2010

guest

Neuromodulation 2010: The way ahead

(Chair: Prof. Francois Alesch)

Vienna, Austria
September 8th-12th, 2010

Edited by

Thomas Mandl
Johannes Martinek
Manfred Bijak
Hermann Lanmüller
Winfried Mayr
Melitta Pichler

Published by

Center for Medical Physics and Biomedical Engineering
Medical University of Vienna, Vienna Medical School
AKH 4L
Waehringer Guertel 18-20
A-1090 Vienna
Austria

Tel.: +43-1-40400-1984
Fax: +43-1-40400-3988

http://www.fesworkshop.org
ISBN 978-3-900928-09-4

Qualität durch Kompetenz

Schuhfried has six decades of experience in designing and producing electrotherapy devices. We work closely with key scientists and reseachers to ensure that our product development takes full account of the latest research as well as practical experience. Our products cover the whole range of physical medicine and rehabilitation.



Sonostat 133 ®
Ultraschalltherapie



Stimulette r4x



Stimulette den2x



Stimulette rx



Stereodynator ®

DR. SCHUHFRIED
MEDIZINTECHNIK GMBH

a-1090 wien . van swieten-gasse 10
fon: (+43-1)405 42 06 . fax: (+43-1)405 44 64
info@schuhfriedmed.at . www.schuhfriedmed.at

Scientific Committee

Francois Alesch
Brian Andrews
Julie Armstrong
Christine Azevedo-Coste
Rik Berkelmans
Manfred Bijak
Jane Burridge
Ugo Carraro
Imre Cikajlo
Alberto Cliquet-Jr.
Glen Davis
Ross Davis
Sam Eljamel
Simona Ferrante
Paolo Gargiulo
David Guiraud
Thordur Helgason
Andy Hoffer
Ursula Hofstoetter
Kenneth Hunt
Jonathan Jarvis
Roman Kamnik
Thierry Keller
Gon Khang
Klaus Koch
Hermann Lanmueller
Richard Lauer
Young-Hee Lee
Thomas Mandl
Johannes Martinek
Winfried Mayr
Karen Minassian
Dong Ming
Tatjana Paternostro
Dejan Popovic
Mirjana Popovic
Milos Popovic
Feliciano Protasi
Dietmar Rafolt
Frank Rattay
Martin Reichel
Janez Rozman
Ruediger Rupp
Michael Russold
Stefan Sauermann
Thomas Schauer
Martin Schuettler
Kazunori Seki
Thomas Sinkjaer
Brian Smith
Thomas Stieglitz
Rune Thorsen
Peter Veltink
Ken Yoshida

Table of Contents

Anniversary Session.

Vienna FES Workshops: 1983-2010 3
Winfried Mayr

Neuro-Motor Rehabilitation in reference to Control Theory 5
Gerhard Vossius

The role of materials biocompatibility for FES-applications 11
Hanns Plenk

Dropped Foot Stimulator: From the first idea to a patient satisfactory device 13
Paul Taylor

The views of people with spinal cord injury about the use of Functional Electrical Stimulation 16
Jane Burridge, Maggie Donovan-Hall, Caroline Ellis-Hill, Bridget Dibb, Lisa Tedesco Triccas, David Rushton

Session 1. Technology

Technical challenges with cochlear implants and the Medel cochlear implant company 23
Erwin Hochmair

The limits of hermeticity test methods for micro-packages 25
Anne Vanhoestenberghe, Nick Donaldson

On the Stability of PEDOT as Coating Material for Active Neural Implants 28
Tim Boretius, Martin Schuettler, Thomas Stieglitz

Active Books: a practical way to increase the number of stimulation channels for FES after SCI? 31
Nick Donaldson, Anne Vanhoestenberghe, Xiao Liu, Nooshin Saeidi, Andreas Demosthenous, Martin Schuettler

Towards the development of an integrated stimulator for Active Books . . . 34
Xiao Liu, Andreas Demosthenous, Anne Vanhoestenberghe, Nick Donaldson

Sacro-lumbar Anterior Root Stimulator Implant for Exercising 37
Antoine Nonclercq, Anne Vanhoestenberghe, Pablo Aqueveque, Dominik Cirmirakis, Nick Donaldson

Diaphragm Pacing with Endovascular Electrodes 40
Joaquin Andres Hoffer, Bao Tran, Jessica Tang, James Saunders, Colin Francis, Rodrigo Sandoval, Ramasamy Meyyappan, Surbhi Seru, Helen Wang, Marc-Andre Nolette, Almira Tanner

Flexible shaft electrodes for transdural implantation and chronic recording 43
Birthe Rubehn, Chris Lewis, Pascal Fries, Thomas Stieglitz

Session 2. Future Applications 1

Bioimpedance based measurement system for a controlled swallowing neuro-prosthesis 49
Holger Nahrstaedt, Thomas Schauer, Rainer O. Seidl

Surface electrical stimulation to assist laryngeal elevation for swallowing rehabilitation in dysphagia 52
Hiroaki Kuno, Naosuke Yamamoto, Toshiyasu Yamamoto, Yoichiro Aoyagi, Akio Tsubahara

The effect of an abdominal FES training protocol on pulmonary function in tetraplegia 55
Angus Mclachlan, Henrik Gollee, Alan Mclean, David Allan

Optimisation of electrode placement for abdominal muscle stimulation . . . 58
Henrik Gollee, Graham Henderson

Session 3. Future Applications 2

Semi-closed loop tremor attenuation with FES 65
Lana Popovic, Nebojsa Malesevic, Igor Petrovic, Mirjana Popovic

Microscopic Magnetic Stimulation 68
Giorgio Bonmassar, Daniel Freeman, Shelley Fried, John Gale

Displaying Centre of Pressure Location by Electrotactile Stimulation Using Phantom Sensation 71
Serge Pfeifer, Ozan Çaldıran, Heike Vallery, Robert Riener, Alejandro Hernandez Arieta

A switched capacitor method for crosstalk reduction in vestibular nerve stimulators 74
Tim Perkins, Nick Donaldson, Andreas Demosthenous, Dai Jiang

Modulation of seizure susceptibility by spinal cord stimulation 77
Kristian Rauhe Harreby, Cristian Sevcencu, Johannes Jan Struijk

Safe neuromuscular electrical stimulator designed for elderly people 80
Matthias Krenn, Michael Haller, Manfred Bijak, Ewald Unger, Christian Hofer, Helmut Kern, Winfried Mayr

Session 4. Controls, Sensors, Algorithms - non invasive 1

Spinal involvement and muscle cramps in electrically-elicited muscle contractions 87
Roberto Merletti, Alberto Botter, Marco Alessandro Minetto

Event Detection for Gluteal or Hamstring Stimulation During Walking in Neurological Patients 93
Noreha Abdul Malik, Paul Chappell, Duncan Wood, Paul Taylor

Can the coherence between two EMG signals be used to measure the voluntary drive in paretic muscles? 96
Runhan Luo, Jonathan Norton, Nick Donaldson

Stimulus-response curves: Effect of recording site and inter-electrode distance 99
Ernest Nlandu Kamavuako, Dario Farina

A Preliminary Study of Muscle Fatigue Evaluation Using M-waves elicited by additional pulses for Rehabilitation with FES 102
Naoto Miura, Takashi Watanabe, Hiroshi Kanai

Torque Prediction Based on Evoked EMG in Fatiguing Muscle Toward Advanced Drop Foot Correction 105
Qin Zhang, Mitsuhiro Hayashibe, Bertrand Sablayrolles, Christine Azevedo-Coste

Output-Error Model System Identification for FES-driven control of Knee Extensor Muscles 108
Aikaterini Koutsou, Juan Camilo Moreno, Eduardo Rocon, Juan Alvaro Gallego, Jose Luis Pons

Session 5. Controls, Sensors, Algorithms - non invasive 2

Automatic real time procedure for adjusting the stimulus intensities to ensure reliable measurements of the H-reflex recruitment curve 115
Emilia Ambrosini, Simona Ferrante, Alessandra Pedrocchi, Thomas Schauer, Holger Nahrstaedt, Riccardo Mazzocchio

Use of an inverted pendulum apparatus for the study of closed-loop FES control of the ankle joints during quiet standing 118
John Tan, Jose Zariffa, Albert Vette, Cheryl Lynch, Kei Masani, Milos Popovic

Mapping Method Using A Super Multi-Electrical Stimulation Device 121
Takuya Watanabe, Yoshihiko Tagawa, Naoto Shiba

A Study on Feedback Error Learning Controller for FES: Generation of Target Trajectories by Minimum Jerk Model 124
Takashi Watanabe, Keisuke Fukushima

Can non-invasive electrical stimulation of the brain (ESB) modify the resting-state functional connectivity of the motor cortex? A proof of concept fMRI study 127
Gad Alon, Steven Roys, Rao Gullapalli

Session 6. Control, Sensors, Algorithms - invasive

Performance of implanted multi-site EMG recording electrodes: In vivo impedance measurements and spectral analysis. 133
Sören Lewis, Heiko Glindemann, Michael Friedrich Russold, Stephanie Westendorff, Alexander Gail, Thomas Dörge, Klaus-Peter Hoffmann, Hans Dietl

Selectivity of longitudinal versus transverse tripolar stimulation of median nerve in pigs using a multicontact nerve cuff electrode 136
Mathijs Kurstjens, Winnie Jensen

Development of an Implantable Myoelectric Sensor for Advanced Prosthesis Control 139
Daniel Merrill, Joseph Lockhart, Phil Troyk, Richard Weir, David Hankin

An experimental setup for stimulation selectivity measurement - variability of the muscle responses to the constant stimulus 142
Paweł Maciejasz, Wiesław Marcol, Roman Paśniczek, Thomas Dörge

EMG recordings of triceps brachii muscle in rats during downhill locomotion 145
Dirk Arnold, Bernd Faenger, Agnes Huebner, Hans-Christoph Scholle

In vivo electrical stimulation of rat triceps brachii muscle to identify intramuscular electrical sensitive points 148
Bernd Faenger, Nikolaus-Peter Schumann, Dirk Arnold, Roland Grassme, Martin Fischer, Hans-Christoph Scholle

Stimulation selectivity of an interfascicular electrode in the sciatic nerve of rabbits 151
Thomas N. Nielsen, Cristian Sevcencu, Johannes Jan Struijk

Characterization of peri-infarct, intra-cortical motor cortex responses during reaching task in a chronic animal model of ischemic stroke 154
Winnie Jensen, Michael Vognsen Nielsen, Kasper Juhl Graesboell Ottesen, Lars Christian Fjeldborg

Session 7. Modeling

Development of a method for estimating unit conduction velocity using spectral analysis of the action potential 161
Shaoyu Qiao, Ken Yoshida

3D-ColorComputer Tomography assessment: monitoring of muscle recovery in SCI patients treated with electrical stimulation 164
Paolo Gargiulo, Ugo Carraro, Egill Fridgeirsson, Pall Jens Reynisson, Thordur Helgason

Enhancement of vowel encoding for cochlear implants by adding a high frequency signal: a modelling study 167
Liliana Paredes, Cornelia Wenger, Frank Rattay

Current-distance relations for microelectrode stimulation of pyramidal cells 170
Cornelia Wenger, Liliana Paredes, Frank Rattay

Improving Stimulation, Recording, and Modeling Tools and Techniques for Retinal Implant Development 173
Saso Jezernik, Giovanni Dandrea, Bohdan Kolomiets, Milan Djilas, Bertrand Cahuzac, Robin Ladmiral, Andreas Kuhn, Christophe Beesau, Lucia Cadetti, Serge Picaud, Jose Sahel

Session 8. Upper Extremity

Preliminary comparison between haptic and electrical stimulation adaptive support for upper extremity motor training 181
Matjaž Zadravec, Jakob Oblak, Imre Cikajlo, Zlatko Matjačić

Toronto Rehabilitation Institute's Functional Electrical StimulationTherapy for grasping in traumatic incomplete spinal cord injury: Randomized Control Trial 184
Naaz Kapadia, Vera Zivanovic, Julio Furlan, B.Cathy Craven, Colleen McGillivray, Milos Popovic

Multicenter clinical trial of Myoelectrically-controlled FES (MeCFES) for assisting hand function in subjects with tetraplegia - study of user population, orthotic effect and ADL use 188
Rune Thorsen, Davide Dalla Costa, Sara Chiaramonte, Luca Binda, Tiziana Redaelli, Eugenio Occhi, Ettore Beghi, Roza Converti, Maurizio Ferrarin

Computer vision for selection of electrical stimulation synergy to assist prehension and grasp 190
Strahinja Dosen, Grethe Kiehn Kristensen, Behamin Bakhshaie, Marco Pizzolato, Maros Smondrk, Jana Krohova, Mirjana Popović

Session 9. Lower Extremities

Twenty-five year stimulation of the common peroneal nerve 197
Janez Rozman, Polona Pečlin, Janez Krajnik

An EMG based system for assessment of recovery of movement 200
Nadica Miljkovic, Jovana Kojovic, Milica M. Jankovic, Dejan B. Popovic

Polymyography during hemiplegic walking: Implications for control of FES 203
Ivana Milovanović, Milica Djurić-Jovičić

Effects of FastFES Gait Training on Mechanical Recovery in Post-Stroke Gait 206
Nils Hakansson, Trisha Kesar, Darcy Reisman, Stuart Binder-Macleod, Jill Higginson

Perspectives of Peripheral Functional Magnetic Stimulation in the Rehabilitation of Central Pareses 209
Johann Szecsi, Stefan Götz, Andreas Straube

The time dependence of oxygen uptake and evoked torque during prolonged isometric sub-tetanic NMES. 212
Conor Minogue, Brian Caulfield, Louis Crowe, Madeleine Lowery

Activation threshold and contraction dynamics of quadriceps femoris heads measured with ultrasound imaging : a pilot study 215
Matthias Krenn, Lukas Kneisz, Cristina Hanc, Dietmar Rafolt, Manfred Bijak, Radu V. Ciupa, Winfried Mayr, Christian Kollmann

Brain activation during active, passive and FES-induced movements: a feasibility fMRI study 217
Marta Gandolla, Claudia Casellato, Simona Ferrante, Giancarlo Ferrigno, Giuseppe Baselli, Franco Molteni, Alberto Martegani, Tiziano Frattini, Alessandra Pedrocchi

Session 10. INS Session.
Neuromodulation 2010: The way ahead

Deep brain stimulation - current and future indications 223
F Alesch

Psychiatric indications - a new challenge in deep brain stimulation 223
A Erfurth

Shaping the electrical field - a concept for improving neurostimulation ... 223
L Manola

Neuromodulation and magnetic resonance imaging - conflicting partners? 223
W Kainz

Session 11. Lower Extremities, SCI

Home-based FES in SCI: Recovery of tetanic contractility drives the structural improvements of denervated muscles 227
Ugo Carraro, Helmut Kern

Restoring Stepping After Spinal Cord Injury Using Novel Electrical Stimulation and Feedback Control Strategies 230
Brad J. Holinski, Kevin Mazurek, Dirk G. Everaert, Vivian K. Mushahwar, Richard B. Stein

Active arm involvement in the rehabilitation of walking after spinal cord injury: a case study 233
Laura Elena Alvarado Pacheco, Robert J. Ogilvie, Su Ling Chong, Vivian K. Mushahwar

Optimal walking trajectories estimation using wavelet neural network for FES-assisted arm-supported paraplegic walking 236
Vahab Nekoular, Abbas Erfanian

The effects of intermittent electrical stimulation with varying load and stimulation paradigms for the prevention of deep tissue injury 239
Cara A. Curtis, Su Ling Chong, Vivian K. Mushahwar

Repeated Bout Effect During Eccentric FES cycling: Pilot Data 242
Che Fornusek, Glen M Davis

Cardiopulmonary responses to active and electrically stimulated stepping, with robotics assistance in early-stage spinal cord injury 244
Colm Craven, Henrik Gollee, Mariel Purcell, David Allan

Effects of Recovery after Fatigue on M-wave vs Torque Relationships during Isometric FES-induced Contractions 247
Glen Davis, Eduardo Estigoni, Che Fornusek, Richard Smith

Session 12. FES and Human Motor Control 1

Neural control of posture and locomotion 255
Tatiana Deliagina

Neural control of human posture and movement: Modifications of monosynaptic lumbosacral posterior root-muscle reflexes 256
Ursula Hofstoetter, Karen Minassian, Winfried Mayr, Frank Rattay, Milan Dimitrijevic

Neurophysiology of the human lumbar locomotor pattern generator 259
Karen Minassian, Ursula Hofstoetter, Keith Tansey, Frank Rattay, Winfried Mayr, Milan Dimitrijevic

Marked multi site stimulator of the lumbar posterior roots as a tool for studies of the locomotor pattern generator in humans 262
Manfred Bijak

Session 13. FES and Human Motor Control 2

Human neurophyiology of the voluntary motor tasks 267
John Rothwell

Computation in neuroscience of conducting and processing capabilities of the human nervous system 268
Frank Rattay, Karen Minassian, Ursula Hofstoetter, Simon Danner, Winfried Mayr, Milan Dimitrijevic

Can FES device be also a tool for assessment of motor control 271
Winfried Mayr

Session 14. FES and Human Motor Control 3

Comparison of neuromuscular stimulation to exercise 275
Gerta Vrbova

Scientific Poster Presentations.

1100-Channel Neural Stimulator for Functional Electrical Stimulation Using High-Electrode-Count Neural Interfaces 279
Scott Hiatt

Functionning of Sacro-Lumbar Anterior Root Stimulator Implant 282
Pablo Aqueveque, Antoine Nonclercq, Anne Vanhoestenberghe, Dominik Cirmirakis, Nick Donaldson

Development of a Thin-Film Array for Cortical Stimulation 285
Benjamin Townsend, Iain Stitt, Gerhard Engler, Andreas K Engel, Birthe Rubehn, Thomas Stieglitz

An Energy-Efficient and Multiple-Waveform Stimuli Generator for Visual Cortex Microstimulation 288
Md. Hasanuzzaman, Mohamad Sawan, Rabin Raut

Therapeutic FES with distributed units 291
Nenad Jovicic

Implantable pressure sensor for detecting the onset of a bladder contraction - preliminary results 294
Jacob Melgaard, Nico Rijkhoff

Methods for in vitro study of electrical current and potentials distribution in layered biological tissue 297
Nebojša Malešević, Goran Bijelić

Iterative learning control for FES of the ankle 300
Robert Nguyen, Silvestro Micera, Manfred Morari

Blink prosthesis for facial paralysis patients 303
Daniel McDonnall, M. Douglas Gossman, K. Shane Guillory

Effects of the number of pulses on evoked sensations in pairwise electrocutaneous stimulation 306
Bo Geng, Ken Yoshida, Winnie Jensen

Development of a Wearable Sensory Prosthetic Device for Patients with Peripheral Neural Disturbances 309
Kunihiko Mabuchi, Hirotaka Niiro, Makoto Shimojo, Masanari Kunimoto, Masatoshi Ishikawa, Takafumi Suzuki

Cortically controlled functional electrical stimulation: a neuroprosthesis for grasp function 312
Christian Ethier, Emily R. Oby, Matthew J. Bauman, Sonya P. Agnew, Lee E. Miller

Dependence of implantation angle of the transverse, intrafascicular electrode (TIME) on selective activation of pig forelimb muscles 315
Aritra Kundu, Winnie Jensen, Mathijs Kurstjens, Thomas Stieglitz, Tim Boretius, Ken Yoshida

High Performance Motion Control by Neuro-Muscular Electrical Stimulation applied to the Upper-Limb 318
Christian Klauer, Thomas Schauer, Jörg Raisch

Reduction of the Onset Response in High Frequency Nerve Block with Frequency and Amplitude Transitioned Waveforms 321
Niloy Bhadra, Meana Gerges, Emily Foldes, Michael Ackermann, Narendra Bhadra, Kevin Kilgore

Optimization of a Tremor-Reduction Algorithm for Asynchronous Stimulation of Independent Motor-unit Groups 324
Andrew Wilder, Richard Normann, Gregory Clark

Including Non-ideal Behaviour in Simulations of Functional Electrical Stimulation Applications 327
Cheryl Lynch, Geoff Graham, Milos Popovic

Influence of back muscle strength on Vertebral Stress 330
Kazutoshi Hatakeyama, Toshiki Matsunaga, Yoshinori Ishikawa, Kohei Ohtaka, Mineyoshi Sato, Satoaki Chida, Motoyuki Watanabe, Akiko Misawa, Kana Sasaki, Takenori Tomite, Takayuki Yoshikawa, Daisuke Kudo, Takehiro Iwami, Yoichi Shimada, Kiyomi Iizuka

Motion analysis of low-intensity back muscle exercise using a three-dimensional musculoskeletal model 333
Takayuki Yoshikawa, Toshiki Matsunaga, Michio Hongo, Takenori Tomite, Kana Sasaki, Daisuke Kudo, Mineyoshi Sato, Satoaki Chida, Kazutoshi Hatakeyama, Takehiro Iwami, Yoichi Shimada

A Review on Functional Electrical Stimulation in China 335
Dingguo Zhang

Cortical change and functional recovery of upper limb by therapeutic electrical stimulation with chronic hemiplegic patient: a case report 339
Kana Sasaki, Toshiki Matsunaga, Akiko Misawa, Takenori Tomite, Takayuki Yoshikawa, Daisuke Kudo, Satoaki Chida, Mineyoshi Sato, Kazutoshi Hatakeyama, Yoichi Shimada

Therapeutic Electrical Stimulation through Surface Electrodes for Hemiplegic Shoulder Subluxation - Comparative study of the low-frequency stimulation method and the Russian method 341
Daisuke Kudo, Toshiki Matsunaga, Takenori Tomite, Kana Sasaki, Takayuki Yoshikawa, Mineyoshi Sato, Satoaki Chida, Kazutoshi Hatakeyama, Yoichi Shimada

Improving the Hemiplegic Hand Function by FES using Direct Myoelectric Control 343
Rune Thorsen, Marco Cortesi, Johanna Jonsdottir, Ilaria Carpinella, Daniela Morelli, Rosa Maria Converti, Maurizio Ferrarin, Anna Casiraghi

EMG-triggered Neuromuscular Electrical Stimulation Combined with Motor Point Block to Improve on Hand Function in Hemiplegic Patients with Severe Spasticity 346
Young Hee Lee, Jong Hoon Lee, Eun Young Yoo, Soo Hyun Park, Ik Sun Choi, Young Ho Kim

Effect of combined peripheral motor electrical stimulation and anodal transcranial direct current stimulation(tDCS) in stroke patients 349
AR Ko, Young-Hee Lee, Jongsang Son, Young Ho Kim

Neuroprosthesis for finger rehabilitation and independent user application: Testing with one patient 352
Arna Oskarsdottir, Thordur Helgason

Repetitive Exercises using Electrical Stimulation and a Robot Arm for Upper Extremities: a pilot study 355
Satoaki Chida, Toshiki Matsunaga, Mineyoshi Sato, Kazutoshi Hatakeyama, Takenori Tomite, Kana Sasaki, Takayuki Yoshikawa, Daisuke Kudo, Takehiro Iwami, Tomoya Kosaka, Yhoichi Shimada

FES-assisted cycling training can improve cycling performance, cardiorespiratory ftiness, strength, gait and functional activity following an 8-week, home-based training program - a case report 358
Samuel Lee, Ann Harrington, Calum McRae

Bi-Moment Chair for the Measurement of Joint Moments 360
Kylie de Jager, Nick Donaldson, Di Newham

Combined video game and neuromuscular stimulation based training 363
Dimitry Sayenko, Matija Milosevic, Mark Robinson, Kei Masani, Kristina McConville, Milos Popovic

A Comparative Study on Electrical Stimulation and Magnetic Stimulation as for the Muscle Contractility and the Pain Perception 366
Tongjin Song, Khang Gon, Sun Hee Hwang, Bum-Suk Lee, Da-Woon Jung, Dong-Gu Kim, Dae-Sung Park, Jei Cheong Ryu, Sung Jae Kang

Gait cycle detection using 3-axes linear accelerometers & gyroscopes in hemiplegic patients. 369
Takenori Tomite, Yoichi Shimada, Toshiki Matsunaga, Kana Sasaki, Takayuki Yoshikawa, Daisuke Kudo, Mineyoshi Sato, Satoaki Chida, Kazutoshi Hatakeyama, Takehiro Iwami

Movement of Ankle Plantar flexor and Subjective Pain by Monophasic Electrical Stimulation 372
Tatsuto Suzuki, Takashi Watanabe, Ryuichi Saura, Hironobu Uchiyama

The dynamics of cortical reorganization associated with voluntary and peripheral electrical stimulus 375
Simona Denisia Iftime Nielsen, Michael James Grey, Thomas Sinkjaer, Omar Feix do Nascimento

A biofeedback treatment based on FES to recover the medial hamstring use in stroke patients suffering of stiff legged gait 378
Simona Ferrante, Emilia Ambrosini, Paola Ravelli, Giancarlo Ferrigno, Franco Molteni, Alessandra Pedrocchi

Reducing the upper body effort during FES-assisted arm-supported standing up in paraplegic patients 381
Ali Seyedi, Abbas Erfanian

Use of ultrasound current source density imaging (UCSDI) to monitor electrical stimulation of denervated muscles and fiber activity, some theoretical considerations 384
Bjorg Gudjonsdottir, Paolo Gargiulo, Thordur Helgason

Joint reaction force of lower extremities during rowing in non-disabled individuals 387
Toshiki Matsunaga

Anniversary Session

(including Podium discussion with FES users)

Vienna FES Workshops: 1983-2010

Winfried Mayr

Center for Medical Physics and Biomedical Engineering, Medical University of Vienna, Austria

The Vienna International Workshop on Functional Electrical Stimulation (FES) is a triennial event that started in 1983 on initiative of Herwig Thoma. The workshop was held on varying locations in and near the Austrian capital Vienna. Colleagues from all over the world have joined us for this meeting over the years, many of them regularly. The workshop provides FES related information in actual and condensed form, always on an interdisciplinary basis integrating technical, biological and medical sciences in the whole spectra from basic to applied research. The workshop documentation is based on proceedings with short-papers. The meanwhile 10 proceeding books cover 27 years of FES history including a lot of material that has never been published elsewhere and are completely available in digital form.

Looking through this little FES library shows topics of permanent interest as well as coming and going trends. The two big success stories Cardiac Pacemaker and Cochlear Implants were strongly represented in the first workshops and disappeared to specific conferences, as they became wide and complex research fields of their own accompanied by an impressive commercial background. Spinal Cord Injury (SCI) Rehabilitation remained of constant importance throughout the years. The emerging success stories were smaller and commercially less spectacular, but nevertheless of unquestionable benefit for the users. E. g. Sacral Anterior Root Stimulator, Phrenic Pacing, Grasping- and Gait-Support Systems provide direct impacts in persons quality of live, and to a certain extend an equilibrium between availability on the market and still ongoing research efforts has been achieved. The same is true for many therapeutical approaches, traditionally pain and spasticity treatment or neuromuscular training. Those are more and more seen as complementary and synergic with functional restoration and over time we see a clear development from electrical braces versus therapeutic methods to integrative functional solutions taking advantage of plasticity of neural and neuromuscular structures. We see special application topics like Cardiomyoplasty or use of muscles to provide energy for cardiac assist devices, with extremely strong efforts for a limited time span ending as suddenly as they were started. Though the early high expectations were disappointed the research output remained valuable and supported other research branches. In parallel to the mentioned applications technological development is mirrored from miniaturization of electronics and power supply solutions via biomaterial research, sensors and control to biotelemetry.

In our actual edition we notice a clear focus on spinal cord stimulation which is known from classical anti-pain and anti-spasticity therapy and the important Brindley sacral anterior root stimulation system. Novel approaches in part still address improvements in these classical applications, others develop more in direction of selective central stimulation of efferences to elicit specific peripheral motor functions. Stimulation of afferences at the spinal level to control and modify the activities of the "spinal brain", the neuronal networks for movement control, known as e. g. central pattern generator (CPG), lumbar locomotion pattern generator (LLPG), seems extremely promising for the development of more efficient clinical rehabilitation strategies. Another topical accumulation is visible on the field of stroke and hemiplegia and in particular aiming in functional improvements of impaired upper and lower extremity. This research has been important throughout all our workshops and underlines the increasing actually needs of effective rehabilitation concepts for the growing population of elderly. A third trend we notice is a revival of implant technology. FES implants had been seen as a priority in the earlier years of FES. Due to limited achievements for many applications, high costs and lack of acceptance by the patients research topics drifted to non-invasive solutions in the 90th. In the actual reports we notice many attempts on implantable electrodes with optimized selectivity and complex electronic solutions based on contemporary capabilities. These developments are accompanied by advanced biosignal recording and sensor techniques and complex control strategies that give hope that this time "closing the loop" in complex neuroprostheses could have better chances then ever in history of FES.

Finally let's not forget the fresh and unconventional ideas that spice up the discussions and fertilize new development. They have accompanied us through all the years and many of them appeared just once, some developed to something greater. In older issues we find things like influencing the electrical field distribution in the tissue by injecting metal particles, artificial muscles – polymers that contract in electrical field or focused non-invasive stimulation by applying constant magnetic field in combination with focused ultrasound. In the 2010 edition a neuroprosthesis for reactivation of the paralyzed eye lid and minimal invasive phrenic pacing via endovascular electrodes to support respiratory weaning strategies are examples for those special novelties.

Neuro-Motor Rehabilitation in reference to Control Theory

Vossius Gerhard

Institute of Biomedical Engineering, Karlsruhe Institute of Technology, Karlsruhe, Germany

Abstract

Rehabilitation of the Neuro-Motor-System incorporates the physical, neurological – and psychological – aspects of this domain. Whereas the treatment of the deficits of the physical part of the domain is already well developed, so far little attention has been paid to the structure of the networks built by the nerve cells to create the functional capabilities we observe. In order to execute its control tasks appropriately, the brain, CNS, has theoretically to provide sufficient perceptibility of the surrounding environment and the internal state of the body as well as guidability of the body movement. This comprises in our case a multilevel Closed Loop structure including appropriate References. In addition Dynamic Stability of the system, an Undirectional Information Flow and the creation of Reference Patterns have to be granted.

At least two of these prerequisites are distinctly hurt: The noise accompanying the information flow through the computing networks with their large number of nerve cells is fast adding up to large amounts of uncertainty. Assuming e. g. a realistic noise level of 1% per nerve cell and an average number of 500 000 cells per segment of the spinal cord it is quite obvious, that there have to be specialized structures to make up for this deficit of precision. –. There are indications that the spastic reactions, e. g .after an injury, are involving at this level. Secondly: The sufficient perceptibility does not adequately exist. The higher the level and the degree of complexity in the hierarchy of the system the more this effect is pronounced at the reference and control at level.

The regular and specific properties of the neuro-muscular control system can be related to the therapeutical and rehabilitation procedures. This way one gains a better insight into the background of the system which supports e. g. the treating of spasticity, the restoration of normal motor control, and the relieve of hurting, the patient bothering effects accompanying chronic diseases as MS, ALS or Parkinson disease. Using Electrical Stimulation the contact to the inflicted centres of the CNS may be made non invasively via the skin.

Keywords*: Control theory, Electrical Stimulation, Free Will, Rehabilitation, Sensor-Motor-Control*

Introduction

Life, also in its simplest form, foots on its basis at the cybernetic principles of order, of structure. This dimension of order is principally independent from the other physical dimensions WIENER [1], it is orthogonal to the latter, as MARKO [2] proved. The knowledge of the nature of this dimension of order evolved mainly from the development of communication and control theory. WIENER named it Cybernetics and its basic quality Information. Its two major parts are Information and System Theory.

There is a certain drive, to burry the cybernetic as a scientific discipline. When it evolved, it was fast loaded with fashionable expectations. Everyone tried to jump on the "band-wagon". Now this ballast is being stripped off – as a fortune for science – and one returns to matter. And nature is going on to populate the earth on this principle.

Our universe foots completely on the other physical domains. The cybernetic structures including information flow and processing are imbedded in them for their realization. As a consequence this results in certain restrictions of the original inherent power of the cybernetic structures due to limitations of their physical host.

The Sensor-Motor-System, the topic of this talk, is subject to these conditions. Its mode of operation is determined on this basis.

During recent years more and more effort has been made to improve the rehabilitation procedures by establishing a more effective contact from the outside to the sensor-motor-centers of the CNS. This objective might be all the more achieved all the better one understands the processes generating the observable functions truly, by this being able to interact with the appropriate motor centers using matching loci and patterns.

So far our knowledge about this topic is rather limited. We know a number of neurophysiologic modes of operation comprising limited numbers of nerve cells or some mathematical descriptions of specific motoric functions. But as soon as one approaches the domain of higher, more complex

functions, today one is able to locate them better and better refined within the brain, but is not able to find out how they are really attained. In Neuro-Motor Rehabilitation this latter aspect has not yet been too closely tackled. Therefore I shall start out by comparing the fundamental properties of system theory to their realization in the nervous system of man.

Cybernetic Aspects of the Sensor-Motor-System

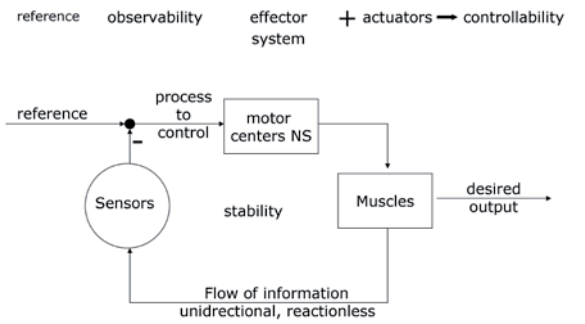
The physical basis of the system, the layout of the "hardware" structure, is encoded in the genes. The genetic level is determining the frame of what is functionally realizable. It is controlled by so-called epigenes and other chemical structures in which the information is encoded. How far this control is open or closed loop and reaches into the neural domain or being also functional directly effective is not yet known. This specifies the frame, the borderlines of the total hierarchy of the CNS with its information processing capability altogether attainable, as well as certain initial properties to start out and conduct the individual development of the anatomical structure of the brain, the functional faculties are embedded in. Looking on the CNS from a cybernetic aspect it consists as a system of self-contained components with unidirectional in- and outputs communicating by information flows. Evolution took great care of developing the nervous synapses granting unidirectionality. The computing, information processing is executed in an analog mode, which is unfortunately more susceptible to errors stemming from noise and systematic errors, especially in systems comprising larger numbers of elements. These errors, attained to each decoupled element, are fast summing up. Taking in consideration that every specific function has in most cases being build up by combinations of multiply interconnected single nerve cells, one may imagine, how fast the error grows beyond being acceptable. This is especially the case if one keeps in mind that our brain consists altogether of about 19 to 23 billions nerve cells and even one segment of the spinal cord contains averagely 500 000 nerve cells, each with a modestly estimated noise level of 1%.
Technically one circulates this problem to a large extent by digitalization and gains this way also access to much higher resolutions, including another advantage:
Information structures may be implemented in hierarchical systems horizontally by adding structures with equal, vertically with higher, more complex, more powerful faculties. In systems based on analog procedures these properties are much more limited.

Basic Functions of the Nervous System

We are not familiar with the calculation procedures the brain uses to organize the nerve cells with its synapses to fulfill its task. One may observe just the outcome. The brain has generally a stable mode of operation – otherwise life would not be possible – and it may on special requests produce high exactness.
The true functional domain handling the on-line information processing of the internal state of the body is neural based in conjunction with chemical components, e. g. hormones. The higher the level in the hierarchy of the nervous system, the more complex the structures, the larger the body of nerve cells being involved, the more a neuronal base has to be established for reducing the "error-pool" accompanying the lumped cooperation of the nerve cells and granting the background for domiciling the functional sphere. The increase of the supporting base might lead to a limiting cycle.
Disorders at this level might lead to functional disruptions at the higher levels. E. g. spasticity can be such a reaction, preventing all normal ways of action. Applying electrical stimulation pulses of low frequency to the region afflicted, the spasticity ceases accompanied by a carry-over effect. Subsequently the effect is consolidated by slowly raising the frequency and normal function is returning. Stimulation of the healthy sensor-motor system does not produce any additional side effects if applied adequately [3].

Levels of Control

Simple scheme of the control loop of motor functions



A simple scheme of the control loop of the sensor-motor system, fig. 1., shows its basic components.
In the case of man we have well structured multi level control systems incorporated into a larger system unit finally coordinating the about 200 degrees of freedom and the references which are gained from various sources inside and outside the moving body, creating a copy of the time changing conditions it has to operate in.
For each effector, e. g. arm, the capability has to be established on the one side to direct it at any point in space within its range and on the other one to trace its movement to the same extends in order to control it adequately. In analogy to KALMAN´s specifically for linear situations introduced terms "Controllability" and "Observability" I want to use here as a general frame not requesting presuppositions "Guidability" and "Perceptibility". Guidability is sufficient if it is able to meet its attributed tasks perceptibility if it can ensure this.
The level of control itself is, simplified composed of a lower stage caring for the peripheral parts of the local control system and an upper one using evidently a variety of eligible strategies to establish sufficient guidability and perceptibility, by this resisting consistant descriptions. From here on at the latest commences a certain alternative to select from various modes of executing a movement, although still unconscious but trainable.
Looking at the control in man from this aspect the guidability is rather well equipped. At the lower stages this is also true for the perceptibility. But higher up in the hierarchy the sufficiency of the latter is fading. The range between fast responsiveness, normal model based prediction to compensate for the reaction-time and fast almost completely model dependent artistic or sports performances exists an enlarging gap in the online-perceptivity. This has more and more to be closed by copying and modeling support without adequate feedback. One pictorial result of this shortcoming is the need of a trainer to improve performance.
A missing secure representation of the state of the muscular system leads also to the so-called sleeping functions: After a local damage in a motor center causing a central paralysis, this might persist even when the damage has been cured completely. By adequate electrical stimulation the muscles can be "enlivened" again and further on integrated into the normal movement patterns [4, see also there for more lit.].
On the other hand the widespread interconnectivity of the various parts of the sensor-motor system having led to distinct dysfunctions being evoked by damage within one of them. These dysfunctions can be corrected by electrical stimulation applied to the skin of the adjoined dermatomes. An example may illustrate this: A patient suffering from ALS, Amyotrophic Lateral Sclerosis, the 1. and 2. motor neurons are increasingly in number destroyed. This results in a central or peripheral paralysis of the adjoined motor units. The paralysis is not only restricted to the cells afflicted, it is much more extended. By stimulation this secondary effect can be largely reversed. E. g. a patient being still capable of walking slowly and insecure on leveled ground can use again a staircase up and down quite naturally and unassisted without in need of hand-rails. The stimulation is accompanied by a longer after-effect. Therefore daily stimulation gives him a good part of functional ability not yet restricted back.
Unfortunately the stimulation is by no way able to cure the cause of the disease, and the moveability is fading with its progress!!
But it allows him a better life in the frame of the still existing muscle force.
An analogous experience has been made with a patient suffering from Parkinson disease, being psychically and physically in a severely reduced state: She was completely emotionless with a collapsed bearing, walking with short, slow, draping steps being assisted by her father. She was a short while ago presented to Mrs. Eck and me, whether it might be possible to improve her bodily impairment. In the beginning we had already a certain success applying stimulation. In the third session, by trying to improve the bearing of the trunk, during 15 min. of stimulation the patient started to erect the trunk, not only her trunk arose but also the entire muscular system gained tonus, she changed to a vivid, normal, merry mood, stood up and walked quite naturally and even lively. Apparently after about three hours came a certain backlash with a return to the former state. Being obvious, that it had not been taken care for her too adequately, a special clinic solved her problem. She was able to return to work again. The stimulation was applied to the skin – non invasively – as in all other cases mentioned here.
In general often it is possible to improve the motoric situation of patients suffering from chronicle diseases, e. g. MS [3], especially by reducing spasticity and improving mobility and, as a side effect, reducing pain. The method contains surely a quite not yet exploited potential, above all in cases otherwise not treatable.

Levels of Coordination and Reference

The coordination and reference creating systems are in man confronted with the same problems as at the higher stages of control. The internal and external conditions are changing their characteristics, valid perceptibility is limited and the gap has to be closed by restricted copying and time requiring modeling procedures. In addition all of this has to be on-line adapted, updated. The coordination level has to be closely interconnected with the control and the reference level because it is dependent from the state of the periphery and the guiding patterns generated by the reference level to create well organized outputs.
In man a broad multi-multifold of references have to be generated to serve the belonging specific control loops and vice versa these states have to be reacquired because most of the reference values are not prefixed but have to be extracted from all the system parts being incorporated in the respective tasks. This way the reference is also partly generated using feedback from the output it has itself initiated. That may result in a state of free-floating which might be dangerous, if the system is not caught in time. The higher the level the greater the danger to miss the real point.
All these considerations presented so far concerning the sensor-motor-system are also analogous true up to the conscious high intellectual levels, taking into account their characteristics and boundary conditions. E. g. one may notice the implications whether the real world is recognized truly or functionally – and how strongly one may cling to this in the latter case.
In general man has been gifted with the domain of conscious objective abstraction and as a consequence the enormous artificial enrichment of the sensory sphere permitting a complete new view of the world. This reduces also the lack of independence at the reference level and the gap of the perceptivity remarkably, but can not close it completely, especially in the non abstract domain. However this topic will here not be covered further.

Conclusions

One of the main purposes of this talk is, to turn the attention to the domain of control of the field of rehabilitation. Rehabilitation and its research background are intensively occupied by special parts of the field. But when treating patients suffering from severe deficits it is always the complete scope being asked for as a reference to judge the state of the patient and consequently to select and fit the therapeutic procedures into the total picture, to restore this as good as possible.

Control theory is the best possible background to serve the above objective because evolution developed it along the cybernetic line, being the principle to embed the task to be achieved in.
The levels of the total system are: (genetic) – neuronal base – control – coordination – reference.
Due to the complexity of the total system, the flexibility within each level and in conjunction with the other levels, there exist no simple, unique solutions to describe more complex functions. Right now the therapeutic procedures are in most cases bound to use the sensory plain as an input to the sensor-motor-system, then to depend on the systems own information processing power and use the muscular motor-power, being restricted to choose the right input patterns and to load the muscles in an appropriate manner.
The more we want really to communicate interactively with the nervous system, the more a drastic different approach would be required. Then one might be aware how powerful a tool control theory can be, as it has already been proven in simpler cases.

Off the Track

The variability man possesses to create and execute his movements and, which is not limited to this case but also to different motives for taking action, rises the question, whether if he chooses consciously between different actions, does this happen on the base of his own “free will” or whether he does not at all have the possibility of choice because what he interprets as his own decision is already in advance genetically determined. From today’s point of view the natural scientific facts are: Life is based on the cybernetic principles of order, of structure not depending upon the kind of substance the structures is made of. The information is encoded in the lay-out of the structure. In the beginning of evolution of life the carrier of the information was only chemical based, that is concerning the genes so till today. In the course of evolution this way to develop higher information structures was not too successful, for what reason is not known. Instead the nervous system is developing more and more, although this is a tedious way. It handles on-line all the enormous amount of information we foot on during our life. But for reproduction the base of transferring information is solely chemical and the genes control the development of the new offspring including the frame of the functional capacity being available by the brain.
Considering the functional state of the brain, primarily the potential to execute his own free choice

exists, being extended upwards in the hierarchy of the brain, not being unlimited but being confined by its cybernetic, physiological, physio-chemical borderlines from a natural-scientific point of view. Selecting the action is also modified by different motives e. g. moral ones and generally bounded by reasons as the intellectual capacity, education, experiences gained a. s. o.
But whatever releases the initiative to take action, to decide about its goal, whether it is determined by a gene or by mans free will, this question can not be settled today. We are not yet able to detect, whether the decision is somewhere laid down genetically, preferable within the center controlling the process centrally, or whether it results from (carefully) considering there in. We know that the genes have a certain upward influence, but we don't know whether there exists also a certain nervous feedback down to the genetic level to execute some control on its part or not. This is only to answer if we are able to describe the system structure exactly. Thus right now we have to live with the uncertainty – and act.

Acknowledgements

First of all I want to congratulate the Vienna Group to their 10th jubilee arranging the Vienna Symposium on Electrical Stimulation of patients being motoricly handicapped. It was always and is today an important opportunity to summaries and spread the state of art in the field. This was offered always with the famous Vienna charm we enjoyed and have to thank for so much. Of course we have to thank them also for the body of scientific work emerging from Vienna in former times especially by the initiative and guidance of Prof. Thoma, e. g. inventing the so-called "Karussel"-Stimulation of the phrenic nerve. Developing with his group a reliable implantable stimulator he helped patients being high level spinalized by restoring a key function to lead a much better life. I may be allowed to wish the group all the best for the future, permitting them to grow and flourish.

References

[1] Wiener N.: Cybernetics, The Technology Press, Cambridge, Mass. 1948

[2] Marco H.: Physikalische und biologische Grenzen der Informationsübermittlung. Kybernetik 2 (1965) p. 274-284

[3] Vossius G., Frech R.: Parameters controlling antispastic electrical stimulation: clinical application & theoretical considerations, in: Pedotti A., Ferrarin M., Quintern J. et al., Neuroprothetics from research to clinical applications, Springer Berlin-Heidelberg-New York (1996) p. 437-446

[4] Vossius G.: Correcting Sensor-Motor Disorders by Means of Structured Electrical Stimulation – Quoted Neuromodulation, Biomed Tech 53 (2008) Suppl.1; p. 173-182

Author's Address

Prof. em. Dr. med. Gerhard Vossius
eMail: elsmarie.vossius@t-online.de

The role of materials biocompatibility for FES-applications

Plenk Hanns Jr.

Bone & Biomaterials Research, Institute for Histology & Embryology, Medical University of Vienna, Austria

In functional electrical stimulation (FES), the materials in contact with the biological environment are primarily the implanted electrodes and their insulation, and secondarily the packaging of stimulator and leads connecting the stimulator with the electrode. Choosing the electrode material, the tissue response to the material, a possible immunological reaction to the bulk material or released constituents, the resulting electrode-tissue impedance, and the radiographic visibility have to be considered. Metallic electrodes, made of stainless steel, or of more inert gold, platinum, platinum-iridium, titanium nitride, tungsten and tantalum, are mainly used and readily visible on radiographs, but also conducting polymer coatings seem promising for better long-term performance. Increasing the surface area and roughness of the electrode will enhance the tissue contact and the signal delivery, but will also affect the tissue response. The growth of a fibrous tissue capsule around the electrode, determining the electrode to cell/tissue impedance, is due to the inevitable inflammatory tissue response which can be influenced by drug release from the electrode tip. Corrosion of electrode metals and alloys may be accompanied by allergic reactions, negatively affecting the tissue response. The preferred electrode insulating materials are polyimide and glass, both being more or less resistant and thus compatible in the aggressive biological environment. The packaging materials for stimulators and leads are mainly silicon- or polyurethane-based, and their long-term performance will also depend on relative motion in the various implant bed situations.

Dropped Foot Stimulator: From the first idea to a patient satisfactory device

Taylor P.N

Department of Clinical Sciences and Engineering, Salisbury District Hospital, Salisbury, UK

p.taylor@salisburyfes.com

Abstract

The Odstock Dropped Foot Stimulator (ODFS) came about to address a clinical need: to improve the mobility of patients with stroke, MS and incomplete spinal cord injury. This paper describes the journey from initial prototype through clinical trial, clinical service and commercialisation. Significant factors in this journey are described.

Introduction

FES for correction for dropped foot in hemiplegia was first put forward by Liberson et al. in 1960. They demonstrated the provision of dorsiflexion by stimulation of the common peroneal nerve timed to the gait cycle using a switch under the heel. By provision of "function" from controlled electrical stimulation the term Functional Electrical Stimulation was coined and the rest as they say is history. Despite promising clinical results significant clinical use of the techniques was limited to a few specialist centres and barely used at all in the UK.

The Odstock Dropped Foot Stimulator (ODFS) was original designed as a solution to improve walking for an individual patient who had dropped foot due to incomplete C6 SCI in 1987. We tried a commercial available device but found it did not have sufficient output for this individual. Hence a bespoke device was made. After about two weeks use of the device walking distance was increased from 2 or 3 steps to over 100m with a walking frame. At about the same time a 2 channel version of the device was constructed for another person with incomplete SCI Brown-Séquard syndrome who required knee extension in stance in addition to dorsiflexion in swing. This device enabled short distance ambulation with a walking frame where no walking was possible without FES. Both devices were constructed analogue and discreet logic circuitry and footswitches based on force sensitive resistors.

Development

The devices were tried with other patients including those with MS and stroke. The clinical engineer worked directly with the patients with the assistance of the physiotherapist allowing direct contact with clinical problems. Hence solutions could be quickly devised, tested and further refined. Through this process the functionality of the device was iteratively improved. A test switch was added to allow easy adjustment of stimulation level and electrode positions. The original fixed time of stimulation was replaced adaptive timing where the stimulation was ended as well as begun by the foot switch. An "extension" facility was added that prolonged the stimulation past heel strike, providing an eccentric contraction of the anterior tibialis, lowering the foot to the ground. Perhaps most significantly an adaptive threshold for detecting when weight was removed or returned to the foot switch was devised. This enabled stimulator to automatically search for a switching point, correcting for drift in FSR resistance over time and also automatically adjusting to the gait of a heavy adult or small child. This innovation significantly improved the clinical usability and reliability of the devices.

RCT

In 1993 A randomized controlled trial (RCT) was conducted to evaluate the effect of the Odstock Dropped Foot Stimulator (ODFS) on effort and speed of walking in hemiplegic patients with dropped foot[1, 2]. Thirty- two chronic post-stroke (>6 months) subjects were randomized to either a treatment group receiving stimulation with the ODFS and concurrent physical therapy or a control group receiving physical therapy alone. During the first month of the trial, all subjects received 10 sessions of physical therapy. Each session was approximately one hour. Evaluations of walking speed over a distance of 10 meters were collected at baseline, 4 weeks, and 12 weeks following the initial device set-up. Comparisons were made between mean walking speed at baseline and mean walking speed at the conclusion of the study for each group. At 12-weeks follow-up, a mean increase in walking speed of 20.5% was observed for the treatment group (when the stimulator was in use) and 5.2% in the control group. The Physiological Cost Index (PCI), a measure of walking efficiency, was also evaluated in this study. Improvement was also demonstrated via a reduction in PCI at the conclusion of the study compared to baseline. The treatment group had a 24.9% reduction of PCI (when the stimulator was in use) whereas the control group had a 1% reduction. During the course of this trial, no significant carryover effect of stimulation with

the ODFS device was observed since there were no significant improvements in walking speed in the treatment group without the use of stimulation

Clinical Service

Following the RCT the results were presented to the South and West Regional Health Authority Development and Evaluation Committee, the body that at the time was responsible for giving the go-a-head for new services in the Hospital. Their evaluation included cost benefit QALY (Quality Adjusted Life Years) analysis. The QALY gain was calculated using a combination of data including change in walking speed and physiological cost index, change in Hospital Anxiety and Depression Index (HAD) and change in a mobility score derived from a custom designed questionnaire closely aligned with the Health Related Quality of Life (IHQL). After 12 weeks of intervention it was calculated that the FES group received a QALY gain of 0.065 while the physiotherapy group had a gain of 0.023, a difference of 0.042. At 1996 prices this gave a cost per QALY of £10,037 over 5 years. In 2010 the report was re-examined and costs per QALY calculated for current prices[15]. This gave a cost per QALY of £39,047 at one year and between £13,524 and £19,237 at five years. However, this analysis assumes that a comparison is made with an individual who receives physiotherapy. In clinical practice the ODFS is used as a long term aid while physiotherapy is rarely received for more than a few weeks. It may therefore be fair to attribute the whole of the QALY gain seen by FES users rather that the difference between FES and Physiotherapy interventions. This gives a cost per QALY gain of £25,230 at 1 year and between £8,738 and £12,431 at 5 years.

Following permission, a clinical service was begun in 1996. However, the hospital's rehabilitation department was not in a position to take up the service so instead the service was run by the Medical Physics Department and was provided by the same staff who had worked on the RCT, part time while working on other research. Unusually, this resulted in physiotherapists being directly employed by a clinical engineering department and clinical engineers being involved in service provision. Mixing research and clinical service enabled researches to focus on real clinical issues and for intervention to be taken to the clinic more easily. It was also decides to continue with the same main outcome measures as the RCT, walking speed and PCI (Physiological Cost Index). This enabled audit of the FES service and it was subsequently demonstrated that results were at least as good as the RCT and for the first time a training benefit was demonstrated from using FES for the correction of dropped foot.

Technology transfer

A condition for the funding of the RCT was that at the end of the project a two day training course would be given to teach clinicians from other centres the techniques we had learned. This implies that the clinicians who were trained would have access to the ODFS for their own patients hence the department extended its small sale production of devices. In fact a decision was made that devices would only be supplied to clinicians who had been trained in the use of FES. This was to ensure that clinical results obtained would remain at a high standard, protecting the reputation of the technique and the equipment. In 1998 CE marking for medical devices became compulsory in the UK. If we were to continue to supply these other clinics we either had to find a commercial partner to take over production and produce the devices under an approved quality system or become able to CE mark devices our selves. As the market was small no commercial organisation was interested in what was seen as risky new technology, our best option was to establish our own quality system and become registered with the Medical Devices Agency as a manufacturer of medical devices. (In 2005 FDA approval for the USA was obtained through the 510k procedure.) As demand grew, production was subcontracted to local manufactures but control of quality and distribution remained with the department.

Through word of mouth a demand for further courses was developed, resulting in a continuous series of courses, approximately 200 being run by 2010. To support the clinicians using the devices, detailed device documentation describing the clinical application was developed. This was further supported by a web page (www.salisburyfes), FES Newsletter and clinical meetings. The intention was to create a community of FES clinicians who could support each other through sharing best practice.

In 2006 the Hospital created a spin out company Odstock Medical Limited (OML) to handle device production and sales and also clinical FES service provision. OML was England's first NHS (National Health Service) owned company. This enabled greater commercial freedom to operate and for the first time advertising. Up to that point promotion had been though educational activity only. However, the FES courses remain to this day the main promotional tool and training is still compulsory. Refinement of the ODFS and associated devices continued thought this period and in 2009 the latest version, the ODFS Pace was released, bringing together the experience of the previous years into a smaller digital unit. The ODFS Pace is designed as a holistic clinical tool both for orthotic dropped foot correction and gait training in physiotherapy where other muscles such as gluteal, quadriceps, calf or hamstring muscles can stimulated in active gait training or in cyclic exercise.

In 2009 the National Institute for health and Clinical Excellence (NICE) produced guidance recommending the use of FES for dropped foot within the NHS. While this does not make it obligatory that the NHS funds FES, it does make it a recognized intervention for routine use. In 2010 further analysis of the cost effectiveness of FES was produced indicating an almost identical QALY gain as calculated 14 years previously. Evidence for reduction of falls following FES use,

improvement in quality of life and efficacy in MS were also published in 2010.

Conclusion

The main drivers in the development of the ODFS have been the need to respond to clinical need and clinical demand, providing solutions at costs sustainable within the NHS. In many ways, through necessity it has been a "cottage industry" approach to technology transfer and commercialisation. However this has enabled establishment of a new clinical technique within the UK's NHS system and enable many thousands of patients to benefit from FES.

Acknowledgments

The ODFS was developed under funding from the Department of Health who also funded the first RCT. The RCT in MS was funded by the MS Trust.

References

1. Liberson, WT; Holmquest, HJ; Scot, D; et al (1961) Functional electrotherapy: Stimulation of the peroneal nerve synchronized with the swing phase of gait of hemiplegic patients. *Archives of Physical Medicine and Rehabilitation, 42:101-105.*

2. Taylor PN and Swain ID. Odstock Dropped Foot Stimulator system and peripheries. Patents applied for: UK, 0014968.2, 0021215.9 and 0021223.5; USA 09/652081; and Canada 2.317232, 2001.

3. Burridge JH, Taylor PN, Hagan SA, Wood DE, Swain ID. The effect of common peroneal nerve stimulation on quadriceps spasticity in hemiplegia. *Physiotherapy*, 83(2): 82-89, 1997

4. Burridge J, Taylor P, Hagan S, Wood D, Swain I. (1997) The effects of common peroneal nerve stimulation on the effort and speed of walking: A randomised controlled clinical trial with chronic hemiplegic patients. *Clin Rehabil* 11. 201-210.

5. Swain ID, Taylor PN, Burridge JH, Hagan SA, Wood DE. Report to the development evaluation committee Common peroneal stimulation for the correction of drop-foot (1996) http://www.salisburyfes.com/dec.htm

6. Taylor PN, Burridge JH, Wood DE, Norton J, Dunkerley A, Singleton C, Swain ID. Clinical use of the Odstock Drop Foot Stimulator - its effect on the speed and effort of walking. *Archives of Physical Medicine and Rehabilitation,* 80: 1577-1583, 1999.

7. Swain ID, Taylor PN. The clinical use of functional electrical stimulation in neurological rehabilitation. *In:* Horizons in Medicine 16 – Updates on major clinical advances. Ed. Franklyn J. Pub. Royal College of Physicians, ISBN 1-86016-233-9, London, pp. 315-322, 2004.

8. National Institute for Health Clinical Excellence (NICE). Functional Electrical Stimulation for drop foot of central neurological origin N1733 1P ISBN 84629-846-6 Jan 09 & Treating drop foot using electrical stimulation N1734 1P ISBN 1-84629-847-4 Jan 09 http://www.nice.org.uk/Guidance/IPG278

9. Economic Report. Functional Electrical Stimulation for dropped foot of central neurological origin. CEP10012. Published by the NHS Purchasing and Supply Agency Feb 2010 www.dh.gov.uk/cep

10. JE Esnouf, PN Taylor, GE Mann, CL Barrett. Impact on falls and activities of daily living of use of a Functional Electrical Stimulation (FES) device for correction dropped foot in people with multiple sclerosis. Mult Scler accepted for publication 10th feb 2010

11. Barrett CL, Taylor PN. The effects of the Odstock Drop Foot Stimulator on Perceived Quality of Life for People with Stroke and Multiple Sclerosis. Neuromodulation 2010 13, 1, pp: 58-64

12. CL Barrett, GE Mann, PN Taylor and P Strike. A randomized trial to investigate the effects of functional electrical stimulation and therapeutic exercise on walking performance for people with multiple sclerosis. Mult Scler. 2009 Apr;15(4):493-504

The views of people with spinal cord injury about the use of Functional Electrical Stimulation

Burridge JH[1], Donovan-Hall M[1], Ellis-Hill C[1], Dibb B[2], Tedesco Tricas L[1], and Rushton D[3]

[1] School of Health Sciences, University of Southampton, Southampton, UK,

[2] Brunel University, London, UK [3]Frank Cooksey Rehabilitation Unit, London, UK

Abstract

This paper reports a qualitative study employing a focus group design. The study explored the views of people with SCI, healthcare professionals and researchers about the current and future use of FES, with the aim of identifying barriers to the translation of research into clinical practice and to provide qualitative data to inform the direction of future research. Eight focus groups were conducted with people with SCI, their carers and healthcare professionals. The groups included people with and without experience of FES. Five themes were identified: decision to use FES; physical improvements; lack of resources; importance of sensation and the future use of FES. From the perspective of people with SCI, benefits of FES extended beyond conventional measures of efficacy and cost-effectiveness to more subtle effects on well-being and participation in society. A need for a better appreciation of the psychosocial issues associated with the use of FES was identified by all groups. The information gathered in the focus groups will inform the design of a series of questionnaires currently being developed that will be applied to a large sample of the SCI community in the UK and the US. Questionnaires will be completed via the internet, telephone and snail-mail. Results of the questionnaire will provide the evidence needed to define guidelines for the direction of future clinical practice, research and development of FES for SCI.

Keywords: *spinal cord injury; rehabilitation; qualitative research; focus groups; users' perceptions of FES*

Introduction

For nearly half a century Functional Electrical Stimulation (FES) has been used in the treatment and management of physical problems encountered by people with Spinal Cord Injury (SCI), such as bladder and bowel control, pain relief and management and improvement of movement. Despite intensive research and development, only a small percentage of people who could potentially benefit use FES do in fact use it; illustrating a problem in translating research into clinical practice.

Repair of the spinal cord by regeneration and obtaining the ultimate 'cure' is the greatest hope for people with spinal cord injury (SCI) [1]. However, in the absence of a cure, improving quality of life, function and mobility and enhancing self care are the day to day primary goals [2, 3]. A possible means of improving the everyday quality of life of people with SCI is the use of FES.

It is important to ensure that future developments are user-led and fulfill the needs of people with SCI.

The aim of this study was to explore views of people with SCI, healthcare professionals and researchers about the current and future use of FES. The aim was to identify barriers to the translation of research into clinical practice and to provide qualitative data to inform the direction of future research.

Material and Methods

The design of the study was qualitative and employed a focus group approach. A total of eight focus groups each lasting between 90 and 120 minutes were carried out with the following groups of participants:

One with researchers involved in the development of FES (n = 6),

Two with people with SCI who had experience of using FES (n = 11) and two with people with SCI who had no experience of using FES (n = 9)

Two with clinicians currently using FES (n = 6) and one with clinicians with no experience of using FES (n = 2)

People with SCI and clinicians were recruited from spinal centres throughout the UK. Researchers were recruited from a FES researcher's network.

SCI participants were selected using a purposive sampling technique to ensure that the sample was diverse in terms of age, time from injury, level and severity of injury (including complete and

incomplete paraplegic and tetraplegic participants), whether they were wheelchair dependent or independent and whether they had or had not had previous experience of using FES.

The data was analysed using thematic analysis [4].

Results

The following five categories of themes were identified relating to:

1. Decision to use FES. For example healthcare professionals discussed concerns over the suitability of patients for FES and screening issues. It was felt that caution was needed in initially presenting FES to patients and some healthcare professionals were fearful of raising patients' hopes and expectations, or giving false hope. Despite the need to be cautious in suggesting FES to participants with SCI, it was felt important to provide patients with an informed choice and give them enough information to be able to make this decision. It was clear from the discussions with both the healthcare professionals and the participants with SCI that the patient often initiated the use of FES.

The healthcare professionals also felt that '*commercial*' and '*outside sources*' were often involved in initial suggestions of FES. They talked about having to '*deal*' with companies and cycling reps, and how patients could be at the risk of being given medical advice or sold equipment from people who may not have had the necessary training.

Some participants thought that the *'hassle'* or '*effort'* of using FES often outweighed the benefit. Concerns were raised about the use of implanted systems that would make an individual unsuitable for neuro-regeneration treatment in the future.

2. Physical improvements

As would be expected, perceived physical benefits of using FES mainly related to improvements in muscle activity and function. Among the participants taking part, FES had been used to stimulate movement, help with standing and walking, strengthen and stimulate muscles, and improve bladder control and sexual function.

Healthcare professionals viewed some FES devices as having preventative benefits, such as the prevention of pressure sores and use in cardiac pacing. It was also found that purely cosmetic and physically improvements were important to patients with participants discussing improvements in reduction in '*flabbiness*' and *'A piece of equipment that would give a person with a SCI the opportunity of working at a greater cardiovascular level, for things like type 2 diabetes, obesity and coronary hear disease'.*

Participants with SCI perceived that improvements in everyday quality of life were a key psychological benefit of using FES. One participant felt that they would have been *'housebound'* without the use of a drop-foot stimulator. Another participant discussed how a bladder implant had *'completely changed'* her life as she could sleep through the night and attend more social activities. Healthcare professionals also described the psychological importance of being able to carry out activities of daily living, such as eating without help and performing activities such as FES rowing and cycling, which could help people with SCI feel able to participate in the same activities as able-bodied people.

3. Lack of resources

Resource issues, such a lack of equipment and training, were a main barrier to the uptake and continuing use of FES. This often led to concerns regarding parity between patients and the need to ensure FES was offered to all suitable patients and not just those who asked for it. Issues around screening and checking for suitability of patients, and the lack of agreed protocols and procedures regarding the application of FES were also identified as key areas that needed to be addressed.

4: Importance of sensation

Some participants expressed the view that there was a desire for 'sensation' and not just motor function and talked about the importance of 'feeling', especially when discussing the use of FES for sexual function.

5: Future use of FES

Healthcare professionals discussed the need for further research and evidence supporting the efficacy of FES and how the research needed to be linked to clinical guidelines and application. It was also discussed how FES needed to be developed to look less experimental and needed to be more user friendly and patient-led.

Participants with SCI also made several suggestions for improving the design of FES systems. It was felt that the size and shape of stimulators could be improved to make them smaller and less intrusive. Wires were often problematic and it was suggested that wireless and implanted devices were needed.

Discussion

As with all qualitative research, the findings of this study have provided knowledge and understanding of the subject rather than definitive answers. The study has though provided the information needed to design a series of questionnaires which will be used to explore the extent to which the beliefs identified by the participants are held by the wider SCI community. The questionnaires are currently being developed and will be applied to a large sample of the SCI community in the UK and the US via the internet, telephone and snail-mail. Results of the questionnaire will provide evidence needed to define guidelines for the direction of future clinical practice, research and development of FES for SCI.

Conclusions

Four groups of participants from the SCI community: people with SCI, their carers, healthcare professionals and researchers have expressed their views on the current and future use of FES in SCI. Key barriers to use were identified: lack of knowledge about what is effective and available and when, and with whom, FES should be used. Provision of FES across the UK was thought to be uneven.

From the perspective of people with SCI, benefits of FES extended beyond conventional measures of efficacy and cost-effectiveness to more subtle effects on well-being and participation in society. A need for a better appreciation of the psychosocial issues associated with the use of FES was identified by all groups. The information gathered in the focus groups will inform the design of a series of questionnaires.

These findings can be seen as a starting point to try and understand issues regarding the current and future use of FES. We have started to provide an understanding of issues related to the translation and application of FES research into clinical practice and illustrated some of the critical issues that require further investigation.

Acknowledgements

We would like to acknowledge the financial support for this and the current study from the SCI charity 'INSPIRE', www.inspire-foundation.org.uk

References

[1] Ragnarsson KT. Functional electrical stimulation after spinal cord injury: current use, therapeutic effects and future directions. *Spinal Cord* 2008; **46**: 255-274.

[2] Rupp R Gerner HJ. Neuroprosthetics of the upper extremity: clinical application in spinal cord injury and challenges for the future. *Acta Neurochirurgica Supplements* 2007: **97**: 419-426.

[3] McDonald JW, Becker D. Spinal cord injury: promising interventions and realistic goals. *Am J Phys Med Rehabil* 2003; **82**: S38-S49.

[4] Braun V, Clarke V. Using thematic analysis in psychology. *Qualitative Research in Psychology* 2006; 3:77-101.

Session 1

Technology

Technical challenges with cochlear implants and the Medel cochlear implant company

Hochmair Erwin

Institute for Ion Physics and Applied Physics, Leopold-Franzens-University Innsbruck, Austria

Early cochlear implants (CI) were based on single site stimulation. The first widely used system, the House-implant, may be thought of as being the secondary coil of a transformer directly driving a shallow intra-cochlear electrode. The stimulation signal – an amplitude modulated 16 kHz-carrier – generated by audio circuits in a body worn processor is supplied via the external primary coil mounted on an ear hook. CI-research at the TU in Vienna began in 1975 with the first successful implantation of an eight-channel microelectronic implant in 1977. In the following years especially the wideband-analog technology had been developed providing open speech understanding to a considerable portion of patients implanted. Advantages of the analogue system over contemporary systems using pulsatile multi-channel stimulation was its faithful representation of pitch – a large percentage of its wearers enjoyed listening to music – and its low power consumption, which in the early 90s allowed the development of the first BTE (= behind the ear) speech processor. Fortunately a number of developments paths which later turned out to be a dead-end road were not taken. These include modiolus hugging electrodes, bipolar stimulation, conditioner pulses, and parameter extraction from the speech signal. The latter method tries to avoid channel interaction problems by extracting a few parameters from the speech signal (e.g. pitch frequency, second formant and later additional formants and their respective amplitudes) to generate very simple low-rate stimulation pulses over several channels. After roughly eight years of a finally unsuccessful cooperation with the 3M-company in Minnesota, USA the Vienna CI Group moved to Innsbruck and founded the Medel Company there. In the course of its rapid growth Medel – in cooperation with the Institute of Applied Physics at the University of Innsbruck – developed power-thrifty multi-channel implants in hermetic ceramic and in titanium packages implementing the CIS-strategy, which is, despite many attempts worldwide to enhance or replace it, still the workhorse processing strategy in cochlear implants. Highlights and firsts of the development at Medel include the first multi-channel BTE-processor, the deep insertion electrode, bilateral implantation, parallel stimulation, and CIs for tinnitus suppression in unilaterally deaf patients. So far the speech understanding provided by the so called continuous interleaved sampling strategy (CIS-strategy) developed by B.W. around 1990 is unsurpassed. It provides adequate temporal and spatial resolution by sufficiently fast sampling of the envelopes of a number of band pass filtered signals. It addresses the channel interaction problem by interleaving non-simultaneous stimulation pulses. The signal processing for the CIS-strategy is performed either on standard DSP-chips which, due to the fast development of integrated circuit technology consume less and less power, or else on especially designed application specific circuits which reduce power consumption even further and which, together with other improvements, have made ear level devices possible. An actual hot topic is "hearing preservation", a combination of electrode design and surgical technique aiming to preserve residual hearing despite electrode insertion into the cochlea. This is the basis for the combined electric and acoustic stimulation via EAS, i.e. the combination of a hearing aid and a CI in one device. Future developments concern the addition of drug delivery systems to cochlear implants, the totally implantable CI, as well as the evolutionary development of existing CIs, like automatic and remote fitting. Presently Medel is a 900-employee company distributing its products worldwide. It developed into a "hearing aid company" offering a wide range of implants to improve hearing from middle ear implants and cochlear implants for a variety of etiologies to auditory brainstem implants. Besides of the development of cochlear implants several other possible application of electric nerve stimulation are under development.

THE LIMITS OF HERMETICITY TEST METHODS FOR MICRO-PACKAGES

Vanhoestenberghe A[1] and Donaldson N[1]

[1] Implanted Devices Group, University College London, London, UK

Abstract

Hermeticity is crucial for the long-term implantation of electronic packages. Pushed by advances in micromachining, package volumes are decreasing and current leak detection methods are no longer sensitive enough. This paper reviews the limits of the most common methods and exposes their inadequateness for medical electronic applications where the device's life is 50 years or longer.

Keywords: *Micro-packaging, hermeticity, active electrode, functional electrical stimulation, long-term implantation.*

Introduction

As detailed elsewhere in these proceedings [1], one way to increase the number of stimulation channels in an implant is by using active electrodes, where some of the electronics is embedded with the electrodes. The embedded IC may be protected from corrosion by enclosing it in a dry atmosphere in a hermetic micro-package. To minimise the package size we propose to bond a silicon cap directly onto the silicon wafer, covering only the active area [2]. The choice of a sealing method is crucial as it will directly influence the hermeticity of the package, hence the lifetime of the implant.

Methods

Hermeticity testing

We are primarily concerned with the ingress of water vapour from the environment into the package over the implant's lifetime (50 years). Methods to measure the hermeticity of a package and what values of the measured leak rate are acceptable are defined in military standards (method 1014.13 of MIL-STD-883, method 1071 of MIL-STD-750 and appendix C of MIL-PRF-38534G). There are discrepancies between standards but the most stringent limit, for internal volumes smaller than 10 mm^3, is a leak rate $\leq 5\ 10^{-9}$ $cm^3.s^{-1}$ of dry air at 25 ºC and 1 atm. These standards also suggest a maximum acceptable moisture level of 5000 ppm at 100 ºC (6.7 % relative humidity at 37 ºC), corrected (lowered) for packages of internal volume smaller than 10 mm^3 sealed in a furnace or with applied pressure. As will be shown in this paper, the leak rates rejection limits are not suitable for the lifetime expected from an implant. Further, the physical detection limits of the methods described in the standards are too high for our application, i.e. a package with a leak rate lower than the lowest detectable rate may still let in too much moisture over time. This statement only echoes what has been found in other engineering disciplines [3–5]. Most of the recent work on hermetical packaging has been concerned with micro-electro-mechanical systems (MEMS) where the focus is on the entrance of air inside a cavity with a low internal pressure. Our interest is to prevent (or estimate) the ingress of water vapour inside a package that may, depending on the sealing method, be filled with a dry gas at or above atmospheric pressure. It is important, for the advance of implant technology, to demonstrate simply the limits of hermeticity testing in our fields and encourage alternative thinking on the subject.

A note on leak rate units

The units used in the military standards, $atm.cm^3.s^{-1}$, leads to rates only valid at the given measurement temperature. If the device is used at a different temperature, this rate must be converted to $mol.s^{-1}$ then translated to the new temperature. Therefore, in the rest of this paper, leak rates will be expressed in $mol.s^{-1}$. For comparison, 1 $mol.s^{-1}$ corresponds to a flow rate of $25.4*10^3$ $cm^3.s^{-1}$ at 37 ºC and a partial pressure difference of 1 atm.

Table 1: Conversion factors for leak rates measured using He

Gas	He	H_2O	Air
Molecular weight (g)	4	18	28.7
Conversion	1	0.471	0.373

The limits of fine leak tests: Helium detection

The most common method for fine leaks is the detection of a tracer gas using a mass spectrometer. Helium is often used due to its rarity in normal atmosphere. The packages under test are "bombed" in a helium chamber at high pressure for a given time then quickly transferred to the detector. The lower leak limit of a good helium detector is of the order of 10^{-16} mol.s^{-1}. Using a simplification of the Howl and Mann equation, this limitation on the measured leak rate may be converted to a limitation on the "standard" or "true" leak rate. That is the leak rate of helium for a partial pressure difference of 1 atm at 25 ºC. The lowest true rate that can be detected with this method is dependent on the cavity volume, bomb time and pressure. Assuming a cavity of a few mm^3, a bomb time of 12 hours at 5 atm and a lowest detectable helium leak rate of $2*10^{-16}$ mol.s^{-1}, the lower limit of the standard rate is of the order of 10^{-14} mol.s^{-1}. An alternative to the bombing method, known as "backfilling", is to fill the package with a fraction of helium prior to sealing and test it shortly afterwards. The true leak rate for helium may then be approximated as the measured rate divided by the helium fraction. So far, all rates are for the leakage of helium, a gas with smaller molecules than water. For the prediction of moisture ingress the helium leak rate must be converted to a water leak rate using the following formula: $L_{H_2O} = \sqrt{M_{He} / M_{H_2O}}\, L_{He}$.

The conversion factors for air, water and helium are given in table 1. These conversions however are of limited use as a leak channel may simply be too small for a larger molecule, especially polar ones as in H_2O (over-estimation of L) and the leak rate may be affected by chemical reactions between the gas and the seal.

Other leak detection methods

There are two other fine leak detection methods proposed in the MIL standards. Using a radioactive tracer gas (mix of krypton-85 and air), equivalent standard leak rates as low as 10^{-15} mol.s^{-1} may be detected. Optical detection relying on the deflection of the cap is popular for full wafer bonding but the lowest reported equivalent standard leak rates are in the range of 10^{-13} mol.s^{-1}. One further method that achieves lower leak rates is cumulative helium leak detection (CHD), where the helium leak rate is measured over time. Manufacturers of detection equipment (Pernicka), claim leak rates measurements limits as low as 10^{-14} atm.cm^3.s^{-1} or 10^{-18} mol.s^{-1}. However the formula for conversion to a standard rate is not given.

Other methods exist and Millar has reviewed a total of 10 methods of hermeticity testing applied to MEMS cavities [3]. She concludes that none of the external methods set in the military standards, nor those developed more recently, are suitable for the small cavity volumes and high hermeticity requirements typical of MEMS. Only in situ methods, using some form of pressure sensor, can achieve a relevant leak rate detection.

Results

The time taken for the partial water vapour pressure $P_{H_2O,in}$ inside a package of volume V, leaking at a true rate L_{H_2O} to reach a given pressure is calculated using equation:

$$t_1 - t_0 = \frac{V}{L_{H_2O}} \ln\left(\frac{\Delta P_0}{\Delta P_1}\right)$$

where $\Delta P_i = P_{H_2O,out} - P_{H_2O,in}$ at instant t_i and $P_{H_2O,out}$ is at all time the saturation pressure of water vapour at 37 ºC. After testing a package, and converting if necessary the measured rate to the true helium rate L_{He}, V/L_{He} may be calculated to find the time before $P_{H_2O,in}$ reaches a set limit. This fraction, at a given temperature and pressure difference, is a useful parameter to compare the performances of different packages. This is illustrated in figure 1. For the purpose of illustration, 5 partial water vapour pressure limits are displayed on the graph. The first two limits, 2994 and 5000 ppm, are set in MIL-STD-883H, 5000 is a general value and 2994 is corrected for a cavity smaller than 10 mm^3 sealed in a heated furnace (350 ºC in this case). Greenhouse suggests using the partial pressure of a volume of water

Table 2: Leak testing methods and their lowest detectable leak rates (expressed as true helium leak rates).

Method	Optical deflection	He bombing	krypton-85	He backfilling	CHD
Comments		Pb = 5 atm, tb = 12 h, V=1 mm^3		100 % He	
True helium leak rate (mol.s^{-1})	10^{-13}	10^{-14}	10^{-15}	10^{-16}	10^{-18}

sufficient to form 3 monolayers of water on all internal surfaces upon condensation [4]. This value is dependent on the package's inner surface area. In fig.1, the package dimensions were: 4 x 2.5 x 0.1 mm. Finally, two relative humidity limits are plotted, 10 and 99 %.

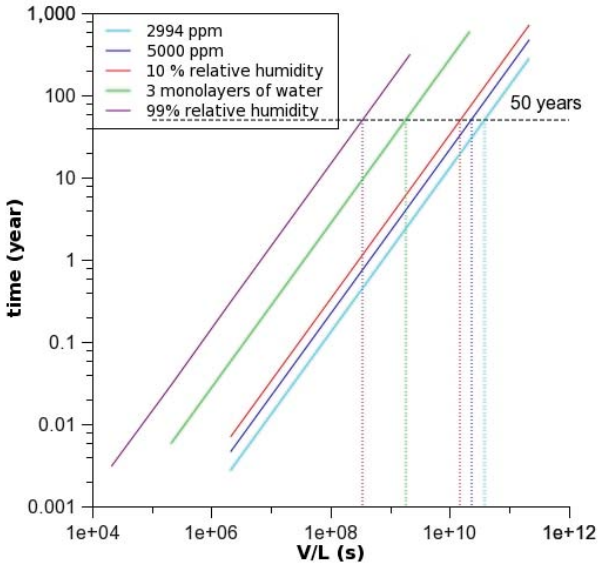


Fig. 1: Time to reach a given partial water vapour pressure limit as a function of V/L for 5 different limits.

Discussion

For a set "time to limit", whatever the limit be defined as, a reduction of the cavity's volume requires an equivalent reduction of the leak rate. However, what is the maximum relative humidity inside the package before failure occurs? For applications where corrosion is the most likely cause of failure, the onset of corrosion related damages needs to be linked to a relative humidity inside the package. The presence of traces of salts with low vapour pressure will encourage water formation at low relative humidities [6]. Once a maximum relative humidity is set, the highest acceptable leak rate may be computed. To illustrate this, table 3 shows the true rates acceptable to guarantee that a 1 mm^3 package will not reach a given relative humidity within 50 years. These are at the limit of what is currently achievable.

Table 3: Minimum true He leak rates for a time to limit of 50 years at 37 ºC for a 1 mm^3 internal cavity.

Limit	L ($mol.s^{-1}$)
Corrected ppm (2994)	$1.03*10^{-18}$
5000 ppm	$1.63*10^{-18}$
10% relative humidity	$2.64*10^{-18}$
3 monolayers of water	$2.17*10^{-17}$
99% relative humidity	$1.14*10^{-16}$

Conclusions

In packages where corrosion is the most likely cause of failure, humidity should be kept low. Currently, the lowest detectable leak rates are not low enough to guarantee acceptable relative humidity levels over the lifetime of the implant. If the humidity cannot be estimated from tests prior to implantation, one alternative is to monitor it after implantation. Humidity sensors may be integrated on the surface of the circuit with only a small increase in overall package dimensions. There are however major design challenges to overcome if the sensors are to be sensitive, stable and precise enough to detect very low humidity levels and slow increases over years [7]. This simple presentation of the issues related to hermeticity testing relies on the assumption that a safe limit for the relative humidity is known. This safe limit will depend on the application, the surface contamination and more.

References

[1] N. Donaldson et al., "Active books: a practical way to increase the number of stimulation channels for FES after SCI?," in these proceedings, 2010.

[2] A. Vanhoestenberghe, J. Evans, X. Liu, N. Saeidi, M. Schuettler, A. Demosthenous and N. de N. Donaldson (in press), "Active Implantable Electrodes: Micro-Manufacturing with Embedded IC," Sensors Review.

[3] S. Millar and M. Desmulliez, "MEMS ultra low leak detection methods: a review," Sensor Review, vol. 29, no. 4, pp. 339–44, 2009.

[4] H. Greenhouse, Hermeticity of electronic packages. William Andrew Publishing, 2000.

[5] Y. Tao and P. Malshe, "How accurate mil-std-883e helium bomb and bubble test methods are for small cavity chipscale packages," Advancing Microelectronics, vol. 45, no. 3, pp. 22–30, 2008.

[6] A. D. Marderosian and C. Murphy, "Humidity threshold variations for dendrite growth on hybrid substrates," in Proc. 15th Annual Reliability Physics Symposium, pp. 92–100, Apr. 1977.

[7] N. D. N. Saeidi, A. Demosthenous and J. Alderman, "Design and fabrication of corrosion and humidity sensors for performance evaluation of chip scale hermetic packages for biomedical implantable devices," in Proc. of European Microelectronics and Packaging Conference, pp. 1–4, 2009.

Acknowledgements

The authors thank the UK EPSRC for financial support.

First Author's Address

Dr. Anne Vanhoestenberghe
Implanted Devices Group
University College London
annevh@medphys.ucl.ac.uk

On the Stability of PEDOT as Coating Material for Active Neural Implants

Boretius T, Schuettler M, Stieglitz T

Department of Microsystems Engineering-IMTEK, Laboratory of Biomedical Microtechnology, University of Freiburg, Germany

Abstract

This paper is about the stability of PEDOT coatings under high loads of current pulses. Test parameters were chosen to match many peripheral nervous system (PNS) applications in regard of charge injection, pulse width and repetition frequency. PEDOT coatings were characterized with electrochemical impedance spectroscopes (EIS) and pulse tests. No decrease in charge injection capacities could be detected after ten million pulses, suggesting a stable coating for at least this time frame with superior properties in regard of conventional platinum electrodes.

***Keywords**: PEDOT, electrode, stability, pulse test, characterization*

Introduction

One of the most challenging aspects in functional electrical stimulation (FES) is the transfer of charge over the phase boundary of metallic conductor (electrode) and tissue. Since metallic conduction is based on electron flow and tissue conduction on ion flow, a transition has to occur which is mediated by the electrode in use. These reactions can basically be capacitive, i.e. charging and discharging of the electrode-electrolyte double layer, or faradic, which involves oxidation and reduction of surface confined species. Prominent examples for these mechanisms are titanium nitride (TiN) or tantalum/Ta_2O_5 for capacitive transition and iridium oxide or PEDOT (poly-ethylenedioxythiopene) as faradic material. Pt and PtIr alloys are special cases since faradic reactions are restricted to a surface monolayer and, hence, are called pseudocapacitive [1]. In general, capacitive charge-injection is preferable to faradic injection since no chemical species are created/consumed during a stimulation pulse. Furthermore, changes of electrolyte composition and finite rates of faradic reactions can lead to irreversible processes which may cause electrode or tissue damage (i.e. corrosion and alteration of pH-value). However, charging the double-layer of an electrode-electrolyte interface by capacitive means yields in only small charge injection capacities (Q_{inj}), since the charge per unit area at an interface is also small, and is often not sufficient to stimulate targeted structures like peripheral nerve fascicles [2]. Hence, it is of upmost importance to consider carefully which electrode material or coating is to be used and what restrictions, e.g. water window or stability under stimulating conditions, are implied.

This paper reports on the stability of PEDOT as coating material for stimulating electrodes under high loads of current pulses which was reported earlier to turn the polymer into an insulator and, thus, limits the actual use of this coating [3]. The goal of this research is to determine the count of current pulses which can be safely injected into the electrolyte without loosing the conductive properties or passing the water window, respectively.

Material and Methods

Preparation of samples:

Test electrodes were manufactured using micromachining techniques in a class 1000 cleanroom. Samples consist of a polyimide-platinum-polyimide stack (5µm-300nm-5µm in thickness), whereas active sites and interconnection pads are opened by reactive ion etching (RIE). Connection was done with zero insertion force adapters (ZIF), whereas the samples incorporate different electrode diameters ranging from 40 to 120 µm. In this study, however, 80 µm diameter electrodes were solely used.

The electrolyte for deposition of PEDOT was made up with following recipe: 0.1 M EDOT (Cat # 483028 Sigma–Aldrich) was doped with 0.05 M pTS (Cat # 152536 Sigma–Aldrich) in a 1 part acetonitrile : 1 part deionised (DI) water solution and used within two months after synthesis [4]. The polymer coating was electrodeposited using galvanostatic mode of a gain-phase analyzer with a

potentiostat (Solartron 1260 & 1287, Solartron Analytical, Farnborough, Hampshire, UK) in combination with the software CorrWare (version 3.1 by Scribner Associates Inc., Southern Pines, NC, USA) at 1 mA/cm^2 for 10 min in a three electrode setup, consisting of a Pt counter electrode and an Ag/AgCl (3M) reference electrode.

Characterization

Test samples were characterized by electrical impedance spectroscopy (EIS) and pulse testing. EIS measurements were done with the three electrode setup described above. Impedance spectroscopy was conducted with excitation amplitudes of 10 mV from 1 Hz to 100 kHz on a regular basis (e.g. immediately after deposition and after 3 million cycles) in phosphate buffered saline solution (PBS; 7.4 pH). To inject current pulses a custom made 12-channel pulse tester was developed, incorporating improved Howland current pumps and circuits to subtract the voltage drop over the access resistance [5]. Applied pulses were rectangular, biphasic and charge balanced in nature with a pulse width of 200 µs and a frequency of 25 Hz. Pulsing was done in non-agitated PBS solution (0.5l, regularly refilled with DI water) against a large area stainless steal counter electrode; temperature and pH value of the electrolyte were measured once per day. For PEDOT an injected charge of 20 nC (100µA x 200µs) was chosen and the voltage across the phase boundary (V_{PB}) was continuously monitored. Since, loss of conductive properties within the coating yields in increased charging of the phase boundary, while the injected charge is held constant, V_{PB} is expected to rise towards the limits of the water window. Hence, the criterion for exclusion is passing the limits of PEDOTs water window (-0.9-0.6V vs. Ag/AgCl). As reference material, a non-coated platinum electrode was tested in the same way, but pulsed to the safe limits of platinum's water window (-0.6–0.8V vs. Ag/AgCl) and the required current was measured. Additionally, the access resistance R_A of PEDOT and Pt was measured once per day.

Results

After electrodeposition of PEDOT, samples were optically inspected using a light microscope. The coating appeared black in colour and was confined to the actual electrode site, i.e. it didn't creep over the boundary of platinum and polyimide which suggests a coating thickness below 5 µm.

EIS measurements showed a significant decrease in mean impedance, cut-off frequency (f_g) and phase angle theta after PEDOT deposition (see Fig. 1, n=10). At 1 kHz, impedance decreased from 113 kΩ to only 4.7 kΩ and the phase angle was increased from -76.5 ° to -8.4 ° for Pt and PEDOT, respectively. Cut-off frequency was decreased from 20 kHz for platinum to 25 Hz for PEDOT. After 3 million load cycles no difference was found neither in impedance nor phase angle measurements.

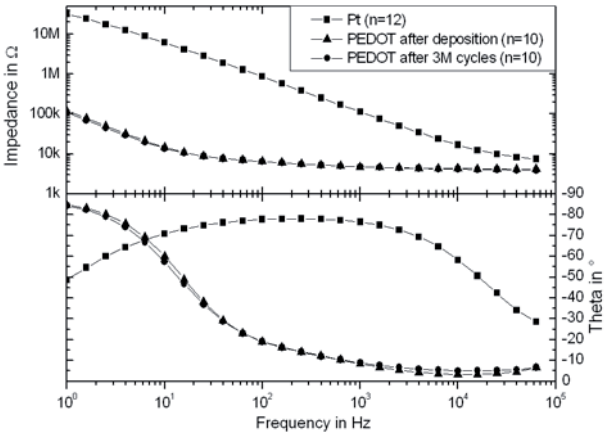


Fig. 1: Electrical impedance measurement of pure platinum and PEDOT coated electrodes.

Pulse tests were conducted for 10 million cycles on 10 electrodes coated with PEDOT. Figure 2 shows the voltage across the phase boundary after 100k and 10M cycles (upper graph) and the fixed current pulse with a charge of 20 nC (lower graph). Note that the voltage drop (iR) over the access resistance (R_A) is already subtracted. The access resistance was measured to 4.5 kΩ and 12 kΩ for PEDOT and Pt respectively, and stayed constant over the 10M pulses. These results are in accordance with the EIS measurements (5.3kΩ with PEDOT and 10.4kΩ for Pt).

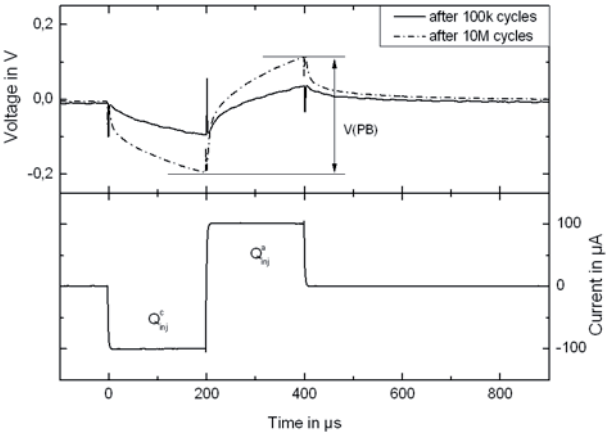


Fig. 2: Pulse test: upper graph depicts the voltage over the phase boundary after different load cycles. Lower graph shows one current pulse.

Peak-to-peak voltages over the phase boundary V_{PB} were measured and the mean values including standard deviations (rms) are depicted in Fig. 3 (upper graph; n=10). Since the water window for PEDOT is situated between -0.9 and 0.6V vs.

Ag/AgCl, the “water window line” would be situated at 1.5V and served as exclusion criterion, but was never met with any of the tested electrodes. Neither was any limit of safe charge injection, cathodic or anodic, met within these 10M pulses. The lower graph in Fig.3 shows the current needed to drive the platinum electrode, which served as reference material, to the safe limits of charge injection. The current stayed constant throughout the experiment which suggests that no faradic or irreversible processes occurred.

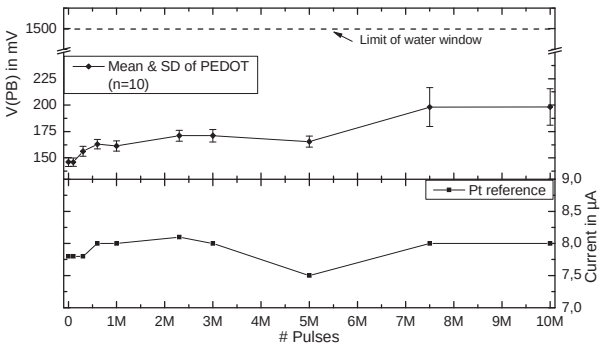


Fig. 3: Upper graph shows the mean peak-to-peak voltage across the phase boundary. Lower graph gives the current needed to drive platinum reference electrodes to safe limits of charge injection.

Discussion

PEDOT coatings were able to decrease the impedance about 95 % when compared to the original platinum electrodes and showed a much stronger resistive behaviour in EIS measurements suggesting properties comparable to iridium oxide coatings. A loss of conductivity could not be seen within the 10M pulses delivered to the electrodes which contradicts another report where PEDOT lost its conductive property after about 24k cycles in a cyclo voltammetric (CV) measurement [3]. This may be caused by another dopant which was used in the other study (PSS rather than pTS) or by an unconventional water window in which the CV was recorded (0-0.6V vs. Ag/AgCl).

Conclusions

The aim of this study was to investigate whether PEDOT is a useful material for stimulating electrodes or if the conductive property of this polymer decreases over time or pulse counts. Therefore, typical values for PNS applications were chosen, e.g. 20 nC of charge injection, 200 µs pulse width and 25 Hz repetition frequency, to model a “realistic” testing environment. Mortimer et al. reported on pulse counts for hand prosthesis and concluded that approximately 200k pulses per day were necessary to operate such a device [6]. In this context it could be shown that PEDOT is a feasible material for stimulating electrodes with superior properties compared to platinum for subchronic experiments. The durability lies in a range of at least 10M pulses or 50 days, but is expected to be much higher since the peak-to-peak voltage across the phase boundary reached merely 13 % of the available range of the water window.

Acknowledgements

Many thanks go to Rylie Green for supplying the recipe of PEDOT and its deposition parameters. The authors would also like to thank the European Union for funding this work under grant CP-FP-INFSO 224012/TIME.

Author’s Address

Name: Tim Boretius
Affiliation: University of Freiburg, Department of Microsystems Engineering-IMTEK
email: boretius@imtek.de
homepage: www.imtek.de/bmt

References

[1] S. F. Cogan, "Neural Stimulation and Recording Electrodes," *Annu Rev Biomed Eng*, vol. 10, pp. 275-309, 2008.

[2] P. M. Rossini, S. Micera, A. Benvenuto, J. Carpaneto, G. Cavallo, L. Citi, C. Cipriani, L. Denaro, V. Denaro, G. Di Pino, F. Ferreri, E. Guglielmelli, K. P. Hoffmann, S. Raspopovic, J. Rigosa, L. Rossini, M. Tombini, and P. Dario, "Double Nerve Intraneural Interface Implant on a Human Amputee for Robotic Hand Control," *Clinical Neurophysiology*, 2010.

[3] N. Peixoto, K. Jackson, R. Samiyi, and S. Minnikanti, "Charge Storage: Stability Measures in Implantable Electrodes,"*31st Annual International Conference of the IEEE EMBS, Sept.2-6, 2009, Minneapolis, Minnesota, USA* 2009, pp. 658-661.

[4] R. A. Green, N. H. Lovell, and L. A. Poole-Warren, "Cell Attachment Functionality of Bioactive Conducting Polymers for Neural Interfaces.," *Biomaterials*, vol. 30, no. 22, pp. 3637-3644, 2009.

[5] M. Schuettler, M. Franke, T. B. Krueger, and T. Stieglitz, "A Voltage-Controlled Current Source With Regulated Electrode Bias-Voltage for Safe Neural Stimulation," *J Neurosci Meth*, vol. 171, no. 2, pp. 248-252, 2008.

[6] J. T. Mortimer, "Electrodes for Functional Electrical Stimulation 10," Progress report for NIH Neural Prosthesis Program, 1999.

Active Books: a practical way to increase the number of stimulation channels for FES after SCI?

Donaldson N[1], Vanhoestenberghe A[1], Liu X[1], Saeidi N[1], Demosthenous A[1], Schuettler M[2]

[1] University College London, United Kingdom [2]IMTEK, University of Freiburg, Germany

Abstract

Progress in FES after spinal cord injury using motor neuron stimulation requires an implant that allows more stimulation channels but will be acceptable to informed volunteers. Stimulation of nerve rootlets allows more channels, probably with good reliability; much relevant useful clinical information is available from past usage of sacral anterior root stimulators. This paper outlines the main technical challenges presented by rootlet stimulation.

***Keywords**: Active Book; Nerve Root; Rootlets; Stimulation; FES.*

Introduction

In the 1970s and 1980s, there were more human trials of implanted stimulators for restoring leg function after spinal cord injury (SCI) than in recent years. This diminution is certainly not because the problem has been solved. Several reasons are apparent: Europeans have become more averse to risk; there is the possibility of the 'cure' for spinal cord injury (perhaps remote); and the patient group is relatively small to amortise the industrial investment while regulations have grown into a greater obstacle to human testing. But over this period, technology has advanced so that neuroprostheses may now be possible that would not have been thirty years ago.

Our goal is to develop an implant for restoring lower-body function; specifically to allow cyclic exercises (cycling and rowing), to control the bladder and improve bowel evacuation. Elsewhere in these Proceedings, we describe the SLARSI 10-channel nerve root stimulator that we hope soon to use in human trials [1]. 8 of these 10 channels are for leg muscle stimulation at anterior roots L3-S1. Eight is the same number of channels as we use for FES-cycling with surface electrodes on quadriceps, hamstrings, triceps surae and gluteal muscle groups [2]. Power output during FES cycling is low and this is partly due to low metabolic efficiency [3]. A recent experiment by Duffell *et al*. [4] suggested that low efficiency is due to crude activation of muscles which is inherent in the use of so few stimulation channels.

Looking further ahead, how can the leg muscles be activated better but in a way that can be attempted in a human trial? Several methods have been suggested. Those where electrodes are close to the target muscles, whether cable-connected or wireless (*Bions*), seem to be too unreliable [5]. Mushahwar & Horch proposed microstimulation by 1536 electrodes on 8 combs in the motor neuron pools of the lumbar spinal cord [6] but this has not been attempted in man. More radical proposals are based, not on stimulating motor neurons but more dorsal sites so as to evoke complex motions, for example from the central pattern generators [7]. However, there is much to learn before complex motion methods could reasonably be attempted in people with SCI.

In contrast, a great deal of clinical experience has been gained from Sacral Anterior Root Stimulators, mostly with intrathecal electrodes, used to restore bladder & bowel function [8]. After laminectomy, anterior nerve roots can be separated from posterior roots then trapped in *electrode books*. These implants are highly reliable [9] with high success rates [8]. The roots may be damaged by rough handling during surgery but anterior roots nearly always recover (whereas damage to posterior roots is usually permanent) [8]. At stimulation intensities required for skeletal muscles (i.e. low compared to parasympathetic nerves for the bladder), most patients without complete cord lesions will not find it too painful [10] so the method may be used with most SCI patients. In SARS, sacral deafferentation is beneficial and is usually performed intentionally as part of the treatment [8]. We have tested Lumbar Anterior Root Stimulators [11,12,13,14] where deafferentation is not intended but, if it occurs inadvertently, is unlikely to have much effect on muscle tone or spasticity [15]. Some neurosurgeons further separate the roots into smaller strands, so as to be sure that sensory fibres

are not trapped over the electrodes; this shows that further separation is possible in practice. A similar approach is used in selective dorsal rhizotomies.

Each root comprises fibres from several rootlets that emerge from the cord. Typically there are about 8 [16]. Because the anterior horn cells for each muscle are grouped within the grey matter of the cord in *pools* [17], it seems possible that each rootlet is more muscle-specific than the root (but we can not find any evidence for this conjecture). However, if it is true, a rootlet stimulator would give more selective but direct muscle activation. Given that the leg muscles are innervated from L2 to S2 (6 levels), the number of channels needed would be about (6 levels)×(8 rootlets/root)×(2 sides)=96 channels.

Technical Challenge

In whole-root stimulators [10], each root is trapped in a *slot* over a stimulating tripole. There are two or more slots in each *book*, which lies in the spinal canal surrounded by the *cauda equina*. Each tripole must be electrically isolated to prevent cross-talk [18]. Each book is connected by a cable to a stimulator that is usually implanted on the costal margin. These cables pass through *grommets* [10] at the dura that prevent CSF leakage. Given that high-reliability implantable cables have only a few separate helical wires [19], the number of channels is constrained by the number of cables that can pass through the grommet which surgeons have restricted to 5. Thus SLARSI is limited to 5 books and 10 channels [1].

Obviously this restriction would be avoided by multiplexing the stimulation current but this implies having electronic switches within the spinal canal and in intimate proximity to the nerves. The *Active Books* project is an exploration of the feasibility of this idea. To be feasible, many requirements must be met which will be outlined in the following sections.

Blocking Capacitors

µF-size capacitors in series with the electrodes are the orthodox method for ensuring electrical safety under fault conditions. They also can ensure that the electrodes are discharged between pulses if a convenient passive circuit is provided. However they are too large to incorporate in an Active Book. We developed a high-frequency integrated stimulation method for safety under single-fault conditions [20] but it required too much silicon area (0.38 mm^2/mA) for the 8mA/channel required.

Electrical Safety

We therefore defined an output stage, of the layout described in [21], that should be safe by using fault detection or, where that is difficult, redundancy. The cables pose a risk, since they carry direct supply currents and may fatigue-fracture exposing the wires. The protocol therefore allows µA-level DC leakage tests to be performed on the cables before the ICs start drawing significant current [22].

Packaging

Placing the electronic components inside a metal package is impractical. One possibility is to encapsulate the integrated stimulator IC only in polymer, which means that the polymer-chip interface will be exposed to saturated water vapour, and this must not deteriorate for many years of implantation. However, long term tests done at 85%RH have shown electrolytic damage to passivation layers in the high field regions over biased tracks [23]. The trend toward smaller structures therefore higher field strengths in IC technology means that this effect is becoming an increasing problem. An alternative is to use wafer-bonding methods to bond a cap over the active circuits so that only low-field strength regions are exposed to high water vapour pressure. We show elsewhere that the hermeticity of these caps can not be measured by leak rate [24]. However, if a thin-film humidity sensor can be fabricated as part of the integrated circuit [25], high internal humidity can be detected in routine house-keeping procedures.

Electrode Fabrication & Encapsulation

Schuettler *et al.* [26] have developed a method to make planar electrode arrays by cutting Pt foil on silicone rubber with a laser, and then spinning on more silicone as an overcoat. We hope to form tripoles in this way, which are then bent over arch-formers and clamped into a mould to form the book structure [27]. *Fingers* from each electrode will be joined directly to the output pads of the IC by rivet-bonding before moulding silicone to encapsulate the joints. The structure is shown in Figure 1.

Conclusion

This paper introduces the *Active Books* project that aims to develop implantable multi-channel stimulator for helping people with SCI remain healthy. The short-term aim is to demonstrate a system suitable for rootlet stimulation with 20 channels. The technology is challenging but, if successful, is likely to be applicable to other implants in which the electronics is very close to a compliant electrode structure.

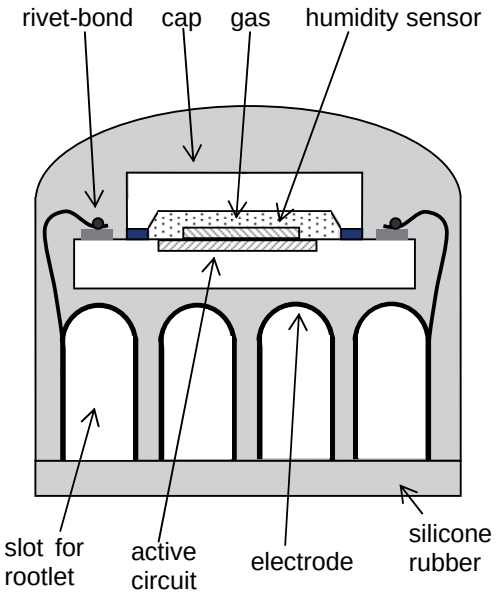


Figure 1

References

[1] Nonclercq *et al.*, these proceedings.

[2] Perkins TA Donaldson N Fitzwater R Phillips GF Wood DE Leg powered paraplegic cycling system using surface Functional Electrical Stimulation. Artificial Organs, 26(3), 297-298, 2002.

[3] Hunt KJ Saunders BA Perret C Berry Allan HDB Donaldson N Kakebeeke TH. Energetics of paraplegic cycling. Eur. J. Appl. Physiol., 101:277–285, 2007.

[4] Duffell LD Donaldson N Newham DJ. Why is the metabolic efficiency of FES cycling low? IEEE TNSRE, 17(3), 263-9, 2009.

[5] Rushton DN. Choice of nerve roots for multichannel leg controller implant. *Advances in External Control of Human Extremities,* vol. X, D. Popovic, Ed. Belgrade: Yugoslav, Committee for Electronics and Automation, 99-108, 1990.

[6] Mushahwar VK & Horch KW. Proposed specifications for a lumbar spinal cord electrode array for control of lower extremities in paraplegia. IEEE TRE, 5(3), 237-43, 1997.

[7] Courtine G *et al.* Transformation of non-functional spinal circuits into functional states after the loss of brain input. Nature Neurosci., 12(10), 1333-44, 2009.

[8] Brindley GS. The first 500 patients with sacral anterior root stimulator implants: general description. Paraplegia. 32(12):795-805, 1994.

[9] Brindley GS. The first 500 sacral anterior root stimulators: implant failures and their repair. Paraplegia. 33(1):5-9, 1995.

[10] Brindley GS Polkey CE Rushton DN Cardozo L. Sacral anterior root stimulators for bladder control in paraplegia: the first 50 cases. Journal of Neurol. Neurosurg. Psych. 49(10):1104-14, 1986.

[11] Donaldson N Perkins TA Worley ACM. Lumbar root stimulation for restoring leg function. Methods: Stimulator and measurement of muscle actions. Artificial Organs, 21, 247-249, 1997.

[12] Rushton DN Donaldson N Barr FMD Harper VJ Perkins TA Taylor PN Tromans AM. Lumbar root stimulation for restoring leg function: results in paraplegia. Artificial Organs, 21, 180-182, 1997.

[13] Donaldson N Rushton D & Tromans T. Neuroprostheses for leg function after spinal-cord injury. Lancet, 350, 9079, 711-712, 1997.

[14] Perkins TA Donaldson N Hatcher NAC Swain ID Wood DE Control of leg powered paraplegic cycling using stimulation of the lumbo-sacral anterior spinal roots. IEEE TRE 10(3), 158-164, 2002.

[15] von Koch CS, Park TS, Steinbok P, Smyth M & Peacock WJ Selective posterior rhizotomy and intrathecal Baclofen for the treatment of spasticity. Ped Neurosurg, 35, 57-65, 2001.

[16] *Atlas of Neuroanatomy,* Netter, Saunders, 2006.

[17] Romanes GJ. The motor cell columns of the lumbo-sacral spinal cord of the cat. J. Comp. Neurol., 94, 313-63, 1951.

[18] Donaldson N Rushton DN Perkins TA Wood DE Norton J Krabbendam A. Recruitment by motor nerve root stimulators: significance for implant design. Med. Eng. Phys, 25(7), 527-37, 2003.

[19] Donaldson PEK. The Cooper cable: an implantable multiconductor cable for neurological prostheses. Med. Biol. Eng. Comput. 21(3):371-4, 1983.

[20] Liu X Demosthenous A Donaldson N. An integrated implantable stimulator that is fail-safe without on-chip blocking capacitors' IEEE TBCS, 2(3), 231-44, 2008.

[21] Langlois P Demosthenous A Pachnis I Donaldson N. High-power integrated stimulator output stages with floating-discharge over a wide voltage range for nerve stimulation. IEEE TBCS 4(1), 39-48, 2010.

[22] Liu *et al.*, these proceedings.

[23] Osenbach JW. Water-induced corrosion of materials used for semiconductor passivation. J. Electrochem. Soc., 140(12), 3667-675, 1993.

[24] Vanhoestenberghe *et al.*, these proceedings.

[25] Saeidi N Demosthenous A Donaldson N Alderman J. Design and fabrication of corrosion and humidity sensors for performance evaluation of chip scale hermetic packages for biomedical implantable devices. EMPC 2009 (Eur), 1-4, 2009.

[26] Schuettler M Stiess S King B Suaning GJ. Fabrication of implantable microelectrode arrays by laser-cutting of silicone rubber and platinum foil. J. Neural Eng., 2, 121-8, 2005.

[27] Vanhoestenberghe A. Implantable electronic devices technology challenges for long-term human implantation. Sens. Rev. (UK), 29(4), 345-8, 2009.

Acknowledgements

We thank the UK EPSRC for grant support.

First Author's Address

Prof. Nick Donaldson
Implanted Devices Group
University College London
nickd@medphys.ucl.ac.uk

Towards the development of an integrated stimulator for *Active Books*

Liu X[1], Demosthenous A[1], Vanhoestenberghe A[2], Donaldson N[2]

[1] Department of Electronic and Electrical Engineering, University College London, London WC1E 7JE, UK

[2] Department of Medical Physics and Bioengineering, University College London, London WC1E 6BT, UK

Abstract

This paper presents a brief overview of the circuit design of an integrated stimulator for a distributed stimulation system to reduce the number of implanted cables. The integrated stimulator will be part of the electrode assembly and is specifically intended for use with Active Books *within the spinal canal. Because the space is very limited, no blocking capacitors are used. The electrodes will be passively discharged. The design allows for the stimulating tripoles to be isolated and the anode current ratio to be adjusted to avoid cross-talk to adjacent nerves. Stimulus intensity is primarily set by pulse width and cathode currents of 1, 4 or 8mA can be selected. Humidity in the micro-package will be measured as a safety precaution and the communication protocol to control the stimulator is briefly described.*

Keywords: *Active Books, integrated stimulator circuits, humidity sensor.*

Introduction

This paper describes the integrated circuits that have been designed for the Active Books introduced in the companion paper [1]. Figure 1 shows an illustration of an electrode book with embedded integrated stimulator.

The implanted part of the system comprises a *hub* that has the inductive receiver and power supply regulator. This will be at a convenient site such as the costal margin. 5-wire cables will run from the hub to each book. In this design, each book has four slots and there can be up to four books connected to the hub. The hub synchronises the 4 books with their *INOUT* lines. The communication protocol can be expanded to more slots and/or more books.

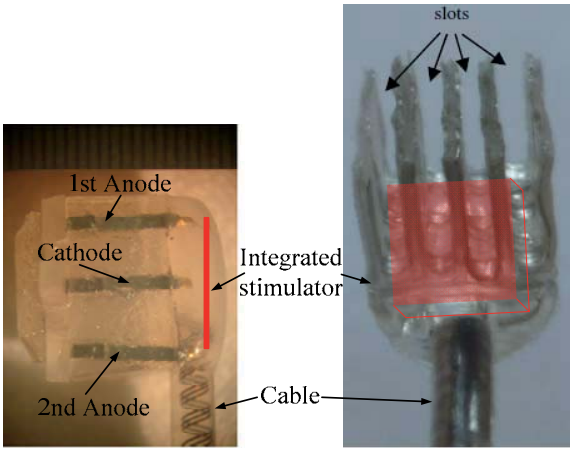


Fig. 1: Illustration of an electrode book with embedded integrated stimulator. (a) Side view; (b) End view (4-slot). (best viewed in colour)

Design

Specification

The integrated stimulator to go in the books must meet the following requirements:

1. It must be small enough to be mounted on the electrode book and not need any off-chip components.

2. To avoid cross-talk between channels, each slot will have an independent tripole, i.e., one central cathode flanked by two outer anodes. The two anodes should be driven by independent current sources, adjustable in relative amplitude so that

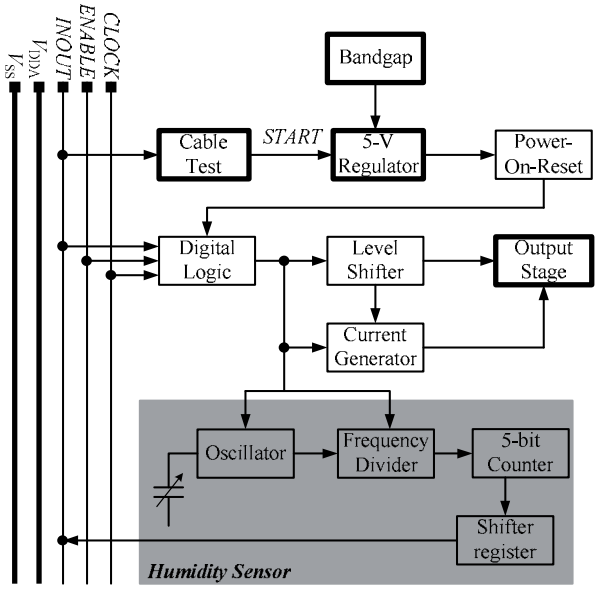


Fig. 2: Functional block diagram of the designed integrated stimulator. Bold outlines indicate high-voltage modules.

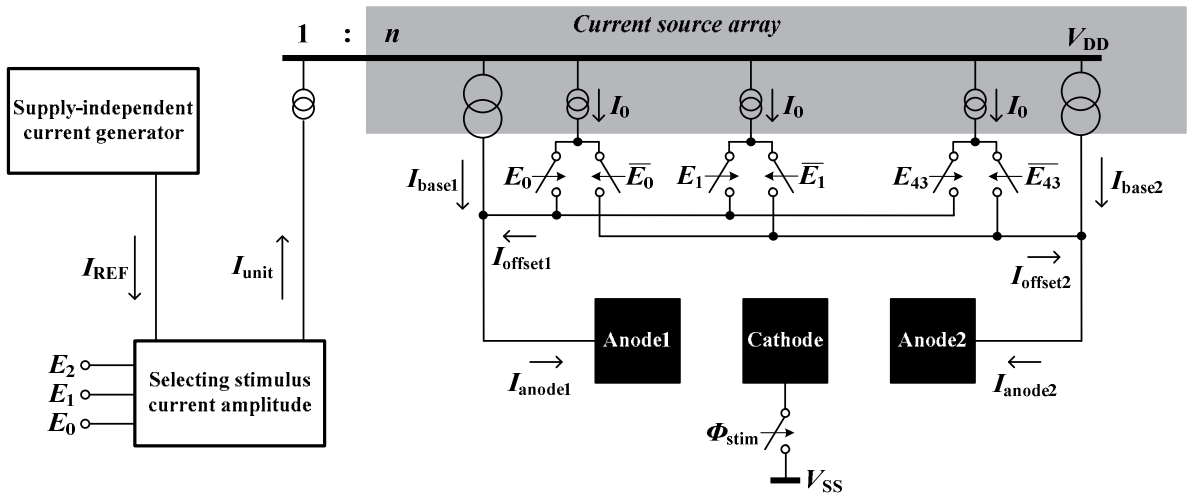


Fig. 3: Stimulus current generator circuit.

there can be no current outside the slot.

3. There is a test mode in which bias is applied from the hub between the wires of the cables and the leakage currents are measured while the stimulator circuits in the books remain quiescent. The current consumption of the stimulator circuits in the quiescent mode must be small enough to make the possible harmful leakage current dominate the leakage reading. Cable failures can thus be detected.

4. Another house-keeping test is to monitor the in-package humidity.

The above requirements have been met by corresponding circuit blocks in the designed integrated stimulator. Figure 2 shows the functional block diagram of the stimulator, driven by five different wires, *CLOCK*, *ENABLE*, *INOUT*, V_{DDA} and V_{SS}.

Stimulation

18V is applied between V_{DDA} and V_{SS}. The channels are selected serially by signals from the hub on *CLOCK* and *INOUT*. The duration of each stimulus pulse is defined by the *ENABLE* signal. All these signals are 0 to 5V logic where 0 is V_{SS}. Only *INOUT* is bidirectional and only *INOUT* is book-specific; all other lines are common. An on-chip regulator provides 5V supply for the digital circuits.

With four books each of four channels, sixteen altogether, while stimulating at 20Hz, there is one pulse on each *INOUT* line every 50ms, with trains of *CLOCK* and *ENABLE* pulses. This is all that is necessary for normal stimulation, adjusting stimulation parameters and interrogating humidity.

Quiescent Mode

To enter the normal mode, V_{DDA} must be high and *INOUT* must have been high at least once since V_{DDA} went high. This turn-on logic procedure ensures that the stimulator will not be turned on accidently during the cable test. In the quiescent mode, the stimulator circuits are expected to draw less than 1μA from the supplies. This means that bias could be applied to each of the wires in the cable relative to the other four for long enough to measure the leakage current drawn from the hub.

Command protocol

Occasionally commands can be sent by sequences of trains of different lengths on the *CLOCK* line. At present, the available commands are: humidity measurement, change to stimulus current (on all channels), and change to the anode current ratio on a particular channel (i.e., a slot). For example, the sequence C18-C17-C16 means that the humidity should be measured, where Cn is a train of n pulses clocked into the stimulator. Note that all commands must be closed by C16 to be valid. Commands are of high and low security, depending on their effect. High security requires a longer correct heading: two pulse trains (C20 followed by C19) before the command itself, while non-stimulation related commands, such as humidity measurement, only requires a low-security heading, i.e., C18 at the beginning of the sequence.

Stimulus current generator

Figure 3 shows the stimulus current generator for driving a tripole. The source unit generates a 2.3μA reference current, I_{REF}, independent of the supply voltage. I_{REF} is scaled up by 1, 4, or 8 times as 1, 4 or 8mA stimulus current is required. This scaled-up unit current, I_{UNIT}, is further increased by either 200 or 196 times for the raw anodic currents, denoted as I_{base1} and I_{base2} in the figure. *Anode1*, *Cathode*, *Anode2* in the figure are three equally spaced electrodes within a book slot. If the inter-electrode impedance of *Anode1-Cathode* is the same as *Anode2-Cathode*, simple generators that supply equal stimulus current for either anode will

Table I: Different anodic current ratio

Cases	$I_{A1}=I_{base1}+I_{offset1}$ (=? $\times I_{REF}$)	$I_{A2}=I_{base2}+I_{offset2}$ (=? $\times I_{REF}$)	Exact ratio $(\frac{I_{A2}-I_{A1}}{I_{A1}})$	Closest approx.
1	**200**	**196**+*44*	20%	20%
2	**200**+*2*	**196**+*42*	17.8%	18%
3	**200**+*4*	**196**+*40*	15.7%	16%
4	**200**+*6*	**196**+*38*	13.6%	14%
5	**200**+*8*	**196**+*36*	11.5%	12%
6	**200**+*10*	**196**+*34*	9.5%	10%
7	**200**+*12*	**196**+*32*	7.6%	8%
8	**200**+*14*	**196**+*30*	5.6%	6%
9	**200**+*16*	**196**+*28*	3.7%	4%
10	**200**+*18*	**196**+*26*	1.8%	2%
11	**200**+*20*	**196**+*24*	0	0%
12	**200**+*22*	**196**+*22*	-1.8%	-2%
13	**200**+*24*	**196**+*20*	-3.6%	-4%
14	**200**+*27*	**196**+*17*	-6.2%	-6%
15	**200**+*29*	**196**+*15*	-7.9%	-8%
16	**200**+*32*	**196**+*12*	-10.3%	-10%
17	**200**+*34*	**196**+*10*	-12.0%	-12%
18	**200**+*37*	**196**+*7*	-14.4%	-14%
19	**200**+*39*	**196**+*5*	-15.9%	-16%
20	**200**+42	**196**+2	-18.2%	-18%
21	**200**+44	**196**	-19.7%	-20%

suffice. However, due to manufacturing tolerances and non-idealities after implantation, such as off-midline electrode placement, electrode deformation during and after implantation, growth of connective tissue encapsulating the electrode, or a non-uniform nerve within the electrode cuff [2], there will be a mismatch in the electrode impedance between two anode-cathode pairs. To compensate for the mismatches and confine the electrical field within the slot, an offset compensation circuit, consisting of 44 unity current sources (see Figure 3) is proposed. In our design, each anodic current is the summation of the base current, I_{base}, and the offset current, I_{offset}. By assigning certain amount of unity current sources to one anode and the rest to the other anode, anodic currents in different ratios are obtained. Table I shows the +20% ~ -20% current ratio in steps of approximately 2%.

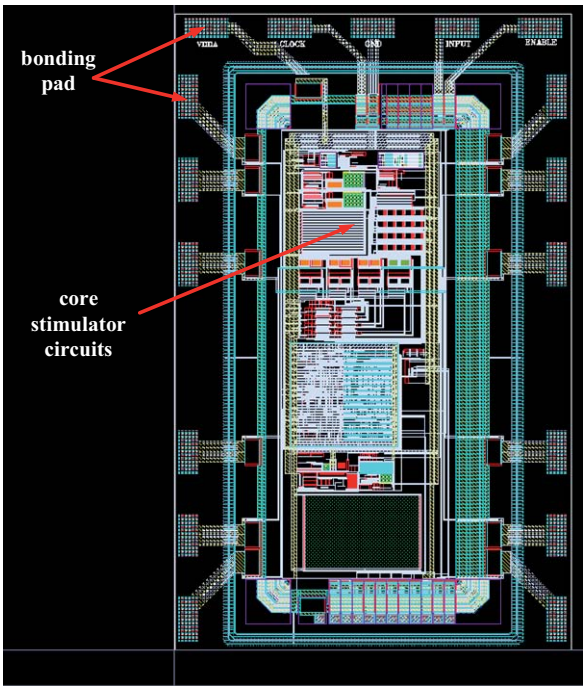


Fig. 4: Layout of the complete integrated stimulator.

Humidity sensor and bi-directional data

The in-package humidity will be monitored by a capacitive sensor. The change of capacitance is to be converted into the change of frequency by an oscillator, as shown in Figure 2. In a given time, the number of cycles is counted and then the output of the counter is modulated on the *INOUT* line by a parallel-in-serial-out shift register.

Size

The chip has been designed in a 0.6-µm CMOS process (Figure 4). The size of the complete integrated circuits is approximately 20mm^2, smaller than the cross-section area of the electrode book which is about 35mm^2. On the top are the pads for connecting to the cable. The twelve pads on the left and right are connected to four tripoles. The contact area of those IO pads has been enlarged to 400µm×170µm for two rivets per bonds per pad.

Conclusions

This paper has presented a brief overview of the design of an integrated stimulator for isolated tripoles with pulse currents up to 8mA adjustable between the anodes. The electrodes are to be passively discharged without blocking capacitors. This integrated stimulator is intended for use in a distributed system, in particular with *Active Books* in the spinal canal. At the time of writing, samples are being fabricated.

References

[1] Donaldson N, Vanhoestenberghe A, Liu X, Saeidi N, Demosthenous A, and Shuettler M, "Active books: a practical way toward increasing the number of stimulation channels for FES? " accepted for presentation in *IFESS* 2010.

[2] Struijk J and Holsheimer J, "Transverse tripolar spinal cord stimulation: Theoretical performance of a dual channel system," *Med.Biol. Eng. Comput.*, vol. 34, no. 4, pp. 273-279, 1996.

Acknowledgements

The authors wish to thank the UK Engineering and Physical Science Research Council (EPSRC) for supporting this project under grant number EP/F009593/1.

Author's Address

Dr Xiao Liu
Analogue and Biomedical Electronics Group
University College London, London WC1E 7JE
x.liu@ee.ucl.ac.uk
http://www.ee.ucl.ac.uk/~xliu

Sacro-lumbar Anterior Root Stimulator Implant for Exercising

Nonclercq A[1], Vanhoestenberghe A[1], Aqueveque P[1], Cirmirakis D[2], Donaldson, N[1]

[1] Implanted Devices Group – University College London, London, United Kingdom

[2] Electronics and Electrical Engineering – University College London, London, United Kingdom

Abstract

Functional Electrical Stimulation has been used since 1970s for providing patients with thoracic spinal-cord injury (SCI) with leg, urinary and sexual functions. After recognizing that people with SCI tend to suffer ill-health due to the secondary effects of inadequate exercise, much work has been done on using functional electrical stimulation (FES) for cycling and rowing using surface electrodes. However, applying the electrodes is tedious and few of those who start FES training continue. It is now timely to develop an implanted stimulator for these functions that will allow this to be done without taking so much of the users´ time to apply surface electrodes. The Implanted Devices Group (IDG), University College London, is currently developing a new Sacro-lumbar Anterior Root Stimulator Implant (SLARSI) system to improve quality of life of patients and reduce the cost of healthcare. This paper assesses the pros and cons of this new implant by comparing it with a previous lumbar anterior root stimulators implant (LARSI), also developed by the IDG.

***Keywords**: FES exercising, FES-cycling, LARSI, SARSI, urological functions, sexual functions.*

Introduction

People with spinal-cord injury (SCI) tend to suffer ill-health due to the secondary effects of inadequate exercise especially by the large muscles of the legs. Substituting the arms, such as in wheelchair sports, is liable to cause injury to joints of the shoulder and therefore is not ideal for long-term maintenance of fitness. Much work has been done on using functional electrical stimulation (FES) for cycling and rowing using surface electrodes. Cycling and rowing can be enjoyed as sports if sufficient training is maintained. Surface-electrode FES-cycling systems are now commercially-available and it is generally acceptable for patients to use them without supervision.

Games and races in sports halls may be exciting but to build up and maintain the muscles, FES exercise must be frequent (at least three times per week) which means that it probably must be done at home. However, applying the electrodes is tedious and few of those who start FES training continue. An implant that is always available, so that the patient only needs to transfer onto the exercise machine, might make FES exercise much more practicable.

In the 1990s, the Implanted Devices Group (IDG) trialled lumbar anterior root stimulator implants (LARSI) in two patients in the hope of providing a method for standing and stepping. However, after two years of practice, one of the two subjects implanted was only able to take 24 consecutive steps before needing to sit down, and her standing posture is still very unsatisfactory. Yet, she was able to cycle with the muscle combinations available [1]. She was therefore the first person to demonstrate FES cycling using nerve root stimulation (See Fig. 1) and has cycled over 1 km on several occasions [2].

Based on this experience, the IDG is now working on a Sacro-Lumbar Anterior Root Stimulator implant (SLARSI). The first aim of this implant is exercising. However, it also will allow bladder voiding and the recovery of some sexual functions by sacral anterior root stimulation.



Fig. 1: FES cycling.

This paper assesses the pros and cons of this new SLARSI by comparing it to the LARSI, previously developed by the IDG.

Comparing the SLARSI with previous LARSI

The LARSI system [1, 3] consists of an R.F. coupled multiplexed receiver implant with intradural book electrodes trapping the anterior spinal roots from L2 to S2 on both sides. The controller, worn externally, powers and controls the implant via a transdermal transmitter, which is placed immediately over the receiver implant when in use.

Compared to the LARSI, that was research based, the aim of the SLARSI is to provide the patients with a tool they can use daily to improve their quality of life and their health. The two systems differ in many ways, detailed in the following paragraphs.

Focus on rehabilitation

The LARSI system was originally intended for standing and stepping, but has failed to show satisfactory results for those aims (see Introduction). Cycling and rowing are more practical activities than walking, safer and without the strenuous effort of standing up and balancing. They are much simpler to control because the feet are fixed to pedals or foot-rests so the motion of the body is highly constrained.

The current project is therefore focussed on cycling and rowing, for exercising and thus long-term health, rather than walking. In this way, the implant system is designed to be integrated in a seamless manner to a recumbent tricycle or rower (e.g. through the use of a shaft encoder).

Functions

Besides exercising, patients who opt for SLARSI will also be able to empty their bladders by S3 stimulation and to regain some sexual functions by S2 stimulation (SARS technique). Those functions were not available using the LARSI.

However, patient suffering from detrusor overactivity will have to decide whether or not to undergo a rhizotomy. Some urologists consider that deafferentation should be avoided because it is destructive and irreversible so might preclude the patient from benefitting from future new neuroregenerative therapies.

If they do not want a deafferentation, and they are content to continue to empty their bladder by self-catheterisation, they would continue to use anticholinergics or Botox injections as before to prevent incontinence.

Electrode arrangement

The LARSI electrodes were configured as tripoles with connected anodes, as shown on Fig. 2a [4]. This electrode arrangement was attractive because only one wire is necessary for all anodes of a book. Three tripoles were used per book on a four wires cable. It was advantageous because all the wires need to pass through a *grommet* in the dura, where space is restricted.

Unfortunately, a high level of cross-talk was found in the implanted patients. To solve this problem, the electrode arrangement proposed in Fig. 2b is used in the SLARSI system. By using separate tripoles, the current is confined to the slot, hence stimulation should only occur under the active cathode.

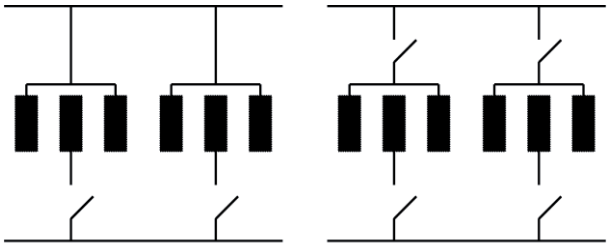


Fig. 2: Electrode arrangement.

Technology improvement

Since the LARSI implant was designed about twenty years ago, it did not benefit from modern technology. Improvements of the new SLARSI system include:

- bidirectional communication (to and from the implant) that will inform the user of the state of the implant, humidity level, electrode loads, etc.;
- a custom integrated circuit for the implant that will reduce the size and power consumption, while allowing independent stimulation of each slot;
- a larger range of current amplitude for the output stage;
- an integrated transmitter that will be smaller and more robust;
- a smaller external control box with a friendlier user interface, and a data logger that will be able to monitor the state of the implant, electrode loads and patient use.

This combination of technological advances will allow a state of the art implant uniquely adapted for nerve root stimulation.

Reliability and risk management

As far as possible, the SLARSI system design is similar to that of the Sacral Anterior Root Stimulator Implant (SARSI), which has been successfully used in many countries throughout the world [5], because this simplifies the process for getting permission to carry out experimental implantations. For the same reasons, the LARSI system was also based on SARSI.

More precisely, when possible, components and materials are the same. Furthermore, the surgical procedure will also be based on SARSI system, because it has proven to be very reliable, especially compared to FES implants with intramuscular electrodes. About 3000 SARSIs have been implanted, generally with good clinical outcomes [6].

Work achieved

The whole system is currently under development. The implant system bidirectional communication was successfully tested using two FPGA. The output stage was also successfully tested in an ASIC (Fig. 3). The final implant ASIC is now being designed, including both the communication and the new output stage architecture. The transmitter specification and architecture have both been completed, and the transmitter ASIC is also being designed. The control box is being implemented, including the user interface.

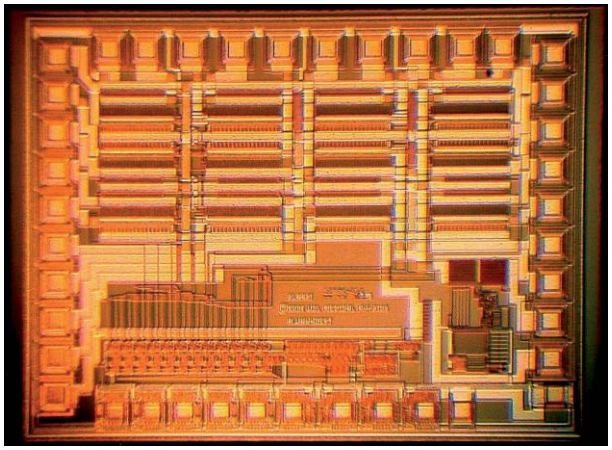


Fig. 3: Output stage ASIC.

Future work

Our first aim is to complete the development of the new SLARSI system and liaise with hospitals where the clinical teams are able to competently implant the system, measure the responses to stimulation and set up the stimulator program for the exercise that the patient will use.

The scientific question is whether the functional anatomy allows useful exercise when stimulating whole roots. If the conclusion is favourable, the method will be transferred to a company. This second step is difficult unless sales increase reasonably quickly after the investment needed to reach regulatory approval (CE Mark, etc).

If we succeed, patients with spinal cord injury will benefit from a commercial product that improves their quality of life while reducing the cost of healthcare. In the longer term, this research also opens new horizons in other related fields such as direct control of paralysed muscles by cortical neurons [7].

References

[1] Perkins TA, Donaldson N de N, Hatcher NAC, et al., “Control of leg powered paraplegic cycling using stimulation of the lumbo-sacral anterior spinal roots.” IEEE Trans Rehab., 10:158-164, 2002.

[2] Perkins TA, Donaldson N de N, Dunkerley AL, et al., “Development of paraplegic leg powered cycling with the Lumbo-sacral Anterior root Stimulator Implant,” in IFESS99: Proc. 4th Annual Conf. IFESS, Y. Handa, Ed., Sendai, Aug. 23–27, 1999, pp. 139–142.

[3] Donaldson N., Perkins T.A. & Worley A.C.M. (1997) "Lumbar root stimulation for restoring leg function. Methods: Stimulator and measurement of muscle actions." Artificial Organs, 21, 247-249.

[4] Donaldson N. de N., Rushton D.N., Perkins T.A., Wood D.E., Norton J. & Krabbendam A. (2003) “Recruitment by motor nerve root stimulators: significance for implant design” Med. Eng. Phys, 25 (7), 527-37.

[5] van Kerrebroeck PEV. “Worldwide experience with the Finetech–Brindley Sacral Anterior Root Stimulator.” Neurourol Urodyn 1993;12: 497–503.

[6] Brindley GS, The first 500 patients with sacral anterior root stimulator implants: general description. Paraplegia, 32:795-805, 1994.

[7] Moritz CT, Perlmutter SI, Fetz EE, “Direct control of paralysed muscles by cortical neurons”. Nature 456:639-42, 2008.

Acknowledgements

P. Aqueveque appreciates the support of postdoctoral project 3100136 of the Chilean Fund for Science and Technology development (FONDECYT).

Author’s Address

Antoine Nonclercq
Implanted Devices Group – Dep. Medical Physics
Malet Place Engineering Building, Gower Street
London WC1E 6BT, United Kingdom
Email: anoncler@medphys.ucl.ac.uk

Diaphragm Pacing with Endovascular Electrodes

Hoffer JA[1,2], Tran BD[1,2], Tang JK[2], Saunders JTW[3], Francis CA[1], Sandoval RA[1], Meyyappan R[1,2], Seru S[1,2], Wang HDY[1], Nolette MA[1,2], Tanner AC[1]

[1]Dept. Biomedical Physiology & Kinesiology, Simon Fraser University, Burnaby, BC, CANADA

[2]Lungpacer Medical, Inc., Burnaby, BC, CANADA

[3]Dept. Plastic Surgery, University of British Columbia, Vancouver, BC, CANADA

Abstract

Patients in intensive care units (ICU) who require mechanical ventilation (MV) for ≥1 week have high risk of medical complications such as ventilator-acquired pneumonia (VAP) and nosocomial infections, are 7X more likely to die in the ICU, and account for 50% of the ICU budget and 1/6 of all hospital in-patient costs in the US. In patients on MV the diaphragm muscle has been shown to atrophy rapidly and profoundly contributing to complications and frequent failure to wean from ventilators. We are developing endovascular electrodes suitable for percutaneous insertion in critically ill patients with only local anaesthesia, intended to electrically pace the phrenic nerves in order to maintain diaphragm strength and resistance to fatigue, improve ventilation, facilitate rapid weaning from MV, shorten the duration of ICU stay, reduce mortality, and decrease overall hospitalization costs. We present proof-of-concept, safety and stability results obtained with prototype electrodes that were implanted in pigs acutely or chronically for up to 3 weeks.

Keywords: *endovascular electrode, transvascular nerve stimulation, diaphragm pacing, phrenic nerve pacing, diaphragm atrophy, intensive care, mechanical ventilation, ventilator-acquired pneumonia, failure to wean.*

Introduction

Patients in intensive care units (ICU) who become dependent on mechanical ventilation (MV) are at high risk of complications such as ventilator-acquired pneumonia (VAP) and nosocomial infections, are seven times more likely to die in the ICU, and account for half the ICU budget and one-sixth of all hospital in-patient costs in the US [1].

Patients who require life-long assisted ventilation can sometimes benefit from electrical "pacing" of the diaphragm, as a partial or full alternative to mechanical ventilation [2]. In the past 30 years about 1,600 adult and paediatric patients have received permanently implanted phrenic nerve pacing systems. However, these systems require complex surgery under general anaesthesia, so they are not a feasible option for fragile ICU patients.

In MV patients in the ICU the diaphragm muscle is known to atrophy rapidly and profoundly [3] which contributes to frequent failure to wean from MV [4]. In order to support the ability of ICU patients to breathe naturally again and successfully wean from MV, we are developing novel, minimally invasive electrodes that can be deployed endovascularly in close proximity to the phrenic nerves and activated to produce rhythmic diaphragm contractions [5].

Nerve stimulation with endovascular electrodes is highly dependent on electrode design, location and orientation. Clinical success will require recruiting the phrenic nerves with low current and with high selectivity, to avoid activating other structures such as the vagus nerves, since they course 2-3 cm medial with respect to the phrenic nerves.

To validate our intravascular electrode designs we modeled the dielectric properties of the vessel wall, fluid and surrounding tissues and determined how these parameters alter the dispersion of the electric field and influence stimulation efficacy for various electrode geometries and locations. Since blood is a highly conductive medium, the stimulation current is substantially reduced by addition of an insulating electrode backing [5]. We subsequently tested intravascular electrode performance in acute and 3-week chronic pig implants. We present here our model predictions and initial findings on electrode selectivity, stability and safety.

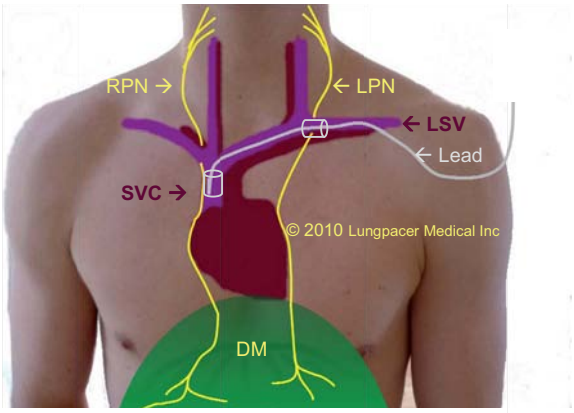


Figure 1: Diagram of target nerves and electrode locations inside central veins. **LPN**: left phrenic nerve **RPN**: right phrenic nerve **LSV**: left subclavian vein **SVC**: superior vena cava **DM**: diaphragm muscle

Material and Methods

We modeled the requirements for selective phrenic nerve activation with COMSOL Multiphysics 3.3a (COMSOL Inc., Stockholm Sweden), a graphical environment useful for changing parameter values that could not be conveniently evaluated in vivo. A 3D conductive media model was used to vary electrode locations, insulation thickness and inter-electrode distances. **Table 1** summarizes the dielectric properties used in our model.

Component	Connective Tissue	Vessel Wall	Blood	Silicone	Nerve
Conductivity [S/m]	0.020	0.027	0.066	10e-4	0.087
Relative Permittivity	25	45	300	11	650

Table 1: Dielectric properties of human tissue [7]

As shown in **Fig. 1**, endovascular electrodes were modeled as deployed inside the left subclavian vein in close proximity to the left phrenic nerve, and inside the superior vena cava, along which the right phrenic nerve courses.

Our model compared relative stimulation efficacy of 2 types of electrodes: an endovascular insulating cuff placed snugly against the vein wall with two electrodes facing outward as described by Hoffer [5] (**Fig. 2A-B**) and a 6F (~2 mm diameter) vessel dilator with two electrodes attached to its outer surface (**Fig. 2C-D**). In both cases, the cathode and anode were placed at 90° from each other in a plane transverse to vein, parallel to phrenic nerve.

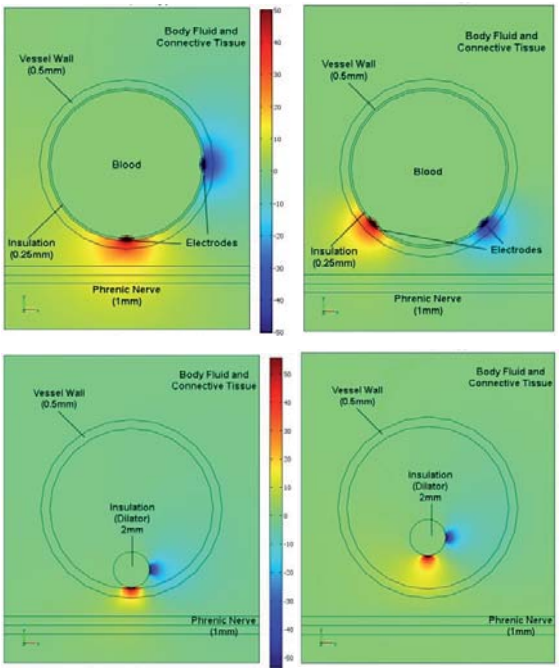


Figure 2: A. cuff with cathode electrode (**red**) optimally located inside vein wall to stimulate the phrenic nerve. **B.** cuff rotated 45° away from its optimal orientation. **C.** 6F dilator with its cathode contacting the vein wall at the optimal location and orientation. **D.** Dilator electrode shown displaced 1.5 mm away from vein wall and nerve.

Following the approvals from the SFU and UBC Animal Ethics Committees, prototype cuff and dilator electrodes (to be described in full detail elsewhere) were endovascularly implanted using the Seldinger technique. Stimulation selectivity, safety and stability properties were tested in nine acute and three 21-day chronic pigs (65 +/- 15 kg).

Model Results

Figs. **2A & C** reveal the powerful effect of placing an insulating wall behind endovascular electrodes. To minimize occlusion of blood flow, we specified cuff cross-section area <10 % of vein lumen area. A 0.5 mm thick silicone cuff (**Fig. 2A**) shields the interior of the vein, resulting in more current flowing out the vein wall and into the nerve than for a similarly placed dilator electrode (**Fig. 2C**). These findings are evident in plots shown in **Fig 3**.

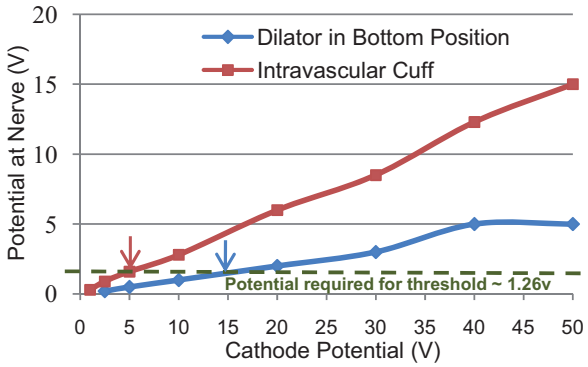


Figure 3. Stimulation potentials reaching the phrenic nerve as function of cathodic potentials generated with **cuff** (**red**) vs. **dilator** (**blue**) endovascular electrodes.

A green dashed line in **Fig. 3** shows the threshold potential (1.26 V; see [6]) required for phrenic nerve stimulation. Our model predicts the endovascular current required to activate a nerve with a shielded electrode (**red arrow**) is 3 times less than required from a lead-type dilator electrode (**blue arrow**).

We estimated the stimulation sensitivity to electrode rotation and/or translation along the vein, by modeling the displacement of each electrode in

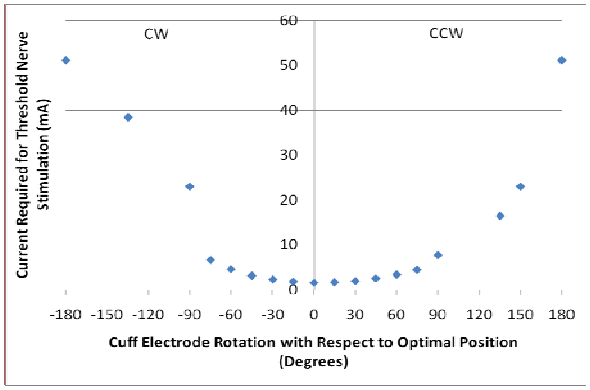


Figure 4: Stimulus efficacy vs. cuff rotation angle.

longitudinal and transverse directions. An example of a cuff electrode rotated 45° away from its optimal position is shown in **Fig. 2B**. Results of rotating the cuff cathode from -180° to +180° with respect to optimal position are plotted in **Fig. 4**. The model predicts that 90° rotation away from the optimal position results in a 5-fold reduction in nerve stimulation efficacy, and 180° rotation results in 50-fold reduction in stimulation efficacy.

The dependence of stimulation efficacy on distance between electrode and nerve is modeled in **Fig. 5.** Advancing the cathode toward and then past the target nerve results in a steep parabolic function. If the cathode is placed just 2 cm away from its optimal location, our model predicts nearly 10-fold reduction in efficacy of transvascular stimulation.

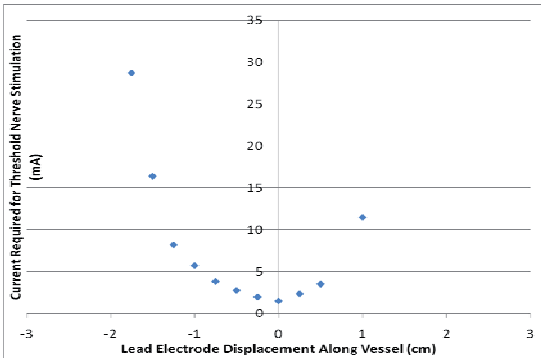


Figure 5: Model of efficacy vs. distance along vein.

Pig Implant Results

We mapped in acute and chronic pigs the threshold currents required for left phrenic nerve recruitment as function of electrode depth into the vein, and found fundamental agreement with model predictions. **Fig. 6** shows a representative result**.**

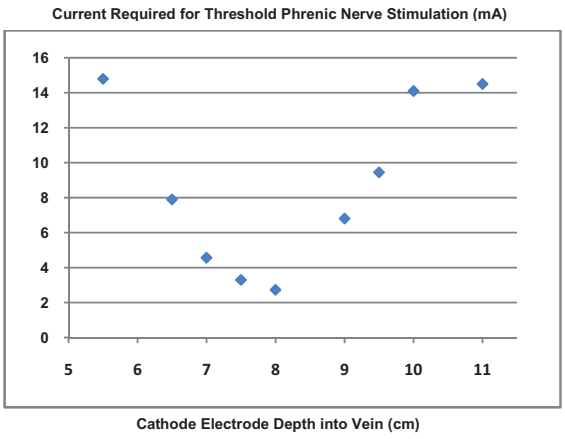


Figure 6: Left phrenic nerve stimulation efficacy as a function of electrode depth into vein (Chronic Pig #1).

Balanced biphasic pulses of 180 µs phase duration were used. Electrode placements within 1 cm from the nerve required stimulus currents ≤ 2 mA, but when the electrode was moved along the vein in either direction, away from the nerve, threshold currents increased rapidly in parabolic fashion.

In 3 pigs, endovascular electrodes were aseptically implanted and left in situ for 3 weeks. Electrode performance was assessed under anaesthesia on days 1, 11 and 21. Stimulation properties remained stable and the pigs remained healthy and gained weight normally throughout the testing period.

Discussion

Our model results provide guidelines for designing endovascular electrodes that maximize target nerve stimulation efficacy and also minimize unwanted stimulation of other structures. Stimulus efficacy is strongly dependent on electrode position with respect to both the vein wall and the target nerve, and is greatly improved by placing an electrically insulating barrier between the electrodes and blood inside the vein. Our results in anaesthetized pigs are consistent with these model predictions.

Conclusions

Effective transvascular diaphragm pacing in ICU patients will require deployment of endovascular electrodes within 1 cm from each phrenic nerve. Insulated endovascular electrodes that are stably positioned for diaphragm pacing are unlikely to produce unwanted stimulation of vagus nerves, since the latter course ≥2 cm away from the phrenic nerves in the regions of interest.

References

[1] Dasta JF. Daily cost of an intensive care unit day: the contribution of mechanical ventilation. Crit Care Med, 33:1266-71, 2005.

[2] Creasey G et al. Electrical stimulation to restore respiration. J Rehab Res and Dev, 33:123-132, 1996.

[3] Levine S et al. Rapid disuse atrophy of diaphragm fibers in mechanically ventilated humans. N Engl J Med, 358:1327-35, 2008.

[4] Vassilakopoulos T, Petrof BJ Ventilator-induced diaphragmatic dysfunction. Am J Respir Crit Care Med, 169: 336–341, 2004.

[5] Hoffer JA Transvascular nerve stimulation apparatus and methods. US patent application 60/887031, 2008.

[6] Elefteriades J et al. Long-term follow-up of pacing of the conditioned diaphragm in quadriplegia. PACE, 25:897-906, 2002.

[7] Miklavčič D, Pavšelj N, Hart FX Electric properties of tissues. Wiley Encyclop Biomed Engineering, 2006.

Acknowledgements

Funded by NSERC I2I phase I and phase IIb grants (JA Hoffer, PI) and by Lungpacer Medical, Inc.

Author's Address

hoffer@sfu.ca www.lungpacer.com

Flexible shaft electrodes for transdural implantation and chronic recording

Rubehn B[1,2], Lewis C[3], Fries P[3], Stieglitz T[1,2]

[1]Laboratory for Biomedical Microtechnology, Department of Microsystems Engineering – IMTEK, University of Freiburg, Freiburg, Germany

[2]Bernstein Focus Neurotechnology – Freiburg/Tübingen, Freiburg, Germany

[3]Ernst Strüngmann Institute in Cooperation with Max Planck Society, Frankfurt, Germany

Abstract

Local field potentials (LFPs) recorded from different brain areas can serve as useful signals to understand the interaction of different brain regions during information processing. In this work, we present a flexible shaft electrode which is designed to be chronically implanted into different brain areas in order to measure LFPs. We demonstrate a novel implantation concept for penetrating the dura mater and inserting the flexible shaft electrode into gray matter with help of an insertion tool. A first test electrode was fabricated by microsystems technology and was hybrid assembled to be used with an insertion tool made from standard tungsten rods. A brain phantom (agar gel covered with polyethylene foil) was used to confirm the insertion principle. In vivo, the implant was able to penetrate the cortical tissue and LFPs were recorded from the visual cortex of a cat. However, in this first trial, the implant could not be implanted through the pia or dura mater.

Keywords*: polyimide, flexible, neural implant, local field potential, MEMS, insertion*

Introduction

We have shown in a previous study that long-term stable LFPs can be recorded by means of a subdurally implanted electrode array based on a thin, micromachined polyimide (PI) foil [1]. After recording from the two-dimensional cortical surface, a next step in understanding the interaction between different brain regions during information processing would be to transfer the two-dimensional into a three-dimensional array and to record not only at the surface but within the brain tissue. If a number of shaft electrodes each comprising a linear array of electrode sites is distributed over the cortex and inserted at the cortical areas of interest, a three-dimensional grid of electrode sites is obtained and LFPs can be recorded from different brain areas as well as different tissue depths. The single shaft electrodes presented here have a small, thin shank, enabling them to be inserted through very small holes (400 µm in diameter) in the skull where the underlying dura mater is then penetrated. This approach is significantly less invasive than the surgery required for the implantation of the large epicortical electrode array [1]. It is anticipated that these small holes will be closed spontaneously by the surrounding skull after surgery, minimising post-surgical complications. By using PI as the substrate material, shaft and cable are flexible and move with the brain tissue, while the connector is attached to the surface of the skull. This should help to improve stability and quality of electrophysiological recordings. However, shaft electrodes are supposed to have two contrary properties. First, they have to be stiff during insertion into brain tissue. Second, after insertion, they have to match the brain's modulus of elasticity in order not to damage the surrounding cortical tissue, while the implant's cable must not transfer force from the connector placed on the skull to the brain, which would cause relative motion between the device and the cortex. Thus the device has to be flexible so that the inserted part moves with the brain while the connector part is attached to the skull. This is especially challenging in the case of a flexible shaft electrode which has to penetrate not only cortical tissue but the tough dura mater. In this work, we present an implant which serves as a first step towards the three-dimensional electrode array setup described above, together with the development of a novel implantation technique.

Materials and Methods

Implant Design

To fulfil the contradicting requirements of stiffness during the insertion and flexibility during the course of a long-term implantation, we developed a custom insertion tool for the shaft electrodes. While the shaft itself is flexible, the insertion tool is used to penetrate the dura mater. The tool comprises a tungsten rod with a diameter of 100 µm and a tapered tip, and two tungsten rods with diameters of 50 µm and blunt tips. The thicker rod is

glued between the two thinner ones protruding beyond them (Fig. 1). Tungsten was chosen as it is a standard electrode material in electrophysiology and tungsten rods are known to be stiff enough to penetrate the dura mater [2].



Fig. 1. Schematic of the insertion tool consisting of one tapered (100 µm diameter) and two blunt (50 µm diameter) tungsten rods glued together with epoxy.

For the implantation, the tapered rod slides into a U-shaped profile which is glued to the back of the shaft's tip (Fig. 2). The whole assembly is intended to be inserted into the brain, with the tapered tip of the rod penetrating the dura mater while the two blunt rods bear against the back of the U-profile, pushing it through the hole in the dura mater and into the tissue. Since it is attached to the U-profile, the flexible shaft is inserted into the brain matter. After placing the shaft at the right position, the tungsten insertion tool is withdrawn, leaving the PI shaft and the U-profile in the brain.

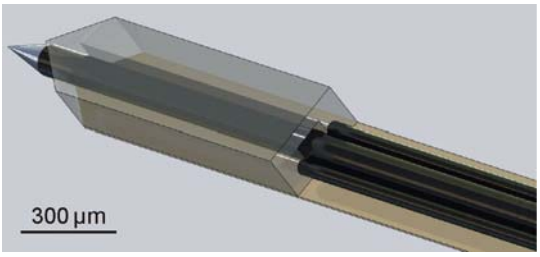


Fig. 2. Schematic of the tip of a shaft electrode with U-profile glued beneath it. The shaft's tip shown from below with the insertion tool inserted into the U-profile.

The U-profile, made of SU-8, has a cross-section of 270 µm by 185 µm and a length of 1 mm. With its cross-sectional dimensions, it is in the range of standard rod microelectrodes. With such electrodes, normal electrophysiology can be found even after many penetrations of the same cortical tissue. Our design has the advantage that only the U-profile has these dimensions and is stiff. The PI shaft directly behind the U-profile tip is very flexible and merges in a 75 mm long cable with a cross-section of 270 µm by 10 µm which mechanically decouples the shaft and the connector part helping the U-profile to float in the tissue. During insertion, the cortical tissue is pushed aside by the U-profile passing and can then relax due to the thin shaft following. Thus, it is anticipated that the implant will cause even less damage than standard rod microelectrodes. The linear electrode array consists of 8 rectangular electrode sites with an area of 100 µm by 500 µm and a pitch of 1 mm.

MEMS Processing and Assembly of the Shaft

The MEMS-processed electrode shafts were made of a 300 nm thick sputtered platinum layer, defining electrode sites, conductor paths and solder pads, sandwiched between two 5 µm thick spin-coated PI foils [1]. The U-profiles were produced in a cleanroom with standard MEMS-technology equipment. A silicon wafer was plasma coated with a C_4F_8 release layer. Two layers of SU-8 (SU-8 3025 and SU-8 3050 respectively; MicroChem Inc., Newton, MA, USA) were spin-coated on the wafer and structured with UV light. The first 24 µm thick layer forms the U-profile cover, whereas the second layer has a thickness of 160 µm and defines the walls of the U-profile.



Fig. 3. Cross-section of the U-profile on a wafer substrate during MEMS-processing.

The U-profile was detached from the wafer using tweezers. With the tip of a needle, a small amount of epoxy (UHU plus endfest 300, UHU GmbH, Bühl, Germany) was applied on the bottom of the profile walls. The U-profile was attached to the rear side of the electrode shaft by tweezers. After aligning the SU-8 profile to the PI shaft, the device was put on a hotplate for 5 min at 70 °C to accelerate the curing of the glue. SMD connectors were soldered directly onto the PI foil. Subsequently, epoxy glue was applied between the connectors and the PI foil to mechanically secure the soldering sites.

Artificial Brain Model

To evaluate the insertion method, a brain phantom was made of an agar gel (1.8 wt% agar powder in water) simulating the cortical tissue, and was covered by a polyethylene (PE) foil which represented the meninges (standard household cling wrap with a thickness of 10-20 µm) [3].

In Vivo Experiment

The experiment was conducted according to the guidelines of the Society for Neuroscience and the German law for the protection of animals, approved by the local government's ethical committee, and overseen by a veterinarian. In one cat, anaesthesia was induced with ketamine and maintained with a mixture of 70% N_2O, 30% O_2 and halothane (0.4%–0.6%). The cat was paralyzed with pancuronium bromide applied intravenously

(Pancuronium, Organon, 0.15 mg kg^{-1} h^{-1}). The right hemisphere was exposed by a trepanation over striate cortex (area 17). The insertion tool was mounted on a microdrive and the flexible shaft electrode was attached to it with sugar solution. The microdrive speed was manipulated by hand and the shaft was inserted perpendicular to the cortex to a depth of about 3 mm.

Results

The shaft and U-profile were successfully assembled. The two parts could be accurately aligned and the glue could be applied without blocking the U-profile's channel (Fig. 4). Electrode impedances ranged from 10 kΩ to 20 kΩ at 1 kHz.

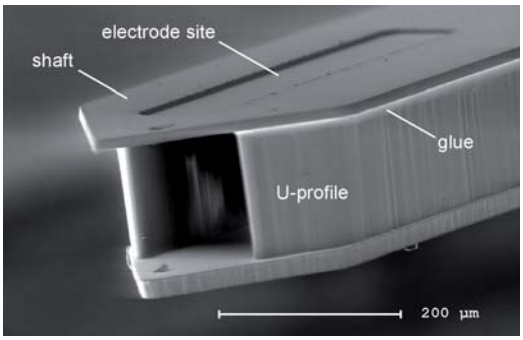


Fig. 4. Scanning electron micrograph of a hybrid assembled shaft electrode tip.

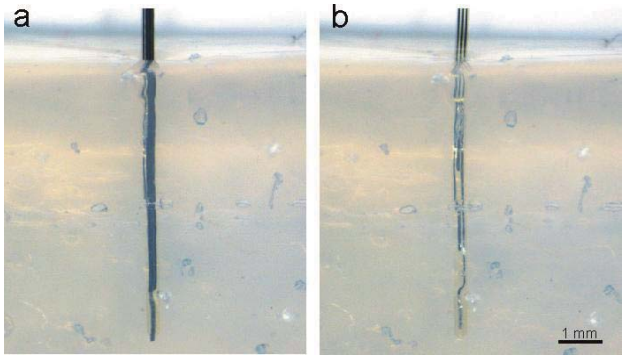


Fig. 5. Insertion of a shaft into the brain phantom. (a) Positioning of the shaft with help of the insertion tool, (b) shaft after withdrawing the insertion tool.

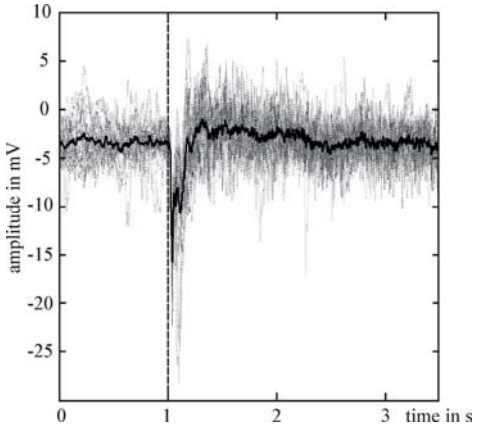


Fig. 6. Event related potentials in the LFP signal. 20 single trials are depicted in grey, the average response in black and the onset of the visual stimulus (downward scrolling grating) at 1 s.

The insertion tool was able to easily penetrate the PE foil of the brain model and to insert the shaft at the desired depth of the gel (Fig. 5a). After withdrawing the insertion tool, the shaft remained at its position (Fig. 5b). The working principle was confirmed by the successful repetition of the insertion procedure for 15 times. The in vivo experiment showed that the insertion tool combined with the flexible implant was easy to handle. However, while the shaft could be inserted into the cortex, it was not possible to insert it through the closed dura or pia mater. After insertion, LFPs could be recorded. Fig. 6 depicts event related potentials to a given visual stimulus.

Discussion

Although the feature size of the U-profile was small, it could be easily glued to the shaft by using tweezers and a standard stereo microscope. While the shaft could be successfully implanted into the cortex, further refinement of the design has to be done in order to be able to also penetrate the dura mater. The quality of the LFP signals was excellent and showed the good applicability of our electrode in intracortical LFP recording.

References

[1] Rubehn B, Bosman C, Oostenveld R, Fries P, Stieglitz T. A MEMS-Based Flexible Multichannel ECoG-Electrode Array. J Neural Eng, 6(3):036003, 2009

[2] Hubel DH. Tungsten Microelectrode for Recording from Single Units. Science, 125: 549-550, 1957

[3] Haj Hosseini N, Hoffmann R, Kisban S, Stieglitz T, Paul O, Ruther P. Comparative Study on the Insertion Behavior of Cerebral Microprobes. Proc 29th Annual International Conference of the IEEE EMBS, Lyon, France. 2007

Acknowledgements

This work was supported by the German Federal Ministry of Education and Research (BMBF grant 01GQ0830). The authors want to thank Christian Henle for taking the SEM picture.

Author's Address

Name Birthe Rubehn
Affiliation Laboratory for Biomedical Microtechnology, Department of Microsystems Engineering - IMTEK, University of Freiburg
Georges-Koehler-Allee 102
79110 Freiburg, Germany

email rubehn@imtek.de
homepage www.imtek.de/bmt

Session 2

Future Applications 1

Bioimpedance based measurement system for a controlled swallowing neuro-prosthesis

Nahrstaedt H[1], Schauer T[1], Seidl RO[2]

[1] Control Systems Group, Technische Universität Berlin, Berlin, Germany

[2] Klinik für Hals-, Nasen-, und Ohrenkrankheiten, Unfallkrankenhaus Berlin, Berlin, Germany

Abstract

Dysphagia has a huge impact on the quality of life. In this contribution, a measurement system is presented which allows an assessment of the swallowing process. Additionally, the system detects aspiration. Basis of the system is a two-channel bioimpedance measurement at the neck which can be extended by an EMG recording from the larynx's musculature. The feasibility of aspiration detection was experimentally demonstrated on an animal model. The proposed measurement may be used in both therapy and diagnosis of dysphagia. Within this contribution the idea of a controlled neuro-prosthesis is outlined.

***Keywords**: Dysphagia, Bioimpedance, EMG, Larynx, Aspiration detection, Neuro-prosthesis, Airway, Swallowing, Intramuscular electrical stimulation.*

Introduction

Swallowing is a complex vital process that takes place either consciously or sub-consciously depending on the current phase of the swallowing. Controlled by cortical processes, which are coordinated in the brain stem (pattern generators), multiple muscles have to be activated in a timely manner for a swallow.

Swallowing disorders (dysphagia) can lead to serious complications, including malnutrition and pneumonia, which may be fatal. The complete closure of the larynx and its timing take a central role in safe swallowing, especially since the larynx is a bifurcation between trachea and oesophagus. In case of closure failure, a transfer of saliva, liquid or food into the airway (aspiration) takes place, which may have the consequences described above.

The causes of swallowing disorders are mostly severe head injuries and strokes. Every second stroke patient suffers from dysphagia, which is chronic in one quarter of the patients [1].

The primary objective of rehabilitation is the restoration of disturbed functions by, for example, sensory stimulation or teaching of special swallowing techniques. Necessary conditions for success are sufficient cortical potential after the injury and an existing connection from the cortex to the muscles. If this connection is lost or the muscles cannot be sufficiently controlled, a rehabilitation of the swallowing process is not possible. Hence, the patient is dependent on a diet via feeding tube and a tracheal cannula.

In these cases, electrical stimulation of the external laryngeal muscles as a therapeutic approach seems to enhance the swallowing process [2]. Another possibility is to stimulate the internal laryngeal muscles such that the vocal cords close and aspiration can be prevented [3]. In both cases intramuscular stimulation seems to be superior to transcutaneous stimulation [4-5]. The stimulation has to released in a timely manner. In previous studies the stimulation was triggered either by the patient himself via a hand-switch [3] or by the electromyography (EMG) of submental muscles [5]. However, neither method is able to adapt to the swallowing success or skills of the patient.

One approach to evaluate the swallowing success could be the measurement of the bioimpedance (BI). Impedance is defined as the relation of voltage to current over an electrical conductor. There are two possible methods to measure BI.

In the two-point method, the voltage is measured directly over the current electrodes. The current, which is induced into the patient through the current electrodes, causes a voltage drop across the electrode-skin contact. As this resistance is time-variant, it will lead to a measurement error. This undesirable effect can be avoided by using the four-point measurement method. The voltage is recorded separately over additional electrodes by a high impedance instrumentation amplifier. Since no current can flow through the voltage electrodes,

there is no disturbing time-varying voltage drop across the electrode-skin contact. The instrument we have developed supports both methods.

A four-electrode method using separate current and voltage electrodes is applied for a transcutaneous measurement of bioimpedance in the neck as proposed in [6]. In previous work [7], it was shown that the BI is correlated to the distance from the hyoid bone to the thyroid cartilage, a measure of airway closure during swallowing. In this work, it is further examined whether such BI measurements can also be used for the detection of aspiration. A measurement system based on two combined BI measurements could then serve as a sensor concept for a regular swallowing neuro-prosthesis.

Idea and concept of a BI controlled swallowing neuro-prosthesis

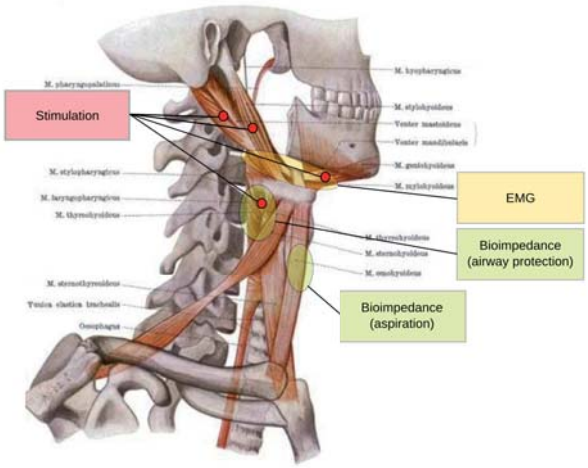


Fig. 1: Model of the measurement and stimulation system as basis for a swallowing neuro-prosthesis

The goal of the BMBF-funded research project BigDysPro is the development of a controlled neuro-prosthesis that supports swallowing by stimulating the appropriate muscles using intramuscular electrodes. The system continuously assesses the success of the stimulation using BI measurements and adjusts to the needs of the patient accordingly. For a synchronized start of swallowing and stimulation, the remaining residual activity of the muscles is recorded by EMG measurements and acts as a trigger for the stimulation. If the patient chokes despite these measures, the device is able to detect this from the BI measurement and triggers a protective cough or throat-clearing induced by a further stimulation. In Fig. 1, the stimulation and measurement areas are shown. For the measurement of airway closure, changes in the BI at the level of the epiglottic vallecula are acquired. Aspiration detection takes place though electrodes on the thyroid cartilage at the level of vocal cords.

Material and Methods

We have developed a measuring system which allows two independent BI measurements and provides four channels of EMG. The BI can be acquired in parallel using two EMG channels.

Current source

The device has two identical galvanically isolated current sources, which operate at one of eight available current settings (max. 135 µA) and can handle a maximal impedance of 2 kOhm. One current source generates a sinusoidal current with a frequency of 50 kHz, while the second current source is set to a frequency of 100 kHz. When measuring, these two frequencies are easily distinguishable from another. Thus, two independent BI measurements can be performed simultaneously.

In the current sources, which drive a current through a patient to the device ground, measurement errors can occur if one part of the current flows capacitively to the device ground instead of flowing entirely through the patient. This may happen when the therapist touches the patient. In contrast to this, the current source we used features a differential design so that such effluent currents can be compensated. To avoid DC components in the current, which may endanger the patient, one Y1-capacitor is connected in series to each output terminal.

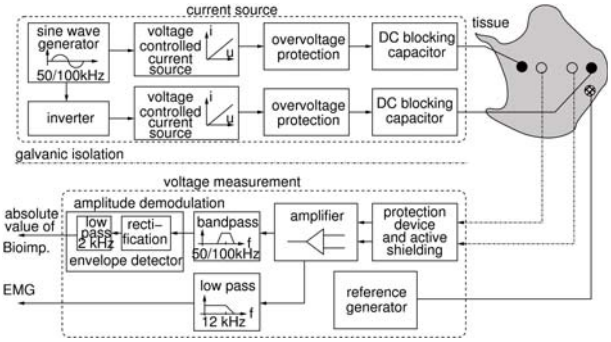


Fig. 2: Structure of a BI / EMG measurement channel

Voltage measurement

Each of the four amplifiers (INA128, TI) features input protection resistors which protect the patient attached to the device from any dangers in case of failure. In addition, protection diodes ensure that the instrumentation amplifier is not damaged. With this setup it is possible to measure during an active electrical stimulation. Fig. 2 shows the structure of one BI / EMG measuring channel.

EMG-Measurement

In order to extract the EMG from measurement data, the amplified signal of the analogue input is filtered with a 12 kHz low-pass filter. Thus, the

high-frequency voltage parts deriving from the BI are removed.

Demodulation

An amplitude demodulation circuit extracts the amount of BI from the measured sinusoidal signal. First, the signal is bandpass filtered in order to isolate the measuring frequency. Next, the signal is rectified and low-pass filtered. The processed signal corresponds to the amplitude of the sine wave and therefore to the amount of the measured BI.

Micro-controller and connection to a PC

The processed analogue signals (up to 4 EMG and 2 BI signals) are sampled simultaneously by a 24-bit A/D converter (ADS1278, TI) with a frequency of 4 kHz. The micro-controller (STM32F103, STM) sends the data to a PC via a galvanically isolated serial-USB converter.

Results

A central part for the development of the described neuro-prosthesis is an aspiration detection. Aspiration is defined as the passage of liquids or solids through the larynx below the vocal cords. At the moment, only a radiological examination can reliably prove that aspiration has occurred. To test the feasibility of an aspiration detection BI, measurement tests have been performed on an animal larynx. A fresh bovine larynx was prepared in a way that it could be suspended freely in order to convey liquids through it. The bioimpedance measurement was recorded using the four-point measurement method. The electrodes were placed at the level of the vocal cords.

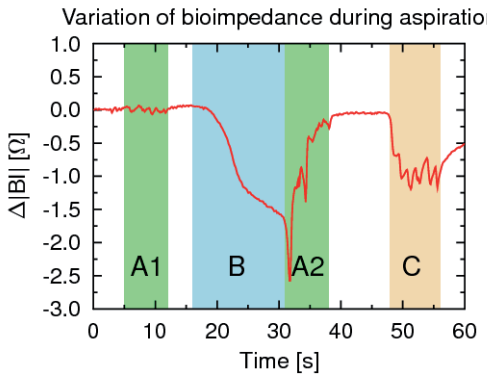


Fig. 3: Measurement result during the passage of various fluids through the larynx. A1 - water, B - yoghurt, A2 - water, C - buttermilk

Various fluids have been inserted into the larynx with a pipette. The respective time segments are marked and plotted in Fig. 3 together with the measured change of BI over time. Water (section A1) causes only small changes in the BI. As yoghurt (section B) is viscous and rinse down very slowly, the BI reacts in a delayed manner. In section A2, yoghurt that still has been present in the larynx, is rinsed down by water and caused peaks in the BI. The respective maximum is reached if and only if some liquid has passed the position of the electrodes near the vocal cords. In section C, buttermilk has been dispensed intermittently, which explains the oscillations in the trace. The deflection of BI is a function of the liquid (electrolyte content changes).

Conclusions

The presented measurements on an animal larynx show that BI may be suitable for detecting aspiration. In order to validate the complete measuring system, comparative studies of patients using videofluoroscopy are needed. The introduced measuring system will be of major help in further developing the described neuro-prosthesis.

References

[1] Prosiegel M, Neurogene Dysphagien: Leitlinien 2003 der DGNKN, *Neurol. Rehabil.*, vol. 9, 157-181, 2003.

[2] Burnett TA, Mann EA, Cornell SA, et al., Laryngeal elevation achieved by neuromuscular stimulation at rest, *Journal of Applied Physiology*, vol. 94, 128-134, 2003.

[3] Broniatowski M, Grundfest-Broniatowski S, Tyler DJ, et al., Dynamic laryngotracheal closure for aspiration: a preliminary report, *Laryngoscope*, vol. 111, 2032-2040, 2001.

[4] Ludlow CL, Humbert I, Saxon K, et al., Effects of surface electrical stimulation both at rest and during swallowing in chronic pharyngeal Dysphagia, *Dysphagia*, vol. 22, 1-10, 2007.

[5] Leelamanit V, Limsakul C, Geater A, Synchronized electrical stimulation in treating pharyngeal dysphagia, *The Laryngoscope*, vol. 112, 2204-2210, 2002.

[6] Kusuhara T, Nakamura T, Shirakawa Y, et al., Impedance pharyngography to assess swallowing function, *J Int Med Res*, vol. 32, 608-616, 2004.

[7] Schauer T, Seidl RO, Nahrstaedt H, Erfassung der pharyngealen Schluckphase durch Bioimpedanz-Messung, *Automatisierungstechnische Verfahren für die Medizin (8. Workshop)*, 47-48, 2009.

Acknowledgements

This work was partly funded through grant by the German Federal Ministry of Education and Research (BMBF) within the project BigDysPro (FKZ 01EZ1007A).

Author's Address

nahrstaedt@control.tu-berlin.de

Surface electrical stimulation to assist laryngeal elevation for swallowing rehabilitation in dysphagia

Kuno H[1], Yamamoto N[1], Yamamoto T[1], Aoyagi Y[2], Tsubahara A[2]

[1] Okayama University of Science, Okayama, JAPAN

[2] Kawasaki Medical School, Kurashiki, JAPAN

Abstract

In this study, we investigated a basic surface electrode stimulation method to support laryngeal elevation in patients with pharyngeal dysphagia. Subjects were 12 healthy men and 7 patients with pharyngeal dysphagia. Digastric and stylohyoid muscles were stimulated by the silver-textile surface electrodes covering the muscle belly. Laryngeal elevation by the electrical stimulation (ES) during liquid (water, 3ml) swallowing movement was measured by digital video camera and pressure transducer. Trajectory of laryngeal elevation demonstrated a hysteresis loop. Elevation distance of the larynx increased with a rise of stimulus strength. Laryngeal elevation by ES was 76.0% in healthy subjects and 86.6% in patients in comparison with liquid swallowing. ES for the laryngeal elevation may assist a part of the swallowing reflex.

***Keywords**: Surface electrical stimulation, Dysphagia, Laryngeal elevation.*

Introduction

Recently, the application of Functional Electric Stimulation (FES) has come to be paid to attention to dysphagia. The surface electric stimulation (ES) of this study is noninvasive attacks, and may also promise the effectiveness of sensory nerve stimulation.

In the swallowing therapy, it is one of the important functions to be able to cause the rise-up movement of the hyoid bone. In 2002, the first commercially available stimulator (VitalStim) was developed in the USA for swallowing rehabilitation [1]. It stimulates the infrahyoid and suprahyoid muscles by comparatively small surface electrodes (0.5 in^2) on the skin over the throat area. At that time, a physiologic role of each muscle was not examined enough in VitalStim, and the program for the movement generation has not been proposed. According to the recent research of Tsushima et al. (2009) during normal swallowing, the hyoid moves up and forward [2]. The geniohyoid, mylohyoid, and digastrics muscles lift the larynx, and its movement is assumed to settle toward the mandible.

Humbert et al. (2006) and Ludlow (2010) examined the effect of stimulation of the surface electrode type [3, 4]. They indicate that it is necessary to pay attention to the stimulating timing so that the stimulation of hyoid depressors may have the possibility to bring aspiration (or misswallowing). Lastly, it is pointed out that a further verification is needed to the clinical effectiveness of ES.

We hypothesized that the surface ES of the suprahyoid muscles; digastrics and stylohyoid muscles, can assist laryngeal elevation, which is a similar rise-up motion of the hyoid bone during normal swallowing. The final goal of our research is to develop the electrical stimulator for swallowing rehabilitation.

Material and Methods

Subjects

Subjects were 12 healthy male volunteers (between 21 and 23 years of age) and 7 patients with pharyngeal dysphagia. Informed consent was provided before examination.

Experimental protocol

Liquid (water, 3ml) swallowing movement was estimated by EMG, accelerometer, digital video camera and pharyngeal pressure transducer. EMG was obtained from masseter, digastrics, geniohyoid, and mylohyoid muscles [5]. Wireless three-axis accelerometer was attached on a hyoid bone. Elevation distance of the larynx was measured by image analysis software (ImageJ, NIH) from a digital video camera image. Pharyngeal pressure was measured by pressure transducer which placed on epipharynx, oropharynx, hypopharynx and esophageal entrance.

ES was done with the experimental constant-voltage type stimulator (8 channels) [6], and a biphasic burst-stimulating wave was modulated with the rectangular (or sine) wave of 5 kHz carrier frequency. The polarization voltage between the skin and the electrode was compulsorily discharged for about 10ms by using optical switching technique. In addition, the surface electrode was made from the silver-nylon woven cloth, and the size of the electrode has been adjusted to cover muscle belly.

Results and Discussion

Firstly, on the rectified EMG around the submental region (figures, not shown), the acceleration amplitude of the hyoid bone in the normal swallowing movement pattern, the starting point of acceleration wave was almost synchronized with muscular discharges of the mylohyoid and geniohyoid muscle, which reflects elevation of the thyroid cartilage by the swallowing movement.

Figure 1 shows one example of elevation distance of larynx with stimulus strength. Dotted line shows liquid swallowing movement, solid line shows elevation of larynx using ES and bold solid line shows stimulation pattern. Elevation distance of larynx increased with a rise of stimulation voltage and was saturated in more than 35V. It seems that it is a maximum of elevation by ES. The elevation distance pattern almost accorded with a stimulation pattern. Therefore, it can select appropriate stimulus pattern and strength for the patients.

Figure 2 shows elevation distance of larynx in healthy subjects (a, b) and patients (c, d). Left side of figures were liquid swallowing, and right sides of figures were elevation of larynx using ES. Elevation distance had a slightly smaller with ES, in comparison liquid swallowing movement.

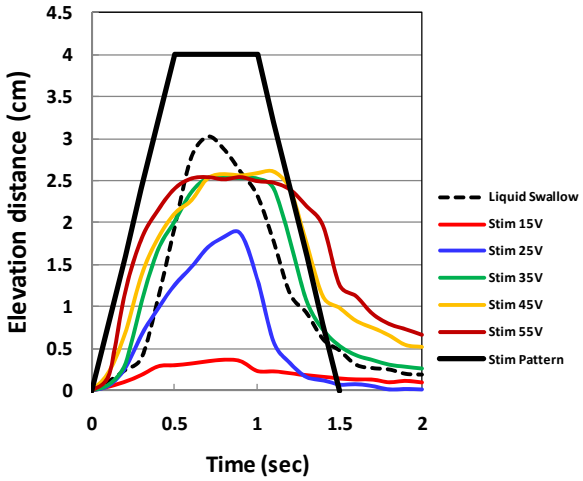


Fig.1 One example of elevation distance of larynx with stimulus strength. Dotted line shows liquid swallowing movement, solid line shows elevation of larynx using ES, and bold solid line shows stimulation pattern.pattern.

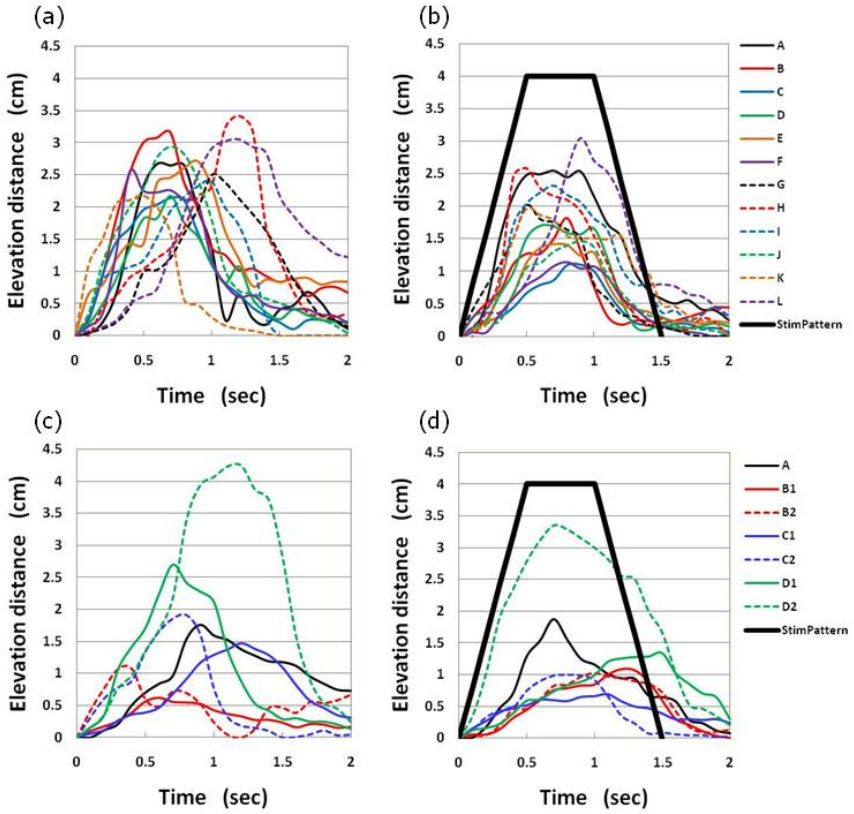


Fig.2 Elevation distance of larynx in healthy subjects (a, b) and patients (c, d). Left side of figures were liquid swallowing, and right sides were elevation of larynx using ES. Bold solid line (b, d) shows stimulation pattern.

Elevation of larynx by ES was 76.0% in healthy subjects and 86.6% in patients in comparison with liquid swallowing. The electrodes must be placed carefully, because the elderly has a wrinkle and slack of the skin. Burnett et al. (2005) showed that the normal subjects could start ES by manual switch for swallowing [7]. It is necessary to evaluate sensory function of oral cavity, a finger function, and a cognitive function when the patients handle the switch.

Figure 3 shows pharyngeal pressure change in epipharynx, oropharynx, hypopharynx and esophageal entrance. Pharyngeal pressure of healthy subject shows positive pressure in epipharynx, oropharynx, hypopharynx, and negative pressure in esophageal entrance (a). On the other hand, positive pressure of patient was lower than healthy subject, and negative pressure did not happen (b). On the other hand, ES caused negative pressure of esophageal entrance of patient (c). We conclude that elevation of larynx by ES assist to generate negative pressure of esophageal entrance and may facilitate swallowing movement.

Conclusions

In this study, we investigated a basic research of surface ES to assist laryngeal elevation. As a result of having compared with liquid swallowing movement, the ES was able to elevate a larynx to assist swallowing reflex movement.

References

[1] Wijting Y: Neuromuscular Electrical stimulation in the treatment of dysphagia-A summary of the evidence. VitalStim therapy, 2-25, TI Anode UK PVT Ltd, 2010.

[2] Tsushima C, Saitoh E, Baba M, Yokoyama M, Fujii W, Okada S, Uematsu H: Hyoid movement and laryngeal penetration during sequential swallowing. J Med Dent Sci, 56: 113－121, 2009.

[3] Humbert IA, Poletto CJ, Saxon KG, Kearney PR, Crujido L: The effect of surface electrical stimulation on hyolaryngeal movement in normal individuals at rest and during swallowing. J Appl Physiol, 101: 1657–1663, 2006.

[4] Ludlow CL: Electrical neuromuscular stimulation in dysphagia: current status. Current Opinion in Otolaryngology & Head and Neck Surgery, 18:159-164, 2010.

[5] Okitsu T, Arita M, Sonoda S, Ota T, Hotta F, Honda T, Chino N: The surface electromyography on suprahyoid muscles during swallowing, Jpn. J. Rehabil. Med., 35: 241-244, 1998 (in japanese).

[6] Yamamoto T, Ohshima J, Hamade S: Multichannel TES system for the neuromuscular reeducation. 2nd International FES Symposium, 3 pages, 1995.

[7] Burnett TA, Mann EA, Stoklosa JB, Ludlow CL: Self-triggered functional electrical stimulation during swallowing, J Neurophysiol, 94: 4011–4018, 2005.

Acknowledgements

Finally, we express our thanks that a part of this research was supported by the Ministry of Education, Culture, Sports, Science and Technology of Japan through a Financial Assistance Program of the Social Cooperation Study (2006-2010), and the Scientific Research (c) (19500466, 21500500).

Author's Address

Name: Hiroaki Kuno
eMail: kuno@are.ous.ac.jp

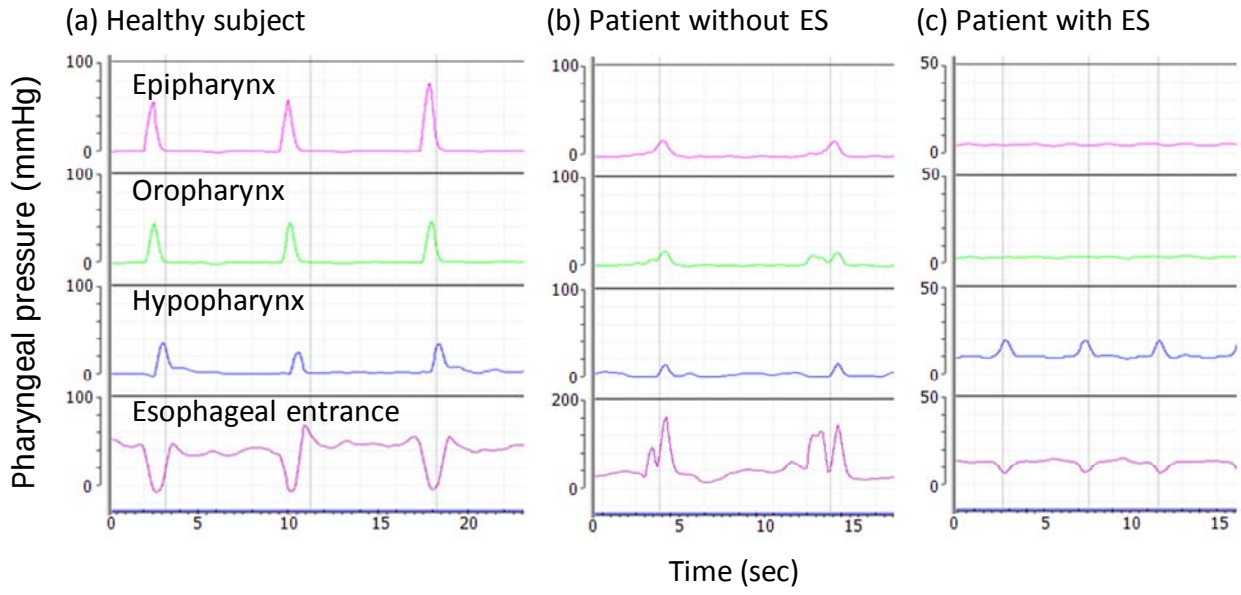


Fig.3 Pharyngeal pressure change in epipharynx, oropharynx, hypopharynx and esophageal entrance. Figures were healthy subject (a) and patient (b, d).

The effect of an abdominal FES training protocol on pulmonary function in tetraplegia

Mclachlan A J[1,2], Gollee H[1,2], M[c]Lean A N[2,3], Allan D B[2,3]

[1] Centre for Rehabilitation Engineering (CRE), University of Glasgow, Glasgow, Scotland

[2] Scottish Centre for Innovation in Spinal Cord Injury, http://www.scisci.org.uk

[3] Queen Elizabeth National Spinal Injuries Unit (QENSIU), Southern General Hospital, Glasgow, Scotland

Abstract

Tetraplegia may result in significant paralysis of the breathing muscles. Decreased forced vital capacity (FVC), forced expiratory volume in one second (FEV_1), peak expiratory flow rate (PEF) and maximum expiratory pressure (MEP) can result in significant respiratory compromise. It has been shown that abdominal functional electrical stimulation (FES) can augment the above measurements of pulmonary function in single session cross sectional studies. We investigate the effects of an abdominal FES training program on unassisted pulmonary function tests (PFT), FES-assisted PFT and the effectiveness of FES-assisted PFT compared to unassisted PFT. The results from six tetraplegic subjects showed increases in unassisted FVC, FEV1 and PEF and FES-assisted FVC after the training intervention, followed by a decrease during the detraining period, although only the changes in FES-assisted and unassisted FVC were found to be statistically significant. Large inter and intra-subject variability was found in terms of the effectiveness of stimulation which may have affected the FES-assisted FEV_1 and PEF results. We conclude that an abdominal FES training program can be used as a muscle strengthening tool that can increase unassisted PFT in tetraplegia.

Keywords: *Spinal cord injury (SCI), tetraplegia, respiratory function.*

Introduction

Spinal cord injury (SCI) to the cervical region (tetraplegia) may result in significant paralysis of the intercostals and abdominal muscles. A decreased forced vital capacity (FVC), forced expiratory volume in one second (FEV_1) and peak expiratory flow rate (PEF) indicate significant respiratory compromise [5] as can changes in the maximum expiratory pressure (MEP) and the ability to cough [4]. The resulting respiratory complications are one of the leading causes of rehospitalisation and death in tetraplegia [1].

Functional electrical stimulation (FES) has been shown to improve the above pulmonary function tests (PFT) but only in single session cross sectional studies [3]. It is predicted that an increase in PFT will relate to an improved cough and a reduction in respiratory complications [2]. Studies have investigated training paradigms that incorporate abdominal FES [4] but no research with a training program based exclusively on abdominal FES and its effect on unassisted and FES-assisted PFT has been reported. An advantage of this type of training program is that it can be carried out without distracting the patient from other activities.

We investigate the effects, in tetraplegic subjects, of a three week incremental training program and the subsequent de-training period on PFT. We examine the changes in unassisted PFT, FES-assisted PFT and the efficacy of FES-assisted PFT compared to unassisted PFT. It is hypothesised that a positive effect will be seen in each of the above situations over the course of the training period.

Material and Methods

Subjects

As part of an ongoing programme of FES augmented ventilation, results from six patients are reported. Table 1 gives a summary of the patient details. All subjects were ventilator independent but with reduced vital capacity and good response to surface abdominal FES.

Table 1 Subject details

Subject	Sex	Age [yr]	Height [cm]	Post-injury [months]	Level	AIS
S1	M	25	168	96	C4	A
S2	M	53	187	8	C6	C
S3	M	52	178	4	C3	C
S4	M	18	173	27	C6	A
S5	M	20	183	4	C6	A
S6	M	18	183	2	C5	C

Study protocol

The protocol used in this study is summarised in Table 2.

Table 2 Outline of study protocol

Week	1	2	3	4	5	6	7	8
Training [min/day]		20	40	60				
Assessment	1	2			3			4

Each subject underwent three weeks of abdominal FES muscle training which incremented from 20 minutes per day in the first week to 60 minutes per day in the third week. Training was carried out up to 5 times per week. In addition to the training sessions we required that each subject participated in four assessment sessions. Each assessment session was conducted at the beginning of the week marked in Table 2. Assessments A1 and A2 are baseline measurements that were used as a control period before the intervention began. A3 assessed the impact of training and A4 was used to determine any de-training effect that may have occurred.

Pulmonary Function Tests (PFT)

FVC, FEV_1 and PEF were determined from forced vital capacity tests using a spirometer (Microloop), while MEP was measured with a mouth pressure meter (MPM, both Micromedical, UK). Each test (FVC and MEP) was first carried out unassisted followed by a FES-assisted test. A successful test was considered when three attempts were obtained that were within 20% of each other, up to a maximum of 5 attempts.

Functional Electrical Stimulation (FES)

FES was applied to the rectus abdominus and external oblique muscles bilaterally using transcutaneous electrodes. Biphasic stimulation was delivered at 30Hz, with a constant current (25 to 110 mA) and variable pulsewidth (30 – 500 μs) with a programmable stimulator (RehaStim, Hasomed GmbH, Germany).

At each assessment session the stimulation current was set individually for each muscle group until a strong even contraction was observed across the abdomen at a pulsewidth of 50μs. The pulsewidth was increased during the MEP test until a plateau was reached. These stimulator settings were then used for the stimulated FVC test. For both tests, stimulation was manually triggered by the researcher to correspond to the subject exhaling. Stimulation was delivered until the end of the maneuver.

During the training sessions the stimulation period was set to match the patient's breathing rate with a duty cycle of 50%. The stimulation was manually synchronized so that stimulation onset matched the start of expiration. The stimulation current and starting pulsewidth were set to those values which had produced the highest MEP during the most recent assessment session. To compensate for muscle fatigue the pulsewidth was increased throughout the training session to maintain a consistent level of abdominal movement as judged by visual inspection.

Analysis

Due to the difference in absolute respiratory function between subjects, the results were normalised for each subject to their baseline performance (A1), allowing comparison of results between subjects. To test for statistical significance a Friedman test was performed. If significance was found then a post-hoc multiple comparison test with Tukey's honestly significant difference criterion was used to determine in which interval the significance lay. In both tests the significance level was set at $p<0.05$.

Results

In most cases subjects tolerated the stimulation well and a strong contraction of the abdominal muscles was achieved. With S2, one side of the abdomen did not respond well to the stimulation resulting in an uneven contraction. S3 experienced discomfort in response to the stimulation which limited the maximal stimulation intensity which could be used.

Unassisted and FES-assisted FVC, FEV_1, PEF and MEP at each of the assessment sessions are shown in Figure 1 and 2, respectively. Statistical significance was found for the changes in FVC between assessments for the unassisted and FES-assisted PFT. In both cases, the multiple comparison test revealed significant changes between A2 and A3 and no significant changes between A1 and A2 or between A3 and A4.

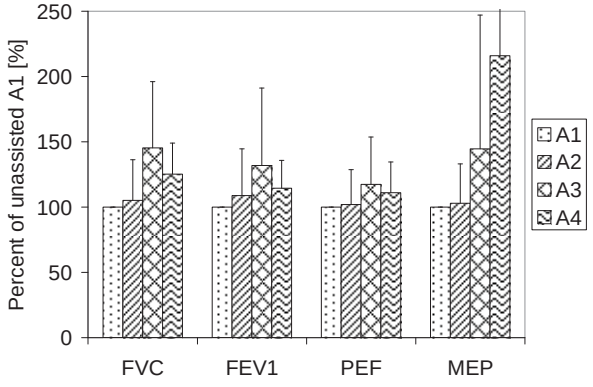


Figure 1 Unassisted group PFT results (mean ± standard deviation) at each assessment session. Results are normalised and expressed as a percentage of unassisted PFT at A1.

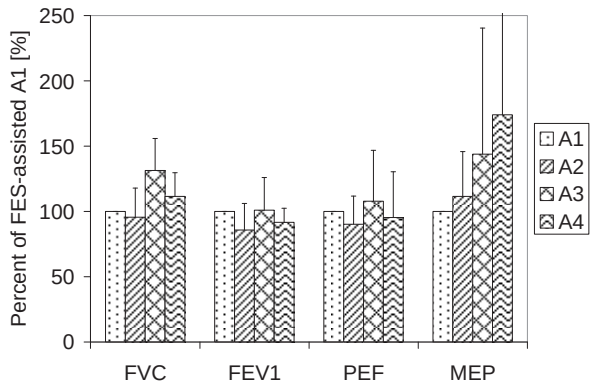


Figure 2 FES-assisted group PFT results (mean ± standard deviation) at each assessment session. Results are normalised and expressed as a percentage of FES-assisted PFT at A1.

Discussion

Unassisted FVC, FEV_1 and PEF all improved over the training period (between A2 and A3). There was a slight increase in the baseline period (between A1 and A2) which suggests some natural recovery in these patients. The increase over the training period (between A2 and A3) was followed by a drop in the de-training period (between A3 and A4). This shows that the increases seen between A2 and A3 can, at least partly, be attributed to the influence of the training intervention.

A similar pattern can be observed for FES-assisted PFTs from A2 to A4. However this was preceded by a drop in PFT during the baseline period (A1 to A2), making the results less clear. Detailed analysis of individual results showed large variations in the effect of FES on PFTs throughout the intervention and between subjects. This shows an inconsistent influence of abdominal FES on the PFT.

While the changes in FVC were significant, the trends observed in FEV_1 and PEF did not reach significance level. This study included a small number of subjects, with variations in level and severity of injury, time post injury and age, resulting in a complex case mix which limits the statistical analysis of the data.

MEP (both unassisted and FES-assisted) increased from A1 to A4. On closer examination of the results it was found that this increase was due to an individual subject, S3. Removing this subject from the pool showed no general trend or statistically significant change in MEP in response to the training protocol. Since this subject had the highest injury he had initially the greatest difficulty performing this test, but appeared to improve his ability to use his neck muscles to support respiration throughout the study. Removing S3 from the subject pool for the FVC test had no marked effect on the results discussed above.

Conclusions

A progressive FES training intervention leads to increases in unassisted FVC, FEV1 and PEF. Respiratory function decreases when the training intervention is discontinued, indicating that continued application is necessary to sustain long term improvements in breathing function. The outcome of FES-assisted PFTs showed large variability, suggesting an inconsistent influence of abdominal FES on FVC and MEP tests which require substantial volitional effort and coordination from the subject.

References

[1] Diana D Cardenas, Jeanne M Hoffman, Steven Kirshblum, and William McKinley. Etiology and incidence of rehospitalization after traumatic spinal cord injury: a multicenter analysis. *Arch Phys Med Rehabil*, 85(11):1757–1763, Nov 2004.

[2] Pao-Tsai Cheng, Chia-Ling Chen, Chin-Man Wang, and Chia-Ying Chung. Effect of neuromuscular electrical stimulation on cough capacity and pulmonary function in patients with acute cervical cord injury. *J. Rehab. Med.*, 38(1):32–36, 2006.

[3] W. E. Langbein, C. Maloney, F. Kandare, U. Stanic, B. Nemchausky, and R. J. Jaeger. Pulmonary function testing in spinal cord injury: effects of abdominal muscle stimulation. *J Rehabil Res Dev*, 38(5):591–597, Sep-Oct 2001.

[4] Bonsan B Lee, Claire Boswell-Ruys, Jane E Butler, and Simon C Gandevia. Surface functional electrical stimulation of the abdominal muscles to enhance cough and assist tracheostomy decannulation after high-level spinal cord injury. *J Spinal Cord Med*, 31(1):78–82, 2008.

[5] W. S. Linn, R. H. Adkins, H. Gong, and R. L. Waters. Pulmonary function in chronic spinal cord injury: a cross-sectional survey of 222 southern california adult outpatients. *Arch Phys Med Rehabil*, 81(6):757–763, Jun 2000.

Acknowledgements

Angus Mclachlan acknowledges the Carnegie Trust for the Universities of Scotland for funding his PhD research.

Author's Address

Angus J Mclachlan
Centre for Rehabilitation Engineering, University of Glasgow, Glasgow, Scotland, UK
amclachl@eng.gla.ac.uk
www.gla.ac.uk\cre

www.scisci.org.uk

Optimisation of electrode placement for abdominal muscle stimulation

Gollee H[1], Henderson G[1]

[1] Centre for Rehabilitation Engineering, University of Glasgow, Glasgow, UK

Abstract

High level tetraplegic individuals have partial or complete paralysis of their breathing muscles, leading to respiratory complications. Functional electrical stimulation of the abdominal wall muscles through surface electrodes can improve respiratory function. In this study the aim was to find the optimum number and position of the electrodes for abdominal stimulation, based on the response to a stimulation burst. Effectiveness of abdominal stimulation was judged by the resulting movement of the abdominal wall which was measured using a piezoelectric belt worn around the abdomen. Pairs of stimulation channels were applied bilaterally in three different positions: anterior, lateral and posterior. In addition to the response to stimulation of single channel pairs, combinations of anterior & lateral and lateral & posterior channels were evaluated, resulting in five different settings. Experiments were conducted with 10 able bodied individuals. Results show that (i) overall the combination of lateral & posterior channels resulted in the strongest response, (ii) in most subjects, the lateral channels resulted in a comparable response to the stimulation of two channel pairs, and (iii) in some subjects the strongest response was obtained from the anterior channel pair. This suggests that the optimal electrode placement may depend on individual factors such as body shape and composition.

Keywords: *tetraplegia, abdominal muscle stimulation, optimal electrode placement.*

Introduction

Because of partial or complete paralysis of their breathing muscles, people with tetraplegia are at increased risk of respiratory complications which are a leading cause of death in the spinal cord population [1]. Electrical stimulation of abdominal muscles during expiration can improve respiratory function in these patients [2,3]. As the abdominal muscles are stimulated they contract which increases the intra-abdominal pressure and reduces lung volume. This can lead to a larger expiration flow and improved cough, and subsequently increased inspiratory volume.

In previous studies [3], four stimulation channels were used: two channels in anterior locations close to the ubilicus stimulate the mm. rectus abdominis, while the other two channels which are positioned more laterally stimulate the lateral abdominal muscle group (mm. transversi and mm. obliqui ext. et int.) on both sides. A previous anatomical study [4] has indicated that a larger part of the abdominal muscles is stimulated by laterally located electrodes since these lie directly over the nerves that supply the abdominal muscles in the midaxillary line.

Lim et al. [5] have previously investigated the optimal electrode placement for abdominal stimulation, using single twitch responses. They confirmed that stimulation at the posterolateral location is more effective than stimulation at the anterior site.

The aim of this study is to determine the optimal location of electrodes for abdominal muscle stimulation using stimulation bursts, rather than single twitch responses. The stimulation response is determined by evaluating the change in abdominal girth during application of the burst.

Abdominal muscle movement will be quantified by measuring changes in abdominal girth, using a piezoelectric belt. It has been shown that this approach can be used to measure respiratory function [6], and this technique has been previously used with electrical muscle stimulation [7]. By using a direct measurement of the abdominal muscle movement, it is possible to quantify the effect of the stimulation and to exclude the influence of any involuntary response on the subject's breathing function. For a given stimulation intensity, a more optimal placement of the electrodes will be characterised by a stronger movement of the abdominal wall.

Material and Methods

Subjects

A total of 10 healthy subjects were recruited to take part in the study (7 male, 3 female, 22-39 years old). All experimental procedures where approved by the local ethics committee at the

University of Glasgow, and subjects gave written informed consent.

Functional Electrical Stimulation

A total of eight surface electrodes (Axelgaard PALS Platinum, 3.3cm x 5.3cm) were positioned bilaterally on the abdomen in one of two setups: In setup I (based on [4]), two stimulation channels were place at the anterior position, close to the ubiliucs while a second pair of stimulation channels was positioned over the lateral abdominal muscle group. In setup II (similar to that in [5]), one pair of channels was in the same lateral location as for setup I, while the second channel pair was placed more posterior. For each channel, electrodes were positioned along the superior-inferior axis. We investigated a total of five channel combinations: single channels on both sides, corresponding to the setups described above (*anterior, lateral, posterior* positions), and combinations of two channels on both sides (*anterior*+*lateral*, *lateral*+*posterior*).

Stimulation was applied using a programmable stimulator (RehaStim, Hasomed GmbH, Germany) connected to a laptop PC. For each pair of channels, stimulation intensity was progressively increased until a level was reached which was high enough to make the abdominal muscles contract while still being comfortably tolerated by the subjects. A constant stimulation frequency of 30Hz was chosen, and stimulation currents ranged from 25 to 40mA, with pulsewidths between 150 and 250μs.

To measure changes in abdominal girth, subjects wore a piezoelectric belt (ProTech, USA) positioned around the abdomen which was connected to the PC through a custom-made amplifier [7] and a DAQ-card (6024E, National Instruments, USA). The response of the piezoelectric belt in response to stretching had been calibrated in separate experiments to ensure a linear output in the range of interest for these experiments. The stimulation was synchronised with the subject's breathing based on the flow measured by a portable spirometer (Microloop, Micromedical, UK) via a low dead-space facemask [3]. Data recording and stimulation control were implemented in Matlab/Simulink.

During the experiment, subjects were asked to breathe normally. Stimulation was applied in random order in one of the five channel combinations described above, for one minute, followed by one minute without stimulation. The duration of the stimulation bursts which were automatically synchronised with the subject exhaling, was 1 second.

Data analysis

The signal obtained from the piezoelectrical belt was integrated to obtain a measure of displacement, and the change in abdominal girth, λ, was determined for each breath. For each subject, the mean change of abdominal girth during quiet breathing periods without stimulation, $\bar{\lambda}_{nostim}$, was calculated. The changes in girth during breathing with stimulation were normalised by this value, $\lambda_{norm} = \lambda / \bar{\lambda}_{nostim}$.

Results

Figure 1 shows a comparison of the normalised changes in abdominal girth, averaged over all subjects. The largest response for stimulation of a single channel pair was obtained for the *lateral* position. The combination of *anterior* and *lateral* channels resulted in a comparable abdominal movement, while the strongest response was obtained for the combination of *lateral* and *posterior* channels.

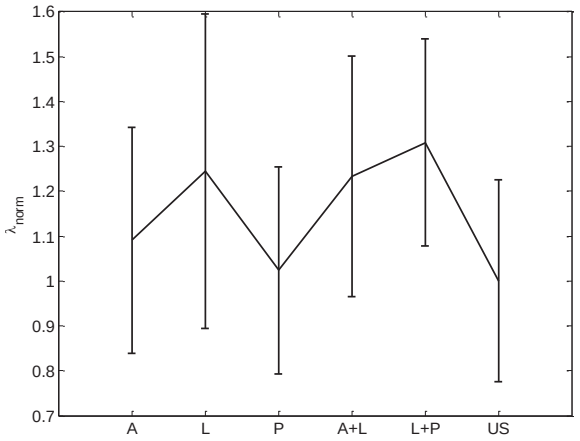


Fig. 1: Normalised change of abdominal girth (mean +/- standard deviations over all subjects) for different channel combinations (A−*anterior,* L−*lateral,* P−*posterior,* A+L−*anterior*+*lateral,* L+P−*lateral*+*posterior*) and un-stimulated breathing (*US*).

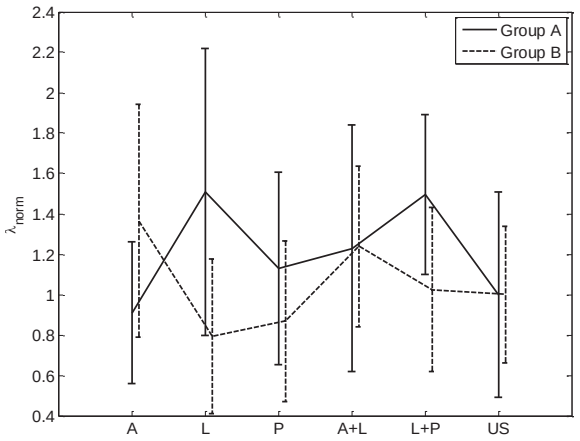


Fig. 2: Normalised change of abdominal girth (mean +/- standard deviations) for different channel combinations for two subgroups of subjects.

When analysing results for individual subjects, the overall trend seen in figure 1 could only be observed in 6 subjects (Group A). In the remaining 4 subjects (Group B), stimulation of the *anterior* channels resulted in larger movements than stimulation of the *lateral* channels (see figure 2). Combination of *anterior* and *lateral* channels resulted in the largest movement for combined channel stimulation in Group B, although this was smaller than the response to stimulation of the *anterior* channels on their own.

Discussion

This study shows that stimulation of the lateral positions created more abdominal wall movement for more subjects than any of the other tested single channel positions. Overall the largest abdominal wall movement was obtained when the *lateral* and *posterior* channels were combined. Stimulation of the *anterior* and *posterior* channels on their own had the smallest effect. This is consistent with the results reported in [5] for single twitch responses were large electrodes at the posterolateral positions (equivalent to the combination of *lateral* and *posterior* channels here) resulted in the strongest response. Our previous study [4] had shown that the nerves that supply a large mass of abdominal muscles are stimulated by electrodes placed in the lateral positions, which provides a possible underlying reason for these being the most effective.

Analysis of individual responses revealed that the overall response described above could be observed in 60% of the subjects, while for the remaining 40% the strongest response was seen for the anterior stimulation channels. For the group in which the strongest response was observed at the lateral position, additional stimulation of the posterior channels did not increase the overall response.

A possible explanation for the different stimulation responses in the two groups might be inter-subject variations in the amount and distribution of body fat at the stimulation site. This could explain that stimulation of the lateral muscles was less effective in some individuals.

Conclusions

The main aim of this study was to find the optimum number and positions of electrodes for abdominal stimulation. Despite the large variation in the results, more subjects had a larger abdominal wall movement during stimulation of the lateral positions than the anterior and posterior positions. For some subjects the stimulation of anterior positions was more effective.

While the combination of lateral and posterior channels was overall the most effective, in most individuals the stimulation of a single channel resulted in comparable abdominal wall movement.

This suggests that a test should be carried out with each subject when undergoing abdominal stimulation to determine the optimum stimulation position for this individual. This would allow to potentially use only one pair of stimulation channels instead of two in those subject were appropriate. Being able to use fewer stimulation channels reduces the effort required for donning and doffing the electrodes, facilitating the practical use of abdominal muscle stimulation as a standard technique in clinical and rehabilitation practice.

References

[1] C. P. Cardozo, “Respiratory Complications of Spinal Cord Injury”, J Spinal Cord Med, vol 30(4), pp. 307–308, 2007

[2] S. H. Linder, “Functional electrical stimulation to enhance cough in quadriplegia,” Chest, vol. 103, pp. 166–169, Jan 1993.

[3] H. Gollee, K. J. Hunt, D. B. Allan, M. H. Fraser, and A. N. McLean, “A control system for automatic electrical stimulation of abdominal muscles to assist respiratory function in tetraplegia,” Med Eng Phys, vol. 29(7), pp. 799–807, 2007.

[4] S. Bell, J. Shaw-Dunn, H. Gollee, D. B. Allan, M. H. Fraser, and A. N. McLean, “Improving respiration in patients with tetraplegia by functional electrical stimulation: An anatomical perspective,” Clin Anat, vol. 20, pp. 689–693, Aug 2007.

[5] J. Lim, R.B. Gorman, J.P. Saboisky, S.C. Gandevia and J.E. Butler, “Optimal electrode placement for non-invasive electrical stimulation of human abdominal muscles” J Appl Physiol vol 102, pp.1612-1617, 2007.

[6] B.E. Pennock, “Rib cage and abdominal piezoelectric film belts to measure ventilator airflow, J Clin Monitor Comp, vol 6, pp. 276–283, 1990

[7] H. Gollee and S. Mann “Measurement of respiratory activity during abdominal muscle stimulation”, In Proc 8th Automed Workshop, pp. 49–50, Berlin, Germany, March 2009

Author’s Address

Henrik Gollee
University of Glasgow
h.gollee@eng.gla.ac.uk
http://www.gla.ac.uk/cre

Session 3

Future Applications 2

Semi-closed loop tremor attenuation with FES

Popović L. Z.[1,4], Malešević N. M.[1,4], Petrović I. N.[2], Popović M. B.[3,4]

[1] Fatronik, Belgrade, Serbia

[2] Institute for Neurology, KCS, Belgrade, Serbia

[3] SMI, Department of Health Science and Technology, Aalborg University, Denmark

[4] Faculty of Electrical Engineering, Belgrade, Serbia

Abstract

We present a closed-loop system for tremor suppression based on the inertial sensors and FES. The proposed algorithm is able to extract information about tremor from the inertial sensors and send stimulation pulses to a pair of antagonist muscles in real-time, out-of-phase with tremor. This strategy suppressed more than 80% of tremor RMS value in one representative Parkinson's disease patient.

Keywords: Tremor, FES, suppression, Parkinson's disease.

Introduction

Tremor is a rhythmic, involuntary muscular contraction which is usually most severe in upper limbs [1]. Tremor can be highly indisposing in everyday living simple activities such as holding a cup, writing, unlocking the door, etc. When it becomes highly noticeable, a person is additionally exposed to a social embarrassment. Tremor is usually controlled by medication, but in many cases the therapy is not effective enough and the appearance of numerous side effects can be a limiting factor. In very severe cases, when no medications help, the surgical procedure of Deep Brain Stimulation is proposed [2].

The alternative approach in tremor suppression based on surface Functional Electrical Stimulation (sFES) was first introduced by the group from the University of Alberta, Edmonton, Canada led by Prof. Prochazka [3, 4]. Although the findings were encouraging, no further results were published. Most recently, two research groups, European partners on TREMOR FP7 project [5] and Nanyang Technological University Biorobotics group [6], continued the research with FES driven tremor attenuation of upper limbs. The system should rely on closed-loop control, based on signals recorded from inertial sensors and/or Electromyography (EMG) recordings. The imperative is that the voluntary motion is not disturbed. FES should only influence tremor.

This paper presents progress in tremor suppression FES system development. We explain basic structure of the algorithms used to extract tremor from inertial sensor data and to control stimulation pulses in real-time, out of phase with tremor. Furthermore, we present the results obtained from one representative Parkinson's disease patient.

Material and Method

Subject

The subject was a 68 year old woman with Parkinson's disease for 15 years, tremor scale 3. She signed informed consent approved by the local ethics committee and voluntary participated in the study.

Apparatus and setup

All the programs presented in this paper were designed in Matlab Simulink environment (MathWorks R2007b, Natick, MA) and run with the Windows XP operating system. Data was acquired with PCMCI-6062E NI DAQ Card (National Instruments) with 1 kHz sampling rate. Motion in the wrist was sensed with two IDG-300 gyroscopes placed on the dorsal side of the hand and on the distal forearm (Fig.1). Wrist angular motion was obtained by subtracting the two signals from gyroscopes. For the stimulation of extensors and flexors we used two UNA-FET stimulators [7] and four self adhesive Pals platinum electrodes. Stimulators can be externally triggered with standard TTL pulses. When the trigger is on the high level, stimulation is on, while the trigger low level turns the stimulation off. Stimulation frequency and pulse width were set to 40Hz and 250 μs, respectively. Current intensities were set to minimal values which elicited wrist flexion

(20mA) and extension (22mA) of the patient. Patient was seated comfortably in a chair, with the forearm supported on the armrest.

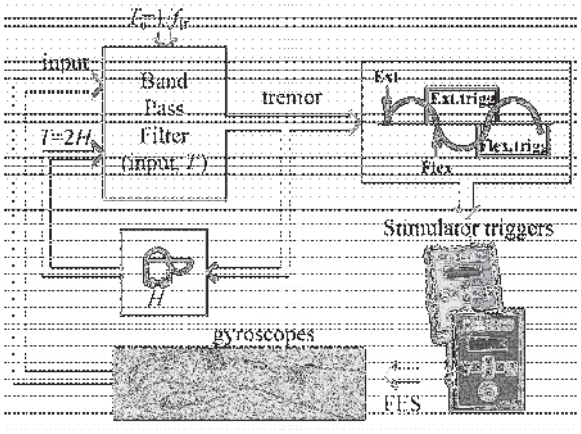


Fig.1. Diagram of closed-loop FES system for tremor suppression.

Program description

First step in designing a closed-loop system for tremor suppression was the development of the program for real-time tremor extraction from the inertial sensor data. Inertial sensors record both, tremor and voluntary movement component. If we want to suppress tremor without disturbing the voluntary movement, we need to separate these two components. Tremor is considered to be a quasi-stationary oscillatory signal with frequency changing slowly over time. Therefore, we decided to use Butterworth 2nd order band-pass filter, augmented with the ability to constantly adapt its center frequency (f_a) according to the dominant frequency of the filter output, Fig.1. The filter transfer function is:

$$H(s) = \frac{\beta\omega_a s}{s^2 + \beta\omega_a s + \omega_a^2}$$

where β=sqrt(2), and ω_a=2πf_a. Since filter has a zero phase at the center frequency, the signal content at f_a passes through with a zero delay and no attenuation. In order for filter to work properly, f_a has to be initially set to a value close to the tremor frequency, f_{tr}. From that point on, filter center frequency is calculated as 1/2H, where H (half-period) is the time between the two consecutive zero crossings of the filter output. Gradually, filter will self-adapt its center frequency until it reaches the tremor instantaneous frequency. Moreover, it will also track the slow changes in tremor frequency over time. The filter performance is explained in details elsewhere [8].

Second part of the program is designed to send trigger pulses to the stimulators in order to elicit muscle contractions out-of-phase with tremor. Real-time tremor estimation from the first part of the program is used to determine the previous tremor cycle onset moment. Based on the quasi-stationary oscillating nature of the tremor, we adopted the assumption that two subsequent cycles (e.g. two extensions of the wrist) have equal durations and that the information from the previous cycle can be used to generate stimulation pulses for the next cycle, Fig.1. Each time a zero crossing is detected, trigger is sent to the corresponding stimulator after a time delay of 7H/8-D, and it lasted for 10H/8, where the tremor half-period, H, and time delay between the stimulation and the movement onset, D are already identified. Short-time co-contractions lasting H/8 between two phases of stimulation (e.g. switching from extension to flexion) were introduced in order to avoid strong and unpleasant twitch generation.

Experiment

The experiment comprised three phases. In the first phase, the patient was asked to keep the arms outstretched in front of the body during 30s. No stimulation was applied. This recording was used to determine the tremor dominant frequency, f_{tr}, in order to preset the filter center frequency, f_a. In the second phase, stimulation was applied to the wrist flexor and extensor muscles to produce 2 Hz oscillations in the wrist. Tremor is commonly of higher frequency than 2 Hz, therefore, oscillations induced by the stimulation are easily separable from those originating from tremor. This recording was used to determine a time delay between the stimulation and movement onset, D. Finally, the stimulation was applied to suppress wrist oscillations by sending bursts of current pulses out-of-phase with tremor, Fig.1.

Results and discussion

Parameter values obtained from the first two experiment phases are provided in Table.1.

Age	Disease	f_{tr}	D
68	PD	5Hz	40ms

Table 1. PD patient parameters (f_{tr}- tremor dominant frequency, D- time delay between the stimulation and the movement onset).

In the first approach, we presumed that the contractions produced by stimulation would only

attenuate tremor intensity, and that the frequency and phase of the movement would be preserved.

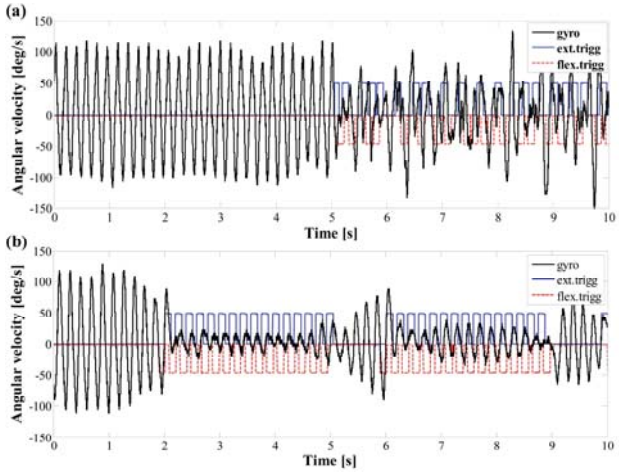


Fig. 2. Results for the (a) closed-loop and (b) semi closed-loop FES tremor suppression. Trigger profiles are symbolically presented pointing up and down to suggest the action on the opposing muscles. When the line is close to zero, the trigger is inactive, otherwise it is active and the stimulation is delivered to the respective muscle nerve.

Results showed that in the periods when no stimulation was applied (0-5s in Fig.2a) the frequency of the wrist movement was approximately constant. When the stimulation started (5s) the frequency and phase of the movement in the wrist were altered by FES (5-10s, Fig.2a). This modified regime of tremor oscillation was no longer providing valid information about movement induced by tremor. Without the proper information about tremor onset in each cycle the closed-loop system became unstable. Pulses were sent in irregular intervals, with wrong timings and as a result not out-of-phase with tremor all the time. Not only that FES didn't suppress tremor, but it produced strong and unpleasant, low frequency twitches in the wrist. Instead, we tested a somewhat different approach, i.e semi-closed loop tremor supression. We used the fact that tremor frequency varies very slowly with time, and presumed that constant stimulation frequency could be adequate for as long as several seconds. Hence, we modified the algorithm to update the frequency and phase for one second (closed-loop period) and to send triggers with constant frequency for the next three seconds (open-loop period), repeatedly (Fig.2b). In this case, the results showed noticeable decrease in the tremor amplitude during FES (2-5s and 6-9s). The RMS value of wrist angular velocity was decreased from 67.99 in the first 2s without stimulation to 12.26 in the next 3s (first period of stimulation, 2-5s), which is less than 20% of the initial tremor value.

Conclusions

The proposed algorithm was used with the data from the inertial sensors to send stimulation pulses to a pair of antagonist muscles in real-time, out-of-phase with tremor. This strategy suppressed more than 80% of tremor RMS value in one PD patient with tremor frequency of 5 Hz. However, the algorithm requires short adaptation periods without stimulation in order to adapt the parameters (tremor frequency and phase) used in the open-loop control periods. This requirement could be omitted by employment of an additional information source - EMG recordings. EMG can provide valuable information about tremor onset; therefore it could be used to trigger the stimulation in each cycle. In further experiments, we will evaluate more patients with different types of tremor.

References

[1] Anouti A and Koller WC, Tremor disorders - Diagnosis and management, Western Journal of Medicine 162(6): 510-513, 1995.
[2] Benazzouz A and Hallett M, Mechanism of action of deep brain stimulation, Neurology 55(12), 2000.
[3] Prochazka A, Elek J, and Javidan M, Attenuation of pathological tremors by functional electrical stimulation I: Method, Annals of Biomedical Engineering 20(2): 205-224, 1992.
[4] Javidan M, Elek J, and Prochazka A, Attenuation of pathological tremors by functional electrical stimulation II: Clinical evaluation, Annals of Biomedical Engineering 20(2): 225-236, 1992.
[5] http://www.iai.csic.es/tremor/index.htm
[6] http://www3.ntu.edu.sg/mae/centres/rrc/biorobotics/projects/patho.htm
[7] UNA-FET. http://www.unasistemi.com/
[8] Popovic LZ, Sekara TB and Popovic MB, Adaptive band-pass filter (ABPF) for tremor extraction from inertial sensor data, Comput. Methods Programs Biomed., in press, 2010.

Acknowledgment

Research supported by the EU FP7 project TREMOR (#224051). UNA sistemi provided stimulators.

Author's Address

Author: Lana Popović
Institute: Fatronik Serbia
Email: lana.popovic@etf.rs

Microscopic Magnetic Stimulation

Bonmassar G[1], Freeman DK[2,3], Fried SI[2,3] and Gale JT[4]

[1] A.A. Martinos Center, Harvard Medical School, Charlestown, USA

[2] Center for Innovative Visual Rehabilitation, Boston Veterans Administration Healthcare System, Boston, USA

[3] Department of Neurosurgery, Massachusetts General Hospital and Harvard Medical School, Boston, USA

[4]Nayef Al-Rodhan Laboratories for Cellular Neurosurgery and Neurosurgical Technology, Massachusetts General Hospital, Boston, USA

Abstract

We present a novel, electrode-less technology for stimulation of neural tissue using magnetic fields generated by microscopic coils. Such micromagnetic stimulation (μMS) is based on Micro-Electro-Mechanical Systems (MEMS) and overcomes many challenges faced by traditional metal electrodes used in neural prostheses. Stimulation coils are encapsulated with biocompatible materials, thus preventing inflammatory responses due to the presence of foreign materials. Because the coils are electrically insulated from the tissue, they are MRI compatible – unlike traditional electrodes that can cause tissue damage through induced currents from RF fields within the MRI. The size of the encapsulated coils is small relative to traditional electrodes, measuring a few hundred microns. This may improve control over the spatial region of neural activation. In order to test whether μMS could elicit responses from neurons, we used cell-attached patch clamping to record action potentials from retinal ganglion cells. The coils were positioned approximately 100-200μm above the ganglion cell soma under visual control. Ganglion cells were found to elicit robust spiking in response to micromagnetic stimulation, demonstrating proof-of-principle for the use of μMS in neural prostheses.

Keywords: *magnetic stimulation, neural prostheses, retinal ganglion cells*

Introduction

The use of electrical stimulation as a means of treating neurological diseases has expanded dramatically in recent years. Deep brain stimulation (DBS) is being evaluated for treatment of chronic pain, depression, Tourette's Syndrome, and is a commonly accepted method for the treatment of Parkinson's Disease [1]. Retinal prostheses have demonstrated the ability to elicit spatially patterned vision in subjects who have been blind for many years [2]. Cochlear implants have achieved remarkable success in restoring hearing to hundreds of thousands of otherwise deaf individuals [3]. Despite these successes, methods using electric stimulation have several limitations. Metal electrodes cause inflammatory reactions that result in scar tissue covering the electrode. Such devices are not MRI-compatible because induced currents can be generated in the stimulation electrodes as a result of the applied RF signals, causing dangerous heating of the tissue. Also, the ability to control the spatial and temporal pattern of elicited neural activity remains limited with electric stimulation. For example, in DBS treatment of Parkinson's Disease, the incidental activation of passing axons from the limbic system cause side effects, including cognitive and mood changes [1].

The use of magnetic stimulation is being investigated as an alternative to electric stimulation in neural prostheses. Applying time-varying electrical currents to metal coils generates a magnetic field. In turn, this magnetic field will induce electrical currents in nearby conductive materials. Such induced currents can be applied to neural tissue to elicit activity with the goal of achieving some medical benefit. For example, Transmagnetic Stimulation (TMS) uses large coils placed on the skull to modulate neural activity using strong magnetic fields (e.g., > 1 Tesla). Unfortunately, TMS coils and associated power supplies are very bulky – this is necessary in order to generate the large current levels involved. In addition, TMS does not allow for spatially precise patterns of neural activity to be generated, limiting its clinical benefit.

In order to overcome some of limitations experience by conventional stimulation methods, we propose the use of magnetic stimulation via *microscopic* coils that can be implanted in the brain in close proximity to the target neurons. This approach has several attractive features. The ability to bring the coils close to the target neurons will likely decrease the amount of energy required to elicit activity (e.g. magnetic field intensity falls off with the cube of distance). Also, because of the small size of the coils, the ability to control the spatial pattern of neural activity will be improved relative to TMS or DBS with large metal electrodes. Furthermore, by electrically insulating the coils, such a device will be both biocompatible and MRI–compatible.

Material and Methods

-*μMS coils:* Commercial multilayer thin film RF inductors were soldered using a 15 mils 44 resin core solder on the tip of 34 AWG copper

wire with polyimide enamel inner-coat and polyurethane over coat. The two wires were then inserted in a 1mm diameter Polyetheretherketone tubing 150 mm in length and electrically connected to a BNC connector. The 1mm tube was inserted and the BNC was glued to larger diameter tubing that allowed for securing the magnetic microstimulator to the micromanipulator.

The stimulation coils (red arrow in Fig. 1, Left) had a quartz, non-magnetic core. The core was made of a ceramic base, which is non magnetic and ideal for MRI use. The coil was soldered to a BNC connector through two fine 34 AWG copper wires, and coated with dielectric polymer (Gardner Bender, Milwaukee, WI) for insulation (red paint in Fig. 1, Left). Silicone (type II, GE) was used to seal the tubing on both sides. The single μMS coil prototype was tested at 7T to measure the spatial extent of the field generated by the micro-coil. We scanned the coil inside a cylindrical phantom containing water with gre sequences with resolution of $1mm^3$ isotropic (96 slices, dist. factor = 20%, TR = 10ms, TE = 3.9ms, Phase Encoding Direction (PED): R→L, 2 averages, Flip Angle=40°) and $500\mu m^3$ isotropic (PED: H→F). The MRI-images of a phantom containing the μMS coils (Fig. 1, Right) show the resulting magnetic field. This illustrates the principle that MRI may be used for imaging the magnetic field generated by the μMS coils in excitable tissue.

- *μMS Insulation*: The μMS coils were thoroughly tested to make sure that leaking currents were minimal during the magnetic stimulation experiments. If present, such currents could have produced the observed neural response. The coils were coated with a Xylene based dielectric varnish (Gardner Bender, Milwaukee, WI) and then were submersed in physiological saline together with an electrode. The impedance between the μMS coil (considering both terminals) and the electrode was measured immediately before and after each experiment to test for insulation (> 50MΩ).

- *μMS Drive:* A generator (AFG3021B, Tektronix Inc., Beaverton, OR) was connected to a 1,000 W audio amplifier. The output of the amplifier was connected to a BNC splitter so that the signal sent to the μMS coil was monitored with a scope (DPO3012, Tektronix Inc., Beaverton, OR). We delivered pulse trains of 20Hz for 0.5sec using pulse widths of 3ms. Stimulus amplitude was increased until a spiking response could be elicited. The maximum stimulus amplitude applied to the coils was 46V.

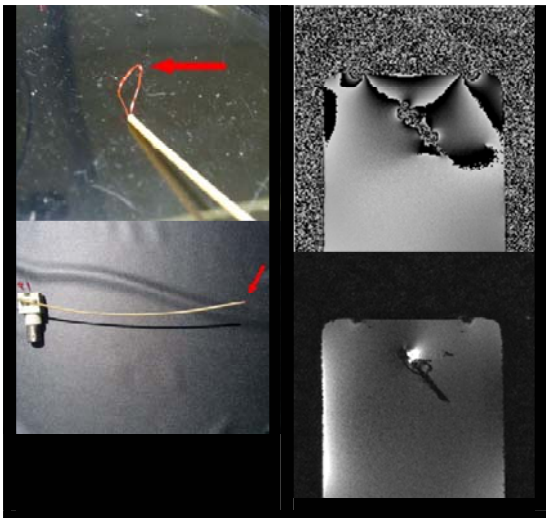


Figure. 1: Left: *A μMS prototype with a single coil Right: On the top are the phase and on the bottom are the magnitude GRE images of Stimulation ON minus Stimulation OFF*

- *Electrophysiology*: The care and use of animals followed all federal and institutional guidelines, and all protocols were approved by the Subcommittee of Research Animal Care of the Massachusetts General Hospital. New Zealand White Rabbits were anesthetized with xylazine/ketamine and their eyes removed. The retina was isolated and mounted photoreceptor side down on Millipore filter paper. Patch pipettes (4-8 MΩ) were used to make small holes in the inner limiting membrane, and ganglion cells with large somata were targeted under visual control. Spiking was recorded with a cell-attached patch electrode filled with superfusate. Two silver-chloride-coated silver wires served as the ground and were positioned at opposite edges of the recording chamber, each approximately 15 mm from the targeted cell. The retina was continuously perfused at 4 mL/min with Ames solution (pH 7.4) at 36°C, equilibrated with 95% O2 and 5% CO2. The light stimulus was projected onto the retina from below through an LCD projector (InFocus). Given that most cells we encountered had no spontaneous firing of action potentials, light stimulation was used to determine (1) that a spike recording had been established for a given cell and (2) the shape and size of the action potentials for comparison to magnetic stimulation. Data acquisition and stimulus triggering was controlled by custom software written in LabView (National Instruments) and Matlab (Mathworks).

Results

In our current preparation, ganglion cells generally did not fire spontaneous action potentials. Therefore all spikes were elicited by stimulation. First, light stimulation was used in order to determine if a successful recording was established, and to estimate the size and shape of action potentials so

that they can be easily recognized followed magnetic stimulation. Then, after positioning a microscopic coil directly above the ganglion cell soma by ~100-200μm, a pulse train was applied to the coils. Stimulus amplitude was gradually increased until the presence of spikes was detected. This generated a large stimulus artifact (Figure 2A, arrow) that would drown out any action potentials that occur during the stimulus. However, immediately following the stimulation pulse, it was clear that ganglion cell fired action potentials consistently in response to each pulse for the duration of the stimulus (Figure 2A, asterisks). Examining the response to a single pulse (Figure 2B), a burst of spikes can be seen with inter-spike intervals on the order of 10ms, corresponding to a firing rate of ~100Hz. This response level is near maximal for many types of retinal ganglion cells [4], suggesting μMS has potential applications in retinal prostheses.

Previous work has shown that in response to direct electric stimulation, ganglion cells fire a single spike per stimulation pulse [5]. However, activation of neurons presynaptic to the ganglion cell is known to generate a burst of spikes. This suggests that the burst of spikes seen here may result from the activation of excitatory bipolar cells known to provide synaptic input to the ganglion cells.

Conclusions

This paper demonstrates that magnetic fields generated with microscopic coils can elicit spiking from nearby neurons. The use of μMS in neural prostheses offers several advantages to conventional methods of stimulation such as TMS or electric stimulation with metal electrodes. Further study is needed to determine the physiological mechanisms responsible for generating spiking in response to magnetic stimulation.

Author's Address

Giorgio Bonmassar, PhD
Assistant Professor
Harvard Medical School
A. Martinos Center
Massachusetts General Hospital
Building 149, 13th Street
Charlestown, MA 02129
email: giorgio@nmr.mgh.harvard.edu

Acknowledgements

This work was supported in part by the National Institute of Neurological Disorders And Stroke (R01 NS037462), in part by the National Institute of Biomedical Imaging and Bioengineering (R01EB006385), in part by the National Center for Research Resources (NCRR) (P41-RR14075), and in part by the MIND institute.

1. Wichmann, T. and M.R. Delong, *Deep brain stimulation for neurologic and neuropsychiatric disorders.* Neuron, 2006. **52**(1): p. 197-204.
2. Caspi, A., Dorn, J.D., McClure, K.H., Humayun, M.S., Greenberg, R.J., McMahon, M.J., *Feasibility study of a retinal prosthesis: spatial vision with a 16-electrode implant.* Arch Ophthalmol, 2009. **127**(4): p. 398-401.
3. Wilson, B.S. and M.F. Dorman, *Cochlear implants: current designs and future possibilities.* J Rehabil Res Dev, 2008. **45**(5): p. 695-730.
4. O'Brien, B.J., et al., *Intrinsic physiological properties of cat retinal ganglion cells.* J Physiol, 2002. **538**(Pt 3): p. 787-802.
5. Fried, S.I., Hsueh, H. A., Werblin, F. S., *A method for generating precise temporal patterns of retinal spiking using prosthetic stimulation.* J Neurophysiol, 2006. **95**(2): p. 970-8.

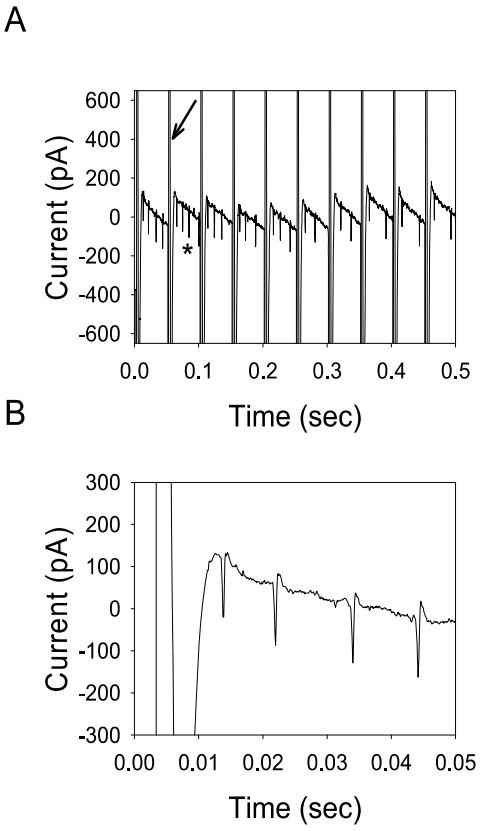


Figure. 2: *A. The spiking response (*) of retinal ganglion cells can be seen in response to a train of magnetic pulses presented at 20Hz. The stimulus artefact is denoted by an arrow. B. Zooming in on the response to the first pulse in (A), a clear burst of biphasic spikes can be seen. This confirms that such microscopic coils can generate sufficient power to elicit spiking from neurons.*

Displaying Centre of Pressure Location by Electrotactile Stimulation Using Phantom Sensation

Pfeifer, S[1], Çaldıran, O[1], Vallery, H[1], Riener, R[1], Hernandez Arieta, A[2]

[1] Sensory-Motor Systems Lab, ETH Zurich & Medical Faculty, University of Zurich, Switzerland

[2] Artificial Intelligence Laboratory, University of Zurich, Zurich, Switzerland

Abstract

Amputees not only lack motor function, but also sensory feedback of the missing limb. It has been shown that lower-limb amputees can improve certain gait characteristics when they perceive additional information about the kinematics and kinetics of their prosthetic leg. In this paper, we address the question whether it is feasible to provide centre of pressure location information via electrotactile displays by exploiting the phantom sensation phenomenon, where relative intensity of two electrode pairs is used to encode position between them, creating a single illusory stimulus. Four healthy subjects were asked to identify different locations or movement patterns of the illusory stimulus on a discrete scale under static and dynamic conditions. These stimuli resembled CoP patterns in different locomotor activities. An average recognition accuracy of 73% (std. dev. 17%) was achieved under static conditions, and of 71% (std. dev. 11%) under dynamic conditions. This indicates that the proposed display and mapping can be used to present centre of pressure location, and future work will focus on evaluation with patients.

Keywords: *sensory substitution, electrocutaneous stimulation, tactile phi phenomenon, prosthetics*

Introduction

Above-knee amputees using a conventional prosthesis receive only limited sensory feedback. To some extent, they perceive ground contact by forces transmitted to the stump, but they can hardly perceive the exact location of the centre of pressure (CoP). It is hypothesized that this limited perception contributes to the reduced abilities of above-knee amputees to walk downhill [1]. To restore these lost functions, sensory substitution has been suggested, where unimpaired sensory receptors are used to replace the function of the missing ones. As an example, vibration on the skin of the residual limb can encode grasping force in a prosthetic hand [2]. Tactile sensations can also be elicited by pulsed currents passing through the skin, more commonly known as electrotactile stimulation. One advantage of electrotactile displays over vibrotactile displays is their low power consumption [3]. It has been shown that feeding back heel and toe pressure by modulating stimulation intensity of two separate electrode-pairs on the back and on the front of the stump, proportionally to the respective pressure, improves gait symmetry in lower-limb amputees [4]. An interesting psychophysical phenomenon is the tactile phi phenomenon, or the phantom sensation. When two tactile stimuli are presented at adjacent locations with equal intensity, they are not perceived individually, but as a single stimulus between the two stimuli [5], [6]. When their relative intensity changes, the apparent location moves towards the stronger stimulus. This allows the use of only two stimulation sites to convey information on a continuously varying location.

In this study, we investigated how well different electrotactile phantom sensations can be discriminated, in order to find out whether the phantom sensation could be used to encode the location of the CoP. In the first condition, subjects had to discriminate five different static stimuli. In the second condition, subjects were asked to identify six dynamic patterns that are inspired by CoP patterns occurring during different locomotor activities. The findings shall later be used to design a lower-limb sensory substitution system.

Material and Methods

Electrotactile Phantom Sensation

The phantom sensation as described earlier can be evoked by two pairs of electrodes with a small distance between them (around 4 cm), which are stimulated with different relative intensities. If the intensities change linearly, the perceived stimulus intensity decreases when the perceived stimulus moves to the midpoint between the electrodes. To keep this perceived intensity constant, the two intensities can be modulated in a nonlinear, e.g. logarithmical, fashion [5].

Experimental Setup and Protocol

Four able-bodied male subjects (24, 26, 27 and 30 years old) participated in a feasibility study. We

used an electrotactile stimulator that was developed at the Artificial Intelligence Lab. It is voltage-based and was set to provide biphasic square pulses at 4 kHz on two channels, each channel corresponding to one pair of electrodes. The intensity of each channel was modulated by changing the duty rate of the biphasic pulse, while the amplitude was constant at 12 V for both channels. We used self-adhesive multilayer hydrogel electrodes (square, size 25 cm^2); one pair of electrodes was placed with the lower edge 2 cm above the Spina Iliaca Posterior Superior. The lower edge of the other pair was placed 4 cm above the upper edge of the lower pair (Fig. 1). The pulse frequency of 4 kHz and the electrode placement used in this study were based on previous studies [7]. Once the electrodes were in place, they were calibrated to a minimum intensity slightly below the sensory thresholds and a maximum intensity that was clearly perceivable but still comfortable. During the experiments, the stimulus intensities were always scaled between these thresholds.

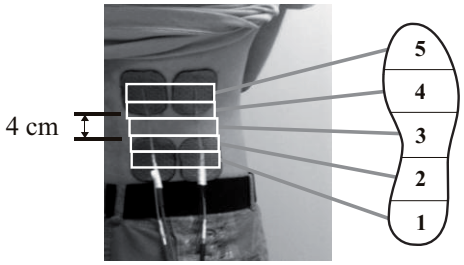


Fig. 1: Electrode placement and mapping to foot sole.

Static Localization Task

The region between the electrodes was divided into five discrete regions, which would correspond to five regions on the foot (Fig. 1), region 1 corresponded to the lower pair stimulated at maximum intensity, and region 5 corresponded to the upper electrode pair being stimulated at maximum intensity. Signal duration was 1 s. The training phase started with displaying all regions sequentially, twice. Thereafter, subjects had to identify the active region in five subsequent training trials. Subjects were told the correct answer after each trial. In the test phase, each region was displayed four times in random order (20 trials in total). After each trial, the subject had to indicate on a virtual foot sole placed in front of them, as displayed in Fig. 1, which region had been active. Once the answer was given, the next trial was performed. This training and test procedure was performed twice, once with the linear mapping and once with the logarithmic mapping; the order of the two conditions was randomized between subjects.

Dynamic Localization Task

In this task, simple moving patterns were displayed to the subject, moving from one region in Fig. 1 to another at a constant speed, by continuously modulating the relative intensity of the two electrode pairs; the patterns were chosen inspired from patterns that occur in different locomotor activities (Table 1). All patterns were presented in 2 versions, one of duration 0.5 s, and the other of duration 1 s. In the training phase, all patterns were displayed by the stimulator and the subject was told which pattern it was. At the beginning of the training session, all patterns of duration 0.5 s were displayed in the order presented in Table 1, first in descending order, and then in ascending order. After that, all patterns of duration 1 s were shown in the same order. In the test phase, each pattern was shown three times for both durations, in a random order, yielding 36 displayed patterns. The subject was asked to identify the start point and end point of each pattern. The training and test phase were performed twice, once with the linear mapping and once with the logarithmic mapping; the order of the two conditions was randomized between subjects.

Pattern	Corresponding activity
1→5	Level-ground walking
1→3	Downhill walking
3→5	Uphill walking
5→1	Walking backwards
5→3	Stair descent (toe first)
3→1	Stair descent (toe overlaps step edge)

Table 1: Different moving sensation patterns; e.g. 1→5 indicates a moving stimulus from region 1 to 5.

Results

Static Localization Task

The averaged recognition accuracy resulted in a 73% recognition rate for the linear mapping and 69% for the logarithmic one (Fig. 2).

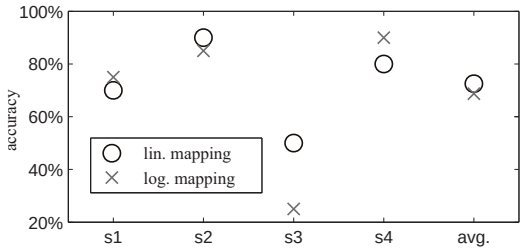


Fig. 2: Individual and avg. static recognition accuracy.

With the exception of two single answers, all of the misclassified regions were found neighbouring the stimulated region (Fig. 3).

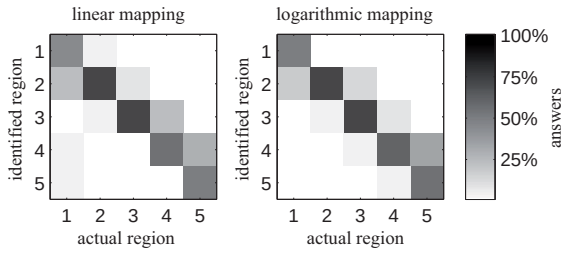


Fig. 3: Actual and identified static regions (avg.).

Dynamic Localization Task

All subjects achieved a higher accuracy for the slower patterns of 1s duration in both linear and logarithmic mappings (Fig. 4). For the linear mapping, the average accuracy observed was 83% for the patterns of 1 s, and 58% for the patterns of 0.5 s duration. For the logarithmic mapping, these accuracies were 71% and 64% respectively.

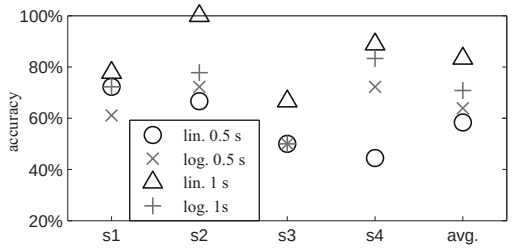


Fig. 4: Individual and avg. dynamic recognition accuracy for 0.5 s and 1 s duration patterns.

With the linear mapping, pattern 1→3 and 3→1 were often confounded; the same can be stated for pattern 3→5 and 5→3. With the logarithmic mapping, other misclassifications appeared more often (Fig. 5).

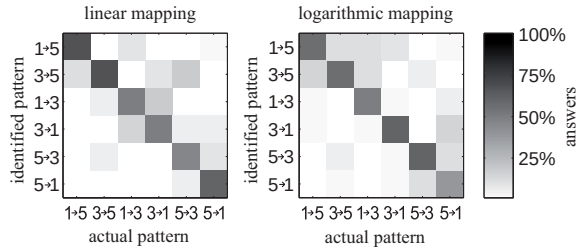


Fig. 5: Actual and identified dynamic patterns (avg.).

During the experiments, the subjects reported that the stimulus was perceived as a spread sensation rather than a single point, especially in the static condition.

Discussion

While a clearly localized phantom sensation could not be evoked in most situations, especially in the static condition, which corresponds to findings from other researchers [6], subjects could still distinguish the different stimuli with a good accuracy (Fig. 2, Fig. 4) on a two-channel electrotactile display. We observed no clear difference between linear and logarithmic mappings.

Conclusions

In this paper, we showed that a two-channel electrotactile stimulator can be used to display different location sensations in one dimension; they can be interpreted as CoP locations. Having a practical daily-life application for amputees in mind, the electrodes were attached on the lower back, close to the missing limb. While the tactile resolution on the lower back is not very high, and subjects only had very little time to familiarize with the system, they were able to distinguish five regions and dynamic patterns with a good accuracy. Future work will address whether this display is helpful for amputees during gait.

References

[1] Franchignoni F, Giordano A, Ferriero G, Orlandini D, Amoresano A, and Perucca L. Measuring mobility in people with lower limb amputation: Rasch analysis of the mobility section of the prosthesis evaluation questionnaire. Journal of Rehab. Med., 39:138–144(7), March 2007.

[2] Pylatiuk C, Kargov A, and Schulz S. Design and evaluation of a low-cost force feedback system for myoelectric prosthetic hands. JPO: Journal of Prosthetics and Orthotics, 18(2):57–61, 2006.

[3] Kaczmarek KA, Webster JG, Bach-y Rita P, and Tompkins WJ. Electrotactile and vibrotactile displays for sensory substitution systems. Biomedical Engineering, IEEE Transactions on, 38(1):1–16, Jan. 1991.

[4] Sabolich JA and Ortega GM. Sense of feel for lower-limb amputees: A phase-one study. Journal of Prosthetics and Orthotics, 6(2):36–41, 1994.

[5] Alles DS. Information transmission by phantom sensations. Man-Machine Systems, IEEE Transactions on, 11(1):85 –91, March 1970.

[6] Izumi T, Hoshimiya N, Fujii A, and Handa Y. A presentation method of a traveling image for the sensory feedback for control of the paralyzed upper extremity. Systems and Computers in Japan, 19(8):87–96, 1988.

[7] Seps M. Electrotactile sensory substitution. Master's thesis, University of Zurich, 2010.

Acknowledgements

This work was supported by the "Gottfried und Julia Bangerter-Rhyner Stiftung", the ETH Research Grant "ETHIIRA" and the SNF Grant k-23k1-116717/1. We also thank Selina Bühler, Thomas Böni, Rainer Burgkart, and Eric J. Perreault for their valuable advice.

Author's Address

Serge Pfeifer
Sensory-Motor Systems Lab, ETH Zurich
serge.pfeifer@mavt.ethz.ch

A SWITCHED CAPACITOR CROSSTALK REDUCTION METHOD FOR VESTIBULAR NERVE STIMULATORS

Perkins TA[1], Donaldson N[1], Demosthenous A[2], Jiang D[2]

[1] Implanted Devices Group, University College London, London, UK

[2]Electronic & Electrical Engineering Dept, University College London, London, UK

Abstract

A method has been found for reducing crosstalk between the channels of a 3-D vestibular nerve stimulator implant. By separating the power supplies for the individual stimulation channels, it was found possible to reduce stimulation crosstalk by a factor of nine. A 3-D vestibular nerve prosthesis may accordingly be provided without the need for temporal separation of stimuli to keep crosstalk below physiological threshold. A more normal perception of head rotation for the restoration of balance for patients with chronic bilateral vestibular deficit should therefore be possible.

Keywords: *Crosstalk reduction, FES multichannel implant, vestibular nerves, balance restoration.*

Introduction

Crosstalk reduction between sets of stimulating electrodes sharing the same conductive body fluid has long been a problem [1]. However multiple bulky transformers would not fit in a small implant set in the mastoid bone. The 'Continuous Interleaved Sampling' (CIS) strategy for reducing stimulus crosstalk in multichannel implants has been described [2, 3]. By fixing the stimulation frequency and allocating a separate time slot to each channel, only one channel is stimulated at once. This technique works well for the cochlear [4], perhaps because auditory frequency perception is encoded mainly by position along the cochlear.

Perception of head angular rotation is coded by frequency modulation in the ampullary branches of the vestibular nerves [5]. An implant which provides 3 independent frequencies of stimulation for these nerve branches in the 3 orthogonal Semi Circular Canals (SCC) could restore perception of head rotation in patients with chronic bilateral vestibular deficit. As there is no equivalent of the positional coding in the cochlear, CIS may be unable to restore 3-D vestibular sensation. The small space in the SCC virtually precludes low crosstalk cuff electrodes, open dipoles being the only alternative. With no guarantee of favourable orientation, open dipoles in the expected close proximity are a recipe for excessive crosstalk.

Santina et al [6] proposed a multichannel vestibular stimulator, again reducing crosstalk by temporal separation. This involved deferring the stimulation for one of two channels if they 'clashed' due to momentary phase synchronisation of the 'independent frequencies'. The resulting delay in stimulation could exceed the limit (of about 0.25%) in frequency change that would alter rotation perception significantly. A method which allows stimulation simultaneously, but still keeps crosstalk below physiological threshold, is therefore desirable.

Material and Methods

Charge balanced stimulator:

Fig. 1 shows the charge balanced stimulator used.

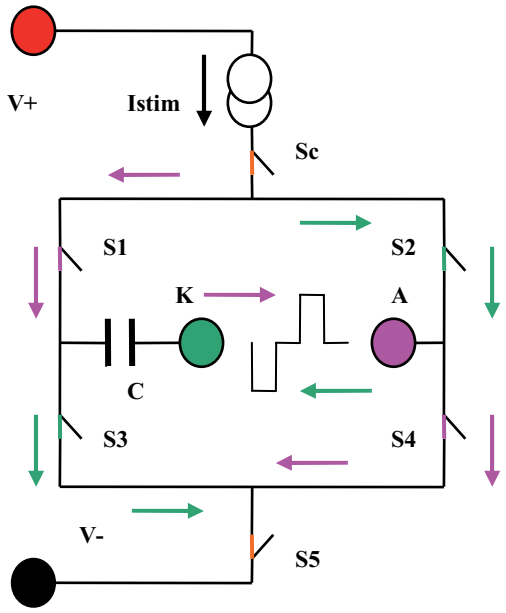


Fig. 1: Charge balanced bipolar stimulator. Switches S1 to S4, in 'H' configuration, steer stimulus current Istim for the cathodal and anodal electrode pulses.

The constant current generator providing Istim is activated following closure of the isolation

switches Sc and S5. Initially switches S2 and S3 are closed to steer stimulation current via anode A to give a negative going pulse on cathode K. S2 and S3 are then opened for an intra pulse interval (perhaps of 10% of the cathodal phase duration [6]). The subsequent S1 and S4 switch closure is timed to give an exactly balancing anodal pulse, reversing the direction of current in the electrodes. Sc and S5 can then be opened to isolate the electrodes during the inter pulse interval. For safety, the blocking capacitor C is included to ensure no dc is passed through the electrodes, even in fault conditions.

Power supply and electrode isolation:

Fig. 2 shows the circuitry needed to transfer power and the required stimulus parameters from the system's 'Master' supply and logic to one of the 'Slave' stimulators, using switched capacitors.

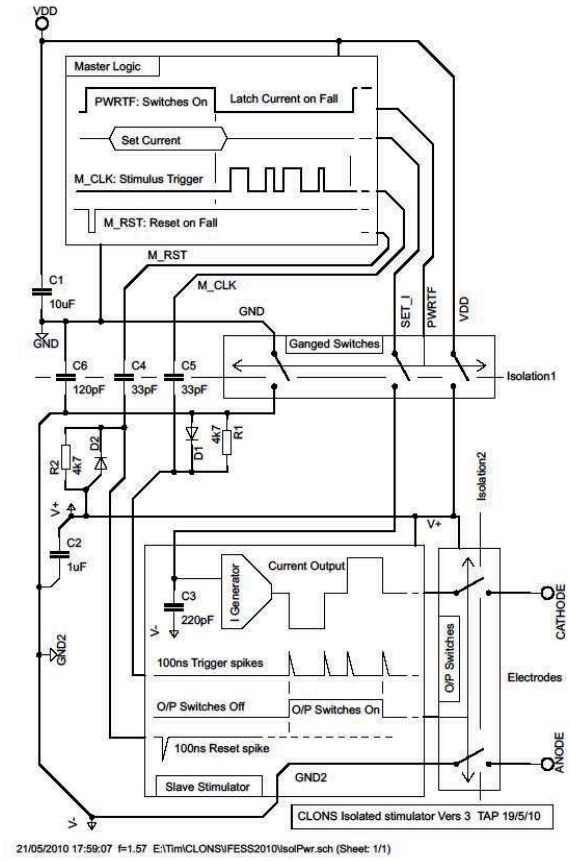


Fig. 2: Arrangement for transferring power and stimulation data from the 'Master' supply and logic to an isolated 'Slave' stimulator. Power transfer via the 'Ganged Switches' occurs when the stimulator is NOT stimulating, while PWRTF is high. When PWRTF is low and the 'Ganged Switches' are off, stimulation can proceed via the 'O/P Switches' which are only on DURING stimulation (as per Sc and S5 of Fig.1). So isolation between 'Master' circuitry and electrodes is maintained.

The power required by the slave stimulator is drawn from the master supply while power transfer line 'PWRTF' is high. A 1uF capacitor C2 maintains enough voltage for the stimulation while 'PWRTF' is low.

The timing for the stimulator is provided by a master clock signal 'M_CLK' which steps the slave stimulator through the stimulation sequence via capacitor C5. The active low master reset 'M_RST' (again via a capacitor, C4) ensures the slave stimulator stimulation keeps the correct count from power on onwards. C6 represents capacitance between the master and slave power supplies. The values for C4-6 should be small enough for the total switching charge during stimulation to be below 1nC, which we believe is below the threshold for physiological effect. The purpose of the sample and hold capacitor C3 is to store the stimulus current programming voltage 'SET_I' during stimulation. Similar circuitry is repeated for the other stimulation channels.

Note the circuit can ensure switches along line 'Isolation1' and those along 'Isolation2' are never on at the same time. The electrodes for one channel are then free to float in potential with respect to the master supply and hence to the electrodes for the other channels in the same physiological fluid. During stimulation the electrode pairs for each channel should float to the potential which minimises crosstalk, avoiding the cross currents inevitable if the power supplies for each channel are shared.

A prototype circuit following the Fig. 2 scheme was assembled using standard CMOS and discrete components, to demonstrate the concept prior to committing the design to an ASIC suitably small for implantation.

Results

The prototype was tested with two pairs of open dipole electrodes in a saline bath. These dipoles were held facing each other on a spacing of about 2mm, ie in the worst case crosstalk condition expected for a vestibular nerve implant. The resulting oscillographs are shown in Fig. 3. In this figure's upper panel, the 'STIMV' trace records the voltage across an open dipole electrode set for 1mA pulses. This trace was taken with a differential probe with 20 fold attenuation, so the pp voltage on the electrodes is 606mV rather than the 30.3 mV delta Y shown. During 'stimulation' the master and slave power supplies were disconnected. The erratic GND2 trace shows it was indeed floating in this period.

In the bottom panel the differential probe was connected to the second dipole in the saline bath. This second dipole was not connected to the other

two supplies. It had a 10kΩ resistor across it and the 1.375mV delta Y figure implies 27.5mV pp across this second dipole. This indicates 2.75uA pp of crosstalk in this second dipole for 1mA of stimulation in the first dipole.

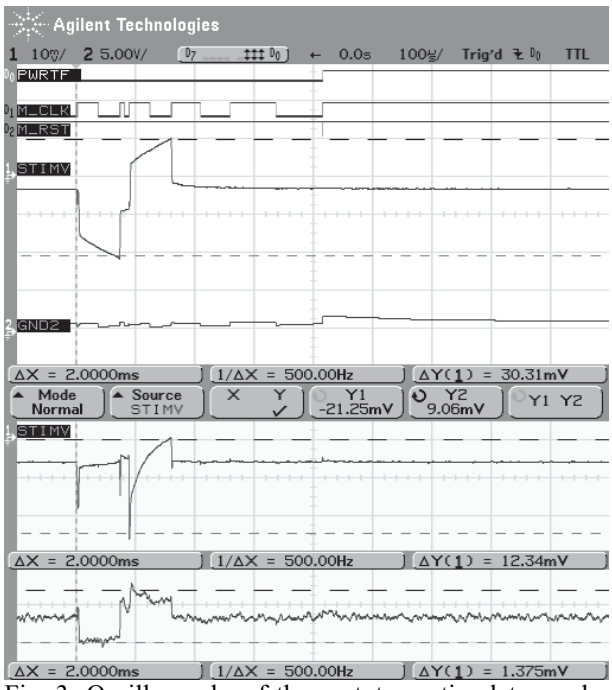


Fig. 3: Oscillographs of the prototype stimulator under test. Two sets of open dipole electrodes were mounted parallel and facing each other with a separation of 2mm in isotonic saline. The PWRTF, M_CLK and M_RST lines were as per Fig. 2. Note 'scope earth was on master GND and probe 2 on GND2. The waveforms were averaged over 256 cycles to eliminate the noise of the differential probe used to measure the voltage across the dipoles. STIMV in the upper panel: voltage across first dipole with 1mA pulses. Middle panel: voltage across second dipole sharing a supply rail with the first. Bottom panel: voltage across second dipole with floating supply.

The middle panel shows the voltage across the second dipole, but this time sharing a common supply rail with the first. In this trace the crosstalk in the second dipole for 1mA pulses in the first was 247mV pp, some 9 times greater than when the supplies were kept separate and allowed to float.

Discussion

It seems there is a very useful reduction in crosstalk if the stimulator supplies are all kept separate. Most of the capacitors needed in the circuitry are small enough to be included on the ASIC. The 1uF capacitors for each of the 3 slave supplies would probably need 0603 'off chip' packages. The 10uF smoothing capacitor for the master supply would need a 1206 package. Nevertheless, despite the capacitor bulk, it should all fit in a behind the ear implant (in the mastoid bone). The test circuit used ordinary FETs and standard CMOS parts which all have integral diodes to power rails ie a pair of diodes in series with the two power switches was needed for each slave supply to allow it to float. Such diodes can be omitted if XFAB's XT06 technology (with no parasitic diodes) is used for the ASIC.

Conclusions

The nine fold reduction in crosstalk found on test demonstrates there is a feasible method for reducing crosstalk between simultaneously activated channels in a multichannel stimulator implant. This method obviates the need for the delays of the stimulation queue of Santina et al's proposal [6]. The switched capacitor supply separation method described here may therefore be useful in preventing distressing disturbance of 3-D rotation perception in vestibular nerve stimulator patients.

References

[1] Mundl WJ. Measuring crosstalk and minimizing it in multiple stimulation arrangements. Med. & Biol. Engng, 4, 409-410, 1966.

[2] Wilson BS, Finley CC, Lawson DT, Wolford RD, Zerbi M. Design and evaluation of a continuous interleaved sampling (CIS) processing strategy for multichannel cochlear implants. J. Rehabil. R. & D, 30(1), 1993, 110-116.

[3] Constandinou TG, Georgiou J, Toumazou C. A Partial-Current-Steering Biphasic Stimulation Driver for Vestibular Prostheses. IEEE TBCAS, 2(2), 2008, 106-113.

[4] Zeng FG, Rebscher S, Harrison W, Sun X, Feng H. Cochlear implants: system design, integration and evaluation. IEEE Reviews Biomed. Eng. 1, 2008, 115-142.

[5] Gong W, Merfeld DM. Prototype neural semicircular canal prosthesis using patterned electrical stimulation. Annals Biomed. Eng. 28, 2000, 572-581.

[6] Santina CCD, Migliaccio AA, Patel AH. A multichannel semicircular canal neural prosthesis using electrical stimulation to restore 3-D vestibular sensation. IEEE Trans. Biomed Eng. 54(6), 2007, 1016-1030.

Acknowledgements

This work is part of the EU supported CLONS project.

Author's Address

Tim Perkins
UCL Dept of Medical Physics & Bioengineering,
Malet Place Engineering Building, Malet Place,
Off Torrington Place, LONDON WC1E 6BT
tap@mephys.ucl.ac.uk

Modulation of seizure susceptibility by spinal cord stimulation

Harreby KR[1], Sevcencu C[1] and Struijk JJ[2]

[1] Center for Sensory-Motor Interaction, Dept. Health Science and Technology, Aalborg University, Denmark

[2] Medical Informatics Group, Dept. Health Science and Technology, Aalborg University, Denmark

Abstract

Epidural spinal cord stimulation (SCS) is one of the most commonly used forms of electrical stimulation therapy. Via the dorsal column nuclei the fibres activated during SCS innervate the thalamus, a structure which has been shown to be highly involved in the generation of ictal activity. In this work we investigate how SCS affects seizure susceptibility.

Rats were divided into a sham stimulated group (control, n = 8), a 4 Hz SCS group (n = 6) and a 54 Hz SCS group (n = 8). Tonic-clonic seizures were induced by infusion of a pentylenetetrazole (PTZ) solution (50mg/kg) over a period of 10 min. Seizure susceptibility was quantified by assessing the seizure onset latency (SOL), number of seizures (NoS) and the total seizure duration (TSD).

4 Hz SCS significantly increased seizure susceptibility, whereas 54 Hz SCS induced a weak trend towards reduced seizure susceptibility.

SCS could modulate seizure susceptibility. If these effects are valid in humans low frequency SCS should be avoided. Further research is necessary to investigate if SCS parameters can be optimized to inhibit seizures.

Keywords: *spinal cord stimulation, epilepsy, rat, pentylenetetrazol.*

Introduction

Since the pain alleviating effect of SCS was discovered in the 1960's, this treatment has become the most used form of electrical stimulation therapy [1,2].

The dorsal column fibres activated during epidural SCS innervate structures in the spinal cord via collaterals and reach the thalamus via the dorsal column nuclei. While the inhibition of abnormal activity in the spinal dorsal horns seems to be the primary reason for pain alleviation, also supraspinal structures such as the thalamus may be involved [3,4]. The thalamus has been shown to be involved in the generation of epileptic seizures and in particular the generation of the spike-and-wave (SW) electroencephalographical activity seen during absence seizures [5]. Moreover, it has been shown that stimulation of various thalamic structures at low frequencies (below 10 Hz) induces cortical synchronization and seizures [6].

Considering the innervations of the thalamus during SCS, we hypothesized that SCS may also influence the seizure susceptibility. In the current work we therefore investigated the effect of SCS on seizure susceptibility, when performed at low frequency (4 Hz) and at the typical frequency range used for pain treatment (54 Hz)

Material and Methods

Experimental procedures

Sprague-Dawley rats (weight = 465 – 620 g) were anesthetised and the electrocorticogram (ECoG) and electrocardiogram (ECG) were recorded using electrodes screwed into the cranium and 1-lead ECG [7]. Electromyograms (EMG) were recorded using wire electrodes inserted in triceps brachii and soleus muscles. After exposing the cervical vertebrae (C), the two contacts of a custom made SCS electrode (stainless steel wires mounted on a plastic strip, 2 mm longitudinal spacing) were slid in the epidural space of C2. All signals were recorded at 10 kHz for later offline processing.

Rats were randomly divided in three groups: sham stimulated (no SCS, controls), 4 Hz SCS and 54 Hz SCS. Control rats stabilised for 20 min following surgery. In the stimulated rats, the SCS electrode was centred to the spinal midline by adjusting the electrode position while observing neck muscle responses elicited by 1 Hz SCS. After a 10 min stabilisation period, the stimulation current was determined by setting the stimulation frequency to the assigned value (4 or 54 Hz, bipolar 2x200 μs pulses) and increasing the current until minor contractions were seen in the neck.

Following this procedure, the stimulated rats were left to stabilise for additional 10 min.

After 5 min (300s) of baseline recording, SCS was started. After additional 5 min, a 10 min intra-venous infusion of PTZ initiated (50 mg/kg) to induce seizures (T = 0 s in Fig. 1). Recording and SCS outlasted PTZ infusion by 5 min.

Offline analysis

Prior to evaluation of the recordings, stimulation artifacts were removed by interpolating between measurements prior to and after each stimulation pulse. The start of a distinctive type of ECoG activity associated with tonic muscle activity was defined as seizure onset and the end of the ECoG activity associated with clonic muscle activity as seizure offset (Fig. 1, [7]). Seizure susceptibility was evaluated using SOL (defined as the time from PTZ infusion onset to seizure onset), NoS and TSD. Multivariate analysis of variance followed by Hotelling's Trace with a Bonferroni corrected significance level ($p < 0.05$) was used to test differences between individual groups.

Results

PTZ infusion induced one or more tonic-clonic seizures in all rats (Fig. 1). Stimulation was conducted at 313 ± 73 µA (mean ± STD) and 298 ± 83 µA in the 4 Hz and 54 Hz SCS groups, respectively. Although no muscle contractions were observed, SCS evoked EMG responses in the frontal limbs could not be avoided.

4 Hz SCS induced persistent large evoked SW responses, except during seizure and the immediate post-ictal period of ECoG depression (Fig. 1). In contrast, 54 Hz SCS did only trigger a smaller ECoG response at stimulation onset.

The control group had a SOL of 289 s, a NoS of 2.75 and a TSD of 132 s. Compared to controls, 4 Hz SCS significantly shifted all evaluated seizure parameters towards increased seizure susceptibility (Fig. 2). Although 54 Hz SCS did not significantly change any of the investigated parameters, all parameters expressed a trend towards reduced seizure susceptibility. Multivariate statistics showed that the 4 Hz group deviated significantly ($p = 0.01$) from the control group whereas the 54 Hz group did not ($p = 0.35$).

Discussion

This study shows that low frequency (4 Hz) SCS induces SW-like activity and increases seizure susceptibility. Although not statistically significant, 54 Hz resulted in a small trend towards decreased seizure susceptibility.

In contrast to our results, Ozcelik et al. showed that 2 Hz SCS, decreases inter-ictal spiking frequency

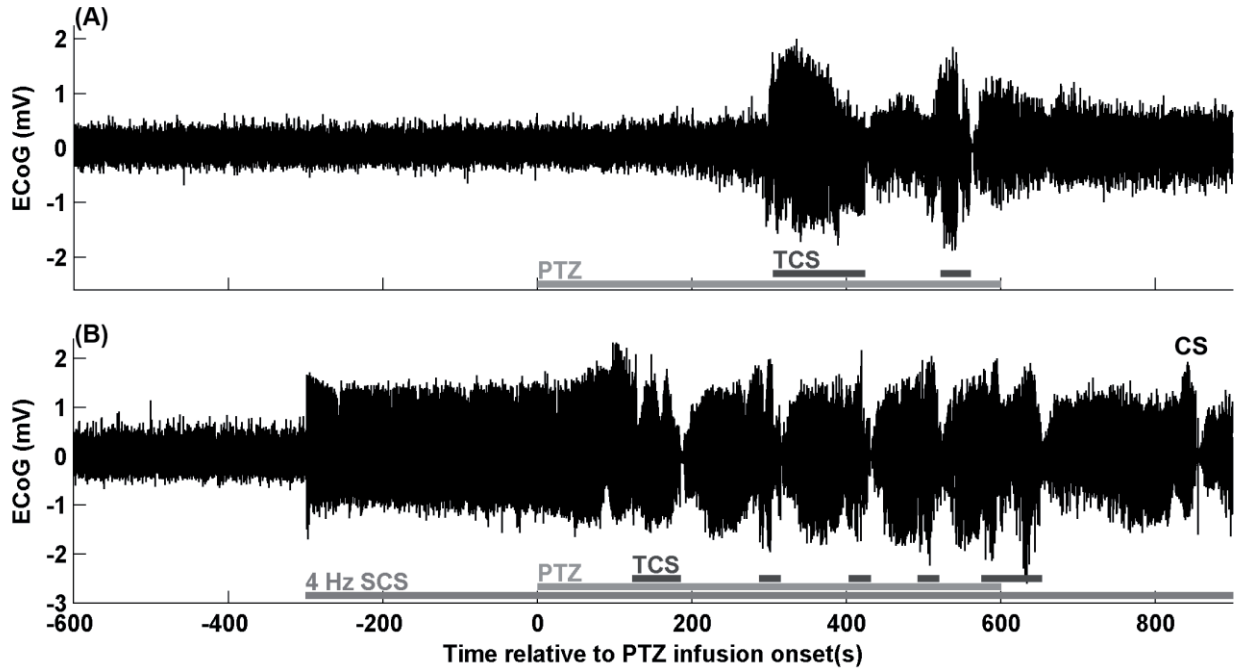


Fig. 1 ECoG recordings. (A) ECoG from a control rat. PTZ-infusion is started at T = 0 s and continued for 600 s. During PTZ-infusion (PTZ, light gray bar) the ECoG gradually becomes more spiky and two tonic-clonic seizures (TCS, dark gray bars) are triggered. (B) 4 Hz SCS (medium gray bar) induces large SW-like complexes. During TCSs, the evoked SW activity is replaced by spontaneous ictal activity. Post-ictally, the evoked SW activity gradually returns and develops into new seizures. The last period with post-ictal ECoG depression is preceded by a clonic-only seizure (CS). This type of seizures was only seen in the 4 Hz stimulated group.

in a penicillin rat epilepsy model [8]. The differences between those results and ours may be caused by the lower stimulation currents (max 100 μA) used by Ozcelik et al., which may not have been sufficient to generate the pro-convulsive cortical synchronization seen in our study.

Our results with SCS are similar to those with direct stimulation of thalamic nuclei. Where low frequency stimulation (<10 Hz) induces SW activity and triggers seizures [6], but may inhibit seizures when performed at higher frequencies (>20 Hz) [9].

The PTZ rat model has previously been used for evaluating the effect of peripheral nerve stimulation on seizure susceptibility, such as vagus and trigeminal nerve stimulation [10,11]. The results of these evaluations have been consistent with later findings in humans [12,13]. However, given that the number and type of fibres activated during SCS will depend on the dimensions of the spinal cord and the stimulation electrode, extrapolating these results to humans should be done with caution.

Conclusions

Our results show that 4 Hz SCS is pro-convulsive in a rat model. If this is valid in humans, such low frequencies should be avoided. On the other hand, 54 Hz SCS caused a weak trend towards decreased seizure susceptibility and further studies are neccesary to investigate if SCS can be optimized to inhibit seizures.

Acknowledgements

This work was supported by the Danish National Advanced Technology Foundation. We wish to thank the staff at Aalborg Biomedical Laboratory for their generous help during our experiments.

References

1. Shealy CN. Electrical inhibition of pain by dorsal column stimulation: Preliminary clinical report. Anesth Analg 46:489, 1967.
2. Kunnumpurath S. Spinal cord stimulation: principles of past, present and future practice: a review. J Clin Monit Comput 23:333, 2009.
3. Oakley JC. Spinal cord stimulation: mechanisms of action. Spine 27:2574, 2002.
4. Kishima H. Modulation of neuronal activity after spinal cord stimulation for neuropathic pain H215O PET study. Neuroimage , 2009.
5. Blumenfeld H, Coulter DA.) (2008) Thalamocortical Anatomy and Physiology. In:E. Jerome and T. A. Pedley. (eds) Epilepsy: A comprehensive testbook. 2nd ed.: Lippincott Williams & Wilkins Philadelphia.
6. Mirski MA, Rossell LA, Terry JB, Fisher RS. Anticonvulsant effect of anterior thalamic high frequency electrical stimulation in the rat. Epilepsy Res. 28:89-100, 1997.
7. Kristian Rauhe Nielsen, Cristian Sevcencu and Johannes J. Struijk. Vagus Nerve Activity based prediction of epileptic seizures in rats. Proceedings of the 13th Annual conference of the International Functional Electrical Stimulation Society - "From Movement to Mind"; 21/09/2008;De Gruyter; 2008.
8. Ozcelik L, Acar F, Cirak B, Suzer T, Coskun E, Tahta K, et al. The influence of cervical spinal cord stimulation on induced epileptic discharges in rats. Brain Res 1135:201-205, 2007.
9. Hamani C, Hodaie M, Chiang J, del Campo M, Andrade DM, Sherman D, et al. Deep brain stimulation of the anterior nucleus of the thalamus: effects of electrical stimulation on pilocarpine-induced seizures and status epilepticus. Epilepsy Res 78:117-123, 2008.
10. Woodbury DM, Woodbury JW. Effects of vagal stimulation on experimentally induced seizures in rats. Epilepsia 31 Suppl 2:S7-19, 1990.
11. Fanselow EE, Reid AP, Nicolelis MA. Reduction of pentylenetetrazole-induced seizure activity in awake rats by seizure-triggered trigeminal nerve stimulation. J.Neurosci. 20:8160-8168, 2000.
12. DeGiorgio CM. Pilot study of trigeminal nerve stimulation (TNS) for epilepsy: a proof-of-concept trial. Epilepsia 47:1213, 2006.
13. Ben-Menachem E. Vagus-nerve stimulation for the treatment of epilepsy. Lancet Neurol 1:477-482, 2002.

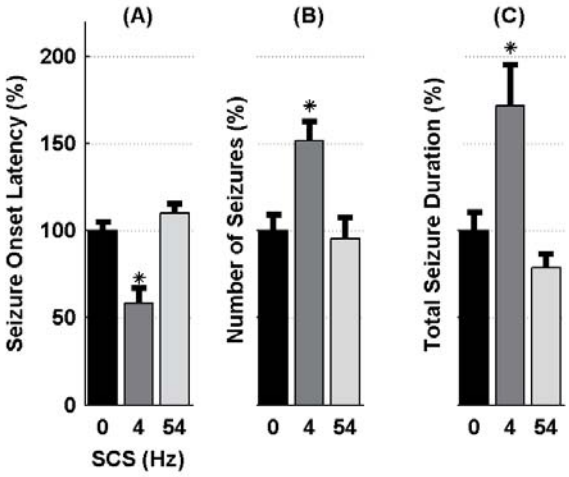


Fig. 2 The evaluated seizure parameters depicted relative to the control group. Significant ($p < 0.05$) deviations from the control group are marked with an asterisk (*). 4 Hz SCS significantly increases seizure susceptibility in all parameters. The 54 Hz SCS shows a weak trend towards a decrease in seizure susceptibility.

Author: Kristian Rauhe Harreby
Institute:Center for Sensory-Motor Interaction (SMI)
Street: Frederik Bajers Vej 7D2
City: 9220 Aalborg
Contry: Denmark
Email : krauhe@hst.aau.dk

Safe neuromuscular electrical stimulator designed for elderly people

Krenn M[1], Haller M[1], Bijak M[1], Unger E[1], Hofer C[2], Kern H[2,3], Mayr W[1]

[1] Center for Medical Physics and Biomedical Engineering, Medical University of Vienna, Austria
[2] Ludwig Boltzmann Institute of Electrical Stimulation and Physical Rehabilitation, Vienna, Austria
[3] Department of Physical Medicine and Rehabilitation, Wilhelminenspital Wien, Austria

Abstract

A stimulator for neuromuscular electrical stimulation, especially suiting the requirement of elderly people with reduced cognitive abilities and coordination, was designed. The ageing of skeletal muscle is characterized by a progressive decline in muscle mass, force and condition. Muscle training with neuromuscular electrical stimulation reduces the degradation process. The discussed system is intended for stimulation of the posterior and anterior thigh.

The core of the stimulator hardware is a multi-processor structure where each output-stage is controlled by its own microprocessor (Microchip Technology Inc.). A central controller unit allows using the stimulator as a stand-alone device. To set up the stimulation sequences and to evaluate the compliance data a PC is connected to the stimulator via wireless data link. The stimulator has four biphasic constant voltage stimulation channels. Additionally, each channel has an analog input to measure the evoked myoelectric signal (M-wave).

To help elderly people to handle the stimulator by themselves the user interface is reduced to four input buttons, start / stop training and increase / decrease of the stimulation amplitude. For safety reasons, the electrode impedance is measured during stimulation.

***Keywords**: FES, aging muscle, electrical stimulation, compliance management, M-wave.*

Introduction

An age-related reduction of muscle mass and strength is often associated with reduced mobility. Lauretani et al [1] reported a decrease of isometric muscle strength of 51% and 43% in 75-85 year old women and men, respectively, compared to young subjects (20 to 29 years). This decrease is often related to dysfunction of mobility in the elderly and is a predictor of future disabilities. Muscle training can dramatically improve the muscle strength, power and functional abilities of elder individuals [2, 3].

This paper introduces a neuromuscular electrical stimulator (NMES) for muscle training of elderly people. A significant improvement of muscle strength is reported in [4], where NMES-training is performed on elderly women between 62 and 75 years. Also in animal models [5] electrical stimulation of elderly shows positive effects.

Many portable stimulator designs are described in literature. These devices have successfully enabled standing and walking in persons with paraplegia [6-8]. Design rules of the presented stimulator are easy usability and a safety protocol that protects the elderly even in case of improper handling. The safety protocol is based on measurements of the electrode impedance and functional feedback such as evoked myoelectric signal and accelerometric detected muscle motion. Additionally, the stimulator stores the compliance data on a memory card.

Material and Methods

The introduced portable transcutaneous stimulator (Fig. 1) consists of a central unit and four stimulation channels. Each channel is designed modular [9] and includes an output stage and measurement module. The multi-processor structure breaks down the design to simple tasks and implements them on several microcontrollers (Microchip Technology Inc., Chandler AZ, USA).

Central control unit

A microcontroller (PIC24, Microchip Technology Inc.) controls all major tasks of the stimulator to provide a stand-alone operation. Essential in the modular design is a bus communication. A master/slave structure with addressable slaves like I2C and SPI are used to set the output stage and the measurement module. The stimulation protocol and the compliance data are stored on a SD card. A real time clock is used to synchronize the stored data especially in long-time run for home use.

USB and Bluetooth are used for the stimulator-computer communication. Via this data-link, the stimulation protocols are programmed and the compliance data are finally stored and evaluated on a computer. The necessary USB-isolation is achieved with a bidirectional isolation amplifier

(ADuM4160, Analog Device Inc., Norwood MA, USA).

Measurement module

Electrode impedance, evoked myoelectric signal (M-wave) and surface motion are measured during stimulation. For safety reason the impedance of the electrodes is monitored. The stimulation process will be terminated if an error occurs. Several publications [10, 11] present a circuit to measure the EMG during electrical stimulation, especially for EMG-triggered NMES. In our case, the M-wave is used for a functional feedback of the training intensity. The amplifier has a gain of 1000V/V and a bandwidth from 15Hz to 1000 Hz. The surface muscle motion is measured with a three axial accelerometer (LIS331DLF, STMicroelectronics Geneva, CH). The twitch response gives a second functional feedback during low-frequency stimulation. Furthermore, the three dimensional acceleration signals are used to determine the thigh orientation.

Output stage

The constant voltage stimulation impulses are generated with a full bridge circuit (A3953, Allegro MicroSystems Inc., Worcester, USA) supplied by a DC/DC step-up converter (MAX668, Maxim Integrated Products Inc., Sunnyvale CA, USA). The output stage has a double fault protection against DC current with capacitors.

Measurement of M-wave

During electrical stimulation, the detected surface myoelectric signal is contaminated by a stimulation artifact. This effect is impaired by near distance between stimulation and measurement electrodes. After the stimulation impulse has ceased, the full bridge circuit of the output stage can be driven in two different settings. First, all switches are open and second, both electrodes are grounded via the transistors S3, S4 (Fig. 2,A). The impact of these two modes was tested on the anterior thigh. Large stimulation electrodes (10x13cm) were use and the M-wave was measured at the rectus femoris.

Results

M-wave, Output characteristic

Fig. 2 shows M-wave and the stimulation impulse at the different configurations of the full bridge output. The capacitance of stimulation electrodes is much faster discharged with the grounded electrodes (Fig. 2,B-C). Therefore, the stimulation artifact during M-wave measurement is reduced (Fig. 2,D-E).

Stimulation protocol

The constant voltage stimulation impulses are rectangular and biphasic. Stimulation patterns are programmed independently for each channel, which allows very flexible training protocols.

Discussion

The constant voltage source increases safety because the subject is prevented from localized high current densities. A disadvantage of this method is that the applied stimulation intensity is dependent on the electrode impedance. Monitoring of the stimulation current provides valuable information regarding the actual intensity.

Input options are kept as simple as possible. The user can only influence the stimulation amplitude and start or stop of the training session. An important element of the system is the storage of the compliance data. All training sessions and measurements are recorded on the SD card, which allows a scientific use of the stimulator in clinical trials.

References

[1] Lauretani F, Russo CR, Bandinelli S et al., Age-associated changes in skeletal muscles and their effect on mobility: an operational diagnosis of

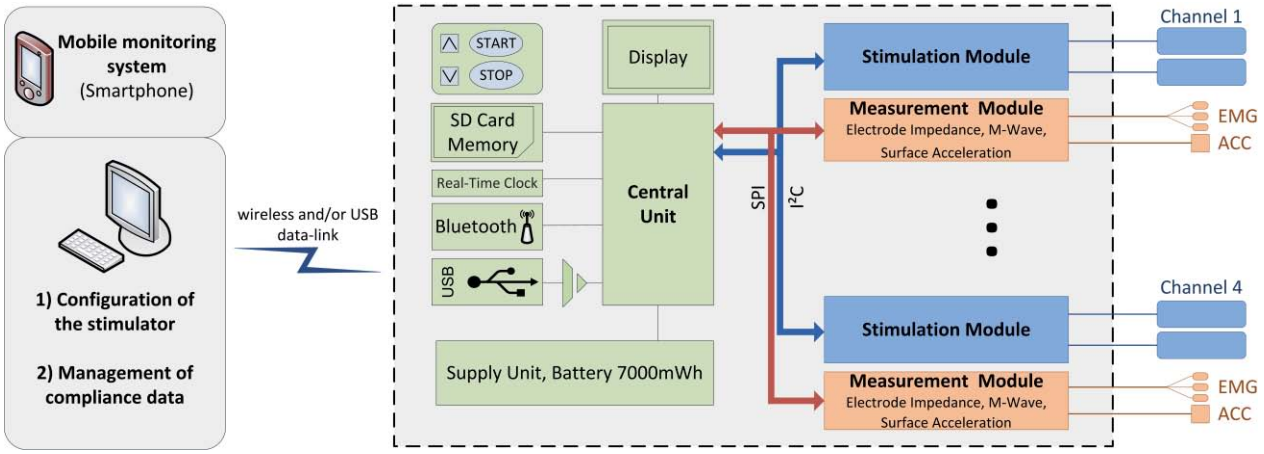
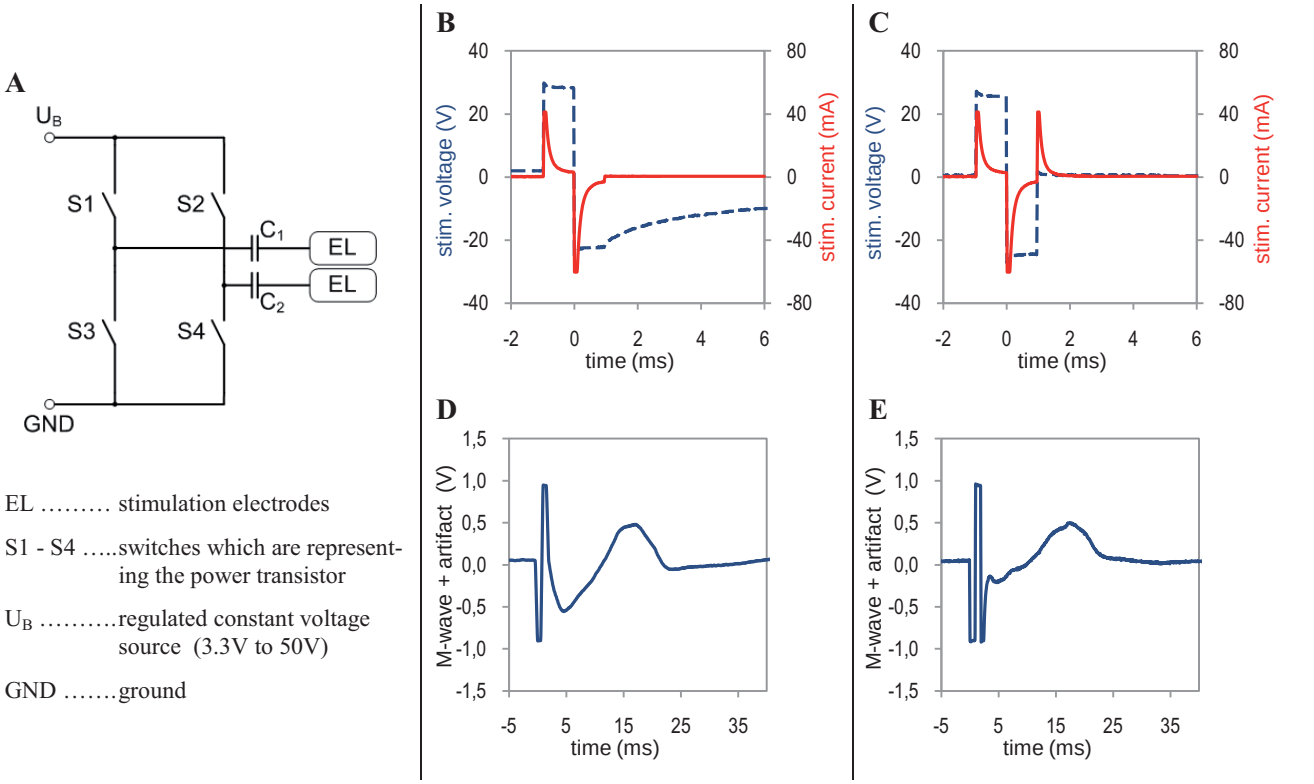


Fig. 1: Block diagram of the neuromuscular electrical stimulator.



EL …… stimulation electrodes

S1 - S4 …..switches which are representing the power transistor

U_B …….regulated constant voltage source (3.3V to 50V)

GND …….ground

Fig. 2: Schematic drawing of the output stage (A). Stimulation voltage (dashed line) and current (continuous line) are plotted for different modes of the bridge circuit. After the stimulation impulse has ceased all switches are open (B) and secondly, the electrodes are grounded (C). Evoked myoelectric signal (M-wave) and the stimulation artifact are plotted in the same two modes of the H-bridge – with open switches (D) and with short-circuited electrodes (E).

sarcopenia, J Appl Physiol, vol. 95, no. 5, pp. 1851-1860, Nov, 2003.

[2] Macaluso A, and De Vito G, Muscle strength, power and adaptations to resistance training in older people, Eur J Appl Physiol, vol. 91, no. 4, pp. 450-72, Apr, 2004.

[3] Kern H, Kovarik J, Franz C et al., Effects of 8 weeks of vibration training at different frequencies (1 or 15 Hz) in senior sportsmen on torque and force development and of 1 year of training on muscle fibers, Neurol Res, vol. 32, no. 1, pp. 26-31, Feb, 2010.

[4] Paillard T, Lafont C, Soulat JM et al., Short-term effects of electrical stimulation superimposed on muscular voluntary contraction in postural control in elderly women, J Strength Cond Res, vol. 19, no. 3, pp. 640-646, Aug, 2005.

[5] Putman CT, Sultan KR, Wassmer T et al., Fiber-type transitions and satellite cell activation in low-frequency-stimulated muscles of young and aging rats, J Gerontol A Biol Sci Med Sci, vol. 56, no. 12, pp. 510-519, Dec, 2001.

[6] Bijak M, Mayr W, Rakos M et al., The Vienna functional electrical stimulation system for restoration of walking functions in spastic paraplegia, Artif Organs, vol. 26, no. 3, pp. 224-227, Mar, 2002.

[7] Simcox S, Davis G, Barriskill A et al., A portable, 8-channel transcutaneous stimulator for paraplegic muscle training and mobility - A technical note, Journal of Rehabilitation Research and Development, vol. 41, pp. 41-51, Jan-Feb, 2004.

[8] Popovic MR, and Keller T, Modular transcutaneous functional electrical stimulation system, Med Eng Phys, vol. 27, no. 1, pp. 81-92, Jan, 2005.

[9] Bijak M, Hofer C, Lanmuller H et al., Personal computer supported eight channel surface stimulator for paraplegic walking: first results, Artif Organs, vol. 23, no. 5, pp. 424-7, May, 1999.

[10] Thorsen R, and Ferrarin M, Battery powered neuromuscular stimulator circuit for use during simultaneous recording of myoelectric signals, Med Eng Phys, vol. 31, no. 8, pp. 1032-1037, Oct, 2009.

[11] Muraoka Y, Development of an EMG recording device from stimulation electrodes for functional electrical stimulation, Front Med Biol Eng, vol. 11, no. 4, pp. 323-333, 2002.

Acknowledgements

This work was supported by the European Union, EU-Intereg IVa 2008-2013: N00033

Author's Address

Matthias Krenn
Medical University of Vienna
Center for Medical Physics and Biomedical Engineering
matthias.krenn@meduniwien.ac.at
www.zmpbmt.meduniwien.ac.at

Session 4

Control, Sensors, Algorithms – non invasive 1

Spinal involvement and muscle cramps in electrically-elicited muscle contractions

Merletti R[1], Botter A[1], Minetto MA[1,2]

[1] Laboratory for Engineering of the Neuromuscular System (LISiN), Department of Electronics, Politecnico di Torino, Italy (www.lisin.polito.it)

[2] Division of Endocrinology, Diabetology and Metabolism, Department of Internal Medicine, University of Torino, Italy

Abstract

Electrical stimulation of innervated muscles has been investigated for many decades with alternations of high and low clinical interest in the fields of stroke, SCI rehabilitation, and sport sciences. Early work demonstrated that afferent fibers have lower thresholds and are usually activated first (therefore eliciting an H-reflex). In the case of nerve trunk stimulation, the order of recruitment is mostly conditioned by the axonal dimension and excitability threshold. In the case of muscle motor point stimulation, the spatial distribution of nerve branches plays a predominant role. Sustained stimulation produces a progressive increase of force that is often maintained in subsequent voluntary activation by stroke patients. This observation suggested a facilitation mechanism at the spinal and/or supraspinal levels. Such facilitation has been observed in healthy subjects as well, and may explain the generation of cramps elicited during stimulation and sustained for dozens of seconds after stimulation has been interrupted. The most recent interpretations of facilitation resulting from peripheral stimulation focused on pre- (potentiation of neurotransmitter release from afferent fibers) or post-synaptic (generation of "Persistent Inward Currents" in spinal motor neurons or interneurons) mechanisms. The renewed attention to these phenomena is once more increasing the interest toward electrical stimulation of the neuromuscular system. This is an opportunity for a structured investigation of the field aimed to resolving elements of confusion and controversy that still plague this area of electrophysiology.

Keywords: *neuromuscular electrical stimulation, electromyography, spinal motor neuron, central torque, muscle cramps.*

Introduction

Neuromuscular electrical stimulation (NMES) of peripheral nerves is commonly used (and frequently abused) to generate muscle contractions for both neuromuscular testing and rehabilitation, "prehabilitation" (i.e., pre-operative conditioning of muscles), training purposes [1].

Surface NMES can be applied using a pair of electrodes in monopolar or bipolar configuration (one small stimulation electrode and a large one far away, closing the current, or two similar electrodes on the same muscle). NMES is commonly viewed as a technique to "disconnect" the investigated (portion of) muscle from the central nervous system and to activate only one (or a portion of one) muscle at a time at a controlled frequency and with a stable motor unit pool. However, several lines of evidence indicate a considerable involvement of different neural structures during NMES [2,3]. It has even been suggested that NMES provides a multimodal "bombardment" of the central nervous system [1], which results in spinal motor neuron facilitation [4-6] and increased cortical activity and cortico-spinal excitability [7]. Interestingly, not only neural involvement may occur during a single NMES session, but also short- and long-term neural adaptations can be triggered by NMES protocols (NMES-induced plasticity), as demonstrated by: a) persistence of the NMES benefits after the stimulation is turned-off, as demonstrated by Vodovnik and Rebersek in 1973 [8] (e.g., functional improvements during and after ankle dorsiflexion stimulation in neurological patients with drop foot); b) increases in muscle strength after only a few sessions of NMES training, with no concurrent variations in muscle fiber size and functional/enzymatic properties; c) increases in muscle strength for the homologous contralateral muscle after unilateral NMES training (a phenomenon referred to as "contralateral limb effect" or "cross-education").

This contribution will be focused on the "acute" involvement of the spinal motor neurons that occurs during NMES, a phenomenon that is based on a reflexive motor neuron recruitment and that is very likely responsible for involuntary muscle phenomena that persist after the stimulation end, such as muscle cramps.

NMES-induced "central torque"

Conventional NMES involves pulse widths between 100 and 400 μs and frequencies between 20 and 50 Hz. This stimulation paradigm preferentially activates motor axons without obvious sequencing related to motor unit type [9] but related to excitability threshold in the case of nerve stimulation and to geometrical distribution of axonal branches in the case of muscle motor point stimulation. During a sustained bout of conventional NMES, the torque first increases and then progressively decreases and a "slowing" of the surface EMG signals occurs due to the development of fatigue [10]. This "slowing" is described by a progressive widening of the M-wave, due to progressive decrease of muscle fiber conduction velocity, and results in progressive compression of the EMG power spectrum and of its mean and median frequencies.

Differently, during wide-pulse (1 ms) high-frequency (50-100 Hz) NMES, torque increases significantly beyond that elicited by conventional NMES and does not decrease during the course of the stimulation: this phenomenon has been referred to as "central torque" (Figure 1) [4-6]. It has been demonstrated that the underlying mechanism is the reflexive recruitment of spinal motor neurons (which activates motor units in the normal physiological recruitment order): in fact, the "extra" force could not be elicited following peripheral nerve block [6]. Interestingly, it has been observed that a weak involuntary contraction (associated with EMG activity) often persists even after the wide-pulse high-frequency NMES is turned-off, thus indicating that the electrically-elicited sensory volley may trigger either bistable discharge of motor neurons (i.e., already recruited motor neuron firing at a higher frequency following the burst) or self-sustained discharge of motor neurons (i.e., recruitment and sustained discharge in previously silent motor units). Bistable and self-sustained discharge are consistent with the development of persistent inward currents in spinal motor neurons and interneurons. Further, a possible role for the cortex in the development of the central torque can not be excluded, as well as a pre-synaptic mechanism related to the potentiation of neurotransmitter release from afferent fibers.

Independently of the physiological mechanism(s) underlying the "extra" force that can be elicited during and after stimulation, the use of a wide-pulse high-frequency stimulation paradigm is promising for rehabilitation medicine [11].

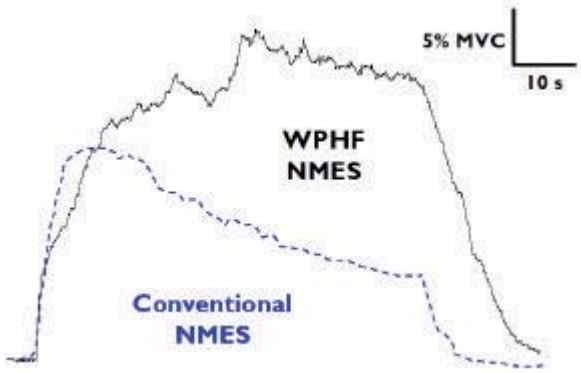


Fig. 1: Representative example of force traces detected from the biceps brachii muscle of a healthy subject during conventional NMES (dashed blue line) and wide-pulse high-frequency NMES (continuous black line).
WPHF (wide-pulse high-frequency) stimulation: 1 ms pulse width, 100 Hz, 6 mA.
Conventional stimulation: 100 μs pulse width, 25 Hz, 50 mA.
MVC: maximal voluntary contraction.

NMES-induced muscle cramps

A cramp can be defined as a sudden, involuntary, and painful contraction of a muscle or part of it, self-extinguishing within seconds to minutes, associated with electrical activity (involuntary repetitive discharge of motor unit action potentials in a large muscle area) [11].

Fig. 2 shows an example of spatio-temporal development of a cramp of the abductor hallucis muscle (elicited by means of electrical stimulation of the main muscle motor point) detected by a two-dimensional array of surface electrodes after the end of the stimulation train.

Muscle cramps are generally considered to be neurogenic [12], although there is still debate on whether cramps have peripheral or central origin. It has been demonstrated that the electrical stimulation of a peripheral nerve [13] or of the muscle motor point [14,15] can trigger involuntary muscle activities, such as fasciculations and cramps, that may last for several seconds after the stimulation end. Concurrent detection of surface EMG signals from both the stimulated and the synergistic muscles showed involuntary EMG activity of the stimulated muscle (after the stimulation end), with no activity detectable from the synergistic muscle. Fig. 3 shows an example of temporal development of a cramp of the medial gastrocnemius muscle, without concurrent involvement of the lateral gastrocnemius or spreading of the cramp from one head to the other. Since the two gastrocnemii muscles work in synergy during a voluntary contraction, the

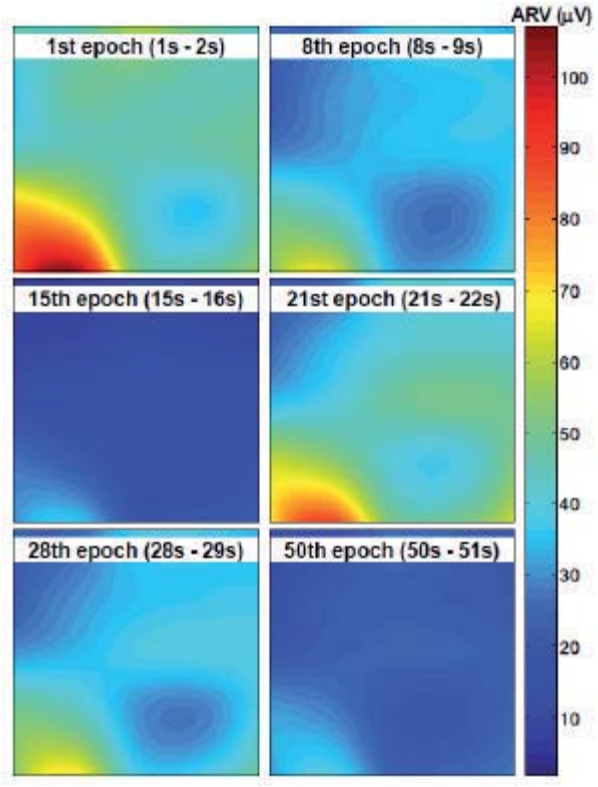


Fig. 2: Example of spatio-temporal development of a cramp of the abductor hallucis muscle detected with a two-dimensional array of surface electrodes (6 rows x 5 columns, circular electrodes, 2-mm diameter, 5-mm interelectrode distance in both directions). Each graph represents the surface EMG average rectified value (ARV) distribution over the skin surface determined over a 1-s epoch and was obtained using bicubic spatial interpolation of ARV estimates between single differential channels of the two-dimensional array. The cramp developed in a small muscle area, then decreased in size and intensity until it disappeared after about 10–15 s, then re-occurred after 20 s in the same portion of the muscle.

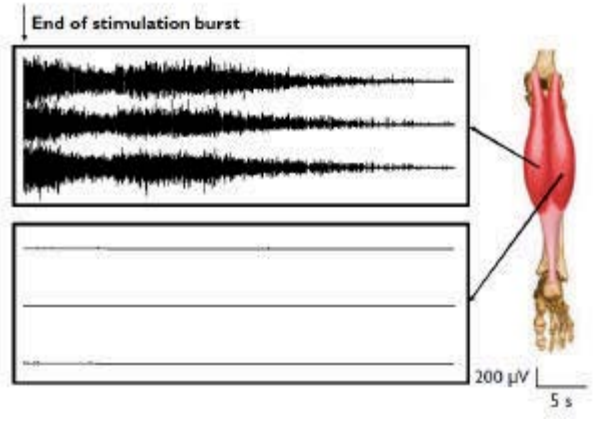


Fig. 3: Top: example of cramp discharge (three bipolar EMG signals detected with a linear array after the end of the stimulation burst) for the medial gastrocnemius muscle of one subject. Bottom: no EMG activity is evident in the surface EMG recording of the lateral gastrocnemius muscle. No concurrent involvement of the two muscle heads or spreading of the cramp from one head to the other can be observed.

observed patterns of EMG responses provided clear evidence for the involuntary nature of the elicited muscle activity [15].

The factors critical for cramp induction were the frequency of the stimulation burst [13-15] and the shortening of the muscle during the stimulation [13]. Similarly to the persistence of an involuntary contraction after the wide-pulse high-frequency NMES is turned-off, the development of the cramp (that is, the maintenance of the involuntary muscle contraction after the end of the stimulation) involves spinal pathways, as indicated by the analysis of motor unit behaviour during electrically-elicited cramps. In fact, it has been demonstrated that: a) motor neurons of a cramping muscle discharge action potentials at rates comparable with those reported for voluntary contractions, but with larger discharge variability [16]. The high discharge variability is likely related to the afferent inputs that motor neurons receive, which can be inhibitory and excitatory, and thus generate greater noise than that in voluntary contraction; b) motor unit discharge rate decreases over time during cramp development [16,17]: this decrease may be associated to reflex inhibition of the motor neuron pool [17]; c) motor unit derecruitment rate during cramp extinction is in the range 5-8 pps [16], which corresponds to the minimal rate at which motor neurons discharge action potentials in voluntary contractions; d) the shape of the action potentials repeats consistently over time during cramp development and extinction [16,17]. Altogether, these results indicate that it is unlikely that motor unit action potentials are generated at the intramuscular terminal branches of motor neuron axons and support the hypothesis of involvement of spinal pathways in cramp development and extinction.

Implications and conclusions

NMES is one of the most common techniques used for maintaining muscle quality (therapeutic electrical stimulation, TES). NMES delivered to recruit motor units through a reflexive pathway may be advantageous for both TES purposes and treatment of muscle atrophy as it may recruit primarily slow motor units which are not preferentially activated using conventional NMES. The preferential recruitment of slow motor units (if proven) could allow to prevent or reduce the slow-to-fast transition of muscle fibers that is associated with immobilization and disuse. However, the induction of muscle cramps may be an undesired result of the stimulation procedure if the electrically-excited muscles shorten during the

stimulation. We recommend that electrical stimuli be delivered under strictly isometric conditions and, if is possible, with the muscles in a lengthened position.

References

[1] Maffiuletti NA. Physiological and methodological considerations for the use of neuromuscular electrical stimulation. Eur J Appl Physiol, in press.

[2] Enoka RM. Activation order of motor axons in electrically evoked contractions. Muscle Nerve, 25: 763-764, 2002.

[3] Vanderthommen M, Duchateau J. Electrical stimulation as a modality to improve performance of the neuromuscular system. Exerc Sport Sci Rev, 35: 180-185, 2007.

[4] Collins DF, Burke D, Gandevia SC. Large involuntary forces consistent with plateau-like behavior of human motoneurons. J Neurosci, 21: 4059-4065, 2001.

[5] Baldwin ER, Klakowicz PM, Collins DF. Wide-pulse-width, high-frequency neuromuscular stimulation: implications for functional electrical stimulation. J Appl Physiol, 101: 228-240, 2006.

[6] Collins DF. Central contributions to contractions evoked by tetanic neuromuscular electrical stimulation. Exerc Sport Sci Rev, 35: 102-109, 2007.

[7] Mang CS, Lagerquist O, Collins DF. Changes in corticospinal excitability evoked by common peroneal nerve stimulation depend on stimulation frequency. Exp Brain Res, in press.

[8] Vodovnik L, Rebersek S. Improvements in voluntary control of paretic muscles due to electrical stimulation. Neural organization and its relevance to prosthetics - 1973. In: Lojze Vodovnik Collected Works. Miklavcic D, Kotnik T, Sersa G (eds). Ljubljana, Slovenia: University of Ljubljana, Faculty of Electrical Engineering, pp. 105-120, 2003.

[9] Gregory CM, Bickel CS. Recruitment patterns in human skeletal muscle during electrical stimulation. Phys Ther, 85: 358-364, 2005.

[10] Merletti R, Rainoldi A, Farina D. Myoelectric manifestations of muscle fatigue. In: Merletti R, Parker PA (eds). Electromyography. Physiology, engineering, and non-invasive applications. Hoboken, USA: J. Wiley - IEEE Press, pp. 233-258, 2004.

[11] Miller TM, Layzer RB. Muscle cramps. Muscle Nerve, 32: 431-442, 2005.

[12] Layzer RB. The origin of muscle fasciculations and cramps. Muscle Nerve, 17: 1243-1249, 1994.

[13] Bertolasi L, De Grandis D, Bongiovanni LG, et al. The influence of muscular lengthening on cramps. Ann Neurol, 33: 176-180, 1993.

[14] Minetto MA, Botter A, Ravenni R, et al. Reliability of a novel neurostimulation method to study involuntary muscle phenomena. Muscle Nerve, 37: 90-100, 2008.

[15] Minetto MA, Botter A. Elicitability of muscle cramps in different leg and foot muscles. Muscle Nerve, 40: 535-544, 2009.

[16] Minetto MA, Holobar A, Botter A, et al. Discharge properties of motor units of the abductor hallucis muscle during cramp contractions. J Neurophysiol, 102: 1890-1901, 2009.

[17] Ross BH, Thomas CK. Human motor unit activity during induced muscle cramp. Brain 118: 983-993, 1995.

Acknowledgements

Authors are grateful to Dr. Nicola A. Maffiuletti and Prof. Dario Farina for their careful review of the final version of this contribution and to Dr. Silvestro Roatta for providing the data presented in Fig. 1.
Musculoskeletal Image is from the University of Washington "Musculoskeletal Atlas: A Musculoskeletal Atlas of the Human Body" by Carol Teitz, M.D. and Dan Graney, Ph.D.
The Author's work related to this contribution was supported by Compagnia di San Paolo Project "Neuromuscular Investigation and Conditioning in Endocrine Myopathies (NICEM)" and Regional Health Administration Project "Ricerca Sanitaria Finalizzata 2009".

Author's Address

Roberto Merletti, Alberto Botter
Laboratory for Engineering of the Neuromuscular System, Politecnico di Torino, Torino, Italy
roberto.merletti@polito.it, alberto.botter@polito.it

Marco A. Minetto
University of Torino, Molinette Hospital and Laboratory for Engineering of the Neuromuscular System, Politecnico di Torino, Torino, Italy
marco.minetto@unito.it

Event Detection for Gluteal or Hamstring Stimulation During Walking in Neurological Patients

Abdul Malik N[1], Chappell P.H[1], Wood D.E[2,3], Taylor P.N[2]

[1] School of Electronics and Computer Science, University of Southampton, Southampton, UK

[2] Department of Clinical Sciences and Engineering, Salisbury District Hospital, Salisbury, UK

[3] School of Design Engineering and Computing, Bournemouth University, Poole, UK

Abstract

An algorithm to detect when the tibia is vertical is presented. Its intended use is to trigger a functional electrical stimulation (FES) device for either the rotation or extension of the hip (gluteal stimulation) or flexion of the knee (hamstring stimulation) in neurological patients. The algorithm comprises a correlation coefficient calculation and a set of threshold rules. Data from a healthy subject has been used as a sample window for the correlation coefficient calculation for all the neurological patients. The sample window chosen detects correctly the events in five out of seven patients. For one patient, a sample window selected from the same patient data has been used successfully in the detection. All the results have showed no missing events during walking when compared to a footswitch.

***Keywords**: tibia vertical event, FES, detection algorithm, neurological patients, gait.*

Introduction

Gait disorders due to weak or paralysed muscle groups or spasticity of the antagonist muscle groups are common in neurological patients. These disorders affect the quality of life of patients as their walking efficiency decreases, more effort is needed to walk and there is an increased risk of falls. Stimulation of the peroneal nerve during the swing phase of the gait to lift the foot by dorsiflexing and everting the ankle has shown an improvement in the gait of patients [1]. As well as drop foot, there are also other problems contributing to the gait disorder such as reduced knee flexion during swing, knee hyperextension in early and terminal stance, and excessive hip flexion/adduction at heel strike.

Stimulation of gluteal or hamstring muscles can further improve the gait of neurological patients [2, 3], but the timing of stimulating these muscle groups, such as following the normal muscle activity times, is critical. Currently, the footswitch sensor is used to trigger the stimulator for drop foot correction, however the events detected by the footswitch do not coincide with the events needed to stimulate other muscle groups such as hamstring or gluteal muscles. It is very difficult to achieve the right timing with the current sensor as it does not detect events during a gait cycle except for foot contact with the ground. A study of a normal muscle activity from a search of the literature suggests that the gluteal muscles start their contraction at about 6% and hamstrings 20% of the gait cycle before initial heel contact. So the closest event is chosen when the tibia is vertical (TV). Therefore an alternative sensor that can provide more information throughout the gait such as angle and acceleration is required; this has been developed [4] and is used here in detecting when the tibia is vertical by using an algorithm comprising a correlation coefficient calculation and a set of rules with a threshold method. The detected events could be used to trigger stimulation of the gluteal or hamstring muscles prior to heel strike resulting in hip extension/abduction or to prevent knee hyperextension.

Methods

The Protocol

Seven neurological patients who were currently using the Odstock Two-channel FES device (O2CHS) at the time of the trials have been recruited. Four of the participants had multiple sclerosis, two have had a stroke and one person has a spinal cord injury C4/5 incomplete tetraplegia. All participants were medically stable, able to walk with and without a stimulator and single-side affected. The study was granted ethical approval by the Wiltshire Research Ethics Committee and the participants gave informed consent. Each patient was asked to walk with and without stimulation in a gait lab for about 4 metres in each trial.

The Experimental Set Up

Two dual axis accelerometers (LIS2LO2AS4 from STMicroelectronic) were used to derived the angle and linear acceleration of a segment in a gravitational field with respect to the horizontal plane [4]. A sensor unit was attached to the thigh, shank and foot of both lower limbs for the kinematic measurements as shown in Figure 1. Two footswitches were placed under the heel and the first metatarsal head of the foot for both limbs; these were used as reference sensors. The data was captured using two data acquisition systems (DAQ6015, DAQ6036E) from National Instrument Ltd connected to two laptops. A remote switch was used to start and stop the data collection at the same time. The sampling rate used was 1kHz and the sensor unit bandwidth was set to 500Hz. The data was analysed off-line using Matlab® R2006b.

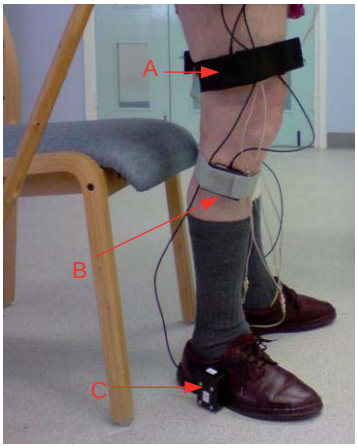


Figure 1: Sensor units attachment to both lower limbs. Right lateral view. (A: thigh segment, B: shank segment and C: foot segment)

The Detection Algorithm

From the accelerometer data the foot segment angle of the affected side has been used in the event detection. The algorithm used to detect the event consists of correlation coefficient calculation and a set of rules with a threshold method. The correlation coefficient value was calculated for the foot segment angle from the patients and a sample window taken from a healthy subject. From the correlation coefficient value obtained, a set of rules with a threshold method was employed to detect the desired event. The set of rules are as follows:

i) Search for the negative threshold (t_n) (refer to Figure 2(b)), once the negative threshold (t_n) is reached, start counting for T_{fl} (time frame 1). Within T_{fl} the positive threshold (t_p) must be reached and the first maximum value (m) after the positive threshold (t_p) is reached is where the event occurred. If within the T_{fl} the positive threshold (t_p) is not reached then no event occurred and the algorithm will start again.

ii) Once an event is detected, start counting for T_{f2} (time frame 2). Within the T_{f2} any detection will be cancelled. After T_{f2} has ended, the algorithm returns to (i).

Results

Figures 2 and 3 show an example of the event detection algorithm output in Patient 1 and Patient 3 during walking. The algorithm employed a sample window from a healthy subject for Patient 1 while for Patient 3 a sample window selected from the same patient data was used.

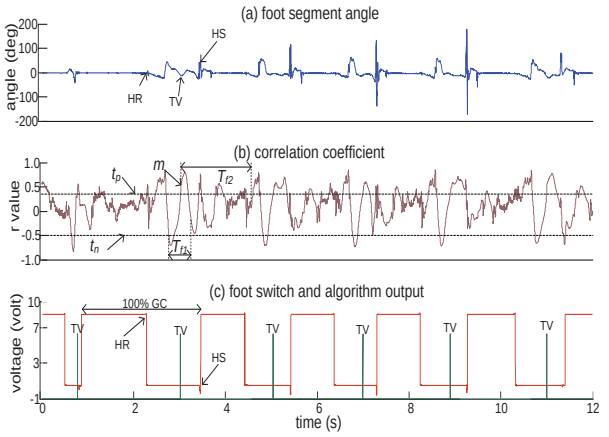


Figure 2: Patient 1 walking with stimulation. (a) foot segment angle with respect to horizontal plane (b) correlation coefficient value calculated from foot segment angle with a sample window from a healthy subject. (T_{fl}=0.55s, T_{f2}=1.5s, t_n=-0.5 and t_p=0.35) (c) heel switch and algorithm output. (HS=heel strike, HR=heel rise, TV=tibia vertical event, GC=gait cycle, m=first maximum point, t_n=negative threshold, t_p=positive threshold, T_{fl}=time frame 1, T_{f2}=time frame 2)

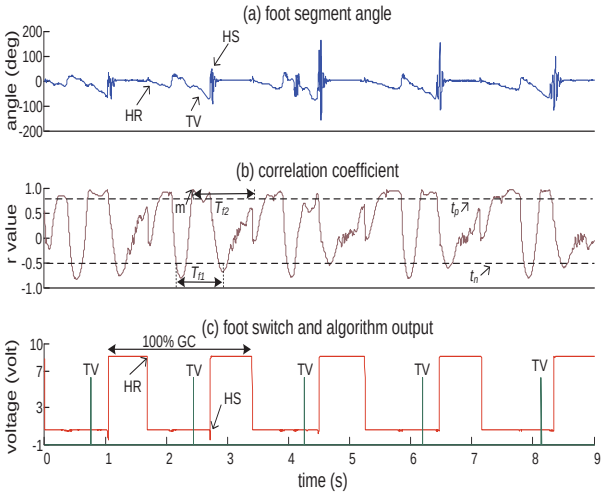


Figure 3: Patient 3 walking without stimulation. (a) foot segment angle with respect to horizontal plane (b) correlation coefficient value calculated from foot

segment angle with a sample window from the same patient data. (T_{f1}=0.80s, T_{f2}=1s, t_n=-0.5 and t_p=0.8) (c) heel switch and algorithm output.

Table 1 summarises the results of the tibia vertical events detection in six neurological patients. There were no missing events.

Table 1: Tibia vertical events detection. (TE=time event, GC=gait cycle and IC=initial contact)

Patient	No. of events detected	Mean of stride time (s)	Mean ± SD (TE % of GC before IC)	Mean ± SD (TE in % of GC before IC compared to 13% of GC before IC)
1	37	2.56	20.47±8.06	7.47±8.06
2	50	1.39	19.05±5.41	6.05±5.41
3	16	1.76	14.10±2.79	1.10±2.79
5	53	2.12	28.91±7.71	15.91±7.71
6	36	1.73	19.67±5.53	6.67±5.53
7	39	1.88	17.02±5.79	4.02±5.79

There was a problem with the data obtained from Patient 4, therefore it was not possible to make an analysis and no result is reported.

Discussion and Conclusions

The tibial vertical event is reported to occur at about 13% of the GC before the initial heel contact in normal gait [5]. The results obtained from the experiment showed that the events detected are between 14-29% of GC before initial contact. This difference is possibly due to the delay of the heel strike events detected by the footswitch. There may be other physical reasons for this difference but further research is required. Furthermore, the detection algorithm uses the first maximum of the correlation coefficient value after the positive threshold as the time of the event occurred, but the exact time of the event occurring should be at the most maximum correlation coefficient value. However, most of the events were detected earlier than the actual event and this would allow a delay to be introduced, for example to trigger the stimulation. The detection algorithm has an advantage of comparing a threshold with the correlation coefficient for the event detection as the correlation coefficient is within -1 to 1 only and not dependent on individual absolute values. The segment angle has a larger range of values and will vary between the subjects, making the threshold more difficult to set.

The detection algorithm has detected the desired events for five patients using the same sample window from a healthy subject and for one patient using a sample window from their own data. It is a remarkable result of this research, that the data from one healthy subject and not a combination from several people has been used to detect correctly and accurately the events. It is hypothesised that more events could be detected using the algorithm with different selective sample windows. It is anticipated that the algorithm can be executed in a microcontroller producing a very small timing delay between event detected and delivery of stimulation pulses.

References

[1] J. H. Burridge, K. Elessi, R. M. Pickering, and P. N. Taylor, "Walking on an Uneven Surface: The Effect of Common Peroneal Stimulation on Gait Parameters and Relationship Between Perceived and Measured Benefits in a Sample of Participants With a Drop-Foot," *Neuromodulation,* vol. 10, pp. 59-67, 2007.

[2] I. A. Wilkinson and P. N. Taylor, "Retrospective study of patients using Funcional Electrical Stimulation for drop foot correction and increased hip stability," in *9th Annual Conference of International FES Society*, Bournemouth, UK, 2004, pp. 305-307.

[3] P. A. Wright, J. H. Burridge, D. J. Ewins, G. E. Mann, D. L. McLellan, I. D. Swain, P. N. Taylor, and D. E. Wood, "The Compustim 10B in stroke: control algorithms and patient selection criteria," in *4th Annual Conference of International FES Society*, Sendai, Japan, 1999.

[4] N. Abdul Malik, P. H. Chappell, D. E. Wood, and P. N. Taylor, "Measurement of the relative joint angle and acceleration of the lower limb during walking," in *13th Annual Conference of International FES Society*, Freiburg, Germany, 2008.

[5] J. Perry, *Gait analysis normal and pathological function*. Thorofare, N.J.: SLACK, 1992.

Acknowledgements

This work comprises a component of PhD studies of the first author, sponsored by the Ministry of Higher Education of Malaysia and International Islamic University of Malaysia.

Author's Address

Noreha Abdul Malik

ESD Group, School of Electronics and Computer Science, University of Southampton, UK.
nam06r@ecs.soton.ac.uk

Can the coherence between two EMG signals be used to measure the voluntary drive in paretic muscles?

Luo R[1], Norton J[2], Donaldson, N[1]

[1] Implanted Devices Group, University College London, UK

[2] Department of Surgery
University of Alberta Hospital/Stollery Children's Hospital, Edmonton, Alberta

Abstract

Coherence is found in EMG-EMG signals during voluntary contraction of the muscles that work synergistically. This is resultant from the shared drive of motor units to the different motorneuron pools [1]. We would like to study the relationship of EMG signals between different muscle pairs during FES cycling using the coherence analysis. The hypothesis is that the frequency at which the coherence between two synergistically activated muscles peaks is related to the voluntary drive and is not influenced by the stimulation with suitable frequency. If that is the case, coherence can then serve as an indication of presence of voluntary drive and could be used for feedback control of FES cycling.

***Keywords**: EMG, Coherence, Pooled coherence, FES cycling, Voluntary drive.*

Introduction

We are trying to find a way to measure of voluntary drive to the muscles in incomplete SCI patients during FES cycling. A controller can then use this measurement to adjust the stimulation intensity accordingly. The possibility of using the rms EMG signal from short time windows in the time domain as an input to the controller of a stimulator was discussed previously [2]. Here we introduce EMG-EMG coherence as an alternative input to the controller. Challenges to using the subject's voluntary drive to control the stimulation of FES cycling include the presence of large stimulation artefacts. We hypothesise that the frequency at which the coherence between two synergistically activated muscles peaks is related to the voluntary drive and is not influenced by the stimulation frequency. Coherence can then serve as an indication of presence of voluntary drive and could be used for feedback control of FES cycling.

Coherence can be used to examine the relationship between two time series in the frequency domain [3]. An EMG signal measured at successive times spaced uniformly is considered to be a time series. In able-bodied subjects, EMG-EMG coherence is found in certain frequency bands in muscles that co-contract during common motor tasks [4-7]. It is generally stronger in two frequency bands: lower frequency coherence at 5-18Hz and higher frequency coherence at 24-40Hz. The lower one is thought to arise subcortically while the higher frequency is thought to originate from the cortex[8]. It may therefore be possible to identify the source of drive to the muscles by inspecting the coherence between their EMGs.

Methods

Coherence measures the similarity of two signals in their frequency contents. The coherence C_{xy} between two signals x and y is defined as follows:

$$C_{xy} = \frac{|G_{xy}|^2}{G_{xx}G_{yy}} \quad (1)$$

Where G_{xy} is the cross-spectral power density between x and y, and G_{xx} and G_{yy} are the power spectral density of x and y respectively [9]. The power density describes how the power of the time series is distributed in the frequency domain. It is the Fourier transform of the autocorrelation function. Coherence values vary between 0 and 1. Unity indicates that x and y are perfectly matched, and zero shows that x and y are completely unrelated.

Theoretically, coherence should only be used for stationary data due to the nature of the Fourier transform. Therefore data collected at the onsets and offsets of muscle contractions, in which the data changes rapidly, should not be included. It is also difficult to perform coherence analysis on short segments of data. For the cycling process, there is not enough quasi-stationary EMG data within one revolution because the region of muscle co-activation is very short. One solution is to combine the selected EMG data from many revolutions which then will give us enough data to generate meaningful coherence. This method is called "pooled coherence" [9]. The new problem is

that when combining the EMG data from many revolutions, there are discontinuities at the boundaries of the data. To solve this problem, the data is passed through Hanning windows to smooth the ends of the data without significantly affecting the bulk of the data points.

To test the hypotheses, three experiments were conducted on a semi-recumbent tri-cycle (trike). Five able-bodied subjects were recruited for each experiment. The subjects were asked to cycle following a metronome beating once per second. In this way the cycling cadence was kept roughly constant. Simple differential EMG amplifiers were used for the experiments without stimulation; and blankable EMG amplifiers were used for the ones with stimulation.

The aim of Experiment 1 was to find coherence from different muscle pairs during cycling. EMG from three different muscles, Vastus Medialis (VM), Vastus Lateralis (VL) and Rectus Femoris (RF) were recorded bilaterally for 3 minutes. Coherence was calculated for each muscle pair. The coherence plots between each pair of the muscles from both legs were also compared.

The rms EMG amplitude from a time window increases with increasing effort levels [2]. For the coherence analysis, we select EMG signals from a time window in each revolution, so it is necessary to look at how the amplitude and frequency of the significant coherence changes with effort levels. In Experiment 2, a cycling computer was used to control the resistance applied to the back tyre of the trike. Five randomised effort levels were used in each test.

Two points were investigated in Experiment 3: 1) whether the coherence would be influenced by stimulation; 2) the effect of changing the stimulation frequency on the coherence spectra. This was done by using a gated stimulator running at 15Hz, 20Hz and 30Hz in three tests, each performed at the same effort level. Stimulation pulses were applied to the left VL during its activation range, while recording from both VL and VM. These frequencies were chosen because they fall in the range of the coherence peaks and are commonly used for FES. The stimulation pulses were triggered by a commutator signal, the timing of which was determined by the crank angle.

For all three experiments, the sampling frequency was 5 kHz. An average of 600+30(SD) ms EMG data was selected in each revolution and then passed through a Hanning window. The resultant data clips are joined together and then rectified before being analysed using a modified version of Neurospec V2.0 in MATLAB [10].

Results

Results for Subject A:

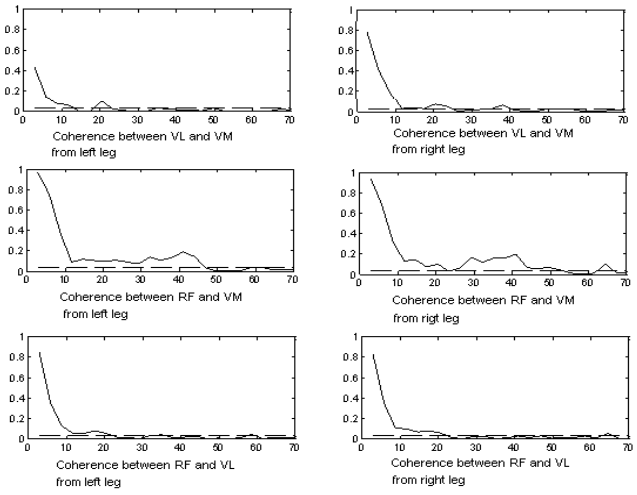


Fig 1: Coherence (y-axis 0-1) plot versus Frequency (x-axis 0-70Hz) between different muscle pairs during cycling without stimulation. The dashed lines in Fig 1, Fig 2 and Fig 4 are the 95% confidence limits.

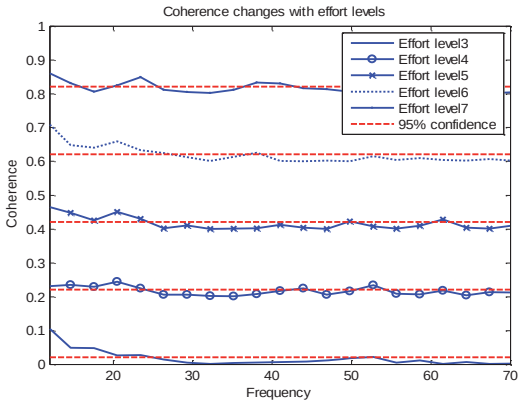


Fig 2: Coherence between VM and VL for 5 effort levels during cycling without stimulation. Successive plots are offset by 0.2 for clarity.

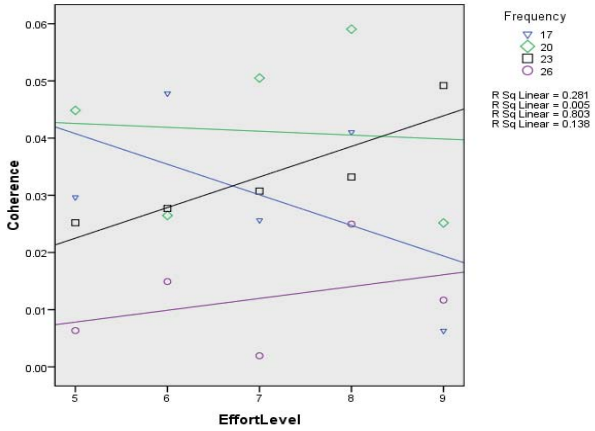


Fig 3: Coherence at effort levels 5-9 for frequencies between 17-26Hz

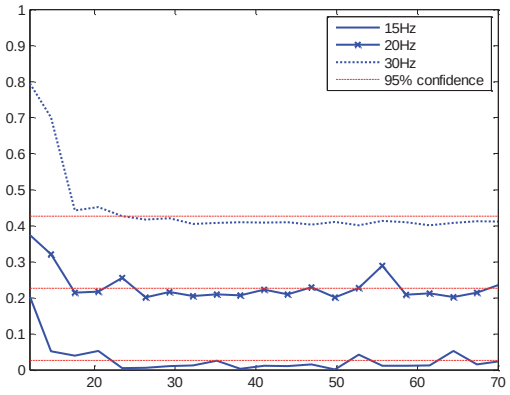


Fig 4: Coherence plot between VM and VL for different stimulation frequencies.

Discussion

Any data below 10Hz is ignored as it is most likely due to motion artefacts. Fig 1 shows how the shape of the coherence curves differ for different muscle pairs for Subject A. Coherence values above the 95% confidence limits are considered to be significant. For the VM and VL pair, there is a single peak around 20Hz, while there is a wide range of frequencies with significant coherence for the RF and VM pair. For all three muscle pairs, we can say that they share a high coherence around 20Hz. Comparisons of coherence spectra from all 5 subjects show: 1) Similarity between the same pair of muscles in opposite legs; 2) Different shapes for different muscle pairs; 3) Different shapes for a given pair of muscles between subjects; 4) Different peak frequencies between subjects.

Coherence peaks appear at about the same frequency for different effort levels as shown in Fig 2 (between 20-25Hz for Subject A). Fig 3 shows the coherence against different effort levels at the frequencies where the coherence is significant (17-26Hz for Subject A). At 23Hz, the coherence shows an increasing trend with the effort levels, as well as a high R^2 value of 0.803. This is also true for the other 4 subjects, although at different frequencies (17-33Hz) and with R^2 values ranging from 0.673 to 0.803.

Fig 4 shows the effect of changing stimulation frequency to the coherence spectra for VM and VL. The coherence peaks remain in the same range as when there was no stimulation, which implies that the stimulation did not cause false peaks in the coherence spectra.

Conclusions

Significant coherence can be found between muscles that work synergistically. The coherence between different muscle pairs varies in pattern and shape. We do not always get a single peak frequency, instead a range of significant coherence may be found. The feasibility of using the area under the coherence curve as an indication of effort level needs to be investigated. For all 5 subjects, there is a frequency at which the coherence is positively related to the effort levels between VM and VL. Therefore when there is no stimulation, coherence during cycling at certain frequencies may be used as an indication of how much effort the subject is making. Further experiments still need to be done to check if this is still the case when using stimulation.

In these experiments, three minutes of data were recorded for each test. This is rather long compared to the 15s of recording used for the time domain analysis [2]. We are looking to reduce recording time for the coherence analysis.

References

[1] Farmer S, Gibb J, Halliday D, Harrison L, James L, Mayston M, et al. Changes in EMG coherence between long and short thumb abductor muscles during human development. The Journal of Physiology 2007;(579):389-402.

[2] Luo R, Fry M, Donalson N. A statistical approach to myoelectric control of FES cycling. 2010.

[3] Rosenberg JR, Amjad AM, Breeze P, Brillinger DR, Halliday DM. The Fourier approach to the identification of functional coupling between neuronal spike trains. Prog Biophys Mol Biol 1989;53(1):1-31.

[4] Baker SN, Olivier E, Lemon RN. 20 Hz coherent oscillations in cortical and EMG recordings from a monkey performing a precision grip task. Journal of Physiology-London 1996 Jul;494P:64-5.

[5] Baker SN, Olivier E, Lemon RN. Coherent oscillations in monkey motor cortex and hand muscle EMG show task-dependent modulation. Journal of Physiology-London 1997 May 15;501(1):225-41.

[6] Kilner JM, Baker SN, Salenius S, Jousmaki V, Hari R, Lemon RN. Task-dependent modulation of 15-30 Hz coherence between rectified EMGs from human hand and forearm muscles. Journal of Physiology-London 1999 Apr 15;516(2):559-70.

[7] Kilner JM, Salenius S, Baker SN, Jackson A, Hari R, Lemon RN. Task-dependent modulations of cortical oscillatory activity in human subjects during a bimanual precision grip task. Neuroimage 2003 Jan;18(1):67-73.

[8] Brown P. Cortical drives to human muscle: the Piper and related rhythms. Progress in Neurobiology 2000 Jan;60(1):97-108.

[9] Amjad AM, Halliday DM, Rosenberg JR, Conway BA. An extended difference of coherence test for comparing and combining several independent coherence estimates: Theory and application to the study of motor units and physiological tremor. Journal of Neuroscience Methods 1997 Apr 25;73(1):69-79.

[10] Halliday D. NeuroSpec 2.0 User Guide. 2008.

Stimulus-response curves: Effect of recording site and inter-electrode distance

Kamavuako EN, Farina D

Center for Sensory-Motor Interaction (SMI), Department of Health Science and Technology, Aalborg University, Aalborg, Denmark

Abstract

This paper investigates whether the indexes of the stimulus-response (SR) curves of human motor nerves depend on the recording site and on the inter-electrode distance (5-35mm) in 18 healthy subjects. SR curves were measured by stimulating the peroneal nerve, with the compound muscle action potential (CMAP) recorded on the tibialis anterior muscle using a linear adhesive array of 8 electrodes. Each SR curve was characterized using the threshold intensity of stimulation to obtain 5, 10, 50, 90 and 95% ($I_{5\%}$, $I_{10\%}$, $I_{50\%}$, $I_{90\%}$, and $I_{95\%}$) of the CMAP computed on the basis of four parameters (peak, area, peak-to-peak, and total area). The results showed no significant differences between recoding sites and inter-electrode distances. Although no significant difference was found between parameters, the peak-to-peak value had the most consistent threshold intensities across inter-electrode distances. It is concluded that electrode positioning along the direction of the muscle fibers and inter-electrode distance do not have a significant influence on the characteristics of the normalized SR curve.

Keywords: *Stimulus-response curve, CMAP, Electrical stimulation.*

Introduction

A stimulus-response (SR) curve is a graphic display of the compound muscle action potential (CMAP) size in response to stimuli of increasing intensity [1]. SR curves have found applications in the assessment of the muscle fibers in individual motor units (MUs) [1] and in the study of the recovery functions of muscle fibers [2, 3]. The typical recording schemes are the belly-tendon configuration, the bipolar derivation or the linear array of electrodes. There is no standardization on the optimal recording site or the inter-electrode distance, which can allow comparison across studies. The aim of this study was to investigate whether the threshold intensities obtained from SR curves were dependent on the recording site and inter-electrode distance.

Materials and Methods

Subjects

The experiments were conducted on 18 healthy men (age range, 21 - 32 yrs, and mean 25.4 yrs) in accordance with the Declaration of Helsinki and approved by the local ethical committee. Subjects gave written informed consent to the experimental procedures.

Electrical stimulation and EMG recordings

CMAPs were recorded from the tibialis anterior muscle of the right (dominant) leg. Ag-AgCl surface electrodes were used for electrical stimulation. CMAPs were elicited with electrical stimulation of the peroneal nerve using a voltage-controlled current-source stimulator (NoxiSTIM, JNI Biomedical A/S, Aalborg, Denmark). The bipolar stimulation was applied with one electrode just below the head of the fibula and the other at the popliteal fossa along the medial border of the biceps femoris tendon [3]. The two electrodes were at a distance of ~10 cm.

The EMG signals were detected in bipolar derivation with a linear adhesive array of 8 electrodes (5-mm inter-electrode distance) located between the innervation zone and the distal tendon. The location of the main innervation zones was estimated from signals recorded in test contractions with a dry array of electrodes. The adhesive array was oriented along the direction of the muscle fibers. Signals were amplified with gain 1000 by a multi-channel surface EMG amplifier (EMG16, LISiN, Torino, Italy), band-pass filtered (20-500 Hz), A/D converted on 12 bits (resolution: 2.44μV per least significant bit), and sampled at 10 kHz. The ground electrode was placed at the ankle of the left leg.

Procedures

The subjects sat comfortably on a dental chair. After placement of the stimulating and EMG electrodes, the right leg was fixed to a custom made pedal for ankle joint stabilization with the knee extended at 135º. The SR curves to single stimuli were determined for all recordings. A custom written LabVIEW program increased the amplitude of a 0.2-ms test stimulus in steps of 6% from sub-threshold level to the level at which three consecutive responses gave no further increase in the amplitude of the CMAPs. The sub-threshold level was manually set at the beginning of each experiment.

Data analysis

Each SR curve was normalized with the maximum value and the threshold intensities $I_{5\%}$, $I_{10\%}$, $I_{50\%}$, $I_{90\%}$, and $I_{95\%}$ for a response of 5%, 10%, 50%, 90%, and 95% of the maximum response were estimated with linear interpolation. The SR curves were determined as the relation between current intensity and the following parameters: 1) *peak* and 2) *area* of the first negative peak of the CMAP, 3) *peak-to-peak* amplitude and 4) *total area* under the CMAP.

In the first step we analyzed if there was a difference between recording sites for all parameters. In the second step, the effect of inter-electrode distance (5 to 35 mm) was investigated. Inter-electrode distances were obtained by summing consecutive bipolar recordings. A three-way analysis of variance (ANOVA) with factors the parameters (*peak, area, peak-to-peak, total area*), the recording sites and intensities ($I_{5\%}$, $I_{10\%}$, $I_{50\%}$, $I_{90\%}$, $I_{95\%}$) was used to compare the SR curves. ANOVA was also applied for analyzing the effect of inter-electrode distance (5, 10, 15, 20, 25, 30, 35 mm). P-values less than 0.05 were considered significant. In the third step, we normalized all threshold intensities by $I_{50\%}$ and we quantified the standard error (SE) across distances in order to study which parameter had the smallest sensitivity to inter-electrode distances.

Results

Figure 1 shows an example of normalized SR curves computed using the *area* of the first negative peak from seven channels from one subject. There was no significant difference in SR curves between different recording sites (P=0.260). However a trend was observed between parameters (P=0.067) with *total area* having values far away compared to the other three parameters. Comparison between different inter-electrode distances showed no significant difference either between parameters (P = 0.240) or between distances (P=0.506).

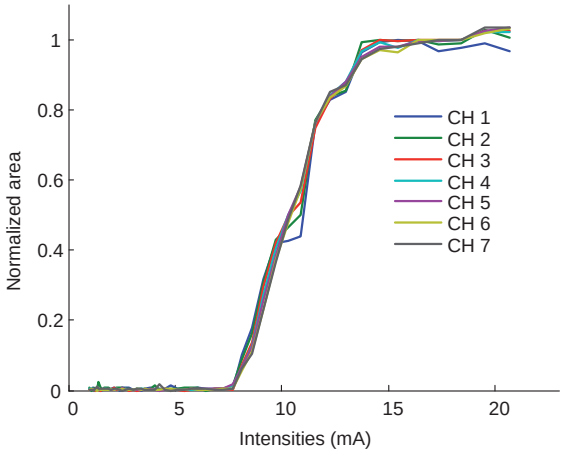


Figure 1: Representative illustration of SR curves computed based on the area of the first negative peak of the compound muscle action potential for different channels or recording sites.

To compute the spread, we first averaged across subjects and then computed the SE across distances for each normalized threshold intensity and each parameter. The results that are summarized in Table 1 show that *peak-to-peak* parameter had the lowest SE; that is it produced the most consistent results across inter-electrode distances.

Table 1: Standard Error (SE) values computed across inter-electrode distances as a measure of consistency for different parameters (*Peak, Peak-to-peak, area, total area*) and normalized intensities ($I_{5\%}/I_{50\%}$, $I_{10\%}/I_{50\%}$, $I_{90\%}/I_{50\%}$, $I_{95\%}/I_{50\%}$)

	Peak	Peak-to-Peak	Area	Total area
$I_{5\%}/I_{50\%}$	0.0092	0.0034	0.0077	0.0067
$I_{10\%}/I_{50\%}$	0.0055	0.0022	0.0022	0.0088
$I_{90\%}/I_{50\%}$	0.0053	0.0042	0.0066	0.0035
$I_{95\%}/I_{50\%}$	0.0079	0.0070	0.0164	0.0070
Mean	0.0070	**0.0042**	0.0082	0.0065

Discussion

This study investigated the dependency of the SR curves on the recording site and inter-electrode distance along the direction of muscle fibers. The results showed that normalized threshold intensities ($I_{5\%}$, $I_{10\%}$, $I_{50\%}$, $I_{90\%}$, $I_{95\%}$) do not statistically depend neither on the recording site nor on the distance between the electrodes.

These results indicate that if the electrodes are positioned along the direction of the propagation of the CMAP, the intensity indexes computed from the SR curves will be statistically the same. This result is a consequence of the propagation of the CMAP along the fiber direction with an almost unchanged shape (Fig. 2).

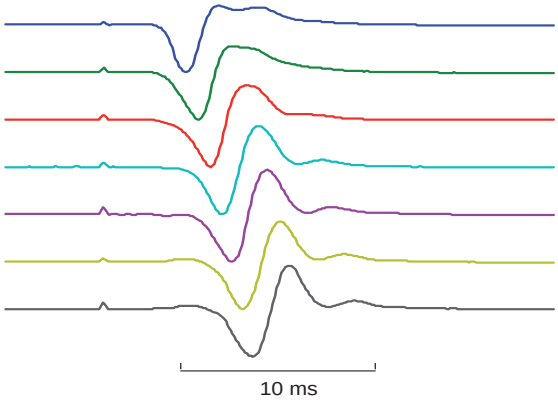


Figure 2: Example of multisite recording showing propagation of the CMAP from one subject. The shape of the CMAP changes slightly at different channels.

Furthermore, the results also indicate that in bipolar recording configuration, the distance between the two electrodes does not influence the SR curve as long as both electrodes are placed along the direction of propagation. This is due to the normalization procedure that compensate for changes in amplitude due to the recording derivation.

Our investigation did also include the difference between four parameters (*Peak, Peak-to-peak, area, total area*) of the CMAP that can be used to compute the SR curve. We found no significant difference between these parameters, although the *total area* of the CMAP was the one most sensitive to changes in recording site. Furthermore the parameters provided statistically equal values of intensities across different inter–electrode distances. However we recommend the use of *peak-to-peak* of the CMAP as the optimal parameter because it showed the lowest standard error across distances, thus providing the most consistent normalized threshold intensities.

Conclusion

The present study has shown that the SR curve does not depend on the recording site or on the inter-electrode distance along the propagation of muscle fibers. This result indicates that results from different studies can be compared if the electrodes are placed along the direction of the muscle fibers between the innervation zone and tendon regions, even if different locations and inter-electrode distances are used.

References

[1] Henderson RD, Ridall GR, Pettitt AN, McCombe PA, Daube JR. The stimulus-response curve and motor unit variability in normal subjects and subjects with Amyotrophic Lateral Sclerosis. Muscle Nerve 2006; 34:34-43.

[2] Kamavuako EN, Hennings K, Farina D. Velocity recovery function of the compound muscle action potential assessed with doublet and triplet stimulation. Muscle Nerve. 2007; 36: 190-196.

[3] Kamavuako En, Farina D. Time-Dependent Effects of pre-conditioning activation on muscle fiber conduction velocity and twitch torque. Muscle nerve 2010; in press.

[4] Lee HJ, Delisa JA. Manual of nerve conduction study and surface anatomy for needle electromyography. 4 ed, Lippincott Williams & Wilkins 2005, USA

Author's Address

Name: Ernest Nlandu Kamavuako

Affiliation: Center for Sensory-Motor Interaction (SMI), Department of Health Science and Technology, Aalborg University, Fredrik Bajers Vej 7- D3, 9220 Aalborg, Denmark

email: enk@hst.aau.dk

homepage: www.hst.aau.dk/~enk

Name: Dario Farina

Affiliation: Center for Sensory-Motor Interaction (SMI), Department of Health Science and Technology, Aalborg University, Fredrik Bajers Vej 7- D3, 9220 Aalborg, Denmark

email: df@hst.aau.dk

homepage: www.hst.aau.dk/~df

A Preliminary Study of Muscle Fatigue Evaluation Using M-waves elicited by additional pulses for Rehabilitation with FES

Miura N[1], Watanabe T[1,2], Kanai H[1,2]

[1] Graduate School of Engineering, Tohoku University, Sendai, Japan

[2] Graduate School of Biomedical Engineering, Tohoku University, Sendai, Japan

Abstract

Early occurrence of muscle fatigue is one of problems on FES. We focused on using M-waves elicited by the additional pulses in muscle fatigue evaluation during rehabilitation training with the surface stimulation system. In this report, a preliminary test of measurement of M-waves elicited by the additional pulses was performed under the two conditions: knee extension force production under the isometric condition and knee extension angle control by fuzzy controller based on the cycle-to-cycle control. The change in M-wave elicited by the single pulse in a burst stimulation for FES was less relevant result against decrease of force production under the isometric condition and increase of burst duration under the knee extension angle control during the muscle fatiguing. The decreasing of the M-wave elicited by the 2nd pulse of a double-pulse was observed with both experiments. These results suggest that M-waves elicited by the additional pulses would provide useful information for muscle fatigue evaluation.

Keywords: *FES, fatigue, M-wave, double pulse, cycle-to-cycle*

1. Introduction

The therapeutic effects during rehabilitation with FES have been shown to improve muscle strength [1-2] and muscle recruitment [2-3]. The repetitive movement therapy mediated by the electrical stimulation has the potential to facilitate motor relearning [4].

However, early occurrence of muscle fatigue is one of problems on FES. Therefore, condition of activity of electrically stimulated muscle is considered to provide useful information for training with electrical stimulation.

Surface electromyographic activity elicited by electrical stimulation (M-wave) has a possibility of being used as an indicator of the muscle fatigue. We proposed using M-waves elicited by additional pulses inserted into a stimulus pulse train in muscle fatigue evaluation, and found the effectiveness of using the M-waves for prolonged continuous electrical stimulation under the isometric condition [5-6].

This study focused on using the M-wave for muscle fatigue evaluation in training with surface FES applying repeated burst pulses. In this report, M-waves elicited by additional pulses inserted into repetitive burst stimulation pulses were tested preliminary under the isometric condition and knee extension angle control.

2. Experimental Methods

The vastus lateralis were stimulated through surface electrodes (SRH5080, Sekisui Plastics), and M-waves were measured repetitive under the following two conditions with 3 neurologically intact subjects.

a) Knee extension force production under the isometric condition

b) Knee extension angle control by the cycle-to-cycle control

The subjects were seated in the chair (Musculator GT-30, OG Giken), and relaxed his legs during experiments.

In the measurement condition a), muscle force produced by bursts of electrical stimulation was measured with M-waves under the isometric condition. The burst duration of stimulation pulses was 750ms (15 pulses in a burst), since the burst duration to produce the maximum knee extension angle from the neutral position was 500ms to 1,000ms in our preliminary experiment. Stimulus burst pulses with and without an additional pulse were applied alternately in one experimental session (Fig. 1). An additional pulse was inserted into a stimulus burst after the fifth pulse because the shape of M-wave varied in the first few pulses in a burst [7]. Therefore, the 5th pulse and the additional pulse consist of a “double pulse". The inter pulse interval (IPI) of the double-pulse was 2ms, 2.5ms and 3ms, which was changed in turn. The time interval between stimulation bursts was set at 1s and fixed in one experimental session.

In the measurement condition b), knee joint angle was controlled by regulating burst duration of

stimulation pulses by the fuzzy FES controller based on cycle-to-cycle control [8-9]. Electric goniometer (M180, Penny & Giles) was used to measure the knee joint angle. Knee joint angle at the resting was approximately 75 degree, and target angle was 30 degree (0 degree means full knee extension). The additional pulses were inserted into stimulus burst pulses under the same condition as the measurement condition a).

In one experimental session, the number of repetitive stimulation was more than 200 in both experiments. Pulse setting was monophasic pulse, 50ms period, 0.3ms width. Pulse amplitude was determined to develop full knee extension by a stimulation burst. The output signals of EMG amplifier, the goniometer and the force transducer (DTG-20, DIGITECH) were recorded by personal computer through AD converter (sampling frequency: 20kHz for M-wave and force, 40Hz for joint angle). The M-wave data for about 1.5ms including stimulation period were removed and set to 0mV to remove the artifact of electrical stimulation pulse. The M-wave elicited by the 2nd pulse of a double pulse was obtained by subtracting the M-wave elicited by the 4th pulse from the M-wave elicited by the double pulse in the same stimulation cycle [5-6].

3. Result and Discussion

Fig. 2 shows an example of the M-waves elicited by the 4th, 5th (double-pulse) pulse in the same stimulation cycle and the derived M-wave by the additional pulse under the isometric condition. As shown in this figure, the M-waves by the additional pulse were appropriately derived. However, under the angle control, there was a little difference between the 4th and the 5th M-waves without additional pulse. Although the difference was small, the deriving method of the M-wave by the additional pulse will be studied in more detail.

Fig. 3 shows an example of the measurement results under the condition a). The force production decreased as the number of cycles increased because of muscle fatigue elicited by the burst stimulation.

Fig. 4 shows an example of the measurement results under the condition b). Since the mean value of stimulus burst interval and the number of stimulus pulse in a burst was 1.0±0.1 sec and 9.3 ±3.3 pulses, the condition of applied electrical stimulation is considered to be similar as the measurement condition a). The burst duration increased in the early stimulation cycles, and decreased until about the 30th cycle, afterward increased as the number of cycles increased. After the 30th cycle, the burst duration increased because of muscle fatigue elicited by the burst stimulation.

As seen in Fig. 3, the peak-to-peak amplitude of M-wave elicited by the 4th pulse in a burst pulse (VM4th) increased in the early stimulation cycles, afterward decrease as the number of cycles increased. In our previous study under the isometric condition, high correlation coefficients between the force and the amplitude of the M-wave in long lasting constant electrical stimulation were found [5-6]. However, correlation coefficient between the force and VM4th was negative value in two subjects (Subject A:-0.34, Subject B:-0.67, Subject C:0.95). VM4th under the condition of knee extension angle control as shown in Fig. 4 was increased against the burst duration increased after about the 30th cycle. From these results of VM4th, it is suggested that the change in the amplitude of the M-wave elicited by the single pulse for FES control in a burst does not provide effective information of muscle fatigue for repeated activation by FES.

The peak-to-peak amplitude of the M-wave elicited by the 2nd pulse of a double-pulse (3ms interval: VMD3m, 2.5ms interval:VMD2.5m, 2ms interval: VMD2m) decreased is both condtion a) and b). The decrease of the M-wave elicited by the 2nd pulse of a double-pulse was larger with shorter interval of double-pulse in the early cycles as seen in the previous report [5-6]. In general, the double-pulse stimulation is used to measure the refractory period, and the large size of motor unit is known to

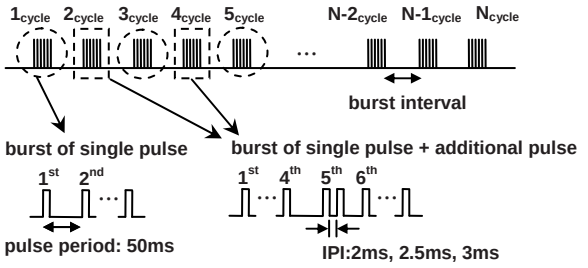


Fig.1 Stimulus pulse condition

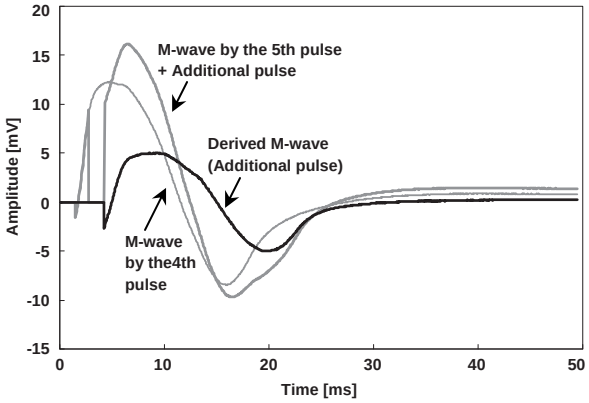


Fig.2 Example of the M-waves in the same stimulation cycle and the derived M-wave by the additional pulse under the isometric condition.

have short refractory period [10]. The decrease of the amplitude of the M-wave elicited by the 2nd pulse of a double-pulse is considered to be related to the decrease of the number of activated motor units that have longer refractory period than pulse interval of double-pulse. Therefore, it is suggested that the M-wave elicited by the 2nd pulse of a double pulse can provide information of muscle fatigue.

4. Conclusion

In this paper, M-waves elicited by the additional pulses were tested preliminarily under the condition of repeated stimulation in training with surface FES. The M-wave elicited by the single pulse in a burst could not provide effective information of muscle fatigue for repeated stimulation. The amplitude of the M-wave elicited by the 2nd pulse of a double-pulse showed decrease in the early cycles depending on the IPI of double-pulse with increasing fatigue. M-waves elicited by the additional pulses are expected to provide useful information of muscle activation state. Further studies are necessary to find an effective evaluation method for muscle fatigue using M-wave.

References

[1] Granz M, et al., "Functional Electrostimulation in poststroke rehabilitation: a meta-analysis of the randomized controlled trials," Arch Phys Med Rehabil, 77: 549-553, 1996

[2] Yan T, et al., "Functional Electrical Stimulation Improves Motor Recovery of the Lower Extremity and Walking Ability of Subjects With First Acute Stroke: A Randomized Placebo-Controlled Trial," Stroke, 36: 80-85, 2005

[3] Nwesam CJ, and Baker LL, "Effect of an electric stimulation facilitation program on quadriceps motor unit recruitment after stroke," Arch, Phys Med Rehabil, 85: 2040-2045, 2004

[4] Sheffler LR, and Chae J, "Neuromuscular electrical stimulation in neurorehabilitation," Muscle & Nerve, 35-5: 562-590, 2007

[5] Watanabe T, et al., "A possibility of using M-waves evoked by double pulses for evaluating muscle fatigue on FES control," Abstract Book of 4th International Congress of the International Neuromodulation Society, 259, 1998 (Joint Meeting with the 3rd Annual Conference of IFESS)

[6] Watanabe T, et al., "The Possibility of Using M-waves Related to Double Pulses for Evaluating Muscle Fatigue in FES Control," Trans. of Japanese Soc. Med. and Biolog. Eng., 38-1: 42-48, 2000 (in Japanese)

[7] Arifin A, et al., "Design of Fuzzy Controller of the Cycle-to-Cycle control for Swing Phase of Hemiplegic Gait Induced by FES," IEICE Trans. Inf. & Syst., E89-D-4: 1525-1533, 2006

[8] Watanabe T, et al., "Preliminary Tests of a Practical Fuzzy FES Controller Based on Cycle-to-Cycle Control in the Knee Flexion and Extension Control," IEICE Trans. Inf. & Syst., E92-D-7: 1507-1510, 2009

[9] Miura N, et al., "A Preliminary Test of Muscle Fatigue Evaluation Using M-wave for Rehabilitation with Electrical Stimulation," Abstract Book of 14th Annual Conference of IFESS society, 99-101, 2009

[10] Horcholle-Bossavit G, et al., "Activation of Cat Motor Units by Paired Stimuli at Short Intervals," J. Physiol. 387: 385-399, 1987

Acknowledgements

This study was supported in part by the Ministry of Education, Culture, Sports, Science and Technology of Japan under a Grant-in-Aid for Scientific Research (B), and the Saito Gratitude Foundation.

Author's Address

eMail:naoto.miura@bme.tohoku.ac.jp

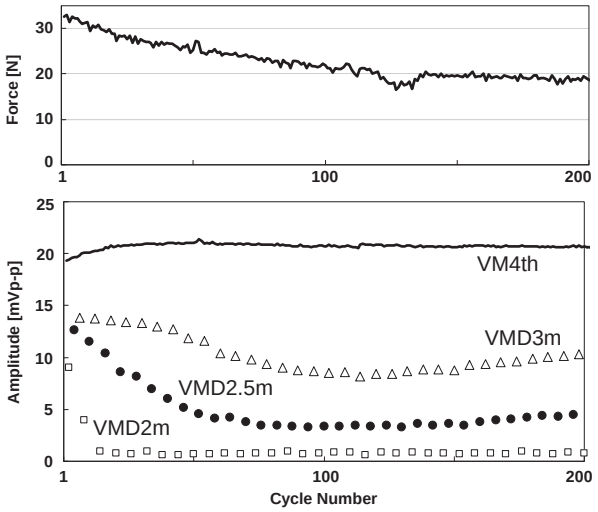


Fig.3 Knee extension force production under isometric condition. (Subject A). Force (Top) and peak-to-peak amplitude of each M-wave (Bottom) are shown.

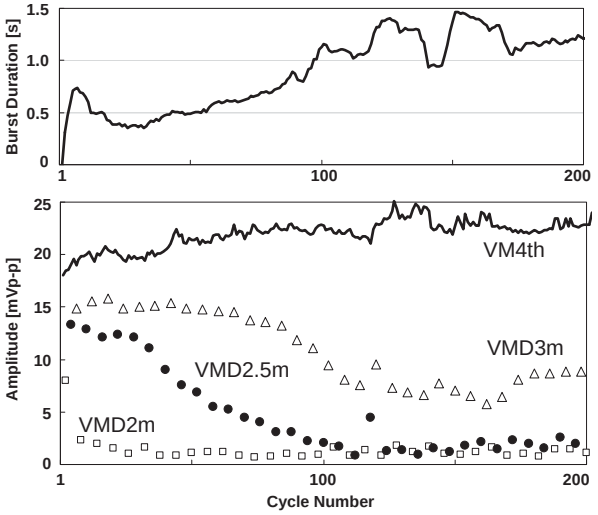


Fig.4 Knee extension angle was controlled by fuzzy controller based on the cycle-to-cycle control. (Subject A). Burst duration (Top) and peak-to-peak amplitude of each M-wave (Bottom) are shown.

Torque Prediction Based on Evoked EMG in Fatiguing Muscle Toward Advanced Drop Foot Correction

Zhang Q, Hayashibe M, Sablayrolles B, Azevedo-Coste C

DEMAR project, LIRMM - INRIA, Montpellier, France

Abstract

Electrical stimulation (ES) has been applied since 1961 for the correction of hemiplegic drop foot. One main drawback of the technique is the occurrence of early fatigue. Therefore, it is essential to predict force generation for precise ES closed loop control when the stimulated muscle becomes fatigued. This work aims to predict ankle torque using stimulus evoked EMG (eEMG) during different muscle fatigue states. Five healthy subjects participated in our study. Conventional stimulation for drop foot correction was applied by surface stimulation in sitting position. The results showed that during long-term stimulation the generated torque gradually declined due to muscle fatigue, the muscle activity (EMG) performed quite differently in different fatigue level. In this work, we carried out the torque prediction with an adapted parameters model according to muscle fatigue state by reidentification using the latest measurement. The prediction was improved with 21%~90.9% comparing to the fixed parameters model. The results revealed a promising approach to use evoked EMG for fatigue compensation in the application of drop foot correction.

Keywords: *drop foot correction, muscle fatigue, stimulus evoked EMG, electrical stimulation*

Introduction

Hemiplegic drop foot (DF) is a condition resulting from stroke where the subject cannot lift his or her foot or dorsiflex [1]. The lack of dorsiflexion results in a dragging of the leg and as a result has a significant impact on the person's gait [1]. Electrical stimulation (ES) is one of the existing solutions which are used to correct drop foot. Many researchers paid most attention to get optimal stimulation intensity profiles for the affected leg. An optimised stimulation envelope to reproduce the EMG pattern observed in the tibialis anterior (TA) during healthy gait was proposed in [1]. The changes in TA activity with walking speed was further considered to enable adaptive FES intensity envelope in [2]. A method providing with precise timing adaptation of the ES pattern to ensure a good coordination of the healthy and affected legs was proposed in [3]. However, in practice, the clinical implementation of ES for drop foot correction in hemiplegia is a challenging task. One of the challenges is the rapid onset of fatigue on the stimulated muscle. Thus, it is required to adjust stimulation parameters to provide optimal and tolerable treatment with minimal muscle fatigue. In previous researches, optimal stimulation patterns or modulation of stimulation parameters were proposed to reduce fatigue. However, no consensus was reached to date. Moreover, fatigue phenomenon is unavoidable with repetitive or prolonged stimulation and it usually occurs fast with ES on paralyzed muscles. Therefore, it is essential to predict force generation for precise ES closed loop control when the stimulated muscle becomes fatigued.

The aim of this work is to predict ankle torque preliminarily in healthy subjects for the application of ES induced ankle dorsiflexion. In our study, we propose to identify the eEMG-torque model adaptively to improve torque prediction.

Material and Methods

Experimental Setup

Five healthy subjects participated in this study. A commercial stimulator (Prostim) was used to induce sufficient dorsiflexion. The active (cathode) stimulating electrode was placed over the common peroneal nerve and the indifferent (anode) was placed over the TA muscle. The isometric ankle torque was measured by a calibrated dynamometer (Biodex), interfaced with an acquisition system (Biopac MP100). The subjects were seated on the chair with their right ankle at 90^{o}, while the foot was strapped on the pedal. Evoked EMG activity of TA was collected using bipolar surface electrodes. The electrodes were positioned on the TA muscle along muscle fiber direction with 20mm interelectrode spacing. The reference electrode was placed on the patella. The EMG signal was amplified (gain 1,000) and sampled at 4KHz.

Experimental Protocol

For each subject, the first step of the experiment is to find the optimal stimulation location, that is, inducing pure dorsiflexion but tolerable and painless. The second step is to find supramaximal stimulation amplitude. In order to imitate hemiplegic walking situation, sequences of 2s stimulation and 2s rest were applied during 30mn. Stimulation consists of a trapezoidal envelope with pulse width modulation. Each 2s stimulation train consists of 0.4s ramp-up, 1.2s plateau and 0.4s ramp-down. The maximum pulse width and stimulation frequency were fixed at 350 μs and 40Hz for all subjects.

Signal Processing

The stimulation artifacts were removed by means of blanking window to extract muscle response (Mwave) signal. The measured torque was offset with respect to the baseline of the torque measurement without stimulation. The torque data was lowpass filtered (6^{th} order, cutoff frequency 100Hz). The measured eEMG data was lowpass filtered (6^{th} order, cutoff frequency 300Hz). The eEMG data was divided into epochs with each epoch containing one Mwave. The mean absolute value (MAV) of eEMG was calculated every 9 Mwave through moving average. The mean torque during the same time window was simultaneously computed.

The measurements of torque and eEMG were used to identify the parameters of mathematical models for ankle torque prediction. A Hammerstein model was adopted to represent the contraction dynamics as proposed in [4]. The eEMG-torque model is shown as follows:

$$y(t) = \sum_{i=1}^{l} a_i[y(t-i)] + \sum_{j=1}^{m}\sum_{k=1}^{n} b_{jk}[x(t-j)]^k + c_0$$

Where *y(t)* is the torque output at time *t*, *x(t)* is the input, in this study, it is the MAV value of eEMG. The term c_o is used to fit any offset of the output torque. We chose *n=3* as in [4]. Different model order *(l,m)* was assumed to identify and validate the model. Finally we chose model order *l=3, m=4* to minimize the prediction error. A recursive least squares method was used to fit these parameters.

For model identification, past measured torque is used as the past torque *y(t-i)*. For torque prediction, past predicted torque is used as the past torque. In this case, model output $\hat{y}_p(t)$ based on the identified parameters can be computed as follows:

$$\begin{aligned}\hat{y}_p(t) \quad = \quad & f[x(t-1), x(t-2), ...x(t-m), \\ & \hat{y}_p(t-1), \hat{y}_p(t-2), ...\hat{y}_p(t-l)]\end{aligned}$$

When force measurement is not available, this approach makes it possible to use evoked EMG as a synthetic force sensor. The predicted torque was initialized at zero when no stimulation was delivered to the muscle. Mean-squared prediction error (MSE) is used as prediction performance index.

Results

For each subject, in order to observe the global change tendency in torque and eEMG, the peak torque and peak MAV during every 2s stimulation train were calculated and then normalized by the maximum values during the whole stimulation duration. We found that during 30mn stimulation the torque represented potentiation and fatigue, the muscle activity represented different feature in different muscle condition. Fig. 1 showed the changes in torque and MAV of eEMG with fatigue in subject1. In the initial 4mn, the torque and eEMG varied in parallel. From time 4mn to 18mn, the torque and eEMG dissociated. From 18mn to 30mn, they maintained parallel change tendency. We also found this kind of time-varying properties in the variation of eEMG and torque in all other subjects. The dissociation due to muscle fatigue condition was also found in [5]. Therefore, it is difficult to obtain precise torque prediction using a fixed eEMG-torque model especially in prolonged stimulation.

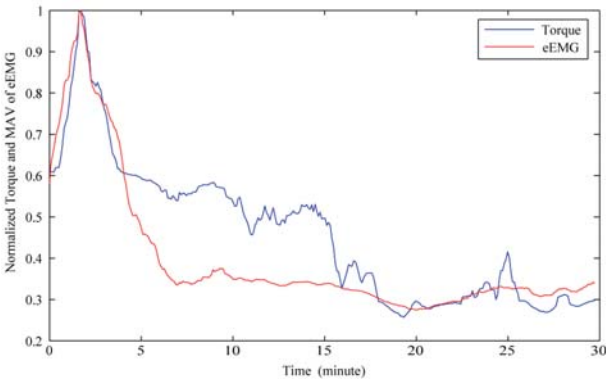


Fig. 1: The transition of the torque response and MAV of eEMG by stimulation in subject2. The results are normalized by the maximum values in the whole test.

In order to validate the model, we adopted two methods: 1) fixed parameters model as proposed in [4] and 2) our method based on adapted parameters model. For each subject, the eEMG data was divided into sets with each set containing 6 trains (33s). Each set of 6 trains was subdivided into two epochs with each epoch containing 3 trains (16.5s). In the first approach, we applied the initial 16.5s data in first set to identify model and fixed the model parameters to predict all the following ankle torque. In the second approach, we applied the data during the first epoch (16.5s) in each set to identify

model. Then the obtained parameters were used to predict the torque just during the adjacent epoch (16.5s) in the same set. The process was repeated for every set during the whole stimulation duration.

The prediction results of two approaches in subject2 were shown in figure 2. Test1, Test2 and Test4 indicate three different muscle states. MSE1 and MSE2 respectively indicate the prediction error with fixed and adapted model. 30mn stimulation resulted in torque loss from (a) 100%, to (b) 60%, until (c) 20% mainly due to muscle fatigue. The prediction with fixed model became less precise over time. Nevertheless, the torque prediction was greatly improved with adapted model.

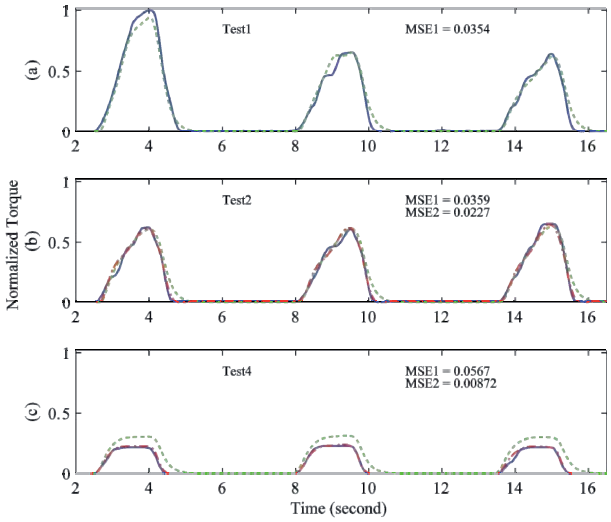


Fig. 2: The measured torque and predicted torque based on evoked EMG in different muscle fatigue state in subject2. The measured torque (blue), the predicted torque with fixed model (green dotted) and the predicted torque with adapted model (red dashdotted) are shown. The results are normalized by the maximum value in the whole test.

We validated the two approaches in all 5 subjects and summarized the prediction performance as shown in TABLE I. Test1~Test4 indicate different muscle condition. We can find that the prediction is less precise or difficult with the fixed model (e.g. test2, test3 in subject1) during long-term repetitive stimulation. However, when the model was reidentified with the latest data as our approach did, the prediction errors were greatly reduced as shown in TABLE I. The prediction with adapted model was improved with 21%~90.9% comparing to the fixed parameters model in all subjects.

Discussion and Conclusions

Our study focuses on the prediction of ankle torque based on evoked EMG in the context of ES drop foot correction during different muscle fatigue states. Five healthy subjects participated in the experiments. During 30mn stimulation applied in isometric conditions, the torque declined in all subjects. The eEMG and the torque represented time varying dissociation properties. However, eEMG-torque relationship was gradually varied relating to muscle fatigue condition in each subject. Therefore, despite the dissociation between eEMG and torque, we were able to apply our adapted eEMG-torque model to highly improve prediction performance comparing to fixed model which was commonly used in previous researches. Thereby, the effect of adapted identification should be significant and this approach has great potential for contribution of ES closed loop control with fatigue consideration. The future work includes to validate the results in hemiplegic subjects, to extend the present method to on-line automatic identification and adaptive control of electrical stimulation for fatigue compensation towards advanced drop foot correction.

TABLE I

SUMMARY OF THE PREDICTION ERROR OBTAINED WITH FIXED OR ADAPTED eEMG- TORQUE MODEL

Subject	Model	Mean Square Error			
		Test1	Test2	Test3	Test4
S1	Fixed	0.0317	0.175	0.14	0.0876
	Adapted	/	0.0158	0.0138	0.0218
S2	Fixed	0.0354	0.0359	0.039	0.0567
	Adapted	/	0.0227	0.0223	0.00872
S3	Fixed	0.0505	0.0473	0.0448	0.0651
	Adapted	/	0.0373	0.0206	0.0342
S4	Fixed	0.0586	0.0854	0.0846	0.0734
	Adapted	/	0.0592	0.0328	0.0402
S5	Fixed	0.0256	0.0512	0.156	0.104
	Adapted	/	0.0178	0.0256	0.0476

References

[1] D. T. O'Keeffe, A. E. Donnelly and G. M. Lyons. The Development of a Potential Optimized Stimulation Intensity Envelope for Drop Foot Applications. IEEE Transactions on Neural Systems and Rehabilitation Engineering, 11: 249-256, 2003.

[2] C. A. Byrne, D. T. O'Keeffe, A. E. Donnelly, et al. Effect of Walking Speed Changes on Tibialis Anterior EMG during Healthy Gait for FES Envelope Design in Drop Foot Correction. Journal of Electromyography and Kinesiology, 17: 605-616, 2007.

[3] R. Héliot, C. Azevedo, and B. Espiau. Functional rehabilitation: Coordination of artificial and natural controllers. Rehabilitation Robotics, I-Tech Education and Publishing, Vienna, Austria, 2007.

[4] A. Erfanian, H. J. Chizeck, and R. M. Hashemi. Using Evoked EMG as a Synthetic Force Sensor of Isometric Electrically stimulated muscle. IEEE Transactions on Biomedical Engineering, 45: 188-202, 1998.

[5] C. K. Thomas, R. S. Johansson, and B. Bigland- Ritchie. EMG Changes in Human Thenar Motor Units With Force Potentiation and Fatigue. Journal of Neurophysiology, 95: 1518-1526, 2006.

Output-Error Model System Identification for FES-driven control of Knee Extensor Muscles

A.D. Koutsou, J. C. Moreno, E. Rocon, J. Gallego and J. L. Pons

Bioengineering Group, CSIC, Spain

Carretera de Campo Real km 0,200 Arganda del Rey, Madrid, SPAIN

Abstract

The biomechanical model of the lower limb musculoskeletal function can be useful when designing and adapting an assistive system in case of impaired control of the limbs or individual joints, e.g. knee injuries, spinal cord injuries (SCI), etc. In particular, FES-driven neuroprostheses can be used to assist impaired leg function. Simple but accurate models are required as tools that assist in tuning such neuroprostheses. This work presents a methodology to identify a non-analytical model of the human knee extensors under Functional Electrical Stimulation (FES) of extensor muscles. A unique model of the swing knee extension of individual subjects is subjected to system identification, based on information provided by a knee brace instrumented with rate gyroscopes. The model identification method was tested with healthy an injured knees. The estimated knee joint velocities verify that theadapted polynomial models can be used to predict the muscle extensors performance in a swinging leg free motion.

***Keywords**: FES, hybrid systems, systems identification.*

Introduction

FES is an effective solution in recovery of motion functions in SCI subjects, [1]. During the last two decades a plethora of studies have been based on FES-based systems that promote or recover leg ([2], [3], [4], [5], [6]), or foot ([7]) functions. Simple but realistic models are a requirement for robust control of the human limbs in a wearable application. Thus, muscle models play an important role in the analysis of motor control and the design of neuroprostheses, [8]. In particular, FES-driven neuroprostheses to assist impaired walking function require some modelling approach that enables tuning the controller. A useful model characterizes the essential characteristics of the muscle [9].

One approach is to build an analytical model based on the knowledge of the physical rules of the system under study; a second approach is to find an experimental, non-analytical model. The former option (also called black-box model) offers the advantage of simplicity in parametric tuning between subjects and useful input-output mapping. Furthermore, it constitutes a good alternative for systems with multiple non-linear features. In this work, a system identification method, based on experimental data, is proposed to model the knee joint response to electrical stimulation of the extensor muscles. The ultimate goal of the model is to serve as a tool for parametric tuning of FES-driven leg neuroprostheses.

Material and Methods

Experiments were conducted with a healthy subject (Subject 1) without a history of knee injury and a subject with a reconstructed anterior cruciate ligament (Subject 2). In these experiments, the quadriceps muscles where stimulated with surface electrodes and the resulting motion was measured. Data collected was used to build the input data set to test the identified models.

Experimental Setup

The subjects were instructed to sit with the leg resting freely (this state constitutes the reference initial position) while the FES system induces sequences of extensions, see fig. 1. The subjects were asked to be relaxed and avoid voluntary movements. Three transcutaneous stimulation electrodes were placed on the quadriceps group. The subjects wore a knee brace, which was equipped with rate gyroscopes that supply the angular velocity of the knee extension. The goal of the stimulation was to generate accurate and repeatable isometric knee extensions while sitting with the leg resting freely.

The stimulation sequence was a burst of 1 second followed by a pause of 3 seconds. Different combinations of stimulation parameters were

tested with each subject. In order to optimize the selection of the stimulation parameters combinations, the Federovs' algorithm was used. Each combination of stimulation parameters was repeated 10 times, and the gyroscopes were recording the angular velocity of the obtained knee extension.

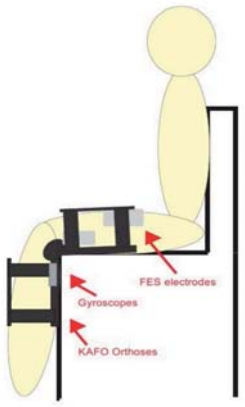


Fig. 1: Experiment set-up. The subject is sited with the legs in 90 degrees of flexion.

Testing Data for Modelling

The input test data are the stimulation frequency and amplitude; the output test data is the angular velocity measured by the rate gyroscopes. A data set was collected per each combination. Each data file contained the angular velocity obtained in each repetition.

System Identification Method

System identification is done using the input output test data. Model identification was performed with Matlab's (Mathworks) system identification toolbox. The Output-Error (OE) model structure is a parametric ARMAX model that describes the system dynamics separately from the stochastic dynamics. This model structure has been chosen as it provides a general-linear polynomial model that reduces to the output-error model by neglecting a noise model.

Estimation of model order was performed by testing multiple OE models (in the range of 1:10 orders) with a testing data set. The lowest OE model was chosen. The OE uses the least square estimation algorithm to determine the best model parameters.

For the purpose of model validation, we studied its performance in predicting the output per each combination of parameters. The prediction corresponds to minimizing one-step ahead prediction, which typically favors the fit over a short time interval. For the total signal fitting, input was used to quantify the relative importance of the fit in the specific frequency range and was optimized for output simulation applications.

Results

The best model fitting to the testing data was provided with by the OE model of 4 order. In particular, for subject 1, the model is described by:

$$y(t) = [\frac{B(q)}{F(q)} \cdot u(t) + e(t)],$$

where

$$B = \begin{bmatrix} -0.01257 & -0.0249 \\ 0.01303 & 0.05131 \\ 0.01175 & 0.03782 \\ 0.1222 & 0.008417 \end{bmatrix} \quad F = \begin{bmatrix} -0.5767 & -2.816 \\ 0.01303 & 2.518 \\ 0.01175 & -0.58 \\ 0.1222 & -0.1212 \end{bmatrix}$$

Figure 2 illustrates the results with respect to the testing data. The model estimation results for the tested parametric combinations are presented in table 1.

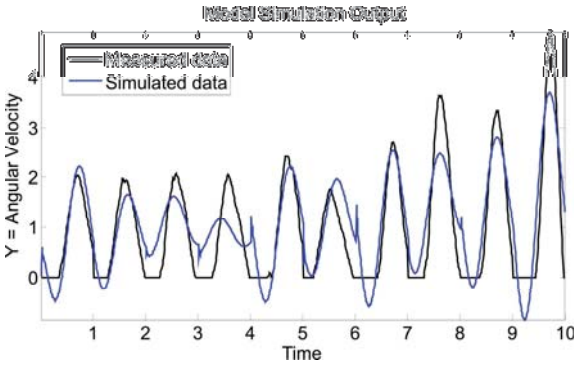


Fig. 2: Simulation Output for the identified model of the swing knee motion (rectus femoris stimulation) (subject 1). Fit 51.55%.

The estimated knee joint velocities of our model were similar to the velocities measured by rate gyroscopes during electrical stimulation of the muscles. This verifies that our selected modelling approach can be used to predict the muscle performance for a given task in which the knee joint is extended while the leg moves freely, e.g. during the swing phase of gait. The output estimation of the second subject, with a reconstructed anterior cruciate ligament was not as satisfactory as the in the health subject. The problem we had to front here was the high sensibility of the subject that did not permit us to collect a representative data set for the model identification method (only 3-6 from 10 combinations). Even so, the mean Estimation Fit was 72.46% for the Rectus Femoral muscle and 80.07% for the muscle group.

Conclusions

A non-analytical system identification method of a FES-driven knee joint has been presented and tested. The proposed methodology represents a practical means to identify muscle activation profiles to control the human knee joint, suitable for combination with mechanical knee braces. The muscle model identification is a critical step in various clinical applications, [10]. Moreover, this approach relies on the use of small and low-cost inertial measurement units that are of practical use in rehabilitation and functional compensation applications (e.g. gait recovery in SCI) where hybrid systems are required, [11]. The method can be practical for the design of the FES strategy in individual cases. In further work, we will introduce means to perform dynamic adaptation of the muscle, taking into account the effects of muscle fatigue. Also, experiments with a wide number of healthy subjects will be performed in order to account for intra-subject variability in the assessment of performance of the method. A knee joint control strategy for SCI subjects will be implemented based on the presented procedure and tested with patient case studies.

Combination		Estimation Fit
Frequency	Amplitude	
50	40	92.06%
60	40	89.47%
70	40	86.4%
90	40	84.62%
40	45	86.47%
100	45	88.98%
30	50	83.07%
60	50	83.64%
30	55	86.75%
30	60	79.45%
	Mean	86.09%

Table 1. Swing knee motion output estimation results (subject 1).

References

[1] Dejan B. Popovic and Thomas Sinkjaer. Control of Movement for the Physically Disabled. Springer-Verlang, London, 2000.

[2] T. Houdayer, A. Barriskill, R. Davis, Z. Milijasevic, and R. Cousins. The praxis and minax fes systems for functional restoration in sci. Bioengineering Conference, 2002. Proceedings of the IEEE 28th Annual Northeast, pages 189–190, 2002.

[3] Dai R., Stein R. B., Andrews B. J., James K. B., and M Wieler. Application of tilt sensors in functional electrical. IEEE Transactions on Rehabilitation Engineering, 4(2):63–72, 1996.

[4] Marsolais E. B. and Kobetic, R. Functional Electrical Stimulation for Walking in Paraplegia* The journal of Bone and joint surgery, 1987, 69, 728-733

[5] Popovic, D., Stein, R. B., Oguzt6reli, M. N., Oguztreli, M. N.; Lebiedowska, M., Jonic, S. & Member, S. Optimal Control of Walking with Functional Electrical Stimulation: A Computer Simulation Study IEEE Trans. Rehab.. Eng, 1998, 7

[6] Spadone R., Merati G., Bertocchi E., Mevio E., Veicsteinas A., Pedotti A., and M. Ferrarin. Energy consumption of locomotion with orthosis versus parastep-assisted gait: a single case study. International Spinal Cord Society, 41:91–104, 2003.

[7] Burridge J., Haugland M., Larsen B., Svaneborg N., Iversen H., Brogger Christensen P., Pickering R., and T Sinkjaer. Long-term follow-up of patients using the actigait implanted drop-foot stimulator. The Journal of Hand Surgery: Journal of the British Society for Surgery of the Hand, 26:459–464, 2005.

[8] Guayhaur Shue, Patrick E. Crago, and Howard Jay Chizeck. Muscle-joint models incorporating activation dynamics, moment-angle, and moment-velocity properties. IEEE Transactions on Biomedical Engineering, 42(2):212–222, February 1995.

[9] Hassan El Makssoud, David Guiraud, and Philippe Poignet. Mathematical muscle model for functional electrical stimulation control strategies. In Proceedings of the 2004 IEEE International Conference on Robotics & Automation, pages 1282–1287, New Orleans,LA, April 2004.

[10] J.C. Moreno, N. Bonsfills, E. GÃ³mez, J.L. Pons, Towards a new concept to the neurological recovery for knee stabilization after anterior cruciate ligament reconstruction based on surface electrical stimulation, Association for the advancement of assistive technology in Europe AAATE 2009.

[11] J.C. Moreno, A.D. Koutsou, J.L. Pons, The Rehabot-Knee Project approach for recovery of neuromuscular control of the knee with controllable braces, EFRR 2009.

Acknowledgements

This work has been done with partial financial support of the Ministerio de Educación y Ciencia (Contract DPI2008-06772-C03-01) in the framework of the project “REHABOT, Sistemas avanzados EEF y UMI para el desarrollo de soft-robots en el ámbito de la robótica de rehabilitación”.

Author’s Address

Bioengineering Group, CSIC

km. 0.2 La Poveda, Arganda del Rey, Madrid, Spain 28500

kkoutsou@iai.csic.es

http://www.iai.csic.es/users/gb/

Session 5

Control, Sensors, Algorithms – non invasive 2

Automatic real time procedure for adjusting the stimulus intensities to ensure reliable measurements of the H-reflex recruitment curve

Ambrosini E[1], Ferrante S[1], Pedrocchi A[1], Schauer T[2], Nahrstaedt H[2], Mazzocchio R[3]

[1] NearLab, Bioengineering Department, Politecnico di Milano, Milan, Italy

[2] Control Systems Group, Technische Universität Berlin, Germany

[3] Sezione di Neurofisiologia Clinica, Dipartimento di Scienze Neurologiche, Neurochirurgiche e del Comportamento, Siena, Italy

Abstract

Variability in the H-reflex can make it difficult to identify significant changes using traditional analysis techniques. This study presents an automatic real time procedure to adjust tibial nerve stimulus intensities to ensure reliable soleus H-reflex measurements. The procedure consists of 3 steps: (1) an acquisition of a full recruitment curve (RC); (2) a sigmoidal fitting of the ascending limb of the H-reflex RC to compute stimulus intensities needed to evoke the maximal H amplitude (H_{max}) and the 50% of H_{max} (H_{50}); (3) reliable repeated-measurements of both H_{max} and H_{50}. Furthermore, the procedure can detect when changes in the H-reflex RC occur and redetermine the optimal stimulation intensities. Tests on one healthy subject were carried out both at rest and during voluntary contraction of the triceps surae muscle to provide a first validation of the procedure reliability. Significant differences were found between the 2 experimental conditions in the amplitudes of H_{max} and H_{50} and in the homosynaptic depression, as found in literature. The procedure may be used at rest, during muscle contractions and could be particularly useful in prolonged experiments or after fatiguing exercises. Between-day and inter-subjects analyses will be next performed to fully validate the procedure.

***Keywords**: H-reflex, recruitment curve, stimulus constancy*

Introduction

The Hoffmann (H)-reflex has been used widely to measure spinal excitability changes in motor control experiments [1]. Despite extensive reviews, variability of the H-reflex can make it difficult to identify significant changes using traditional analysis techniques. For instance, it is possible that H-reflex changes described in previous studies may have been due to a small number of stimuli being delivered, or a shift in the recruitment curve (RC) because of movements of stimulating electrode/ nerve, and/or recording electrode/muscle relationship [2]. Furthermore, the size of the M-response can also change during different muscle lengths and experimental conditions [1].

Rupp et al. demonstrated that keeping the stimulation intensity constant to evoke the maximal resting H-reflex after a sustained muscle contraction can underestimate the H-reflex facilitation occurring after exhaustive exercise. It is therefore more appropriate to redefine the optimal stimulation intensity to evoke it [3].

In literature, most of the studies on between day reliability of the H-reflex consider only one point of the RC. A recent study suggested that the entire RC should be investigated to ensure both between conditions and between days reliability [2]. However, it is rather time consuming to check whether the stimulus intensity needed to obtain the maximal H-reflex has to be adjusted, as eliciting a full H-reflex RC can take up to 10 min. On the other hand, it would be crucial to acquire more than one point of the RC to obtain more information on changes in spinal excitability.

Considering these methodological constraints, the study aims at the design of a system able to acquire and store reliable measures of the H-reflex in 2 different points of the RC. In addition, the system is able to calibrate itself automatically performing RC and adjusting stimuli intensities when needed.

Material and Methods

To illustrate the automatic procedure, one healthy subject took part in the study. The subject was seated with the knee angle kept constant at 120°.

Instrumentation

The H-reflex was recorded from the soleus muscle using EMG electrodes in a bipolar configuration [1]. The posterior tibial nerve was stimulated in the popliteal fossa through a monopolar adhesive electrode. The anode was placed above the patella. The stimuli were 1 ms monophasic pulses. The EMG was sampled at 2048 Hz. The EMG envelope (obtained applying a high-pass filter, rectification and low-pass filter at 5 Hz to the raw EMG) was displayed to the subject.

Experimental procedure

In each experimental condition, the automatic algorithm started with the acquisition of a RC. The stimulus intensity was increased in steps of 2 mA

starting just below H-reflex threshold. When H-reflex amplitude began to decline the stimulus intensity was increased in steps of 20 mA till evoking the maximal M wave.

The H-reflex peak-to-peak amplitudes computed on the ascending limb of the RC were fitted using the following sigmoid function [4]:

$$H(s) = \frac{H_{max}}{1 + e^{m(sH_{50} - s)}} \quad (1)$$

where $H(s)$ is the H amplitude at a given stimulus intensity (s); H_{max} is the upper limit of the curve calculated as the mean of the values above the 95% of the largest one (also the standard deviation, *SD*, on this interval was computed); m is the slope of the function; sH_{50} is the stimulus at 50% of H_{max}. The sH_{50} and m were optimized by a non linear least square method. The following parameters were computed on the fitted RC: stimulus intensity needed to evoke the first point above the 95% of the largest H amplitude (sH_{max}); the M amplitude elicited by sH_{max} (M_{Hmax}); the stimulus intensity corresponding to the maximal M amplitude (sM_{max}) and its peak-to-peak amplitude (M_{max}).

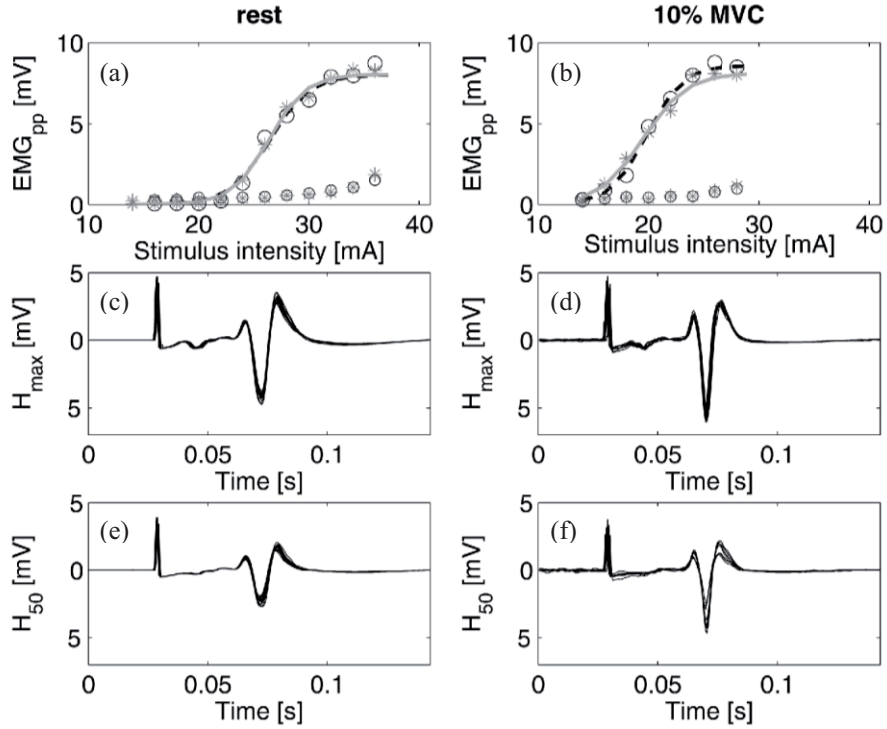
Once the parameters were obtained, the protocol started: a first stimulus at sH_{max} was sent; if the H amplitude was considered reliable (H amplitude within $H_{max} \pm SD$ and the M amplitude within $M_{Hmax} \pm 95\%\ M_{Hmax}$), a second sH_{max} was sent after 1 s. When the H amplitude was outside its confidence interval, an acquisition of a new RC began and new parameters were automatically computed. Instead, if the H amplitude was repeatable but the associated M amplitude was not, the stimulus intensity was increased or decreased by 2 mA. Once a train of 4 reliable couples of sH_{max} was sent (the interval between 2 consecutive couples being 10 s), an analogous train of 4 stimuli to evoke H_{50} was delivered. The same current correction applied to elicit the last reliable H_{max} was added to sH_{50} and used to evoke the H_{50}. After both trains, M_{max} was evoked. If the M amplitude was within $M_{max} \pm 95\%\ M_{max}$, a second train started; otherwise a new RC was required. The acquisition ended after the third elicited M_{max}. The procedure was tested at rest and at 10% MVC.

Data processing and analysis

In both conditions, mean values and standard deviations of the reliable H_{max}, H_{50}, and M_{max} obtained were computed. Furthermore, for each reliable couple of H_{max}, the homosynaptic depression, *HD*, i.e., the ratio between the second and the first H amplitude [1], was determined.

Results

Panels (a) and (b) in Fig. 1 depict the fitted H-reflex RC obtained at rest and at 10% MVC before the procedure (dashed line). A second RC (solid line) was elicited at the end of the protocol to check that no changes in the RC occurred.



	rest	10% MVC
H_{max} [mV]	7.22 (0.46)*	8.54 (0.31)*
M_{Hmax} [mV]	0.77 (0.03)	0.78 (0.05)
HD [%]	59 (9)*	83 (5)*
H_{50} [mV]	3.95 (0.42)*	5.34 (1.28)*
M_{H50} [mV]	0.46 (0.01)	0.45 (0.09)
M_{max} [mV]	17.16 (0.45)	17.60 (0.12)

Fig. 1: Panels (a) and (b) show the H and the corresponding M data obtained before (o) and after (*) the procedure at rest and at 10% of MVC, respectively. The fitted $H(s)$ computed before (dashed line) and after the procedure (solid line) are also depicted. The muscular responses evoked by sH_{max} and sH_{50} are shown (at rest, panels (c, e) and at 10% MVC (panels (d, f)). All the computed parameters (mean values and standard deviations, in brackets) are reported in the table. The asterisks indicate significant differences between the 2 experimental conditions (t-test, $p<<0.05$).

As evident from the figure, the 2 curves were very repeatable, particularly at rest. Panels (c) and (f) represent all the reliable EMG responses evoked by sH_{max} and sH_{50} during the procedure in both experimental conditions. Also in this case the repeatability of the signals is noticeable and confirmed by mean values and standard deviations of M and H amplitudes reported in table. The statistical analysis shows that *HD* is significantly lower at rest than at 10% MVC (t-test, $p<0.05$), while both H_{max} and H_{50} are significantly higher at 10% MVC than at rest. No differences were found between the correspondent M amplitudes. These results confirm what already found in literature [5].
To outline the potentiality of the automatic procedure, two cases in which adjustments of the stimulus intensities are needed to ensure reliable H-reflex measurements are unfolded. In the first case (Fig. 2 panel (a), a RC was obtained (dashed line); then, before starting the protocol, an artificial change in the position of the stimulating electrode was provoked. The procedure automatically decreased the stimulus intensity by 2 mA to elicit both H_{max} and H_{50}. The acquisition of a second RC (solid line) at the end of the protocol confirmed a solid shift between the 2 curves. Whereas, panel (b) shows an example of physiological changes in the H reflex excitability: 3 different RCs were obtained at rest, at 10% and 20% MVC. A stronger muscle contraction produced a RC shifted towards lower stimulus intensities and an increased H_{max} as already well-known from the literature [5].

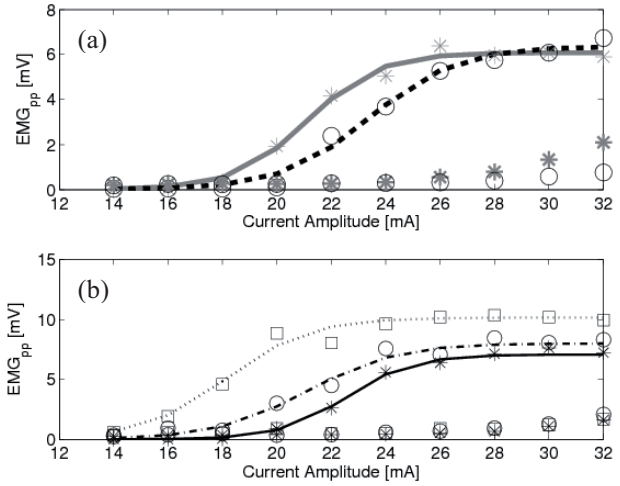


Fig 2 Panel (a) show the H, the corresponding M data and the fitted $H(s)$ before ('o', dashed line) and after ('*', solid line) moving the stimulating electrode. Panel (b) reports the H, the corresponding M data and the fitted $H(s)$ obtained at rest ('*', solid line) at 10% MVC ('o', dash-dot line) and at 20% MVC ('□', dotted line).

Discussion

This study is one of the first attempts to provide a real time automatic procedure to measure accurately the H-reflex excitability. This procedure offers reliable measurements in 2 different points of the RC: H_{max} and H_{50}. H_{50} was chosen because it is widely sensitive to modulations in reflex excitability, but it is also characterized by a very small M-wave less responsive to configurational changes and not exploitable to ensure stimulus constancy [1]. Therefore, H_{max} was also evoked because its corresponding M-wave is large enough to estimate and control stimulus constancy.
A crucial potentiality of the procedure is that it can detect when changes in the H-reflex RC occur and, therefore, it automatically adjusts the stimulus intensities to ensure reliable measurements. The procedure can also perform a complete re-calibration (full RC) lasting less than 3 minutes.
Finally, the procedure may be used at rest, during movement or isometric muscle contractions.
These features make the system particularly useful in prolonged experimental settings or after fatiguing exercises. In both conditions, the changes occurring in the RC and in the M_{max} [1] can be compensated automatically. Between-day and inter-subjects analyses will be next performed to fully validate the procedure. A comparability of H amplitudes between subjects and conditions will require a normalization of the H-response to a physiological constant such as M_{max} [6].

References

[1] Zehr EP Considerations for use of the H-reflex in exercise studies. Eur J Appl Phys, 86:455-468, 2002.

[2] Brinkworth RSA, Tuncer M, Tucker KJ, et al. Standarization of H-reflex analyses, J Neur Met, 162:1-7, 2007.

[3] Rupp T, Girard O, Perrey S. Redetermination of the optimal stimulation intensity modifies resting H-reflex recovery after a sustained moderate-intensity muscle contraction. Muscle Nerve, 41:642-50, 2010.

[4] Klimstra M, Zehr EP. A sigmoid function is the best fit for the ascending limb of the Hoffmann reflex recruitment curve. Exp Brain Res,186:93–105, 2008.

[5] Stein RB, Estabrooks KL, McGie S et al. Quantifying the effects of voluntary contraction and inter-stimulus interval on the human soleus H-reflex. Exp Brain Res, 182:309–319, 2007.

[6] Crone C, Hultborn H, Mazières L, et al. Sensitivity of monosynaptic test reflexes to facilitation and inhibition as a function of the test reflex size: a study in man and in the cat. Exp Brain Res 1990; 81:35-45

Acknowledgements

This work was partly supported by the German-Italian University Centre within the Vigoni Project.

Author's Address

emilia.ambrosini@mail.polimi.it

Use of an inverted pendulum apparatus for the study of closed-loop FES control of the ankle joints during quiet standing

Tan JF[1,2], Zariffa J[1,2,3], Vette A[1,2], Lynch C[1,2], Masani K[1,2], Popovic MR[1,2,3]

[1] Rehabilitation Engineering Laboratory, Institute of Biomaterials and Biomedical Engineering, University of Toronto, Toronto, Canada

[2] Rehabilitation Engineering Laboratory, Toronto Rehabilitation Institute, Toronto, Canada

[3] Edward S. Rogers Sr. Department of Electrical and Computer Engineering, University of Toronto, Toronto, Canada

Abstract

The restoration of arm-free standing in individuals with paraplegia can be accomplished with the help of functional electrical stimulation (FES). An experimental device, the Inverted Pendulum Standing Apparatus (IPSA), is used to study closed-loop FES control of the ankle joint. The IPSA uses the ankle muscles of a sitting subject to balance an inverted pendulum that mimics the subject's body during quiet stance, thereby overcoming the safety issues associated with studying standing in individuals with paraplegia. We used the IPSA to evaluate the ability of proportional-derivative and proportional-integral-derivative (PD and PID, respectively) controllers to regulate quiet standing in an individual with a T3-T4 complete (AIS A) spinal cord injury (SCI). The controllers were able to regulate balance of the inverted pendulum. However, while the controller gains and FES stimulation parameters were chosen based on simulations and experimental calibration, they did not prove adequate to compensate for the day-to-day variability in the subject's muscle strength, creating the need for adjustments prior to every trial. Although the controller output exhibited a saturated phasic profile, we conjecture that increasing the ankle stiffness (by changing the subject's position from sitting to standing) may help to achieve a more physiologically realistic tonic profile.

Keywords: *Functional electrical stimulation, inverted pendulum, real-time control, rehabilitation devices, human factors in medical devices, human performance/force assessment, medical device design processes*

Introduction

Spinal cord injury (SCI) is a serious neurological condition that frequently leads to paralysis and a range of impairments that severely degrade the quality of life of individuals with SCI. These impairments include the inability to stand, walk, grasp, and sit, as well as secondary complications such as pressure sores (ulcers), respiratory complications, urinary tract infections, spasticity, scoliosis, and depression. One of the simplest ways to alleviate some of these secondary complications is to get individuals with SCI to stand [1]. For individuals with SCI, there are therapeutic benefits to standing, such as bone loading, extending the joints, improving blood flow, and activating muscles. In addition, standing allows these individuals to communicate with people at eye level, reach for items that are normally inaccessible when using a wheelchair, transfer more easily, and perform other activities of daily living that cannot be carried out while seated [2].

Material and Methods

An experimental device, the Inverted Pendulum Standing Apparatus (IPSA) shown in Fig 1, was used to study closed-loop FES control of the ankle joint, which used the ankle muscles of a sitting T3-T4 complete (AIS A) subject to balance an inverted pendulum, thereby overcoming the safety issues associated with studying standing in individuals with paraplegia.

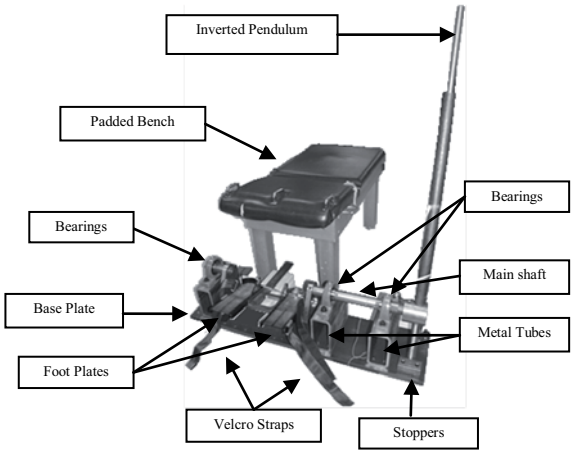


Fig 1: Inverted Pendulum Standing Apparatus (IPSA) with seated bench

A padded bench was provided for the subject to sit on while Velcro straps securely held the subject's feet on the foot plates which could move in the

anterior-posterior direction. The foot plates were connected to the inverted pendulum through a single shaft, which translated the rotational motion from the foot plates to the inverted pendulum (weighing 17.2kg)

A Keyence LK-2500 laser (Keyence, Japan) was used to track the angular position of the pendulum and was interpreted by a real-time PD/PID controller implemented on a personal computer installed with MATLAB 7.1 using Windows Target toolbox. The controller modulated the Compex Motion stimulator output. The Compex Motion stimulator is a programmable, multipurpose, transcutaneous, functional electrical stimulation system developed by Drs. Popovic and Keller [3]. The current pulses were delivered to the subject's plantarflexors (the muscles primarily responsible for quiet standing). A reference angle of 5 degrees (to the vertical) was used for the controller to track.

The stimulation waveform used was a rectangular, biphasic, monopolar pulse waveform, with a pulse duration of 300μs at a stimulation frequency of 40Hz. The amplitude was varied from 0 to 80mA.

Controller parameters were modified for different trials and were tabulated in Table 1. The selection of these gains was based on the gains used by [4], followed by a trial and error process in an attempt to increase controller response time (through K_d) and reduce the mean error (through K_i).

Gains and maximum amplitudes used during sessions				
Trial #	**K_p** $Nm{\cdot}rad^{-1}$	**K_d** $Nm{\cdot}s{\cdot}rad^{-1}$	**K_i** $Nm{\cdot}s^{-1}{\cdot}rad^{-1}$	**Max Amp.** mA
1	750	350	0	63
2	750	350	0	60
3	95	50	0	60
4	700	250	0	54
5	700	200	20	60
6	700	180	20	52
7	700	180	20	48
8	700	120	20	55
9	700	350	20	58

Table 1: Gains and maximum stimulation pulse amplitudes used during controller experiments.

Results

Table 2 summarizes the performance of the trials for each controller listed in Table 1. The second column provides the length of time during which the controller was able to balance the inverted pendulum about the 5 degree reference angle, and the third column provides the error between the mean angle during the time the pendulum was balanced and the reference angle (5 degrees from the vertical) set by the controller.

The most successful trial was trial 6 with a PID controller (k_p = 700 $Nm{\cdot}rad^{-1}$, k_d = 180 $Nm{\cdot}s{\cdot}rad^{-1}$, k_i = 20 $Nm{\cdot}s^{-1}{\cdot}rad^{-1}$) which was balancing the pendulum around an angle of 5 degrees for almost 90 seconds (Fig. 2).

Trial #	Length (s)	Error (%)
1	29	28
2	27	1
3	10	138
4	29	11
5	55	7
6	87	4
7	60	10
8	23	27
9	33	46

Table 2: Length of time pendulum was balanced and mean error from reference balance point of 5 degrees

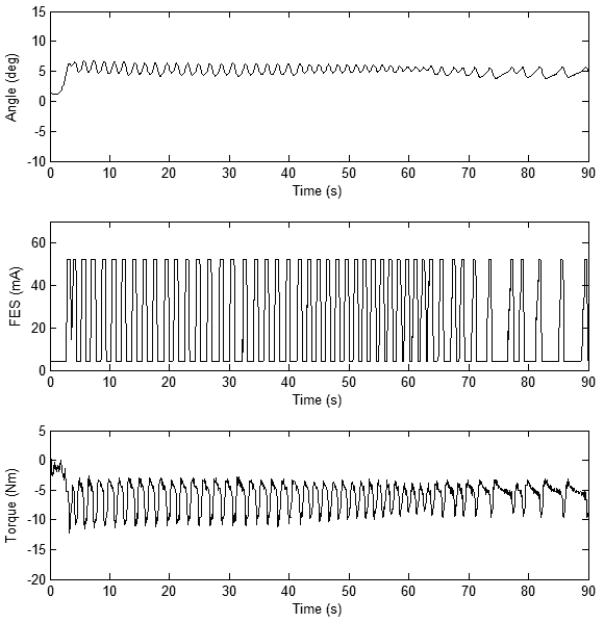


Fig 2: Results for trial 6 with a PID controller (k_p = 700 $Nm{\cdot}rad^{-1}$, k_d = 180 $Nm{\cdot}s{\cdot}rad^{-1}$, k_i = 20 $Nm{\cdot}s^{-1}{\cdot}rad^{-1}$, ref = 5 degrees) and a maximum amplitude of 52 mA.

Discussion

The IPSA is advantageous for the development of a standing neuroprosthesis for individuals with SCI, as it provides a safe mechanism through which some aspects of a quiet standing neuroprosthesis can be studied. It can potentially investigate such issues as the muscle strength requirements for successful standing in an individual with SCI. The pendulum weight and moment of inertia were significantly lower than that of the subject due to substantially weakened muscles of the subject due to chronic SCI (classified as T3-T4 complete AIS A)

Although balance of the pendulum was accomplished with a PD/PID controller, as shown in Figure 2, the control signal was saturated in both directions (the same behaviour was observed in all

trials). This pattern effectively activated the muscles then relaxed them with each pendulum sway. This phasic mode of operation differs from that observed in the quiet standing of able-bodied individuals [5].

One possible reason for the difference is that the IPSA setup does not take into account the passive torque that is normally exerted during quiet standing by the stiffness of the ankle joint. Recent work has compared the contributions of active and passive torques during quiet standing and demonstrated that, in an able-bodied subject, the majority of the torque required to keep the individual from falling was provided by passive torques (80-85%) [6]. With this in mind, we would expect that a subject's ability to balance the IPSA would improve by placing the subject in a standing frame while they use the IPSA to increase the passive torque around the ankles. We conjecture that this may be enough to stabilize the swing of the pendulum.

The controller gains are also crucial, but despite our use of simulations to guide our choices, refining these values is challenging because of the time-varying nature of the muscles' performance. None of the gain combinations explored produced a tonic mode of operation, which would be more physiologically realistic than the phasic behaviour observed. It is possible that the phasic operation may not be completely detrimental to the system, given that it allows for short windows for the muscles to recover after contracting. Nonetheless, phasic contractions lead to larger pendulum sway and do not match the physiological behavior exhibited by the able-bodied individuals.

The performance of the controller depends on the accuracy of the calibration map that converts the desired torque value into stimulation amplitude of the FES device. Our assumption in this study was that the calibration of the controller could be accomplished by measuring the torque generated by the ankles during isometric contractions. However this proved to be inaccurate for controller experiments, since for each trial, the maximum amplitude of the stimulator had to be adjusted, scaling the torque-stimulation relationship by a gain. The need for this adjustment was due to the day-to-day variability of the subject's muscle performance. From our experience with this and other subjects with complete SCI, this variability can be dramatic and stochastic in nature, requiring the development of more effective methods to compensate for this variability.

Lastly it should be noted that due to the limited time the subject participated in the study, there weren't enough trials to draw any statistical relevance as related to the gains of the controllers.

Conclusions

This study has shown that, in certain cases, it is possible to use PD/PID control to artificially activate and control paralyzed muscles to balance an inverted pendulum. Although the controller output exhibited a saturated phasic profile, we conjecture that increasing the ankle stiffness (by changing the subject's position from sitting to standing) may help to achieve a more physiologically realistic tonic profile. In the next phase of the study, we will attempt to retrofit the IPSA with a standing frame to allow the same experiment to be carried out on a subject in a standing position.

References

[1] Bajd T, Munih M, Kralj A. "Problems associated with FES-standing in paraplegia". Technology and Health Care, 7(4):301-308, 1999.

[2] Veltink PH, Donaldson N. "A Perspective on the Control of FES-Supported Standing", IEEE Transactions on Rehabilitation Engineering, 6(2): 109–112, 1998.

[3] Popovic MR, Keller T. "Modular Transcutaneous Functional Electrical Stimulation System". Medical Engineering and Physics, 2004.

[4] Vette AH, Masani K, Popovic MR. "Implementation of a physiologically identified PD feedback controller for regulating the active ankle torque during quiet stance". IEEE Trans. on Neural Systems and Rehabilitation Engineering, 15:235-243, 2007.

[5] Masani K, Popovic MR, Nakazawa K, Kouzaki M, Nozaki D. "Importance of body sway velocity information in controlling ankle extensor activities during quiet stance". Journal of Neurophysiology, 90: 3774-3782, 2003.

[6] Vette AH, Masani K, Nakazawa K, Popovic MR. "Neural-mechanical feedback control scheme generates physiological ankle torque fluctuation during quiet stance". IEEE Tr. on Neural Systems and Rehabilitation Engineering, 18(1):86-95, 2010.

Acknowledgements

This work was supported by Canadian Institutes of Health Research (MOP-69003), Natural Sciences and Engineering Research Council of Canada (249669), Ministry of Health and Long Term Care in Ontario and Toronto Rehabilitation Institute.

Author's Address

John Tan
Rehabilitation Engineering Laboratory
jf.tan@utoronto.ca / www.toronto-fes.ca

Mapping Method Using a Super Multi-Electrical Stimulation Device

Takuya Watanabe[1], Yoshihiko Tagawa[1], Naoto Shiba[2]

[1] Kyushu Institute of Technology, Kitakyushu, Japan

[2] Kurume University, Kurume, Japan

Abstract

Many functional electrical stimulation (FES) devices use surface electrical stimulation (SES). However, most such devices are unable to reproduce task-oriented motions such as pinching or flexing of individual fingers. We have reported reproduction of such motions using SES based on a mapping method that specifies the distribution of the target muscles from the skin surface. Nevertheless, mapping method presents some problems such as a lack of objective estimation and long processing time. To solve these problems, we plan to develop a new FES system that includes an auto-mapping function using acceleration sensors. We have developed a prototype system and have reproduced some motions using a stimulation device that has 192 stimulation channels.

***Keywords**: FES, Orthosis, Stimulation device, Daily FES*

Introduction

Functional electrical stimulation (FES) is a method used to restore paralyzed limb function. Many researchers have reported the effects of FES. Some FES devices have been developed for restoring hand function. For example, Ring et al. [1] and Snoek et al. [2] designed and assessed a neuroprosthetic FES device for the hand, called the "NESS Handmaster," which uses surface electrical stimulation (SES). Knoutson et al. [3] developed and assessed a contralaterally controlled FES (CCFES) system that hemiplegic patients can control with the impaired hand. Furthermore, Prochazca et al. [4] developed a bionic glove that can control the FES of muscles by detecting voluntary wrist movement. Swain et al. [5] pointed out the importance of adequate gripping and stable prehension when a hand/arm prosthesis is controlled automatically.

Most FES devices used today cannot reproduce task-oriented motion. For example, the NESS Handmaster can only perform a grasping motion. If a new device can be developed to reproduce task-oriented motions such as the individual movement of fingers, then patients' quality of life (QOL) will be improved considerably.

To resolve the disadvantage described above, we suggest the "mapping method," which specifies the distribution of the target muscles from the skin surface. Using this method, we reproduced the flexion of individual fingers, adequate gripping, and stable prehension by SES. Moreover, we confirmed that this method is applicable to support spinal cord injury (SCI) patients with C6 level immobility. We conducted 20 min of therapeutic electrical stimulation (TES) training during sessions held 2–3 times a week (total 28 weeks) [6]. We assessed the effect of this TES training by quantitative tracking of the patients' movement trajectories with a 3-SPACE (Polhemus Inc., USA) apparatus and sequential MRI imaging. Results show improvement in hand motion when the patients were stimulated, but no improvement was found in voluntary motion [7].

This result serves as a reminder that home-based daily FES training is extremely important. To realize daily FES, the mapping method requires enhancements to achieve more objective estimation and shorter processing time. Here, we propose a new FES device that includes an automatic mapping function using sensor feedback.

This paper describes 1) the mapping method, 2) the structure of the prototype of the new FES device, and 3) the evaluation of the prototype system.

Mapping method

The mapping method is one method of specifying the distribution of the target muscles from the skin surface. The mapping procedure is the following:

Step 1) Identify the motor points of individual muscles.

Step 2) Raise the current intensity of the device; we investigate the points found in Step 1) to clarify the SES area while observing the muscle's stimulated contractions.

Step 3) Establish the maximum tolerable level of stimulation for each muscle.

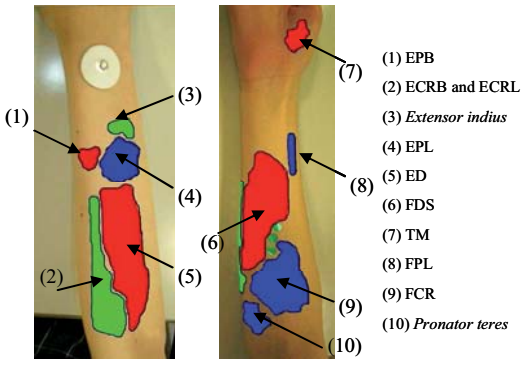


Fig. 1: Result of mapping method.

Figure 1 shows one result of the mapping method applied to C6 level SCI patients.

The present mapping method has some problems: 1) long processing time (it takes about 2 hr to complete); 2) lack of objective evaluation; and 3) maintaining constant pressure of the stimulator probe.

TES for SCI patients

Using results of the mapping method, we undertook TES training with two SCI patients, each with stable C6 level (1 male and 1 female, 5 and 6 years after injury, respectively) [6] [7].

This training was conducted for 20 min during sessions held 2–3 times a week (total 28 weeks). We assessed the effect of this TES training by quantitative tracking of the patients' movement trajectories with a 3-SPACE (Polhemus Inc., USA) apparatus and sequential MRI imaging (Fig. 2). We measured almost identical dimensions of every image and found little muscular hypertrophy (Table 1). We also found improvement in hand motion when the patients were stimulated. However, no improvement was found in voluntary motion. From these results, we concluded that the FES system should be used daily. In fact, Ring et al. described the importance of daily FES training [1].

New FES system

Our goal is to produce a new FES system that includes the following: 1) an automatic mapping function using acceleration sensors attached on fingers and hand; 2) an FES function that can realize task-oriented motion by stimulating specified muscles; and 3) grip strength or wrist angle controls using sensor feedback.

Prototype system

Figure 3 portrays an FES system prototype. It consists of a PC, a PC-controlled stimulator, and an orthosis with stimulation electrodes. The PC-controlled stimulation device has 192 stimulation channels. Moreover, about 150 electrodes of 1 cm diameter are attached to the inside surface of the orthosis for adequate fixed pressure (Fig. 4). This system is expected to resolve the problems of the mapping method described above. If 10 s are taken to evaluate muscle contraction induced by one channel's electrical stimulation, then the processing time of all channels will be about 1500 [s]. Some sensors are necessary to establish automatic mapping.

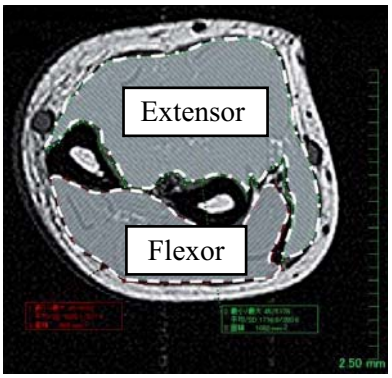


Fig. 2: MRI image.

Table 1: Muscular hypertrophy

Female subject	Flexor muscles [mm^2]	Extensor muscles [mm^2]
Before TES	537	1040
After 4 mo TES	608	1082
After 7 mo TES	620	1087

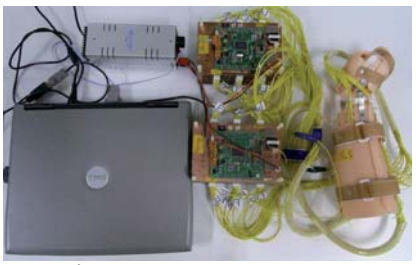


Fig. 3: Prototype system.

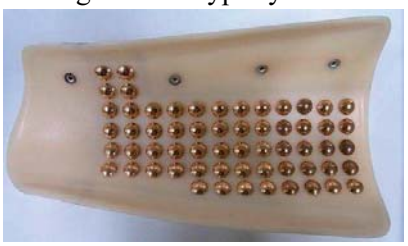
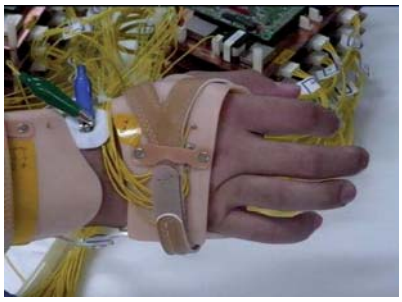


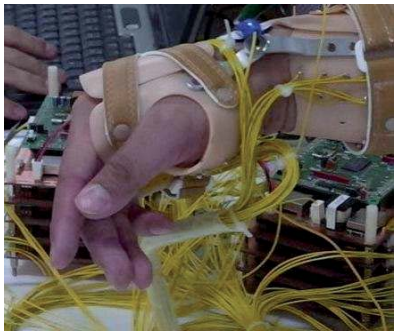
Fig. 4: Attached electrodes.

Experiment

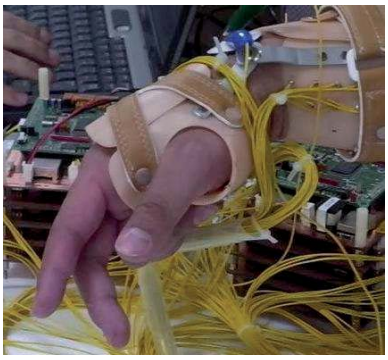
Using the prototype system, we stimulated the muscles of the hand and forearm of a healthy person (23 years old, male). To observe the muscle's stimulated contractions, electrodes were activated one-by-one to stimulate the corresponding small area of the muscle. This process continued until the whole area had been checked. Figure 5 shows stimulation results for (a) the extensor digitorum (ED), (b) the flexor digitorum superficialis (FDS), and (c) the flexor carpi radialis (FCR), together with results for the same responses in manual mapping.



(a) Muscle contraction (ED)



(b) Muscle contraction (FDS)



(c) Muscle contraction (FCR)

Fig. 5: Experimental results.

Future study

We plan to add accelerometers and pressure sensors to the FES system prototype to realize more objective estimation or automatic mapping. We will investigate, from a practical perspective, the feasibility of automatic mapping and daily FES use to reproduce task-oriented motions. We intend to design a GUI interface that can help us process them at given intensity, selection of muscles for the FES, and so on. Furthermore, we will estimate the relation between the subject's motor intention and stimulated motor output using near infrared spectroscopy (NIRS).

References

[1] H. Ring N. Rosenthal. Controlled Study of Neuroprosthetic Functional Electrical Stimulation in Sub-Acute Post-Stroke Rehabilitation. J. Rehabil. Med., 37: 32-36, 2005.

[2] G. J. Snoek MJ IJzerman, FACG in `t Groen, et al. Use of the NESS Handmaster to restore handfunction in tetraplegia: clinical experiences in ten patients. Spinal Cord, 38: 244-249, 2000.

[3] J. S. Knutson T. Z. Hisel, M. Y. Harley. A Novel Functional Electrical Stimulation Treatment for Recovery of Hand Function in Hemiplegia: 12-Week Pilot Study. Neurorehabilitation and Neural Repair, 23-1: 17-25, 2009.

[4] A. Prochazka M. Gauthier, M. Wieler, et al. The Bionic Grove: An Electrical Stimulator Garment That Provides Controlled Grasp and Hand Opening in Quadriplegia. Arch. Phys. Med. Rehabil., 78: 608-614, 2007.

[5] I. D. Swain, J. M. Nightingale. An Adaptive Control System for a Complete Hand/Arm Prosthesis. J. Biomed. Engng., 2:163-166, 1980.

[6] T. Watanabe Y. Tagawa, N. Shiba. Surface Electrical Stimulation to Realize Task Oriented Hand Motion. EMBC 2009: 662-665, 2009.

[7] T. Watanabe Y. Tagawa, N. Shiba. Mapping Method for a Surface Electrical Stimulation and Effect of TES on SCI Patients with C6 Level. 14th Annual IFESS conference 2009: 49-50, 2009.

Acknowledgements

This work was supported in part by a Ministry of Education, Culture, Sports, Science and Technology Grant-in-Aid for Scientific Research (B) 20360118.

Author's Address

Name: Takuya Watanabe

Affiliation: Kyushu Institute of Technology

eMail: i344228t@tobata.isc.kyutech.ac.jp

homepage:
http://lab.cntl.kyutech.ac.jp/~tagawa/index.html

A Study on Feedback Error Learning Controller for FES: Generation of Target Trajectories by Minimum Jerk Model

Watanabe T[1], Fukushima K[2]

1 Dept. Biomedical Eng., Graduate School of Biomedical Eng., Tohoku University, Sendai, Japan

2 Dept. Electrical and Communication Eng., Graduate School of Eng., Tohoku University, Sendai, Japan

Abstract

In our previous studies, the Feedback Error Learning (FEL) controller was found to be applicable to FES control of wrist joint movements. However, sinusoidal trajectories were only used for the target joint angles and the artificial neural network (ANN) was trained for each trajectory. In this study, focusing on two-point reaching movement, target trajectories were generated by the minimum jerk model. In computer simulation tests, ANNs trained with different number of target trajectories under the same total number of control iteration (50 control trials) were compared. The Inverse Dynamics Model (IDM) of the controlled limb realized by the trained ANN decreased the output power of the feedback controller and improved tracking performance to unlearned target trajectories. The IDM performed well when target trajectory was changed every 1 control trial during ANN training.

Keywords: feedback error learning, tow-point reaching movement, minimum jerk model

Introduction

The Feedback Error Learning (FEL) controller was found to be applicable to FES control in our previous studies of wrist joint control by computer simulation and with neurologically intact subjects [1]. The FEL controller was composed with a multichannel proportional- integral- derivative (PID) controller [2] as a feedback controller and an artificial neural network (ANN) as a feedforward controller as shown in Fig.1. The ANN realizes the Inverse Dynamics Model (IDM) of the controlled limb by learning using outputs of the feedback controller.

The target joint angles, however, were only sinusoidal trajectories of 2-DOF or 1-DOF movements in the previous studies. In addition, the ANN was trained for each target trajectory. These conditions are not practical for clinical applications.

In this study, focusing on two-point reaching movement, target trajectories were generated by the minimum jerk model [3]. ANN training condition was examined by changing target trajectory in some different way during the training.

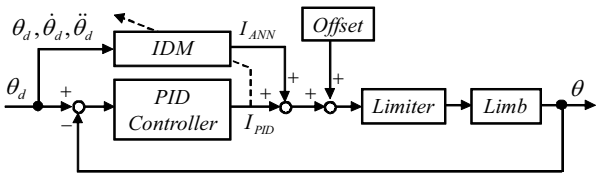


Fig.1: Block diagram of the FEL controller for FES. θ_d and θ represent the desired and the measured joint angles. The ANN learns with the outputs of the PID controller while controlling limbs.

Methods

Generation of Target Trajectories

In this study, the tracking control was performed on 2-DOF movements of the wrist joint (the dorsi/palmar and the radial/ulnar flexions). Since the single wrist joint were controlled, the minimum angular jerk model was used for the generation of the target trajectories. This model can generate an appropriate trajectory with small amount of calculation.

The following cost function was minimized to plan the trajectory:

$$C_\theta = \frac{1}{2}\int_0^{t_f} \left\{ \left(\frac{d^3\theta_1}{dt^3} \right)^3 + \left(\frac{d^3\theta_2}{dt^3} \right)^3 \right\} dt \qquad (1)$$

where t_f is the movement time. θ_1 and θ_2 shows dorsi/palmar and radial/ulnar flexion angles, respectively. Trajectories for two-point reaching movements are derived analytically as shown below:

$$\begin{aligned} \theta_1(t) &= \theta_1^s + (\theta_1^f - \theta_1^s)(15T^4 - 6T^5 - 10T^3) \\ \theta_2(t) &= \theta_2^s + (\theta_2^f - \theta_2^s)(15T^4 - 6T^5 - 10T^3) \end{aligned} \qquad (2)$$

where θ^s and θ^f are joint angles at the starting and the terminal points, respectively. $T = t/t_f$ is

normalized movement time ($0 \le t \le 1$).

Computer Simu1ation

Target trajectories were generated in the rectangular area on the joint angle plane with the center at 0deg (30deg in the direction of the radial/ulnar flexion and 50deg in the direction of the dorsi/palmar flexion). First, three points (A, B and C) were determined randomly. The target was moved from the origin (center) to the point C through the points A and B. The target was stopped at each point for 1sec and moved between two points for 2sec (Totally 10sec for each target). Each movement trajectory between two target points was generated based on Eq.(2).

The IDM was trained with the fixed iteration number of control (50 trials) using the generated target trajectories under the following conditions:

a) PID control only (without training)
b) 1 target trajectory
c) 5 trajectories changed every 10 control trials
d) 10 trajectories changed every 5 control trials
e) 50 trajectories changed every 1 control trials

where 3 sets of target trajectory were examined for each training condition b) ~ e).

Learning and control performance was examined by computer simulation with musculoskeletal model. Three different subject models were prepared, whose parameters were adjusted to the muscle properties of 3 normal subjects, respectively. Stimulated muscles were the ECR, the ECU, the FCR and the FCU. A three-layered ANN was used as a feedforward controller. The inputs of the ANN were time series of angles, angular velocities and angular accelerations of target movements at continuous 6 times, from n to n+5 (50ms interval). The ANN connection weights were updated after one control trial with the error back-propagation algorithm. Three initial patterns of the connection weights were prepared for each training condition.

Fifty unlearned target trajectories were prepared for evaluation of IDM learning. Mean error (ME) and root mean square (RMS) value of PID controller outputs were calculated for the evaluation as follows:

$$ME = \frac{1}{N}\sum_{n=1}^{N}\left|e(n)\right| \qquad (3)$$

$$RMS = \sqrt{\frac{1}{N}\sum_{n=1}^{N}\left\{I_{PID}(n)\right\}^2} \qquad (4)$$

where N is the total number of sampled data. ME was calculated for each movement direction and RMS was done for each muscle.

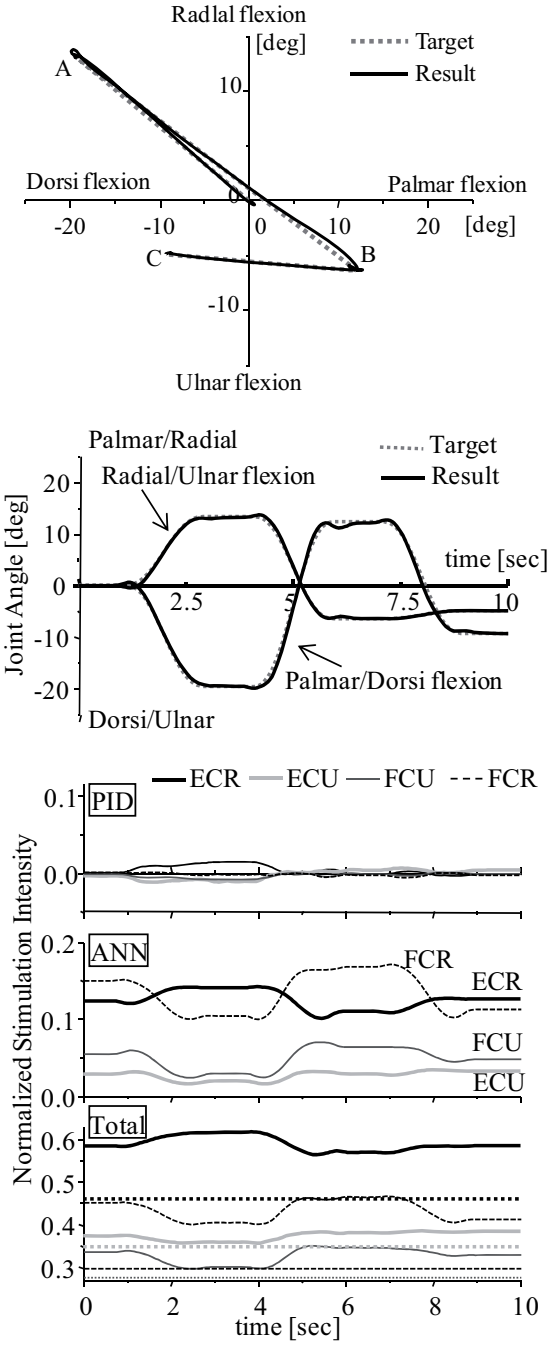


Fig.2 An example of control result for unlearned target trajectory (subject A, training condition e)). Joint angles, stimulation outputs of PID controller and ANN, and total output are shown. The dotted lines on the total output show stimulation thresholds.

Results

An example of control result for unlearned target trajectory is shown in Fig.2. Although the PID controller without the IDM showed delay in response, the FEL controller for FES (FEL-FES controller) performed good tracking decreasing the delay and output of the feedback controller to small values. Values of ME and RMS were decreased to 0.26deg from 1.13deg and to 0.005

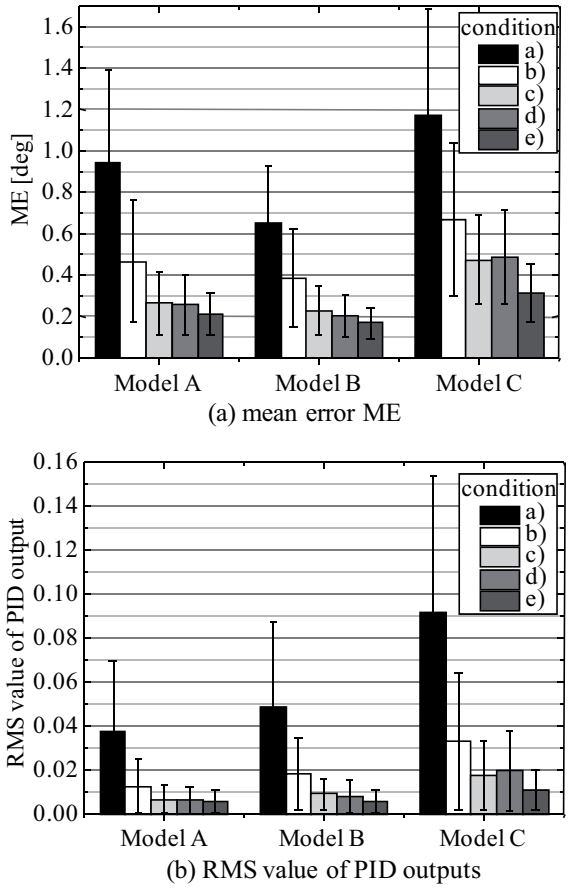


Fig.3 Evaluation results of ANN training. Average value and SD is shown for each training condition. For each training condition, 50 evaluation targets were controlled on 9 ANNs that were trained by different 3 sets of trajectory and different 3 patterns of initial connection weights.

from 0.044 by using the IDM, respectively in the case of Fig.2.

ME and RMS values of PID controller outputs were summarized in Fig.3. The training condition e) showed the minimum ME and RMS value of PID outputs. Variations of those values also decreased with the training condition e). Although the condition b) using one target trajectory improved the PID controller, ME and RMS values were larger than other three conditions. There is no large difference between the conditions c) and d).

Discussion

The FEL-FES controller improved tracking control of the targets including two-point reaching movements generated by the minimum jerk model decreasing delay, ME and RMS value of PID outputs. Since the IDM can acquire nonlinear characteristics of electrically stimulated musculoskeletal system, control performance would be improved. In addition, the learning type controller can decrease burden to users and medical staffs in controller parameter tuning for a lot of muscles. Therefore, the FEL-FES controller is expected to be effective clinically.

When ANN was trained with the same total number of iteration of control, increasing the number of target trajectories was effective. Especially, changing the target every control trial was most effective. This result suggests that the ANN was trained appropriately by using various target positions and movement velocities rather than repeated training with same target, even if training data is used only one time. In this paper, all target trajectories included 1sec staying at 4 points (center, A, B and C) and 2sec movement between 2 points. It is expected to test various target movements including different movement time, different number of positions and so on considering practical application.

Conclusions

Target trajectories for FEL controller for FES were generated by the minimum jerk model. In computer simulation tests, the IDM of the controlled limb realized by training the ANN decreased the output power of the feedback controller and improved tracking performance to unlearned target trajectories. The IDM performed well when target trajectory was changed every 1 control trial during ANN training.

References

[1] Kurosawa K, Futami R, Watanabe T, et al. Joint angle control by FES using a feedback error learning controller. IEEE Trans. Neural Systems & Rehab. Eng., 13(3): 359-371, 2005.

[2] Watanabe T, Iibuchi K, Kurosawa K, Hoshimiya N. A method of multichannel PID control of two-degree-of-freedom wrist joint movements by functional electrical stimulation. Systems and Computers in Japan., 34(5): 25-36, 2003.

[3] Flash T and Hogan N. The coordination of arm movements: An experimentally confirmed mathematical model. J. Neuroscience, 5(7): 1688-1703, 1985.

Acknowledgements

This study was partly supported by the Ministry of Education, Culture, Sports, Science and Technology of Japan under a Grant-in-Aid for Scientific Research (B), and the Saito Gratitude Foundation.

Author's Address

Takashi Watanabe
Dept. Biomedical Eng., Graduate School of Biomedical Eng., Tohoku University
nabet@bme.tohoku.ac.jp

Can non-invasive electrical stimulation of the brain (ESB) modify the resting-state functional connectivity of the motor cortex? A proof of concept fMRI study

Alon G, Roys S, Gullapalli RP.

Purpose: To develop and test an innovative method to obtain fMRI data during the application of non-invasive tDCS.

Materials and Methods: One subject participated in 5 MRI sessions. Functional images (Siemens 3T Tim Trio scanner, 8-channel head coil) were acquired using single-shot EPI T_2^*-sensitive sequence (TE = 30 ms, TR = 3s, 1.8 × 1.8 mm^2 in-plane resolution and a FOV of 23 cm) using 36 axial slices (4 mm thick) with no gaps between slices. A high resolution T1-weighted MPRAGE (TE = 3.44ms, TR = 2s, TI = 900ms, flip angle = 9º, 72 slices, slice thickness 2 mm, 0.898 × 0.898 mm^2 in-plane resolution and a FOV of 23 cm) was acquired for anatomic reference.

In each session, two resting state scans were separated by two tDCS scans and one functional activation scan involving the motor cortex. The functional scan was a self paced finger-thumb apposition task. Block design was used with 20s-On and 20s-Off for a total of 8 cycles. In tDCS sessions 1-3, 2 mA of direct current was applied for 6.45 min placing the positive electrode over the right primary motor area of the cortex and the negative electrode over the supra-orbital area on the left side of the head. In session 4-5 we applied a pulsed tDCS stimulator (tPDCS) with identical electrodes size and positions.

Data were analyzed using AFNI (Robert Cox, NIH) and MATLAB (MathWorks Inc., Natick, MA). Images were corrected for slice timing, registered, blurred with a 6mm FWHM Gaussian blur, and intensity normalized. For motor fMRI analysis, the general linear model (GLM) was used to determine the voxels that were significantly correlated with the motor task paradigm. For fcMRI, 7mm spherical regions of interest (ROIs) were drawn centered on the right M1 and left M1 regions, guided by the fMRI results. The resting-state time series from the voxels in the RM1 ROI were averaged and the resulting time series used as a regressor in the GLM analysis of resting state data. The functional connectivity maps thus obtained were thresholded at 0.65 of the maximum R^2 value, and then combined to give overlap maps for each of the 3 resting-state conditions (non-simulated, tDCS, and tPDCS). Voxels that were above the 0.65 threshold in all of the scans for each condition were considered “highly active” seed voxels (HASV).

Results: The ROI were the left and right M1 regions. During rest, the number of HASV in the left M1 were 401 compared to 65 HASV in the right M1, indicating 84% vs. 16% activity. tDCS increased the left M1 HASV to 564 and decrease the right M1 HASV to 19 (a 97% vs. 3% activation). Pulsed tDCS increase both the left (698) and right (168) HASV while decreasing the left M1 percentage to 76% and increasing the right M1 to 24%.

Conclusion: This maybe the first-ever in-vivo demonstration that non-invasive tDCS can affect fMRI recording of the motor cortex's resting-state. tDCS and pulsed tDCS may have different effect on fMRI derived hemodynamic response within the brain.

Session 6

Control, Sensors, Algorithms – invasive

Performance of implanted multi-site EMG recording electrodes: In vivo impedance measurements and spectral analysis.

Lewis S[1], Glindemann H[1], Russold M[1], Westendorff S[2], Gail A[2], Dörge T[3], Hoffmann K-P[3], Dietl H[1]

[1] Otto Bock HealthCare GmbH, Duderstadt, Germany

[2] German Primate Center, Göttingen, Germany

[3] Fraunhofer Institute for Biomedical Engineering, St. Ingbert, Germany

Abstract

The presented work is part of the development of a fully implantable EMG recording system for control of upper limb prosthetic devices. In the following, investigations on the usability of an implantable thin film electrode with multiple recording sites for intramuscular EMG are presented. Electrodes were implanted epimysially on the musculus deltoideus of a rhesus macaque. To our knowledge, this is the first investigation of such electrodes for muscular EMG recordings. Ingrowth was monitored by periodic impedance measurements over eight weeks after implantation. Increase of impedance plateaued after four weeks indicating a completed encapsulation of the electrodes. EMG was recorded during relaxation and reproducible voluntary contractions of the muscle. Power spectral analysis confirmed that EMG signals with a frequency content of up to 1.2 kHz could be recorded. During contraction the signal at 200 Hz was four orders of magnitude higher than during relaxation.

Keywords: *intra muscular EMG, implanted electrode, impedance, electrode ingrowth.*

Introduction

Recent developments of prosthetic limbs have resulted in increased functionality. Latest prosthetic hands offer a high number of degrees of freedom and sometimes even the movement of individual fingers. The challenge now is to provide adequate control signals for these devices.

State of the art is the use of surface EMG electrodes. Surface EMG records compound muscle activation and has a limited capacity to detect signals from deeper or smaller muscles. Moreover, differentiation of signals from different muscles (close to each other) is poor. It also frequently is influenced by movement artefacts and its sensitivity to changes in skin condition.

One approach to overcome this problem is the use of intracorporal signals. In transcarpal amputees who are still able to control the muscles in their forearm and amputees who underwent targeted muscle reinnervation [1] a high number of independent, intuitively controlled signals could be obtained by means of implanted electrodes recording intramuscular EMG.

The work presented here ultimately aims at controlling an upper extremity prosthesis by means of a new type of permanently implanted EMG electrode. Previously the first tests of the electrodes were reported [2]. Here we will report on in-vitro EMG recordings and first impedance measurements for eight weeks following implantation. We also report on a preliminary analysis of signals from the relaxed and contracted muscle.

Material and Methods

Animal model

For permanent recording of EMG three electrode arrays were implanted epimysially into the musculus deltoideus of one rhesus macaque. Suitable locations were chosen frontal, lateral and dorsal on the muscle with a distance of approximately 2 cm between electrode arrays. Electrodes were connected to a connector housing placed on the skull of the animal via subcutaneous cables. For follow-up investigations the monkey was placed in a monkey chair. The animals performed repeatable directed voluntary movements with his arm, thus generating reproducible contractions of the muscle under investigation. Animal care and all experimental procedures were conducted in accordance with German laws governing animal care.

Electrode arrays

The electrode arrays were fabricated in a micro technological process [3]. Each of the electrode arrays (Fig. 1) consisted of a 20 µm thick polyimide structure carrying five platinum recording sites with a surface area of 1 mm^2 and an inter-contact distance of 4 mm.

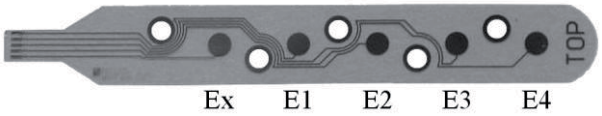


Fig. 1: Electrode array. Dark circles are the recording sites. White circles are suture holes for electrode fixation.

Two of the implanted electrodes had smooth platinum surfaces and one was coated with micro porous platinum [4].

Impedance measurement

Prior to implantation, impedance of electrodes with smooth and coated recording sites was measured in-vitro in saline (0.9% NaCl) to quantify the effect of coating on impedance reduction.

To monitor the process of electrode encapsulation, impedance measurements were carried out during implantation as well as two, four and eight weeks postoperatively. Impedance was measured between all possible combinations of recording sites of each electrode.

A custom built impedance measurement system was used [5]. The system applied a current of 1 μA_{RMS} consisting of a linear combination of frequencies from 1 Hz to 10 kHz between two recording sites. The resulting voltage was measured and decomposed into the induced frequencies by FFT, which allowed the calculation of the impedance at each frequency separately.

EMG measurements

Eight weeks after implantation EMG signals were recorded using a biosignal acquisition device (g.USBamp, g.tec). The signal was band-pass filtered with a pass band from 2 Hz to 2 kHz and sampled at 4.8 kHz. Spectral density of the recorded EMG signals was calculated in MATLAB (The MathWorks, Inc.) using Welch's method.

Results

Impedance in vitro

The reduction of impedance achieved by microporous coating of the contact surfaces is most dominant at low frequencies (Fig. 2). At 1 Hz impedance is reduced by 66.8% (330 kΩ). This reduction declines to 31.7% (1 kΩ) at 1 kHz. Coating of contact surfaces also reduces the introduced phase shift in the range of 8° to 12°.

Due to the loss of signals from the coated electrode within two weeks after implantation no further comparison between smooth and coated electrodes was possible.

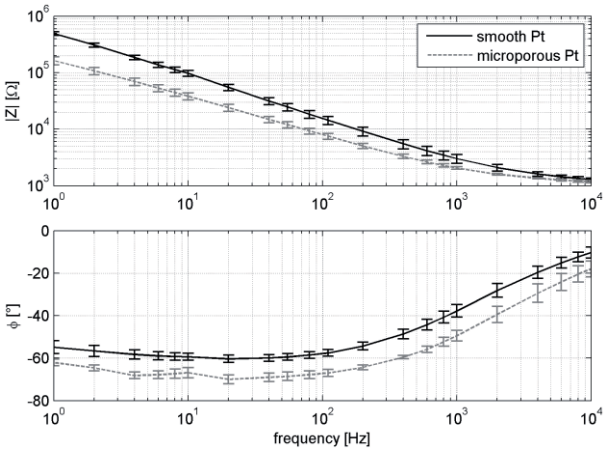


Fig. 2: Bode Plot of electrode impedance in saline of electrodes with smooth and coated surfaces.

Impedance of implanted electrodes

As shown in Fig. 3, impedance of the smooth electrode just after implantation is lower than the impedance measured in vitro, but at the same time showing a very similar course of the curve. The phase shift shows a decrease nearly logarithmic to frequency.

Two weeks after implantation impedance increases over the whole frequency range while the graph maintains a similar course. The introduced phase shift is increased for frequencies below 400 Hz.

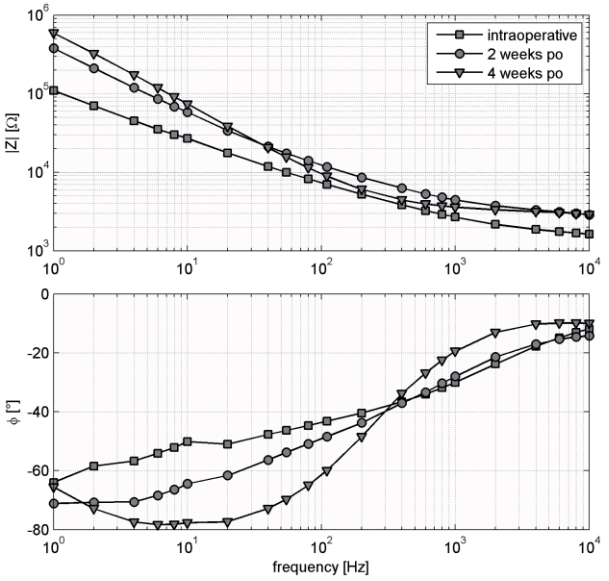


Fig. 3: Bode Plot of averaged impedance (all combinations of Ex-E4) of a smooth electrode over time after implantation.

Four weeks after implantation impedance is further increased for frequencies lower 35 Hz and also slightly reduced for higher frequencies. The course of the magnitude also shows a more pronounced bend at the transition towards nearly constant magnitudes around 1 kHz. The phase shift is further increased for frequencies up to 400 Hz and decreased for higher frequencies, reaching a

constant value of -10° above 4 kHz. Changes in electrode impedance plateaued four weeks after implantation.

Spectral differences between passive and activated muscle

Power spectral densities during activity and relaxation were calculated (Fig. 4) to evaluate the sensitivity to muscle activity.

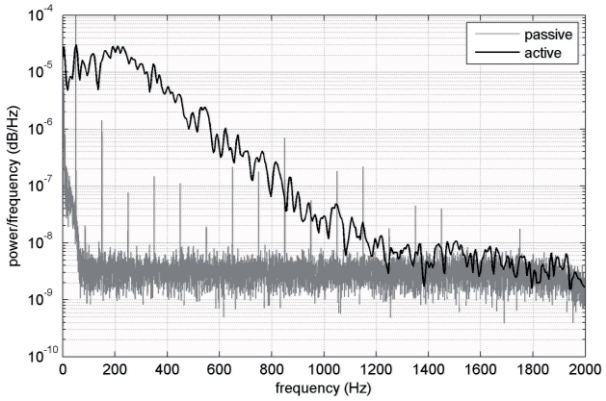


Fig. 4: Power spectral density estimate of recorded data during relaxation (passive) and movement (active) of the arm.

Power spectral density during relaxation of the muscle shows a constant frequency content from 70 Hz up to 2 kHz (onset of the low-pass filter). The spikes shown (Fig. 4) are the harmonics of the 50 Hz artefact which was intentionally not filtered. During contraction power spectral density is increased for frequencies up to 1.2 kHz with a peak at 200 Hz resulting in a clearly distinguishable power spectrum. At 200 Hz four orders of magnitude were observed between the signals (Fig. 4).

Discussion

Impedance was reduced in in-vitro and in intra-operative measurements by the microporous coating. Due to the loss of signals from the coated electrode the benefit of such electrodes in chronic conditions could not be investigated.

Impedance measurements showed considerable changes in electrode impedance over time following implantation. Magnitude of changes decreased over time and plateaued after a period of four weeks indicating a complete incorporation of the implanted electrodes.

The results confirm that the electrodes used are suitable to record intramuscular EMG for up to eight weeks. We were able to clearly distinguish activation and relaxation of the investigated muscle. We therefore conclude that the electrode is of interest for use in an implanted system for long-term permanent recording of intramuscular EMG.

Chronic long-term stability for more than 8 weeks will be investigated in follow-up experiments.

Additionally we will concentrate on further analysis of the recorded signals with an emphasis on efficient detection of muscle activity.

Conclusions

The applied electrodes were able to record intramuscular EMG for up to eight weeks after implantation. A clear discrimination between contracted and relaxed muscle could be made by offline analysis of the recorded data. Electrode impedance plateaued four weeks after implantation, indicating a complete incorporation of the electrodes at this point in time.

References

[1] Kuiken T-A, Dumanian G A, Lipschutz R D, Miller L A, Stubblefield K A, “The use of targeted muscle reinnervation for improved myoelectric prosthesis control in a bilateral shoulder disarticulation amputee”, Prosthetics and Orthotics Int., 28: 245-253, December 2004

[2] Ruff R, Poppendieck W, Gail A, Westendorff S, Russold M, Lewis S, Meiners T, Hoffmann K-P, “Acquisition of Myoelectric Signals to Control a Hand Prosthesis with Implantable Epimysial Electrodes” [submitted to IEEE EMBS 2010]

[3] Hoffmann K-P, Koch K P, Dörge T, Micera S, “New Technologies in Manufacturing of Different Implantable Microelectrodes as an Interface to the Peripheral Nervous System”, Proceedings of the 1 st IEEE/RAS-EMBS International Conference on Biomedical Robotics & Biomechatronics, 414-419, Feb 2006.

[4] Poppendieck W, Dörge T, Hoffmann K-P, “Optimization of microporous platinum coatings for neural microelectrodes”, Proceedings of the 13 th Annual Conference of the IFESS, 319-321, Sep 2008.

[5] Searle A, Kirkup L, “Real time impedance plots with arbitrary frequency components”, Physiol. Meas. 20: 103-114, 1999.

Acknowledgements

This work was supported by the German Federal Ministry of Education and Research under Grant 16SV3695.

Author’s Address

Sören Lewis
Otto Bock Healthcare Products GmbH
mail@soeren-lewis.de

Selectivity of longitudinal versus transverse tripolar stimulation of median nerve in pigs using a multicontact nerve cuff electrode

Kurstjens M, Jensen W

Center for Sensory-Motor Interaction, Dept. of Health Science and Technology, Aalborg University, Denmark

Abstract

The objective of the present study was to investigate the stimulation selectivity of a multicontact cuff electrode in a large nerve animal model. A cuff electrode with 6 contacts equally spaced around the inner circumference and two outer ring contacts was acutely implanted on the median nerve in pigs. The selectivity of activation of 7 forelimb muscles when applying monophasic stimulation in the commonly used longitudinal tripolar configuration (LTC) was compared to that when using the transverse tripolar configuration (TTC). Results showed that, depending on the electrode contact, current pulse amplitude and stimulation configuration used, up to 4 muscles were activated with 100% selectivity in a single animal. Using TTC increased selectivity compared to LTC for individual muscles but not the total number of muscles that was activated selectively and larger current amplitudes were needed to obtain activation. More sophisticated stimulation paradigms capable of targeting additional fascicles located more centrally in the nerve trunk will be needed in the future to provide sufficient number of control channels for advance degree of freedom upper limb prosthetic devices.

Keywords: *Selective electrical stimulation, nerve cuff electrode.*

Introduction

Functional neuromuscular stimulation is a technique whereby electrical excitation of neural tissue is used to elicit artificial control of paralyzed musculature [1]. For restoration of motor function, coordinated control over many muscles is necessary. To achieve this, a neural interface is needed that can selectively activate different fascicles in the nerve that each innervate a different muscle. Different types of extra and intra neural electrodes are currently available, but only nerve cuff electrodes have long shown the ability to provide a chronic reliable interface.

Selective activation of peripheral nerve using a cuff electrode with multiple contacts can produce selective activation of different muscles innervated by that nerve trunk and has been investigated extensively in different animal models as well as human [e.g. 1-4], but the degree of selectivity is limited. Most of these studies involved an electrode design where the number of tripolar channels (typically four, arranged circumferentially around the nerve) is in the order of number of fascicles contained in a lower limb nerve trunk (sciatic nerve) on which the electrode was applied. However, in case of upper limb application, the number of fascicles that are contained within the main target nerves (radial, median and ulnar nerve) and the number of muscles that they innervate are several times larger. The more traditional 4-channel cuff design may therefore not be sufficient in upper limb application. Few studies have applied cuff electrodes with more channels [5,6]. A 6-channel cuff offered better stimulation selectivity than a 4 channel cuff on the radial nerve in pigs [5], but was not used on the median nerve so far.

The aim of the present study was to investigate the stimulation selectivity of a 6-channel cuff electrode in upper limb in a large nerve pig model. Results will provide a base for future comparison with ongoing studies investigating the stimulation selectivity of multichannel thin-film intrafascicular electrodes in the same animal model [7,8].

Material and Methods

Animal preparation

All experimental procedures were approved by the Animal Experiments Inspectorate under the Danish Ministry of Justice. Experiments were carried out on six female Landrace-Yorkshire pigs placed under general anaesthesia (Isoflurane). With the animals in supine position, access to the left median nerve was achieved through the axilla. A multi-contact cuff electrode was placed around the median nerve (six 0.5 x 0.5 mm contacts equally spaced at 60° intervals around the inner circumference at cuff center, 1mm wide ring contacts at each end approx. 4 mm from the middle).

Bipolar patch electrodes were sutured on the surface of seven muscles, as close to the innervation points as possible. Five flexor muscles were chosen (M1: flexor digiti II, M2: flexor carpi radialis, M3: flexor digit superficialis, M4: flexor carpi ulnaris, M5: flexor digit superficialis (deep belly)) and two extensor muscles (M6: extensor carpi radialis, M7: brachialis).

Electrical stimulation

A programmable, multichannel electrical stimulator (STG2008, Multi Channel Systems) was used to apply controlled current pulses to the different electrode contacts. Cathodal stimulation was performed with the center electrode contacts in a longitudinal tripolar configuration (LTC) in all pigs, and transverse tripolar configuration (TTC) using shorted neighbour center contacts in three pigs. Applied pulses were monophasic, rectangular pulses with amplitudes ranging from 20 µA to 800 µA (duration 100 µs, frequency 2 Hz, 5 repetitions per level, 20 stimulation levels). The stimulation sequence was controlled via a USB connection between the stimulator and a laptop computer.

Data acquisition and analysis

The EMG activities from seven lower forelimb muscles were recorded in response to extra neural stimulation. The EMG activity was streamed to hard disk (HD24, Alesis) for offline analysis. The offline analysis consisted of band-pass filtering (20 Hz to 2 kHz), quantifying the peak-to-peak amplitude (V_{pp}) and normalizing the value to the maximum V_{pp} obtained for each muscle in the experiment. A response threshold of 10% of maximum activation was then defined for each channel [4]. A selectivity index (SI) was calculated for each muscle as the ratio between the response of that particular muscle and the sum of all muscles responses. An SI of 100% corresponds to only one of the muscles being active.

Results

Longitudinal stimulation

Fig. 1 shows the selectivity of muscle activation as function of current amplitude when using the TLC stimulation configuration in pig 4. The absence of SI values at the lowest current levels indicates that all muscle responses stayed below the threshold. Electrode contacts 1-3 activated first the whole flexor muscle group M1-M5 before full activation occurred (i.e. all muscles were recruited simultaneously). Contacts 5 and 6 showed selective activation of the flexor muscles M6 and M7. A SI of 100% was obtained for M3 and M7, using contacts 4 and 5 respectively. There was a tendency across all animals that per contact the selectivity was largest for two muscles. The number of muscles for which selective activation was achieved in the other pigs varied from 1 to 5, see Table 1.

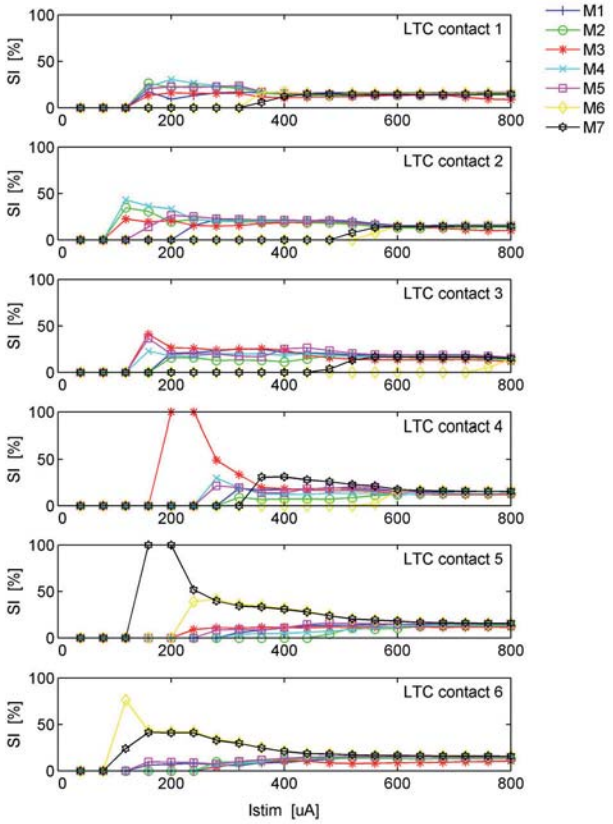


Fig. 1: Selectivity index plotted as function of current pulse amplitude obtained for the LTC configuration in pig 4.

Transverse stimulation

Applying the TTC stimulation configuration increased the overall selectivity in pig 4, see Fig. 2. However, larger current amplitudes were needed to exceed response threshold and the number of muscles with 100% selectivity did not change. For contact 5, all of the muscles were not activated sufficiently over the full current range. In all three animals, TTC showed large selectivity for one muscle per electrode contact, and low or none for the other muscles or no muscle activation at all.

Pig	TLC	TTC
# 1	M4	-
# 2	M4	-
# 3	M1, M2, M3, M5	-
# 4	M3, M7	M3, M7
# 5	M3, M5, M7	M1, M4, M5
# 6	M1, M3, M6	M1, M3, M6

Table 1: Overview across all pigs showing all muscles for which a SI of 100% was obtained.

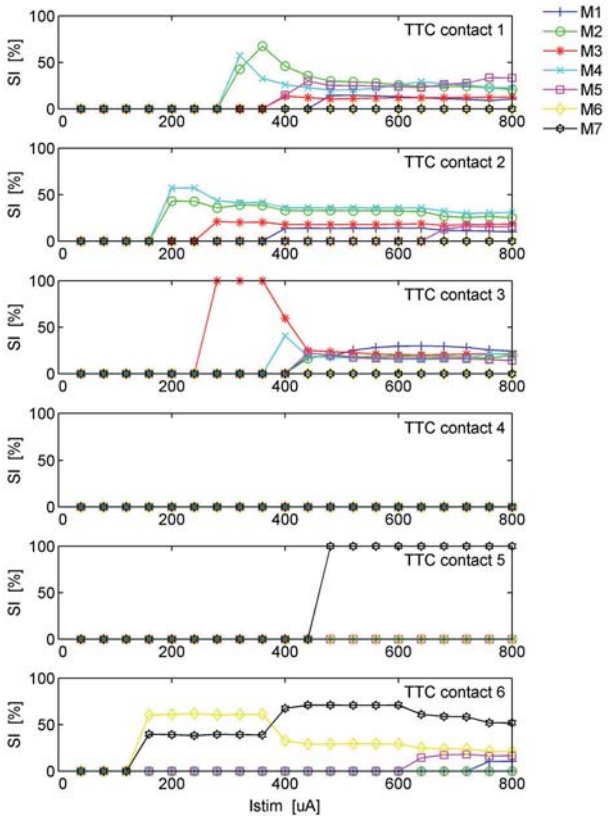


Fig. 2: Selectivity index as function of current pulse amplitude obtained for the TTC configuration in pig 4.

Discussion

Muscle recruitment as function of current amplitude was typical for the stimulation strategies used [1-6]. Obtained SI values were largest at the lower current levels when only the fascicle closest to the electrode contact was activated. At increasing current levels, "spill-over" excitation occurred in neighbouring fascicles and more muscles were activated leading to a SI equal for all muscles when full activation was reached.

Selectivity of muscle activation could possibly be improved by using more sophisticated stimulation paradigms such as the use of transverse steering currents [1,2] to activate localized regions deeper in the nerve trunk, or improvements in electrode design when more is known about the fascicular organization of the nerve trunk.

The present study focussed primarily on the degree of selectivity of activation. The relevance of the amount of actual activation was not considered here and remains an issue for future study.

Conclusions

The results of this study suggest that the fascicles of the most selectively activated muscles were located in the periphery of the nerve bundle. Selectivity depended on the electrode contacts as well as current amplitude used. TTC increased selectivity for individual muscles when compared to LTC stimulation, but larger current amplitudes were needed to obtain activation. More sophisticated stimulation paradigms capable of targeting additional fascicles located more centrally in the nerve trunk are needed to provide sufficient number of control channels for advance degree of freedom upper limb prosthetic devices.

References

[1] Sweeney JD, Crawford NR, Brandon TA. Neuromuscular stimulation selectivity of multiple-contact nerve cuff electrode arrays. Med & Biol Eng Comput, 33: 418-425, 1995.

[2] Grill WM, Mortimer JT. Quantification of recruitment properties of multiple contact cuff electrodes. IEEE Trans Rehab Eng, 4: 49-62, 1996.

[3] Navarro X, Valderrama E, Stieglitz T, et al. Selective fascicular stimulation of the rat sciatic nerve with multipolar polyimide cuff electrodes. Restor Neurol Neurosci, 18: 9-21, 2001.

[4] Polasek KH, Hoyen HA, Keith MW, et al. Human nerve stimulation thresholds and selectivity using a multi-contact nerve cuff electrode. IEEE Trans Neural Sys Rehab Eng, 15: 76-82, 2007.

[5] Schuettler M, Riso RR, Dalmose A, et al. Selective stimulation of pig radial nerve: comparison of 12-polar and 18-polar cuff electrodes. Biomed Tech (Berl), 47 Suppl 1 Pt 2: 696-699, 2002.

[6] Deurloo KE, Holsheimer J, Bergveld P. Nerve stimulation with a multi-contact cuff electrode: validation of model predictions. Arch Physiol Biochem, 108: 349-359, 2000.

[7] Kurstjens M, Jensen W, Yoshida K. Selective activation of pig forearm muscles using thin-film intrafascicular electrodes implanted in the median nerve. Proceedings 13th Ann conf IFESS: 279-281, 2008.

[8] Kundu A, Jensen W, Kurstjens M, Stieglitz T, Boretis T, Yoshida K. Dependence of implantation angle of the transverse, intrafascicular electrode (TIME) on selective activation of pig forelimb muscles. This meeting.

Acknowledgements

This study was supported by the Danish National Advanced Technology Fund (J. 005-2005-1).

Author's Address

Mathijs Kurstjens, PhD
Center for Sensory-Motor Interaction (SMI),
Department of Health Science and Technology,
Aalborg University, Fredrik Bajers Vej 7-D3,
DK-9220, Aalborg, Denmark.
eMail: mku@hst.aau.dk
homepage: www.smi.hst.aau.dk

Development of an Implantable Myoelectric Sensor for Advanced Prosthesis Control

Merrill DR[1], Joseph Lockhart[1], Troyk PR[2], Weir RF[3], Hankin DL[1]

[1] Alfred E. Mann Foundation for Scientific Research, Santa Clarita, CA, USA

[2] Sigenics Inc., Lincolnshire, IL, USA

[3]Rehabilitation Institute of Chicago, Chicago, IL, USA

Abstract

Modern hand and wrist prostheses afford a high level of mechanical sophistication, but the ability to control them in an intuitive and repeatable manner lags. Commercially-available systems using surface electromyographic (EMG) or myoelectric-control can supply at best two degrees-of-freedom (DOF), most often sequentially controlled. This limitation is partially due to the nature of surface-recorded EMG, for which the signal contains components from multiple muscle sources. We report here on the development of an implantable myoelectric sensor (IMES) using EMG sensors that can be chronically implanted into an amputee's residual muscles. Because sensing occurs at the source of muscle contraction, a single principal component of EMG is detected by each sensor, corresponding to intent to move a particular effector. This system can potentially provide independent signal sources for control of individual effectors within a limb prosthesis. The use of implanted devices supports inter-day signal repeatability. We report on efforts in preparation for human clinical trials, including animal testing, and a first-in-human proof of principal demonstration where the subject was able to intuitively and simultaneously control two DOF in a hand and wrist prosthesis.

Keywords: *myoelectric sensor, prosthesis control, EMG, electromyographic*

Introduction

Out of approximately 100,000 people in the USA with upper limb loss [1], 57% are transradial (below elbow) amputees [2], [3]. About 80% use a prosthesis [4], of which 50% are myoelectric-controlled [5] and 50% are body-powered and controlled. In myoelectric control, electrodes on the skin of the residual limb detect electric potentials from underlying muscles (electromyograms, or EMGs). These EMG signals contain components from several active muscles in the residual limb [6]. Algorithmic processing has been attempted for differentiation of distinct signal sources, but this technique is not optimized. A maximum of four independent surface EMG sites can be located on a residual limb [7], and typically only two sites are used in an agonist-antagonist (flexor/extensor muscles) arrangement.

In a three-state, two-site EMG controller, rapid co-contraction of extensors and flexors switches between the modes of hand opening/closing and wrist supination/pronation. Sequential control is slow and unintuitive; thus many amputees abandon their prostheses since it is easier to perform tasks with their intact hand.

Mechanical prostheses have been developed with high numbers of degrees-of-freedom (DOF), including the DARPA RP2007 DEKA arm with 18 DOF, and the DARPA RP2009 Applied Physics Laboratory arm with over 25 DOF. Unfortunately, the lack of independent control sources, lack of simultaneous multi-DOF control ability, and lack of repeatable control sources limits commercially available transradial prostheses to at best two DOF with sequential control.

We have previously reported on development of the Implantable Myoelectric Sensor (IMES) system [8], [9] which uses devices chronically implanted into the residual muscles of an amputee's arm using minimally invasive surgical techniques (Fig. 1). By using a stable EMG sensor implanted within the source muscle, a single principal component of EMG is detected. These signals, corresponding to the intent to move a particular part of the anatomy, can be decoded and used to drive the appropriate effectors in a prosthesis. By using an implanted device, we have mitigated the problem of multiple-component EMGs inherent in surface recording. By using a leadless telemetered device, we have mitigated the infection risk present with any transcutaneous recording system, as well as issues with inter-day donning and doffing electrode placement.

We report here on our further development of the system in preparation for deployment into clinical trials for prosthesis control.

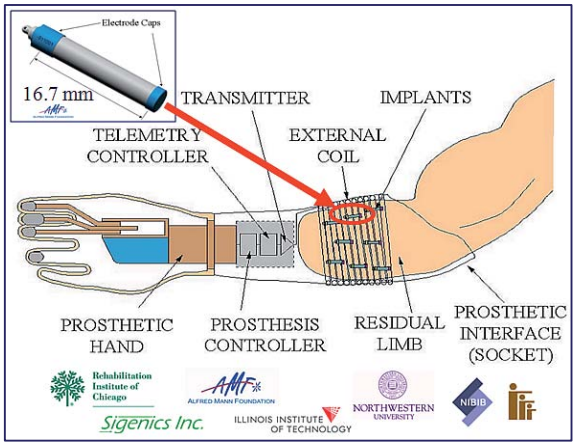


Figure 1: Schematic of the Implantable Myoelectric Sensor System. Implant devices are 2.4 mm dia. x 16.7 mm length, and act as differential amplifiers. One or more devices can be implanted into gross muscle, and telemeter EMG data to an external coil connected to a telemetry controller (TC). The TC passes the EMG to the prosthesis controller to drive a prosthesis.

Material and Methods

IMES Technical Description

The implanted sensors receive power and commands from an external telemetry controller (TC) driving a coil that will ultimately be built into an amputee's prosthetic socket. Each implant acts as an independent differential amplifier connected to two electrodes (on the ends on the implant) to detect the EMG generated during muscle contraction. The implants transmit the EMG signals as digital data over a transcutaneous magnetic link to the TC, which then reforms the analog EMG signals for presentation to a prosthesis controller. Each implant is housed in a hermetic, biocompatible ceramic package originally developed by the Alfred Mann Foundation (AMF) for the Radio Frequency Microstimulator (RFM). These packages have a qualified benign lifetime in-vivo of 80 years.

The system is designed to telemeter EMG data on one of two bands. Integrated EMG (band 1) is the format used in commercial myoelectric systems, thus allowing for direct replacement of surface recordings to drive current myoelectric prostheses. Raw EMG capability (band 2) has been designed to support future advanced control algorithms requiring higher sampling rates. The frame-based transmission scheme uses 32 time slots per frame, which can be assigned to individual IMES to optimize sample rates for a particular set of implants. In the human demonstration reported here, four IMES were used. Band 1 was set for 120 samples/s/IMES (480 samples/s aggregate). Band 2 was not used in the demonstration, but is capable of transmitting raw EMG signals at 444 frames/s, which for four IMES yields 3,552 samples/s/IMES (14,208 samples/s aggregate).

Animal Experiments

Three cats were each implanted with two IMES sensors into the tibialis anterior and lateral gastrocnemius muscles [9]. Bi-weekly recordings were taken for 12 months. Chronic stability was evaluated using statistical markers in the power spectral density. X-rays were taken at post-implant and 6 and 11 months post-implant.

Nine IMES sensors were implanted into the forearm of a rhesus monkey. Simultaneous recordings have been taken for over two years while the monkey performed individuated and combined finger flexions on a manipulandum [10]. Off-line pattern recognition was performed using a parallel linear discriminant analysis (LDA) to decode finger activity. A second monkey has subsequently been implanted with IMES. This experiment is ongoing.

First-in-human demonstration

To demonstrate proof of principle, a human volunteer was acutely implanted with four pairs of fine wire bipolar electrodes into the supinator, pronator teres, extensor digitorum, and flexor digitorum muscles (Fig. 2). The leads exited the forearm percutaneously and were connected to four IMES implants, contained within the TC external coil. On the same volunteer, four pairs of surface EMG electrodes were placed over these same muscles. A two-DOF hand and wrist prosthesis (Motion Control, Salt Lake City, UT, USA) was driven by either the four pairs of intramuscular (IMES) recordings or the four surface recordings, allowing a head-to-head performance comparison. The comparison was video recorded.

Results

Animal Experiments

The signal content recorded from chronic cats was stable over time, and x-rays indicated no migration of devices. All devices operated without problems throughout the study.

In the chronic monkey experiment, EMG from different IMES demonstrated very little cross-correlation. Training was stable across data sets that were collected months apart.

The animal experiments suggest that IMES implants do not migrate over time and yield stable EMG signals.

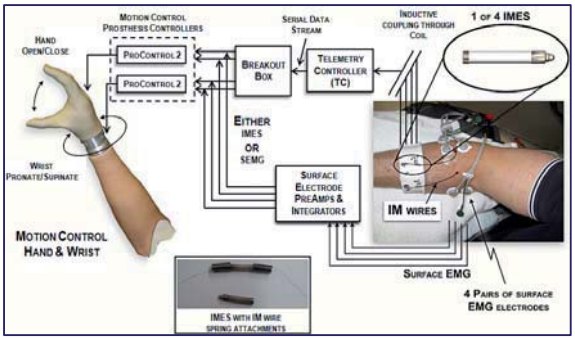


Figure 2: System used in 2 DOF prosthesis control demo. Fine wire intramuscular electrodes were attached to the IMES electrodes via springs. The coil is not shown so the IMES cuff can be seen.

First-in-human demonstration

The IMES control system provided excellent tracking of the prosthesis to the movement of the natural hand in an intuitive manner, demonstratively better than the control obtained with the surface electrodes. The combined time for IMES parameter setup and training of the volunteer was about one hour. Using the IMES devices the volunteer was able to simultaneously and intuitively control two DOF, in a manner which could not be matched with the surface control system.

Discussion

An IMES system has been designed and tested which we believe will offer superior control, relative to surface EMG, for upper limb prostheses. We have demonstrated the stability of control signals in chronic animals and simultaneous two-DOF control in a human volunteer.

We are now continuing with design verification, which will be followed by miniaturization of the telemetry controller for incorporation into a prosthesis shell in preparation for human clinical trials.

Conclusions

The implantable myoelectric sensor offers promise as a stable control signal sensor which will allow acquisition of independent principal components of EMG from distinct muscles, thus mitigating the problem of multiple-component EMGs inherent in surface recording, and facilitating true intuitive and simultaneous multiple-DOF prosthesis control.

References

[1] Ziegler-Graham K, MacKenzie EJ, Ephraim PL, et al. Estimating the prevalence of limb loss in the United States: 2005 to 2050. Arch Phys Med Rehab 89: 422-29, 2008

[2] Kay H and Newman J. Relative incidence of new amputations. Orth Prosth 29: 3-16, 1975

[3] Glatty HW. A statistical study of 12,000 new amputees. Southern Med J 57: 1373-78, 1964

[4] Biddiss EA and Chau TT. Upper limb prosthesis use and abandonment: A survey of the last 25 years. Prosth Orth Intl 31: 236-57, 2007

[5] Whiteside SR, et al. Practice Analysis Task Force. American Board for Certification in Orthotics and Prosthetics, Inc. Alexandria, VA 2000

[6] Basmajian J and De Luca C. Muscles alive: Their functions revealed by electromyography. 5th ed. Baltimore, MD. Williams and Williams. 1985

[7] Ajiboye AB and Weir RF. A heuristic fuzzy logic approach to EMG pattern recognition for multifunctional prosthesis control. IEEE Trans Neural Sys Rehab 13: 280-91, 2005

[8] Weir RF, Troyk PR, DeMichele G, Kerns D. Technical details of the implantable myoelectric sensor (IMES) for multifunction prosthesis control. Proceedings of the 2005 IEEE Engineering in Medicine and Biology 27th Annual Conference, Shanghai, China, 7337-40, 2005

[9] Weir RF, Troyk PR, DeMichele GA, et al. Implantable myoelectric sensors (IMESs) for intramuscular electromyogram recording. IEEE Trans Biomed Eng 56: 159-71, 2009

[10] Greger B, Baker J, Scheme E, et al. Continuous detection and decoding of dexterous finger flexions with implantable myoelectric sensors. IEEE Trans Neural Sys Rehab Eng, in print, 2010

Acknowledgements

The authors would like to acknowledge the help of Alex Birdwell of the Biomechatronics Development Laboratory, Rehabilitation Institute of Chicago, in acquiring the intramuscular signals.

Author's Address

Daniel R. Merrill
Alfred E. Mann Foundation for Scientific Research
P.O. Box 905
Santa Clarita, CA 91380 USA
danm@aemf.org

An experimental setup for stimulation selectivity measurement - variability of the muscle responses to the constant stimulus

Maciejasz P[1], Marcol W[2], Paśniczek R.[1,3], Dörge T.[4]

[1] Institute of Metrology and Biomedical Engineering, Warsaw University of Technology, Warsaw, Poland

[2] Department of Physiology, Medical University of Silesia, Katowice, Poland

[3] Department of Rehabilitation, Medical University of Warsaw, Warsaw, Poland

[4] Department Medical Engineering & Neuroprosthetics,
Fraunhofer Institute for Biomedical Engineering IBMT, St. Ingbert, Germany

Abstract

Selective nerve stimulation may allow decreasing an invasiveness of procedures aiming at restoration of the sensory and motor function lost due to neurological disorders or injuries. The beneficial application of selective stimulation in medicine is however often hindered by duration of procedures necessary for the setting of the stimulation parameters.

To find a method allowing for quick determination of the stimulation parameters producing a specified response, an experimental setup has been developed. The setup comprises a programmable current stimulator with signal analyzer and computer with experimental software that controls the operation of the stimulator and processes signals (EMG, ENG, force, displacement, etc.) recorded in response to the stimulation.

To verify the reliability of the system, preliminary experiments on rats have been conducted. The sciatic nerve has been stimulated with the use of a 12-polar cuff electrode. A MEMS gyroscope has been attached to the paw. The value of the rats paw's angular displacement in response to the stimulation has been used as an indicator of muscle response to the stimulation. A series of various stimuli have been generated three times. During each series, each stimulus was repeated three times. Intra- and inter-series response variability for each stimulus has been calculated.

The inter-series variability of responses to the same stimulus was significant and higher than intra-series variability. However, the spectra of all responses recorded during each series were similar. It has been also observed that stimuli of various duration and amplitude, but same charge per phase and stimulation contacts combination, produced similar responses.

The variability of the muscle response to the constant stimulus may have both technical and physiological causes. In practical application, e.g. neuroprostheses, this variability may be difficult to be avoided. Therefore, close-loop control of stimulation parameters may be necessary in order to precisely control activation level of effectors by selective stimulation of nerve fibres.

***Keywords**: selective stimulation, peripheral nerves, cuff electrode, rats, inertial sensors*

Introduction

In neuroprosthetics, direct nerve stimulation is used for restoration of sensory and motor functions lost due to neurological disorders or injuries [1]. It has been shown that the use of multi-contact electrodes can allow for activation of various effectors by changing stimulation contacts and parameters [2]. It is believed that this technique might help to restore lost functions with higher precision and lower invasiveness. However, determination of pulse parameters resulting in selective activation of effectors is time consuming, what hampers the application of selective stimulation in medicine.

Our work aims at developing algorithms for fast determination of nerve stimulation parameters allowing for an activation of the specified effectors. For that purpose we have developed an experimental setup. In order to determine reliability of the setup, preliminary experiments have been conducted.

Material and Methods

The setup

The setup consists of a computer with especially developed control software and a prototype of the programmable current stimulator with embedded signal analyzer. The software enables the control of all stimulation and acquisition parameters, as well as processing, logging and visualization of acquired data. The current stimulator, model PULSEGEN/ANA-16-10, has been developed for the purpose of that project by Creotech Ltd. (Poland). It has 16 current outputs and 8 inputs for signal acquisition. Pulse duration and amplitude on

each output channel can be independently adjusted with precision up to 62 ns and 8 µA, respectively. The sampling rate of input channels is 60 kHz with a resolution 8 bit.

Experimental procedure

In order to verify the reliability of the experimental setup, a series of experiments on rat has been conducted. All procedures have been approved by the Local Ethics Committee. The rat was anaesthetised with chloral hydrate (0.42 g/kg body weight). A 12-polar cuff electrode (Fraunhofer IBMT, fig. 1) has been implanted around the right sciatic nerve. A dual axis gyroscope (LPY530AL, STMicroelectronics) has been attached to the right paw. The rat's leg just above the ankle has been attached to the stereotactic frame in such a way, that the movement of the leg above ankle was constrained, but movement of the paw was not restricted.

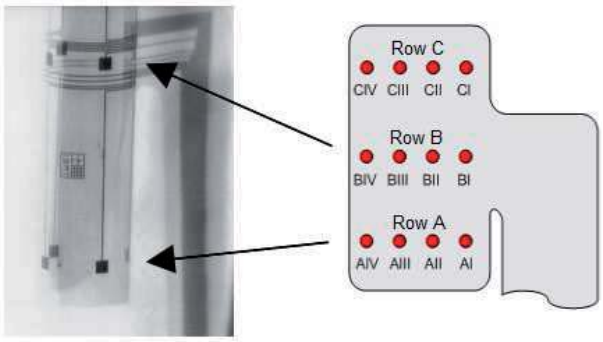


Fig. 1: 12-polar cuff electrode [3] (left) and symbols of stimulating contacts used in the paper (right).

Three series of various monopolar rectangular stimuli have been generated. During each series, each stimulus was repeated 3 times. The minimal delay between pulse repetitions was 400 ms and the delay between each series was 40 minutes. During each stimulation series same stimuli in the same order have been generated.

Each time one of the contacts from row B (Fig. 1) was anode. The corresponding contacts at rows A and C (i.e. A1 and C1 for contact B1) have been grounded. In some cases second contact from row B has been used as a "steering electrode" [4]; it could be anode, cathode or grounded. The amplitude of stimulus generated through the first stimulating contact (main pulse) was 50, 100, 200 or 400 µA. The amplitude of the "steering pulse" was always (if any) 50 or 100% of the main pulse (but in some cases with opposite polarity). Pulse durations of 10, 20 and 40 µs have been used. The main and the steering pulses were generated concurrently and had the same duration.

Response variability estimation

After each stimulus the angular velocity of the rat's paw was recorded and the ankle's angular displacement (flexion/extension and ad-/abduction) has been calculated. For each stimulus intra-series (F_{intra}) and inter-series (F_{inter}) variability of angular displacement normalised to the mean displacement value has been calculated. Only angular displacements higher than 0,5° have been taken under consideration.

$$F_{intra} = \frac{\sum_{i=1}^{3}\sqrt{(\bar{x}_k - x_i)^2 + (\bar{y}_k - y_i)^2}}{3}\,\frac{100}{\sqrt{\bar{x}_k{}^2 + \bar{y}_k{}^2}}$$

$$F_{inter} = \frac{\sum_{k=1}^{3}\sqrt{(\bar{x} - \bar{x}_k)^2 + (\bar{y} - \bar{y}_k)^2}}{3}\,\frac{100}{\sqrt{\bar{x}^2 + \bar{y}^2}}$$

where:

k - series number

x_i, y_i - ankle ab-/adduction x_i and flexion/ extension y_i values recorded for the particular repetition of the stimulus during a specified series

$\bar{x}_k, \bar{y}_k$ - mean ab-/adduction $\bar{x}_k$ and flexion/ extension $\bar{y}_k$ values recorded for the stimulus during a specified series

$\bar{x}, \bar{y}$ - mean ab-/adduction $\bar{x}$ and flexion/ extension $\bar{y}$ values recorded for the stimulus during all series.

Results

In Fig. 2, mean values of maximal displacements recorded during the third stimulation series for various stimuli are presented. Plots for the first and the second stimulation series were very similar to the one presented. The circled area indicates the highest concentration of the observed responses. These responses probably correspond to the situation when all or almost all fibres within the nerve were stimulated.

High variability of the displacements recorded for the same stimuli during the experiment has been observed. The mean value of the intra-series variability F_{intra} was 5.8 (SD=8.99), 4.25 (SD=4.21) and 4.88 % (SD=4.12) during the first, second and third series, respectively. The mean value of the inter-series variability for all stimuli F_{inter} was 12.26 % (SD=9.91).

In Fig. 3, angular displacements recorded for selected stimuli without steering pulses are presented. Each point corresponds to mean paw

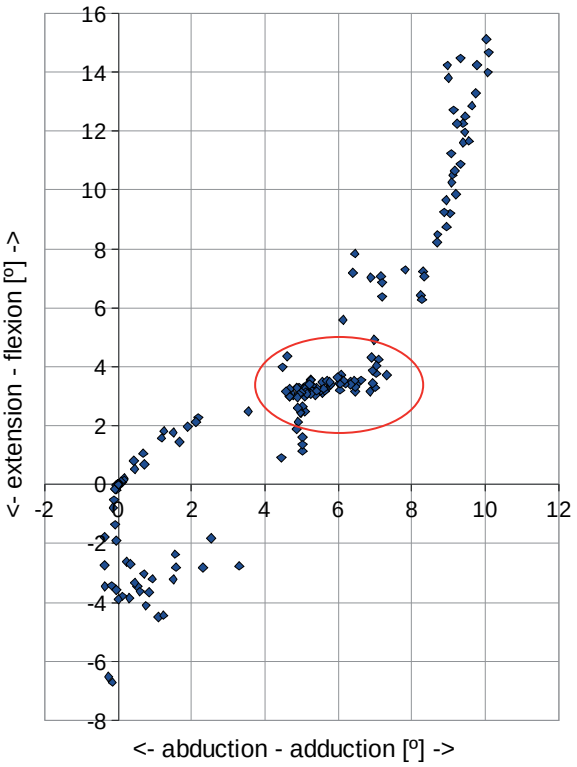


Fig. 2: Mean maximal displacements recorded during the third stimulation series for various stimuli.

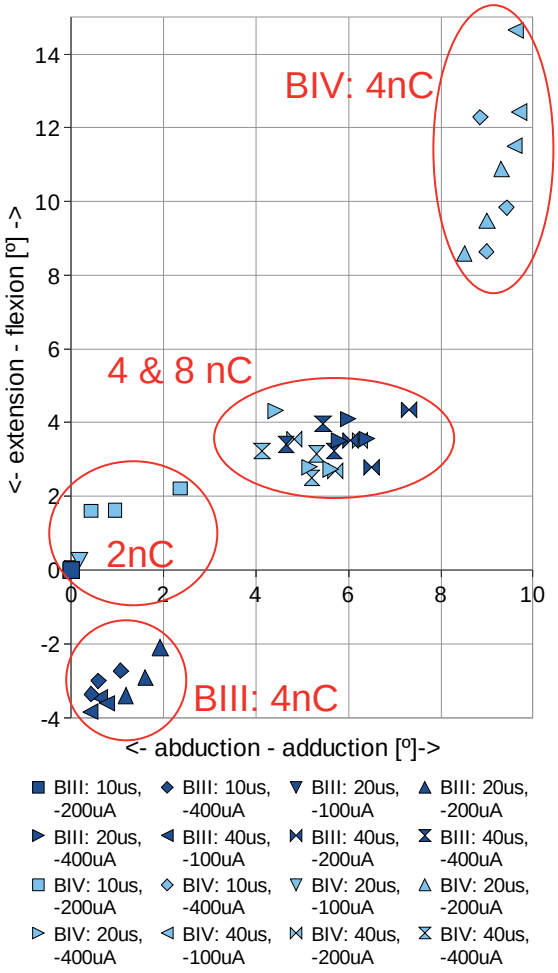


Fig. 3: Angular displacements recorded for selected stimuli during various stimulation series.

displacement in response to a particular stimulus during particular stimulation session. Variability of responses to the same stimulus during various series can be observed. It is also possible to distinguish areas with responses only to stimuli of particular charge and (in some cases) stimulating contacts combination.

Discussion

The variability of the response to the same stimulus could have a number of reasons. Among them are: response measurement error (drift of sensor), nerve impedance change (e.g. due to swelling), alternating influence of the anaesthesia on the nerve excitability, muscle fatigue due to prolonged stimulation. To some extent the variability of the muscle response to the same stimulus may be also normal physiological behaviour.

Conclusions

In practical application (e.g. neuroprostheses) it may be difficult to avoid variability of responses to the same stimulus. Therefore close-loop control of stimulation parameters and frequency may be necessary to achieve the precise control of effectors activation by selective stimulation of nerve fibres.

References

[1] Hoffmann KP, Dehm J [Eds.]. VDE-Studie zum Anwendungsfeld Neuroprothetik. VDE, Frankfurt, 2005

[2] Prodanov D, Marani E, Holsheimer J. Functional electric stimulation for sensory and motor functions: progress and problems. Biomed Rev, 14: 23-50, 2003

[3] Koch KP. Neural prostheses and biomedical microsystems in neurological rehabilitation. Acta Neurochir Suppl, 97:427-434, 2007

[4] Sweeney JD, Ksienski DA, Mortimer JT. A nerve cuff technique for selective excitation of peripheral nerve trunk regions. IEEE Trans Biomed Eng. 37:706-715, 1990

Acknowledgements

This work has been supported by the European Union in the framework of European Social Fund through the Warsaw University of Technology Development Programme.

Author's Address

Paweł Maciejasz
Institute of Metrology and Biomedical Engineering
Warsaw University of Technology
ul. Sw. A. Boboli 8, 02-525 Warszawa, Poland
eMail: pawel.maciejasz@gmail.com

EMG recordings of triceps brachii muscle in rats during downhill locomotion

Arnold D.[1], Faenger B.[1], Huebner A.[1], Scholle H.Ch.[1]

[1] Division for Motor Research, Pathophysiology and Biomechanics, Department for Trauma-, Hand and Reconstructive Surgery, University Hospital, Friedrich-Schiller-University Jena, Germany.

Abstract

With the presented study a data base is being built which should allow the comparison of EMG data of the triceps muscle of rats before and after training and / or electrostimulation. The triceps brachii muscle of rats showed strong activities during the stance phases of the foreleg. The muscle consists of a medial, lateral and long head. The medial head is covered by the two other heads and was not further examined in this study. The triceps brachii muscle in general is well investigated. The distribution of the different fibre types (von Mering & Fischer 1999) and the position of its motoneurons (Lucas-Osma & Collazos-Castro 2009) as well as the activation pattern for walking on a horizontal treadmill (Biedermann et al. 2000, Scholle et al. 2001 and Schumann et al. 2002) are sufficiently known. Furthermore the point of electrical sensitivity was identified with a new developed intramuscular multi-channel electrode (Faenger et al. 2009). In the presented study this electrode (MED-El) was used for investigations of the activation pattern during downhill locomotion on a motor driven treadmill. The activity of the long head reached a maximum before and during touch down of the hind limb, which is in contrast to normal locomotion. An additional activation peak was also observed in the lateral head directly after touch down. The modified motor control reflects in the different activation pattern. This could be explained with the changed acting forces.

Keywords*: triceps brachii muscle, EMG, intramuscular multi-channel electrode, motor control, rats*

Introduction

The long and the lateral head of the triceps brachii muscle of rats are under investigation in this study. The long head originates at the caudal border of the scapula and the lateral from the greater tubercle as well as from the neck of the humerus. They insert at the olecranon process of the ulna. Beside investigations of fibre type and motoneuron distributions the spatiotemporal activation pattern of rats' triceps brachii muscle during locomotion on a horizontal treadmill was revealed (1, 2, 3, 4). The activity shifted from central regions to the surface of the muscle. The long head was activated shortly before ground contact to dispose the hind limb of the touch down. During the stance the activity of the lateral head increased and exceeded this of the long head to stabilise the elbow joint.

The downhill locomotion demanded a modified activation. Up to now there are no studies which investigated the pattern of activity of the triceps brachii muscle during this kind of locomotion. To reveal the activation pattern the activity of both muscle heads were for the first time recorded during downhill locomotion. The muscle activation patterns of walking on a horizontal and an inclined treadmill were compared to expose the differences (1, 2, 3). This is needed for the next step of our study which is going to be the exercise of the triceps brachii muscle by downhill locomotion and physiological stimulations. These results should be indicating if this is an effective training for this muscle. Subsequently the electrostimulation should be similar to the physiological pattern to support the exercise.

In former studies matrix electrodes were fixed on the muscle surface to measure the myoelectrical activity (1). In a recent study a new intramuscular multi-channel electrode was developed. It enables measurements of muscle activity as well as the stimulation of muscles and different muscle regions (5). The new electrode worked very well with only the period of application as limiting factor. A new modified cardiac pacemaker electrode (MED-EL) was tested in current investigations because of its higher durability. This electrode is more inflexible and until now it was not possible to fix it reliably within the heavy moving triceps brachii muscle for more than a few days.

Material and Methods

Subjects:

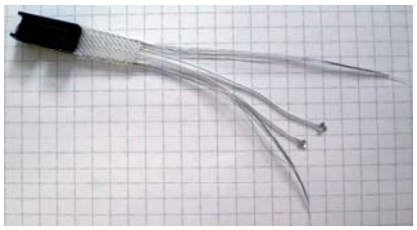
The experiments were carried out on 4 female adult rats (HanWistar). All animals were kept according to the German animal welfare regulations. The experiments were registered and

approved by the Committee for Animal Research of the Freistaat Thüringen, Germany.

Electrodes:

A new array platinum electrode with 16 channels (8 per raw) was used. The single electrodes are embedded in silicon. Just the outside is silicon free to allow the registration of muscle activity. All as well as the reference electrode are connected to a 20 pin micro connector (ODU Germany). They were manufactured by MED-EL (Austria) (Fig. 1).

A)



B)

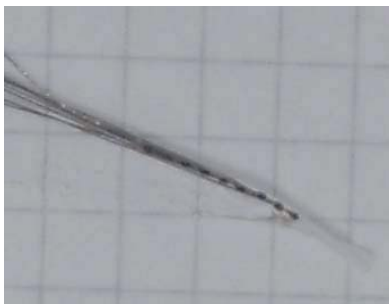


Fig. 1: A) Multi-channel array electrode, B) electrode in higher magnification

Surgery:

The animals were anaesthetized with isofluran. The nape and the foreleg were shaved; skin incisions in the nape and over the triceps brachii muscle were connected by a subcutaneous tunnel. Electrodes were implanted and fixed in the long and lateral head of the muscle. The micro connector was positioned in the nape and fixed with not absorbable sutures. Afterwards the skin incisions were closed.

EMG measurements and analysis:

EMG recordings started at the third postoperative day. The animals were connected to an amplifier box and walked downhill on a motor driven treadmill. The treadmill was tilted about 15° and the speed was adapted to the preferred pace of each animal. The EMG data recording (10-700 Hz, sampling rate 4000 Hz, 0,488 µV/bit) and the high-speed videography (300 frames/s) were synchronised.

For data analysis the frames of touch down and lift off of the hind limbs were identified from the high-speed videos. Those frame times were used in the raw EMGs as markers and RMS profiles (root mean square) were calculated over 1150 stance phases.

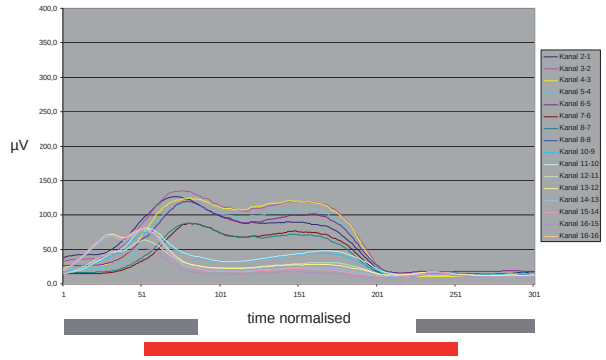
Stimulation:

After the EMG recordings an intermittent stimulation (2-3 mA, 30 Hz, 250 µs pulse width / Stiwell MED-EL) of the muscle was tested. The muscle reaction was observed. No force measurements were carried out.

Results

The activation patterns of the long and the lateral head of the triceps brachii muscle differ clearly (Fig.2A). The first activity in both muscle heads takes place at the end of the swing phase considerably before touch down of the foreleg. Maximum activity of the *C. longum* peaks two times - the first time before and the second during touch down. During the stance phase the activity decreases and in the second half it increases again. The basic level is reached before lift off. The activity of the lateral head achieves its maximum shortly after touch down. The activation profile forms nearly a plateau and ends at the same time as the activity of the long head. RMS-profiles of one muscle head differ within the amplitude but have identical shapes.

A)



B)

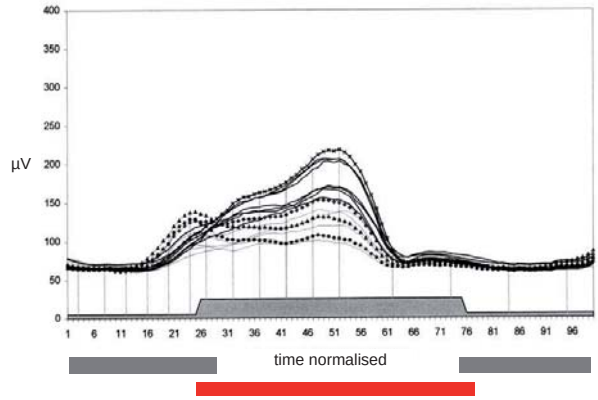


Fig. 2.: A) Bipolar RMS-profiles of *C. laterale* (1-8) and *C. longum* (9-16), stance phase ipsilateral and contralateral foreleg during downhill locomotion; B) Bipolar RMS-profiles of *C. laterale* (line) and *C. longum* (dots) during walking on a horizontal treadmill (modified after 3.)

As long as EMG measurements could be carried out it was also possible to stimulate the muscle. The single electrode position determines how strong the muscle contracts.

Discussion

The activation pattern revealed for walking on a horizontal treadmill (1, 2, 3, 4, 5, Fig.2B) differs from the pattern in the presented study in two points in spite of the same walking speed. During downhill locomotion the activity of the *C. longum* reached two maxima before touch down. This muscle head acts as a fine tuning tool to prepare the foreleg for ground contact (1, 2, 3, 4, 5). Because of the tilted treadmill the foreleg has to be stretched out further and counteracts against the higher acceleration. Therefore the motor control of the muscle has to be different which is reflected in the modified activation pattern. In the *C. laterale* the maximum of activity in normal locomotion occurs in the second half of the stance phase (1, 2, 3, 4, 5) whereas the maximum in this investigation appears shortly after touch down. Because of the downhill locomotion the weight increases with the acceleration force. The lateral head has to stabilise the elbow joint against this higher weight in spite of the inappropriate conditions (lever, inertia, modified angel).

Conclusions

The presented study reveals the so far unknown activation pattern of the triceps brachii muscle during downhill locomotion. The EMG measurements exposed that the activation patterns of the *C. longum* and the *C. laterale* are modified compared to the horizontal walking. The additional stretching of the foreleg requires an additional activation of the muscle and the elbow joint needs earlier stabilisation during the stance phase because of the higher acceleration of the animal. The data results in the cognition that the downhill locomotion is an effective exercise for the triceps brachii muscle of rats. Additionally we will try to adjust the stimulation parameters to the revealed physiological activation pattern to optimize the supporting stimulation.

References

1: Biedermann F, Schumann NP, Fischer MS, Scholle HC. Surface EMG-recordings by using a miniaturised matrix electrode: a new technique for small animals. J Neurosci Methods, 97: 69-75, 2000.

2: Scholle HC, Schumann NP, Biedermann F, Stegeman DF, Grassme R, Roeleveld K, Schilling N, Fischer MS. Spatiotemporal surface EMG characteristics from rat triceps brachii muscle during treadmill locomotion indicate selective recruitment of functioneally distinct muscle regions. Exp Brain Res, 138: 26-36, 2001.

3: Schumann NP, Biedermann FHW, Kleine BU, Stegeman DF, Roeleveld K, Hackert, R, Scholle HC. Multi-channel EMG of the M. triceps brachii in rats during treadmill locomotion. Clin Neurophysiol, 113: 1142-51, 2002.

5: Faenger B, Schumann NP, Arnold D, Grassme R, Scholle HC. Dynamic intramuscular activation patterns of the rats triceps brachii during locomotion – comparison between supra- and intramuscular multichannel EMG. Acta Physiologica International Joint Meeting, Acta physiologica 186(1): 245, 2006.

6: Lucas-Osma AM, Collazos-Castro JE. Compartmentalization in the triceps brachii motoneuron nucleus and its relation to muscle architecture. J Comp Neurol. 516:226-239, 2009.

7: von Mering F, Fischer MS. Fibre type regionalization of the forlimb muscles in to mammalian species, *Galea musteloides* (Rodentia, Caviidae) and *Tupaia belangeri* (Scandentia, Tupaiidae), with comments on postnatal myogenesis. Zoomorphol 119:117-126, 1999.

Acknowledgements

Supported by:

MED-EL Austria

Special thanks to IVTK Jena

Author's Address

Dr. rer. nat. Dirk Arnold

Division for Motor Research, Pathophysiology and Biomechanics

Department for Trauma-, Hand- and Reconstructive Surgery, University Hospital Jena
Friedrich-Schiller-University Jena

Erfurter Street. 35, 07743 Jena, Germany

e-mail: dirk.arnold@med.uni.jena.de

In vivo electrical stimulation of rat triceps brachii muscle to identify intramuscular electrical sensitive points

Faenger B.[1], Schumann N.P.[1], Arnold D.[1], Grassme R.[1/2], Fischer M.S.[3], Scholle H.Ch.[1]

[1] Division for Motor Research, Pathophysiology and Biomechanics, Department for Trauma-, Hand and Reconstructive Surgery, University Hospital, Friedrich-Schiller-University Jena, Germany.

[2] Berufsgenossenschaft Nahrungsmittel und Gaststätten, Geschäftsbereich Prävention Erfurt, Germany.

[3] Institute of Systematic Zoology and Evolutionary Biology with Phyletic Museum, Friedrich-Schiller-University Jena, Germany

Abstract

Earlier studies aim at a precise characterisation of intramuscularly varying recruitment patterns within M. triceps brachii (Biedermann et al. 2000, Faenger et al 2006). For physiologically justified FES (functional electrical stimulation) it is a primary condition to know more about inter- and intraindividual activation patterns. To protect the delicate muscle structure we developed, in cooperation with MED-El®, a flexible and atraumatic full silicone coated array electrode. This electrode can be used for intramuscular EMG measurements and for electrical stimulation. The aim of this study was to identify intramuscular electrically sensitive points in rat's triceps brachii muscle. Additionally Sihler´s staining and EMG measurements have been used to identify and display details about the intramuscular position of the electrode plate in relation to nerve branches. Results show that the maximum time of feasible continuous stimulation varied between a few seconds and several hours, depending on the electrode plate position being the stimulation position. Positions of motor end plates do not correspond to the positions of longest excitability. Considering the histological results, pairs of electrodes which could be stimulated for a long period of time were located very close to nerves or an intramuscular plexus. Around the surfaces of the electrode plates that can hardly stimulate the muscle non or only very thin nerves can be found.

***Keywords**: electrical stimulation, EMG, Sihler´s staining, motor end plate, multi-channel electrode, intramuscular electrical sensitive point*

Introduction

The effects of electrical stimulation on muscle are not fully known, but muscle fatigue is a limiting factor in functional electrical stimulation (FES). Muscle activation patterns have been investigated in several experimental studies [1, 2, 3, 4]. The results show that individuals have a very stabile EMG patterns for cyclic movements. Thus, there probably is a possibility to significantly reduce muscle fatigue by stimulating the muscle with help of these patterns. This could lead to a more physiological FES. Therefore, it is essential to identify electrical sensitive points in the muscle. It was published that there are indications for such areas in the muscle. In this study we started to identify intramuscular, electrically sensitive points in rat's triceps brachii muscle. Sihler´s staining has been used to display details about the electrode plate position in relation to nerve branches [5, 6]. Additional EMG was used to locate the motor end plates.

Material and Methods

Subjects:

The experiments were performed on 4 female adult rats (strain Wister), body mass between 246 and 311 g. All animals were kept according to the German animal welfare regulations. The experiments were registered and approved by the Committee for Animal Research of the Freistaat Thüringen, Germany.

Electrodes:

For stimulation and for additional EMG measurements we used our self-developed flexible and atraumatic full silicone coated platinum array electrode (Fig. 1). Two array electrodes (9 channels each, array with equal spacing between all adjacent electrodes) were placed into the M. triceps brachii - one array in the C. longum and the other one in the C. laterale (Fig. 1).

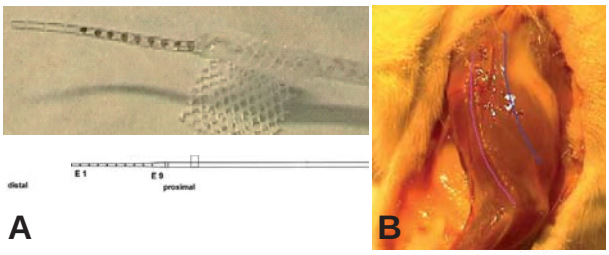


Fig. 1: Electrodes and orientation. A: Array electrode, B: Array electrode positions in M. triceps brachii.

C. longum, C. laterale

EMG measurements and analysis:

EMG-recordings started at the second postoperative day. The EMG was recorded (10-700 Hz, sampling rate 4000 Hz, 0,488 µV/bit) simultaneously with high-speed videography (Fig. 2).

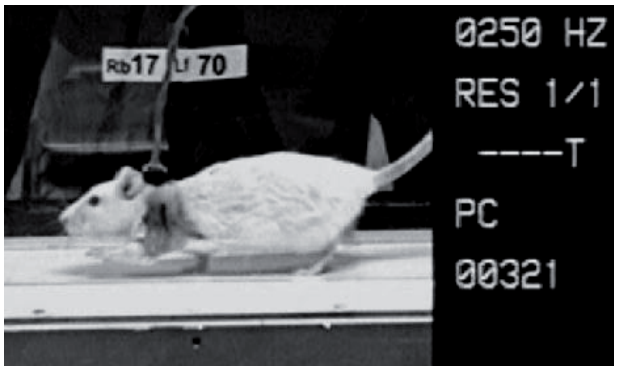


Fig. 2: Rat connected to the amplifiers during locomotion on a motor driven treadmill.

Stance phases were identified by the foot-down and foot-up points via the high-speed videos. Single steps were selected with respect to artefacts, ECG-complexes and gait mode.

In the EMG data the motor endplate activation can be localized and the following propagation along the muscle fiber can be traced (Fig. 3).

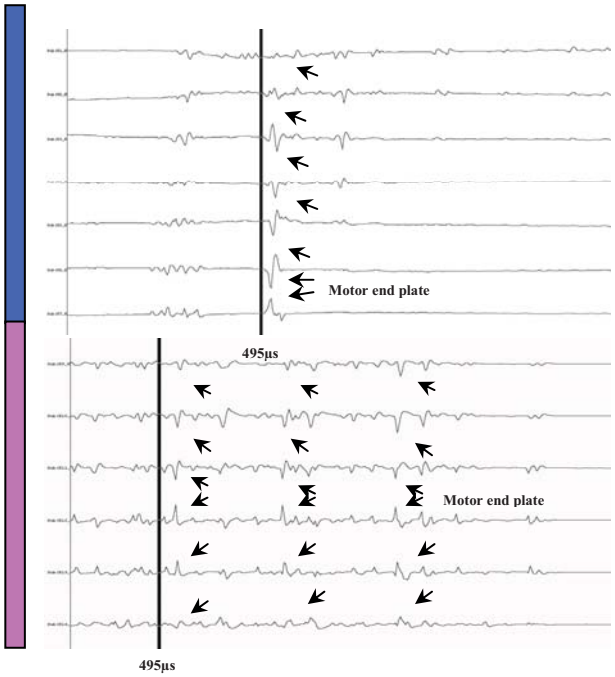


Fig. 3: Bipolar EMG signals during locomotion on treadmill. The motor endplates are located at the point of reversion of polarity.

↙ Motor end plate and propagation

C. longum, C. laterale

Sihler´s staining:

After finishing the stimulation procedures the stimulated muscle was stained with Sihler's staining to locate the electrode positions in relation to the nerve branches. This kind of staining allows a high resolution view at the nerve branches.

Stimulation:

An intermittent stimulation with a positive, rectangularly shaped signal of 1–7 mA at a frequency of 40 Hz with a pulse wide of 200 µs was applied to the muscle. Two seconds of stimulation were followed by a period of a two second stimulation pause. Rising and declining flanks took 0.5 s each.

Results

The stimulation time to fatigue (until no further muscle contraction could be registered) of different electrode pairs was measured in each of the four animals. The length of time period of respective stimulation is shown for one animal in Fig. 4 and Fig. 5.

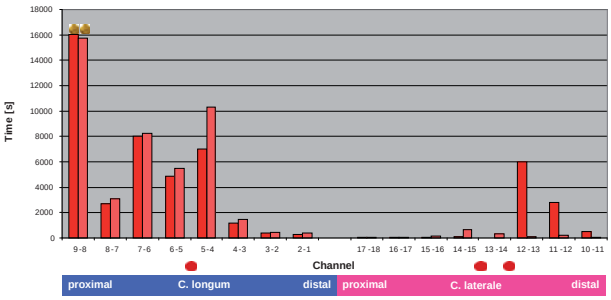


Fig. 4: Stimulation time and localisation of motor end plates.

● motor end plate, ● even longer stimulation periods possible

Channels 1–9 were located in the C. longum (channel 9 most proximally and channel 1 most distally in the muscle) whereas the channels 10–18 were sited in the C. laterale (channel 18 most proximally and channel 10 most distally) of M. triceps brachii. The brown circles on top of some of the bars in the diagram point out the channels that could have been stimulated even longer. In those cases the stimulation was stopped to defend the life of the animal from the long period of anesthesia. The data show that the C. longum can be stimulated longest in the proximal region whereas the longest stimulation period in the C. laterale is in the distal region. According to EMG-analysis the circles beneath the diagram point out the positions where motor end plates are located. It seems to be no correlation between the

positions of motor end plates and the regions where longest stimulation is possible.

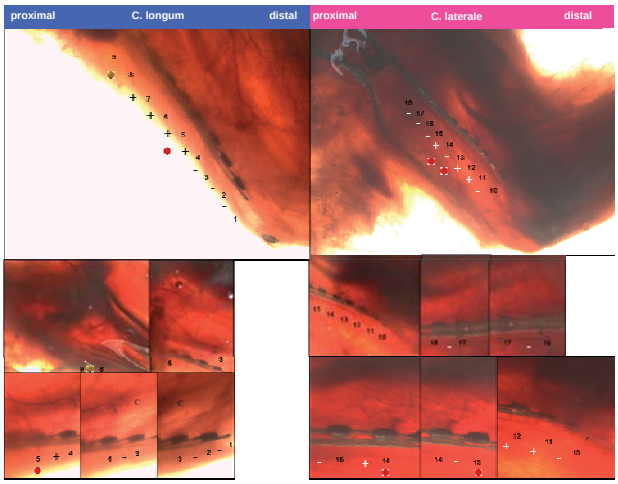


Fig. 5: Electrode plate position and nerve staining with Sihler's staining. Different views of rat foreleg.

-: hard to stimulate, +: good to stimulate, longer stimulation periods possible, Motor end plate

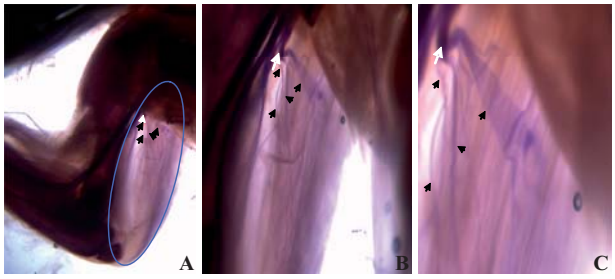


Fig. 6: Nerve staining with Sihler´s staining. Rat, right foreleg, ventral view.

C. longum innervating nerve nerve branches

Discussion

The analysis of the stained preparations show that pairs of electrodes that can stimulate the muscle for a long period of time are located very close to nerves or a plexus. However, around the surfaces of the electrode plates that can hardly stimulate the muscle non or only very thin nerves can be found (Fig. 5). In all 4 animals the most proximal electrodes in the C. longum can stimulate the muscle longest. With help of Sihler's preparations can be demonstrated that those electrodes are positioned close to the region where the innervating nerve enters the muscle. Since this is the region the nerve begins to branch out into the muscle belly the cross section area of the nerve is accordingly large (Fig. 6).

Conclusions

Our results show that the potential stimulation duration of the C. longum is longer than that of the C. laterale. While the position with the longest possible excitability is located proximally in the C. longum, such a region is found more distally in the C. laterale. The duration of feasible continuous stimulation varied between a few seconds and several hours. The longest uninterrupted stimulation duration was 4 hours 45 minutes, and an even longer stimulation would be theoretically possible. In consideration of the animal anaesthesia time the stimulation duration was restricted. Overall, the positions of the motor end plates do not correspond to the positions with the longest possible excitability of the triceps brachii muscle.

References

[1] Biedermann F, Schumann NP, Fischer MS, Scholle HC. Surface EMG-recordings by using a miniaturised matrix electrode: a new technique for small animals. J Neurosci Methods, 97: 69-75, 2000.

[2] Faenger B, Schumann NP, Arnold D, Grassme R, Scholle HC. Dynamic intramuscular activation patterns of the rats triceps brachii during locomotion – comparison between supra- and intramuscular multichannel EMG. Acta Physiologica International Joint Meeting, Acta physiologica 186(1): 245, 2006.

[3] Scholle HC, Schumann NP, Biedermann F, Stegeman DF, Grassme R, Roeleveld K, Schilling N, Fischer MS. Spatiotemporal surface EMG characteristics from rat triceps brachii muscle during treadmill locomotion indicate selective recruitment of functionally distinct muscle regions. Exp Brain Res, 138: 26-36, 2001.

[4] Schumann NP, Biedermann FHW, Kleine BU, Stegeman DF, Roeleveld K, Hackert, R, Scholle HC. Multi-channel EMG of the M. triceps brachii in rats during treadmill locomotion. Clin Neurophysiol, 113: 1142-51, 2002.

[5] Sihler C. Über eine leichte und sichere Methode ,die Nervenendigung an Muskelfasern und Gefässen nachzuweisen. Verhandl. D. Berl. Gesellsch., Archiv f. u. Ph., Physiol. Abthlg., 202-208, 1895.

[6] Wu BL, Sanders I. A technique for demonstrating the nerve supply of whole larynges. Arch Otolaryngol Head Neck Surg., 118(8): 822-7, 1992.

Acknowledgements

Supported by:

MED-EL® and BMBF, No.: 01EZ0335.

Author's Address

Dipl.- Biol. Bernd Faenger

Division for Motor Research, Pathophysiology and Biomechanics
Department for Trauma-, Hand and Reconstructive Surgery, University Hospital Jena
Friedrich-Schiller-University Jena, Bachstr. 18
07740 Jena, Germany
e-mail: Bernd.Faenger@med.uni-jena.de

Stimulation selectivity of an interfascicular electrode in the sciatic nerve of rabbits

Nielsen TN[1], Sevcencu C[1], Struijk JJ[2]

[1] Center for Sensory-Motor Interaction, [2]Medical Informatics Group, Department of Health Science & Technology, Aalborg University, Aalborg, Denmark

Abstract

The choice of electrode for functional electrical stimulation systems is a compromise between selectivity and invasiveness; high selectivity is desirable to obtain maximum functional control, but if the surgical procedure induces too high risk the electrode will not be acceptable for human use. Current literature on peripheral nerve electrodes has focused mainly on extra-neural and intrafascicular electrodes. The current study presents a new interfascicular electrode that could simplify implantation of the electrode because it does not require the nerve to be freed of blood vessels and connective tissue. The electrode was implanted in the sciatic nerve of nine rabbits and was capable of fully activating the tibial and peroneal nerve branches with high selectivity (SI = 0.98±0.02, mean±SD) in all animals. Implantation of the electrode was simple and the interfascicular electrode could be an interesting alternative in applications where freeing the nerve is complicated by blood vessels e.g. the vagal nerve. Further studies are needed to investigate the stability and safety of the electrode in chronic experiments.

***Keywords**: Interfascicular electrode, nerve stimulation, stimulation selectivity, peripheral nerves, animal experiments.*

Introduction

Neural prosthetic devices utilizing stimulation of peripheral nerves are in use for multiple applications today, including vagal nerve stimulation to treat epilepsy, sacral nerve stimulation to treat urinary and faecal incontinence, phrenic nerve stimulation for ventilator assistance, and peroneal nerve stimulation for correction of foot-drop [1, 2]. A large variety of electrodes have been developed to provide the interface of these systems to the nerve, ranging in invasiveness from percutaneous to extra-neural, intraneural and even regenerative electrodes [2].

The most successful electrode for peripheral nerve stimulation has been the cuff electrode, which has been used for many research and rehabilitation applications for several decades, but also intrafascicular electrodes have received considerable interest over the last two decades. The intermediate stage between the cuff electrode and the intrafascicular electrode, i.e. electrode placement among the fascicles, has received less interest.

In a modelling study it was found that an electrode placed in the epineurium just outside a fascicle of the human deep peroneal nerve was unable to stimulate this fascicle selectively with respect to neighbouring fascicles [3]. This is a rather intuitive result since several fascicles were within a relative short distance of the electrode and the impedance of the perineurium must be overcome before the fascicle can be activated. Tyler and Durand 1997 did, however, show that a solution to this problem could be to include a passive element in the electrode that shields non-target fascicles from the stimulating contact [4].

From a surgical point of view implanting cuff electrodes can be cumbersome in some locations due to the requirement to free the nerve of surrounding tissue such as blood vessels, while implantation of intrafascicular electrodes is a relatively invasive procedure as well, requiring the penetration of the perineurium with a sharp needle. An electrode designed to be pushed into the relative soft epineurium without lifting the nerve could provide a relatively less invasive means of placing electrode contacts in close proximity of the nerve fibres. This should provide a current consumption low enough for an implanted system and selectivity at least to the level of activating a single nerve.

In the current study a four-contact interfascicular electrode was developed and tested in the sciatic nerve of nine rabbits. The electrode contained two pairs of contacts, placed on opposite sides of the electrode, shielded from each other by the nylon frame of the electrode. Orienting the electrode so that one contact pair faced the tibial fascicle of the sciatic nerve and the other the peroneal fascicle the electrode demonstrated excellent selectivity in recruitment of the tibial vs. peroneal nerve.

Material and Methods

Surgery

Nine rabbits weighing 3894±216 g (mean±SD) were anaesthetized, the skin was opened in a line from the hip to the knee of the left hind leg and the femoral biceps and semitendinous muscles were split from each other to expose the underlying nerves. The interfascicular electrode was implanted in the sciatic nerve distal of the muscular branch with one pair of contacts facing the tibial fascicle and the other pair facing the peroneal fascicle. This insertion was made using a blunt glass needle to pierce the nerve after which the electrode could be pulled through the channel created by the needle using the nylon suture attached to the electrode. The tibial and peroneal nerves were freed and a cuff electrode was placed around each nerve for recording.

Electrodes

The interfascicular electrode developed for the experiment is illustrated in Fig. 1. It consisted of an 8 mm long piece of flattened 0.63 mm outer diameter Nylon tube with a Nylon suture, used for pulling the electrode into the nerve, and four circular Ag contacts of approximately 0.5 mm diameter. Silver was used for the contacts because it is relatively easy to manipulate and because we sought to investigate electrode properties, not biocompatibility. The contacts were placed in pairs on each side of the flattened tube with 2 mm between the middle of each contact of the pair. The total width of the electrode was less than 1 mm. The suture was fixated with a knot inside the tube, the contacts were glued to the tube wall, and the electrode was filled with silicone. The lead wires were coiled for strain-relieve and soldered onto the four wires of a shielded lead cable.

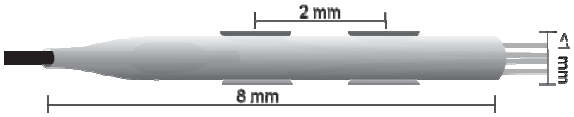


Fig. 1: Illustration of interfascicular electrode with four Ag contacts. Not drawn to scale.

Cuff electrodes for recording were produced according to the technique described by Haugland [5]. The cuffs were 12 mm long and contained three 1 mm wide Pt ring contacts placed with 5 mm between each ring.

Stimulation

Mono-phasic constant current square pulses of 50 µs were delivered by a SD9 stimulator with a PSIU6X isolation unit (Grass Technologies). Recruitment curves were obtained by computer triggered stimulation with 10 single pulses at each stimulation intensity for several intensities, from below recruitment threshold to above full recruitment of the first recruited nerve branch. Stimulation current was calculated from the linear relationship between the voltage output of the SD9 and the constant current output of the PSIU6X.

Recording

Recorded nerve signals were preamplified, amplified, filtered, and further amplified using two AI402 SmartProbes and a CyberAmp 380 (Axon Instruments Inc.). The gain was chosen depending on signal amplitude. The signals were high-pass filtered using a first-order filter with -3 dB frequency of 0.1 Hz and low-pass filtered using a fourth-order Bessel filter with a -3 dB frequency of 10 kHz. In some rabbits it was necessary to increase the corner frequency of the high-pass filter to 1 Hz because of high amplitude low frequency noise. The signals were then digitized at 50 kHz using a PCI-6221 ”M series DAQ” with a BNC-2110 connector block (National Instruments) and stored on a computer for further analysis.

Data analysis

Data analysis was performed off-line using Matlab® (The MathWorks^{TM}). A time-average was generated for each set of 10 stimuli with equal stimulation intensity and the peak-to-peak response (V_{pp}) of the direct nerve volley was calculated from this time average. Each V_{pp} was normalized in each of the nerve branches with respect to the largest V_{pp} obtained during the experiment to express the response as a fraction (f) of full nerve activation.

For each stimulation intensity (I) the selectivity index (S) was calculated as the response of the target nerve branch (b) divided by the sum of the responses of both nerve branches:

$$S_b(I) = \frac{f_b(I)}{f_{tibial}(I) + f_{peroneal}(I)} \qquad (1)$$

in accordance with e.g. [6, 7]. To get a single number to measure the selectivity of the electrode, it was calculated as the mean of the highest achieved selectivity in recruitment of each nerve branch while activating the branch to at least 70% of its maximum, i.e.:

$$\hat{S} = \frac{1}{2}\sum_{i=1}^{2} \max\left\{S_i(I) \mid f_i(I) \geq 0.7\right\} \qquad (2)$$

Adapting the definition provided by Yoo et al [7], a nerve branch was regarded as selectively activated in a functionally relevant way if both the criteria $S_b(I)>0.7$ and $f_b(I)>0.7$ were satisfied.

In addition, the maximally achieved f and the threshold current ($I_{10\%}$), required to produce 10% activation of the nerve branch were obtained.

Results

The interfascicular electrode achieved functional selective stimulation of all 18 nerve branches tested in the experiment with $\hat{S}$ = 0.98±0.02 (mean±SD) and with f up to 0.98±0.04. The selectivity was slightly higher for the peroneal nerve than for the tibial nerve (1.00±0.00 vs. 0.97±0.04, p=0.009 by Mann-Whitney Test) whereas the maximal selective response did not differ significantly (f_{tibial} = 1.00±0.01, $f_{peroneal}$ = 0.96±0.05, p=0.292). The threshold current for stimulating the nerves was $I_{10\%}$ = 415±210µA (0.02µC per stimulus pulse) with the peroneal nerve requiring significantly lower current than the tibial nerve (287±111µA vs. 542±213µA, p=0.003).

Discussion and Conclusions

Electrodes for stimulating of or recording from peripheral nerves have been extensively researched, but designs have focused on either extra-neural electrodes or the more invasive intrafascicular electrodes, while interfascicular electrodes have received very little interest. In this study a new electrode was designed to be easily implanted between the fascicles without isolating parts of the nerve and to provide fascicle selectivity. Implantation of the electrode was smooth; the epineurium was easily penetrated by the blunt needle while the perineurium was left intact. Once a channel was created by the needle the electrode could be pulled into the nerve without much resistance.

The results of the present study demonstrate that the interfascicular electrode presented here is capable of fully activating two fascicles separated by the nylon tube of the electrode with remarkable selectivity ($\hat{S}$ = 0.98±0.02, max(f) = 0.98±0.04).

In the present study the electrode was inserted into the nerve without any difficulty, but it was difficult to see the electrode inside the nerve and therefore also to asses if it still had the desired orientation. The results and observations during explanation do, however, show that electrode placement was successful. In this experiment the electrode was fixated only by the fascicles pushing on the sides of the electrode. No electrode movement was observed in the current experiment, but it remains to be investigated if this passive fixation is sufficient in a chronic environment.

It should be noted that stimulation of multi-fascicle nerves would require a very different design than for a nerve with just two fascicles e.g. topological sectioning of the nerve into more than just two chambers.

For chronic studies it is necessary to develop a non-silver electrode and perhaps to include some means of fixation, e.g. tiles. The presented electrode design should, however, otherwise provide a stable and safe interface to the nerve since it does not penetrate the protective boundary of the nerve, the perineurium, and does not confine the nerve to a limited space, which could lead to pressure damage.

References

[1] Rijkhoff NJ, "Neuroprostheses to treat neurogenic bladder dysfunction: current status and future perspectives," *Childs Nerv. Syst.,* vol. 20, pp. 75-86, Feb. 2004.

[2] Navarro X, Krueger TB, Lago N, Micera S, Stieglitz T and Dario P, "A critical review of interfaces with the peripheral nervous system for the control of neuroprostheses and hybrid bionic systems," *Journal of the Peripheral Nervous System,* vol. 10, pp. 229-258, 2005.

[3] Veltink PH, Van Veen BK, Struijk JJ, Holsheimer J and Boom HBK, "A modeling study of nerve fascicle stimulation," *IEEE Trans. Biomed. Eng.,* vol. 36, pp. 683-692, 1989.

[4] Tyler DJ and Durand DM, "A slowly penetrating interfascicular nerve electrode for selective activation of peripheral nerves," *IEEE Transactions on Rehabilitation Engineering,* vol. 5, pp. 51-61, 1997.

[5] Haugland M, "Flexible method for fabrication of nerve cuff electrodes," in 1996, pp. 359-360.

[6] Deurloo KEI, Holsheimer J and Bergveld P, "Nerve stimulation with a multi-contact cuff electrode: Validation of model predictions," *Arch. Physiol. Biochem.,* vol. 108, pp. 349-359, 2000.

[7] Yoo PB, Sahin M and Durand DM, "Selective stimulation of the canine hypoglossal nerve using a multi-contact cuff electrode," *Annals of Biomedical Engineering,* vol. 32, pp. 511-519, 2004.

Acknowledgements

The authors thank the staff at Aalborg Hospital for their assistance. This study was supported by the Danish National Advanced Technology Foundation.

Author's Address

Thomas Nørgaard Nielsen
Center for Sensory-Motor Interaction (SMI)
Department of Health Science and Technology
Aalborg University, Fredrik Bajers Vej 7D-3
DK-9220 Aalborg, Denmark
Email: thnn@hst.aau.dk

Characterization of peri-infarct, intra-cortical motor cortex responses during reaching task in a chronic animal model of ischemic stroke

Fjeldborg LC[1], Nielsen MV[1], Ottesen KJG[1], Jensen W[1]

[1] Center for Sensor-Motor Interaction, Dept. Health Science and Technology, Aalborg University, Denmark

Abstract

Stroke is a leading cause of disability and mortality worldwide. Neuroplasticity is believed to play a key role in functional recovery. Our objective was to characterize the long-term effect of ischemic stroke on intra-cortical responses obtained from the motor cortex (i.e. the prenumbra zone). Two Sprague-Dawley rats were instrumented with a 16-ch electrode array. Animals were trained to reach and retrieve food pellets. Intra-cortical responses were obtained during behavioral training sessions. Computed PSTH responses revealed similar trends between the animals, i.e we observed an increase in cortical activity in a 150-300 ms interval related to the reaching task (day 0, before ischemic onset), that modulated in both amplitude and time after ischemic onset (decreased activity at Day 4 and 5, increased activity at Day 7). Variability across animals should be expected and must be investigated further. A better understanding of the effect of stroke on motor patterns may assist to a better understanding of the plasticity mechanisms involved in functional recovery in the future.

Keywords*: ischemic stroke, intracortical recordings, motor cortex, functional evaluation, plasticity*

Introduction

Cerebral ischemia is caused by occlusion of the vascular supply in a local region of the brain, and 80-85 % of all strokes are ischemic in nature [1]. A blockage of the blood supply will typically result in an ischemic area that are damaged within minutes or hours (i.e. the 'core'), and a surrounding area that is less ischemic (i.e. the peri-infarct zone or the penumbra). When a part of the motor cortex is destroyed, the result is often loss of control of the peripheral limb or paralysis. The term 'recovery' is referred to as the re-emergence of the exact motor and sensory patterns that were in place before the stroke. Although the neural basis for functional motor recovery it not fully elucidated, it likely involves both structural and functional changes of the neural connectivity [2], including e.g. cerebral reorganization within ipsi or contra-lateral motor areas [4;5]. Previous studies have investigated the plastic changes in the hyper acute, acute and chronic neural changes following ischemic stroke (see e.g. [3][4]). Most animal and human tests assess performance changes [2]. However, the use of intra-cortical recordings has the possibility to study intricate changes of the neural activity. We have previously reported on changes in the intra-cortical motor cortex or sensory responses in the hype acute phase based on intra-cortical recordings [5-7].

The objective of the present work was to characterize peri-infarct, intra-cortical, motor cortex responses in the chronic phase (days) following ischemic stroke. A more detailed understanding of the effect of stroke on the intra-cortical motor patterns is expected to assist to provide a better understanding of the plasticity mechanisms involved in functional recovery.

Materials and methods

Animal preparation

Approval for all experimental procedures was obtained from the Danish Committee for the ethical use of animals. Two male Sprague-Dawley rats (weight of 350-400g) were anaesthetized with a 0.5 ml subcutaneous injections of Ketamine (100 µg/ml), Xylazine (20 µg/ml) and Acepromazine (10 µg/ml). A dose of 0.1 ml / 100 g body weight were aministered every hour. A craniectomy was performed over the primary motor cortex (M1) related to forelimb movement (2-4 mm postal, 2-4 mm lateral relative to Bregma [8]). A 16-channel tungsten micro-wire array (diameter = 100 µm, spacing ~500 µm, depth 1.7 mm) was implanted after retraction of the dura, see Fig. 1A. Two stainless steel bone screws were placed outside the cortical implant area to both serve as ground reference and mechanical stabilization points.

Behavioural training

Prior to electrode implant, we used standard psychophysical techniques to train the rats to perform the reaching task in return for a food reward. Rats were food restricted and maintained on 90% of target body weight. The training cage was a simple, square box where a 1.2 cm opening was place on one side, see Fig. 1B. The pellets were placed at a distance of 2 cm from the opening. When the pellet was successfully retrieved by the rat, a new pellet was manually placed in the same position. To provide synchronization between the reaching task and the intra-cortical signals, a light-sensitive sensor was placed below the pellet, that provided a digital high signal when regular light hit the sensor, i.e. at the point when the rat was removing the pellet. Once the animals successfully retrieved at least 80 pellets in 4 consecutive sessions they received the electrode implant. The number of pellets and the animal's preferred limb usage were tracked.

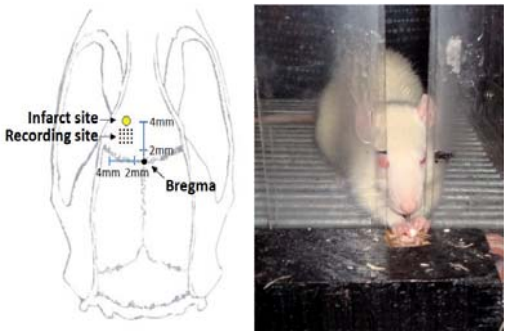


Fig. 1. A) A 16ch microwire array was placed in the M1 area in the hemisphere contra lateral to the rat's preferred limb. A 1.5 mm diameter, ischemic infarct was created anterior to the electrode. B) Functional evaluation task. The rat was trained to reach for and retrieve a food pellet.

Ischemic infarct

A localized, ischemic infarct was created by activation of a photosensitive dye in the animal's blood stream [9]. Rose Bengal dye solution (Aldrich Chemicals, 10 mg/ml saline solution, 0.3 ml/100 g body weight) was administered intravenously through a tail vein catheter while the animal was placed under general anaesthesia. A fiber optic light source of white light (1.5 mm diameter) was lowered through a guide-tube to be positioned directly over the brain surface immediately anterior to the implanted micro-wire array. The target location for the ischemic infarct was chosen to be the border area between the primary somatosensory cortex (S1) and primary motor cortex (M1), anterior to the implanted electrode, see Fig. 1A.

Measurements and data-analysis

The intra-cortical signals were filtered (800 Hz - 8 kHz) before sampling at 24 kHz (Tucker Davis Technologies). On-line spike detection was performed using a lower threshold at approximately 1.5 times the RMS of the raw data. The threshold was determined based on spontaneous motor cortex firing activity before the behavioural sessions began. Neural data were collected before the ischemic infarct (***Day 0***) and at ***Day 4***, ***Day 5*** and ***Day 7*** after the ischemic infarct. Peri-stimulus time histograms (PSTH) were synchronized to the time where the pellets where removed, and the mean was subtracted. For each PSTH, we calculated the mean response in the [0:-100] ms, [-100:-200]ms, [-200:-300]ms, [-300:-400]ms and [-400:-500]ms intervals. These features were compared using a 4-way ANOVA (factors: 'Day after stroke onset', 'Rat', 'Time interval' and 'Distance from stroke core'). A time window of 200 ms correspond to the time ranges analyzed in e.g. [10][11]. Since the synchronization point is where the rat is retracting the paw, we have extended the time window for analysis to 500 ms.

Results

The PSTH responses obtained before the ischemic onset (***Day 0***) and at ***Day 4***, ***Day 5*** and ***Day 7*** after the ischemic onset are depicted in Fig. 2 for both rats. The responses are grouped according to the electrode distance from the ischemic core (corresponding to the ischemic core is on the left side in Fig. 2). Time 0 is the synchronization point that corresponds to the time when the food pellet was retracted by the rat. At ***Day 0*** increased activity was observed 150-300 ms prior to retrieving the food pellet in the majority of the channels, which is believed to be related to the reaching and grasping of the food pellet (i.e. when PSTH'es were calculated with random synchronization points, no modulation in the time window was observed). This is comparable to responses found in healthy rats performing a similar reaching movement [12, 13]. For Rat 1, we observed a clear decrease in the activity in the 150-300m interval at ***Day 4*** and ***Day 5*** we. At ***Day 7*** a marked increase in activity, indicating a re-emergence of activity similar to what was observed prior to stroke onset. A similar decrease in activity was observed at ***Day 4*** for Rat 2, however the decrease was not so prominent at ***Day 5***, and no clear reemergence of activity at Day 7 was observed.

The behavioural performance of the rats was

evaluated by tracking the number of food pellets retrieved and the preferred limb usage (Table 1 and 2). The pellet retrieval rate for Rat 1 did not change over time and the preferred limb usage did not shift, indicating that the effect of the stroke may have been minor. The complete opposite was observed for Rat 2 that increased the pellet retrieval rate over time, and also changed the preferred limb usage. The ANOVA analysis showed that there was a difference in the PSTH responses between rats, the time after stroke onset and the specific PSTH time interval analyzed (results shown in Table 3). However, there was no difference between signals depending on the distance from the stroke core.

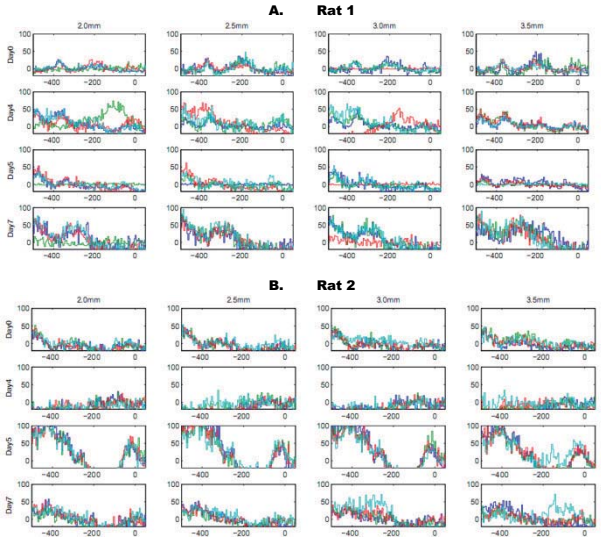


Fig. 2. PSTH responses (with mean subtracted) according to distance from the stroke area, recorded at ***Day 0*** (before ischemic onset), ***Day 4, Day 5*** **and** ***Day 7*** (after ischemic onset) for the two animals. At 0 ms the food pellet was retracted.

	Baseline		Day 4		Day 5		Day 7	
	p/m	Tot	p/m	tot	p/m	tot	p/m	tot
Rat1	3	76	2	74	4	98	3	75
Rat2	5	101	2	97	9	95	8	108

Table 1. Assessment of behavioural performance. The number of pellets pr min (p/m) and the total number of pellets retrieved (tot).

% limb usage	Before		After stoke		Shift in preferred limb
	Left	Right	Left	Right	
Rat 1	19	**81**	18	**82**	No shift
Rat 2	**52**	48	27	**73**	Shift

Table 2. Assessment of behavioural performance. Scoring of preferred limb usage before and after stroke.

Factor	Prob>F
'Rat'	0.00064
'Distance from stroke core'	0.40
'Time interval'	0.00
'Day after ischemic onset´	0.00000016

Table 3. Results from ANOVA analysis

Discussion and Conclusions

Our objective was to characterize the intra-cortical responses in a chronic animal model of ischemic stroke. We analyzed PSTH responses related to a reaching task up to 7 days after the ischemic onset and correlated the responses with the behavioural performance. We observed significant changes of the cortical responses and different behavioral changes following the stroke, which indicate that the animals are applying behavioural compensation strategies. To further evaluate the ongoing neuroplastic changes and the variability among animals, we are currently analyzing data from a larger set of animals.

Author's Address

Winnie Jensen, Center for Sensor-Motor Interaction, Department of Health Science and Technology, Aalborg University, Fredrik Bajersvej 7D-3, 9220 Aalborg, Denmark, wj@hst.aau.dk

References

[1] M.G. Hennerici, J. Bougousslavsky and R.L. Sacco, Stroke, London: Mosby. Elsevier Limited, 2004, .

[2] T.H. Murphy and D. Corbett, "Plasticity during stroke recovery: from synapse to behaviour," Nat.Rev.Neurosci., vol. 10, pp. 861-872, Dec. 2009.

[3] H. Fujioka, H. Kaneko, S.S. Suzuki and K. Mabuchi, "Hyperexcitability-Associated Rapid Plasticity After a Focal Cerebral Ischemia," Stroke, vol. 35, pp. 346-348, 2004.

[4] R.J. Nudo and G.W. Milliken, "Reorganization of movement representations in primary motor cortex following focal ischemic infarcts in adult squirrel monkeys," J.Neurophysiol., vol. 75, pp. 2144-2149, May. 1996.

[5] W. Jensen, P.J. Rousche and T. Chiganos, "A method for monitoring intra-cortical motor cortex responses in an animal model of ischemic stroke," Submitted to the IEEE EMBS Conference, New York, USA 2006, 2006.

[6] T. Chiganos, W. Jensen and P.J. Rousche, "Characterization of rat auditory cortex responses after photothrombotic infarction," Annual Biomedical Engineering Society (BMES) Meeting,Baltimore,USA,Sept.28 - Oct.1,2005., 2005.

[7] T. Chiganos, W. Jensen and P.J. Rousche, "Dynamic Electrophysiolgic Response of Rat Auditory Neurons in Response to Photothrombotic Infarction," Submitted to International Stroke Conference (American Heart Association), Feb 16-18, Gaylord Palms, Kissimmee, Florida, 2005.

[8] J.K. Chapin and C. Lin, "The somatic sensory cortex of the rat," in The Cerebral Cortex of the Rat, R.C. Tees, MIT Press, 1990, ch. 14, pp. 341-379.

[9] B.D. Watson, W.D. Dietrich, R. Busto, M.S. Wachtel and M.D. Ginsberg, "Induction of reproducible brain infarction by photochemically initiated thrombosis," Ann.Neurol., vol. 17, pp. 497-504, 1985.

[10] M. Lauback, J. Wessberg and M.A.L. Nicolelis, "Cortical Ensemble Activity Increasingly Predicts Behaviour Outcomes During Learning of a Motor Task," Nature, vol. 405, pp. 567-571, 2000.

[11] J.K. Chapin, K.A. Moxon, R.S. Markowitz and M.A.L. Nicolelis, "Real-time control of a robotic arm using simultaneously recorded neurons in the motor cortex," Nat.Neurosci., vol. 2, pp. 664-670, 1999.

[12] W. Jensen and P.J. Rousche, "Movement discrimination based on rat primary motor cortex responses," IEEE Conference in Neural Engineering, 2005.

[13] W. Jensen and P.J. Rousche, "Encoding of self-paced, repetitive forelimb movements in rat primary motor cortex," IEEE Conference in Medicine and Biology, San Francisco, 2004.

Session 7

Modeling

Development of a method for estimating unit conduction velocity using spectral analysis of the action potential

Qiao S[1] and Yoshida K[2,1]

[1] Weldon School of Biomedical Engineering, Purdue University, West Lafayette, IN 47907, USA
[2] Biomedical Engineering Dept, Indiana Univ. – Purdue Univ. Indianapolis, Indianapolis, IN 46202, USA

Abstract

We present derivation and computational model predictions of a method to estimate the conduction velocity of an action potential(AP) based upon frequency domain analysis of its spectrum. A tissue filter relationship was derived using reciprocity equations in the frequency domain and transforming the spatial frequency to time frequency. The derived function relates how the single fiber action potential (SFAP) is transformed as a function of conduction velocity. A three-dimensional (3-D) finite element (FE) volume conductor model of a thin-film longitudinal intra-fascicular electrode (tf-LIFE) residing in a nerve fascicle was developed to determine the potential distribution in the nerve fascicle, and further derive the tissue filter function. Single fiber action currents were filtered using the tissue filter function to simulate the predicted AP for different unit conduction velocities. A power spectral density (PSD) analysis was then implemented for the simulated SFAPs to quantify changes in the PSD of the simulated SFAPs. The FE model predicts that the faster conducting fiber, the narrower its temporal weighting function is. This gives rise to a tissue filter function with a broader bandwidth. These factors result in a quantitative change in the PSD of faster conducting fibers, leading to a change shape of the PSD of the AP. Relative changes in landmarks of the PSD can be quantified and used as a predictor of the unit conduction velocity.

Keywords*: Neuroprosthetic electrode, finite element model, weighting function, unit conduction velocity, power spectral density.*

Introduction

Advanced neuroprosthetic electrodes are indwelling devices that are currently being developed to create a bidirectional interface to the nervous system. They are a key enabling technology under development to restore function to those suffering from neurological disorders or injury, and have the potential to restore function to paralyzed limbs, sight to the blind, or hearing to the deaf. The advanced neural interfacing technique derives its selectivity by their ability to observe, classify and track single fiber activity through analysis of shape of the action potential (AP). However, the conduction velocity of the unit has not been used, and could give additional information to enhance unit discrimination.

Previous experiments have shown that the nerve signals have a power spectrum with components between 3 kHz and 7 kHz. Cuff electrodes (placed around and outside the nerve bundle) and longitudinal intra-fascicular electrodes (LIFE) have different spectral distributions. A prior study has described the bimodal spectral distribution of the LIFE in the recording of nerve activity peaking at about 1 kHz and 5 kHz, in contrast to the unimodal spectral distribution of cuff electrode recording peaking at about 2.5 kHz [1]. However, the origins of the bimodal LIFE spectral distribution were not well understood. By exploring the origins of this distribution, we realized that the relative magnitude of power spectral density (PSD) at the peaks of the bimodal distribution was, among other factors, related to the conduction velocity of AP.

Methods

Derivation of the tissue filter equations

A myelinated nerve fiber can be represented as a line of point sources representing the nodes of Ranvier distributed along the nerve fiber. The single fiber action potential (SFAP) recorded by an electrode can be estimated as the convolution of action currents, i_{AC}, distributed at the nodes of Ranvier and the spatial weighting function, $w(x)$, based on the theorem of reciprocity [2]. The weighting function can be appropriately interpreted as the ratio of the simulated electric potential divided by its source current at position x, which has the same dimension as resistance, Ω. Assuming a constant conduction velocity, $x = \theta t$, describes the conduction of the AP, where t is time, and θ is the conduction velocity. Then, the spatial weighting function $w(x)$ can be transformed to a temporal weighting function $w(\theta t)$.

In this paper, we analyze simulated activity from myelinated nerve fibers of different calibers (5, 10 and 20 μm dia.), 0.5 mm away from the electrode. The action current, i_{AC}, at the nodes of Ranvier was simulated based on the Frankenhaeuser-Huxley model [3]. The amplitude of i_{AC} was linearly scaled corresponding to nerve fibers with different

diameters [4]. Since the AP conduction velocity, θ, is proportional to the fiber diameter, D ($\theta \approx 6D$), the amplitude of i_{AC} has a linear relationship with the conduction velocity. The internodal distance (between two nodes of Ranvier), L, also has a linear relationship with the fiber diameter, D ($L = 100D$) [2]. The parameters used for the action current simulation are shown in Table 1.

Table 1: The relationship between the fiber diameter, conduction velocity and internodal distance

Fiber Diameter D (μm)	Conduction Velocity θ (m/s)	Internodal Distance L (mm)
20	120	2
10	60	1
5	30	0.5

The SFAP can be estimated by

$$SFAP(t)=\int_0^t i_{AC}(\tau)\, w[\theta(t-\tau)]\, d\tau \quad . \qquad (1)$$

Taking its Fourier transform results in

$$SFAP(j\omega)=\iint i_{AC}(\tau)\, w[\theta(t-\tau)]\, e^{-j\omega t}\, d\tau\, dt \qquad (2)$$

which can be simplified and represented as

$$SFAP(j\omega)=\frac{1}{\theta} W\left(\frac{j\omega}{\theta}\right) I_{AC}(j\omega) \quad . \qquad (3)$$

Thus the SFAP can be generated by filtering the time or frequency domain representation of the action current with a weighting function, W, which is a function of the unit conduction velocity and the relative position of its nodes of Ranvier to the electrode. The weighting function, linearly scaled by the inverse of the conduction velocity, can be interpreted as a tissue filter function.

Estimation of the weighting function

A reduced three-dimensional (3-D) finite element (FE) volume conductor model of a structure of thin-film longitudinal intra-fascicular electrode (tf-LIFE) residing in a nerve fascicle in a Cartesian coordinate system (Fig. 1(a)), due to the geometric symmetries of the XY and XZ planes, was developed using the Conductive Media DC module of COMSOL Multiphysics 3.4 (Comsol Inc., Burlington, MA, USA) to determine the potential distribution in the nerve fascicle and surrounding tissue, and further derive the tissue filter function.

The geometry of this FE volume conductor model consists of a tf-LIFE with a 20 μm × 20 μm active site (40 μm × 40 μm in the full model) positioned in the center line of a nerve fascicle, through which a 1 μA cathodic current was applied. The fascicle was modeled as a 20 mm long cylinder, with a radius of 1.2 mm along the Z-axis, a 50 μm thick perineurium layer surrounding the fascicle. The surrounding medium outside the nerve fascicle was modeled as a 20 mm long cylinder with a radius of 6 mm, large enough to assume the electric potential boundary conditions set to ground at the top surface of the medium. The governing equation, subdomain conductivities and boundary conditions of the FE volume conductor model are defined in Table 2.

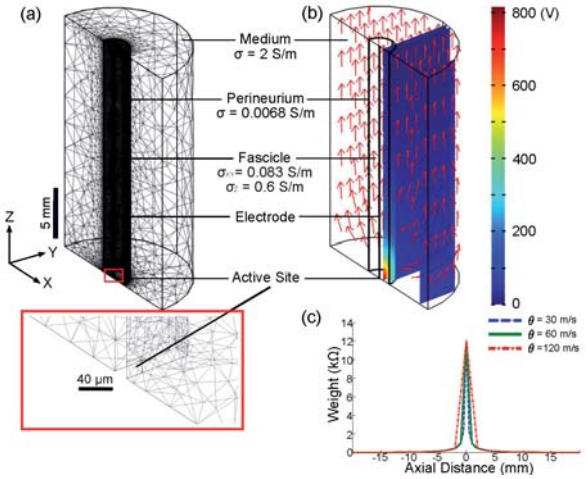


Fig 1: (a) 3-D meshed axial symmetric FE volume conductor model of a tf-LIFE with a 20 μm × 20 μm active site in a nerve fascicle surrounded by tissue. (b) Simulated current density distribution (arrows) in the volume conductor and potential distributions (slices) of planes at 0.5, 1 and 5 mm from the active site. (c) The weighting functions captured from the FE model for three nerve fibers 0.5 mm away from the electrode with conduction velocities of 30, 60 and 120 m/s.

Table 2: Governing equation, subdomain conductivities and boundary conditions of the FE volume conductor model (J: current density; J_n: current density injected into active site; Φ: electric potential, σ: conductivity)

Governing Equation		
$-\nabla\cdot(\sigma\nabla\Phi)=0$		
Subdomain Conductivities		
Fascicle		σ_{XY} = 0.083 S/m σ_Z = 0.6 S/m
Perineurium		σ = 0.0068 S/m
Medium		σ = 2 S/m
Boundary Conditions		
Current Source	$-n\cdot J = J_n$	Active site of the electrode
Continuity	$n\cdot(J_2 - J_1)=0$	Outer layer of the perineurium
Electric Insulation	$n\cdot J = 0$	Body of the electrode; XY and XZ planes; Surrounding surface of the medium
Ground	$\Phi = 0$	Inner layer of the perineurium; Top surface of the medium

The Lagrange-Quadratic element was applied in meshing the FE model, and solved by COMSOL with the specific subdomain conductivities and boundary conditions as defined in Table 2. The weights at the locations of the nodes of Ranvier in the solved model are the unscaled weighting

function. A PSD analysis was then performed on the simulated SFAPs and the derived weighting functions, to quantify changes in the PSD of the simulated SFAPs and estimate the tissue filter function.

Results

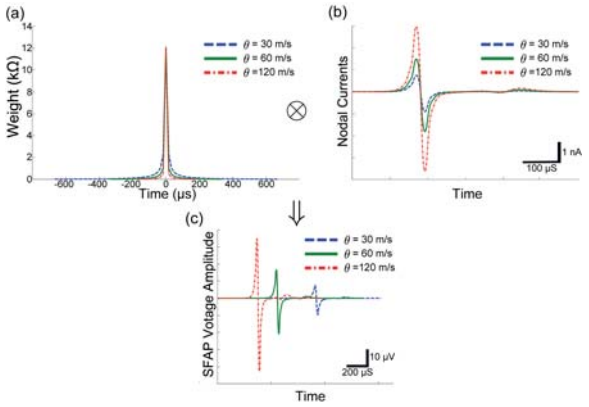


Fig 2: The temporal weighting functions (a), action currents (b) and simulated SFAPs (c) at the conduction velocities of 30, 60 and 120 m/s.

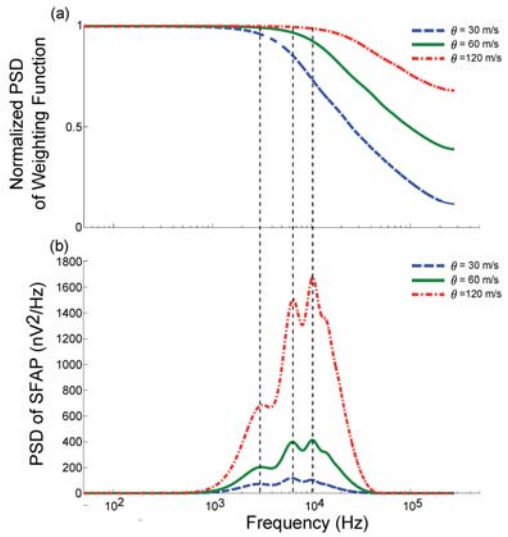


Fig 3: Spectral distribution of the weighting functions (a) and SFAPs (b) at the conduction velocities of 30, 60 and 120 m/s.

Fig. 2(a) shows the transformed weighting functions from the space domain to the time domain. SFAPs at three conduction velocities obtained (Fig. 2(c)) via by convoluting the temporal weighting functions and fiber diameter scaled action currents (Fig. 2(b)). The spectral distributions of the weighting functions are shown in Fig. 3(a) and the corresponding SFAPs are in Fig. 3(b). Magnitudes of the three peaks were measured and are summarized in Table 3. The ratios of Peak2 (~6.5 kHz) to Peak1 (~2.5 kHz) magnitudes of the PSD of SFAPs show a linear relationship (Fig. 4) and could be used as a basis to estimate conduction velocity of SFAPs.

Table 3: The peak magnitudes of the SFAP's PSD for action potentials of three conduction velocities

Peak magnitude of the SFAP's PSD (nV^2/Hz)			
Conduction Velocity (m/s)	Peak1 (~2.5 kHz)	Peak2 (~6.5 kHz)	Peak3 (~10 kHz)
$\theta = 30$	71	117	103
$\theta = 60$	202	397	413
$\theta = 120$	685	1503	1675

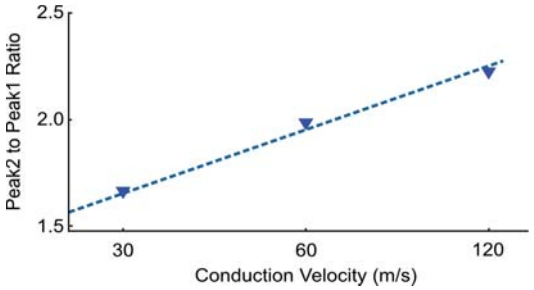


Fig 4: Ratios of the Peak2 to Peak1 magnitudes of the PSD of the SFAPs of 3 different conduction velocities. Peak2 is defined at 6.5 kHz and Peak1 at 2.5 kHz.

Discussion and Conclusions

The results based on the FE model indicate that the faster the conducting fiber, the narrower its temporal weighting function is. This gives rise to a tissue filter function with a broader bandwidth. These factors result in a quantitative change in the PSD of faster conducting fibers, leading to a change shape of the PSD of the action potential. Relative changes in landmarks of the PSD can be quantified and used as a predictor of the unit conduction velocity.

References

[1] Yoshida K and Stein RB. "Characterization of signals and noise rejection with bipolar longitudinal intrafascicular electrodes." *IEEE Trans Biomed Eng,* vol. 46, pp. 226-34, 1999.

[2] Struijk JJ. "The extracellular potential of a myelinated nerve fiber in an unbounded medium and in nerve cuff models." *Biophys J,* vol. 72, pp. 2457-69, 1997.

[3] Frankenhaeuser B and Huxley AF. "The action potential in the myelinated nerve fiber of xenopus laevis as compuated on the basis of voltage clamp data." *J Physiol,* vol. 171, pp. 302-315, 1964.

[4] Marks WB and Loeb GE. "Action currents, internodal potentials, and extracellular records of myelinated mammalian nerve fibers derived from node potentials." *Biophys J,* vol. 16, pp. 655-68, 1976.

Author's Address

Shaoyu Qiao
Weldon School of Biomedical Engineering
Purdue University, West Lafayette, IN 47907, USA
sqiao@purdue.edu

Ken Yoshida
Biomedical Engineering Department
Indiana University – Purdue University Indianapolis,
Indianapolis, IN 46202, USA
yoshidak@iupui.edu

3D-Color Computer Tomography assessment: monitoring of muscle recovery in SCI patients treated with electrical stimulation.

Gargiulo P[1,2], Carraro U[3], Fridgeirsson E.A.[2], Reynisson P.J.[2], Helgason T[1,2]

[1] University Hospital of Iceland, Department of development and consultancy

[2] Reykjavik University, Department of Biomedical engineering

[3]Department of Biomedical Sciences, University of Padova, Italy

Abstract

Muscle tissue composition accounting for the relative content of muscle fibers and intramuscular adipose and loose fibrous tissues, can be efficiently analyzed and quantified using images from Spiral Computer Tomography (S-CT) technology and the associated distribution of Hounsfield (HU) values. Muscle density distribution, especially when including the whole muscle volume, provides remarkable information on the muscle condition. Different physiological and pathological scenarios can be depicted using the muscle characterization technique based on the HU values and the definition of appropriate intervals and the association of such intervals to different colours. Using this method atrophy, degeneration and restoration in denervated muscle undergoing electrical stimulation treatments can be clearly displayed and monitored [1]. The reliability of this tool though depends on S-CT assessment and calibration. To assess imaging quality and the use of HU values to display muscle composition different S-CT devices are compared using a Quasar body scanner [4]. Density distributions and volumes of various calibration elements such as lung, polyethylene, water equivalent, trabecular and dense bone are measured with different scanning protocols and at different points of time. The results show that every scanned element undergoes HU variations, which are greater for materials at the extremes of the HU scale, such as dense bone and lung inhale. Moreover S-CT scanning with low tube voltages (80KV) produces inaccurate HU values especially in bones. In conclusion, 3D-Color S-CT scanning is a powerful follow-up tool that may provide structural information at the mm scale, and thus may drive choice and timing to validate rehabilitation protocols.

Keywords: Three dimensional reconstruction , Modeling, Electrical stimulation, Human muscle, Tissue composition, Denervation, HU scale

Introduction

Spiral CT images provide accurate assessment of patient geometry. Using the information contained in the Hounsfield Unit (HU) data it is possible to account for tissue inhomogeneity. Moreover, density, volume and the 3-dimensional (3D) appearance of a specific region of interest can be computed and measured quantitatively using CT data and special software tools. In this paper is introduced a novel approach based on medical imaging and processing techniques to determine muscle condition and quantify: 1) progression of atrophy in permanently lower motor neuron (LMN) denervated human muscles; and 2) their recovery as induced by functional electrical stimulation (FES). Briefly, we used 3-dimensional reconstruction of muscle belly and bone images to study the structural changes occurring in these tissues in paralyzed subjects after complete lumbar-ischiatic spinal cord injury (SCI). These subjects were recruited through the European project RISE, which aim is to establish a novel clinical rehabilitation method for patients who have permanent and non-recoverable muscle LMN denervation in the lower extremities [2]. Here, we have used medical images to develop 3D models: shape, volume and density changes were measured on each part of the muscles studied. Changes in tissue composition within both normal and atrophic muscle were visualized by associating the Hounsfield Unit values of muscle fibers, fat and loose connective tissue with different colours. This 3D approach is based on the use of HU scale to quantify density changes and therefore require HU value consistency. Indeed there may be a significant difference in absolute CT numbers depending on various physical factors (e.g., kilovoltage, phantom orientation and position in the scan aperture) [3]. These differences must be taken into account when HU intervals are associated to biological tissues. In this work density profiles and HU variation are measured in 3 different Spiral CT devices using a calibration phantom [4]. Different calibration elements and protocols are used to assess the HU intervals as indicator of muscle composition.

Material and Methods

X-ray computed tomography is an imaging method that uses X-rays to produce images of structures 'inside' the body. Each imaged volume element (voxel) is traversed, during the scan, by numerous X-ray photons and the intensity of the transmitted radiation is measured by detectors. The measured intensity profile contains information on the densities the beam encountered on its path through the body (i.e. the denser the regions the weaker the signal). With suitable mathematical methods the measured profiles of each slice are transformed into an image of the structures inside – the image is reconstructed, the grey value corresponding to the linear attenuation coefficient. These coefficients are rescaled to an integer range that encompasses 4096 values, between -1000 and 3095. From these intensity readings, the density or attenuation value of the tissue at each point in the slice can be calculated. This scale is called CT number or Hounsfield unit (HU) and it is expressed by the following formula:

$$CT\ Number = 1000 \cdot \frac{\mu_{pixel} - \mu_{water}}{\mu_{water}} \qquad \text{(eq. 1)}$$

With this scaling, if the linear attenuation coefficient of a given pixel (μ_{pixel}) is equal to that of water, the CT number will be 0.

To assess imaging quality and the use of HU values to display muscle composition 3 different S-CT devices was compared under the conditions simulating those encountered in routine body CT scanning. QUASAR phantom was used for this purpose (Quality Assurance System for Advanced Radiotherapy [4]); it supports the testing of a wide variety of dosimetric and nondosimetric functions on radiotherapy systems, using different calibration elements for measuring both volume and density. Density distributions and volumes of various calibration elements such as lung, polyethylene, water equivalent, trabecular and dense bone are measured with different scanning protocols and at different points of time. Three Spiral CT devices are enrolled into the assessment program: Philips Brilliance 64 CT (which is the device used in practice), GE medical Light Speed 16 CT and Toshiba Aquilon 64 CT.

These measurements require precise positioning of the phantom on the CT scanner couch. The calibration phantom is first placed on the couch, with the Electron Density Ring closest to the CT gantry. The calibration elements are inserted into the phantom Body Oval. For best results, the dense bone and trabecular bone rods are placed opposite to each other, and the water equivalent rod is placed in the center. Then the phantom is aligned through the laser alignment marks on the Body Oval with either the CT suite room lasers or CT scanner lasers. Finally the images are acquired scanning the entire length of the phantom with protocols having tube voltage of 80, 120 and 135 KV. Slice thickness and increment is set constant to 1mm.

Post processing of the data is performed with the programs MIMICS and Excel.

Results and Discussion

The results of this work shows that every scanned element undergoes HU variation. HU variation is greatest for materials at extremes of HU scale: up to 50 HU values using the same protocol. This variation occurs also to elements in middle scale as muscle and water but it is contained within 10 HU. Figure 1 shows the differences in HU conversion among different S-CT devices using the scanning protocol used for the muscle monitoring.

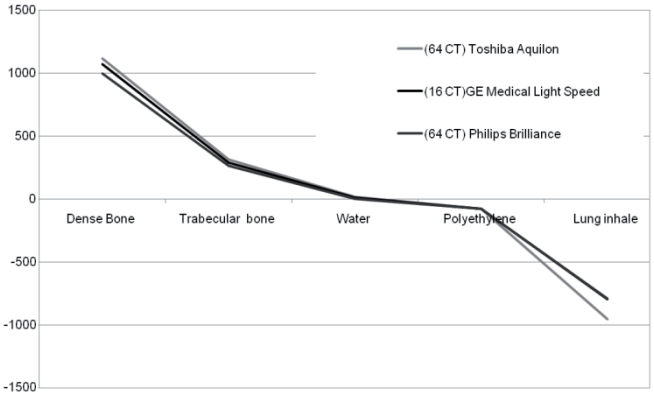


Figure 1: HU differences among different CT scanner devices set at 120KV, which is equal to the value used in muscle monitoring

Figure 2 shows the electron density conversion for different kilovoltage values: Must be noticed that especially for high HU values (representing generally bones) a low tube voltage produce great variation.

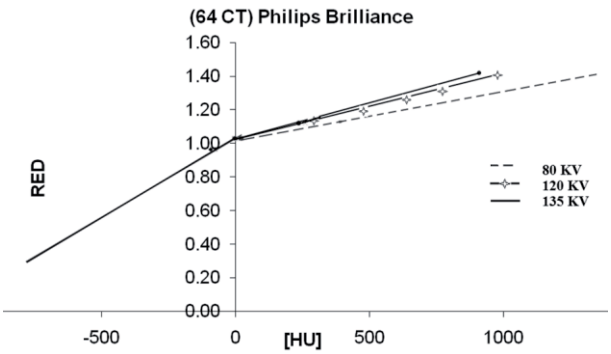


Figure 2: S-64CT Philips brilliance, Electron density - HU scale conversion: Dependence from CT scan protocols 80KV (dashed) 120KV (star) and 135KV (solid line).

Figure 3 shows the Hounsfield variation from time to time and depending on the different kilovoltage values. This variation is less sensible when the kilovoltage used is 120KV.

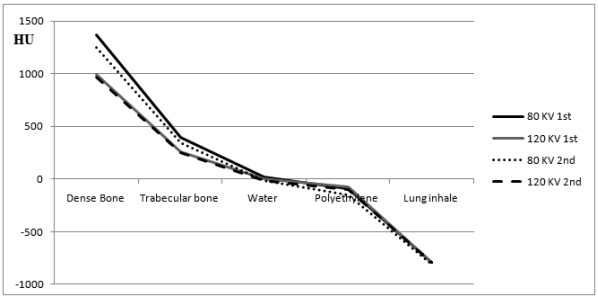


Figure 3: S-64CT Philips brilliance, density differences from time to time.

These results suggest the use of customized HU intervals for studying bone and muscle density changes. These intervals must take into account the type of CT scan device, the used protocol and the HU variability which is greater for materials at the extremes of the HU scale. The empirical evaluation of different tissues in many Spiral CT data allows establishing the following table which shows the HU intervals for the main tissues in the body.

Table 1: is a display of main human tissues and their empirical HU intervals.

Anatomical Tissues	Hounsfield intervals	
	Min	Max
Bone	250	3071
Compact bone	601	1988
Spongial bone	250	600
Normal Muscle	41	80
Dense fibrous connective (Tendons-dense muscle)	81	200
Loose connective (low dense muscle)	-5	40
Fat	-200	-6
Skin	-30	60
Tooth	1200	3071

The use of this approach on rectus femoris muscle volume allows depicting very efficiently muscle tissue composition and structural changes due to long term denervation and FES treatment. In Fig. 4 the HU intervals of table 1 are used to develop the structural 3D appearance of rectus femoris. Fat, loose connective, muscle tissue and fibrous connective are represented individually in 3D. The histogram shows FES treatment allows restoration of muscle fiber (from 42% to 58% after 4 years FES) and sensible decrease of low dense muscle fibers/ loose connective and fat (from 41% to 31% and from 8% to 2% respectively).

Conclusions

In conclusion, 3D-Color CT scanning is a powerful follow-up tool that provides structural information at the mm scale, and thus may drive choices and timings to validate rehabilitation approaches and protocols.

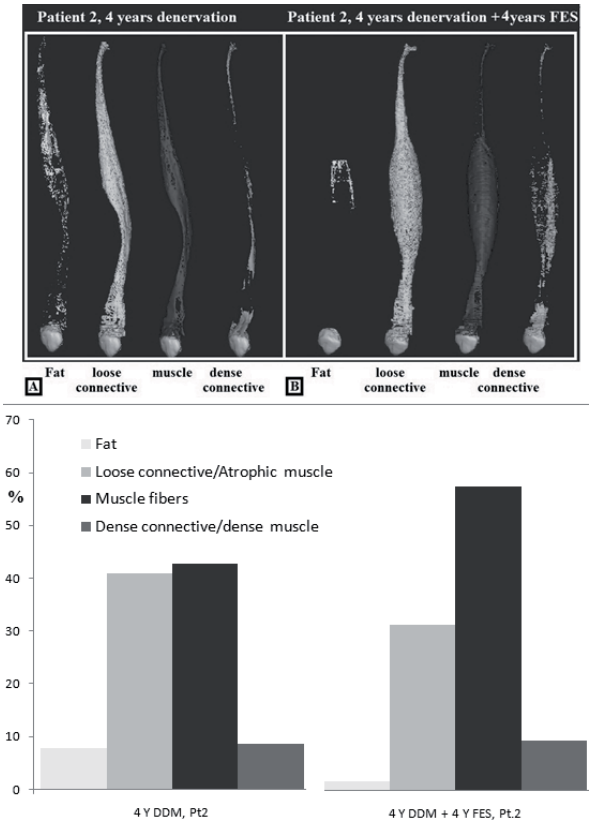


Figure 4: 3D appearance and histogram showing distribution of fat, loose connective, muscle fibers and dense connective in LMN patient after 4 (A) and 8 years (B) from injury during that the muscle have been stimulated with FES (Patient 2)**.**

References

[1] Gargiulo P, Kern H, Carraro U, et al. Quantitative colour 3D CT imaging of human long-term denervated muscle... Neurol Res 2010; 32:13-19.

[2]Mödlin M, Forstner C, Hofer C, at al .Electrical stimulation of denervated muscles... Artif Organs 2005; 29: 203–206.

[3] Levi C, Gray J E, McCullough E C, et al. The unreliability of CT numbers as absolute values. AJR: 139: 443-447, September 1982.

[4] Quasar multi propose body scanner http://www.modusmed.com/quasar_mpbdyphntm.html

Author's Address

Dr. Paolo Gargiulo, Assistant Professor.
University Hospital of Iceland: Dept. of development and consultancy. Armuli 1A, 105 Reykjavik –Iceland.
paologar@landspitali.is, www.ru.is/paolo

Enhancement of vowel encoding for cochlear implants by adding a high frequency signal: a modelling study

Paredes LP[1], Wenger C[1], Rattay F[1]

[1] Vienna University of Technology, Vienna, Austria

Abstract

The outstanding human auditory perception is based on high quality signal transfer between auditory receptor cells and the brain. The healthy afferent fibres of the cochlear nerve generate the neural code involving three different coding principles, unlike modern cochlear implants which solely incorporate the tonotopic principle. Therefore, an important step to improve hearing performance of the electrically stimulated ear might be to include temporal fine structure similar to the natural one. Interesting results using vowels could be obtained by computational evaluation of a multi-compartment model of the human auditory nerve including the initial approach of adding a high frequency signal. This method allows smaller maxima of the source signal to generate spikes and further declines the sharp synchronization of action potentials in a population of excited fibres. Analogue speech stimuli without the supporting effect of a 5 kHz signal causes firing times that are dominated by the fundamental frequency f0 and the refractory behaviour of already stimulated fibres. In contrast to the high frequency method, the variance in firing times and representation of frequencies above 1 kHz are poor.

Keywords: *neural code, cochlear nerve, cochlear implant, computer simulation, temporal theory.*

Introduction

There is an old controversy whether the inner ear uses the place coding principle or the temporal structure of the neural code when transmitting the information of an acoustic signal. The "place theory" introduced by Helmholtz assumed already that: (i) the basilar membrane consists of segments with varying stiffness, (ii) frequency selectivity is based on the resonance of a corresponding part, and (iii) each part is connected with a nerve fibre [1]. The "temporal theory" was put forward by Rutherford, who speculated that each hair cell in the cochlea responds to every tone entering the inner ear [2].

Hundred years later both theories were applied independently as basis for two essentially different signal processing strategies in cochlear implants and auditory perceptions seemed to underline the validity of just one of both theories. Early implants transmitted the electrical stimulus as a continuous voltage, analogous to an amplitude compressed acoustical input to a single active electrode placed in the scala tympani close to the nerve fibres of the auditory nerve [3]. The fact that such single channel methods supported vowel discrimination, contradicts sheer place theory. However, all modern cochlear implants represent acoustic source signals according to the tonotopic organization of the cochlea, i.e., the signal is distributed among multiple channels which are tuned to certain frequencies in relation to the place principle. Neglecting the temporal fine structure of the input is one reason for deficient speech understanding with cochlear implants, especially in noisy environment.

Several authors have added noisy signals to the stimulus in order to improve the temporal firing pattern in cochlear implant users [4, 5], although the noise favours phase locking to the prominent signal components. Another shortcoming is that artificially noise related perceptions are sustained rather than transferring the temporal fine structure of the source signal accurately.

Within this study the possible enhancement of the temporal fine structure, that is representation of the signal maxima, is investigated by adding a subthreshold 5 kHz sinus to the audio signal.

Material and Methods

The primary segments of German vowels from a female speaker are used as analogue stimulus signals with and without an added sinus. Series of both signals with varying intensities are applied to a 27 compartment model of a single human

auditory neuron to examine its stimulation by a small spherical electrode. The resulting firing times represent the response of a group of activated neurons placed at different distances away from the electrode. In more detail, electrode current as a function of time t in [ms] is either

A[μA]*(speech signal),

or including the supporting signal

A[μA]*(sinus(10πt) + speech signal).

The speech was sampled at 16 kHz within the limits -1 to 1.

The bipolar model neuron is a modified Hodgkin-Huxley model which consists of a peripheral process with 5 nodes of Ranvier, an unmyelinated area around the soma and a central process with 6 nodes of Ranvier (Fig. 1). Geometry, electrical parameters and ion channel modelling as well as electrode data are used as in [6]. However, in order to spare computation time the stochastic contributions from ion channel current fluctuations are neglected.

The obtained firing times of the fourth postsomatic node of Ranvier are recorded in order to quantify the enhancement of the temporal fine structure when the sinusoidal high frequency signal is added.

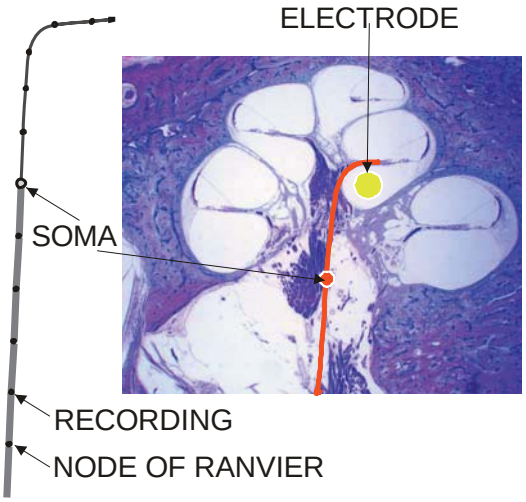


Fig. 1: Compartment model of the cochlear neuron and its position within a human cochlea

Results

The applied sinus signal of maximum studied intensity, i.e., A=715 μA (log A = 2,85 and $A_{threshold}$ = 705μA), causes two spikes within the first 5 ms.

The primary 42 ms of vowel /a:/ generate the spiking times which are shown in Fig. 2 and marked by either triangles in the absence of a sine wave, or by circles which represent the extended signal .

Addition of this rather strong constant sinus signal has two important consequences: First, because of

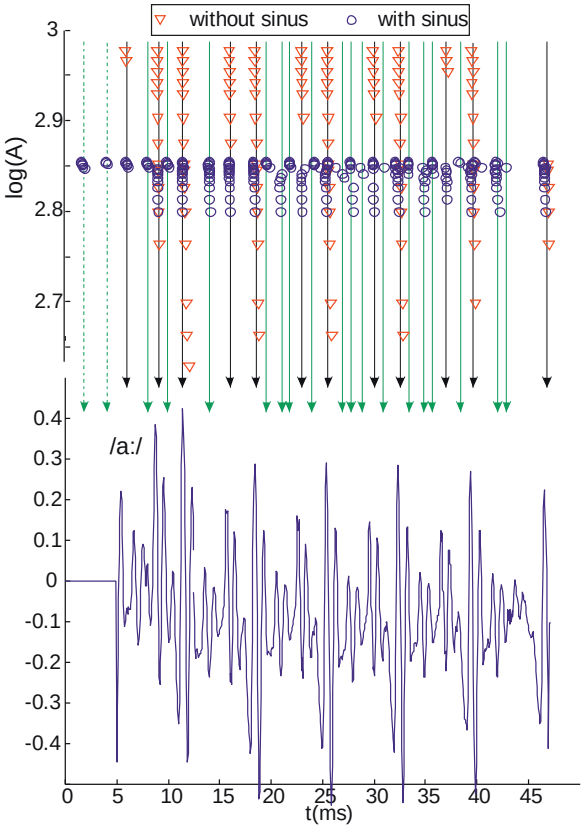


Fig. 2: Stimulus signal /a:/ from a female speaker (bottom) and firing times for different intensities (top). Without high frequency signal the temporal pattern is poor (marked by black arrows). Additional spiking times (green longer arrows) occur by adding the 5kHz sinus. At the vicinity of log(A)=2.85, the best representation of the fine structure could be obtained, then signal values of these amplitudes activate neurons placed far away from the electrode that should contribute to the group response.

the presence of the sinus the cell is no longer at its resting state; instead it is close to the threshold. Therefore, the dynamic range of the audio signal is constricted to a smaller operating window (circles in fig. 2). Second, the representation of the temporal fine structure of the acoustic source is significantly improved by displaying more signal maxima, that is peaks of the audio signal not present because of the refractory behavior appear to cause firing times in fibres placed distant from the electrode.

Discussion

The hearing performance of cochlear implant users is still limited, especially when it comes to speech understanding in noisy environment even the best among all performers show deficits. In order to improve acoustical perception, most of the developers relied on increasing the number of

implant channels confining in the place theory. However, the neural code transmitted in the healthy ear by speech signals indeed has a surprisingly low resolution as demonstrated with Fig. 3, where a 'capture effect' [7] causes large populations of adjacent cochlear nerve fibres to respond rather synchronized to the maxima of the acoustic input [8] resulting in a neurogram containing only a few regions with different firing characteristics.

Next attempts to test this approach should include finding valid parameters for the sinusoidal frequency and its amplitude. Additionally, exploring multichannel strategies with such a method might improve the representation of the temporal fine structure of a source signal.

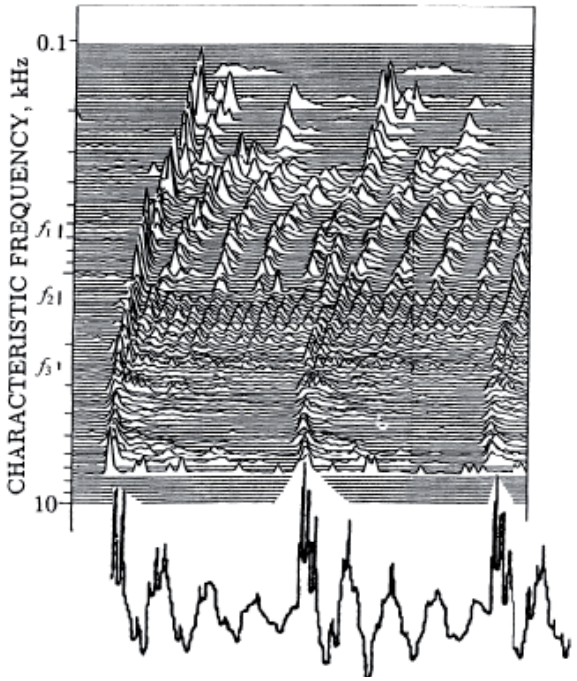


Fig. 3: Firing behavior from 223 cochlear nerve fibres from a single cat that are stimulated repetitively with the synthetic speech signal /da/. The first 20 ms of the stimulus (bottom) evokes firing patterns that are recorded with a delay of about 12 ms in the fibers with high characteristic frequencies and with an additional delay for the low frequencies. Every line represents the beginning of a poststimulus histogram of the firing times of a single fibre. The formant frequencies f1, f2, f3 of the speech signal are slowly changing as marked by vertical bars on the left-hand side of the histograms. The neurogram contains six regions with different firing characteristics. Typically, the peak times in one region are strongly related with some of the maximum values of the speech signal.
The intervals between the peaks in one line are not constant and they are only closely related to the period duration as implicated by the characteristic frequency of the target fibre. The three main maximum values of the speech signal (indicated by interrupted lines at the bottom of the neurogram) which correspond to the fundamental frequency f0 cause pressure waves that are recorded in every part of the cochlea, i.e. these events are seen in every line of the neurogram. From [8], adopted after [9] and [10].

Furthermore, digital signaling strategies should be investigated with reference to this concept.

Acknowledgements

This research project with the presented results was supported by the Austrian Science Funds (FWF) - project 21848-N13.

Corresponding author

Frank Rattay
Institut for Analysis and Scientfic Computing
Vienna University of Technology
A-1040 Vienna, Austria
frank.rattay@tuwien.ac.at

References

[1] Helmholtz H. Die Lehre von den Tonempfindungen als physiologische Grundlage für die Theorie der Musik. Vieweg, Braunschweig. 1863

[2] Rutherford W. A new theory of hearing. J. Anat Physiol 21: 166-168, 1886

[3] Hochmair ES, Hochmair-Desoyer IJ. Percepts elicited by different speech-coding strategies. In Cochlear prostheses, Eds CW Parkins and SW Anderson, Ann NY Acad Sci 405: 268-279, 1983

[4] Morse RP, Evans EF. Enhancement of vowel encoding for cochlear implants by addition of noise. Nat Med 2: 928–932, 1996

[5] Chatterjee M, Robert ME. Noise enhances modulation sensitivity in cochlear implant listeners: stochastic resonance in a prosthetic sensory system? J Assoc Res Otolaryngol 2:159-171, 2001

[6] Rattay F, Lutter P, Felix H. A model of the electrically excited human cochlear neuron. I. Contribution of neural substructures to the generation and propagation of spikes. Hear Res 153: 43-63, 2001

[7] Rattay F, Lutter P. Speech sound representation in the auditory nerve: computer simulation studies on inner ear mechanisms. ZAMM 12: 935-943, 1997

[8] Rattay F. Basics of hearing theory and noise in cochlear implants. Chaos, Solitons & Fractals 11: 1875-1884, 2000

[9] Miller MI, Sachs MB. Representation of stop consonants in the discharge pattern of auditory nerve ®bers. J Acoust Soc Am 74: 502-517. 1983

[10] Shamma S. Speech processing in the auditory system: I. The representation of speech sounds in the responses of the auditory nerve. J Acoust Soc Am 78: 1612-1621, 1985

Current-distance relations for microelectrode stimulation of pyramidal cells

Wenger C[1], Paredes LP[1], Rattay F[1]

[1] Vienna University of Technology, Vienna, Austria

Abstract

*Microelectrodes placed within the densely packed cortical neuronal region are surrounded by many thin processes. Although, dendrites are considered to be functionally different to axons, they also possess voltage sensitive membrane channels. Therefore, dendritic regions are suitable candidates for spike initiation sites when stimulated externally, although they demand for 2-3 times higher thresholds in comparison with thin axons. Simulations based upon recently reported distributions of two types of sodium channels and traced pyramidal cell data accompanied by a simplified model structure enlightened the spike initiation sites for extracellular cortical microstimulation and revealed insights into dendritic excitation patterns. Surprisingly low dendritic threshold values for cathodic stimulation were detected, i.e., 3.3µA for a 0.4 µm diameter fibre excited with a 100µs pulse in 4 µm distance. However, according to the activating function concept the excited region is calculated by 1,414*electrode-distance, therefore a minimum electrode-fibre distance is required as sufficient sodium channels are needed to produce enough intracellular current for spike conduction. The minimum distance for dendritic spike initiation increases with diameter and hinders low current stimulation of thick dendrites. This effect is in contrast to the inverse recruitment order known from FES. Simulations were performed using NEURON and MATLAB.*

Keywords: *microelectrode stimulation, pyramidal cell, dendrite stimulation, computer simulation, multi-compartment model, current-distance relation, activating function.*

Introduction

Modern techniques like patch clamp, immunochemistry and tracing methods develop rapidly and constantly reveal detailed recording data causing deficiencies in theoretical investigations. Therefore, the excitation pattern along the whole neural axis has to be examined to understand the underlying mechanism when low current pulses are applied for cortical stimulation. Consistent with previous work [1] our results confirmed the myelinated axons to be the most sensitive elements for external stimulation, followed by non-myelinaned fibres, whereas the soma is rather difficult to stimulate.

A crucial question concerns the spike generator site. New findings on the distribution of voltage sensitive ion channels revealed the dendrites as possible candidates since they act as independent processing units [2]. Although the inverse recruitment order, causing plenty of problems in FES, states that thick fibres are more excitable, our findings indicate that thin dendrites can be easier stimulated under certain circumstances.

The presented results for dendritic spike initiation are not in accordance with a quadratic current-distance relation that is assumed by many authors without defining which part of the neuron has been examined [3]. Accounting for the fact that most theoretical investigations focus on simulation of intracellular stimulation [4], we applied the activating function concept to a L5 (layer 5) pyramid cell, a typical cortical neuron, to analyze the current distance relations.

Material and Methods

The activation function concept has been connected with a multi-compartment model to test current-distance relations along the neural axis. We assumed a monopolar spherical electrode in an infinite homogeneous extracellular medium with a resistivity of ρ_e = 300 Ohm.cm. Data of a traced pyramidal cell (Fig. 1) revealed a dendritic arbour consisting of 10 basilar dendrites and one apical dendrite consisting of 83 main sections [5]. The 30 µm long soma is followed by the tapering axon hillock and axon initial segment (AIS) of 10 and 50 µm length, respectively, after which a 400 µm long unmyelinated axon proceeds the alternating sequence of the myelinated parts, i.e., the 100 µm long internodes and the node of Ranvier which have a typical length of 1 µm [6]. In accordance with the concept that a branching structure can be

equivalent to a simple cylinder [7] a rectified model neuron with only one simple dendrite has also been examined to keep track of the traveling voltage.

As adopted by data obtained from [6], different ion channels are non-uniformly integrated throughout the functionally distinguished segments and combined with a linear leakage current throughout the cell. $Na_v1.2$ denotes a high threshold sodium current distinguished by the low threshold $Na_v1.6$ as indicated by its reduced half activation voltage $V_{1/2}$ of -41mV compared to the -28mV of $Na_{v1.2}$. One calcium Ca^{2+} and three potassium currents are present, i.e., fast voltage-gated K_v, slow non-inactivating K_m and a calcium dependent K_{Ca} [5].

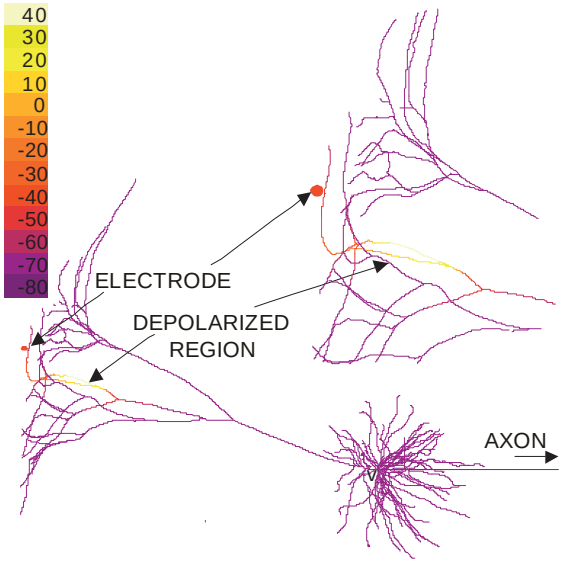


Fig.1. Geometry of the investigated pyramidal cell stimulated by a microelectrode (red circle, compare enlargement) positioned close to a branch of the apical dendrite. Colour legend displays a calculated action potential travelling in direction of the soma. Note that since traced data were only available for the dendrite with diameters in the range of 0.34-4.7µm, the axon was assumed to be a straight line.

Results

Although threshold investigations on current distance relation revealed the AIS to be the most excitable region with the lowest values, i.e., is most likely to be the spike generator site, our results also support active dendritic properties as reported by [2,4,7,8]. Depending on electrode configurations dendrites are capable of developing and successfully transmitting an action potential reflecting the effect of their ion channel composition as demonstrated in Fig. 2. In the subthreshold case the effect of the applied electrical field either fails to stimulate the neuron or the travelling depolarized membrane voltage succeeds to cross the soma and reaches the low threshold AIS region which triggers an action potential. A spike generated by an electrode placed above the dendrite (Fig. 2A) will propagate slowly and cause a delay compared to the spikes generated in the axon (Fig. 2B) due to their increased conduction velocity resulting of both the earlier activation of the Nav1.6 type and the higher sodium channel density.

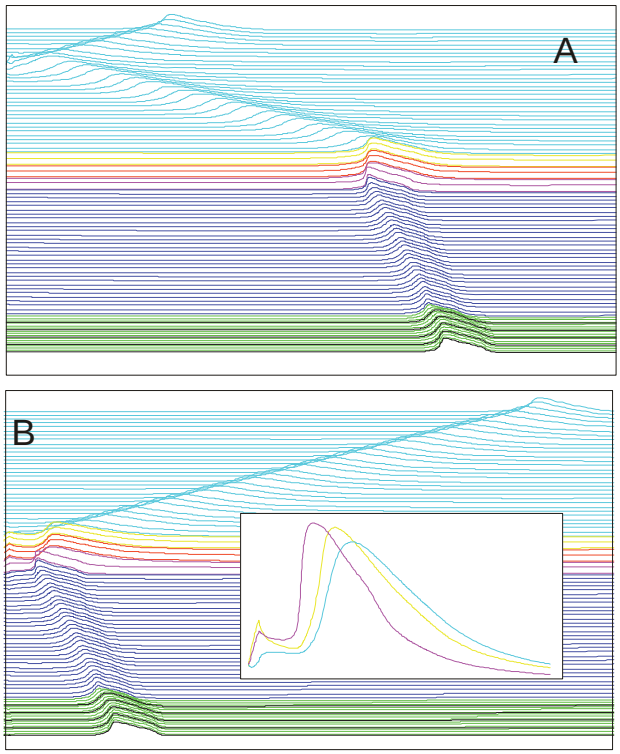


Fig.2. Propagating action potential initiated in the dendrite marked as cyan lines (A) and in the magenta AIS (B). The 100 µm cathodic electrode needs higher threshold in (A) and causes a delay of about 5ms, crossing the yellow soma and red hillock travelling through the blue unmyelinated region to the node-internode region marked in green and black resp.

Comparing the current distance relations along the neural axis showed altering patterns for the different segments. Threshold currents of 100µs monophasic pulses were calculated for changing electrode positions, focussing on different positions along the dendritic tree including thinner and thicker sites as well as branching points. In almost every case cathodic thresholds for dendritc fibres were smaller than anodic, a fact that is also known from peripheral nerve stimulation [9, 10]. Anodic thresholds for 100µs pulses are 7.9, 13, 8.3 and 18 µA for A, B, C and D respectively. The greater variance within the group of thin fibres can be explained by different conditions in the vicinity to a branching point.

A rather linear current distance relation was detected for cathodic stimulation of different dendritic areas (Fig. 3). Caused by the low sodium channel density, a minimum electrode-fibre distance is however required for direct dendritic

spiking, with increasing values for thicker dendrites. Therefore thin branches can profit from the stronger electrical field close to the electrode.

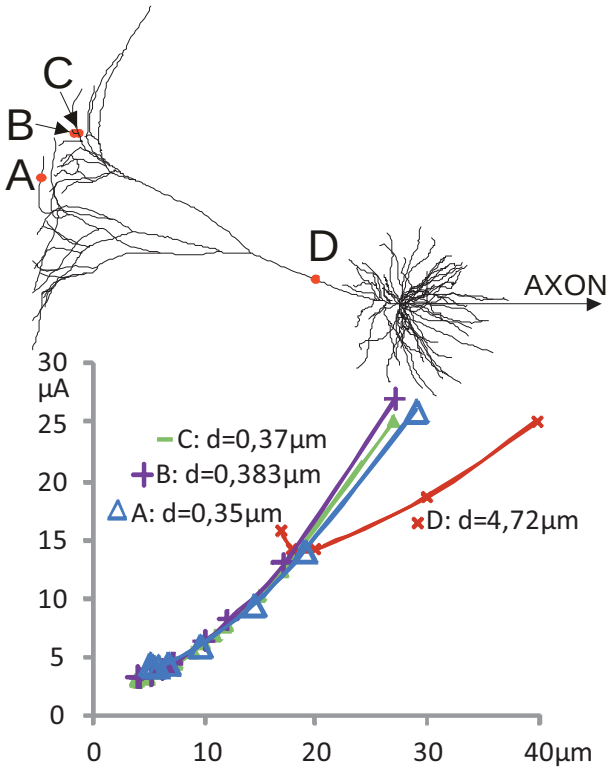


Fig.3. Current distance relation for cathodic stimulation of dendritic branches of four electrode positions A-D. The first marker denotes the minimum electrode-fibre distance for which the dendritic segment is directly excitable. Note that these values are similar for fibres of related diameters and the greatest threshold value of 15.7 µA for the 4.72 µm appears for the thick dendrite

Discussion

When single microelectrodes used for low threshold stimulation are placed within the densely packed cortex, they are surrounded by many thin processes. Due to their abundance dendrites and axons from the terminal region have a bigger chance to be in close proximity, compared to larger elements as soma, axon hillock or even the myelinated axon. Our results further approve the active properties of the dendritic elements what explains recent observations reported by [11] who describe that cell bodies of the primarily stimulated neurons are usually rather far away from the stimulating microelectrodes.

The current distance relations of extracellular stimulation have been studied under quasi-static conditions for monophasic pulses acting on only one specific traced pyramidal neuron limiting the experiments on different branching [7]. In accordance with our results [11] report a minimum biphasic current of 10 µA needed to activate at least one cell with 0.2 µm dendrites and axon.

Further investigations on the dendritic excitation pattern should be concerned with the effect of pulse trains, synaptic activities, backpropagating signals [2, 8], changing sensitive parameters like resistivities, the membrane potential V_m at the soma as well as altering values for the composition of non-uniformely distributed ion channels [4].

Acknowledgements

Austrian Science Fund (FWF), project 21848-N13.

Corresponding author

Frank Rattay
Institut for Analysis and Scientfic Computing
Vienna University of Technology
A-1040 Vienna, Austria
frank.rattay@tuwien.ac.at

References

[1] Rattay F. The basic mechanism for the electrical stimulation of the nervous system. Neuroscience 89(2): 335-346, 1999

[2] Remy S, Csicsvari J, Beck H. Activity-dependant control of neuronal output by local and global dendritic spike attenuation. Neuron 61:906-916,2009

[3] Tehovnik EJ, Tolias AS, Sultan F, Slocum WM, Logothetis NK. Direct and indirect activation of cortical neurons by electrical microstimulation. J Neurophysiol 96(2): 512-521, 2006

[4] Gasparini S, Migliore M, Magee JC. On the initiation and propagation of dendritic spikes in CA1 pyramidal neurons. J Neuroscience 24(49):11046-11056, 2004.

[5] http://senselab.med.yale.edu/ModelDB/ShowModelasp?model=123897

[6] Hu W, Tian C, Li T, Yang M, Hou H, Shu Y. Distinct contributions of Na(v)1.6 and Na(v)1.2 in action potential initiation and backpropagation. Nat Neurosci 12(8): 996-1002, 2009

[7] Kath W. Computational modelling of dendrites. J Neurobiology 64(1): 91-99, 2004.

[8] Larkum ME, Waters J, Sakmann B, Helmchen F. Dendritic spikes in apical dendrites of neocortical layer 2/3 pyramidal neurons. J Neuroscience 27(34): 8999-9008, 2007.

[9] Ranck JB. Which elements are excited in electrical stimulation of mammalian central nervous system: A review. Brain Res 98: 417-440, 1975

[10] Rattay F. Analysis of models for external stimulation of axons. IEEE Trans Biomed Eng 33(10): 974-977, 1986

[11] Histed MH, Bonin V, Reid RC. Direct activation of sparse, distributed populations of cortical neurons by electrical microstimulation. Neuron 63(4): 508-522, 2009

Improving Stimulation, Recording, and Modeling Tools and Techniques for Retinal Implant Development

Jezernik S [1], Dandrea G [1], Kolomiets B [2,4], Djilas M [2], Cahuzac B [3], Ladmiral R [3], Kuhn A [1], Beesau C [3], Cadetti L [2,4], Picaud S [2,4], Sahel JA [2,4,5],

[1] Altran AG, Innovation & Engineering Consulting, Zürich, Switzerland

[2] INSERM, UMR_S968, Institut de la Vision, Paris, France [3] Altran Prime, Levallois-Perret, France

[4] Fondation Ophtalmologique Adolphe de Rothschild (Paris)

[5] Centre Hospitalier National d'Ophtalmologie des Quinze-Vingts, Paris, France

Abstract

Several major challenges still exist with the development of retinal prostheses. These range from surgical approach, implant placement and fixation (epi- vs sub-retinal), to implant design (size and density of stimulation electrode array, biocompatibility, powering), image and stimulus processing paradigms, as well as selective activation of targeted retinal cells. An open challenge is also development, simulation, and test-bench validation of novel stimulation strategies for optimal generation of visual information. This article describes some of research efforts that our team has dealt with in order to contribute to a better and faster development of retinal prostheses. Following results are presented: 1) retinal stimulation/neuronal modeling where different electrode array designs were tested for selective activation of bipolar retinal cells; and 2) development and integration of an on-the-fly stimulus artifact removal scheme into an existing in- vitro setup. Finite-element modeling simulation show that 3D electrode geometries yield a tenfold increase in selectivity compared to a planar structure of similar dimensions. The artefact removal scheme significantly reduces stimulus artifact enabling better recording of stimulus-induced retinal neural activity. Our simulation tools enabled optimization of selective activation of retinal bipolar cells while minimizing ganglionic cell activation at minimal used power.

***Keywords**: selective retinal stimulation, visual prosthesis, stimulation artifact reduction, retinal neuronal model*

Introduction

Patient populations suffering from retinal diseases such as retinitis pigmentosa and age-related macular degeneration can profit from a retinal implant placed into the eye that is used to stimulate the remaining retinal neural network in order to generate useful visual perceptions in the brain. Several research groups are currently developing such implants e.g. [1-3]. Three different systems are currently undergoing clinical European and FDA IDE studies (Second Sight, USA: *www.2-sight.com*, Intelligent Medical Implants, IMI, Germany / Switzerland: *www.imidevices.com* and Retina Implant, Germany: *www.retina-implant.de*) and have already been implanted in several patients.

Retinal implant systems present medical, surgical, and engineering challenges. Two major ones that require substantial future research are achieving high image resolution (visual perception) and achieving high quality of perception. Current systems are able to create only crude visual perceptions [1-3]. One underlying reason is the complexity of the retinal neural network and it's processing [4]. More than 10 different types of retinal cells are inter-connected in complex ways. The healthy retina consists of 3 major layers: the photoreceptor layer, the bipolar cell layer, and the ganglion cell layer (Fig. 1). The mechanism underlying vision starts when photons hit the photoreceptors. Light information is subsequently processed in the bipolar and ganglion cell layers (convergence and codification of visual information) before it is relayed through the optical nerve to higher brain centers. Visual information is thus more strongly coded at the ganglion than at the photoreceptor side of the retina. Because of this, recent attempts are focusing on development of subretinal vs. epiretinal prostheses, where the former are geometrically closer to the bipolar cell layer and can, thus, preferentially stimulate bipolar cells, acting upstream of the information flow [5]. The preferred target for stimulation should be ON cone bipolar cells (normally activated by glutamate released from photoreceptors). The bipolar cells generate sustained graded potentials with depolarization levels between -30 and -60 mV [4]. The goal is thus not to trigger an ON/OFF event in form of action potential (like in peripheral nerve stimulation), but to achieve a desired depolarization level in a controlled way. Graded responses are needed in order to achieve correct dynamic range of excitation. In case of saturated stimulation levels (on/off triggering) we can expect patients only to see white flashes / phosphenes, which is the case with current implants [1]. The cone ON bipolar cells should be activated quasi-continuously (corresponding to dynamic image information) and with implemented lateral

inhibition. The overall retinal stimulation pattern corresponding to whole image needs to be generated in a similar form as described in [3]. This publication presents a new overall paradigm for pre-processing of visual information and subsequent current source stimulation of the retina by application of different spatially and temporally filtered patterns (e.g. slow vs. fast dynamics, gradients for enhanced contrast).

The questions that remain to be answered are how to achieve the selective stimulation of the bipolar ON cells with minimal co-activation of ganglion cells with the subretinal approach while also minimizing the required electrical power, as well as how to validate the stimulation patterns and pre-processing in in-vitro retinal experiments. For latter, when using extracellular microelectrode array recording from the ganglion side of the retina, ganglion firing pattern generated with natural, visual stimuli needs to be compared and matched to the ganglion firing pattern evoked by electrical stimulation of implanted retinal prosthesis. This presents potential means for validation of the overall stimulation paradigm. A previous study [6] has demonstrated that a quasi-natural temporal firing pattern of retinal ganglion cells could also be achieved by using special temporal stimulation profiles.

In our research, we were focusing on the above two questions. We made an attempt to improve the existing multi-electrode array (MEA) experimental setup and have proposed new stimulation configurations verified with new simulation models / tools.

Material and Methods

Recording and Stimulation

The MEA60 (200 3D) recording platform combined with an 8 channel programmable electrical stimulator, a temperature controller, a switch-board, a computer interface and software (all from MCS Multi Channel Systems GmbH) was used for recording and stimulation of retinas extracted from knock-out mice and rats (animal models for targeted diseases). Recordings and stimulations were done with retinas subjected to continuous perfusion with oxygenated Ames medium. The commercially fabricated 3D MEA60 biochips (Ayanda Biosystems, SA) contained arrays of 60 platinum 3D-tip shaped electrodes of the following geometry: rectangular 8x8 matrix arrangement with 200 µm inter-electrode spacing, electrode dimensions 40 x 40 µm; electrode height 50-70 µm; recording noise level was 15-20 µV). For a control comparison of stimulation, another 4-channel custom-made stimulator was used as well. The array is recording from about 350,000 ganglion cells (with 60 contacts). Each contact covers roughly about 6000 cells. Selectivity for recording and stimulation is thus low. For artifact removal, an adaptive template matching algorithm was developed in Matlab (The Mathworks) and was integrated into the MEA environment. This allowed for on-the-fly comparison of raw recordings vs. recordings with adaptively removed stimulation artifacts.

Modeling and Simulation of Selective Retinal Stimulation

Two models were developed and tested. The first model was a 3D FEM model with different electrode geometries and configurations (with returning electrodes). The outputs of this model were electric fields and voltage potential distributions produced with different configurations and with different timings. Configurations generating perpendicular and transverse fields as well as combinations of both were tested. The second model comprised excitation models of bipolar and ganglion cells (similar models to those described in [7-9] were implemented). It was thus possible to calculate which bipolar cells (BC) and ganglion cells (GC) were activated and to compare the selectivity results across different configurations and parameter values (Fig. 1). Following equations were used for excitation calculations (V =potential, Vm = membrane potential):

GC: $$\tilde{V}_m(s) = \lambda^2 \frac{pulse_duration}{2.\tau} . \frac{\partial^2 V_{ext}}{\partial s^2} \geq 15mV$$

BC: $$\tilde{V}_m(s) = \int_{cell} V_{ext} - V_{ext}(s) \geq 5mV$$

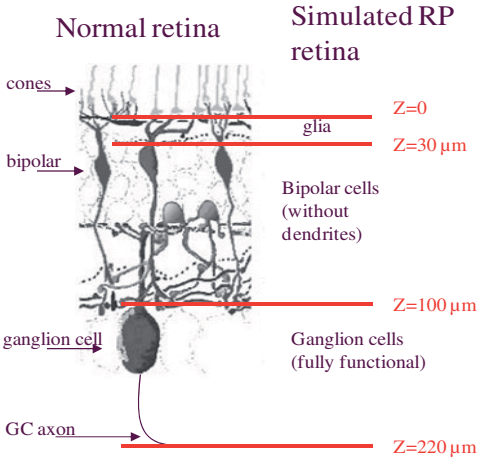


Fig. 1: Retina geometry used in simulations. Stimulation was delivered at z=0. BC@ 30 µm; GC@ 100 µm

The model was also used to evaluate (quantify) the effect of repolarization (anodic) pulses - which are expected to be minimal compared to stimulation (cathodic) pulses.

Stimulation and Retinal Response Modeling

For coupling the above simulation results into a dynamic retinal neuronal model, a model from [10] was used. Computer simulations were performed in order to assist in derivation and to verify/validate optimal temporal patterns of stimulation for production of graded target responses of targeted retinal cells. The nerve cell model represents a simplified retinal network consisting of a certain number of cells that can be taken as representative for retinal modular organization. Focus here was on the temporal evolution of cell hyperpolarization/depolarization in response to dynamic external electrical fields.

Results

For optimal artifact removal, several recordings with different stimuli parameters (10-800 µA and 0.1-1 ms) were performed. Large differences in artifact temporal patterns were observed having non-linear relationship to the input stimuli. Varying artifact responses were observed even between different channels when using the same input stimulus (also due to capacitive coupling, see [11]). This excluded the use of a non-adaptive artifact template. On-line reconstruction of adaptive templates for each recording channel and LSQ error optimization for shape adaptation were needed. Different adaptive algorithms were implemented and tested. One algorithm used adaptive estimation of the artifact template with a time-stretch factor fitting and exponential forgetting. Exponential forgetting weight was also adaptive (using two levels and switching between them; 0.3 and 0.7) depending on the cross-correlation value of the current template and the newest artifact. In case of a largely different new shape, strong forgetting was used. Like this, higher dynamics for artifact adaptation and suppression was achieved. Algorithm performed very well and spike artifacts were removed even when their shape was changing between electrodes or with time and stimulation amplitude (Fig. 2). The algorithm was at the end coded as a plug-in extension to the MAE evaluation software.

In FEM simulations, different planar and 3D electrode configurations and shapes were tested and compared for their efficacy in recruiting bipolar cells and ganglion cells. Also, the effect of different electrode and configuration parameters on selectivity of activation, needed power, and repolarization effects (anodal breakdown) were tested. Example of concentric electrode configuration is shown in Fig.3 together with the area of activated bipolar cells. Concentric electrode configuration achieved strongest lateral decay of electrical fields minimizing cross-talk activation (lateral spread) (see also Table 1).

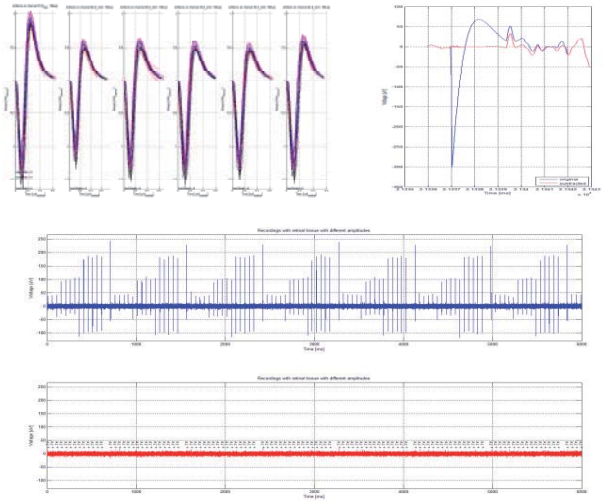


Fig. 2: Stimulation artifacts, their shapes, and artifact removal (red vs. blue traces).

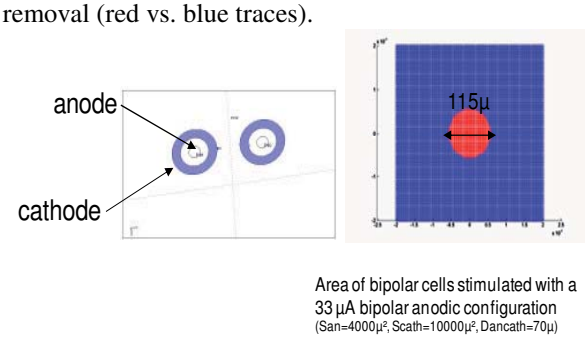


Fig. 3: Testing concentric electrode configuration for activation of bipolar cells (in this configuration, no GC were activated).

Electrode surface, injected current, and pulse duration were highly sensitive parameters for activation of GC. At the tested current levels, GC axons were never activated.

	current µA	power µW	surf. Bipolar µm²	surf. Gangl µm²	remarks
circular	165	960	78600	19300	
rectangular	142	850	79000	20100	aspect ratio 0,3
concentric (D=100µ)	110	658	38800	20400	
cylindric	186	1116	77200	18000	height 12µ
conic	174	1042	84000	19200	height 12µ
conic concentric (D=100µ)	108	647	38800	16400	height 12µ

Table. 1: Simulation results, activation of BC and GC at same electrode surface area, current, pulse duration, and inter-electrode distance.

Furthermore, 3D electrode geometry was found to yield up to a ten-fold increase in selectivity compared to an optimal planar geometry of similar dimensions (Fig. 4). When the activated retinal ganglion cells were identified with the two different configurations/structures (planar and 3D), the 3D electrodes yielded a smaller volume of activation thus allowing generation of more focalized images. Figs. 5 and 6 show results of simulation where electric stimulation fields from 3D model were coupled into a dynamical temporal simulation of a simplified retinal neuronal network.

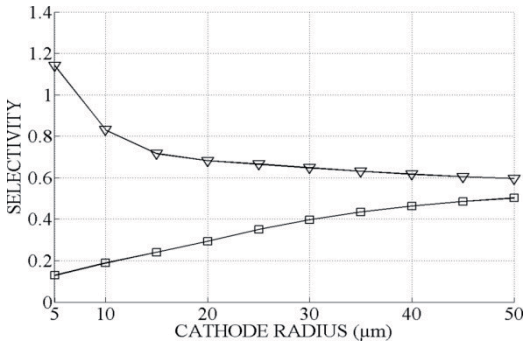
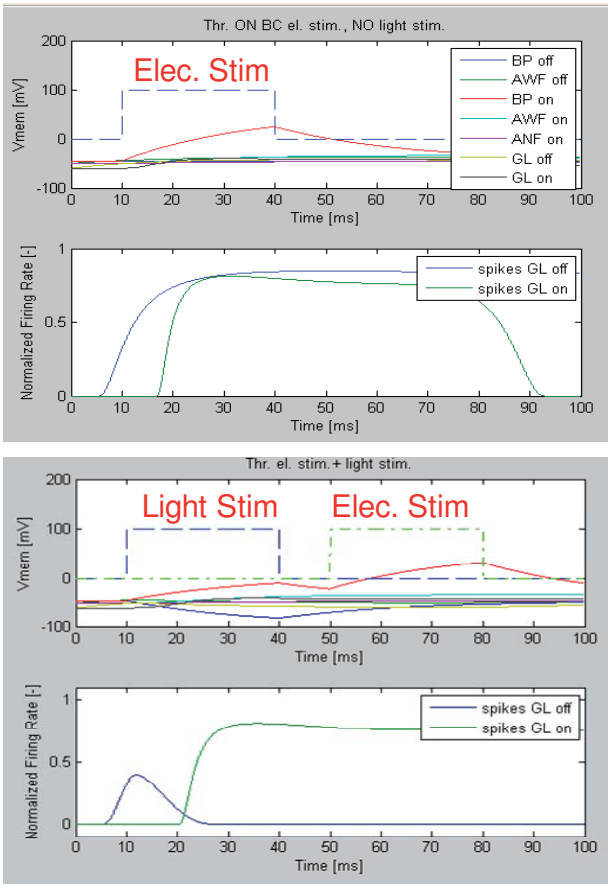


Fig. 4: Simulation selectivity of 3D electrode configuration (triangles) compared to planar (squares) electrode geometry over a range of cathode disc radii.



Figs. 5 and 6: Simulation of a simple retinal network. Top: For suprathreshold stimulation of BC ON cells, spikes are generated at GL ON cells. GL OFF cells are spiking because of lacking light input. Bottom: with el. stimulation, spiking of GL ON cells triggered by initial light stimulus could be maintained.

Discussion

Lots of advances were recently made in the development of retinal implants [2,3,12]. The visual prosthesis is, however, very complex, thus many problems remain unsolved. Here we have presented certain improvements in electrode design, as well as in recording and stimulation techniques and tools that should aid in development of next product generations.

References

[1] Humayun MS, Weiland JD, Fujii GY, Greenberg R, Williamson R, Little J, Mech B, Cimmarusti V, Van Boemel G, Dagnelie G, de Juan Jr, E. Visual perception in a blind subject with a chronic microelectronic retinal prosthesis. Vision Research 43 (2003), pp.2573-2581.

[2] Boston Retinal Implant Project (BRIP): Partners: Massachusetts Eye and Ear Infirmary/ Harvard Medical School, MIT, and Dept. of Veterans Affairs. Link: http://www.bostonretinalimplant.org/

[3] Asher A, Segal WA, Baccus SA, Yaroslavsky LP, and Palanker DV. Image Processing for a High-Resolution Optoelectronic Retinal Prosthesis. IEEE Trans Biomed Eng, Vol. 54(6), 2007, pp.993-1004.

[4] Rodieck RW. The First Steps in Seeing. Publisher: Sinauer Associates; 1st edition (January 15, 1998), ISBN-10: 0878937579, 562 pages.

[5] Jensen RJ and Rizzo JF. Thresholds for activation of rabbit retinal ganglion cells with a subretinal electrode. Experimental Eye Research 83 (2006), pp.367-373.

[6] Fried SI, Hsueh HA. A Method for Generating Precise Temporal Patterns of Retinal Spiking Using Prosthetic Stimulation. J Neurophysiol 95: pp. 970-978, 2006.

[7] Greenberg RJ, Velte TJ, Humayun MS, Scarlatis GN, de Juan E. A Computational Model of Electrical Stimulation of the Retinal Ganglion Cell. IEEE Trans Biomed Eng 1999; 46(5): 505-514.

[8] Rattay F and Resatz S. Effective Electrode Configuration for Selective Stimulation With Inner Eye Prostheses. IEEE Trans Biomed Eng 2004; 51(9): 1659-1664.

[9] Joucla S, Yvert B. Improved focalization of electrical microstimulation using microelectrode arrays: a modeling study. PLoS One. 2009;4(3):e4828

[10] Cottaris NP and Elfar SD. How the retinal network reacts to epiretinal stimulation to form the prosthetic visual input to the cortex. J. Neural Eng. 2000; 2: S74-S90.

[11] Grumet AE. Electric Stimulation Parameters for an Epi-Retinal Prosthesis. Ph.D. Thesis, MIT, Cambridge. 1999.

[12] Sekirnjak C, Hottowy P, Sher A, Dabrowski W, Litke AM, and Chichilnisky EJ. Electrical Stimulation of Mammalian Retinal Ganglion Cells with Multielectrode Arrays. J Neurophysiol 95: pp. 3311-3327, 2006.

Acknowledgements

Authors would like to thank the *Altran Foundation for Innovation* (and its director Christian Le Liepvre) that has enabled and sponsored this project. This work was supported by INSERM, the *University Pierre and Marie Curie* (Paris), the *Fondation Ophtalmologique Adolphe de Rothschild* (Paris), the *Federation des Aveugles de France*, City of Paris, the *Regional Council of Ile de France, Agence Nationale de la Recherche* (ANR TechSan: MEDINAS and RETINE) and the *European Community* for the projects EVI-GENORET (LSHG-CT-2005-512036) and DREAMS (NMP 033345). All recording and stimulation experiments were conducted at INSERM-UPMC (Institute of Vision in Paris, Chair: Prof. Jose Sahel) under supervision of Bohdan Kolomiets and Lucia Cadetti.

Corresponding Author's Address

Sašo Jezernik, Ph.D.
Altran Expert Consultant
Altran Switzerland, Seestrasse 513
CH - 8038 Zürich
saso.jezernik@altran.ch; URL: www.altran.com
Tel.: 0041-76-491-8101

Session 8

Upper Extremity

Preliminary comparison between haptic and electrical stimulation adaptive support for upper extremity motor training

Zadravec M, Oblak J, Cikajlo I and Matjačić Z

University Rehabilitation Institute, Ljubljana, Slovenia

Abstract

Numerous clinical studies have demonstrated that practicing of simple, repetitive and assisted activities effectively reduces motor impairment after neurological insult. This preliminary study investigates the efficacy on human motor learning in upper extremity when assisted by two different support approaches: haptics and electrical stimulation, both controlled with the same adaptive algorithm. Three unimpaired participants, who played a simple game (virtual reality based table football) to learn wrist movements with their inferior arm, participated in the experiment. The evaluation before training without any support was done, followed by the training with adaptive controlled robotic support (RS) and electrical stimulation (ES) and concluded with the evaluation after training. The results show the noticeable improvement in the motor performance of all three subjects regardless of the support method.

***Keywords**: Adaptive control, Motor learning, Upper extremity rehabilitation, Electrical stimulation, Robotic support, Haptics.*

Introduction

Recent studies in neuroscience have demonstrated that the central nervous system can reorganize after neurological injury. It has been demonstrated that intensive movement-based training delivered either by a therapist or haptic robotics – robotic support (RS) reduces motor impairment after neurological insult. There is also a body of clinical evidence showing that the use of Electrical Stimulation (ES) improves motor control. It is known that when stimulation is associated with the person's intention to move the effect is enhanced [1]. In many cases support parameters (delivered either by RS or ES) were manually preset before each session according to temporary working performance of each subject, while during session they remained constant. However, recent clinical results suggest that form of therapy may be more important that its intensity and more importantly that active participation of a trainee is required. Therefore, RS or ES support with fixed control parameters during session is not as effective as a concept "assist-as-needed", which means that only the minimum assistance needed to successfully accomplish a given task will be provided by the robot. The objective of this work was to investigate the efficacy of two different approaches in human motor learning: adaptive ES and adaptive RS.

Methods

Task

Experimental evaluation was carried out by means of Universal Haptic Drive (UHD) [2]. The task for training experiment was a simple football game. Subjects view a football field with a vertical moving player associated with movement of haptic arm, and reference player that shows the reference trajectories to hit ball into the goal. The aim of the game is to achieve as many goals as possible and thereby to learn specific movements. In each attempt the ball comes randomly from one of two possible predetermined directions (Fig. 1). Every time the direction 1 (upper shot) is chosen, subject gets assistance of ES, while for direction 2 (lower shot) the RS is engaged.

Subjects

Three neurological intact right-handed adult males participated in the experiment. Subjects had to train their wrist movements of the inferior arm with the assistance of RS or ES.

Protocol

Subjects had two electrodes placed over the wrist flexor muscles and two electrodes placed over the wrist extensor muscles of inferior hand. Their hands were strapped in UHD's forearm support in a way allowing wrist flexion and extension movements in only 1-DOF as shown from Fig. 2. The experiment was composed of three parts. First part was evaluation before training that consisted of 20 shots on goal (10 upper and 10 lower shots) without any support or showing the reference player. UHD robot was operated in zero impedance mode, meaning that the robot did not apply any support forces. Second part of experiment was training of 100 shots (50 upper and 50 lower, randomly chosen ball direction), visually cued by reference player. Every upper shot the ES was turned on, and in the case of lower shot the RS was provided. After training we did the same evaluation as before it. The experiment lasted approximately 30 minutes.

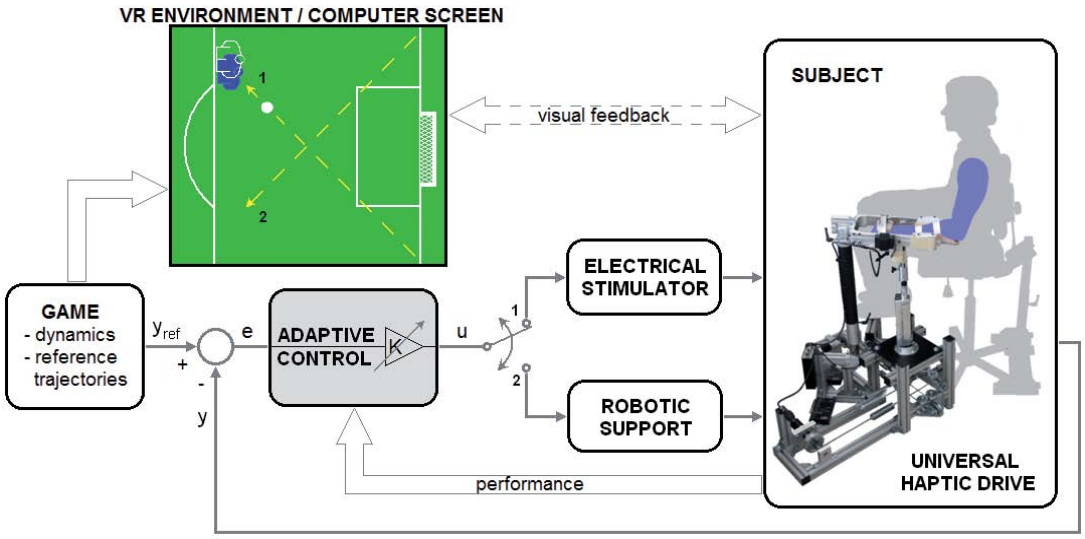


Fig. 1. Block diagram of the experiment. The subject performs the task with UHD's handle bar. Based on the chosen ball direction the subject gets assistance in a form of either electrical stimulation (direction 1) or robotic support (direction 2), which is driven by performance-based adaptive control algorithm.

Support method

Besides visual guidance (reference player) adaptive RS and ES support was implemented separately for each movement direction during training, where support parameters have varied depending on the subject's performance. In this end we define support gain – K through which we determine appropriate level of support that depends on the error between desired and current player position (Eq. 1, Fig. 1).

$$u = K \cdot e = K \cdot \left(y_{ref} - y \right) \tag{1}$$

Level of support has been adapted after two consecutive shot attempts. It decreased in the case of two goals, remain fixed in the case of one goal, and increased in the case of both missed shots as shown in Table 1. According to this adaptation method the RS step was 5% and represent the change of robot's stiffness, which ranged between zero impedance mode (the robot did not apply any support forces) and its maximum value (stiffness 12000 N/m). The ES's minimum and maximum pulse width were preset before each experiment for flexion and extension muscles separately, where minimum value corresponded to the threshold between sensory (SES) and functional (FES) electrical stimulation. Maximal value of pulse width was determined in each subject to acceptable level not provoking discomfort. We used fixed

Table 1. The support method after two consecutive shot attempts.

Shots	*Goals*	*Support*
	0	↑
2	1	=
	2	↓

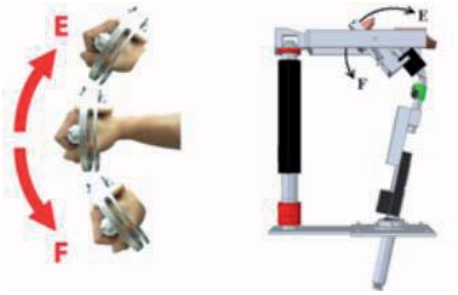


Fig. 2. Wrist flexion and extension movements in UHD's forearm support in a way allowing in 1-DOF.

stimulation frequency, which was 40 Hz. During training the ES's amplitude remained fixed, while pulse duration has been varied in range between 100 and 300μs in steps of 2%. Both support approaches started at 50% ($K_0 = 0.5\ K_{max}$) of their maximum values.

Performance measures

Two performance measures were analyzed to assess subjects' task performance average error and standard deviation of all shots before and after training. Error was defined as an absolute distance from the goal center, when the ball has reached the outline.

Results

Fig. 3 shows the results of supporting curves during training and both evaluations – before and after training, demonstrating similar improvement with both support methods. Table 2 shows percent of performance improvement at the end of training compared to initial assessment. During training the level of assistive ES ranged between 36% and 58%. In the case of lower shots robotic assistance decreased to minimum in all three subjects (bottom left graph of Fig. 3).

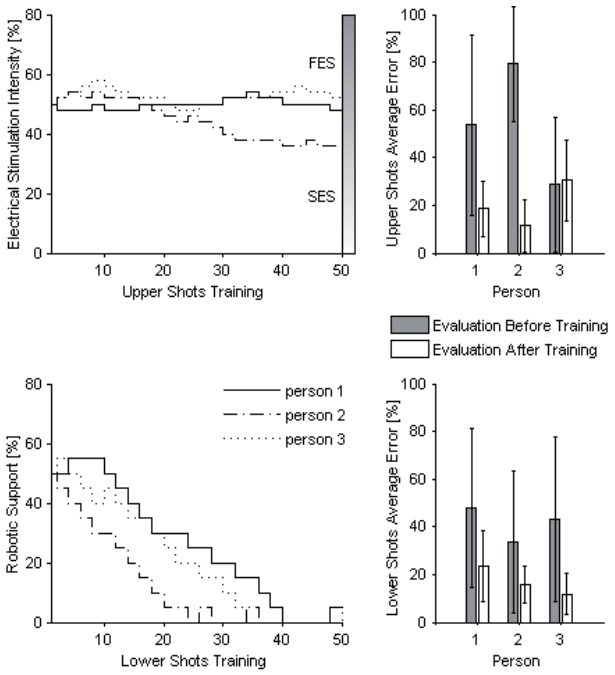


Fig. 3. Results before and after training and corresponding training supporting curves.

Table 2. Evaluation differences between average error before and after training.

Shots	*Person 1*	*Person 2*	*Person 3*	*Group Average*
Upper	65%	86%	-7%	48%
Lower	50%	53%	73%	59%

Discussion and Conclusions

The main aim of this paper was to explore a motor learning task based on two different support approaches. Preliminary results show that both support approaches have similar training effects in selected task of motor learning. We were interested in adapting the ES support in a similar way as is usually done by RS. Therefore, we set the ES for upper shots and the RS for lower shots. The delicate aspect of ES was electrode positioning on the wrist flexors and extensors, which is important to adequately stimulate muscles to do the correct wrist movements. Furthermore, the range of stimulation intensity, which includes minimum and maximum stimulation values for flexor and extensor muscles, should be carefully chosen for effective learning. If the supporting curve is decreasing with increasing number of task repetitions, that is very likely a good and important indicator for effective learning. Such learning can be clearly seen from lower shots training where RS provided assistance (bottom left graph of Fig. 3). In this case all subjects have shown a successful motor learning progress. In the case of upper shots training with ES support the second person has shown similar performance – his supporting curve has been decreasing. The first person's supporting curve, which also showed a significant improvement as well, did not decline, but rather stayed on the same level. There can be several possible explanations why supporting curve did not decrease even though a person has shown successful performance (according to both evaluations). One of them is that the healthy persons, who participated in this experiment, could defy the ES support, so the errors might be greater. Another reason could be our inappropriate choice of predefined desired trajectories. Probably each individual has his own unique way of learning. Therefore, the initial support (50% in our case) may have been different for each individual. In this experiment, we used an adaptation method, where support was adapting after two consecutive shot attempts. In further research different or modified adaptation method could be used. For instance, adaptation method could be based on moving average error of previous repetitions and its support step could also be varied [3]. Another option for motor training could be a modified system, operated by both support approaches simultaneously where motor support would be provided by RS while sensory information would be enhanced by sub-motor threshold ES.

References

[1] De Kroon JR, IJzerman MJ, Chae J, et al. Relation between stimulation characteristics and clinical outcome in studies using electrical stimulation to improve motor control of the upper extremity in stroke. *Journal of Rehabilitation Medicine*, vol. 37, no. 2: 65-74, 2005

[2] Oblak J, Cikajlo I, Matjačić Z. Universal haptic drive: A robot for arm and wrist rehabilitation. *IEEE Trans Neural Syst Rehabil Eng.*, 2010, in press.

[3] Freeman CT, Hughes AM, Burridge JH, et al. An experimental facility for the application of iterative learning control as an intervention aid to stroke rehabilitation. *Measurement and Control*, vol. 40, no. 1: 20-23, 2007

Acknowledgements

This study is supported by the Slovenian Research Agency (ARRS).

Author's Address

Matjaž Zadravec
University Rehabilitation Institute, Republic of Slovenia
matjaz.zadravec@ir-rs.si
www.ir-rs.si

Toronto Rehabilitation Institute's Functional Electrical Stimulation Therapy for grasping in traumatic incomplete spinal cord injury: Randomized Control Trial

Kapadia N[1], Zivanovic V[1], Furlan J[1], Craven B.C.[1, 3], McGillivray C[1], Popovic M.R.[1, 2]

[1] Toronto Rehabilitation Institute, Toronto, Canada.

[2] Institute of Biomaterials and Biomedical Engineering, University of Toronto, Toronto, Canada.

[3] Departments of Medicine and Health Policy Management and Evaluation, University of Toronto, Toronto, Canada.

Abstract

The purpose of this single site randomized control trial was to assess the efficacy of Functional Electrical Stimulation (FES) therapy over conventional occupational therapy in improving voluntary hand function in individuals with sub-acute traumatic incomplete C4-C7 spinal cord injury (SCI). 22 individuals with sub-acute traumatic incomplete SCI were invited to participate in this randomized control trial. All individuals recruited in the study received treatment for both the left and right upper extremities. All 22 individuals recruited in the study received one dose (60 min per day) of conventional occupational therapy for hand function. Over and above 12 of the 22 individuals received an additional dose of conventional occupational therapy while the remaining 10 participants received a dose of FES hand therapy. Therapies were delivered 5 days a week for 8 weeks (40 hours of therapy in total, over and above daily conventional occupational therapy). The primary outcome measure was Functional Independence Measure (FIM). Spinal Cord Independence Measure (SCIM) and Toronto Rehabilitation Institute Hand Function Test (TRI-HFT) were secondary outcome measures. The participants who received FES therapy improved their upper limb function significantly better than the controls as measured by FIM, SCIM upper extremity sub-score, and TRI-HFT. The FES therapy effectively reduced the degree of disability and restored voluntary grasping function in individuals with tetraplegia when compared with conventional occupational therapy.

***Keywords**: Neuroprosthesis, functional electrical stimulation, therapy, spinal cord injury, quadriplegia, grasping and hand function*

Introduction

In individuals who have survived cervical spinal cord injury (SCI), hand function has been singled out as the most important function that these individuals would like restored [1]. In recent decades various therapies, surgical interventions and/or devices have been proposed to improve hand function in individuals with C4-C7 SCI. Amongst these functional electrical stimulation (FES) devices have shown the most promising results[2]. Some FES systems for grasping, also known as neuroprosthesis for grasping, have been successfully commercialized and are typically intended for routine use[3,4].

The purpose of this single site randomized control trial was to examine whether FES therapy is actually able to improve voluntary hand function in adult individuals with incomplete sub-acute C4-C7 SCI. Based on the results of this single-center randomized control trial, one can conclude that SCI individuals who undergo short-term FES therapy can more effectively improve voluntary hand function compared to individuals who receive conventional occupational therapy after SCI.

Methods

Patients with sub acute traumatic SCI (Mean time since injury in days was 58.33 ± 6.55 for the control group and 69.9 ± 14.11 for the intervention group) injury from C4-C7 who were unable to grasp and manipulate objects were invited to participate in the study. A battery of primary and secondary outcome measures was administered at baseline including Functional Independence Measure (FIM), Spinal Cord Independence Measure (SCIM) and Toronto Rehabilitation

Institute Hand Function Test (TRI-HFT)[7]. Participants were randomized upon completion of baseline assessments. All participants in the study received therapy daily, 5 days per week, for the duration of 8 weeks (40 sessions in total). *Conventional therapy* consisted of muscle facilitation exercises, task-specific, repetitive functional training; strengthening and motor control training using resistance to available arm motion to increase strength and stretching exercises. *FES therapy* consisted to performing ADL's while being assisted with electrical stimulation (Fig 1). The stimulation parameters used were: a) balanced, biphasic, current regulated electrical pulses; b) pulse amplitude from 8 to 50 mA (typical values 15-30 mA); c) pulse width 250 μs; and c) pulse frequency 40 Hz. For the intervention group we found that the intensity of current administered needed to be increased over a period of time as the participant became accustomed to the stimulation. Both control and intervention groups received therapy for an equal amount of time and received identical attention. The primary and secondary outcome measures were performed again upon completion of therapy and at 6 month follow up.

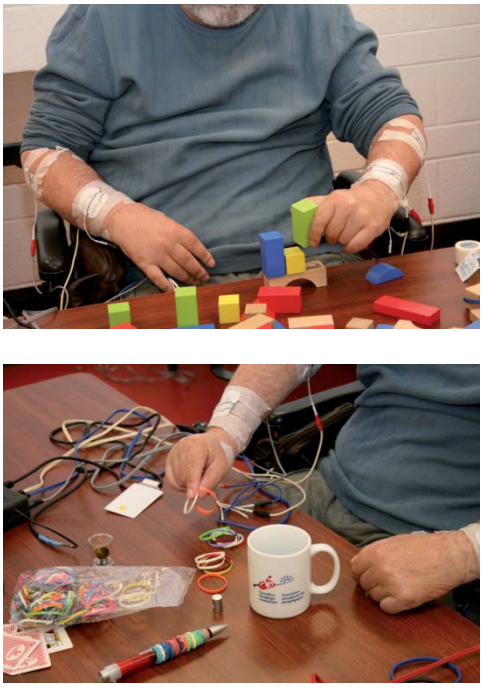


Fig 1. Examples of object manipulation during the FES therapy

Baseline data of intervention and control groups were compared using Fisher's exact test (for categorical variables) and Mann Whitney U test (for continuous variables). Comparisons between the intervention and control groups were carried out using linear regression analysis adjusted for the baseline degree of disability. All data analyses were carried out using SAS program version 9.1 (SAS Institute Inc., USA). Significance was determined at $p<0.05$.

Results

The results of this study suggested that both intervention and control groups improved their upper limb functions due to the therapies provided to them. However, the intervention group, i.e., the one that received FES therapy, improved significantly better as compared to the control group (Table1).

Test	Control		Intervention		p values
	Before	*After*	*Before*	*After*	
FIM	7.8	17.8	8.1	28.2	0.015
SCIM Upper Extremity Sub-score	3.3	6.4	1.9	12.1	<0.0001
TRI-HFT Components					
10 Objects	27.2	38.5	37.1	53.8	0.054
Rectangular Blocks	29.3	38.4	34.7	49.7	0.124
Wooden Bar (Able to Hold)	0.63	0.96	0.8	1.5	0.065

Table 1: FIM, SCIM and TRI-HFT scores before and after therapy for control and intervention group.

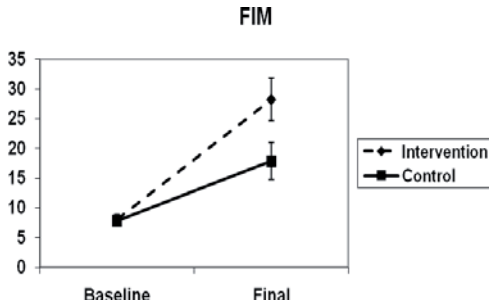


Fig 2. FIM total score at baseline and after the therapy completion for the control and intervention groups (mean ± standard error of mean).

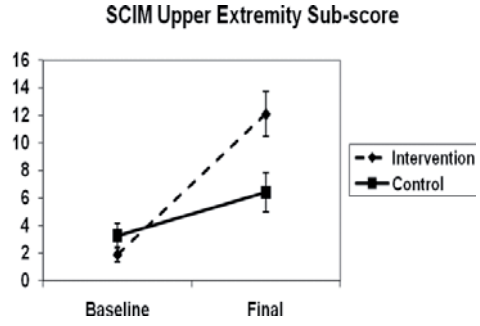


Fig 3. SCIM upper extremity sub-score at baseline and after the therapy completion for the control and intervention groups (mean ± standard error of mean).

Statistically significant improvements were noted in FIM self care scores p= 0.015 (Fig 2.), SCIM upper extremity sub-score p<0.001 (Fig 3), TRI-HFT instrumented cylinder score p=0.033, and TRI-HFT credit card score p=0.035. TRI-HFT total score for manipulation of objects 1 to 10 and the TRI-HFT wooden bar test score had p values 0.0538 and 0.0652, respectively. The only test that did not show statistical significance between intervention and control groups was TRI-HFT nine rectangular blocks test.

Discussion

The results of this study are overwhelmingly positive. Since we have obtained statistically significant results with only 22 participants (12 in control group and 10 in intervention group) and since the variability in the achieved results/function is large, our results clearly show that the intervention group had to have dramatically better improvements in hand function as compared to the control group to achieve statistical significance with such a small sample size. The results of this study as well as some of our previous work stress the importance of applying a surface FES therapy intervention that can be tailored and adjusted to patient needs on a daily basis, and can evolve as the patients improve their function[5,6,7,8]. Furthermore, our findings suggest that if a participant who attempts to execute a grasping task is assisted with the FES therapy to carry out that task, he/she is effectively voluntarily generating the motor command (desire to move the arm, i.e. *command input*). It is suggested that FES therapy is providing the afferent feedbacks (*system's output*), indicating that the command was executed successfully. We hypothesize that by providing both the command input and system's output to the central nervous system (CNS) repetitively for prolonged periods of time, this type of treatment facilitates functional reorganization and retraining of intact parts of the CNS and allows them to take over the function of the damaged part of the CNS[8]. Moreover past literature shows that the combination of performing diverse and meaningful tasks with high repetition, and participant's persistent active engagement (i.e., all participants had to devote 100% of their attention to the tasks performed) plays an important role in retraining voluntary grasping functions[9]. These strategies are fully in tune with recent findings in the field of neuroplasticity and suggest that the proposed FES therapy is potentially another very effective method that can be used to retrain the neuromuscular system.

Conclusion

We conclude that FES therapy is a very effective method of restoring voluntary hand function in individuals with incomplete SCI. We also conclude that FES therapy is effective in retraining the neuromuscular system. This therapy is very easy to administer and requires minimal training on part of the Physiotherapists and Occupational therapists. Donning and doffing the system doesn't require more than 5 minutes. From the logistics point of view this therapy can be easily integrated into already existing occupational therapy programs without a need for additional treatment hours or funds beyond those needed to purchase a programmable FES system.

References

[1]Anderson KD. Targeting recovery: priorities of the spinal cord-injured population. J Neurotrauma.2004; Oct, 21(10):1371-1383. [2]Popovic MR, Thrasher TA. Neuroprostheses. In: Wnek GE, Bowlin GL (eds). Encyclopedia of Biomaterials and Biomedical Engineering. Marcel Dekker: New York, July 2004, pp 1056-1065.

[3]Smith B, Peckham PH, Keith M, Roscoe D. An externally powered, multichannel, implantable stimulator for versatile control of paralyzed muscle. IEEE Trans Biomech Eng 1987; 34(7): 499-508.

[4]IJzerman M, Stoffers T, 't Groen F, Klatte M, Snoek G, Vorsteveld J, Nathan R, Hermens H. The NESS handmaster orthosis: Restoration of hand function in C5 and stroke patients by means of electrical stimulation. J Rehabil Sci 1996; 9(3): 86-89.

[5]Popovic MR, Keller T, Pappas IPI, Dietz V, Morari M. Surface-stimulation technology for grasping and walking neuroprostheses. IEEE Engineering in Medicine and Biology Magazine 2001; 20(1): 82-93.

[6]Popovic MR, Thrasher TA, Adams ME, Takes V, Zivanovic V and Tonack MI, Functional electrical therapy: Retraining grasping in spinal cord injury. Spinal Cord 2006; 44:143–151

[7]Popovic MR, Thrasher TA, Zivanovic V, Takaki J, and Hajek V. Neuroprosthesis for restoring reaching and grasping functions in severe hemiplegic patients. Neuromodulation 2005; 8(1): 60-74.

[8]Thrasher TA, Zivanovic V, McIlroy W, and Popovic MR, Rehabilitation of reaching and grasping function in severe hemiplegic patients using functional electrical stimulation therapy. Journal Neurorehabilitation and Neural Repair, 2008; 22(6):706-714.

[9]Szturm T, Peters C, Otto C, Kapadia N and Desai A, Task Specific Rehabilitation of finger hand function using interactive computer gaming. Archives of Physical Medicine and Rehabilitation, Volume 89, Issue 11, Pages 2213-2217.

Acknowledgements

The work presented in this manuscript was supported by grants from The Physicians' Services Incorporated Foundation and Christopher and Dana Reeve Foundation. Additional financial support for this study

was received from the Toronto Rehabilitation Institute and Ontario Ministry of Health and Long-Term Care.

Authors Address

Naaz Kapadia B.P.T. MSc (Rehab)
Toronto Rehabilitation Institute, Lyndhurst Centre
520 Sutherland Drive, Toronto, ON.
E-Mail: kapadia.naaz@torontorehab.on.ca
www.toronto-fes.ca

Multicenter clinical trial of Myoelectrically-controlled FES (MeCFES) for assisting hand function in subjects with tetraplegia –A study of user population, orthotic effect and ADL use

Thorsen R[1], Dalla Costa D[2], Chiaramonte S[2], Binda L[3], Redaelli T[2], Occhi E[3], Beghi E[4], Converti R[5], Ferrarin M[1]

[1]Biomedical Technology Department - Fond. Don Carlo Gnocchi Onlus, Italy

[2] Spinal Unit, Ospedale Niguarda Ca' Granda, Milano, Italy

[3] Spinal Unit, Ospedale Morelli, Sondalo, Italy

[4] Laboratory of Neurological Disorders, Istituto Mario Negri, Milano, Italy

[5] DAT - Fond. Don Carlo Gnocchi Onlus, Italy

Abstract

A multicenter trial of myoelectrically-controlled FES (MeCFES) for assisting hand function in subjects with C5 - C7 myelopathy and tetraplegia is described. The aim of the study is to test the incidence of potential users, the effectiveness as an orthotic device and the utility for activities of daily living (ADL). Myoelectric signal from the wrist extensors is used for control of direct stimulation of the finger flexors as to enhance the tenodesis grip. Candidate users are asked to use MeCFES in 12 sessions to perform the self selected ADL thought to be facilitated by the device. Of 253 randomly selected clinical records of patients with tetraplegia, 166 met the inclusion criteria. Of 107 eligible subjects who could be contacted, 27 had a positive response to MeCFES and were enrolled. At the end of therapy 14 of them found the device sufficiently useful for use at home. It's estimated that 9% of the tetraplegia population may benefit from the MeCFES method and find it useful for ADL.

Keywords*: Tenodesis, Spinal cord injury, Myoelectric control, Orthosis.*

Introduction

A prior pilot study [1] has indicated that myoelectrically controlled FES (MeCFES) can assist hand function in some subjects with a cervical spinal cord lesion.

This multicenter trial aims to estimate the expected number of persons with SCI who can improve their activities of daily living (ADL) by using a device recording myoelectric activity from the wrist extensors to stimulate relevant muscles of the thumb and finger flexors. A further objective is to test the hypothesis that one surface stimulation channel can provide enough hand function to make a sensible difference for the users. It is assumed that single channel users represent a conservative estimate of the number of multichannel users.

Material and Methods

Clinical records of patients with cervical myelopathy were screened for inclusion (level:C5-C7, age:18-80 yrs. and medically stable). Eligible subjects were assessed clinically. Myoelectric signal from wrist extensors was used to control stimulation of the finger flexors. A Hand Test, self assessment and performance questionnaires were administered. Subjects in whom the MeCFES improved grasping, were invited to use the device in 12 occupational therapy (OT) sessions, while performing relevant self prioritised activities.

The MeCFES system consisted of an amplifier, a signal processor, and a single-channel stimulator. The signal was processed to reduce stimulation responses and the average rectified value was calculated and low pass filtered. This signal exerted a direct control of the stimulation amplitude using a piecewise linear function. As a consequence, the subject has to sustain activation of the controlling muscle (ECR) to maintain a stimulation output. The system was battery powered and could fit in a pocket.

Results

Of N_0 = 253 randomly selected clinical records of patients with tetraplegia, N_1 = 166 (63% of N_0) met the inclusion criteria. All includible subjects were contacted and invited to participate in the study, 52 potential responders could not be seen clinically for logistical reasons and yet 7 could use

the MeCFES but could not participate in OT training for logistic reasons or sudden change in health status. Since the responsiveness to MeCFES for these 59 remained untested, they were excluded from the evaluated sample of 107 subjects. Of this portion of N_2 = 107 subjects, 34 were judged 'non responders' from first interview due to health or functional status and 46 were excluded as non risponders at subsequent clinical examination leaving N_3 = 27 subjects that were enrolled in OT. See flowchart in figure 1 for further explanation.

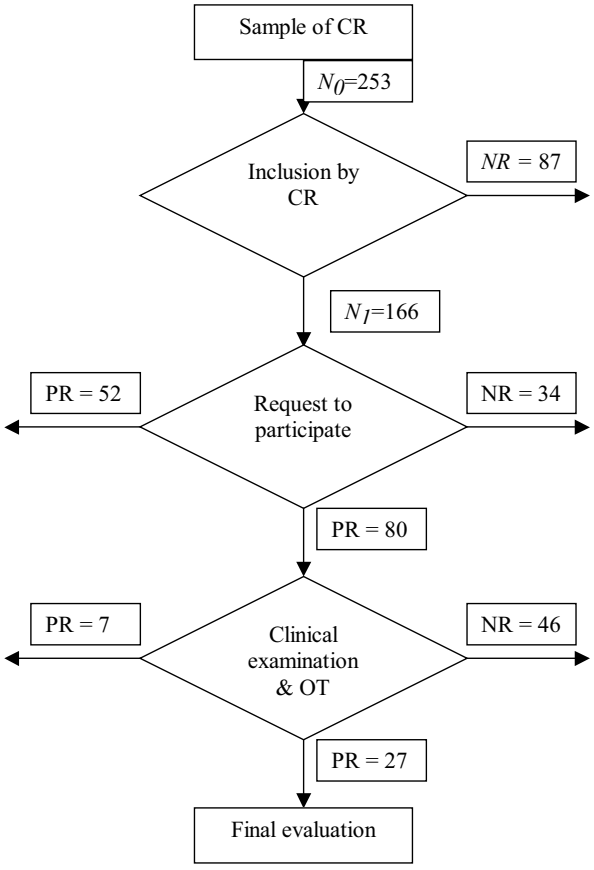


Figure 1. Flowchart of the study. A sample of clinical records (CR) is filtered by inclusion/exclusion criteria and non-responders (NR) are discarded. Possible responders (PR) are requested to participate. Some PR cannot participate in the study and are discarded (to the left). 80 possible risponders are examinated and another 7 PR cannot participate in OT.

The enrolled subjects presented an improvement in hand's function at a first application of the MeCFES device and were enrolled in the MeCFES-assisted Occupational Therapy program. N_r = 14 of the enrolled patients obtained a functional gain and wished to continue use of MeCFES at home if it was available.

C6 was the most frequent lesion level accounting for 78/253=31% of all cases.

Discussion

To summarize: 14 of 107 tested subjects (or 13%) were responding positively to MeCFES. It can be assumed that there would be the same percentage of responders among the untested subjects. Thus we missed 8 (13% of 59) possible responders. The conservative estimate of responders is 14 of 253 subjects yielding 6 % of N_0. Correcting by the fraction of possible risponders that were not tested this could be estimated as (14+8)/N_0 = 9%. We assume that our sample is representative for the population of subjects with a cervical spinal cord lesion present in Italy.

Conclusions

Data suggests that 9% of the tetraplegia population may benefit from the MeCFES method and find it useful for ADL.

References

[1] Thorsen R, Occhi E, Boccardi S, and Ferrarin M. Functional electrical stimulation reinforced tenodesis effect controlled by myoelectric activity from wrist extensors. J Rehabil Res Dev 2006;43:247-56.

Acknowledgements

This work has been supported by the Italian Ministry of Health (Ricerca Corrente IRCCS).

Author's Address

Rune Thorsen,
Fond. Don Carlo Gnocchi Onlus, via Capecelatro, 66 - 20148 Milano Italy
rthorsen@dongnocchi.it

Computer vision for selection of electrical stimulation synergy to assist prehension and grasp

Došen S[1], Kristensen GK[1], Bakhshaie B[1], Pizzolato M[2], Smondrk M[3], Krohova J[3], Popović MB[1,4,5]

[1] Aalborg University, Department of Health Science and Technology, Denmark

[2] University of Padova, Department of Information Engineering, Italy

[3] University of Zilina, Faculty of Electrical Engineering, Slovakia

[4] University of Belgrade, Faculty of Electrical Engineering, Serbia

[5] Institute for Multidisciplinary Research, University of Belgrade, Serbia

Abstract

We describe a method for selection of the grasping synergy of forearm and hand muscles for assisting the hand opening and closing in stroke patients during the therapy of upper extremities. The novelty is the stereo vision system realized with a simple computer peripheral (web camera) and the software which in real-time decides on the grasp type (lateral or palmar) and hand opening requirement (small, middle, large). The test of the vision system in five subjects shows that the overall recognition of the objects size and shape was over 90%, failing only due to shadows and overlapping of the objects in the scene. The vision system is integrated with the four-channel electrical stimulator.

Keywords: *Grasping, Control, Artificial Vision, Electrical Stimulation*

Introduction

The good rehabilitation practice suggests that the recovery of function in stroke patients is benefiting from the intensive task related exercise, especially if applied in the early phase of disability [1]. One of the tools to augment the intensive exercise of the upper extremities is to apply multi-channel electrical stimulation; thereby, allow grasping to stroke patients at the time when they can not do it volitionally. This method, termed Functional Electrical Therapy (FET) was suggested many years ago by Merletti et al., [2], but received the attention again with the availability of new technology such as Bioness H200 [3], Bionic glove [4] and especially Actrigrip and UNAFET [5]. For the effective use of stimulation within FET, the pattern of stimulation needs to be adapted to the type of grasp which entirely depends on the object characteristics (size, shape, and mass). The electrical stimulation integrated into FET [6] contributes to palmar and lateral grasps that are used in more then 90% of the daily activities [7], and uses the preset intensity of stimulation for each of the said modalities. During the therapy session the subjects have to manually select the grasping modality based on the object that is the target.

Recently, we introduced a system comprised of a web camera, distance sensor and laser pointer for the control of prehension of a transradial prosthesis. The system uses computer vision to estimate object properties (size and shape), and sends this information to the rule-based controller which determines the size of hand opening, orientation of the hand vs. the object and type of grasp [8, 9]. This cognitive vision system was mounted onto a five-fingered robotic hand attached to the forearm of a healthy subject (15 subjects) who used it to grasp various 18 objects .

We present the principle of operation of a new stereo web camera system for automatic selection of prehension and grasp implemented on a multi-channel stimulator designed by UNA Sistemi (http://www.unasistemi.com/) as a part of the project TREMOR (http://www.iai.csic.es/tremor/). The stimulator uses the command from the cognitive vision for triggering the prehension/grasping synergy by activating four muscle groups (surface electrodes) (Fig. 1).

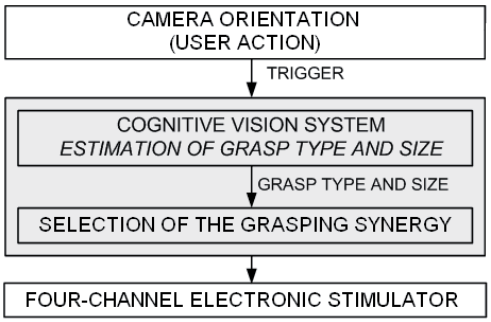


Figure 1: The principle of operation of the cognitive vision system for selection of the stimulation sequence that is appropriate for the object to be grasped.

Web camera stereo vision

The 3D web camera (http://www.minoru3d.com/) was mounted on the dorsal side of the forearm slightly elevated, so that the camera had an unobstructed view of the scene in front of the hand. Each camera from the Minoru stereo pair was calibrated by using Camera Calibration Toolbox for Matlab. The cameras were configured to acquire color (RGB) images at a resolution of 640x480 pixels. The images are visible to the user. The system operates through the following phases (Fig. 1): 1) the user points the cameras so that the target object is central in the scene (multiple objects in the scene) and triggers the control process; 2) the stereo system assesses the distance, and based on the camera calibration data determines the size and shape of the object; 3) the rule-based algorithm decides on the synergy that needs to be implemented [9].

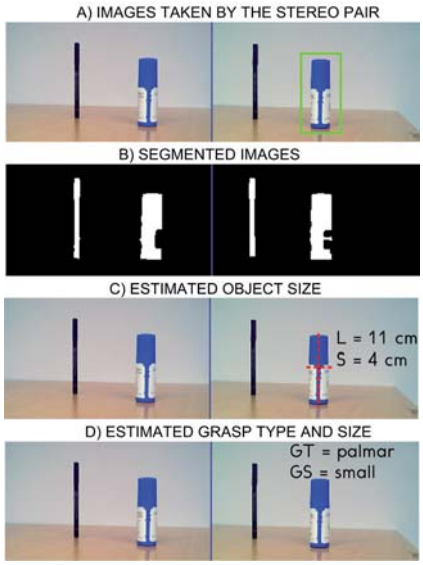


Figure 2: The sketch of the operation of the computer vision for determining the shape and size of the object. The target object is a small bottle (10.5 cm x 3.5 cm). The notations are: L, S – long and short object axes; GT, GS – estimated grasp type and size.

The phases 2 and 3 are further illustrated in Fig 2. The cameras acquire the snapshots of the scene, and the acquired images are stereo rectified (Fig. 2[A]). The objects are then segmented from the background (Fig. 2[B]) by applying Canny edge detection algorithm in the color space and morphological operations of opening and closing. The object that is the closest to the center of the right image is selected as the target for grasping. The lengths in pixels of the object short and long axes are measured. The centers of masses (COMs) of the target object in the left and right image are located, and the disparity, i.e., a difference between the positions of the COMs along the horizontal axis, is computed. The obtained disparity is used to estimate the distance from the stereo system to the target object. By using the estimated distance, focal length of the camera, and the lengths of the object axes in pixels, the lengths of the object axes in centimeters are determined (Fig. 2[C]). Finally, the grasp type and aperture size are selected (Fig. 2[D]) by applying a set of IF-THEN rules mapping the estimated size and shape of the object to an appropriate grasp (e.g., if the object is large and wide use palmar grasp).

Stimulation patterns for lateral and palmar grasps

The electrical stimulation needs to achieve muscle contractions that would lead to hand posture which matches the hand opening and closing to the size and shape of the target object (Fig. 3). The hand posture generation follows principles well defined in motor control literature for grasping of healthy humans, that is, formation of the opposition space. The opposition spaces were assumed in the following manner:

Grasp Type	The opposition space
Lateral	The thumb vs. the radial side of the flexed index finger
Palmar	The thumb vs. the palm with flexed fingers



Figure 3: The palmar and lateral opposition spaces

These two opposition spaces can be formed by stimulating the following muscle groups: thennar muscle group, *flexor profundus digitorum* and *flexor superficials digitorum*. The opening of the hand can be achieved by stimulating *thumb abductor*, *extensors pollicis longus* and *brevis, extensor indicis* and *extensor digitorum communis*. The stimulation profiles were adopted in the form shown in Fig. 4 based on previous research [6].

The selection of the two stimulation synergies is based on information from the vision system (grasp type and size). The intensity of stimulation also uses information from the vision system (size of the object). The intensity levels that correspond to different opening and closing of the hand need to be determined individually by recording the recruitment curves (before the use of the system).

The time line in Fig. 4 shows that the stimulation duration in different phases of prehension and grasping (e.g., hand opening, holding, and closing) can be varied. It was assumed that at the beginning of the therapy the intervals would be set long (≈ 2 s) in order to allow stroke patients to learn how and what to do, and as the skills are being improved

along the therapy the interval would be gradually decreased to the values characteristic for healthy subjects (≈ 0.5 s).

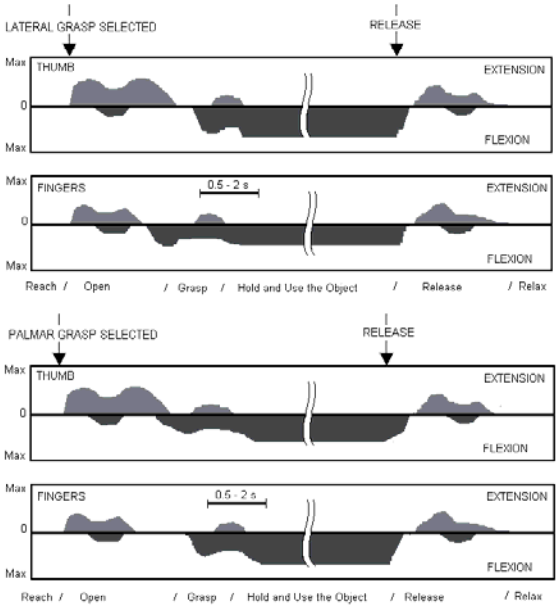


Figure 4: The synergies for lateral (top) and palmar (bottom) grasps. The vertical axes are normalized pulse charges where the level depends on the recognized size of object. The horizontal axis is time.

The actual implementation is envisioned with the system that uses multipad electrodes and protocol described by Popović and Popović [10].

Implementation of the web camera in FET: An example (Fig. 5)

The operation of the vision system was tested in 5 subjects, and the overall success rate of correct recognition was above 90%. The wrong recognition was analyzed by looking at the video that was recorded during the sessions: in all cases shadows and overlapping of objects led to wrong estimate of the size of the shape.

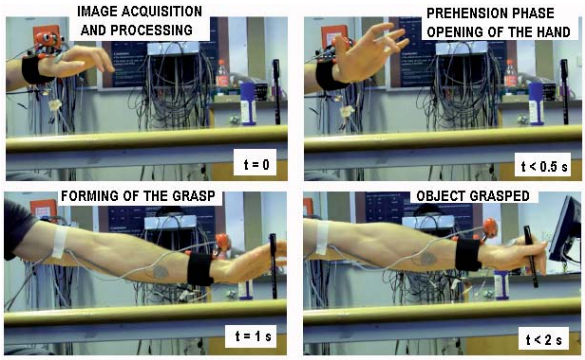


Figure 5: An example showing the use of the cognitive vision system during lateral grasping.

The cognitive vision allows subjects to practice grasping with the most appropriate stimulation sequence. The only volitional activity needed is pointing the camera to the object.

The recognition of the size of the object decreases the level of stimulation and shortens the period of prehension for about 30%.

References

[1] Kroon JR, Lee JH, van der Ijzerman MJ, Lankhorst GJ. The effectiveness of electrical stimulation to improve motor control and function of the upper extremity in stroke. Clin Rehabil.16: 350-60. 2002.

[2] Merletti R, Aćimović R, Grobelnik S, Cvilak G. Electrophysiological orthosis for the upper extremity in hemiplegia: feasibility study. Arch Phys Med Rehabil. 56(12): 507-13. 1975.

[3] http://www.bioness.com/NESS_H200_for_Hand_Rehab.php, accessed on May 11 2010.

[4] Prochazka A, Gauthier M, Wieler M, Kenwell Z. The bionic glove: an electrical stimulator garment that provides controlled grasp and hand opening in quadriplegia. Arch Phys Med Rehabil. 78: 608-14, 1997.

[5] Popović MB, Popović DB, Stefanović A, Schwirtlich L, Sinkjær T. Promoting recovery of reaching and grasping in acute stroke subjects: Functional Electrical Therapy. J Rehab Res Develop. 40(5): 443-54, 2003.

[6] Popović DB, Popović MB, Sinkjær T, Stefanović A, Schwirtlich L. Therapy of paretic arm in hemiplegic subjects augmented with a neural prosthesis: A cross-over study. Can J Physio Pharmacol. 82(8/9):749-56, 2004.

[7] Peckham PH, Knutson JS. Functional electrical stimulation for neuromuscular applications. Annu Rev Biomed Eng. 7:4.1–4.34, 2005.

[8] Klisić Dj, Kostić M, Došen S, Popović DB. Control of prehension for the transradial prosthesis: natural-like image recognition system. J Automatic Control. 19: 27-31, 2009.

[9] Došen S, Popović DB. Cognitive vision system for control of artificial hand. Artif Organs. 2010, in press

[10] Popović DB, Popović MB. Automatic determination of the optimal shape of the surface electrode: Selective stimulation. J Neurosci Meth. 178(1): 174-81, 2009.

Acknowledgements

The works on this project were partly supported by the Ministry of Science and Technology of Serbia, EC funded project HUMOUR FP7-ICT-231724, and InRES project, SCOPES, Switzerland.

Author's Address

Name: Strahinja Došen
Affiliation: Aalborg University, Department of Health Science and Technology, Aalborg, DK
e-mail: sdosen@hst.aau.dk
homepage: http://smi.hst.aau.dk/~sdosen/

Session 9

Lower Extremities

Twenty-five year stimulation of the common peroneal nerve

Rozman J[1], Pečlin P[1], Krajnik J[2]

[1] ITIS d. o. o. Ljubljana, Ljubljana, Republic of Slovenia

[2] University Rehabilitation Institute, Ljubljana, Republic of Slovenia

Abstract

The objective of the report is to summarize the findings after twenty-five year selective electrical stimulation of the common peroneal nerve (CPN) for correction of drop-foot in a 52-year-old left-sided hemiplegic patient. Restoration of a dorsal flexion and eversion of the foot was achieved with selective functional neuromuscular stimulation (FNS) of the particular superficial region of the CPN innervating mostly the tibialis anterior (TA) and partly peroneus longus (PL) and peroneus brevis (PB) muscles. In the last ten years of the twenty-five year period the implant provided very good functional results until the lead wires of the cuff electrode broke out so the implant had to be replaced. In comparison of results with those obtained with the implant implanted ten years before, significant thickening of the CPN at the site of FNS was observed. Within the entire FNS period, conduction velocity of the CPN was slightly reduced. Electrophysiological and biomechanical findings however, have not revealed an explicit functional sign which could be attributed to the damage of the CPN.

Keywords: *Drop foot, peroneal nerve, electrical nerve stimulation.*

Introduction

In 1961, Liberson and colleagues reported the first clinical application of FNS [2]. They used a single-channel peroneal stimulator to activate the ankle dorsiflexors in patients with hemiplegia. Stimulation was synchronized with the swing phase of gait by using a foot switch that allowed activation when the foot was lifted off the ground. Waters et al. (1975) [9] attempted to solve some of the problems with surface electrodes by developing an implantable peroneal nerve stimulator. They reported the results from the use of this implantable stimulator with 16 patients. Significant increases were seen in walking velocity, stride length, and step frequency. However, the authors noted that at a 3-year follow-up, subjects showed encapsulation of the electrodes without any apparent tissue damage. Difficulties with implanted electrodes included the need for surgical re-implantations following electrode displacement. Continued improvement in electrode materials and design performed in our laboratory however, resulted in more predictable and reliable stimulation of muscles [5]. In FNS of a CPN, the recruitment of slow motor units was desired to optimize postural holding and antigravity function while the recruitment of fast motor units was desired when the production of high force or when rapid movements were required. The present study was aimed at demonstrating the results of analysis related to functionality of the implant implanted in a hemiplegic patient and comparing these results with those obtained with the implant implanted ten years before.

Material and Methods

CPN is a terminal division of the sciatic nerve, passing through the lateral portion of the popliteal space to opposite the head of the fibula where it divides into the superficial peroneal, deep peroneal, and recurrent nerves [6]. Muscular branches of the deep peroneal nerve supply the TA, extensor digitorum longus, extensor hallucis longus, peroneus tertius, and extensor digitorum brevis. The superficial peroneal nerve supplies the peroneus PA and PB muscles. At the level above bifurcation of the CPN, tibial fibers lie mostly within the superficial region of the deep peroneal nerve. Therefore, a particular region of the CPN innervating the three aforementioned muscles must be selectively stimulated in order to achieve appropriate functional movement of the foot [3, 5]. The cuff with a platinum electrode shown in Fig. 1a, was constructed considering the results of modelling selective FNS of superficial regions and fibers with different diameters in the CPN by the monopolar stimulating electrode [4, 7, 8]. The stimulus (Fig. 1b), was a current rectangular cathodic component *ic* which could be preset between 1 and 10 mA. The width *tc* of the cathodic component could be set by the patient from 0 to 500 μs, while the frequency *f* and the time delay *td* between the cathodic and the anodic part of the

stimulating pair was preset at 22 Hz and at 50 μs, respectively.

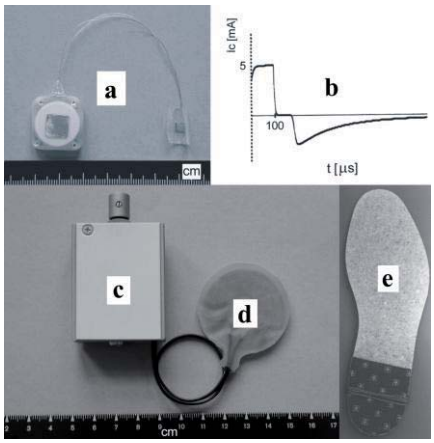


Fig. 1: (a) Implantable stimulator, (b) Stimulating pulse, (c) External unit, (d) Antenna and (e) Foot switch.

The work complied with the principles laid down in the Declaration of Helsinki; Recommendations guiding physicians in biomedical research involving human subjects. Informed consent was obtained from a 52-year-old left-sided hemiplegic male patient.

The implant with two wire loop electrodes placed close to the CPN behind the lateral head of the fibula and providing monophasic voltage-related stimuli was implanted in 1984 and after ten years replaced with a monopolar type. This implant providing very good functional results for the next ten years was replaced with a new monopolar one in March 2008. To activate mainly the TA, PL, and PB during the surgery, the stimuli had to be delivered to the electrode situated close to the corresponding region in the CPN. During fixation of the cuff, the *ic* and *tc* were varied until the optimum movement was obtained. The non-implanted parts of the system are shown in Fig. 2. FNS started 14 days after surgery while the first gait analysis was performed 6 months after surgery.

Results

The results showed that after fifteen years the speed of stimulated gait significantly increased. After twenty-five years, however, the difference in the speed of stimulated and even un-stimulated gait increased even more. It was observed that EMG activity of the left m. triceps surae (TS) was weak during the swing phase. Within the remaining part of the gait cycle a typical sign of spasticity of the TS was observed. Furthermore, ankle goniograms and length of the m. soleus (SOL) and m. gastrocnemius (GAST) demonstrate contractures in TS. However, they were lower when compared to the contractures seen ten years before. Besides missing push off, one consequence of impairment in GAST was also weak knee flexion, especially at the beginning of the swing phase. Consequently, a patient has performed the swing phase with explicit circumduction. The patient compensated for his inability to perform the left swing phase by generating additional power in the knee and hip and with the right side. It could be concluded from EMG of the left TA that this muscle was actually not affected. Therefore, considering the impairment of the plantar flexors and plantigrade foot contact, the pattern of the TA seemed to be almost normal. Both, the shape and the amplitude of EMG activity in the left m. quadriceps (QUAD) seemed almost normal. In the ankle goniogram recorded in the last measurement, a significant move towards dorsal flexion (~10°) could be observed while the shape of the first one was almost identical.

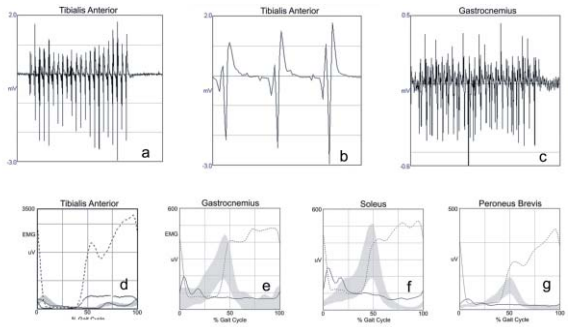


Fig. 2: (Upper) SEMG in the TA graph (a), and graph (b), and GAST graph (c). Graphs (a) and (c) show entire FNS time interval while graph (b) shows a shape of activation in motor units, elicited by an individual stimulating pulse (M-wave). (Lower) Rectified and averaged SEMG in muscles TA, GAST, SOL and PB during FNS. Solid lines-without FNS, dashed lines-with FNS and grey thick line-normative.

It could be seen in Fig. 2 (lower part), representing EMG recorded in TA, PB, SOL and GAST, that all these muscles were stimulated. It was observed that without stimulation there was no normal EMG activity of the flexor TA while EMG activity of the PL could be considered as normal. However, with selective stimulation of the CPN both EMG activity of the TA and PL could be observed. Graphs (a), (b) and (c) in Fig. 3 clearly demonstrate the effectiveness of stimulation by showing a position of center of pressure (COP) along the sole (COPX) and, especially graph (d) by showing the ankle goniogram. Furthermore, correction of ankle inversion, which should be elicited by stimulation of the PL and PB, was favorable in the measurement performed in the year 2000. Dorsal flexion in the swing phase was significantly larger, thus enabling heel contact. A co-activation of TS, elicited by unexpected

stimulation, actually stabilized the ankle at heel contact and additionally contributed to heel contact becoming more steadily. FNS significantly improved the shape of the ankle torque graph in the sagittal plane. However, as a consequence of severely affected TS, amplitude in the mid stance was heavily decreased.

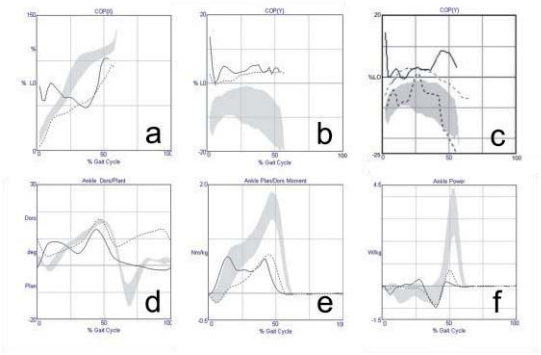


Fig. 3: (Upper) A trajectory of COP along the sole. Graph (a) and graph (b) measured at 2009, graph (c) measured at 2000. (Lower) An influence of FNS on increase in dorsal flexion graph (d), on torque in the ankle graph (e) and, on push off power graph (f). Solid lines-without FNS, dashed lines-with FNS and grey thick line-normative.

In fact, during this interval, TS was only able to produce passive tonic activity. Immediately after heel lift-off, stimulation was turned on, thus causing activity to appear in these muscles and, consequently, contributing to the push off. This could be seen in graph (e) of Fig. 3, showing the torque in the ankle. Results also revealed that left support lasted longer.

Discussion

A system enables highly selective stimulation mainly of those muscles that contribute to strong dorsal flexion and moderate eversion of the hemiplegic's foot. It requires a simple procedure of implantation and is suitable for a wide population of patients. It was observed that motor conduction velocity of the CPN was slightly reduced within the twenty-five-year stimulation perhaps due to the use of a tight elastic band over the implanted region. An examination of the legs did not show a more severe loss of muscle control over the legs and feet and muscles atrophy.

Conclusions

It was shown that even after twenty-five years of usage the implantable gait stimulation system is capable of making a reliable long-term selective activation of FNS of the CP. The highest degree in improvement of gait was provided by obtaining firm heel contact, which enabled for the beginning of support, which become almost normal [10]. However, there was still a lack of normal or stimulated activity in TS in the mid-stance, resulting in an absence of normal push off and knee bending in the swing phase. Partial coactivation of TS during stimulation actually had a functionally favourable effect, since it minimally contributed to push off and stabilized the ankle at approach.

References

[1] Grieve DW. Gait patterns and the speed of walking. Biomed. Eng.1986;3: 119-122.

[2] Liberson WT, Holmquest HJ, Scot D, Dow M. Functional electrotherapy: stimulation of the peroneal nerve synchronized with the swing phase of the gait of hemiplegic patients. Arch Phys 201. Med 1961;42:101-105.

[3] McNeal DR, Bowman BR. Selective activation of muscles using peripheral nerve electrodes. Med & Biol Eng & Comput 1985;23:249-253.

[4] Rattay F. Ways to approximate current-distance relations for electrically stimulated fibres. J Theor Biol 1987;125:339-349.

[5] Rozman J, Krajnik J, Gregorič M. Selective Stimulation of the Common Peroneal Nerve for Hemiplegia: Long-Term Clinical Follow-up. Basic Appl Myol 2004;14(4):223-229.

[6] Sunderland S. Nerve and Nerve Injuries. 2nd ed. Baltimore: WB Saunders; 1978, 925-991.

[7] Sweeney JD, Ksiensky DA, Mortimer JT. A nerve cuff technique for selective excitation of peripheral nerve trunk regions. IEEE Trans 1990;BME-37:706-715.

[8] Warman EN, Grill WM, Durand D. Modeling the effects of electric fields on nerve fibers: Determination of excitation thresholds. IEEE Trans Biomed Eng 1992;BME-39:1244-1254.

[9] Waters RL, McNeal DR, Faloon W, Clifford B. Functional electrical stimulation of the peroneal nerve for hemiplegia. J Bone and Joint Surg 1985;67:792-793.

[10] Winter DA. Biomechanics and motor control of human gait, University of Waterloo Presss, Waterloo, Ontario, Canada N2L 3G1, 1991.

Acknowledgements

This work was funded by the Ministry of Higher Education, Science and Technology, Ljubljana, Republic of Slovenia.

Author's Address

Janez Rozman, Ph. D., ITIS d. o. o. Ljubljana, Centre for Implantable Technology and Sensors, Lepi pot 11, 1000 Ljubljana, Republic of Slovenia. Tel.: +386 1 470 19 13, Fax.: +386 1 470 19 39, E-mail:jnzrzmn6@gmail.com.

An EMG based system for assessment of recovery of movement

Miljković N[1,3], Kojović J[2], Janković MM[1], Popović DB[1,2]

[1] University of Belgrade, Faculty of Electrical Engineering, Serbia

[2] Aalborg University, Department of Health Science and Technology, Denmark

[3] Fatronik Serbia, Belgrade, Serbia

Abstract

We present a polymyography based method to study the recovery after stroke. The method relies on an instrument comprising amplifiers for polymyography, joint angle transducers, software for data acquisition and visual feedback (target and achieved trajectory). The user-friendly, menu driven software allows intuitive use to clinicians. The instrument that we developed can capture up to 16 signals (between -5V and 5 V) which characterize movement (EMG, goniometers, accelerometers, gyroscopes, force sensors, etc.) and send wirelessly processed signals to a host computer. We demonstrate the method and the instrument by presenting a cohort clinical study where we followed EMG during voluntary dorsiflexion in five stroke patients before and after the intensive walking exercise augmented with multi-channel electrical stimulation (Functional Electrical Therapy). The reference data were the recordings from five healthy subjects. We introduced a new measure Rm as the ratio between the median (line which divides the area under the EMG envelope in time domain in two equal regions) in patients and healthy subjects. We show that the recovery of function (dorsiflexion) and Rm were well correlated in this study.

Keywords*: assessment of recovery, polymyography, stroke, synergy, median.*

Introduction

The assessment of recovery of walking in stroke patients is based on clinical scores (e.g., Fugl-Meyer scale, Barthel Index, Functional Ambulation Classification, Berg Balance test, etc.) and quantitative descriptors such as walking speed, symmetry, cadence, stride lengths and duration. The missing element is the central nervous system (CNS) change that is responsible for the recovery. Methods for studying the physiological changes within the CNS are based on imaging (functional Magnetic Resonance Imaging, Near Infrared Spectroscopy [1]) and evoked potentials elicited by Transcranial Magnetic Stimulation [2]. We propose a method which uses polymyography during well controlled movement in order to separate the central pattern generator controlled movement from reflex controlled movement. The control of the movement is left with the patient, and relies on visual feedback provided by the said instrument [3]. The basis for this analysis is a new portable instrument that allows parallel assessment of EMG and kinematics. The instrument that we developed differs from commercially available systems (e.g., DataLOG, Biometrics, Gwent, UK) in the feedback, on-line display during long sessions (up to 2 hours), and 100% error free recordings of up to 16 channels. The instrument is supported by the user friendly software that allows simple clinical application.

Material and Methods

The new instrument consists of a custom designed multi-channel signal conditioner for signals from sensors (e.g., goniometers, force sensing resistors, accelerometers, gyroscopes) and a set of miniature (<15g) low-noise amplifiers (Biovision, Wehrheim, Germany) for acquiring muscle activity (EMG) all connected to the NI USB 6212 A/D card and powered by the USB port. The EMG amplifiers (CMRR>100 dB, gain = 500-2000) are close to the recording sites. The example shown in this paper uses Penny and Giles (Biometrics, Gwent, UK) flexible goniometers (Fig. 1) which output 2.5 ± 2 V for the angle variation between 0 and $\pm\pi$ (resolution of 0.02 radians).

The custom designed software runs in the LabView (National Instruments, Austin, Texas, USA) environment on a miniature portable PC (Sony VAIO VGN-UX1XN). This PC communicates wirelessly by Remote Desktop option with the second host computer used for feedback to the patient and real time inspection and processing of the recordings.

Signals are sampled at 1 kHz by NI USB 6212 A/D connected to the portable computer. The kinematics data are decimated (factor 10). The battery life of the portable computer allows about 2 hours of continuous recordings (the screen turned on), and user can control the recordings on a

remote computer. This wireless design was motivated for prolonged recording sessions in any environment (e.g., walking, standing, reaching), if so required.

Muscles synergies during voluntary dorsi-flexion in healthy subjects and stroke patients

The experiments included 5 healthy individuals (55 ± 6 years of age, 3 female and 2 male, with no known neurological deficit) to collect benchmark data and five post-stroke patients included in the clinical trial analyzing effects of Functional Electrical Therapy (FET) for augmentation of gait, [4]. All subjects signed an informed consent. Patients were evaluated at the entry point to the clinical trial and six months after the entry date.

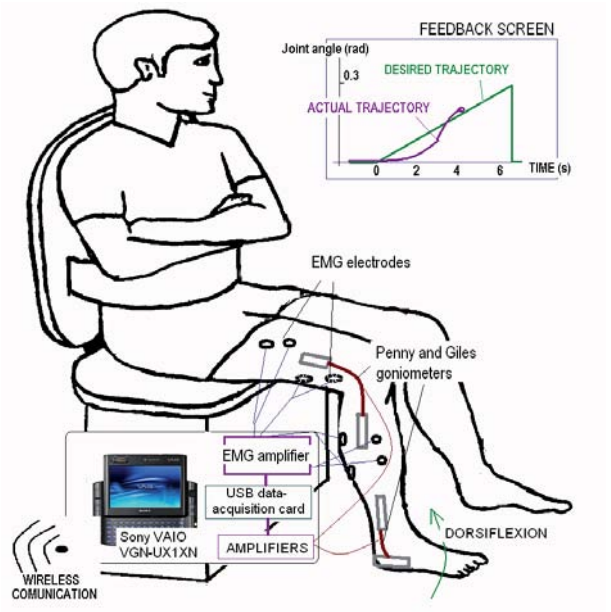


Figure 1: Setup for the analysis of dorsiflexion recovery in post-stroke hemiplegic patients.

The task of the analysis was to evaluate the synergies of major knee and ankle movers during the tracking of the progressive dorsiflexion from neutral to 90 % of maximal angle with right leg (healthy subjects) or paretic leg (patients). We recorded EMG from *Rectus Femoris* m. (RF), *Biceps Femoris* m. (BF), *Lateral Gastrocnemius* m. (LG) and *Tibialis Anterior* m. (TA). Selection of the task followed the well known characteristic of the drop-foot type disability in stroke patients [3].

The setup for the tests of the new instrument is shown in Fig. 1. Electrodes (DS26 disposable surface Ag/AgCl electrodes, Bio-Medical Instruments, Warren, USA) were positioned following the recommendation of SENIAM project [5]. Flexible goniometers (type SG110, Biometrics) were positioned to measure the knee joint angle that should not change, and the ankle joint angle (type F35, Biometrics). All acquired data was normalized to the maximum values for each of the signals using Maximum Voluntary Contraction (MVC) method. Envelope of normalized EMG was calculated by Root Mean Square (RMS) method [6]. Precisely, subjects were asked to dorsiflex to about 90 % of the maximum joint angle flexion (φ_{max}). The straight line between the zero and the φ_{max} was displayed as the target trajectory *vs.* time. Before the tracking test subjects were asked to generate maximum contraction of the four listed muscles in sitting position and the recorded EMG was used as the maximum for normalization [5]. The outcome of the measurement was the averaged normalized value calculated from the results from ten repetitions of the same task. Subjects were asked to rest between the trials to minimize the effects of fatigue.

Results

Averaged and normalized (to maximal angle values) ankle angle trajectories in healthy subjects, and patients before therapy and after therapy together with desired trajectory are given in Fig. 2, top panel. The maximum dorsiflexions were 9±6, 18±4 and 23±5 degrees for patients before and after the FET and for the healthy subjects respectively. The two bottom panels in Fig. 2 show normalized and averaged EMG envelopes for RF and TA muscles in one healthy subject and in one patient before and after FET with the individual variability in percent.

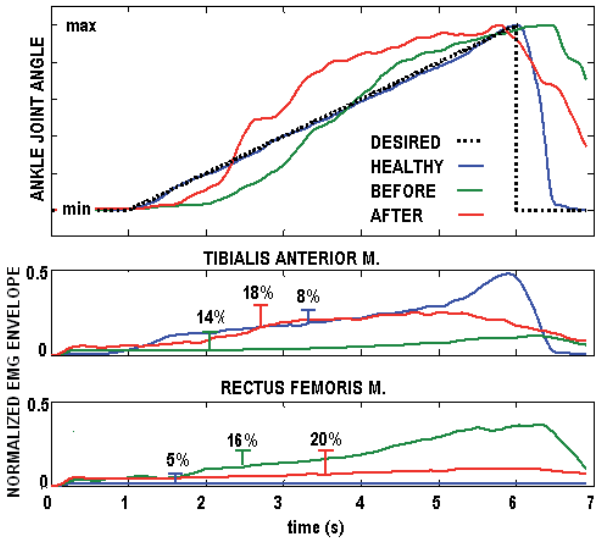


Figure 2: Top panel shows the tracking task: dorsiflexing to the maximum ankle flexion from neutral position. Bottom two panels are normalized and averaged EMG activities for TA and RF for one healthy subject and one patient before and after the FET during the tracking task (percent show EMG variability).

Based on the analysis of the graphs we introduce the median of the normalized EMG envelope as the

level of EMG which divides the area under the EMG envelope in two equal regions. We analyzed the ratio of the medians for patients before and after therapy and median values calculated for each muscle in healthy subjects.

Fig. 3 shows the ratio of averaged median (Rm) for patients before and after the therapy with respect to the values of the healthy individuals. The differences for RF and BF are significantly different before and after therapy, Fig. 3.

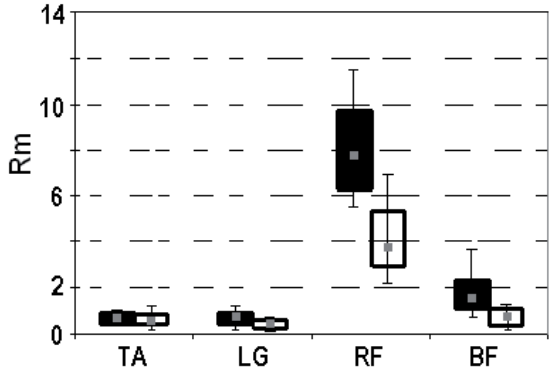


Figure 3: The ratio calculated between the median for subjects before (black) and after (white) the treatment. The ideal Rm value is 1. The values for TA and LG are about 0.9, while the values for the RF and BF are higher.

Discussion

This paper presents an instrument which allows studies of temporal and spatial synergies. The type of results that this instrument provides is illustrated with data collected in a small group of stroke patients who participated in the clinical trial where gait was augmented with electrical stimulation. The synergies analyzed are muscles activation levels during single joint movement which is compromised because of the brain lesion. The movement analyzed was the tracking of the dorsiflexion angle shown on the monitor. The tracking of the target dorsiflexion angle (maximum angle was 9±6 degrees) was delayed compared with the tracking after the therapy where the maximum angles reached values of 18±4, which is almost 80% of the values characterizing healthy subjects (Fig. 2; top panel). Patients before FET had low graduation of TA EMG, and in general low activation of TA in parallel with the high activation of RF, Fig. 2 (bottom panel) which is completely opposite compared with the healthy subjects. Patients after FET had steeper graduation of TA EMG and reached higher activation of TA, in parallel with low activation of RF. This synergy is much closer to the one characteristic for healthy subjects.

The measure of closeness of EMG activities between those recorded in patients and healthy is the Rm. The Rm value was significantly decreased for some muscles, suggesting that control closer to normal was restored (Fig. 3.). This finding could be used for hypothesizing that the recovery of the ability to volitionally control the foot comes from the recalibration and reorganization of cortical activities.

The system presented allows polymyographic and kinematics/dynamics analysis of the movements in the clinical environment. The portability of the system allows also the recordings during free walking for long distances. In this case the feedback needs to be of a different type. The feature of the instrument is the user-friendly software which allows simple selection of the feedback presented to the subjects (e.g. target trajectory, game).

References

[1] Kato H, Izumiyama M, Koizumi H, Takahashi A, Itoyama Y, Near-Infrared Spectroscopic Topography as a Tool to Monitor Motor Reorganization After Hemiparetic Stroke. J American Heart Association, vol. 33: 2032-2036, 2002.

[2] Trompetto C, Assini A, Buccolieri A, Marchese R, Abbruzzese G, Motor recovery following stroke: a transcranial magnetic stimulation study. J Clinical Neurophysiology, vol. 111: 1860-1867, 2000.

[3] Miljković N, Milovanović I, Kojović J, Multi-channel EMG for studying motor control. ETRAN Conference, Vrnjačka Banja, Serbia, vol. 53: ME2.1-ME2.4, 2009.

[4] Kojović J, Đurić-Jovičić M, Došen S, Popović MB, Popović DB, Sensor-driven four-channel stimulation of paretic leg: Functional electrical walking therapy. J Neuroscience Methods, vol. 181: 100-105, 2009.

[5] European concerted action in Biomedical Health and Research Program (BIOMED II): Surface ElectroMyoGraphy for the Non-Invasive Assessment of Muscles – SENIAM, http://www.seniam.org/ (2010)

[6] Burden A, Bartlett R, Normalization of EMG amplitude: an evaluation and comparison of old and new methods. J Medical Engineering and Physics, vol. 21: 247-257, 1999.

Acknowledgements

This work was partly supported by the Fatronik, Serbia.

Author's Address

M. Sc. Nadica Miljković, PhD student
Faculty of Electrical Engineering, Bulevar kralja Aleksandra 73, 11000 Belgrade, Serbia
nadica.miljkovic@etf.rs
http://bmit.etf.rs

Polymyography during hemiplegic walking: Implications for control of FES

Milovanović I[1,2], Djurić-Jovičić M[1,2]

[1] Faculty of Electrical Engineering, University of Belgrade, Serbia

[2] Fatronik Serbia d.o.o, Belgrade, Serbia

Abstract

Clinical practice suggests that intensive walking exercise augmented with functional electrical stimulation (FES) leads to faster and better recovery of walking in hemiplegics. The issue still not resolved is, how to control an FES system to match the needs and capabilities of a stroke patient. We suggest the control based on temporal and spatial synergies which are created by using a block-box model. The input to the black box is the sensors model of gait events, and the output is the set of profiles of muscle activities from the nonparetic leg, acquired from the same patient. In technical terms, we propose the use of an artificial neural network (ANN) for generation of stimulation profiles for FES, and later implementation of sensors driven finite state control for assisting of the walking. This proposal follows our polymyographic studies of walking performance when assisted with a cane and the Walkaround, a device that provides postural control and prevents from falls. The polymyographic analysis revealed substantial differences between the muscle synergies of not only the paretic, but also the nonparetic leg compared to healthy subjects, and strong dependence on assistance used to provide balance while walking. We present here a method how to capture data required for the training of the ANN.

***Keywords**: FES, control, hemiplegia, polymyography.*

Introduction

Providing intensive healthy-like walking training is an important component of rehabilitation of hemiplegic patients [1]. The control of multi-channel electrical stimulation that was designed for assisting of the walking of complete paraplegic patients is not directly applicable, since functional electrical stimulation (FES) in hemiplegic patients operates on muscles that are still partly volitionally controlled; yet, in an altered manner compared to healthy.

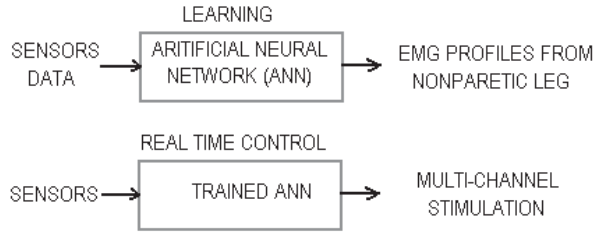


Fig. 1: Sketch of the proposed model of control

The synergistic control that we suggest is based on black-box modeling (Fig. 1), where the inputs are signals from the sensors characterizing the geometry, kinematics and dynamics of the body (system state), and outputs are patterns of muscles activities (actuation) from the nonparetic leg. The procedure comprises off-line training of the artificial neural network (ANN), and use of a determined mapping for real time control of FES. This approach asks for the control to be modified iteratively during training, since the patterns of activities of the nonparetic leg will be changing in parallel with the recovery of walking.

The data presented in this paper are from a hemiplegic patient (56 years of age) in the acute phase of hemiplegia (3 weeks after stroke). The Fugl-Meyer score for lower extremities was 22, patient had no other neurological deficits, and was cognitively ready to follow the instructions. At the time of data collection he could stand on the paretic leg with cane support and ambulate slowly (v = 0.24 m/s) with the cane. The patient signed the informed consent approved by the local ethics committee. It is important to say that single case presentation does not decrease the generality since we propose that in practical applications, control needs to be designed for each subject individually.

Material and Methods

We collected data during two walking modalities: walking assisted by cane (Fig. 2, left panel), and walking assisted with the powered Walkaround® [2] (Fig. 2, right panel). The patient was required to walk along 10-meters long straight-line path. Data from the 8 meters in the middle of the walking event were used for analysis. Both tasks

were repeated several times and typical pattern was considered.



Fig. 2: Experimental set-up: patient walking with a cane (left) and walking supported by the Walkaround (right).

We recorded surface EMG from four muscles of both legs: *Tibialis anterior* (TA), *Gastrocnemius* (GC), *Vastus Lateralis* (VL), and *Biceps Femoris* (BF), We used GS 26 (Bio-Medical Ins.) disposable pre-gelled Ag/AgCl electrodes connected to the Biovision EMG-amplifiers [3] following the procedures suggested in "SENIAM" protocol [4]. We also recorded the ground reaction forces with the insoles instrumented with FSRs [5].

LabView 8.2 software and NI-USB-6212 card connected to Sony Vaio UX Premium Micro PC were used for data acquisition. The sampling rate for EMG signals was 1000 Hz, and 100 Hz for ground reaction forces. The EMG signals were full-wave rectified. Envelope extraction was performed by 4th order low pass Butterworth filter with cut-off frequency 6 Hz.

Results

Figures 2 and 3 show processed normalized EMG signals recorded from the nonparetic and paretic leg of the hemiplegic patient, respectively. EMG patterns during walking assisted with a cane are presented on the left panels and during walking with a Walkaround® on the right panels. Vertical lines show swing/stance transition for the healthy pattern used as the target benchmark, while the swing and stance phases for patient's EMG are shown by horizontal bars.

Muscle activation synergies were quantified by assessing muscle timings and amplitudes. We calculated average muscle amplitude and duration of muscle activity (burst duration) of individual muscles. All parameters were determined on separate WAlking Cycles (WAC). Muscle time parameters were normalized using the walking cycle time, starting from the related heel contact. Normalized EMG was calculated with respect to the maximum EMG, measured for each of the muscles individually at the beginning of the walking session. Maximum EMG was recorded during maximum isometric contraction (MVC) against load.

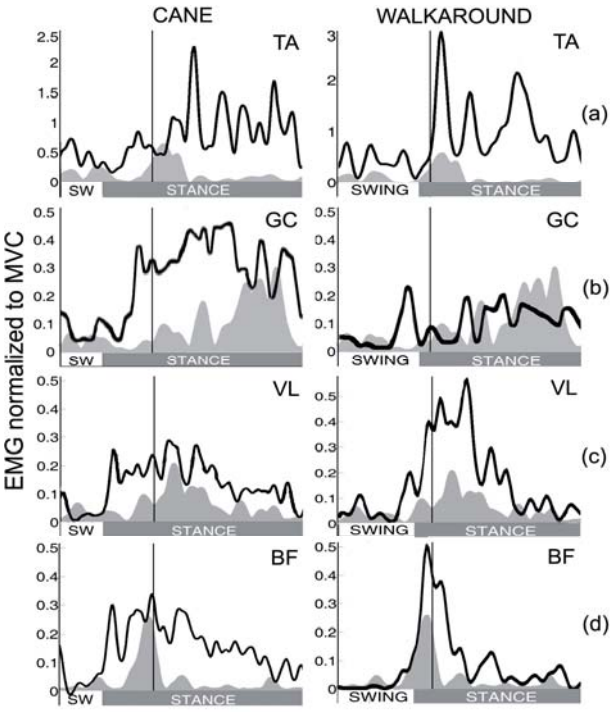


Fig. 3: Normalized EMG patterns for the nonparetic leg (black line) and data from healthy subject (grey area).

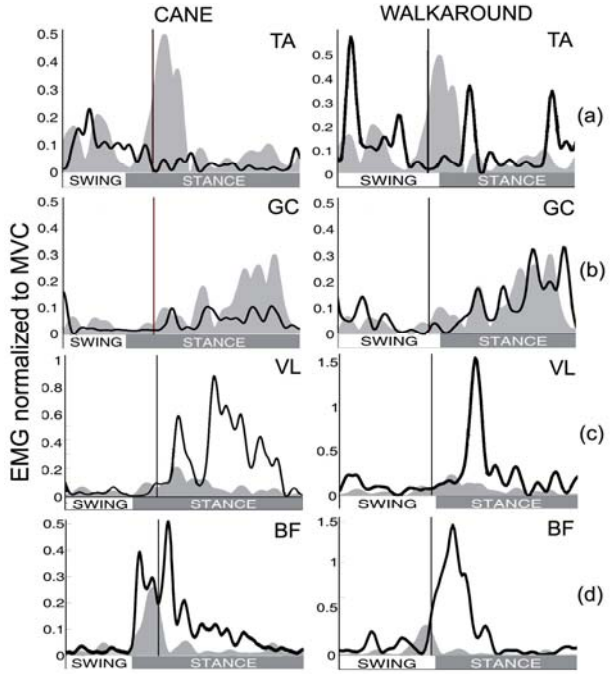


Fig. 4: Normalized EMG patterns for the paretic leg (black line) and data from healthy subject (grey area).

Discussion

When analyzing muscle activities of the nonparetic leg during walking with both assistive devices, we found substantial differences in EMG patterns compared with healthy data (Fig. 3). During walking assisted with a cane, muscle timing parameters indicate prolonged muscle activities of

TA (35% longer), VL and BF (40% and 50% longer, respectively), together with longer TA-GC and VL-BF co-contraction periods (20% and 60% longer, respectively). Walking assisted by the Walkaround® significantly reduced prolonged duration of BF (~ 40%) while TA activity remained abnormal. These atypical synergies in unaffected leg have been reported by others [6, 7], and explained as a compensation for the disturbed control of the paretic leg.

Polymyography of the paretic leg shows the influence of assistive devices on patient's walking and suggests that FES generated synergy should match the type of assistance.

During walking with a cane, as a consequence of inability to dorsiflex the ankle, EMG amplitudes of TA and GC are smaller than normal.

Healthy TA has two major periods of activity, first one during the heel contact, and the second during initial swing (dorsiflexion), which is in accordance with [8]. When walking with a cane, TA muscle activity exists only in a swing phase, while the first period of its activity that stabilizes the foot during loading is missing (Fig. 4a).

As seen in healthy muscle activity of GC (Fig 4b), peak amplitudes constantly increase from mid-stance towards toe-off, where they reach highest values. The highest activity in a toe-off phase is responsible for a body weight push-off provided by GC muscle. However, peak muscle activities of hemiplegic subject walking with a cane reach a plateau early in mid-stance, followed by decrease of peak amplitudes at terminal stance.

BF muscle experiences prolonged duration (34% of WAC) in a stance phase, for about 10% longer than in healthy (around 20%).

In Walkaround®, amplitudes of TA and GC increase up to the levels typical for healthy. TA peak activity during initial heel contact is re-established (Fig. 4a), while GC muscle regains the rise of peak activity at the end of the stance phase (Fig 4b). Activity of BF is shortened to 23% of WAC in healthy.

With both assistive devices, activity of GC muscle resembles the healthy activity, and retains the same pattern when walking with cane and Walkaround®. VL muscle also does not show atypical behavior.

The differences mentioned above point to the need to set the stimulation pattern to the type of assistance. If FES is applied when walking with a cane it is necessary to stimulate TA-GC complex in order to provide leg stabilization during leg loading and sufficient push-off during late stance. This is not the case when walking is assisted by Walkaround®. It is important to notice that when supported by Walkaround®, muscle activities of both legs became closer to healthy pattern, with shorter muscle activities and decreased co-contraction. Better posture alignment and weight bearing in walking with Walkaround® leads to increased stability and less stimulation needed, assessed by EMG.

Conclusions

This study suggests that the design of the strategy of stimulation should be adapted to the type of assistance. The method presented here allows an iterative change of stimulation synergy during the treatment (e.g., once a week). The software that we developed allows this iterative procedure to be used by clinicians.

References

[1] Mazzaro N, Spaich EG, Andersen OK, Grey MJ, Popovic D, Sinkjaer T. Electrical stimulation augmented rehabilitation of hemiparetic gait. 28th IEEE EMBS, New York, 2006.

[2] Veg A, Popovic DB. Walkaround®: mobile balance support for therapy of walking. IEEE Trans Neural Syst Rehabil Eng, 16(3):264-9, 2008.

[3] http://www.biovision.eu/biovision1_en.htm

[4] http://www.seniam.org/

[5] Djurić-Jovičić M, Milovanović I, Jovičić N, Radovanović S. Gait analysis: BUDA vs. GAITRITE. 53rd ETRAN Conference, Vrnjacka Banja, Serbia, 2009.

[6] Hirschberg GC, Nathanson M. Electromyographic recording of muscular activity in normal and spastic gaits. Arch Phys Med Rehabil, 33:217-225, 1952.

[7] Wortis SB, Marks M, Hirschberg GG, Nathanson M. Gait analysis in hemiplegia. Trans Am Neurol Assoc, 76: 181-183, 1951.

[8] Perry J. Gait Analysis, Normal and Pathological Function. Slack Incorporated, NJ, 1992.

Acknowledgements

The work on this project was partly supported by the Ministry of Science and Technology of Serbia.

Author's Address

Milovanović Ivana, PhD student.
University of Belgrade, Faculty of Electrical Engineering, Bulevar kralja Aleksandra 73, Belgrade, Serbia
e-mail: ivana.milovanovic@etf.rs
homepage: http://bmit.etf.rs

Effects of FastFES Gait Training on Mechanical Recovery in Post-Stroke Gait

Hakansson NA[1], Kesar T[2], Reisman D[2], Binder-Macleod S[2], Higginson JS[1]

[1]Department of Mechanical Engineering, University of Delaware, Newark, DE, USA

[2]Department of Physical Therapy, University of Delaware, Newark, DE, USA

Abstract

Stroke leads to gait impairments that can negatively influence quality of life. FES applied during fast walking is an effective gait rehabilitation strategy that can lead to improvements in gait performance, walking speed and endurance, balance, activity, and participation post-stroke. The effect of fast FES gait training on mechanical energy utilization is not well understood. The objective of this study was to test the effects of 12-weeks of FES gait training on mechanical recovery indices of post-stroke gait. Kinematic data were collected from 11 stroke survivors before and after 12-weeks of FES training. Mechanical recovery was calculated from the positive changes in vertical, anterior-posterior, and medial-lateral components of COM energy. The average mechanical recovery increased from 34.5% before training to 40.0% after training. The increase was statistically significant (p=.014). The average self-selected walking speed increased from 0.4m/s to 0.7m/s after the 12-week FES training. The results indicate that the subjects were better able to generate and utilize the external mechanical energy of walking after FES gait training. FES gait training has the capacity to increase the gait speed, improve the mechanical recovery, and reduce the mechanical energy expenditure of stroke survivors when they walk.

Keywords: *FES, stroke, gait, mechanical recovery, training.*

Introduction

Stroke leads to gait impairments such as slowed walking speeds, inter-limb asymmetry, and increased energy consumption [1]. Functional electrical stimulation (FES) applied to the dorsiflexor muscles of stroke survivors is commonly used to address foot-drop, [2] and therefore improve safety, speed, and efficiency of walking [3]. However, FES of the dorsiflexors alone does not address other critical gait deficits such as reduced ankle plantarflexor moment and push-off forces during terminal stance and decreased knee flexion angle during swing. Recent work has shown that delivering FES to multiple muscles during gait, especially to ankle plantarflexors, produces greater immediate improvements in gait compared to the traditional approach of delivering dorsiflexor FES alone [2].

Treadmill training has also recently emerged as an effective gait rehabilitation intervention [4]. Treadmill training at fast speeds can provide several advantages, such as improved cadence and gait symmetry [5]. We developed and tested a novel gait rehabilitation intervention combining functional electrical stimulation (FES) of ankle dorsi- and plantar-flexor muscles and Fast treadmill walking (FastFES). We hypothesized that combining these 2 independent interventions would enable us to correct multiple post-stroke gait impairments (decreased forward propulsion, decreased swing phase knee flexion, decreased trailing limb angle, and footdrop), and thereby produce maximal improvements in walking speed and endurance. The preliminary results show that 12-weeks of FastFES gait training results in improvements in gait performance, walking speed and endurance, balance, activity, and participation post-stroke.

The mechanical recovery index (R) is a measure of the mechanical energy exchange that is preserved through the pendulum-like motion of the whole-body center of mass (COM) during gait [6]. It can provide insights into the effects of FastFES training on post-stroke gait mechanics and energetics, and therefore, help us to understand the mechanisms underlying the FastFES intervention. The objective of this study, therefore, was to test the effects of 12-weeks of FastFES gait training on mechanical recovery indices of post-stroke gait.

Material and Methods

Subjects

Eleven chronic stroke subjects participated in this study. All subjects received medical clearance from their physicians to participate in gait training and gave informed consent to participate in the study which was approved by the University of Delaware Human Subjects Review Board. All subjects could walk for at least 5 minutes continuously at their self-selected speed.

Training

Each subject participated in 12-weeks (3 sessions/week) of gait training. Training sessions comprised five 6-minute bouts of walking with ~5-minute rest breaks between bouts (~30-minutes of

fast walking each session). Training sessions comprised walking practice with and without FES, and also included overground walking. Training speeds were based on participant's maximal walking speed, and progressed every 4 weeks.

FES During Training

During training, FES was delivered using surface electrical stimulation electrodes to the dorsiflexor and plantarflexor muscles. A Grass S8800 stimulator and SIU8TB stimulus isolation unit (Grass Instrument Co, Quincy, MA) delivered the stimulation (30-Hz trains, pulse duration of 300µs, 300ms long). Electrical stimulation timing was controlled using a custom-built real-time controller using input from two compression-controlled footswitches attached to the sole of the forefoot and hindfoot of the subjects' shoes. DF stimulation was applied from when the forefoot switch left the ground until the hindfoot switch contacted the ground (paretic swing phase). PF stimulation was applied from when the hindfoot switch left the ground until the forefoot switch left the ground (paretic terminal stance) [2, 7].

Gait Analysis

Data were collected before and after 12-weeks of training. An 8-camera motion analysis system (Vicon 5.2, Oxford, England) recorded (100 Hz) the positions of 41 retroreflective markers placed on the bony landmarks of the foot, shank, thigh, pelvis, and trunk of the subjects as they walked on an instrumented treadmill (AMTI, Watertown, MA) at their self-selected speed.

Body segment masses were determined from anthropometric data [8] and COM positions were calculated from marker position data using Visual 3D (C-Motion, Rockville, MD). COM positions were low-pass filtered at 6Hz. Segment velocities and accelerations were calculated by taking derivatives of the limb COM positions relative to the whole-body COM and used to calculate segment kinetic and potential energies [6].

Mechanical Recovery

Mechanical recovery was calculated to assess the energy exchange between the vertical, anterior-posterior and medial-lateral directions of the whole-body COM during gait [6, 9]. Mechanical recovery (R) was calculated as:

$$R = \frac{W_v + W_{ap} + W_{ml} - W_{ext}}{W_v + W_{ap} + W_{ml}} * 100\%$$

where W_v, W_{ap}, and W_{ml} are the vertical, anterior-posterior, and medial-lateral components of the whole body external work, W_{ext}, respectively. W_v, W_{ap}, and W_{ml} were calculated by summing the positive changes in vertical, anterior-posterior, and medial-lateral components of energy, respectively, averaged over eight consecutive gait cycles. To account for inter-trial and inter-subject differences, the whole body external work measures were normalized to subject body mass (kg) and distance walked (m).

Data Analysis

Paired-sample t-tests were performed to identify differences between pre-training and post-training average mechanical recovery. Significance was set at $p<0.05$.

Results

The average mechanical recovery across subjects prior to FES training was 34.5% (range 18.4 to 52.9%). After the 12-week FES training, the average mechanical recovery across subjects was 40.0% (range 30.0 to 58.8%). Mechanical recovery increased as a result of FastFES training in all but one subject (Fig. 1). The mechanical recovery levels after FastFES training were significantly higher than the pre-training levels (p = 0.014). Overall mechanical recovery was low relative to healthy adults walking at self-selected or slow speeds [6].

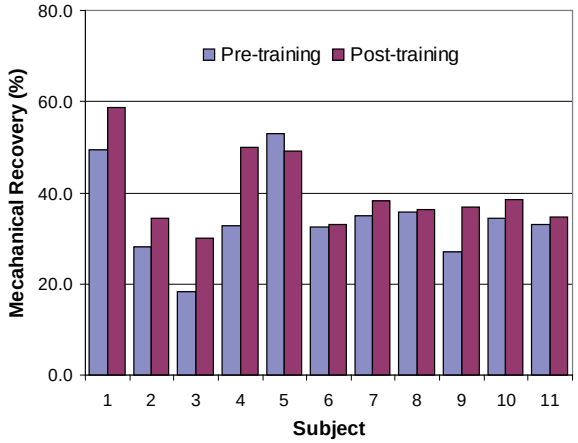


Fig. 1 Mechanical recovery over eight gait cycles for each of the subjects as they walked prior to and after 12 weeks of FastFES training.

Self-selected walking speeds increased for all subjects following FES training. The average self-selected walking speed prior to training was 0.4m/s (range 0.3 to 0.7m/s) and after the training period was 0.7m/s (range 0.4 to 1.0m/s).

Discussion

One important finding of this study was that FastFES gait training resulted in a significant increase in mechanical recovery. Another finding was that self-selected speed increased after 12

weeks of FastFES gait training. Both of these outcomes provide functional benefits for stroke survivors.

It is known that an increase in the walking speed of slow walking stroke survivors is one method to improve mechanical recovery [9]. The change in self-selected walking speed had a confounding effect on the results. The mechanical energy of the COM is directly related to the kinetic energy, and thereby speed, in the anterior-posterior direction, i.e. $\frac{1}{2}mv^2$. Additionally, mechanical recovery exhibits a parabolic relationship with walking speed [6]. Therefore, with increasing speed, some post-stroke individuals may better utilize the mechanical energy exchanges associated with the pendulum-like motion of the body COM. Because we evaluated the subjects at their present self-selected walking speeds, which improved with the training, we cannot determine if the observed improvements would have occurred independent of changes in each subject's walking speeds. However, because increased mechanical recovery and walking speed are meaningful benefits for stroke survivors, we believe this study and its results are meritorious.

The result that mechanical recovery and speed improved after FastFES training indicates that the subjects were better able to generate and utilize the external mechanical energy of walking. This finding implies that the training improved the subjects' ability use the plantarflexors to accelerate the COM vertically up and forward over the base of support. Improved utilization of the plantarflexors in late stance would lead to higher gait speeds, which are associated with increased energy efficiency [10] and mechanical recovery [9] in post-stroke gait.

The observed increased in gait mechanical recovery and speed support the possibility that FastFES training may prolong the beneficial immediate effects of FES applied to the dorsiflexor and plantarflexor muscles, i.e. greater swing-phase knee flexion, greater ankle plantarflexion angle at toe-off, and greater forward propulsion [2]. In turn, prolonged training with FastFES may enable the subjects to learn to adjust their muscle activity patterns so as to gain further improvements in mechanical efficiency.

Conclusions

This study demonstrated that FastFES training has the capacity to increase the gait speed and improve the mechanical recovery of stroke survivors when they walk.

References

[1] P. Zamparo, M. P. Francescato, G. Luca *et al.*, "The energy cost of level walking in patients with hemiplegia," *Scandinavian Journal of Medicine & Science in Sports,* vol. 5, no. 6, pp. 348-352, 1995.

[2] T. M. Kesar, R. Perumal, D. S. Reisman *et al.*, "Functional electrical stimulation of ankle plantarflexor and dorsiflexor muscles: Effects on poststroke gait," *Stroke,* vol. 40, no. 12, pp. 3821-3827, 2009.

[3] P. N. Taylor, J. H. Burridge, A. L. Dunkerley *et al.*, "Clinical use of the Odstock dropped foot stimulator: Its effect on the speed and effort of walking," *Archives of Physical Medicine and Rehabilitation,* vol. 80, no. 12, pp. 1577-1583, 1999.

[4] R. Dickstein, "Rehabilitation of gait speed after stroke: A critical review of intervention approaches," *Neurorehabil Neural Repair,* vol. 22, no. 6, pp. 649-660, 2008.

[5] M. Pohl, J. Mehrholz, C. Ritschel *et al.*, "Speed-dependent treadmill training in ambulatory hemiparetic stroke patients: A randomized controlled trial," *Stroke,* vol. 33, no. 2, pp. 553-558, 2002.

[6] G. A. Cavagna, H. Thys, and A. Zamboni, "The sources of external work in level walking and running," *The Journal of Physiology,* vol. 262, no. 3, pp. 639-657, 1976.

[7] T. M. Kesar, R. Perumal, A. Jancosko *et al.*, "Novel patterns of functional electrical stimulation have an immediate effect on dorsiflexor muscle function during gait for people poststroke," *Physical Therapy;* vol. 90, no. 1, pp. 55-66, 2010.

[8] D. A. Winter, *Biomechanics and Motor Control of Human Movement*, 4th ed. ed., Hoboken: Wiley, 2009.

[9] C. Detrembleur, F. Dierick, G. Stoquart *et al.*, "Energy cost, mechanical work, and efficiency of hemiparetic walking," *Gait & Posture,* vol. 18, no. 2, pp. 47-55, 2003.

[10] D. S. Reisman, K. S. Rudolph, and W. B. Farquhar, "Influence of speed on walking economy poststroke," *Neurorehabil Neural Repair,* vol. 23, no. 6, pp. 529-534, 2009.

Acknowledgements

The authors are grateful to Ben Roewer for his help with Visual 3D. This study was funded by NIH NS 055383 and NIH NR 010786.

Author's Address

Nils Hakansson
Center for Biomedical Engineering Research
University of Delaware
nilsh@udel.edu
http://research.me.udel.edu/higginson/index.html

Perspectives of Peripheral Functional Magnetic Stimulation in the Rehabilitation of Central Pareses

Szecsi J[1], Götz S[2], Straube A[1].

[1]Center for Sensorimotor Research, Ludwig Maximilians University, Munich, Germany

[2]Technische Universität, Munich, Germany

Abstract

Using functional magnetic stimulation (FMS) of the musculature, which is largely supposed to be 'painless', for rehabilitation of patients with partially preserved sensation to support mechanically constrained movements is in principle possible and potentially superior to surface electrical stimulation (FES).
The goal of the project was to develop a procedure and technical means consisting of 1. the mechanical constraint and 2. the peripheral magnetic stimulation supporting the movement. The potential of the magnetic stimulation, originally provided for diagnostic transcranial application, had to be further developed to be used in neurological rehabilitation of central pareses. We report the clinical and technical results.
The optimization steps that we undertook or which are under examination comprise the optimization of the stimulation waveform, the adaptation of the stimulation coil to the requirements of muscle stimulation by increasing the stimulation surface and fitting the geometry of the coil to the shape of the thigh, as well as the adoption of active cooling to assure the required operating time at an effective power level.
In particular, applying large surface coils in patients with incomplete paralysis of the musculature ensures a 2.5-fold increase of the isometric force evoked, compared to FES, an essential requirement for implementation of effective rehabilitative strategies.

***Keywords**: peripheral functional magnetic stimulation, muscle, torque, pain, paresis, cycling.*

Introduction

Most of the literature on functional electrical stimulation (FES) propelled cycling focuses on patients with complete spinal cord injury (SCI), although the population with incomplete paralysis (due to stroke, multiple sclerosis, etc.) by far exceeds the complete SCI population. It is thought that electrical stimulation can also be used in the latter case to achieve mobility (walking or cycling) or for training purposes (ergometry).

However FES cannot be applied in patients with paralysis or paresis, who have at least partially preserved sensation (e.g. due to stroke or multiple sclerosis, MS), at higher stimulation intensities, which are necessary to achieve effective training, because surface stimulation also activates pain receptors located in the skin.

In contrast, by using time-varying electromagnetic fields to induce eddy currents which penetrate the tissue mainly tangentially, repetitive FMS activates the nerve innervating the muscle while only minimally stimulating the skin nociceptors[1].

However, comparing FMS with FES, magnetic stimulators are bulky and more expensive, and they overheat at frequencies used to achieve tetanic contraction. As FMS is more diffuse than FES, it seems to be ideally suited for stimulation producing force (see below) of the large thigh musculature. For the stimulation of small muscles like those of the arm or hand, FES seems to be more suitable.

The goal of the present study is to investigate whether FMS is a superior and 'more painless' alternative to FES under realistic training setups in functional rehabilitation of patients. Here we report an excerpt of the project results.

Material and Methods

As commercially available magnetic stimulators and coils could not achieve sufficient torque to exceed FES, several technical alternatives were considered: increasing discharge energy appeared to be costly and perhaps painful. The optimization of the pulse-shape by varying the number of phases showed inconclusive results. Fitting the geometry of the coil and increasing its stimulation surface was the option we adopted and realized.

Experimental Setup

Therefore torque and pain induced by quadriceps stimulation in 13 subjects with preserved sensation (with chronic progressive multiple sclerosis, MS) were investigated under the following conditions: 1. small vs. large stimulated surfaces of the thigh, 2. varying contraction velocities of the muscle (isometric vs. 15 and 30 rpm isokinetic conditions), and 3. different stimulation modalities: FMS vs. FES. In addition, the role of the placement of the round coil during magnetic stimulation was investigated in 29 subjects with MS.

Measurements

A stationary tricycle equipped with a torque transducer, an incremental encoder and a motorized brake served as the testbed for isometric and isokinetic experiments(Fig. 1). Magnetic (Mag & More GmbH, Germany) and electrical stimulation (Krauth & Timmermann, GmbH, Germany) of the quadriceps muscle controlled by a PC, was possible in a sequential or synchronous manner.

To compare FMS vs. FES measurements the electrodes were first placed on the skin, and the coil was fastened over the electrodes. To investi-



Fig. 1. FMS of the legs in a patient with MS

gate the dependency on the stimulated surface, 4 setups were considered (Fig. 3): FES with small and normal separation electrodes and FMS with a round and a specially manufactured saddle coil (Fig. 2). Thirty randomized stimulation intensities (in the range of 0 to the maximum tolerable amplitudes for that subject and setup) were applied each for FMS and FES. The muscle was alternately stimulated magnetically and electrically (using therefore 2 x 30 bursts at 30 Hz) both in isometric and ergometric situations. Subjects were instructed to estimate their pain or discomfort verbally using a 0-10 scale. During isometric measurements the leg was fixed at 120° crank angle (0° defined by the left, horizontal, backward-pointing crank arm) and during isokinetic experiments the crank was turned by the motor at 15 and 30 rpm. For statistical comparisons Friedmann's nonparametric analysis of variance was used over the four setup conditions.

Technical results

A large-surface, saddle-shaped coil was manufactured (31 x 24 cm) with an inner

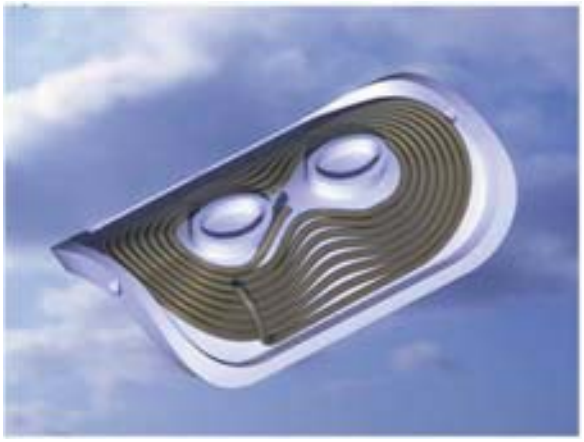


Fig. 2. The saddle-shaped coil with support prepared for active cooling.

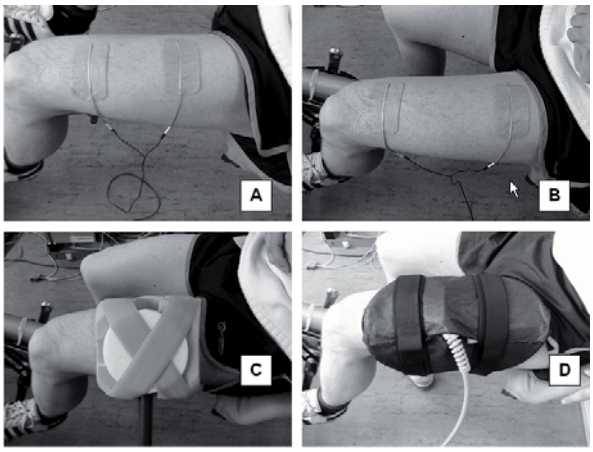


Fig 3. Setups: short(A), normal(B) electrode-distance FES, round-(C) and saddle(D)-coil FMS

cylindrical surface and an aperture angle of 140°. An actively cooled saddle coil(Fig.2) is also available to assure meaningful training times (Table 1).

Clinical results

In persons with preserved sensibility, torque and pain significantly depended on the amount of stimulated surface during FMS, on the muscle contraction velocity during FES and FMS, on the stimulation location during FMS, and on the stimulation modality (FMS vs. FES)[2]. In particular, FMS with a saddle-shaped coil produced more torque ($p < 0.05$, see Fig. 4) and less pain than standard FES ($p < 0.05$).

Further investigations[2] showed that maximal efficacy of stimulation can be achieved in a specific location of the round coil, a proximal ventral lateral position. That means, the coil has to be tilted at 45° in relation to the frontal plane.

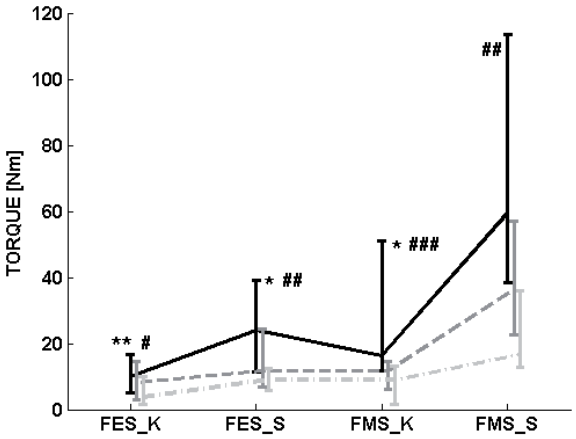


Fig. 4. Dependency of torque in subjects with MS on stimulation modality (FES vs FMS), the amount of stimulated surface (small vs large), and kinematics (isometric (black) vs isokinetic (grey)). FES_K: FES with small separation electrodes, FES_S: FES with standard-separation electrodes, FMS_K: FMS with round coil, FMS_S: FMS with saddle coil. Asterisks: significant differences between, on the one hand, FMS_S and, on the other, FES_K, FES_S and FMS_K under all kinematic conditions (isometric, 15 and 30 rpm) : ** $p < 0.001$; *$p < 0.05$. Hatches: significant differences between isometric and 30 rpm conditions: # $p<0.05$; ## $p <0.02$; ### $p < 0.005$ [2].

The finding could be explained by the fact that more muscle mass will be penetrated in the oblique than in the frontal plane position of the coil, that means more volume-current will be induced in the excitable tissue.

Discussion

Whether the achieved technical possibilities can satisfy the *therapeutic needs* of the rehabilitation of patients with partial pareses is the object of current investigation. It must be emphasized that hardly any dose-response relationships are actually known in rehabilitation yet. Nevertheless empirical data collected during cycle-training supported by stimulation in paresis showed that a varying amount of preserved sensation can be invoked. Therefore training protocols are dependent on the disease causing the paresis, the mobility of the patient and the exhaustion state of the patient (Table 1.). Comparing current technical limitations, especially the thermal conditions of the coil and the power supply lines with the needs of effective therapeutic outcome (Table. 1) shows that training protocols for patients with preserved sensation (stroke, MS) can indeed be performed successfully.

Etiology	Training duration	Intensity	Frequency
Complete or incomplete SCI	20 min – 1 h	50-100%	20-30 Hz
Chronic progressive MS	3 x 2 min oder 3 x 5 min	40-70%	20-30 Hz
Subacute stroke	3 x 5 min	40-70%	20-30 Hz
Chronic stroke	20 min	40-70%	20-30 Hz

Table 1: Proposed training-protocols with FMS

Conclusions

The combined therapeutic system will presumably allow training durations of 20 minutes at the required power to be achieved. This seems to represent a general limitation of functional magnetic stimulation, which is suitable for patients with at least partial preserved sensation. In patients with complete loss of sensation, due to the higher operating expense, electrical stimulation is the method of choice still [3].

References

[1] Saypol JM, Roth BJ, Cohen LG, Hallett M. A theoretical comparison of electric and magnetic stimulation of the brain. Annals of biomedical engineering. 1991;19(3):317-28.

[2] Szecsi J, Gotz S, Pollmann W, Straube A. Force-pain relationship in functional magnetic and electrical stimulation of subjects with paresis and preserved sensation. Clin Neurophysiol. 2010 Apr 9;doi: 10.1016/j.clinph.2010.03.023, in press.

[3] Szecsi J, Schiller M, Straube A, Gerling D. A comparison of functional electrical and magnetic stimulation for propelled cycling of paretic patients. Archives of physical medicine and rehabilitation. 2009 Apr;90(4):564-70.

Acknowledgements

The project “Functional peripheral magnetic stimulation FMS for rehabilitation of patients with central pareses” was funded by the German Federal Ministry of Education and Research (Grant No. 01 EZ 0756)

Author’s Address

Johann Szecsi, MD, e-mail: jszecsi@nefo.med.uni-muenchen.de

The time dependence of oxygen uptake and evoked torque during prolonged isometric sub-tetanic NMES.

Minogue CM[2], Crowe LM[1], Caulfield BM[1], Lowery MM[2].

[1] School of Physiotherapy & Performance Science University College Dublin, Ireland

[2] School of Electrical, Electronic and Mechanical Engineering, University College Dublin, Ireland

Abstract

The purpose of this study was to examine the time course of whole body oxygen uptake and evoked knee torque during a 30-minute session of sub-tetanic isometric neuromuscular electrical stimulation (NMES) of the quadriceps muscles. Five subjects were tested while positioned in a dynamometer which was set up for continuous recording of extensor torque at 60° knee flexion, with simultaneous measurement of respiratory gas volumes using a breath-by-breath analysis system. NMES was applied bilaterally with one pair of large hydrogel electrodes per leg, using a stimulation frequency of 4Hz, phase duration 600μS and a mean current amplitude of 92mA. The oxygen uptake increased over the first 6 minutes to a mean value which was 3.5 (1.0) times the resting level, thereafter stabilizing and gradually reducing at a mean rate of -0.045 (0.051) ml sec^{-1}. This was mirrored by a gradual reduction in output torque over the same period.

Keywords: *NMES, oxygen uptake, fatigue.*

Introduction

NMES-induced isometric exercise has not generally been associated with a significant steady-state aerobic energy component and has therefore not become established as a means of delivering cardiovascular exercise to patients unable to move voluntarily. Although it has been shown that NMES is energetically more costly than voluntary exercise of the same work output, this effect is short lived and the rate of energy conversion cannot be sustained.[1]. Fatigue is a well-known feature of NMES with many contributory factors, one of which is the unphysiological nature of synchronous re-stimulation of the same motor unit pool. NMES is also thought to preferentially select type II motor units, which have less oxidative capacity, and the high stimulation frequency often used can fatigue the neurotransmission process[2].

Low frequency sub-tetanic NMES has been shown to elicit therapeutically significant levels of oxygen uptake ($\dot{V}O_2$) which are sustainable for an hour or more.[3, 4]. There is some reduction in the oxygen consumption rate over time however the actual rate of fatigue has not been assessed to date. The purpose of the present study was to assess the change in $\dot{V}O_2$ and evoked knee torque during a 30 minute session of constant intensity NMES at 4Hz.

Material and Methods

Five healthy male subjects, mean (SD) age 41.2 (10.3), body mass 71.4 (11.7) kg, participated in this study. All subjects provided written informed consent and the data was collected in accordance with a protocol approved by the Ethics Committee of University College, Dublin.

Subjects were positioned in a Cybex dynamometer which was set up for measurement of isometric knee torque of the right leg at 60° knee flexion. The left leg was also restrained isometrically at the same knee angle. The torque signal from the dynamometer was continuously recorded in a data acquisition system (Biopac) at a sampling rate of 200Hz. Two large (12cm x 16cm) hydrogel stimulation electrodes (Axelgaard, Fallbrook, USA) were applied to the quadriceps of each leg and connected to a research stimulator, NT2010, (Biomedical Research, Galway, Ireland), which was programmed to produce a constant current, continuous, symmetric biphasic 4 Hz pulse train up to 200mA peak, with a phase duration of 600μS and an interphase interval of 100μS. The subject was fitted with a face mask connected to a pulmonary gas exchange analysis system, (Quark, Cosmed Italy), which allowed breath-by-breath estimation of oxygen consumed and carbon-dioxide produced. After at least 5 minutes quiet breathing to establish the subject's basal metabolic

rate the stimulation was started. The intensity level selected for each subject had been determined in a previous related experiment as the highest level they were prepared to tolerate indefinitely. This ranged from 84 to 100mA, with a mean level of 92mA. From the torque record, the peak torque per impulse was plotted over time and the torque-time-integral, accumulated over each 10s period, was also calculated. The respiratory exchange ratio, which is the molar volume ratio CO_2:O_2, was also calculated and plotted over time.

Results

The group mean resting $\dot{V}O_2$ rate was 253 (35) ml min^{-1}. The results for a typical sample subject are compiled in Figure 1, and a compilation of the additional $\dot{V}O_2$ uptake and torque-time-integral for all 5 subjects are shown in figure 2.

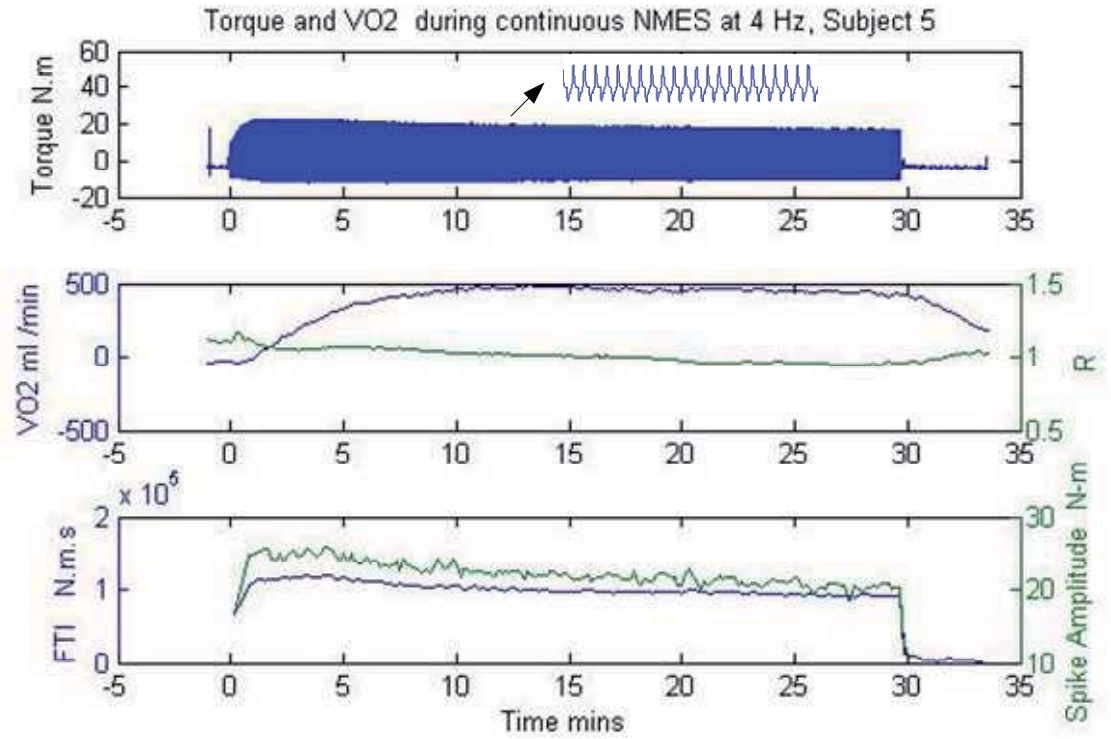


Figure 1. Torque and Respiratory gas record during 30 minutes of NMES at 4Hz for a typical subject. Top: Torque output, with insert expanding to view individual torque impulses. Middle: additional $\dot{V}O_2$ over resting level (left axis) and Respiratory Exchange Ratio R. Bottom: Force Time Integral (left axis) and Spike Amplitude.

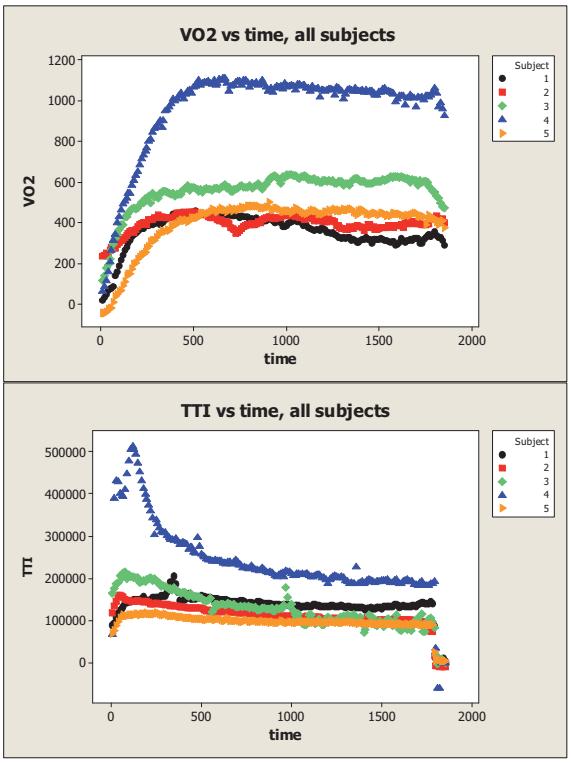


Figure 2. Compilation of individual plots for $\dot{V}O_2$ (top) and Torque Time Integral (bottom) for all 5 subjects.

The mean oxygen consumed at 500s was 878 (279) ml $min^{-1,}$, which corresponds to a multiple of 3.5 (1.0) on the resting rate. Visual inspection of the fatigue curves suggested that, after an initial transient period of approximately 500s, the changes could be modelled by a straight line. The slopes were estimated by linear least squares regression for each subject. The group mean slope for $\dot{V}O_2$ and FTI was -0.045 (0.051) ml sec^{-1} and -0.004 (0.009), N.m respectively. In general, the respiratory exchange ratio R increased rapidly from resting levels indicative of lipid oxidation, to exceed unity briefly, thereafter gradually declined without recovering resting levels.

Discussion.

The principal considerations in designing an aerobic exercise programme based on NMES are the magnitude and the sustainability of the stimulated oxygen uptake during the exercise session. These measurements suggest that isometric stimulation of the quadriceps muscle at 4 Hz produces a significant increase in oxygen uptake that is sustainable, with relatively low declines in both $\dot{V}O_2$ and torque output during a 30 minute session. The slope of the $\dot{V}O_2$ curve suggests that on average the output at 30 minutes will have declined by only 9 % compared to its peak, with a corresponding low level of torque fatigue. This contrasts with torque reductions of at least 40% which have been found using NMES at higher frequencies[5]. The absolute $\dot{V}O_2$ levels during higher frequency stimulation have been generally found to be low [6] , and so the issue of $\dot{V}O_2$ sustainability is moot.

The present study is limited by the small sample size and the fact that only one frequency and one stimulation intensity per subject was used.

[1] M. Vanderthommen, S. Duteil, C. Wary, J. S. Raynaud, A. Leroy-Willig, J. M. Crielaard, and P. G. Carlier, "A comparison of voluntary and electrically induced contractions by interleaved 1H- and 31P-NMRS in humans," *J Appl Physiol,* vol. 94, pp. 1012-24, Mar 2003.

[2] B. Bigland-Ritchie, D. A. Jones, and J. J. Woods, "Excitation frequency and muscle fatigue: electrical responses during human voluntary and stimulated contractions," *Exp Neurol,* vol. 64, pp. 414-27, May 1979.

[3] P. Banerjee, B. Caulfield, L. Crowe, and A. Clark, "Prolonged electrical muscle stimulation exercise improves strength and aerobic capacity in healthy sedentary adults," *J Appl Physiol,* vol. 99, pp. 2307-11, Dec 2005.

[4] P. Banerjee, B. Caulfield, L. Crowe, and A. L. Clark, "Prolonged Electrical Muscle Stimulation Exercise Improves Strength, Peak VO2, and Exercise Capacity in Patients With Stable Chronic Heart Failure," *Journal of Cardiac Failure,* vol. 15, pp. 319-326, 2009.

[5] J. Ding, A. S. Wexler, and S. A. Binder-Macleod, "A predictive fatigue model--I: Predicting the effect of stimulation frequency and pattern on fatigue," *IEEE Trans Neural Syst Rehabil Eng,* vol. 10, pp. 48-58, Mar 2002.

[6] J. Theurel, R. Lepers, L. Pardon, and N. A. Maffiuletti, "Differences in cardiorespiratory and neuromuscular responses between voluntary and stimulated contractions of the quadriceps femoris muscle," *Respir Physiol Neurobiol,* Dec 15 2006.

Correspondence: minogue@bmr.ie

Activation threshold and contraction dynamics of quadriceps femoris heads measured with ultrasound imaging: a pilot study

Krenn M[1], Kneisz L[1], Hanc C[1,2], Rafolt D[1], Bijak M[1], Ciupa RV[2], Mayr W[1], Kollmann C[1]

[1] Center for Medical Physics and Biomedical Engineering, Medical University of Vienna, Austria
[2] Department of Electrical Engineering, Technical University of Cluj-Napoca, Romania

Abstract

The assessment of muscle properties is of great interest for diagnosis of neuromuscular diseases. Ultrasound imaging can be used for analysis of muscle tissue dynamics in clinical practice. We examine the quadriceps femoris heads with different selective electrical stimulation settings. Therefore, electrodes are placed on the motor points of vastus lateralis, vastus medialis and rectus femoris. The femoral nerve is stimulated transcutaneous to activate the vastus intermedius.

Initially the amplitude of the biphasic, rectangular stimulation impulse was increased until the activation threshold of each electrode setup was reached afterwards it was further increased in 5V steps to measure the contraction dynamics of the isometric twitches. The ultrasound measurements of the pilot study show that the vastus intermedius and the rectus femoris are stimulated selective with the different stimulation setups. Selective electrical stimulation and activation patterns are verified with measurements of the evoked myoelectric signal, twitch force and the muscle vibration. This study provides an insight on the behavior of muscle and potential mechanisms of muscle contractions.

Keywords: *m. quadriceps femoris, muscle ultrasound, myoelectric signal, neuromuscular monitoring.*

Introduction

Clinical imaging techniques have become an important tool for muscle assessment. Ultrasound is a particularly promising tool in this regard [1]. One of the advantages of ultrasound is that it is real-time, allowing movement to be imaged.

In [2] a method is described to measure the electromechanical delay of the vastus medialis obliquus and vastus lateralis. In that case the ultrasound image is synchronized with the stimulations impulse. During voluntary contraction the onset time of activation is measured with tissue Doppler imaging (TDI). TDI includes information about velocities of tissue motion [3].

In this study we examine the quadriceps femoris heads with different selective electrical stimulation settings. The main interest was to examine deeper layers of the anterior thigh during electrical stimulation and compare these results with superficial muscle layers.

Material and Methods

Transcutaneous electrically evoked contractions were induced by using two different electrode setups. First, self-adhesive stimulation electrodes (ø 3.2cm) were placed on the motor points of each head of the quadriceps. The counter electrode (10x13cm) was attached to the posterior thigh. Second, the femoral nerve was stimulated

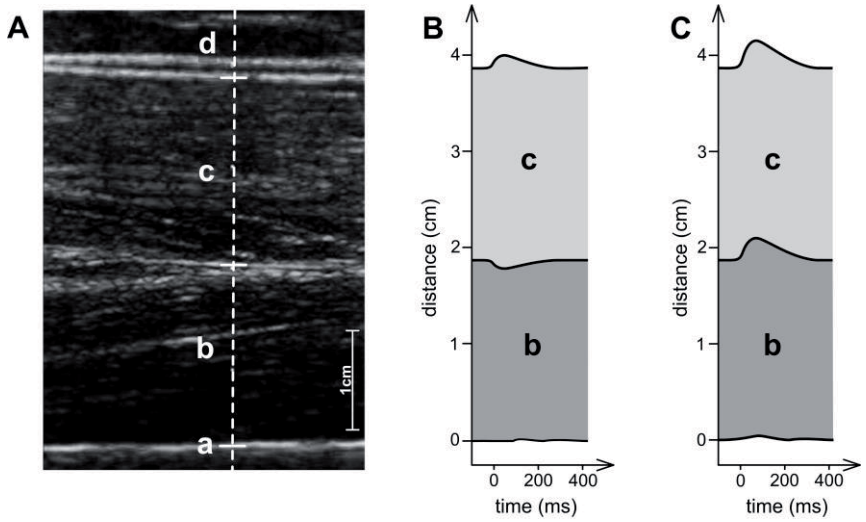


Fig. 1: Longitudinal B-mode ultrasound image of the anterior thigh (A); schematic plots of M-mode images are shown on the right side with different stimulation setups - motor point stimulation of rectus femoris (B) and transcutaneous stimulation of the femoral nerve (C).

a ... femur bone
b ... vastus intermedius
c ... rectus femoris
d ... subcutaneous tissue

transcutaneously using a bipolar electrode. The amplitude of twitch impulse was increased until the activation threshold was obtained and then it was further increased in 5V steps until 29V

A diagnostic ultrasonic device was used with a high frequency linear array probe (7.5MHz). The focus was set on the line between to muscle heads. A gel pad was used to minimize the contact pressure onto the muscle. The longitudinal plane of muscle structure was displayed in B-mode (a two-dimensional diagnostic image of echo-producing interfaces) or M-mode (motion mode; a plot of the tissue structure along a single axis vs. time). Myoelectric signals of the superficial muscles were recorded with surface electrodes. The surface muscle motion was detected with 3-axial accelerometers (LIS3L02 STMicroelectronics, Geneva CH) on each head of the quadriceps. The amplifiers were designed in-house and for the digitalisation a data acquisition card (NI USB-6218, National Instruments Corporation, Austin TX, USA) was used.

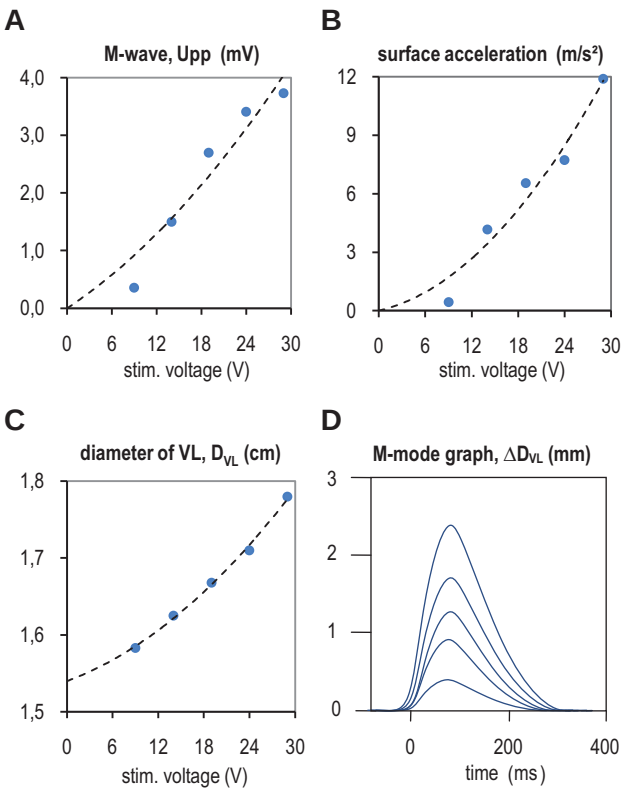


Fig. 2: Electromechanical measurements during motor point stimulation of vastus lateralis (VL) with different stimulation amplitudes; peak-to-peak amplitude of evoked myoelectric signal (A) and peak value of surface acceleration which detects the muscle contraction (B) – both measurements are performed on the muscle belly of VL; maximum muscle diameter during contraction (C); schematic M-mode graphs of the diameter changes of vastus lateralis diameter (D_{VL}) – measured with increasing stimulation amplitudes (D).

Results

The B-mode ultrasound images rectus femoris (RF) and vastus intermedius (VI) are shown in Fig. 1A in longitudinal plane. The fibroadipose septa of the perimysium that surrounds muscle fascicles is seen in this ultrasound image [1]. The schematic M-mode images show the different activation pattern. During RF motor point stimulation (Fig. 1B) only the superficial muscle layer is activated, whereas during stimulation of the femoral nerve (Fig. 1C) both muscle heads are contracted.

Fig. 2 shows electromechanical measurements during electrical stimulation of the motor point of vastus lateralis (VL). The ultrasound image shows the diameter of VL (D_{VL}). Dynamic changes of D_{VL} are observed in the M-mode image (Fig. 1D). All measurements show a similar trend with the increase of the stimulation amplitude from 9V to 29V.

Conclusions

The pilot study shows that ultrasound imaging can provide easy accessible data of dynamic and structural muscle properties. Modern ultrasound devices are providing real-time motion analysis of image points (spackle tracking) which gives accurate data and high time resolution.

The dynamic muscle properties of the quadriceps heads can be studied with these electrode setups of selective motor point stimulation and transcutaneous femoral nerve stimulation.

References

[1] Walker FO, Cartwright MS, Wiesler ER *et al.*, Ultrasound of nerve and muscle, Clin Neurophysiol, 115(3):495-507, 2004.

[2] Chen HY, Liau JJ, Wang CL *et al.*, A novel method for measuring electromechanical delay of the vastus medialis obliquus and vastus lateralis, Ultrasound Med Biol, 35(1):14-20, 2009.

[3] Pulkovski N, Schenk P, Maffiuletti NA *et al.*, Tissue Doppler imaging for detecting onset of muscle activity, Muscle Nerve, 37(5):638-649, 2008.

Acknowledgements

This work was supported by the European Union, EU-Intereg IVa 2008-2013: N00033

Author's Address

Matthias Krenn
Medical University of Vienna
Center for Medical Physics and Biomedical Engineering
matthias.krenn@meduniwien.ac.at
www.zmpbmt.meduniwien.ac.at

BRAIN ACTIVATION DURING ACTIVE, PASSIVE AND FES-INDUCED MOVEMENTS: A FEASIBILITY fMRI STUDY

Gandolla M[1], Casellato C[1], Ferrante S[1], Ferrigno G[1], Baselli G[1], Molteni F[2], Martegani A[2], Frattini T[2], Pedrocchi A[1]

[1] Politecnico di Milano, NearLab (Bioengineering Dept.), Milano, Italy

[2] Valduce Hospital, Costamasnaga (LC), Italy

Abstract

The objective of the present study was to perform a multi-modal analysis of brain activation maps induced by specific motor task execution in healthy subjects. Experimental set-up was composed by fMRI and a motion capture system so as to acquire the effectively executed movement. Ankle DorsiFlexion (ADF) was chosen as analyzed task because of its importance in the gait cycle. The specific goal was to individuate how amplitude affects the related cerebral flow maps in active, passive and electrical stimulated (FES) movements. Firstly FES compatibility with fMRI images acquisition was assessed, for the safety of both subject and device, and for mutual disturbances evaluation. A single subject underwent the block designed experimental protocol and brain activation maps analysis has been performed. First level analysis to compare different execution modalities and different movement amplitudes has been performed and preliminary qualitative results suggest that amplitude affects brain activation maps and that FES movements have an effective relation with motor re-learning, which is not shown in passive movement modality. The long run application is the exploitation of this multi-modal system in the evaluation of neurological patients functional recovery where the definition of the motor tasks could be only partially accomplished depending on the patient residual functionality.

Keywords*: fMRI, FES, Motor control, ADF, rehabilitation, kinematic measurement, functional recovery, Passive movement.*

Introduction

When facing neurological diseases, hemiparesis is not a static phenomenon and some recovery is foreseen depending on the severity of the damage and the choice of the rehabilitation treatment. How do rehabilitative approaches affect brain re-mapping? How does damaged brain re-map single motor tasks? To answer these questions, a preliminary functional study on healthy subjects is needed. fMRI analysis during motor tasks requires an adequate monitoring of the effective executed movement, so as to correctly interpret revealed activation maps. Literature proposes different integrated systems with fMRI and EEG, MEG, strength signals or more commonly EMG [1, 2]. Present work proposes a motion capture system tracking the trajectories of plastic retroreflective markers placed on significant and repeatable skin or bone landmarks. Passive markers don't interfere with the magnetic field of the MRI room and vice versa images acquisition doesn't affect markers recording as demonstrated in a previous study [1].

When facing cortical map activation analysis, it is important to determine how movement parameters affect the extension and the intensity of the activation. Recent studies [2] analyzed the effect of different movement modalities on activation maps during ankle dorsiflexion in healthy subjects. The fall-out of this aspect for rehabilitation is, in fact, crucial. Identification of the most efficient exercise modality for functional recovery re-mapping through the modelling of the after-stroke brain plasticity is of key importance for assessment of patient-designed treatment.

The present work aims to determine how movement amplitude affects cerebral activation maps (e.g. extension and intensity of activation) during active, passive and electrically stimulated ankle dorsiflexion as detected by 1.5 T fMRI in healthy subjects with the simultaneous kinematic recordings. A feasibility study is reported.

Methods

Experimental set-up

The experimental set-up (Fig. 1) is composed by (A) an MRI scanner 1.5T GE Cv/I™, (B) a motion capture system Smart µg™ (BTS, Italy) with (C) three recording cameras enveloped by aluminium foils and (E) an electrical stimulation device current-controlled 8 channel RehaStim pro™ (HASOMED GmbH) with (F) stimulation electrodes arranged as shown in Fig. 1.

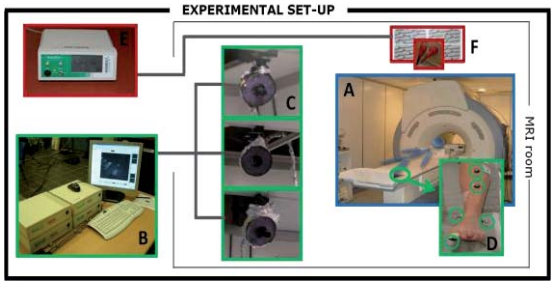


Fig. 1: Experimental set-up.

FES compatibility

FES has only recently been performed during scanning [2,3]. Two resistances were placed in series with both the stimulation electrodes to reduce to security values the maximal current delivered as well as two inductors so as to filter pick-up of gradient fields by the FES device [2]. So as to measure possible induced artefacts of the magnetic field on stimulation currents, we tried the stimulation waveform on a dead chicken because of its skin impedance value similar to the human one. In order to check for images distortion, FES stimulation was made during homogeneous phantom images acquisition and Signal-to-Noise Ratio (SNR) was calculated on each slice using the standard index for image quality (mean of signal/ standard deviation of noise).

Experimental protocol

The experimental protocol had a standard 30 seconds block design with alternate rest and on condition blocks. We proposed six different Ankle DorsiFlexion (ADF) paradigms, combining modalities and movement amplitudes: Active Broad (AB) and Small (AS), Passive Broad (PB) and Small (PS) and FES Broad (FB) and Small (FS). Stimulation was made at tibialis anterior (biphasic current pulses at 20 Hz fixed frequency). Current amplitude was set individually, PulseWidth (PW) was modulated with a trapezoidal shape to induce both phases of ADF (maximum PW 400 µs for FB and 250 µs for FS).

Kinematic data acquisition and analysis

Markers 3D displacements were reconstructed. After ankle angle computation and blocks identification, kinematic parameters of interest were computed (Matlab®).

fMRI data acquisition and analysis

For functional imaging sessions a gradient EPI sequence weighted on T2 was used; TE = 50 ms; TR=3s; flip angle=90°; matrix 128x128; FOV=24cm; voxel size=1.8x1.8x4mm. Padding was placed around the subject's head to minimize head motion. Functional images were realigned, coregistred, segmentated, normalized to standard Montreal Neurological Institute (MNI) space and smoothed. Realignment parameters were assessed for excessive motion. Statistical analysis of fMRI data used a mass-univariate approach based on General Linear Model (GLM). Analysis was carried out separately for each acquisition (SPM8®, Matlab). The results are displayed with a Family Wise Error (FWE) corrected probability $P<0.05$.

Results and Discussion

FES compatibility

SNR percentage loss during FES stimulation resulted to be 3.48% with respect to the standard environment fMRI images acquisition. At least in [4] an SNR loss of about 10% is considered negligible in 3T images acquisition. Accounting for a factor of about 1/2 while analysing 1.5T images [5], we can consider an SNR loss of 3.48% as negligible.

Kinematic parameters analysis

Kinematic recordings allowed to verify for each movement modality that ankle angle for broad and small conditions were significantly different, while frequency was constant through all acquisitions.

Activation maps

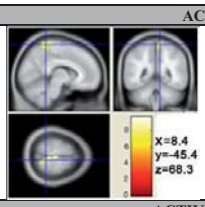
A single subject, female, 36 years old was acquired. Results for Broad movements (Active, Passive and FES) are shown in Fig. 2.

AB movement shows significant activation in controlateral primary motor cortex (M1) and primary sensory cortex (S1), and supplementary motor area (SMA). Bilateral activation is revealed in premotor cortex (PM) and secondary somatosensory area (SII). AS activation map revealed a very small activated cluster corresponding to PM and ipsilateral SMA areas.

PB active areas include controlateral M1 and PM. SMA area does present only controlateral activation; activations in bilateral SII area result to be reduced with respect to AB condition. PS activated areas result to be analogous and comparable in extension with the PB ones.

FB movement shows activation in controlateral M1, S1, SMA and significantly in SII area. The overall activation is widespread in accord with literature [2]. FS activation map shows an overall decreasing of activation with respect to FB, while preserving the same involved areas, but for S1 area that doesn't show any activation. SII activation results to be strongly reduced.

ACTIVE BROAD



KINEMATIC PARAMETERS

Mean angle: (°)

64.83±1.21

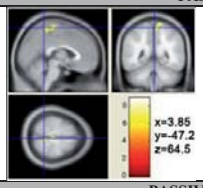
Frequency: (Hz)

0.24±0.01

ACTIVE BROAD > REST

Area	*# voxels*	*x (mm)*	*y (mm)*	*z (mm)*	*T*
SMC	**450**	**6,6**	**-38,2**	**70**	**9,666**
M1	**35**				
PM/SMA	**103**	3	-24	70	9,29
		3	-31	62	8,47
S1	**4**	10	-45	70	8,71
SII	**116**				

PASSIVE BROAD



KINEMATIC PARAMETERS

Mean angle: (°)

31.73±3.19

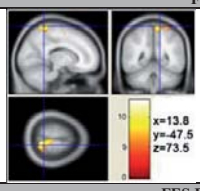
Frequency: (Hz)

0.46±0.10

PASSIVE BROAD > REST

Area	*#voxels*	*x (mm)*	*y (mm)*	*z (mm)*	*T*
SMC	**133**	**6,6**	**-45,4**	**62**	**7,4025**
M1	**6**				
PM/SMA	**24**	3	-25	70	7,18
		1	-31	62	6,48
S1	**--**				
SII	**41**	7	-45	62	7,39
		12	-47	74	6,85

FES BROAD



KINEMATIC PARAMETERS

Mean angle: (°)

39.1±0.04

Frequency: (Hz)

0.21±0.04

FES BROAD > REST

Area	*#voxels*	*x (mm)*	*y (mm)*	*z (mm)*	*T*
SMC	**576**	**10,2**	**-52,6**	**74**	**12,9301**
M1	**37**				
PM/SMA	**103**	5	-27	74	7,84
		3	-26	70	7,77
		3	-33	58	6,17
S1	**14**	7	-36	74	10,49
		14	-42	70	9,78
		39	-35	62	5,62
SII	**103**	10	-53	74	12,93
		30	-45	70	7,07
		5	-40	58	6,25

Fig. 2: Cortical regions significantly activated during active, passive and FES broad ADF. Peak coordinates refers to MNI space. SMC: sensory-motor cortex; T: t-value; M1: primary motor cortex, PM: premotor area; SMA: supplementary motor area; S1: primary sensory cortex; SII: secondary somatosensory area.

Comparative analysis between ADF execution modalities has been done at a first qualitative level. Initial results seem to be related to literature. AB movement shows a general greater activation than PB, particularly in primary S1, SMA and PM area. We found an overall widespread activation during FES sessions, whose significant feature was the increased activation in secondary somatosensory (SII) area. FES ADF has greater activation in SII, S1, SMA areas with respect to active and passive conditions. For what concerns the effect of movement amplitude, it has to be observed that activation is generally reduced from broad to small movement in active and FES ADF movement modalities, whereas the activation between the two passive ADF sessions are comparable.

Conclusions

FES compatibility has been assessed before subject stimulation so as to guarantee subject safety as well as no distortion on image acquisition. Now a day, FES is a well known technique in rehabilitation, however, FES contribution to CNS plasticity still has to be precisely demonstrated and the method discussed in this study could be a valid work hypothesis. Our study, supported by literature findings, opens the doors to possible longitudinal investigations on the effects of rehabilitative therapy on CNS (e.g. movement re-learning) and its correlation with rehabilitation behavioural gains in response to a period of FES or passive treatment, so as to asses better treatment for neurological patients.

Moreover, the amplitude-related activation in active and FES conditions is probably due to the number of shooting motor neurons that are reasonably more numerous if they should induce a broader movement. This is an interesting result because it supports the idea that electrical induced movement has an effective relation with motor re-learning, which is not shown in passive movement modality.

Acknowledgments

This study was supported by grants from Italian Institute of Technology (IIT).

References

[1] Volonterio N et al. Integration between fMRI and motion capture system to evaluate changes in cortical activations after rehabilitation in hemiplegic patients. Proc. IFESS Conference, 256-258, 2008.

[2] Francis S et al. fMRI analysis of active, passive and electrically stimulated ankle dorsiflexion. NeuroImage, 44: 469-479, 2009.

[3] Tasian GE et al. Supraspinal responses to posterior tibial nerve stimulation: a functional magnetic resonance imaging analysis of neuromodulation. AUA 2005, May 21 - 26, 2005.

[4] Scarff CJ et al. Simultaneous 3T MRI and high-density recording of human auditory evoked potentials. NeuroImage, 23: 1129-1142, 2004.

[5] Kruger G et al. Neuroimaging at 1.5T and 3.0T: Comparison of Oxygenation-Sensitive Magentic Resonance Imaging. Magn. Res.in Med., 45: 595-604, 2001.

Author's Address

Marta Gandolla - Politecnico di Milano
marta.gandolla@mail.polimi.it

Session 10

INS Session: Neuromodulation 2010: The way ahead

Deep brain stimulation – current and future indications

Alesch F (Vienna, Austria)

Psychiatric indications – a new challenge in deep brain stimulation

Erfurth A (Vienna, Austria)

Shaping the electrical field – a concept for improving neurostimulation

Manola L (Brussels, Belgium)

Neuromodulation and magnetic resonance imaging – conflicting partners?

Kainz W (Silver Spring, USA)

Session 11

Lower Extremities, SCI

(including presentation by
Stefan Schuy prize laureate)

Home-based FES in SCI: Recovery of tetanic contractility drives the structural improvements of denervated muscles

Carraro U[1], Kern H[2]

[1] Laboratory of Translational Myology, Department of Biomedical Sciences, University of Padova, Italy

[2] Ludwig Boltzmann Institute of Electrostimulation and Physical Rehabilitation, & Department of Physical Medicine, Wilhelminenspital. Vienna, Austria

Abstract

Spinal-cord injury causes muscle atrophy, which is particularly severe when lower motor neurons are involved. We performed a longitudinal study in 25 patients suffering from complete lesion of Conus Cauda from 0.7 to 8.7 years comparing functional and structural thigh muscle properties before and after 2 years of home-based training by Functional Electrical Stimulation (h-b FES). Muscles were electrically stimulated by means of large surface electrodes and a custom-designed stimulator. The poor excitability of the lower motor neuron denervated muscles was improved first by twitch-contraction training and then by tetanic contractions elicited against progressively increased loading. Improvement of thigh muscle properties was estimated by transverse computer tomography scan and force measurements. In addition, needle biopsies of vastus lateralis were harvested before and after the two-years of h-b FES. Twenty out of 25 patients completed the two year h-b FES program, which resulted in: 1. significant increase of muscle size (the cross sectional area of the quadriceps increased from 28.2±8.1 to 38.1±12.7 cm², $p<0.001$, +35%, and the mean diameter of muscle fibers from 16.6±14.3 to 29.1±23.3 μm, $p<0.001$, +75%), accompanied by improvements of the ultra-structural organization of contractile material; and 2. a significant increase in force output during electrical stimulation (from 0.8±1.3 to 10.3±8.1 Nm, $p<0.001$, + 1187%). Important benefits for the patients are the improved cosmetic appearance of lower extremities and the enhanced cushioning effect for seating. The EU Project Rise shows that "home-based FES" is a safe and effective therapy that may maintain life-long physical exercise by active muscle contraction (FES is the only option for denervated muscle) to be used as a procedure to recover tetanic contractility of denervated muscle, and to counteract muscle atrophy in order to prevent long-term complications of SCI.

Keywords: *home-based functional electrical stimulation, denervated muscle, surface electrodes, long impulses.*

Introduction

Long-lasting complete denervation of human muscle resulting from either permanent lower motor neuron (LMN) or peripheral nerve lesions have major consequences on muscle tissue and beyond. During months and years of permanent denervation muscle fibers decrease in size (atrophy), undergo spontaneous activation (muscle fibrillation), and then become un-excitable by surface electrical stimulation using standard commercial stimulators. Muscle fibers will finally disappear being substituted by fibrous and adipose tissue. Leg muscles in LMN paraplegic patients are commonly not treated with Functional Electrical Stimulation (FES) because it is widely accepted that long-term and completely denervated muscles cannot effectively respond. However, recent studies in animal models and humans indicate that: i) in rats severe atrophy does not occur for at least 3-4 months [1,2]; ii) in rabbit, the degeneration of muscle tissue does not appear during the first year of denervation [3-6]; and iii) in humans substitution of muscle fibers with connective and fat tissue (muscle degeneration) starts from the third year onward [7-12]. In addition we recently demonstrated that long term denervated muscle maintain L-type Ca^{2+} current (involved in activation of contraction) longer than the contractile machinery, providing the rationale of a rehabilitation training for human permanently denervated muscles that was developed as a result of clinical observations [13]. However, Electron Microscopy indicates that sarcotubular system and myofibrils decays quite quickly, suggesting that it is best to start h-b FES as soon as possible after SCI [14]. This still leaves a window of opportunity, which may be used to initiate muscle stimulation with the goal of avoiding muscle degeneration.

Material and Methods

The before-mentioned results [1-14] provides the rational for understanding the residual functional characteristics of the long-term denervated muscle and its ability to respond to a new rehabilitation strategy developed in Vienna (Austria). The Vienna training (validated by the results of the EU Project RISE titled: *Use of electrical stimulation to*

restore standing in paraplegics with long-term denervated degenerated muscles) is based on home-base Functional Electrical Stimulation (h-b FES), involving the use of large surface electrodes and custom designed stimulators [7-14]. Since the progression of recovery by h-b FES is inherently slow, patients were clinically evaluated every 12 weeks by physiatrists, who progressively modified the training protocol according to the patient's improvements [9,15].

Results

Two years of h-b FES resulted in: 1. significant increase in size of thigh muscles (Fig. 1) and of the muscle fibers (Fig. 2), accompanied by striking improvements of the ultra-structural organization of contractile apparatus [14]; 2. increase in muscle force output sufficient to perform h-b FES-assisted stand-up and stepping-in-place exercises; 3. evidence that the shorter is the time elapsed from SCI to the beginning of h-b FES the better is the recovery of structure and function of muscle fibers. The reorganization of T-tubules, Ca2+ release units, and of myofibrils that follows h-b FES likely may play a role in the recovered ability of LMN denervated muscles to be stimulated and to respond with tetanic contractions [4,5,6,7,9,14].

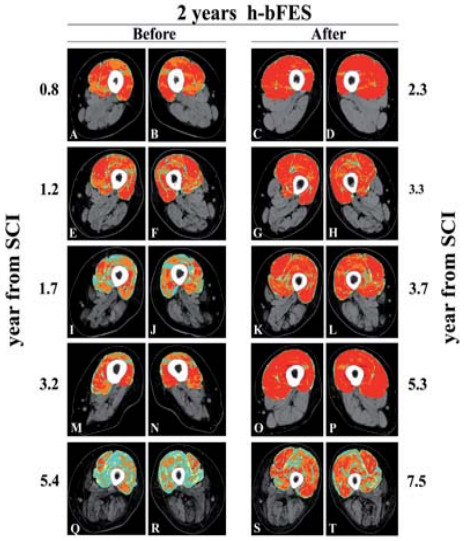


Fig. 1: The cross sectional area of left and right quadriceps muscles in patients starting h-b FES at different time points after denervation increased by two years of home training. The interstitial tissues (which increase with longer denervation periods) decreased in the respective patient after two years of h-b FES

Discussion

At two years, 90% of h-b FES subjects recovered tetanic contractions and 25% of them were able to stand during electrical stimulation in parallel bars. Minimal functional improvements were associated with long time elapses between SCI and initiation of h-b FES and, possibly lower compliance with training. In single case reports, low compliance substantially decreased the effects of training, yet in the same subjects the mass of thigh muscles increased when the patient resumed h-b FES [16-18]. The immediate benefits of h-b FES for the patients are the improved cosmetic appearance of lower extremities, the enhanced cushioning effect for seating and the reduction of leg edema. In addition, further outcomes of our studies are new non invasive imaging procedures designed and implemented to objectively demonstrate the improvements of muscle mass and contractility, despite permanent LMN denervation [7,11,19].

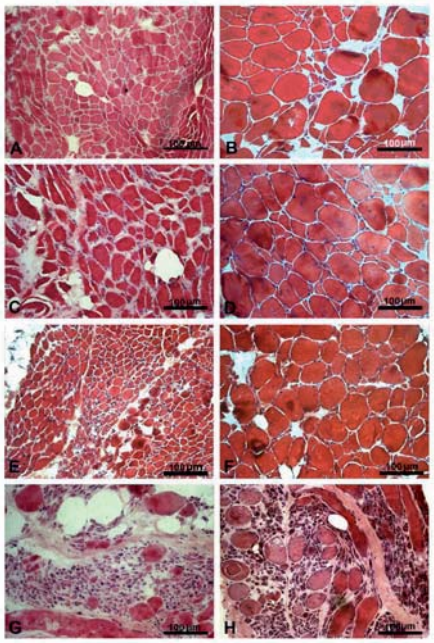


Fig. 2: Hematoxilin and Eosin staining of muscles biopsies harvested from vastus lateralis of LMN paraplegic patients before and after two years of h-b FES. When started earlier than two years after lesion, the h-b FES treatment increases muscle fibers to normal innervated values; however, when h-b FES saw started late, muscle biopsies showed fewer muscle fibers while adipose and fibrous connective tissue did not fully regress.

Conclusions

In the future, h-b FES training could be extended to patients with similar lesions (incomplete LMN denervation of skeletal muscles) and it will be extremely important to determine whether this treatment can also reduce secondary complications related to disuse and impaired blood perfusion (reduction in bone density, risk of bone fracture, decubitus ulcers, and pulmonary thromboembolism).

References

[1] Carlson BM. The Denervated Muscle: 45 years later. Neurol Res 2008;30:119-122.

[2] Adami N, Kern H, Mayr W, et al. Permanent denervation of rat Tibialis Anterior after bilateral sciatectomy: determination of chronaxie by surface electrode stimulation during progression of atrophy up to one year. Basic Appl Myol 2007;17:237-243.

[3] Ashley Z, Sutherland H, Lanmüller H, et al. Determination of the chronaxie and rheobase of denervated limb muscles in conscious rabbits. Artif Org 2004;28:759.

[4] Ashley Z, Sutherland H, Lanmuller H, et al. Atrophy, but not necrosis, in rabbit skeletal muscle denervated for periods up to one year. Am J Physiol Cell Physiol 2007;292:C440-451.

[5] Ashley Z, Salmons S, Boncompagni S, et al. Effects of chronic electrical stimulation on long-term denervated muscles of the rabbit hind limb. J Muscle Res Cell Motil 2007;28:203-217.

[6] Ashley Z, Sutherland H, Russold MF, et al. Therapeutic stimulation of denervated muscles: the influence of pattern. Muscle Nerve 2008;38:875-886.

[7] Kern H, Carraro U, Adami N, Biral D Hofer C, Forstner C, Mödlin M, Vogelauer M, Boncompagni S, Paolini C, Mayr W, Protasi F, Zampieri S. Home-based Functional Electrical Stimulation (h-bFES) recovers permanently denervated muscles in paraplegic patients with complete lower motor neuron lesion. Neurorehabil Neural Repair. 2010 May 11. [Epub ahead of print] PMID: 20460493

[8] Kern H, Rossini K, Carraro U, et al. Muscle biopsies show that FES of denervated muscles reverses human muscle degeneration from permanent spinal motoneuron lesion. J Rehabil Res Dev 2005;42:43–53.

[9] Kern H, Boncompagni S, Rossini K, et al. Long-term denervation in humans causes degeneration of both contractile and excitation-contraction coupling apparatus that can be reversed by functional electrical stimulation (FES). A role for myofiber regeneration? J Neuropath Exp Neurol 2004;63:919–931.

[10] Carraro U, Rossini K, Mayr W, et al. Muscle fiber regeneration in human permanent lower motoneuron denervation: relevance to safety and effectiveness of FES-training, which induces muscle recovery in SCI subjects. Artif Organs 2005;29:87-191.

[11] Kern H, Carraro U, Adami N, et al. One year of home-based Functional Electrical Stimulation (FES) in complete lower motor neuron paraplegia: Recovery of tetanic contractility drives the structural improvements of denervated muscle. Neurol Res 2010; 32 (1) 5-12.

[12] Rossini K, Zanin ME, Carraro U. To stage and quantify regenerative myogenesis in human long-term permanent denervated muscle. Basic Appl Myol 2002;12:277–286.

[13] Squecco R, Carraro U, Kern H, et al. Despite lost contractility, a sub-population of rat muscle fibers maintains an assessable excitation-contraction coupling mechanism after long-standing denervation. J Neuropath Exp Neurol 2009;68:1256-1268.

[14] Boncompagni S, Kern H, Rossini K, et al. Structural differentiation of skeletal muscle fibers in the absence of innervation in humans. Proc Natl Acad Sci U S A. 2007;104:19339–19344.

[15] Kern H, Hofer C, Mayr W, et al. European Project RISE: Partners, protocols, demography. Basic Appl Myol/ European Journal of Translational Myology 2009;19:211-216.

[16] Gargiulo P, Vatnsdal B, Ingvarsson P, et al. Restoration of muscle volume and shape induced by electrical stimulation of denervated degenerated muscles: qualitative and quantitative measurement of changes in rectus femoris using computer tomography and image segmentation. Artif Organs 2008;32:609–613.

[17] Gargiulo P, Vatnsdal B, Ingvarsson P, et al. Computational methods to analyse tissue composition and structural changes in denervated muscle undergoing therapeutic electrical stimulation. Basic Appl Myol/ European Journal of Translational Myology 2009;19:157-162.

[18] Gargiulo P, Kern H, Carraro U, et al. Quantitative colour 3D CT imaging of human long-term denervated muscle. Progression to fibrosis of perimysium and a case report of FES recovery. Neurol Res 2010; 32 (1) 13-19.

[19] Kern H, Hofer C, Mayr W. Protocols for Clinical Work Package of the European Project RISE. Basic Appl Myol/European Journal of Translational Myology 2008;18:39–44.

Acknowledgements

The authors acknowledge support of the EU Project RISE (Contract n. QLG5-CT-2001-02191), of The Austrian Ministry of Science, Vienna (Austria) and of the MIUR project: RISE2-Italy: Evidence-based optimization of home-based therapeutic functional electrical stimulation (hbt-FES) for human denervated muscle (Prot. n. 2008SJ4MRW).

Author's Address

Ugo Carraro, Laboratory of Translational Myology,
Department of Biomedical Sciences,
University of Padova, Italy
eMail: ugo.carraro@unipd.it
homepage:
https://www.biomed.unipd.it/index.php/it/ricerca/groups/139-carraro-group

Restoring Stepping After Spinal Cord Injury Using Novel Electrical Stimulation and Feedback Control Strategies

Holinski BJ[1], Mazurek K[2], Everaert DG[1], Mushahwar VK[1], Stein RB[1]

[1] University of Alberta, Edmonton, Canada

[2] Johns Hopkins University, Baltimore, USA

Abstract

The overall objective of this project is to develop a feedback-driven intraspinal microstimulation (ISMS) system. We hypothesize that sensory feedback will enhance the functionality of stepping by reducing muscle fatigue and adapting to external perturbations. In the current study, the controller was tested with intramuscular stimulation and external sensors (force plates, gyroscopes, and accelerometers). The walking cycle was divided into 4 states that transitioned with external sensory feedback within a preset range of times. Terminations in the swing phase were best served by accelerometer feedback, while gyroscopes were used to terminate the stance phase. Anesthetized cats were partially supported in a sling and bi-laterally stepped overground on a 4-m instrumented walkway. The walkway had variable friction to perturb the controller. In five cats across 7 experimental sessions, the controller (without feedback) produced an average step length of 24.9 ± 8.4 (normalized to foot segment length). Steps were shortened (preventing backward slipping) with the addition of sensory feedback to an average length of 21.8 ± 7.5. Mean peak ground reaction force on each limb also increased from 15.9 ± 7 % to 18.0 ± 4.5 % of body weight with the feedback enabled. The step period was programmed for 1.5 sec. The addition of feedback adapted the average step duration to 1.27 ± 0.25 sec in response to the varying conditions of the walkway. Eventually, this research can be translated into a compact and fully implantable walking prosthesis.

***Keywords**: Intraspinal Microstimulation (ISMS), Intramuscular Stimulation, Dorsal Root Ganglion, Central Pattern Generator (CPG), Sensory Feedback, Walking, Gyroscopes, Accelerometers, Ground Reaction Forces, Walking Prosthesis.*

Introduction

There are currently 1.275 million people affected by spinal cord injury in the United States [1]. Of these, 28.2% have complete paraplegia and reduced mobility. Our laboratory's overall goal is to improve the quality of life of people with paraplegia by increasing their mobility. More specifically, we aim to develop a device which will use functional electrical stimulation (FES) to restore walking. Current FES devices are limited in their ability to restore walking because they are unable to adapt to muscle fatigue and external perturbations which may lead to the user falling [2]. As such, the devices have not been widely adopted. We hypothesize that adding sensory feedback will enhance the functionality of stepping by reducing muscle fatigue and adapting to external perturbations.

The feedback will control intraspinal microstimulation (ISMS) based on either neural recordings from the dorsal root ganglion (DRG) or external sensors. ISMS is a method of electrically stimulating regions of the spinal cord, called motor pools, to produce coordinated movements with less fatigue than with surface stimulation [3]. Nerve cuff electrodes, while decreasing the current required to stimulate a muscle, also unfortunately produce fatigable movements. ISMS activates the intact neural networks below the lesion using low amplitudes (100-200 uA) of current. By changing stimulation parameters in response to feedback and timing, it is possible to modify stepping in real-time.

During normal walking, there is constant feedback provided to the central nervous system (CNS) from specialized cells. These signals can be accessed in the DRG with implantable electrode arrays and provide vital information for the successful coordination of movements. Previously, we have shown DRG recordings can be decoded to provide limb prediction with less than 2 cm error [4].

However, current controller development has utilized intramuscular stimulation and external sensors to allow for rapid iterations of the algorithm. The controller employs intrinsic timing (similar to the central pattern generator) as well as sensory feedback to mimic a physiological walking system. Previous work by Guevermont et al. has

shown that controller algorithms relying solely on either intrinsic timing or sensory feedback produce unstable overground walking [5]. Our purpose for this abstract was to present results from the development of a hybrid controller which utilizes both intrinsic timing and sensory feedback.

Material and Methods

Animal Preparation

All experiments were conducted according to the University of Alberta's Code of Animal Conduct. The cats were anesthetized using isoflurane and subsequently switched to sodium pentobarbital. Stimulation electrodes were inserted percutaneously into 8 muscles of each leg (flexors and extensors of hip, knee and ankle). Walking patterns were induced from direct electrical stimulation of the muscles using trains of biphasic charge-balanced pulses (62Hz, up to 20mA, with on and off ramping). The cat was then transferred to an instrumented walkway and partially suspended in a cart-mounted sling. The cat remained under anaesthesia for the duration of the experiment.

Sensor Preparation

The external sensors, gyroscopes and accelerometers, were calibrated and fixed to the hind limb. The 4-m walkway had separate force plates for each leg. Sensor data were acquired using a Cerebus data acquisition system at 1000 samples/sec. The data were streamed from the Cerebus into Matlab to be processed in real time by custom programs.

Controller

The controller adapted stimulation parameters in real time to create a walking cycle. It contained a state system which divided the walking cycle into four states and restricted the activation of rules to specific states. The states were swing, touchdown, stance and push off. The controller was preset to a walking cycle period of 1.5 seconds with individual weighting of states at 20%, 20%, 20%, and 40%, respectively. There were 13 rules divided into two groups: intrinsic timing rules and sensory feedback rules. The 9 timing rules mimic the intrinsic timing of the CPG. The four IF-THEN sensory feedback rules were: swing to stance transition, stance to swing transition, fatigue compensation, and a safety rule. The fatigue compensation rule increased stimulation amplitudes (typically by 30%) in the stance phase to increase load bearing forces. The safety rule held the load bearing leg in stance while the opposite leg cycled through its walking states until it regained GRF. If feedback rules did not intervene, the state transitions proceeded according to preset timings.

Operators chose the activation thresholds of the IF-THEN rules after analyzing data from trials with the feedback disabled. With feedback engaged, the controller adapted stimulation parameters depending on the current walking state. All sensor data, controller states and kinematics of the leg were recorded.

Results

Results are shown for 5 cats across 7 experimental sessions. The data include 83 trials encompassing both male and female cats with weights of 3.5 to 4.4 kg. Specific trials are used to illustrate the adaptation of the controller to the varying friction of walkway.

Figure 1 shows that without sensory feedback the limb angle (measured from hip to paw) increased in regions of low walkway resistance resulting in the limb extending more backwards.

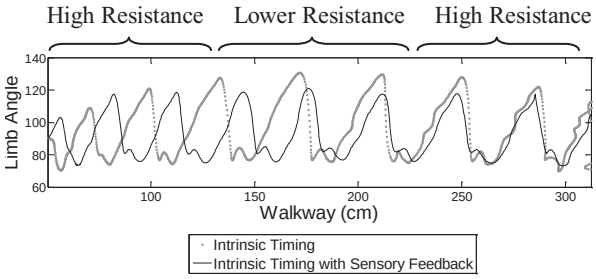


Figure 1: Limb angle (measured from hip to paw) in degrees clockwise from horizontal across the walkway. The traces illustrate the difference between intrinsic timing alone and with the addition of sensory feedback.

With the addition of both transition rules, limb angle adapted to the external perturbation of the walkway. Backward extension of the limb was reduced, which resulted in an increase in the sum of the ground reaction forces. During the intrinsic timing trial, the total load bearing support dropped dangerously low to about 5% of body weight during some steps (Fig. 2). Due to the experimental setup of our sling, 12.5% of body weight is considered full load bearing support for a single hindlimb. With the transition rules, the sum of the GRF's only drops to approximately 10%. This is slightly shy of full load bearing; however it is a marked improvement over intrinsic timing alone.

Looking at the addition of each transition rule individually, we can see the effect they have on stride length during the trial (Fig. 3). Early in the trial, the stride length is less than 10 cm as the cat overcomes static friction and the inertia of the cart.

As the cart begins to move and the resistance of the walkway decreases, stride length differences can be seen for each of the controller algorithms. Intrinsic timing alone resulted in a large stride length of up to 23 cm. The addition of the swing to stance rule decreased it to 16 cm. The greatest decrease in stride length during the low resistance section of the walkway came from adding both swing to stance transitions and stance to swing transitions.

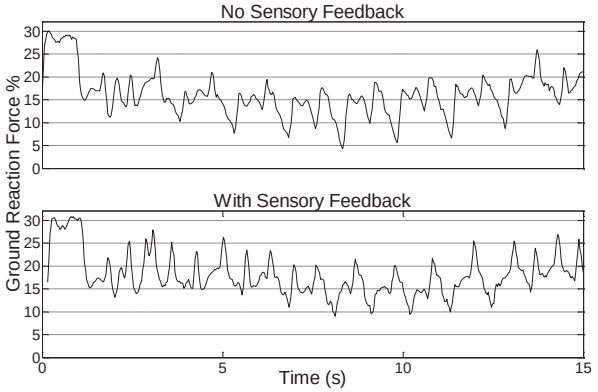


Figure 2: The sum of the vertical GRF's are plotted as a percentage of body weight. The upper pane depicts a trial using only intrinsic timing whereas the lower pane demonstrates the addition of sensory feedback. They are plotted against trial time.

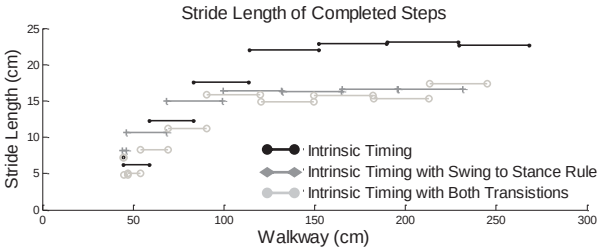


Figure 3: The vertical location of each line represents the stride length for a particular step. The length of the line shows the duration of that step across the walkway. Three trials illustrate the cumulative effect of adding each transition rule.

Across all the successful trials, we saw similar results (Table 1). Inclusion criteria for a successful trial were as follows: the cat walked at least 75% across the length of the walkway and the preset walking cycle duration was 1.5 seconds. Stride length was normalized against the distance from the ankle to the metacarpophalangeal joint. Peak GRF was normalized as a percentage of body mass. Table 1 shows that there is a decrease in the average stride length when using sensory information. There is also a decrease in step duration indicating an increase in the step frequency in response to low resistance sections of the walkway. Finally, the safety of walking improved with increased peak forces with feedback enabled.

Table 1: Summary of 83 Successful Trials

	Intrinsic Timing	with Sensory Feedback
Stride Length (norm.)	24.9 ± 8.4	21.8 ± 7.5
Step Cycle Duration	1.48 ± 0.02 s	1.27 ± 0.25 s
Peak Force	15.9 ± 7 %	18.0 ± 4.5 %

Discussion

In agreement with preliminary evidence presented by Guevermont et al. [2], the combination of intrinsic timing and sensory feedback provides the most functional overground walking. Throughout the regions of least resistance in the walkway, the sensory rules allowed the state transitions to speed up resulting in decreased stride length. This decrease prevented excessive extension and a loss of load bearing ground reaction forces. Load bearing is a critical measure of safety for a functional walking device as it prevents falling.

Conclusions

Future work will replace intramuscular stimulation with ISMS and external sensors with DRG recordings to allow the internalization of the prosthetic device. Eventually, we hope to develop this research into a compact and fully implantable walking prosthesis. This study relies on currently available technologies, some of which are already FDA approved for use in humans. This study will provide a proof-of-principle for application to humans with paraplegia.

References

[1] Christopher and Dana Reeve Foundation, www.christopherreeve.org, accessed May 10, 2010.

[2] Brissot R, Gallien P, et al. "Clinical experience with functional electrical stimulation-assisted gait with Parastep in spinal cord-injured patients." Spine **25**(4): 501-8, 2000.

[3] Mushahwar VK, Collins DF, et al. "Spinal cord microstimulation generates functional limb movements in chronically implanted cats." Exp Neurol **163**(2): 422-9, 2000.

[4] Stein RB, Weber DJ, et al. "Coding of position by simultaneously recorded sensory neurones in the cat dorsal root ganglion." J. Physiol. 560(3): 883-896, 2004.

[5] Guevremont L, Norton JA, et al. "Physiologically based controller for generating overground locomotion using functional electrical stimulation." J Neurophysiol **97**(3): 2499-510, 2007.

Acknowledgements

Funding was graciously provided by AHFMR, CIHR and the Christopher and Dana Reeve Foundation. Special thanks to Sigenics Inc., Rob Rolf and Doug Weber.

Author's Address

Brad Holinski, University of Alberta, bjh2@ualberta.ca

Active arm involvement in the rehabilitation of walking after spinal cord injury: a case study

Alvarado Pacheco L.E.[1], Ogilvie R.J. [1], Chong S. L. [1] & Mushahwar V. K.[1]

[1] University of Alberta, Edmonton, Alberta, Canada

Abstract

The purpose of this study is to evaluate the outcomes of actively involving the arms along with the legs in a rehabilitation program to improve walking after incomplete spinal cord injury (iSCI). Interlimb modulation characterized by the swinging of the arms during walking in humans, involves neuronal pathways between the arm and leg control regions in the spinal cord. However, the arms are not actively involved in locomotion rehabilitation protocols currently in practice. We evaluated this new intervention in one subject with chronic iSCI using a combined arm/leg FES-assisted cycling ergometer. After completing 12 weeks of FES-assisted arm /leg cycling, the participant improved his overground walking ability and now requires one less assistive device for walking more than 10m. Walking speed improved by 23% (10m test), and endurance by 24% (6min test). Improvements in balance according to the Berg scale were observed. Beneficial changes in the activation pattern of leg muscles as well as in foot clearance are reported. The preliminary results suggest that this novel intervention may be effective in improving overground walking in people with iSCI.

Keywords: *Functional electrical stimulation, Cycling, Rehabilitation, Spinal cord injuries, Walking, H-reflex.*

Introduction

While walking and running, humans tend to swing their arms in opposition to the legs. Dietz proposed that during locomotion, interlimb modulation in humans is similar to that found in the cat, and involves both arm and leg control centres in the spinal cord [1]. The interlimb modulation of cutaneous reflexes between the upper and lower limbs was found during walking, but not during standing [2]. After a spinal cord injury, the regular sensory input provided to the spinal cord is interrupted. Therefore, the regulation of motor patterns becomes disorganized including the coordination of arm and leg centres in the spinal cord that is normally present during walking.

Consequently, we believe that the arms can play an important role in the rehabilitation of walking after a spinal cord injury. A few research groups have anecdotally explored this possibility. Their findings highlight that arm position and the reduction of arm weight bearing during body weight supported treadmill training for locomotion facilitates stepping [3]. Also, passive arm movements potentiate the leg motor output (Electromyography) in intact as well as in incomplete spinal cord injured subjects, possibly through interlimb neural pathways [4]. Although a role for the arms in the rehabilitation of walking has been suggested, rehabilitation protocols currently in practice have not involved the arms actively nor systematically measured the benefit that they could have on the recovery of functional walking. Hence, we want to incorporate the arms in a rehabilitation program to improve the ability to walk after a spinal cord injury.

In order to provide regulated sensorimotor input to the spinal cord we will use functional electrical stimulation (FES) of residual neural pathways as required to assist in the rhythmic movement. FES does not only target motor nerves causing a muscular contraction, but also sensory fibres returning to the spinal cord. Therefore, providing regulated input to motor neurons controlling muscles in the arms and legs which coincides with voluntary drive to these neurons could strengthen descending connections from the brain.

Zehr and colleagues found a strong correlation across walking, arm and leg cycling and arm-assisted recumbent stepping, supporting the existence of a common neural network as the regulator of arm and leg rhythmic movements [5]. In order to target this common neuronal network, a task such as FES – assisted cycling which is already available in rehabilitation centres could be used. Therefore, we hypothesize that sensory input during rhythmic arm and leg FES–assisted cycling exercise will regulate the function of the spinal neuronal networks and improve over ground walking after incomplete SCI.

Material and Methods

Case description

One male participant, 46 years old with iSCI at T10 completed the 12 – week arm and leg FES – assisted cycling program. Prior to the program, the participant ambulated with two forearm crutches.

FES-assisted arm and leg cycling:

In order to activate the arms and legs simultaneously, we used a combined arm/leg FES ergometer to generate arm/leg movements resembling the coordination present in natural walking. The study participant had one hour of FES training 5 times a week for 12 weeks. Electrical stimulation was delivered through surface electrodes targeting leg muscles. Since this participant did not need assistance for arm cycling no stimulation was delivered to the arms. Through the progression of the training, the mechanical resistance on the FES – cycling equipment was increased according to the performance of the participant. All parameters regarding intensity of stimulation, speed, resistance and frequency of rest periods were monitored.

Evaluating the effects of FES-assisted arm and leg cycling on walking:

Pre – training, after 6 weeks and after 12 weeks of training the participant was subject to clinical and electrophysiological evaluation. Initially, the level and extent of the lesion were classified using the ASIA Impairment Scale (American Spinal Injury Association). We performed clinical walking, functional and electrophysiological tests. The validated Walking Index for Spinal Cord Injury clinical assessment method [6] was used as well as timed walking tests such as 6 – minute walking and 10 meter walking. We evaluated balance according to the Berg balance scale [7]. To better describe how walking ability improved, we evaluated the muscle activation patterns, kinetics and kinematics during walking.

Evaluating the effects of FES-assisted arm and leg cycling on monosynaptic reflexes:

Since we are interested in investigating the underlying mechanism for the improvements in walking and whether they are a consequence of reorganization of the neuronal networks, we assessed the strength and modulation of the spinal monosynaptic reflex. We used a 1 ms single pulse to electrically stimulate the posterior tibial nerve and measured the H – reflex response in the soleus muscle through surface electromyography.

Results

The results obtained from each assessment session were compared to those obtained at baseline. Initial evaluation according to the ASIA sensory scale indicated severe impairments in the differentiation of light touch/pin sensation. The motor scores were particularly low in left hip flexors, right knee extensors and left long toe extensors. After 12 weeks of training the sensory score indicated improvements in stimulated and non – stimulated regions, Figure 1. The motor score on the right side did not change. On the left side the score decreased from 21 at baseline to 19 after 12 weeks of training even though there was improved range of motion in the hip and ankle. During the post – training assessment, the new range of motion was used resulting in a lower score.

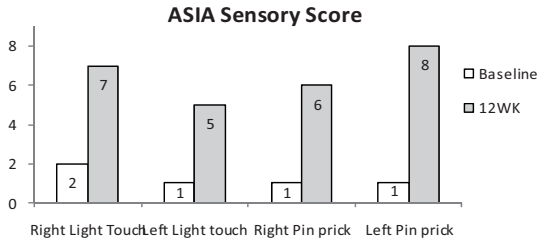


Figure 1. ASIA sensory scores. Only lower extremity regions were evaluated. Maximum score per side = 14.

The participant significantly improved in the endurance, 6 minute – walking test by 23% ($p=0.026$) from a speed of 0.51±0.01 m/s at baseline (Figure 2). Similarly, the results of the 10 – meter walking test indicated an improvement of 24% in speed from an initial speed of 0.45±0.06 m/s.

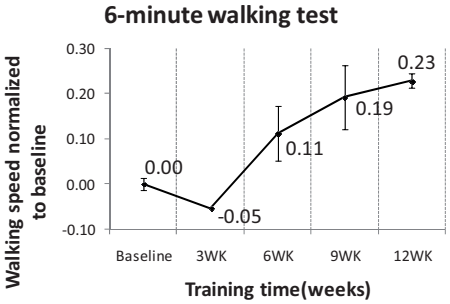


Figure 2: Walking speed measured during an endurance test of 6 minutes (mean±s.d.), pre-training speed = 0.51±0.01 m/s.

After 12 weeks of the training, the participant improved his balance by 9 scale points according to the Berg Balance Scale. This improvement was due to a better ability to stand unsupported, turning while standing, and sitting to standing movements and vice versa.

Kinematics analysis showed that, after 12 weeks of training, there were improvements in foot clearance in the right foot trajectory but not in the left foot trajectory when walking with two crutches (Figure 3). The muscle activation pattern after 12 weeks in left tibialis anterior better resembled that of able – bodied individuals (Figure 4).

Finally, the peak to peak amplitude of the H reflex in the left soleus was reduced by 24% with the muscle relaxed.

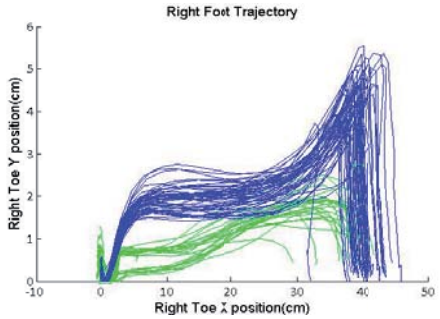


Figure 3. Right foot trajectory at baseline (green) and after 12 weeks (blue) of training. Walking with crutches.

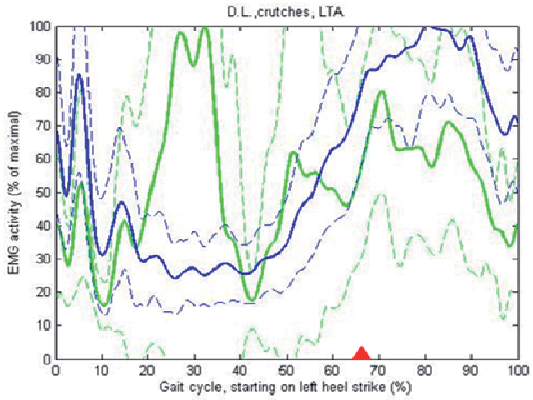


Figure 4. Rectified EMG activity of left tibialis anterior at baseline (green) and after 12 weeks (blue) of training. Red arrow indicates left toe-off.

Discussion

Important walking improvements were observed in this first participant. In particular, improvements in regulation of left dorsiflexion through the step cycle could account for improvements in walking speed and balance. Reduction in reflex excitability of left plantarflexor and the resulting reduction in muscle hypertonicity may also be a mechanism for the improvements in walking speed and posture. Despite the fact that the intervention did not specifically train balance nor involve an upright posture, balance improvements were the most clinically relevant and observable for this subject.

Although not necessary, outside the lab, this participant continues to use the same assistive devices for ambulation that he used before the training. However, he is able to walk faster and with an upright posture. The retention of the improvements in walking and incorporation into daily activities will be another factor to evaluate in the future. Future studies will also evaluate the effectiveness of this intervention relative to conventional locomotor training strategies.

Conclusions

To the best of our knowledge, these experiments represent the first time that the neuronal coupling between networks controlling the arms and legs are exploited to improve walking through FES training. If the FES-assisted arm and leg cycling rehabilitation protocol is, at least, as effective as conventional locomotor training strategies this intervention will be translated to the clinic. While conventional strategies require 3 – 4 physical therapists per client, this approach will have the advantage of requiring the assistance of only one physical therapist.

References

[1] V. Dietz, "Do human bipeds use quadrupedal coordination?," *Trends in Neurosciences,* vol. 25, pp. 462-467, 2002.

[2] E. V. Lamont and E. P. Zehr, "Task-specific modulation of cutaneous reflexes expressed at functionally relevant gait cycle phases during level and incline walking and stair climbing," *Experimental Brain Research,* vol. 173, pp. 185-192, 2006.

[3] A. L. Behrman and S. J. Harkema, "Locomotor Training After Human Spinal Cord Injury: A Series of Case Studies," *Physical Therapy,* vol. 80, pp. 688-700, 2000.

[4] N. Kawashima*, et al.*, "Shaping Appropriate Locomotive Motor Output Through Interlimb Neural Pathway Within Spinal Cord in Humans," vol. 99, ed, 2008, pp. 2946-2955.

[5] E. P. Zehr*, et al.*, "Neural regulation of rhythmic arm and leg movement is conserved across human locomotor tasks," vol. 582, ed, 2007, pp. 209-227.

[6] J. F. Ditunno Jr*, et al.*, "Validity of the walking scale for spinal cord injury and other domains of function in a multicenter clinical trial," *Neurorehabilitation and Neural Repair,* vol. 21, pp. 539-550, 2007.

[7] K. Berg*, et al.*, "Measuring balance in the elderly: validation of an instrument.," *Can J Public Health,* vol. 83 Suppl 2, pp. S7-11.

Acknowledgements

Alberta Heritage Foundation for Medical Research, Spinal Cord Injury Treatment Centre Society – Northern Alberta, Rick Hansen Institute, and Alberta Paraplegic Foundation.

Author's Address

Laura Alvarado Pacheco, Centre for Neuroscience, University of Alberta. lalvarad@ualberta.ca

Optimal walking trajectories estimation using wavelet neural network for FES-assisted arm-supported paraplegic walking

Nekoukar V and Erfanian A

Neuromuscular Control Systems Lab., Neural Technology Research Centre, Department of Biomedical Engineering, Iran University of Science and Technology (IUST), Tehran, Iran

Abstract

One major limitation of arm-supported walking using functional electrical stimulation in paraplegic subjects is the high energy expenditure and the high upper body effort. One major factor that affects the energy expenditure and the high upper body effort during arm-supported FES-assisted walking is the gait pattern. To obtain a gait pattern that lead to minimum handle reaction force (HRF), a method is proposed to find the optimal gait patterns that lead to minimum HRF. For this purpose, a neural network model of the human walking is presented to relate the joint angles to the HRF. Using the neural model, an optimal walking trajectory is determined to minimize the HRF. The experiments were conducted on two paraplegic subjects. The results show that the HRF obtained for optimal gait pattern is less than the measured HRF.

Keywords: *Wavelet neural network, gait, paraplegic, functional electrical stimulation.*

Introduction

For over three decades, many researchers have demonstrated that limited crutch- or walker-assisted walking can be restored in paraplegic subjects by functional electrical stimulation (FES) systems [1]-[2]. Major problem that limits the success of the current motor neuro-prostheses for standing and walking is the high metabolic rate and the high upper body effort observed in paraplegic subjects during the task [3]-[5].

Low-strength of electrically-stimulated muscle and difficulty of controlling multi-link multi-actuator neuromusculoskeletal can be considered as the major factors for high upper body activities and high energy consumption during FES-assisted arm-supported walking.

One major factor that can affect the energy expenditure and the upper body effort is the reference trajectory of walking. In this paper, we present a method to find an optimal trajectory for FES-assisted paraplegic walking and demonstrate that handle reaction force (HRF) can be reduced by defining a suitable walking trajectory.

To find an optimal reference trajectory, a neural model is proposed to relate the joint angles (i.e., ankle, knee, and hip joint angles) with hand reaction forces. The model is identified using a local linear wavelet neural network (LLWNN) [6]. Based on the identified model, an optimal walking trajectory is estimated to obtain the minimum hand reaction force.

Methods

The LLWNN

Local linear wavelet neural network (Fig. 1) is a feed-forward network which is used for approximation, classification, and prediction [6]. The output of a LLWNN is given by

$$y = \sum_{j=1}^{n} v_j Z_j(x) \tag{1}$$

$$v_j = w_{j1}x_1 + w_{j2}x_2 + \ldots + w_{jn}x_n \tag{2}$$

where $x = [x_1, x_2, \ldots, x_n]$ is the input vector, w_{ji} is *i*th weight of the *j*th node and

$$Z_j(x) = a_j^{-1/2}\Psi(\frac{x - b_j}{a_j}) \tag{3}$$

that $\Psi(x)$ is a mother wavelet which is localized in both the time space and the frequency space and $a_i = [a_{i1}, a_{i2}, \ldots, a_{in}]$ and $b_i = [b_{i1}, b_{i2}, \ldots, b_{in}]$ are the scale and transition parameters, respectively.

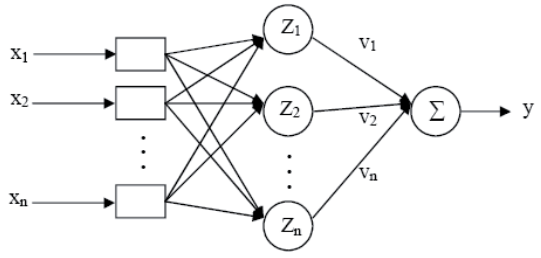


Fig. 1: Schematic of the LLWNN.

Neural Modelling of the Skeletal System

To model the relation between the joint angles of the lower extremities and the HRF, a LLWNN with 6 inputs, 1 output and 12 hidden nodes is used. The input vector is defined as

$$x(t) = [\theta_a(t-1), \theta_a(t), \theta_k(t-1), \theta_k(t), \theta_h(t-1), \theta_h(t)]$$

where θ_a, θ_a and θ_a are the joint angles of the right ankle, right knee and right hip, respectively. The output is the HRF of the right hand at time *t*. The particle swarm optimization (PSO) algorithm [7] is employed to train LLWNN by using the data measured during arm-supported FES-assisted walking of two paraplegic subjects using neuroprosthesis ParaWalk [8].

Optimal Trajectory of Walking

Optimal trajectory of the paraplegic walking $\boldsymbol{\theta}^*(t) = \left[\theta_a^*(t),\ \theta_k^*(t), \theta_h^*(t)\right]^T$ is determined as:

$$\boldsymbol{\theta}^*(t) = \arg\min_{\theta_a,\ \theta_k, \theta_h} \left[\int_{t=0}^{T} f\left(\theta_a(t), \theta_k(t), \theta_h(t)\right) \right] \qquad (5)$$

where $f\left(\theta_a(t),\ \theta_k(t), \theta_h(t)\right)$ is a nonlinear function relating the HRF and joint angles (i.e., the ankle, knee and hip joint angles). The HRF-joint angles relationship f is unknown but can be approximated by using LLWNN. To determine the optimal trajectory $\boldsymbol{\theta}^*$ with minimum hand reaction force, the function f should be minimized (5). In this work, the PSO algorithm is used for optimization process.

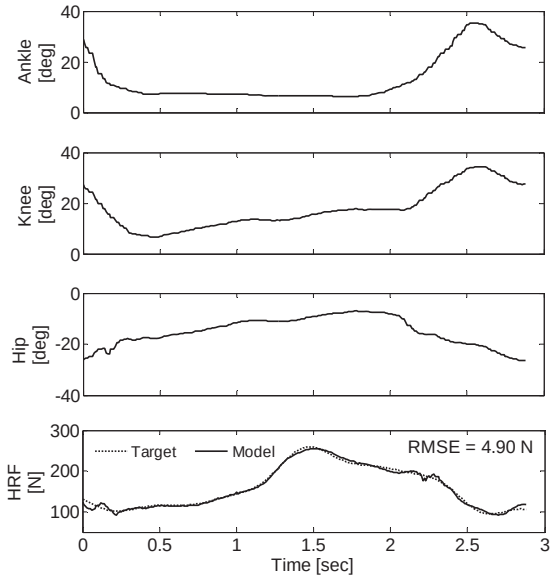
Results

Experimental Procedure

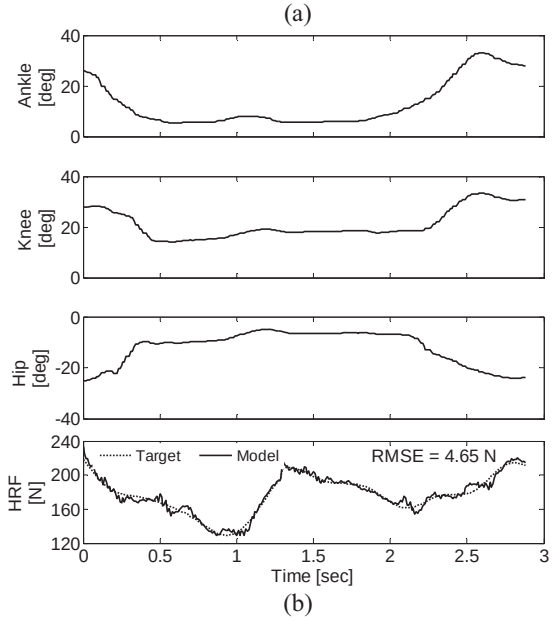
The experiments were conducted on two thoracic-level complete spinal cord injury with injury at T7 (Fig. 2) and T11 levels. The paraplegic subjects were active participants in a rehabilitation research program involving daily electrically stimulated exercise of their lower limbs (either seated or during standing and walking) using ParaWalk neuroprosthesis [8]. The hip, knee, and ankle joint angles were measured by using the motion tracker system MTx (Xsens Technologies, B.V.) which is a small and accurate 3-DOF Orientation Tracker. The hand reaction force was measured by a 3-component piezoelectric force sensor (9602, Kistler, Switzerland) mounted underneath the walker handle. Two pairs of electrodes (1 left, 1 right) over the quadriceps muscle, two pairs over the common personal nerve, and two pairs over the gluteus maximus/minimus muscle. Pulsewidth modulation (from 0 to 700 μsec) with balanced bipolar stimulation pulses, at a constant frequency (25 Hz) and constant amplitude is used to stimulate the muscles.



Fig. 2: A paraplegic subject with injury at T7 level uses ParaWalk to stand and walk.



(a)



(b)

Fig. 3: The joint angles, measured and predicted HRF using the LLWNN for two paraplegic subjects RR (a) and MS (b).

Neural Network Model of Skeletal System

The neural network is trained using the data obtained from one strike of FES-assisted arm-supported walking during the first day of experiment. Then the trained network is used to predict the hand reaction force during subsequent sessions of experiment. Fig. 3 shows the results of the HRF prediction using the LLWNN for both subjects. The root-mean-square (RMS) prediction error for a typical strike are 4.90 N (2.99%) and 4.65 N (4.43%) for subjects RR and MS, respectively.

Optimal Walking Trajectory

The trained LLWNN was used to determine the optimal walking trajectory using the PSO algorithm. Fig. 4 shows the obtained optimal walking trajectory for the subject RR. It can be clearly seen that the HRF for optimal trajectory is less than the measured HRF. The same results was obtained for the subject MS. The average of the optimal HRF is 57.76 N (36.8 N) while the average of the measured HRF is 145.12 N (113.0 N) for the subject RR (MS). The peak of the optimal and measured HRF are 140.48 N (206.0 N) and 244.88 N (285.0 N) respectively, in subject RR (MS).

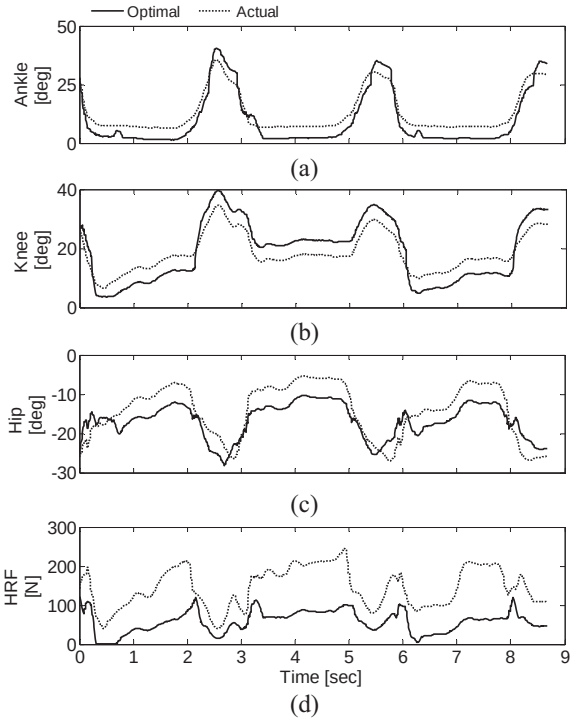


Fig. 4: Result of the walking trajectory optimization for subject RR, (a) ankle joint, (b) knee joint, (c) hip joint, (d) the HRF.

Conclusions and Discussion

In this work, a model was presented for relating the lower extremities joint angles to the hand reaction force using neural network during FES-assisted arm-supported walking in paraplegic subjects. Neural network is a black box model identification technique without requiring information about the physical parameters of the system.

The most important result obtained is that the proposed model is bale to estimate accurately the HRF using only joint angles. The developed model was used to determine the optimal walking trajectory. It was observed that the HRF for optimal trajectory is less than the measured HRF. The results indicate that the HRF was reduced 60.9% and 67.4%, in subjects RR and MS, respectively, during walking with optimal trajectory.

The closed-loop control of walking using the estimated optimal trajectories constitutes the key issue of our current research.

References

[1] Kralj A, Bajd T, Turk R, et al, Gait restoration in paraplegic patients: a feasibility demonstration using multichannel surface electrode FES. J. Rehabil. Res. Dev., 20: 3-19, 1983.

[2] Marsolais EB, Kobetic R, Functional walking in paralyzed patients by means of electrical stimulation. Clin. Orthop. Relat. Res., 175: 30-36, 1983.

[3] Graupe D, Kohn KH, Functional neuromuscular stimulator for short-distance ambulation by certain thoraciclevel spinal-cord-injured paraplegics. Surgical Neurology, 50: 202-207, 1998.

[4] Popović D, Tomović R, Schwirtlich L, Hybrid assistive system – the motor neuroprosthesis. IEEE Trans. Biomed. Eng., 36: 729-737, 1989.

[5] Spadone R, Merati G, Bertocchi E, et al, Energy consumption of locomotion with orthosis versus Parastep-assisted gait: a single case study. Spinal Cord, 41: 97-104, 2003.

[6] Chen Y, Yang B, Dong J, Time series prediction using a local linear wavelet neural network. Neurocomputing, 69: 449-465, 2006.

[7] Nekoukar V, Beheshti MT, A local linear radial basis function neural network for financial time-series forecasting. Applied Intelligence, 2009.

[8] Erfanian A, Kobravi HR, Zohorian O, et al, A portable programmable transcutaneous neuroprosthesis with built-in self-test capability for training and mobility in paraplegic subjects. Proc. 11th Ann. Conf. Int. Functional Electrical Stimulation Society, 2006.

Author's Address

Vahab Nekoukar, Abbas Erfanian
Department of Biomedical Engineering, Iran University of Science and Technology (IUST), Neural Technology Research Centre, Tehran, Iran.
nekoukar@iust.ac.ir, erfanian@iust.ac.ir.

The effects of intermittent electrical stimulation with varying load and stimulation paradigms for the prevention of deep tissue injury

Curtis C[1], Chong SL[2], Mushahwar VK[1,2]

[1] Department of Cell Biology, University of Alberta, Edmonton, Alberta, Canada

[2] Centre for Neuroscience, University of Alberta, Edmonton, Alberta, Canada

Abstract

A pressure ulcer is a medical complication that arises in persons with decreased mobility and/or sensation. Deep pressure ulcers starting at the bone-muscle interface are the most dangerous, as they can cause extensive damage before showing any signs at the skin surface. We proposed a novel intervention called intermittent electrical stimulation (IES) for the prevention of deep tissue injury. In this study, we tested the effects of four paradigms of IES and one conventional pressure relief paradigm in preventing the formation of deep pressure ulcers in rats. Pressures equivalent to 18%, 28%, or 38% of the body weight of each rat were applied to the triceps surae muscle in one limb. Treatment groups received IES every ten minutes for either 5s or 10s and maximal or moderate contraction, or complete pressure removal every ten minutes for 10s. The results showed that conventional pressure relief, emulating a wheelchair pushup every ten minutes, was inadequate for the prevention of deep tissue injury. In contrast, all IES paradigms were equally effective in significantly reducing the extent of deep muscle damage caused by 28% or 38% BW pressure application. This outcome provides important information for the development of an alternative method for pressure ulcer prevention.

***Keywords**: deep tissue injury, intermittent electrical stimulation.*

Introduction

Pressure ulcers are a serious complication associated with loss of mobility and/or sensation. They result from the entrapment of soft tissues between a bony prominence and an external surface. The resulting lesion may involve damage to the skin, fat, and muscle layers, and in extreme cases exposing bone.

The costs to heal a pressure ulcer range from US$15,800 to US$72,680 [1]. The total financial costs to the health care system are between $2.2 and $3.6 billion USD [2] annually, in North America alone.

Pressure ulcers can begin at the surface of the skin and progress inwards. These ulcers are mainly the result of bad nutrition, excessive wetness, and frictional forces applied to the skin [3]. More dangerously, ulcers can begin deep at the bone-muscle interface and progress through tissue layers towards the skin. This type of ulcers has been recently identified as deep tissue injury (DTI). It develops as a result of sustained compressive pressure which leads to: 1) damaging mechanical deformation in muscle tissue, and 2) ischemia and an ensuing cascade of harmful metabolic changes. Because muscle is more susceptible to breakdown due to pressure than skin, this latter class of pressure ulcers can develop unbeknownst to the afflicted individual or their care giver. Once skin signs become apparent, substantial damage to underlying tissue would have taken place.

There are currently several interventions for the prevention of pressure ulcers. These include frequent repositioning of individuals [4-6], as well as the use of specialized cushions and mattresses. Despite these efforts, none of the current interventions has succeeded in decreasing the incidence of pressure ulcers consistently and reproducibly [7,8]. An alternative prevention technique is needed, particularly for ulcers of deep origin.

We have previously shown that intermittent electrical stimulation (IES) can be effective in the prevention of DTI [9]. It was suggested that the IES-evoked contractions allow the muscle to reshape periodically, thus relieving pressure at the bone-muscle interface, restoring blood flow, and increasing oxygen in the tissue. The hallmark feature of IES is the substantially longer "OFF" period relative to the "ON" period of stimulation, which prevents muscle fatigue. To date, the standard IES pattern has been 10s of maximal stimulation once every ten minutes.

The goal of this study was to determine the most

suitable parameters of IES that could be used in clinical settings. More specifically, we investigated the effect of the duration of the "ON" period of IES and intensity of stimulation on its ability to prevent deep muscle damage under varying levels of loading pressure.

Materials and Methods

Experimental Setup and Procedures

Experiments to quantify damage in the deep tissue caused by externally applied pressure were performed in sixty-four adult female Sprague-Dawley rats. All procedures were approved by the University of Alberta animal ethics committee.

Under isoflourane (2%) anaesthesia, constant pressure equivalent to 18%, 28%, or 38% of the rat's body weight (BW) was applied to the triceps surae muscle group in one hind limb. The 38% BW load resembled the load experienced by tissue around the ischial tuberosities (ITs) while sitting on a hard surface [10]. The 28% and 18% BW loads represented the loads experienced when sitting on softer surfaces including wheelchair cushions. Pressure was applied via a 3mm-diameter indenter for two hours (see Fig. 1).

The rats were divided in two groups: one that received stimulation of the experimental limb during the loading period and one that did not. The no IES group included a control subgroup (CG), and a conventional pressure relief subgroup (PG). Rats in CG only received the pressure application, and rats in PG received manual removal of the pressure for 10s every 10 minutes.

The IES group included four subgroups: maximal stimulation for either 5 or 10s (Max5 & Max10), and moderate stimulation for either 5 or 10s (Mod5 & Mod10). Prior to the pressure application, all animals in the IES group were implanted with a nerve cuff around the tibial nerve. *While IES in human volunteers is delivered non-invasively through surface electrodes,* a nerve cuff was necessary in the rat due to the small size of the muscles and the substantial movement between the skin and underlying motor points. Rats in the IES subgroups received the 5 or 10s bouts of stimulation (50Hz, 100µs, charge balanced, constant current) every 10 minutes throughout the period of pressure application. After the two hour period, all rats recovered from anaesthesia and the opioid analgesic, buprenorphine, was administered to ensure comfortable recovery.

Assessing the Extent of Deep Tissue Injury

Between 17 and 24 hours after the removal of pressure, the rats were anesthetized with sodium pentobarbital (i.p., 45mg/kg). Magnetic resonance imaging of both hind limbs was performed in a 3.0T magnet using a custom-built, 8 cm birdcage coil and a T_2-weighted spin-echo sequence. Subsequently, the rats were perfused and the triceps surae muscles from both hind limbs were extracted and prepared for later histological analysis.

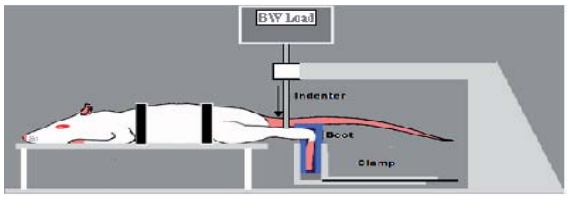


Fig. 1: Diagram showing the apparatus used for applying controlled levels of pressure.

The acquired images were analysed using custom written Matlab codes, allowing the quantification of muscle regions exhibiting edema (see Fig. 2). The contralateral leg was utilized as an internal control for each rat, and the extent of edema in the experimented limb was expressed as a percent of the muscle volume.

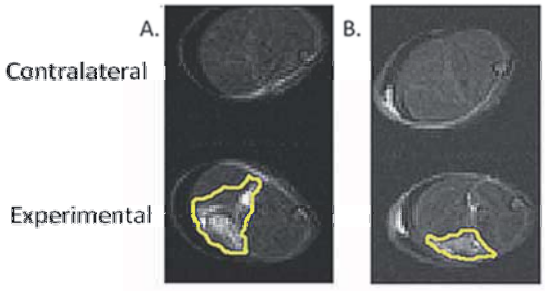


Fig. 2: Quantification of edema with *in vivo* MR; reduction in edema from 60.31% in a CG rat (A) to 31.23% in a Mod10 rat (both loaded with 38% BW).

Results

Effect of IES on Extent of Deep Tissue Injury

As expected, the extent of edema in the control groups (CG) increased significantly with increasing load ($p=0.003$, one-way ANOVA), demonstrating that an increase in pressure corresponds to an increase in muscle damage. The extent of muscle edema in the conventional pressure relief group (PG) was not significantly different from that in the control group for all loading levels, in clear contrast to the outcome seen with IES.

A significant reduction in the extent of edema was produced with IES in the rats that received 28% and 38% BW loading relative to the non-IES groups ($p=0.05$, one-way ANOVA). IES reduced edema by approximately 50% in both groups: from

an average of 28.75% to 13.92% in the 28% BW group and from an average of 43.23% to 23.45% in the 38% BW group. Surprisingly, there were no significant differences between the Max10, Max5, Mod10, and Mod5 groups for both of the higher load groups; all were equally effective in reducing damage in deep muscle tissue (see Fig. 3).

The level of edema in the 18% BW group was variable in this data set. None of the treatments in this group significantly reduced edema produced by the application of pressure.

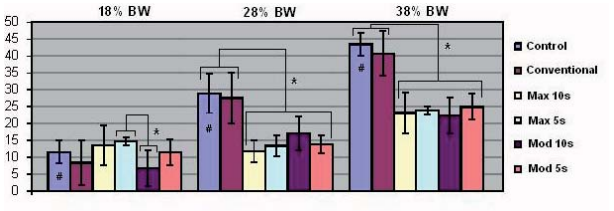


Fig. 3: The average percent of edema in the experimental hind limb in each group for all loads, mean ± SE (*, # significantly different from each other).

Discussion

The results showed that the application of external pressure equal to 28% or 38% BW for durations as short as two hours is enough to generate a significant amount of damage in the deep tissue. The extent of the damage was closely correlated to the level of pressure applied. We found that the muscle indeed is more susceptible to damage than the skin. The outside surface of the skin in all experimental limbs appeared normal and provided no clues regarding the underlying edema in the muscle.

The use of IES showed a significant beneficial effect when applied to muscles exposed to prolonged periods of loading with 28% or 38% BW. Interestingly, conventional pressure relief, which is similar to a person performing wheelchair push-ups, did not show the same beneficial effects obtained by IES. We believe this is due to the dynamic and active nature of the IES-induced contraction which allows not only for a transient increase in blood flow, but also to a sustained increase in oxygen in the compressed tissue [11]. We found that IES worked equally well for all parameters of "ON" period tested, which varied in intensity and duration. This suggests that a 5s-long moderate muscle contraction produced every 10 minutes is adequate for reducing the extent of deep tissue injury. Future studies will explore additional parameters including the longest duration of "OFF" period needed to retain the benefits of IES. Understanding the effect of IES parameters on deep tissue injury will allow for implementation of this approach at its maximal potential.

Conclusions

The results demonstrate that IES reduces the extent of damage in deep tissue even when utilized to elicit 5s-long moderate contractions in the compressed muscles every 10 minutes. When combined with existing pressure relief strategies, IES could provide an effective prophylactic means for preventing the formation of pressure ulcers. Plans are underway for utilizing IES in clinical settings to prevent the formation of pressure ulcers in persons with decreased mobility.

References

[1] Rischbieth H, Jelbert M & Marshall R. Neuromuscular electrical stimulation keeps a tetraplegic subject in his chair: a case study. *Spinal Cord,* vol. 36: pp. 443-445, 1998.

[2] Zanca JM, Brienza DM, Berlowitz D, et al. Pressure ulcer research funding in America: creation and analysis of an on-line database. *Advances in Skin & Wound Care*, vol. 16: pp. 190-197, 2003.

[3] Salcido SB, Fisher JC, Donofrio M, et al. An animal model and computer-controlled surface pressure delivery system for the production of pressure ulcers. *Journal of Rehabilitation Research & Development*, vol. 32: pp. 149-161, 1995.

[4] Grip JC & Merbitz CT. Wheelchair-based mobile measurement of behavior for pressure sore prevention. *Computer Methods & Programs in Biomedicine*, vol. 22: pp. 137-144, 1986.

[5] White GW, Mathews RM & Fawcett SB. Reducing risk of pressure sores: effects of watch prompts and alarm avoidance on wheelchair push-ups. *Journal of Applied Behavior Analysis*, vol. 22: pp. 287-95, 1989.

[6] Merbitz CT, King RB, Bleiberg J, et al. Wheelchair push-ups: measuring pressure relief frequency. *Archives of Physical Medicine & Rehabilitation*, vol. 66: pp. 433-8, 1985.

[7] Thomas DR. Are all pressure ulcers avoidable? *Journal of the American Medical Directors Association*, vol. 4: pp. S43-S48, 2003.

[8] Krause JS & Broderick L. Patterns of recurrent pressure ulcers after spinal cord injury: identification of risk and protective factors 5 or more years after onset. *Archives of Physical Medicine & Rehabilitation*, vol. 85: pp. 1257-64, 2004.

[9] Solis LR, Hallihan D, Uwiera RE, et al. Prevention of pressure-induced deep tissue injury using intermittent electrical stimulation. *Journal of Applied Physiology,* vol. 102: pp. 1992-2001, 2007.

[10] Harrison DD, Harrison SO, Croft AC, et al. Sitting biomechanics Part I: Review of the literature. *Journal of Manipulative and Physiological Therapeutics,* vol. 22: number 9, 1999.

[11] Gyawali S, Solis L, Chong SL, et al. A new potential method for the prevention of pressure ulcers (submitted)

Acknowledgements

Funding for this work was provided by the Canadian Institutes of Health Research and the Alberta Heritage Foundation for Medical Research.

Author's Address

Cara A. Curtis, Research Assistant
caraanne@ualberta.ca

Repeated Bout Effect during Eccentric FES cycling: Pilot data

Fornusek C and Davis GM

Clinical Exercise and Rehabilitation Unit, University of Sydney, Australia.

Abstract

Purpose: *To investigate the potential of electrical stimulation-induced eccentric muscle contractions to enhance the benefits of functional electrical stimulation leg cycle ergometry (FES-LCE) in persons with spinal cord injury (SCI). Initial tests demonstrated that acute bouts of eccentric FES cycling exercise are safe and provide intense exercise to the muscles. Normally-innervated muscle adapts rapidly to repeated bouts of electrical stimulation-induced eccentric exercise. Therefore, in theory paralyzed muscle should adapt to eccentric exercise and allow higher loading to be developed on the muscles and bones of paralyzed lower limbs.* ***Methods:*** *Three experienced FES cyclists with SCI (ASIA A) undertook two sessions of 30-min eccentric FES-LCE (25 rev•min^{-1}) separated by 2 weeks. Standard concentric FES-LCE performance was measured 48hr pre and post each eccentric FES-LCE session.* ***Results:*** *Concentric FES-LCE performance decreased 48hr post eccentric FES-LCE, but less so after the 2nd eccentric cycling session. Additionally, less stimulation was required during the 2nd eccentric cycling session to maintain the desired power absorbance during cycling.* ***Conclusion:*** *Trained paralyzed SCI muscle appears to tolerate and adapt well to eccentric FES-LCE. Continued exposure to eccentric FES-LCE may allow the development of greater muscles forces during FES-LCE.*

Keywords*: Spinal Cord Injury, Eccentric contraction, Cycling Exercise, Electrical Stimulation.*

Introduction

During Functional Electrical Stimulation leg cycle ergometry (FES-LCE), a computer controls electrical stimulation to paretic or paralyzed muscles to elicit the appropriate contractions to pedal a cycle ergometer. Despite bestowing positive health benefits, and the relatively widespread use of FES cycling in research, there has been a slow uptake and uneven application of FES-LCE in SCI rehabilitation. Obstacles include uncertainty whether the perceived benefits exceed the regular training effort invested and whether FES cycling systems build muscle mass or maintain bone density in patients.

Eccentric exercise involves applying stretch-resistance to muscle while it is actively shortening. Low-intensity voluntary eccentric exercise in weak populations (e.g. elderly [1]) has demonstrated substantial improvements in muscle hypertrophy and strength. Recent investigation with paralyzed muscles has suggested that eccentric FES-LCE is technically feasible and safe when performed appropriately [2]. Data from acute eccentric FES-LCE sessions suggested that it might offer a superior training stimulus compared to concentric FES-LCE which is usually employed. Preliminary results showed that substantial force loss was seen 24 hrs following eccentric exercise, but blood borne indicators of muscle damage were not observed suggesting that eccentric FES-LCE does not result in marked muscle damage.

The purpose of this study was to investigate the effect of repeated exposure to eccentric FES-LCE cycling. Non-paralyzed muscle adapts very quickly to eccentric exercise whether induced voluntarily or involuntarily via electrical stimulation [3]. If paralyzed muscle adapts to eccentric exercise then eccentric cycling may be a feasible part of an FES cycling program.

Material and Methods

Three people with SCI (3 ASIA-A) participated in this pilot study. Written informed consent was obtained from all subjects. Prior to commencing the study all subjects had trained with concentric FES-evoked cycling for at least 6 months. For training the subjects usually performed FES-LCE three times per week for up to 45 min.

The experiment involved six FES cycling trials performed over three weeks (Table 1). FES cycling was performed on a custom built FES cycling system based around a Motomed Viva cycle ergometer [4]. In the first and third week the subjects performed two concentric (Mon & Fri) and an eccentric FES cycling trials (Wed). For the second week the subjects returned to their usual

training schedule (FES cycling 2-3 times per week). Stimulation parameters during FES cycling were pulse-width 300 μsec, frequency 35Hz, and maximum pulse amplitude 140mA.

Each concentric cycling session was performed for 30-min at a preset power output using stimulation feedback (pulse amplitude modulation). Eccentric FES cycling was performed at a similar power (absorption) and was produced by stimulating the muscles 180° out of phase compared to concentric cycling firing angles. Stimulation amplitude was recorded during each FES cycling session.

Results

Compared to baseline measurements, concentric cycling performance was reduced 48hr after eccentric FES cycling (Figure 1). Reduction in cycling performance was apparent in the stimulation required to maintain the preset power output (100% vs. 73% maximum stimulation). The reduction in performance was less after the second eccentric cycling session with the stimulation taking longer to reach maximum stimulation (25min vs. 10min). Less stimulation was required to maintain cycling performance during the second eccentric session compared to the first (Figure 2).

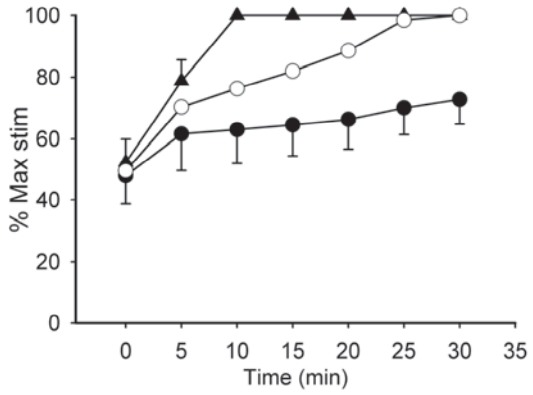


Figure 1 Comparison of stimulation current vs. time for concentric cycling sessions. Key: ● Baseline, ▲ 48h post eccentric cycling 1, ○ 48h post eccentric cycling 2. Error bars represent standard error (N=3).

Discussion

By visual inspection of changes in stimulation amplitude across the exercise sessions, paralysed muscle would seem to demonstrate the repeated bout effect from eccentric exercise. In populations with normal neural innervation, electrically-evoked eccentric exercise has demonstrated the repeated bout effect [3]. This suggests that the repeated bout effect is due to changes in muscle structure and muscle recruitment. Therefore, it is not surprising that paralyzed muscle would also adapt quickly to eccentric FES exercise.

Repeated exposure to eccentric FES cycling exercise might allow paralyzed muscle to develop greater eccentric muscle forces for further improvement in muscle hypertrophy and strength, and bone density.

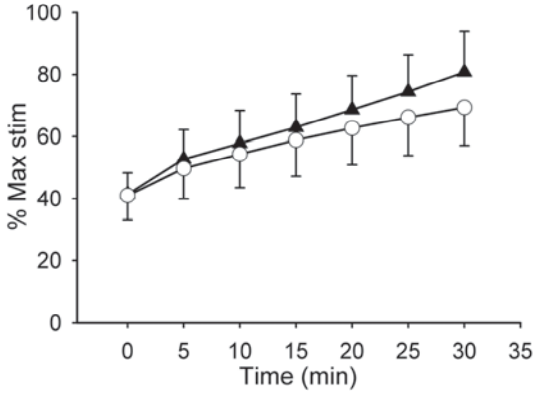


Figure 2 Comparison of stimulation current vs. time for eccentric cycling sessions. Key: ▲ eccentric cycling session 1, ○ eccentric cycling session 2. Error bars represent standard error (N=3).

Conclusions

Trained paralysed SCI muscle appears to tolerate and adapt well to eccentric FES-LCE. However, a carefully designed long-term training study is required to determine the benefits that eccentric FES cycling exercise might confer to persons with muscle paralysis or paresis.

References

[1] LaStayo PC, Ewy GA, Pierotti DD, et al., The positive effects of negative work: increased muscle strength and decreased fall risk in a frail elderly population. J Gerontol A Biol Sci Med Sci, 2003. 58(5): p. M419-24.

[2] Fornusek C, Ahmadi S, Crosbie J, et al. Eccentric Functional Electrical Stimulation Cycling. in *14th Annual International Functional Electrical Stimulation Society Conference*. 2009. Seoul, Korea.

[3] Black CD and McCully KK, Muscle injury after repeated bouts of voluntary and electrically stimulated exercise. Med Sci Sports Exerc, 2008. 40(9): p. 1605-15.

[4] Fornusek C, Davis GM, Sinclair P, et al., Development of an isokinetic functional electrical stimulation cycle ergometer. Neuromodulation, 2004. 7(1): p. 56-64.

Author's Address

Ché Fornusek
Clinical Exercise and Rehabilitation Unit
Exercise, Health, and Performance
University of Sydney
Che.Fornusek@sydney.edu.au

Cardiopulmonary responses to active and electrically stimulated stepping, with robotics assistance in early-stage spinal cord injury

Craven CTD [1,2], Gollee H [1,2], Purcell M [2, 3], Allan DB [2, 3]

[1] Centre for Rehabilitation Engineering, University of Glasgow, Glasgow, UK

[2] Scottish Centre for Innovation in Spinal Cord Injury, Glasgow, UK

[3] Queen Elizabeth National Spinal Injuries Unit, Glasgow, UK

Abstract

Early stage spinal cord injury involves a period of bed rest and low activity. Subsequent co-factors such as low blood pressure and muscle atrophy lead to a decrease in cardiopulmonary fitness. It is proposed here that the introduction of an appropriate training programme during the early stage of injury may attenuate this loss of fitness. This work examined the cardiopulmonary responses of three motor complete and three motor incomplete spinal cord injured subjects to a number of robotics-assisted stepping exercises. Subjects participated in periods of passive, active and electrically stimulated stepping. Increases in a number of cardiopulmonary parameters were observed with some subjects, in response to these exercises. These results show that those with an incomplete SCI may benefit from this form training during the early phase of injury.

Keywords: *spinal cord injury, rehabilitation, functional electrical stimulation, cardiopulmonary, erigo.*

Introduction

Spinal cord injury (SCI) results in partial or complete paralysis and loss of sensation below the level of lesion. In most cases, treatment involves an initial period of bed rest which causes rapid and extensive muscle atrophy in the affected limbs with a subsequent reduction in cardiopulmonary (CP) fitness [1].

Paralysis also inhibits vasomotor control and can result in orthostatic hypotension (OH) with vasodilatation occurring when moving from a supine to an upright position. Venous return and cardiac output are compromised, promoting OH and resulting in syncope or fainting [2]. Physical interventions for the prevention of OH include wheelchair training, compression stockings, passive movements of the legs and tilt table training with an integrated automated stepping device [3].

Delays in rehabilitation can occur as a result of secondary de-functioning due to prolonged bed rest and intractable OH. Active training with robotics assistance may induce positive CP adaptations and counteract the decline in fitness in early stage SCI.

Recent work has shown that some forms of robotics-assisted exercise may have a role in reducing the rate of decline of physical fitness [4, 5]. The aim of this work was to determine if training on a tilt table with an integrated automated stepping device (Erigo, Hocoma, Switzerland) (Fig. 1) can elicit a positive cardiopulmonary response in early-stage SCI subjects, and to investigate any differences in response between volitional stepping and stepping supported by electrical stimulation.



Fig. 1: Tilt table with integrated automated stepper

Methods

Subjects

This study was approved by the NHS South Glasgow and Clyde Local Research Ethics Committee. Six male SCI subjects (Table 1) were recruited from the Queen Elizabeth National Spinal Injuries Unit for Scotland (QENSIU). All subjects provided informed consent prior to participation. Subjects are identified in Table 1 as either motor complete (S_C) or incomplete (S_I).

Table 1: Subject profiles

Subject	Age [yr]	Weight [kg]	Post-injury [wks]	Level	AIS
S_C1	25	60	21	C3	B
S_C2	22	70	16	T4	A
S_C3	18	76	18	T8	A
S_I1	54	81	9	C4	C
S_I2	44	98	40	T2	D
S_I3	53	86	46	T9	C

Exercise protocol

Each subject was asked to participate in a set exercise protocol as identified in Table 2.

Table 2: Testing protocol

Phase	Position	Exercise
1	Supine	No stepping
2	Vertical	Automated stepping
3	Vertical	Automated stepping with volitional input*
4	Vertical	Automated stepping with volitional input* & FES

* motor incomplete subjects only

Each phase of exercise was five minutes in duration. The vertical phases of exercise were carried out at 70° of tilt from horizontal. Stepping speeds that were comfortable for each individual subject were selected and were in the range of 20 – 40 steps/minute.

Cardiopulmonary measurements

Oxygen uptake ($\dot{V}O_2$) (Metamax, Cortex Biophysik GmBH, Germany) and heart rate (*HR*) (Polar S410, Polar Electro Oy, Finland) were continuously measured throughout the experimental session.

Functional electrical stimulation

Transcutaneous neuromuscular electrical stimulation electrodes (PALS Platinum, Axelgaard, Denmark) were placed over the quadriceps (5×10 cm oval), hamstring (5×10 cm oval) and calf (4×6.4 cm oval) muscle groups while the subject was in the supine position. Stimulation was applied automatically and in time with the robotics-assisted stepping (Motionstim, Krauth+Timmermann, Germany). Stimulation frequency and pulse width were fixed at 20 Hz and 300 µs respectively. Stimulation intensities (28 – 100 mA) were adjusted individually for each muscle group. Stimulation intensity was set to maximum for the complete subjects and was set to a level that was comfortable for those subjects with sensation.

Statistical analysis

Data recorded in the fourth minute of each phase of exercise was averaged for each subject. The fourth minute was chosen to allow a sufficient transition from the previous phase to occur. Data from the complete and incomplete subjects were pooled and analysed separately. A repeated measures ANOVA (SPSS v.15.0, IBM, USA) was performed and a Mauchly test with a Huynh-Feldt correction was applied. When applicable a post-hoc Wilcoxon signed rank test was performed.

Results

Baseline (Phase 1) was compared to the passive (Phase 2), active (Phase 3) and electrically stimulated (Phase 4) periods of exercise. Active and electrically stimulated periods of exercise were also compared for the incomplete subjects.

The averaged $\dot{V}O_2$ and *HR* data are presented in Fig. 2 and 3 respectively. $\dot{V}O_2$ was normalised with respect to body weight and all error bars indicate one standard deviation.

$\dot{V}O_2$ and *HR* did not change throughout the passive phases of exercise. No changes were observed during the active phase of exercise (Phase 4) for the complete subjects. An increase was found during the active phases (Phase 3 and 4) of exercise for the incomplete subjects, though these increases were not found to be significantly different from baseline.

A comparison of active (Phase 3) and electrically stimulated (Phase 4) stepping for the incomplete subjects indicates that the addition of FES may elicit an increased $\dot{V}O_2$ and *HR* response over volitional input alone, though these increases were not found to be statistically significant.

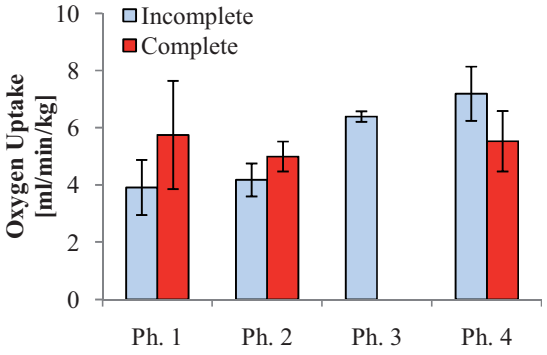


Fig. 2: Phase comparison of oxygen uptake

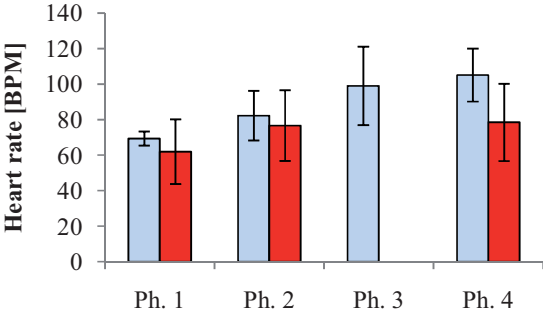


Fig. 3: Phase comparison of heart rate

Figure 3 compares the $\dot{V}O_2$ of a complete and an incomplete subject (S_C2 and S_I2). During Phase 4, the $\dot{V}O_2$ of the incomplete subject is much larger than that of the complete subject. This suggests that there is a CP benefit to volitional participation in this form of robotics-assisted exercise.

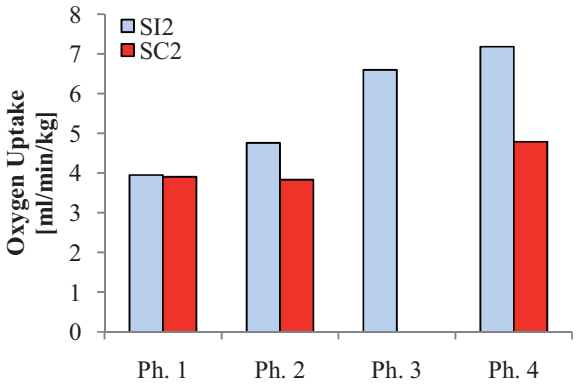


Fig. 4: Comparison of oxygen uptake

Discussion

Increases in CP and vascular parameters were found for the incomplete subjects, who also reported feeling fatigued at the end of the test.

The benefits of applying FES are unclear. Phase 4, the only phase that included FES, also required a degree of volitional input. The magnitude of the FES contribution to the exercise is not quantified and is further questioned by the similar results found in the complete subjects, who were unable to make a volitional contribution to the exercise. No increase in $\dot{V}O_2$ or *HR* were found for the complete subjects in response to FES.

The complete subjects were found to have highly atrophied leg muscles, which may have contributed to the poor responses found. It may be possible to improve their response by extending the intervention with a period of muscle conditioning and by starting training as early as possible to minimise the effects of muscle atrophy.

A spinal lesion at level T6 or above compromises the normal function of the sympathetic nervous system. In this study, no difference was found when comparing the results of those with a high level injury (T6 and above) to those with a low level injury (below T6). However, the small number of subjects tested makes it difficult to conclusively report on the effect of compromised sympathetic nervous function during this form of exercise.

This pilot study included a small and complex case mix and varying time of intervention post injury. Due to these limitations, statistical significance was not found, although clear trends could be observed for the incomplete subjects.

The variable results found in this pilot protocol would not support universal adoption of this type and timing of intervention but would suggest that targeted training may be beneficial in selected groups such as early incomplete injuries.

Conclusions

Oxygen uptake and heart rate were found to increase for incomplete SCI subjects during robotics assisted stepping. This modality of exercise may provide an effective form of cardiopulmonary training in SCI if instituted early, before the onset of extensive muscular atrophy.

References

[1] Bloomfield SA. Changes in musculoskeletal structure and function with prolonged bed rest. Med Sci Sports Ex, 29: 197-206, 1997.

[2] Shibao C, Grijalva CG, Raj SR et al. Orthostatic hypotension-related hospitalization in the United States. Am J Med, 120: 975-980, 2007.

[3] Czell D, Schreier R, Rupp R et al. Influence of passive leg movements on blood circulation on the tilt table in healthy adults. J Neuroeng Rehabil, 1: 4, 2004.

[4] Hunt K, Jack L, Pennycott A et al. Control of work rate-driven exercise facilitates cardiopulmonary training and assessment during robot-assisted gait in incomplete spinal cord injury. Biomed Sig Proc Control, 3: 19-28, 2008.

[5] Pennycott A, Hunt K, Jack L et al. Estimation and volitional feedback control of active work rate during robot-assisted gait. Control Eng Prac. 17: 322-328, 2009.

Acknowledgements

We would like to acknowledge the consultants, nursing staff and physiotherapists at QENSIU and our colleagues from the University of Glasgow whose assistance and input was invaluable in completing this research.

Author's Address

Colm Craven
Centre for Rehabilitation Engineering
James Watt (South) Building
University of Glasgow
Glasgow
G12 8QQ
UK
ccraven@eng.gla.ac.uk
www.gla.ac.uk/cre
www.scisci.org.uk

Effects of Recovery after Fatigue on M-wave vs Torque Relationships during Isometric FES-induced Contractions

Davis GM [1], Estigoni EH [1], Fornusek C [1] and Smith RM [2]

[1] Clinical Exercise and Rehabilitation Unit, [2] Exercise Health and Performance Research Group, The University of Sydney, Australia

Abstract

FES-evoked electromyography (eEMG) has been used to characterize the onset of fatigue in individuals with spinal cord injury (SCI). However, the relationship between eEMG and muscle torque is not always consistent amongst individuals nor over repeated bouts of FES-exercise.

***Purpose**: This study investigated whether the relationship between Torque and eEMG variables remained constant after short recovery periods between repeated bouts of isometric FES contractions.*

***Methods**: Six SCI males volunteered to participate in this study. We employed a custom-built evoked EMG acquisition system to control FES and synchronize myoelectric signals with torque data from a Biodex muscle dynamometer. Each subject performed 3 FES-induced isometric contractions with the knee at 60 deg separated by recovery periods.*

***Results:** Inspection of time curves revealed that key m-wave variables recovered at a faster rate than did muscle torque during and after the 2nd and 3rd contractions. Different patterns emerged between individuals, but there was a clear trend for eEMG data to "recover" more quickly after repeated muscle stimulation.*

***Conclusions**: Since the relationships between m-waves and muscle torque was not consistent between the 3 contractions, the potential use of eEMG signals as a proxy for muscle fatigue must be further investigated. Clinicians may need to re-plan their strategies for using eEMG as feedback for muscle fatigue in SCI individuals and further explore the different causes of fatigue during FES-induced exercise.*

***Keywords**: FES-induced fatigue, Evoked electromyography, Isometric muscle contraction.*

Introduction

Functional electrical stimulation (FES) - evoked exercise can increase leg muscle strength and provide functional outcomes for people with neurological impairments. Cycling, standing, stepping and walking are examples of exercise modes that may be induced via FES [1]. However, muscle fatigue occurs considerably more quickly in the muscles of spinal cord-injured individuals compared to the muscles of able-bodied persons, and especially under FES whereby muscle fibres are activated synchronously by external stimulation pulses [2].

Evoked EMG signals (eEMG; a.k.a. m-waves) are electrical muscle responses generated during FES-evoked contractions. They represent the sum of the action potentials from the activated motor units. Several authors have utilised eEMG signals during FES-evoked exercise to characterize the "quality" of muscle contractions and onset of fatigue in individuals with spinal cord injury [3, 4]. Rapid FES-induced muscle fatigue becomes particularly serious for neurological clinical populations when activating their lower limbs in upright postures, because it may lead to trips, falls [5] or unexpected knee-buckle [6].

We have recently proposed interval training (i.e. short bouts of FES-evoked leg exercise with recovery periods) as an alternative approach to continuous walking for functional gait training in the spinal cord injury (SCI) population [6]. As an adjunct to interval-type gait training, it might be useful if eEMG signals could be used to characterise or predict muscle fatigue in real time.

This study investigated whether the relationship between muscle torque and eEMG variables remained constant after short recovery periods between repeated exercise intervals of isometric muscle contractions induced by FES.

Material and Methods

Subjects:

Six SCI males, with complete or incomplete spinal cord lesions between C7 and T11, aged 45.6±15.7y and 10.5±6y since their injury incident volunteered to participate in this study. All were "experienced" FES users, currently undertaking such exercise at least twice weekly for previous months to years.

Evoked-Electromyography and FES systems

We employed a custom-built computerized evoked-EMG acquisition system − the UniSyd e^2MG [7]− to acquire myoelectric signals with torque data from a Biodex® muscle dynamometer. Bipolar eEMG detection (Noraxon dual, 10mm diameter, 20 mm centre to centre, Ag/AgCl) was deployed to gather myoelectric data. On each subject's bilateral lower limbs, two medium size stimulating electrodes were positioned above and below the quadriceps muscle belly. FES parameters were biphasic pulses, with a frequency of 25Hz, pulse width = 300μs and amplitude up to 140mA as required to attain a desired torque of 40Nm. Each subject performed three FES-induced isometric contractions at 60° knee angle separated by recovery periods (5 min), and muscle torque and eEMG data were pooled from both limbs for later analysis. Contraction intervals lasted from 20s-60s depending upon when muscle forces fell below 40% of their maximal value for the first contraction.

Using the UniSyd e^2MG system, seven variables were extracted and plotted in real-time from the acquired m-waves: (i) positive peak amplitude; (ii) negative peak amplitude; (iii) peak-to-peak amplitude; (iv) peak-to-peak duration; (v) time between stimulus artefact and positive peak; (vi) time between artefact and negative peak; and (vii) m-wave area [8]. In the current paper, only muscle torque [Torque], peak-to-peak amplitude [P2Pamp] and m-wave area [M-area] data have been presented for brevity. For each subject, data have been normalised to 100% representing the highest value for each variable in the first contraction interval.

Repeated-measures ANOVA was employed to determine whether repeated intervals of FES isometric contractions resulted in delayed times to peak for Torque, P2Pamp and M-area. Regression analysis was used to explore relationships between muscle torque, eEMG variables and time. Significance was set to the 95% confidence level ($P<0.05$) and data are shown as mean ± SE.

Results

Fig. 1 portrays from the onset of neurostimulation, that Torque showed a significantly longer time to achieve its maximal value in the second (5.83±0.93s) and third FES intervals (7.64±0.85s) compared to the first (3.24±0.92s) [$P<0.05$]. In contrast, time to maximal P2Pamp only showed a significantly quicker response between the third interval (13.36±1.65s) and the first (16.91±1.32s) [$p<0.05$]. There were no significant differences between contraction intervals for time to greatest M-area.

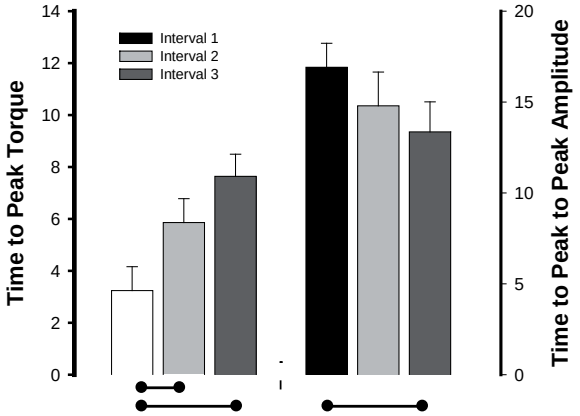


Fig. 1: Time to maximal Torque (left panel) and time to peak P2Pamp (right panel) for FES exercise intervals separated by brief recovery periods. ●● denotes $p<0.05$ between mean contractions. While time to achieve maximum Torque became progressively longer, time to peak P2Pamp shortened.

Fig. 2 and Fig. 3 portray the Torque-time and P2Pamp-time relationships for the first through third FES-evoked contraction intervals. Curves are shown from the point in time where P2Pamp started to decay.

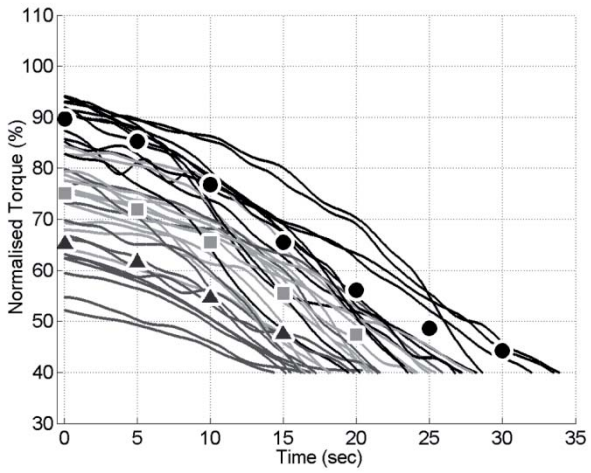


Fig. 2: Decline of normalised torque during the first (black-●), second (light gray-■) and third (dark gray-▲) contraction interval. Interpolation markers fitted by uniform Loess smoothing. Shifting of curves downwards is clearly observed and initial force was lower during each subsequent contraction

Discussion

In the current paper we presented evidence of delayed-onset of muscle contraction force for FES-evoked isometric exercise intervals lasting 20s to 60s duration. Time to peak torque nearly tripled,

from the first to third contraction. In contrast, time from onset of neurostimulation to maximal P2Pamp fell modestly, and was only different between the first and last contractions.

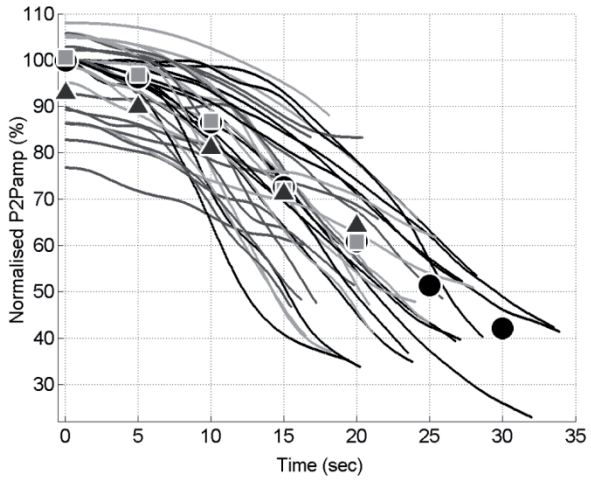


Fig. 3: Decline of normalised P2Pamp during the first (black-●), second (light gray-■) and third (dark gray-▲) contraction intervals. Interpolation markers fitted by uniform Loess smoothing. No shifting of curves is observable and subsequent initial P2Pamp always above 75%

From onset of neurostimulation, while P2Pamp and M-area curves were still increasing towards their maximal values (plateau) during the first FES contraction interval, Torque was already declining with values observed around 90% and 85% of peak, respectively. During this brief period of time, m-wave variables and the Torque were shifting in opposite directions. Consequently, different patterns were observed between them. To reduce this discrepancy, we filtered out samples from Torque and m-wave date obtained during the ascending part of the P2Pamp curves. Logistic sigmoid regression models would then fit P2Pamp curves for most subjects or trials. However, a single sigmoid regression model to fit all variables for all subjects and every trial was not achieved.

Torque data on the muscle dynamometer revealed substantial decrease from the 1st through 3rd contraction, suggesting poor recovery of muscle forces between the FES intervals. Changes appeared to reside within the intercept coefficients of the regression model, with no apparent change of the torque-time slopes. P2Pamp and M-area showed full recovery between contractions 1 and 2; with values occurring above 100% of the first interval for some subjects (this has been termed "m-wave potentiation"). During the third contraction interval, P2Pamp and M-area also presented higher averaged values than the Torque data. No significant differences between contractions 1 and 2 could be detected on the averaged m-wave variables.

Conclusion

Since the relationships between m-waves and muscle torque appeared to be inconsistent between the 3 FES contractions in these SCI subjects, the potential use of eEMG signals as a proxy for muscle fatigue must be further investigated. If FES-evoked interval exercise is to be preferred for gait training [6], then improved "fatigue prediction" from eEMG signals must be achieved.

References

[1] Davis GM, Hamzaid NA and Fornusek C. Cardiorespiratory, metabolic and biomechanical responses during FES leg exercise: Health and fitness benefits. *Artif Organs*, **32**:625-629, 2008.

[2] B. Bigland-Ritchie B, et al, Excitation Frequency and Muscle Fatigue - Electrical Responses During Human Voluntary and Stimulated Contractions, *Experimental Neurology,* **64:**414-427, 1979.

[3] Tepavac D and Schwirtlich L, Detection and prediction of FES-induced fatigue, *Journal of Electromyography and Kinesiology,* **7**:39-50, 1997.

[4] Chang YJ and Shields RK, "Within-train neuromuscular propagation varies with torque in paralyzed human muscle," *Muscle & Nerve,* **26**: 673-680, 2002.

[5] Rushton DN, Functional electrical stimulation, *Physiological Measurement,* 18:241-275, 1997.

[6] Crosbie J, Russold M, Raymond J, Middleton JW and Davis GM. FES-supported interval training following sensorimotor-complete spinal cord injury: a case series. *J Neuromodulation*, **12**: 224-231, 2009.

[7] Estigoni EH, Fornusek C, Song T and Davis GM. A novel system for evoked EMG analysis: Design, construction, and validation. *Proc 14th Annual Conference of the International FES Society*, 88-90, 2009

[8] Estigoni EH, Fornusek C, Song T and Davis GM. Evoked EMG and fatigue during FES-induced muscle contractions: A Critical Review. *Proc 14th Annual Conference of the International FES Society*, 92-94, 2009

Acknowledgements

Mr Estigoni is the recipient of a CAPES award from Brazil, and this paper comprises a portion of his PhD studies

Author's Address

Professor Glen M Davis
Director, Clinical Exercise & Rehabilitation Unit
The University of Sydney, Australia
Glen.Davis@Sydney.edu.au

Session 12

FES and Human Motor Control 1

Neural control of posture and locomotion

Deliagina Tatiana

Department of Neuroscience, Karolinska Institute, Stockholm, Sweden

Maintenance of the basic body posture is a vital motor function based on in-born neural mechanisms. Inability to maintain the basic body posture and equilibrium is one of the major motor disorders following traumatic spinal cord injury, stroke and other neurological conditions. Instability of posture strongly affects locomotion in these patients. Selection of appropriate rehabilitation strategies (including FES) for compensation of locomotor and postural deficits depends largely on an elucidation of corresponding neural mechanisms. We study postural networks, their impairment caused by central and sensory deficits, as well as principles of their interaction with locomotor system, by using animal models. The main conclusions of our study are the following: (i) A number of motor centers (including motor cortex, brainstem and spinal cord) participate in stabilization of body orientation in space. Each of them operates on the feedback principle and generates corrective motor commands if the body orientation is perturbed. (ii) The spinal cord contains neuronal networks underlying spinal postural limb reflexes, which contribute to body stabilization in intact animal. (iii) Perturbations of body orientation during locomotion cause postural corrections, which are well incorporated into the basic locomotor pattern. (iv) Corticospinal and reticulospinal systems mediate interaction of postural and locomotor networks.

Neural control of human posture and movement: Modifications of monosynaptic lumbosacral posterior root-muscle reflexes

Hofstoetter US[1,2], Minassian K[1,2], Mayr W[2], Rattay F[1], Dimitrijevic MR[3,4]

[1] Institute for Analysis and Scientific Computing, Vienna University of Technology, Vienna, Austria

[2] Center for Medical Physics and Biomedical Engineering, Medical University of Vienna, Vienna, Austria

[3] Department of Physical Medicine and Rehabilitation, Baylor College of Medicine, Houston, TX, USA

[4] Foundation for Movement Recovery, Oslo, Norway

Abstract

The stabilization of the basic human body orientation in space relies on continuous motor coordination and dynamic adjustment of sensorimotor transmission, particularly during the execution of postural multi-joint and volitional single joint tasks. The underlying control mechanisms can be assessed by studying monosynaptic spinal reflexes and their movement-induced regulations. To elicit such responses in multiple lower limb muscles bilaterally and simultaneously, we applied a non-invasive technique of transcutaneous spinal cord stimulation. During the execution of controlled postural and volitional multi- and single joint lower limb movements, characteristic task-dependent reflex modifications were demonstrated: (i) The monosynaptic test reflexes were modulated in a way revealing the functional role of the muscles in a particular task. (ii) Information on motornuclei excitability was derived even for muscle groups that were quiescent during that task. (iii) The excitability of motornuclei was modified already in the preparatory phase of a movement, i.e., before its execution. The significance of the present approach lies in that it represents a vital tool to investigate how motor control is triggered and maintained in individuals with intact or altered nervous system functions. Furthermore, it allows evaluating the relation between segmental reflex organization and corrective movements during the execution of motor tasks.

Keywords*: monosynaptic spinal reflexes, posture, motor task, conditioning-test paradigm, sensorimotor transmission*

Introduction

Dynamic task-dependent regulation of spinal reflexes plays an essential role in human motor control and sensorimotor integration [1]. Commonly, the soleus H reflex has been used to assess the efficacy of the transmission from Ia afferents to alpha-motoneurons within the spinal cord [e.g. 2]. Though equivalents to the soleus H reflex can be also evoked in some other lower limb muscles by peripheral nerve stimulation, their selective elicitation is usually difficult to achieve, particularly during movements, and often requires special techniques such as reflex reinforcement [3].

We have previously shown that electrical stimulation applied over the lumbosacral spinal cord via epidurally implanted electrodes or electrodes placed over the body surface can elicit muscle twitches in multiple lower limb muscles bilaterally and simultaneously in subjects with injured or intact nervous system functions [4,5]. When elicited at low frequencies (e.g. 2 Hz) these responses, named posterior root-muscle (PRM) reflexes, were shown to be monosynaptic, segmental reflexes like the H reflex [4,5,6]. Recently, it was demonstrated that the stimulation of the spinal cord with surface electrodes can elicit PRM reflexes in upright standing healthy [7] and spinal cord injured people [8]. Thus, transcutaneous spinal cord stimulation (tSCS), providing afferent input to multiple segmental levels at the same time, presents a potent tool extending classical H reflex studies confined to a single muscle to investigating sensorimotor transmission of numerous lower limb muscles simultaneously.

Here, we aimed at testing the effect of distant, selective motor tasks and postural maneuvers incorporating the whole body on sensorimotor mechanisms regulating the reflex gain of multiple lumbosacral spinal cord segments. In a single subject, we furthermore assessed changes in motornuclei excitability taking place even before the execution of a movement, i.e., during its preparatory phase.

Material and Methods

Subjects

Four healthy subjects (aged 22-34, male) participated to the study. Stimulation and recording protocols utilized in this manuscript were approved by the local ethics committee.

Transcutaneous spinal cord stimulation

Self-adhesive surface electrodes (Schwa-medico GmbH, Ehringshausen, Germany) were used to apply tSCS. To this end, a pair of stimulating electrodes (Ø 5 cm) was placed on the back at T11-T12 vertebral levels, left and right to the spine. A pair of indifferent electrodes (8 x 13 cm) was attached to the abdomen, one on either side of the umbilicus. Both electrodes of each pair were connected to function as a single electrode. Symmetric, biphasic rectangular pulses with widths of 2 ms were delivered by a constant-voltage stimulator. For details see [5,7].

Surface-poly electromyography

Electromyographic (EMG) activity from quadriceps (Q), hamstrings (Ham), tibialis anterior (TA) and triceps surae (TS) bilaterally was recorded with surface electrodes. EMG signals were amplified using Phoenix amplifiers (EMS-Handels GmbH, Korneuburg, Austria) with a gain of 502 over a bandwidth of 20-500 Hz and digitized at 2048 Hz per channel.

Study protocol

Elicitation of PRM reflexes. PRM reflexes were elicited simultaneously in all recorded muscles. The placement of the stimulating electrodes was adjusted as to yield in symmetric bilateral responses. Stimulation intensity was increased until all evoked PRM reflexes had peak-to-peak amplitudes ≥ 100 μV. The reflex nature of the responses was verified by applying double stimuli 50 ms apart; attenuated responses to the second pulse hinted at long refractory periods associated with reflexes. For the conditioning-test paradigms, single stimuli were applied at 0.2 Hz.

Conditioning-test paradigms. For each paradigm, five unconditioned PRM reflexes were elicited followed by five conditioned ones. All responses of a recording were evoked under constant stimulation conditions. In three subjects, following conditioning-test paradigms were utilized: *(i)* unilateral dorsi- and plantar flexion (cycle period 6 s) in one of the lower limbs being unloaded while standing on the contralateral lower limb, with one hand resting gently on a bar; *(ii)* leaning forward and backward at the ankle from neutral standing. In one further subject, PRM reflexes were elicited in supine position during preparation phase of a volitional withdrawal movement performed in response to an acoustic signal.

Data analysis

The peak-to-peak amplitudes of the five unconditioned and conditioned PRM reflexes of each recording were computed and averaged. Mean conditioned responses were normalized with respect to the corresponding averaged controls. In case of unilateral dorsi- and plantar flexion, group results of the three subjects were derived by arranging both lower limbs into the categories ipsilateral or contralateral to the movement. The resulting six values for each muscle were averaged. Data were analysed off-line using Matlab 6.1 (The MathWorks, Inc., Natick, MA, USA).

Results

PRM reflexes in all recorded muscles bilaterally with peak-to-peak amplitudes ≥ 100 μV were elicited on average at 34.3 ± 3.4 V in the three subjects tested in standing position and at 31 V in the subject studied in supine position.

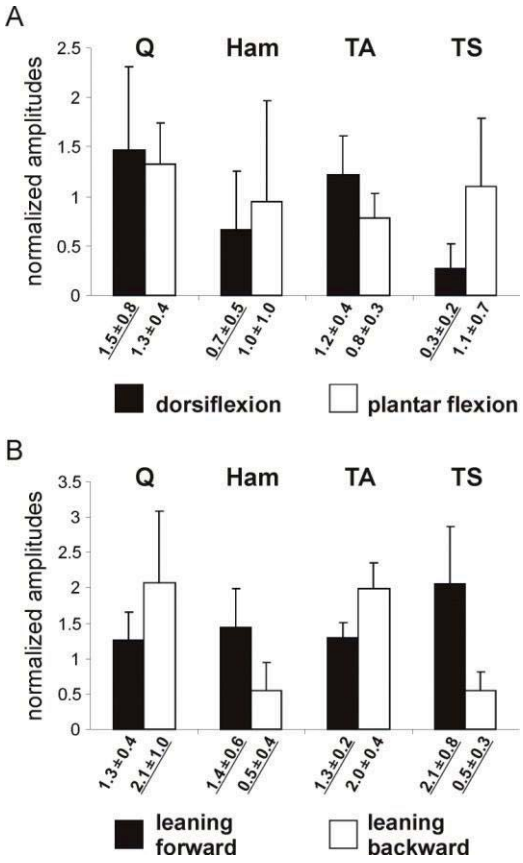


Fig. 1: Bar diagrams and inserted values representing group results of conditioning-test paradigms with peak-to-peak amplitudes of conditioned responses normalized with respect to unconditioned ones. Underlined values marking consistent results found in at least 5 of the 6 lower limbs studied. A, unilateral dorsi- (black bars) and plantar flexion (white bars) while standing on the contralateral lower limb; B, leaning forward (black bars) and backward (white bars) from neutral standing.

Unilateral dorsi- and plantar flexion in standing position. A consistent feature of PRM reflex modulations found in all tested subjects during dorsiflexion (Fig. 1A, black bars) was the suppression of ipsilateral Ham and TS responses

and the facilitation of the ipsilateral Q responses. During plantar flexion (Fig. 1A, white bars), PRM reflex modifications could vary interindividually; responses were either suppressed or facilitated with respect to the unconditioned controls. As compared to dorsiflexion, Ham and TS responses were always larger during plantar flexion (by a factor 1.29 and 6.36, respectively).

Leaning forward and backward at the ankle. Leaning forward was accompanied by facilitated Ham, TA, and TS responses (Fig. 1B, black bars). Leaning backward (Fig. 1B, white bars) resulted in a suppression of the responses of the posterior compartments of the lower limbs (Ham and TS) and a facilitation of the anterior compartments of thigh and leg (Q and TA).

Preparatory phase of a movement. During the preparatory phase of an active withdrawal movement (Fig. 2), facilitation of the Q responses ipsilateral to the planned motor act was revealed. At the same time, all recorded muscles of the contralateral lower limb stabilizing the body posture were facilitated.

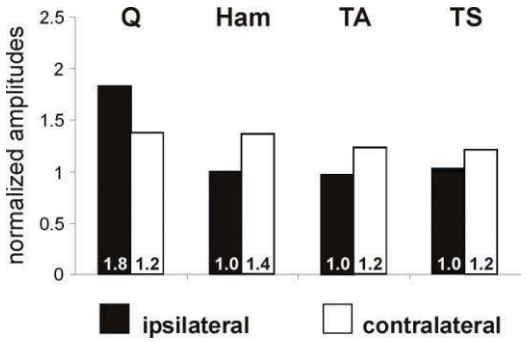


Fig. 2: Peak-to-peak amplitudes (bars and inserted values) of PRM reflexes elicited during the preparatory phase of a fast withdrawal movement normalized to the unconditioned controls. Data derived from a single subject in supine position.

Discussion and Conclusions

The present results demonstrate that PRM reflexes elicited in the lower limb muscles are modified in a way revealing the functional requirements of a particular motor tasks (e.g. attenuation of TS responses during dorsiflexion) and to counteract perturbation of equilibrium (e.g. facilitation of posterior lower limb compartments and TA responses during leaning forward, the latter due to the necessity to stiffen the ankle joint during this task). In particular, the excitability of motoneurons associated with muscles quiescent during a specific task is inhibited. Facilitation of responses elicited during the preparatory phase of a task showed that the motornuclei excitability is modified even before the execution of the movement.

The presented approach opens a new avenue for investigating how motor control is triggered and maintained at the level of the human lumbosacral spinal cord. Expanding the knowledge about the interaction between segmental reflex organization and automatic postural capacities will be crucial in designing new and adjusting already available rehabilitation strategies for restoration of locomotor functions in people with neurological disorders.

References

[1] Pearson KG, Collins DF. Reversal of the influence of group Ib afferents from plantaris on activity in medial gastrocnemius muscle during locomotor activity. J Neurophysiol, 70: 1009-1017, 1993.

[2] Brooke JD, Collins DF, Boucher S, et al. Modulation of human short latency reflexes between standing and walking. Brain Res, 548: 172-178, 1991.

[3] Burke D, Adams RW, Skuse NF. The effects of voluntary contraction on the H reflex of human limb muscles. Brain, 112: 417-433, 1989.

[4] Murg M, Binder H, Dimitrijevic MR. Epidural electric stimulation of posterior structures of the human lumbar spinal cord: 1. muscle twitches - a functional method to define the site of stimulation. Spinal Cord, 38: 394-402, 2000.

[5] Minassian K, Persy I, Rattay F, et al. Posterior root-muscle reflexes elicited by transcutaneous stimulation of the human lumbosacral cord. Muscle Nerve, 35: 327-336, 2007.

[6]Minassian K, Jilge B, Rattay F, et al. Stepping-like movements in humans with complete spinal cord injury induced by epidural stimulation of the lumbar cord: electromyographic study of compound muscle action potentials. Spinal Cord, 42: 401-416, 2004.

[7] Hofstoetter US, Minassian K, Hofer C, et al. Modification of reflex responses to lumbar posterior root stimulation by motor tasks in healthy subjects. Artif Organs, 32: 644-648, 2008.

[8] Dy CJ, Gerasimenko YP, Edgerton VR, et al. Phase-dependent modulation of percutaneously elicited multisegmental muscle responses after spinal cord injury. J Neurophysiol, 103: 2808-2820, 2010.

Acknowledgements

Austrian Science Fund (FWF), Proj.Nr. L512-N13.

Author's Address

Ursula S. Hofstoetter
Institute of Analysis and Scientific Computing, Vienna University of Technology, Vienna, Austria, and Center for Medical Physics and Biomedical Engineering, Medical University of Vienna, Vienna, Austria.
Ursula.Hofstoetter@gmail.com

Neurophysiology of the human lumbar locomotor pattern generator

Minassian K[1,2], Hofstoetter US[1,2], Tansey K[3,4], Rattay F[1], Mayr W[2], Dimitrijevic MR[5]

[1] Institute of Analysis and Scientific Computing, Vienna University of Technology, Vienna, Austria

[2] Center for Medical Physics and Biomedical Engineering, Medical University of Vienna, Vienna, Austria

[3] SCI Research, Shepherd Center, Atlanta, GA, USA

[4] Departments of Neurology and Physiology, Emory University, Atlanta, GA, USA

[5] Department of Physical Medicine and Rehabilitation, Baylor College of Medicine, Houston, TX, USA

Abstract

Human lumbar circuitries isolated from supraspinal structures by spinal cord injury (SCI) have the capability to generate locomotor-like lower limb movements. Continuous multi-segmental afferent input to the lumbar cord produced by epidural electrical stimulation can activate these premotoneuronal structures to generate rhythmic flexion-extension movements of paralyzed lower limbs. The corresponding EMG activities of thigh and leg muscles consist of series of responses to stimulation of posterior root afferents. These posterior root-muscle reflexes demonstrate phase-dependent alterations in amplitude as well as response latency within the rhythmic motor patterns. The data suggest that the human lumbar spinal circuitry can coordinate spatiotemporal patterns of motoneuron firing and select alternative segmental circuitries involved in the generation of rhythmic activity. Recently we described a non-invasive transcutaneous spinal cord stimulation technique of activating lumbar posterior root afferents. We used this technique to apply continuous stimulation in humans with SCI during treadmill stepping assisted either manually or by a robotic gait orthosis. We could demonstrate a phase-dependent augmentation of motor output in motor complete SCI and improved stepping in incomplete SCI subjects. Integrated into multimodality rehabilitation strategies, future biomedical engineering approaches should utilize the 'motor repertoire' of the human spinal cord to ameliorate motor function after injury.

Keywords*: spinal cord injury, spinal cord stimulation, treadmill stepping, spinal pattern generator, locomotion*

Introduction

The mammalian lumbar spinal cord contains neural circuitry that can be activated by a non-patterned drive to generate motor behaviours like stepping. In animals, these central pattern generators can be set into action by continuous electrical stimulation of supraspinal structures and their descending projections [1] as well as afferent pathways of the spinal cord (posterior roots/columns) [2,3]. When epidural spinal cord stimulation (eSCS) became available as a clinical tool, it provided a means to apply continuous stimulation to the posterior lumbar cord structures in humans [4].

We demonstrated that such non-patterned stimulation could produce stepping-like activity in complete spinal cord injured (SCI) persons in supine position [5,6]. The mechanisms for these effects have been attributed to stimulation of afferents within multiple posterior roots with subsequent trans-synaptic activation of lumbar locomotor networks by the tonic input conveyed via axonal collateral branches [6,7].

Recently, we described a method for non-invasive spinal cord stimulation through surface electrodes placed over the lumbar paraspinal and abdominal muscles, so-called transcutaneous spinal cord stimulation (tSCS) [8,9].

The purpose of the current report is to review evidence for the existence of a human spinal pattern generator for locomotion activated by eSCS. Neurophysiological information on the operation of these locomotor circuitries provided by electromyography from paralyzed lower limb muscles in motor complete SCI people will be presented. Finally, we will report our experience using continuous tSCS for enhancing motor output during treadmill stepping assisted manually or by a robotic gait orthosis, the Lokomat, in SCI subjects.

Material and Methods

Subjects

Six subjects with traumatic, complete SCI in a chronic condition participated to the study utilizing eSCS. The effect of tSCS was tested in 2 motor complete and in 4 non-ambulatory, motor-incomplete chronic SCI people.

Epidural spinal cord stimulation

The eSCS system consisted of a cylindrical array with four independent electrodes (Pisces-Quad electrode, Model 3487A, Medtronic, Minneapolis, MN, USA) connected to an implanted programmable pulse generator (Itrel 3, Model 7425, Medtronic), that generated monophasic, charge balanced stimuli with a pulse width of 210 µs. For details see [4,6].

Transcutaneous spinal cord stimulation

The stimulation method utilizes equipment available in electrodiagniostic laboratories and in physical rehabilitation departments. A pair of electrodes (∅ = 5 cm) were placed over the paravertebral skin on each side of the spine at the T11-T12 interspinous space (Fig. 1). Reference electrodes were a pair of rectangular electrodes (8 cm x 13 cm) placed over the abdomen. The two electrodes of each pair were connected to function as a single electrode. Symmetric, biphasic rectangular pulses of 2 ms width were delivered by a constant-voltage stimulator. The paravertebral electrodes were operated as the anode during the first phase of the stimulus pulse. Neural elements were stimulated at the transition from the first to second phase of the biphasic stimulus, when the function of the paravertebral electrodes changed from anode to cathode. For details see [8,6].

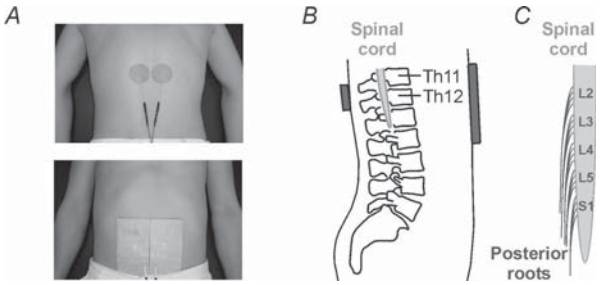


Fig. 1: *A*. Electrode placement for transcutaneous lumbar posterior root stimulation. *B*. Sketch of stimulation electrodes with respect to spine and spinal cord and of *C*. the stimulated posterior roots.

Results

Tonic eSCS at 25-50 Hz in complete SCI persons was effective to produce rhythmic lower limb muscle activities in supine position (Fig. 2). The EMG signals of the induced rhythmic activities consisted of series of compound muscle action potentials (CMAPs) occurring with the stimulation frequency. Each CMAP was a posterior root-muscle reflex (PRM reflex), initiated in large-diameter afferents of lumbosacral posterior roots and detected from the homonymous lower limb muscles. Thus, the muscle activities consisted of series of PRM reflexes, with characteristically modulated amplitudes forming the shape of an EMG burst, followed by phases of PRM reflex suppression.

In addition to amplitude modulations, we found alterations of PRM reflex latency within the rhythmic motor patterns as well as. Bursts during extension-like phases of rhythmic activities were composed of monosynaptic PRM reflexes. During flexion-like phases, these short-latency PRM reflexes were replaced by polysynaptic PRM reflexes in tibialis anterior and other muscles that were co-active. These data suggest that the human lumbar locomotor circuitries can produce coordinated spatiotemporal patterns of motoneuron firing as well as control the phase-dependent selection of segmental circuitries involved in the generation of rhythmic outputs.

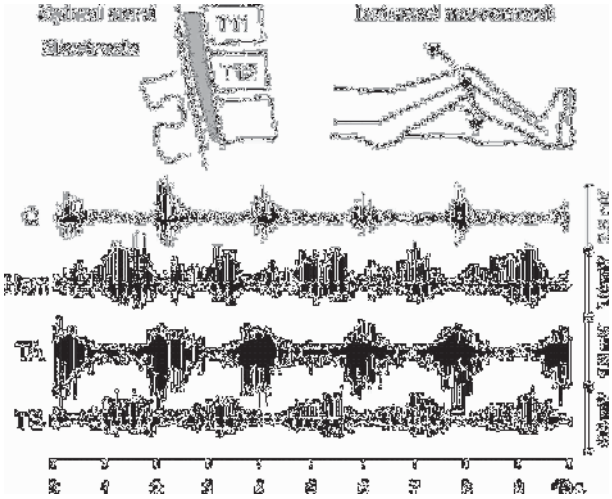


Fig. 2: Locomotor-like activity induced by continuous epidural spinal cord stimulation in a complete SCI individual in supine position. EMG activity of quadriceps (Q), hamstrings (Ham), tibialis anterior (TA), and triceps surae (TS); constant stimulation of posterior lumbar cord with 10 V, 25 Hz.

Continuous tSCS at 30 Hz augmented muscular activity recorded from EMG electrodes placed over proximal and distal flexors and extensors of the lower extremity as with eSCS. Stimulation applied to motor complete SCI subjects at moderate intensities during body weight supported treadmill stepping (BWSTS) considerably increased EMG amplitudes with minor changes of the EMG patterns of the paralyzed lower limb muscles as generated by manually assisted stepping alone. With stronger stimulation, rhythmic activities in the lower limb muscles were generated, but were not linked to the externally imposed gait cycle. The most profound effect of tSCS was seen in the incomplete SCI participants. Sub-motor threshold stimulation at 20-30 Hz (that produced paraesthesiae in the lower limb dermatomes) applied during BWSTS resulted in a gait-phase

appropriate augmentation of lower extremity motor output and improved limb movement (Fig. 3). In the Lokomat, adding loading and increasing gait speed improved EMG output but this was augmented to a greater extent when tSCS was simultaneously supplied.

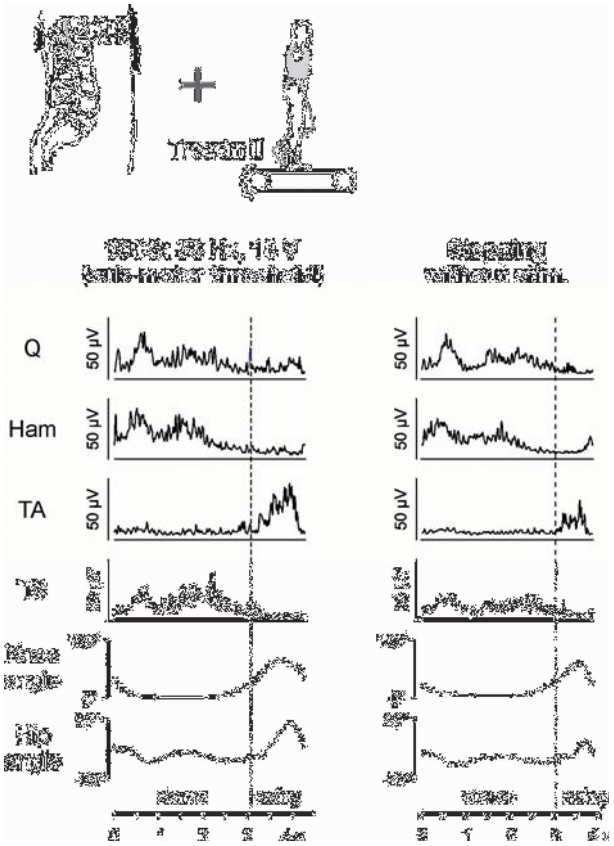


Fig. 3: Modulation of lower extremity motor outputs produced by continuous tSCS at 30 Hz applied to a motor incomplete SCI subject while performing treadmill stepping. Filtered, rectified EMG averaged from 10 step cycles with and without tSCS.

Discussion and Conclusions

The generation of stepping-like lower limb activity in humans does not require connectivity between the brain and spinal cord, when sustained electrical stimulation is delivered to the lumbar posterior roots. Afferent input to the human lumbar cord, when continuously and multi-segmentally provided, can activate premotoneuronal locomotor structures to generate rhythmic flexion-extension movements of the lower limbs.

This 'motor repertoire' of the human spinal cord should have important implications for strategies to improve motor function in humans with SCI or other motor disorders. Minimally-invasive epidural or non-invasive transcutaneous techniques of spinal cord stimulation are promising means to switch the circuits into different operating modes and produce multiple patterns of motor outputs and behaviour. It is very likely that these approaches will have even more potential with further technological development as well as when integrated into multimodality rehabilitation strategies including robotically-assisted locomotor training and FES.

References

[1] Shik ML, Orlovsky GN. Neurophysiology of locomotor automatism. Physiol Rev, 56: 465-501, 1976.

[2] Barthélemy D, Leblond H, Rossignol S. Characteristics and mechanisms of locomotion induced by intraspinal microstimulation and dorsal root stimulation in spinal cats. J Neurophysiol, 97: 1986-2000, 2007.

[3] Lavrov I, Dy CJ, Fong AJ, et al. Epidural stimulation induced modulation of spinal locomotor networks in adult spinal rats. J Neurosci, 28: 6022-6029, 2008.

[4] Pinter MM, Gerstenbrand F, Dimitrijevic MR. Epidural electrical stimulation of posterior structures of the human lumbosacral cord: 3. Control Of spasticity. Spinal Cord, 38: 524-531, 2000.

[5] Dimitrijevic MR, Gerasimenko Y, Pinter MM. Evidence for a spinal central pattern generator in humans. Ann N Y Acad Sci, 860: 360-376, 1998.

[6] Minassian K, Jilge B, Rattay F, et al. Stepping-like movements in humans with complete spinal cord injury induced by epidural stimulation of the lumbar cord: electromyographic study of compound muscle action potentials. Spinal Cord, 42: 401-416, 2004.

[7] Minassian K, Persy I, Rattay F, et al. Human lumbar cord circuitries can be activated by extrinsic tonic input to generate locomotor-like activity. Hum Mov Sci, 26: 275-295, 2007.

[8] Minassian K, Persy I, Rattay F, et al. Posterior root-muscle reflexes elicited by transcutaneous stimulation of the human lumbosacral cord. Muscle Nerve, 35: 327-336, 2007.

[9] Hofstoetter US, Minassian K, Hofer C, et al. Modification of reflex responses to lumbar posterior root stimulation by motor tasks in healthy subjects. Artif Organs, 32: 644-648, 2008.

Acknowledgements

The presented work was supported by the Austrian Science Fund (FWF), Vienna, Austria, # L512-N13, and the Wings for Life Spinal Cord Research Foundation, Salzburg, Austria, # WFL-FR-001/06.

Author's Address

Karen Minassian
Institute of Analysis and Scientific Computing, Vienna University of Technology
Wiedner Hauptstrasse 8-10/101,
Vienna, A-1040, Austria.
Karen.Minassian@gmail.com

Marked multi site stimulator of the lumbar posterior roots as a tool for studies of the locomotor pattern generator in humans.

Bijak M

[Vienna, Austria].

Successful demonstrations in humans showing that it is conceivable by transcutaneous electrical stimulation of lumbosacral roots in man to (1) lead to extension of this technique to studies of posterior root-muscle reflexes {PRMRR] elicited by single stimuli (2) as well by train of stimulation with lower [2-15 Hz] and higher frequency [20-50 Hz]. Single posterior root muscle reflexes resembled H-reflex responses but to the contrast of H-reflexes elicited by stimulation of mixed nerve trunks and recording H-wave in the corresponding muscle group H-wave; transcutaneous PRMRR can elicit simultaneously in a number of spinal cord segments PRMRR, equivalent to plurisegmental H-reflexes. This new exposition of spinal reflex activity with increased frequency reveals different functional configuration of lumbar interneurone and their functional presynaptic modification of spinal motor cells of motor nuclei resulting in a variety of functional movement in subjects with paralyzed lower limbs, due to separation from brain control by occasional traumatic SCI. Therefore, further studies become essential in order to have multisite stimulator with independent control of multiple (>8) stimulating channels in order to examine segmental organization of human lumbar pattern locomotor generator. We shall present technical characteristic of such multistimulator and how stimulation parameters, [strength, frequency, width of single stimuli and trains] and their time and site relation can be programmed and applied in neurophysiological studies of motor control in humans.

1. Maertens de Noordhout A, Rothwell JC, Thompson PD, Day BL, Mardsen CD> Percutaneous electrical stimulation of lumbosacral roots in man. J Neurol Neuroeurg Psychiatry. 1988; 51:174-181.
2. Minassian K, Persy I, Rattay F, Dimitrijevic MR, Hofer C, Kern H.:m Postrior root muscle reflexes elicited by transcutaneous stimulation of the human lumbiosacral cord. Muscle Nerve 2007; 35:327-336.

Session 13

FES and Human Motor Control 2

Human neurophysiology of the voluntary motor tasks

Rothwell John

UCL Institute of Neurology, Queen Square, London, UK

Increasing understanding of the flexible organization of sensorimotor networks in the spinal cord has revealed the large range of behaviors that can be evoked even with relatively unpatterned inputs such as those provided by external stimulation. How does descending volitional input from the cerebral cortex address this circuitry? Are volitional inputs equivalent to "switches" or "tonic external drives" that activate intrinsic self-organizing networks, or is there more direct supervisory control of spinal excitability that updates commands on a moment by moment basis? The question is important in terms of the type of function we might expect to restore after spinal injury following interventions to promote regeneration and reinnervation. I will show that transcranial magnetic stimulation and other imaging methods can be used to investigate the extent of volitional inputs to spinal cord during relatively automatic movements such as gait or stance, and begin to provide some answers to these basic functional questions.

Computation in neuroscience of conducting and processing capabilities of the human nervous system

Rattay F[1], Minassian K[1,2], Hofstoetter US[1,2], Danner S[1], Mayr W[2], Dimitrijevic MR[3]

[1] Institute of Analysis and Scientific Computing, Vienna University of Technology, Vienna, Austria
[2] Center for Medical Physics and Biomedical Engineering, Medical University of Vienna, Vienna, Austria
[3] Department of Physical Medicine and Rehabilitation, Baylor College of Medicine, Houston, TX, USA

Abstract

The enormous parallel activities with up to 10^{16} signals per second hinder detailed simulation of the human nervous system. On the other hand, a single neuron cannot discern through which pathway excitatory or inhibitory information enters the cell. This fact allows to partially substitute the input of descending pathways in cases of injuries by afferent projections that are electrically stimulated in order to drive pattern generators in the spinal cord. The main elements of this network which has to generate the neural patterns for posture and locomotion can be simulated by populations of interacting neurons with rather simple structures. The model concept is based on the central pattern generator of experimental animal and is adapted to account for observations from electrical stimulations of the human spinal cord with implanted and surface electrodes. The tools for human data analysis are multichannel EMG responses that are sharply synchronized with the stimulus pulses. Delays of responses and EMG amplitude modulations are essential elements for model evaluation. Therefore, every simulated neuron that is part of the network model consists of a membrane model of the Hodgkin-Huxley type with an additional stochastic component and a delay representing the temporal influence of signal conduction in axons and synapses.

Keywords: *central pattern generator, spinal cord stimulation, electromyography, posterior root-muscle reflex, computer simulation.*

Introduction

Neural coding within the central nervous system is concerned with how sensory and other information is represented by neurons. In order to reduce computational efforts, most neural network models consist of point neurons, neglecting dendritic geometry. The synaptic activities are often summed linearly to determine spike times that are send without delays to the connected neurons. In comparison with real neurons, the accuracy of these models depend essentially on the formalism for spike development, that can include Hodgkin-Huxley dynamics for the main ion types at the somatic membrane [1,2] or simple rules for synaptic currents that are added until threshold is reached (LIF: the Leaky Integrate-and-Fire Model) [3-5].

In many cases it is of interest which circumstances influence the accumulation of the synaptic inputs. The example in Fig. 1 shows the local excitation of a single dendritic branch of a cortical pyramidal cell, short after external stimulation with a microelectrode in the vicinity of this branch, see [6] for details. In a similar way the same dendritic region can be excited by local excitatory synaptic inputs. Note that subthreshold synaptic excitatory activities in other main branches would not support this spike initiation.

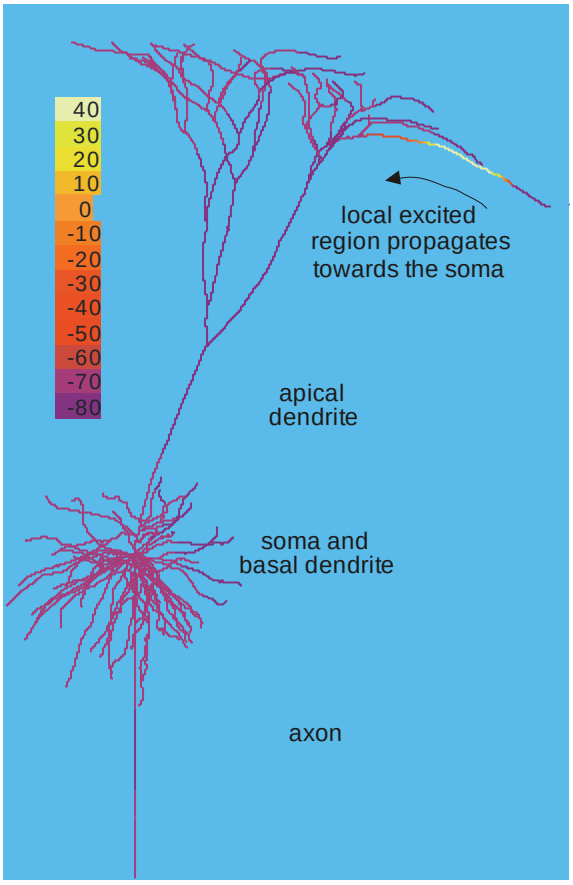


Fig. 1. Simulation of a conducted dendritic spike. Colour codes the transmembrane voltage in mV.

Results

The example of Fig. 1 demonstrates the spatio-temporal dependence of excitatory and inhibitory synaptic events: local concentration along a few 100 µm of synaptic activity within a small time window is most effective and several dendritic domains can operate as individual processing units. In contrast to the apical dendrites, the soma together with all proximate parts of the basal dendrites can be seen as a single processing unit, because of a rather low intracellular resistance between all of these elements.

It is important to note, that the spikes which are finally conducted along the axon do not carry any information about their origin. This principle allows to substitute neural inputs by other pathways, e.g., the neural input from cortico-spinal pathways in humans with spinal cord injuries can be partially replaced by spikes initiated in dorsal root fibers [7,8]. Usually, the dorsal root fibers are stimulated in humans either with epidural electrodes [9] or transcutaneously [10].

Depending on the stimulus frequency the method allows in paralyzed subjects

(i) to reduce spasticity [11],
(ii) to elicit lower limb extension [12],
(iii) to cause stepping-like movements [7, 9]

A simplified scheme of a neural network (Fig. 2) for simulating the characteristic features of the electrically stimulated human lumbosacral cord is a modification of the work presented in [1]. In contrast to the previous explanations related with Fig. 1 it is not necessary to simulate spatial elements like dendritic geometry or the conduction in the axon. This way the computational effort is reduced by a factor 100. Spike conduction from cell to cell is however included as delayed synaptic activity. Every element in Fig. 2 is represented as population of neurons. Stochastic components are included in every neuron (Hodgkin Huxley type) in order to represent ion current fluctuations as expected in the real situation.

Our human experimental data are restricted to multi-channel EMGs, showing sharp synchronization with the train of stimuli, but with a change of the delay indicating a transition from monosynaptic to polysynaptic pathways for higher stimulus frequencies [7-13].

The simulation of the electrically stimulated neural responses demand for a three step procedure:

(i) The electrical potential is calculated along the neural structures that are primarily excited.

(ii) It was shown that these structures are the thickest dorsal root fibers [14, 15]. For a given situation (stimulus frequency, amplitude and electrode positions) the firing pattern of selected sensory axons are evaluated.

(iii) A system of neurons (Fig. 2) is supplied with this artificially generated sensory input that replaces the missing input from the brain. A delay representing the temporal influence of signal conduction in axons and synapses is included.

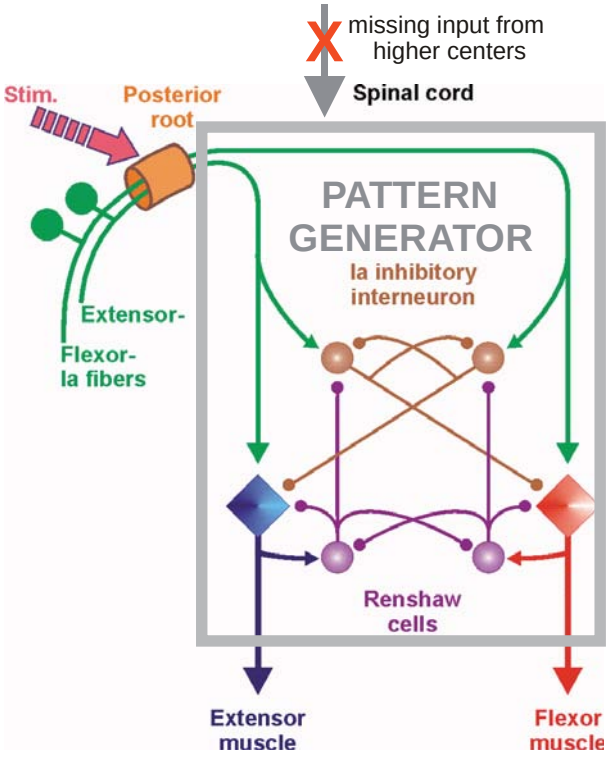


Fig. 2. Neurons of pattern generators of the human spinal cord can be activated through electrical stimulation of afferent axons, thus bypassing the input from the brain.

Conclusions

The human nervous system has many components comparable with the number of stars in the universe, with every neuron like a galaxy when considering the possible synaptic interactions. It is therefore surprising that neural processing can be reduced to some features that are characteristic for those tasks to be solved.

In order to generate for instance stepping like movements in patients with spinal cord injury it is important to send neural signals to the relevant interneurons. These inputs, although coming from other neurons, should have characteristic features similar to the healthy case. Therefore it is not surprising that combing treadmill walking with

electrical lumbar cord stimulation show a better coordination in the EMG patterns of lower extremity muscles in comparison with a single application, that is, either manual guided stepping or electrical stimulation.

Acknowledgements

The presented work was supported by the Austrian Science Fund (FWF), project L512-N13.

Corresponding author

Frank Rattay
Institut for Analysis and Scientfic Computing
Vienna University of Technology
A-1040 Vienna, Austria
frank.rattay@tuwien.ac.at

References

[1] Rybak IA, Shevtsova NA, Lafreniere-Roula M, McCrea DA. Modelling spinal circuitry involved in locomotor pattern generation: insights from deletions during fictive locomotion. J Physiol 577: 617–639, 2006

[2] Fohlmeister JF, Cohen ED, Newman EA. Mechanisms and distribution of ion channels in retinal ganglion cells: using temperature as an independent variable. J Neurophysiol. 103 (3):1357-74, 2010

[3] Dayan P, Abbott LF. Neurons and Neural Circuits – Model Neurons I: Neuroelectronics. In Theoretical Neuroscience, 1st edn, ed. Dayan P & Abbott LF. The MIT Press, Cambridge, USA, 151-194, 2001

[4] Trappenberg TP. Neurons and conductance-based models. In Fundamentals of Computational Neuroscience, 5th edn, ed. Trappenberg TP. Oxford Univ. Press Inc., New York, USA, 13-37, 2007

[5] Izhikevich EM. Simple Model of Spiking Neurons. IEEE Trans Neural Netw 14, 1569-1571, 2003

[6] Wenger C, Paredes LP, Rattay F. Current-distance relations for microelectrode stimulation of pyramidal cells. This volume

[7] Minassian K, Persy I, Rattay F, et al. Human lumbar cord circuitries can be activated by extrinsic tonic input to generate locomotor-like activity. Hum Mov Sci, 26: 275-295, 2007

[8] Minassian K, Hofstoetter US, Tansey K, et al. Neurophysiology of the human lumbar locomotor pattern generator. This volume

[9] Dimitrijevic MR, Gerasimenko Y, Pinter MM. Evidence for a spinal central pattern generator in humans. Ann N Y Acad Sci, 860: 360-376, 1998

[10] Minassian K, Persy I, Rattay F, et al. Posterior root muscle reflexes elicited by transcutaneous stimulation of the human lumbosacral cord. Muscle Nerve, 35: 327-336, 2007

[11] Pinter MM, Gerstenbrand F, Dimitrijevic MR. Epidural electrical stimulation of posterior structures of the human lumbosacral cord: 3. Control of spasticity. Spinal Cord, 38: 524-531, 2000

[12] Jilge B, Minassian K, Rattay F, et al. Initiating extension of the lower limbs in subjects with complete spinal cord injury by epidural lumbar cord stimulation. Exp Brain Res. 154: 308-26, 2004

[13] Hofstoetter US, Minassian K, Hofer C, et al. Modification of reflex responses to lumbar posterior root stimulation by motor tasks in healthy subjects. Artif Organs, 32: 644-648, 2008.

[14] Rattay F, Minassian K, Dimitrijevic MR. Epidural electrical stimulation of posterior structures of the human lumbosacral cord: 2. Quantitative analysis by computer modeling. Spinal Cord, 38, 473–489, 2000

[15] Ladenbauer J, Hofstoetter US, Minassian K, et al. (in press) Stimulation of the human lumbar spinal cord with implanted and surface electrodes: a computer simulation study IEEE Trans Neural Systems and Rehab Eng. Epub available online: http://dx.doi.org/10.1109/TNSRE.2010.2054112

Can FES device be also a tool for assessment of motor control

Mayr W [Vienna, Austria]

Neurological deficits, drop foot, wrist drop, variety of paralysis, paresis, mono, para, tetra, hemip are a result of modified motor control of volitional, automatic postural, reflex activity. FES biomedical approach in the clinical practice is to provide appropriate stimulation of motor points, motor and mixed motor and sensory axons of nerve trunks with appropriate strength, time of stimulation to elicit missing movement or component of it in order to improve human body motor performance. Motor control studies, particularly in the last two decades, extensive studies by multichannel surface electrodes polielectromyography with standard protocols, electrode positioning, amplification, frequency bands [1] and automatic electronic analysis [2,3] help us to learn that there are different features of residual motor control for clinically same or similar neurological deficits. Therefore, it becomes relevant to have insight into the residual motor control of neurological motor deficits, motor control impairment, while we are fitting FES electrophysiological braces. It is critical for the comfort of the fitted person to achieve functional interaction between external control pattern of stimulation and residual motor control of body movement. Enhancement of residual motor control can significantly improve motor performance, endurance after spinal cord, head injury, stroke, multiple sclerosis and other neurological conditions. In the presentation, we shall demonstrate protocol for assessment of residual motor control of upper motor neurone drop foot with the single channel FES stimulator in the outpatient clinic environment. Similar approaches can be applied to assess more complex motor control of the alter features and FES movement restoration. Finally, we shall discuss expected benefits of such practices in providing information, about not only clinical defects, but also underlying neurophysiological mechanism.

1. Sherwood AM, McKay WB, Dimitrijevic MR: Motor Control after sopinal mcord injury: assessment using surface EMG. Muscle Nerve 1996 19(8);m 966-79.
2. McKay WB, Lim HK, Priebe MM, SDtokic DS, Sherwood AM. Clinuical neurophysiological assessment of residual motor control in post-spinal cord injury paralysis. Neurorehabil Neural Repair. 2004 18(3): 144-53.
3. Lim HK, Lee DC, McKay WB, Protas E, Holmes SA, Priebe M, Sherwood AM: Analysis of sEMG during voluntary movement: II Voluntary response index tio change. IEEE Trans Neu Sys Rehab Eng. 2004 12(4): 416-21.

Session 14

FES and Human Motor Control 3

(including general discussion and presentation workshop)

Comparison of neuromuscular stimulation to exercise

Vrbova Gerta

Division of Life Sciences, UCL Gower Str. London, UK

The final structure that is responsible for movement is the motor unit. It consists of the motoneurone, it's axon and the muscle fibers it supplies. Each muscle is composed by a number of different types of motor units. During normal activity as well as exercise these motor units are recruited in a highly organized fashion depending on the excitation of the motoneurones within the central nervous system, which depends on a number of mechanisms such as the size of the motoneurone, as well as excitatory and inhibitory inputs that are impinging upon it. This recruitment order is a rigidly fixed property of the system and for this reason during normal movement or exercise the smallest and most fatigue resistant motor units will always be used first followed by the larger and more fatiguable units. Thus only most intensive exercise can affect the largest and most fatiguable motor units. In contrast, neuromuscular stimulation preferentially recruits these large, fatiguable motor units, since their axons are more excitable by externally applied electrical current. In view of this, the muscle fibers of these motor units will be transformed into fatigue resistant muscle fibers and will be able to participate in electrically elicited movement more effectively. This change of muscle properties of the least active motor units may be useful in situations where after spinal cord injury movement has to be achieved by either activating the central pattern generator of the spinal cord, or elicited by external devices.

Scientific Poster Presentations

1100-Channel Neural Stimulator for Functional Electrical Stimulation Using High-Electrode-Count Neural Interfaces

Hiatt SD[1], Wilder AM[1], Guillory KS[2], Dowden BR[1], Normann RA[1], Clark GA[1]

[1] University of Utah, Salt Lake City, USA

[2] Ripple LLC, Salt Lake City, USA

Abstract

The use of high-electrode-count (HEC) microelectrode arrays in neural prosthetic research has given rise to the need for stimulation hardware capable of generating complex stimulation patterns across hundreds of electrodes. Here we present the design and testing of an expandable, multi-channel, constant-voltage neural stimulator with user-adjustable anodic and cathodic stimulation voltages and electrode biasing voltage. This stimulator has the ability to independently control stimulus rate, timing, duration, and inter-phase interval on each stimulation channel. Channels can be configured to output monophasic or biphasic (anodic or cathodic first) stimulation. The stimulator is designed to function both as part of an integrated HEC Functional Electrical Stimulation (FES) platform or as a stand-alone stimulator. Incorporated into an HEC FES platform, the stimulator was tested in a feline model. Intrafascicular stimuli were delivered to two nerves of the hindlimb via two implanted Utah Slanted Electrode Arrays. The pulse-width modulated constant-voltage stimulator produced graded motor activation similar to that evoked by amplitude-modulated, constant-current stimulation. Further, multi-electrode, multi-nerve submaximal stimulation of the feline hindlimb nerves using the stimulator produced functional, multi-muscle, multi-joint, sit-to-stance behavior.

***Keywords**: functional electrical stimulation, neural stimulator, high-electrode-count microelectrode device, Utah Slanted Electrode Array, intrafascicular multi-electrode stimulation, neuromuscular stimulation.*

Introduction

The introduction of penetrating microelectrode arrays with over 100 independent stimulation sites has made the selective stimulation of many very small populations of neurons possible. However, the high-electrode-count (HEC) of these neural interface devices has made the use of commercially available 1-16 channel count stimulators cumbersome, necessitating the development of HEC stimulators. Without the incorporation of HEC stimulators integrated into HEC FES systems, the ability to investigate neural control strategies for the functional restoration of movement or sensation, and the capabilities of intrafascicular FES cannot fully be realized [1].

To stimulate via hundreds of electrodes independently and simultaneously requires stimulation hardware and software capable of controlling the individual stimulation parameters and timing of each electrode while making the system manageable to a researcher. Several designs for HEC stimulators have been presented, but have been demonstrated with up to 128 independent channels [2,3]. In this paper, we discuss the design, construction, and validation of an 1100-channel pulse-width-modulated, constant-voltage stimulator and its control software. The stimulator is designed to function independently or as part of an integrated HEC FES system. The integrated HEC FES system enables control of complex patterns of stimulator output, and to determine stimulus-response characteristics (EMG, force, or torque recruitment) in an autonomous closed loop manner.

Material and Methods

There are three basic components of the stimulation system: (1) a User Interface and controlling software running on a PC with a high-speed Digital Input Output (DIO) card, (2) a data and power distribution printed circuit board, and (3) several 50-channel constant-voltage stimulator printed circuit boards. Stimulator function begins when a stimulation command is received by the stimulation control software, where it is translated into low-level hardware control signals. These signals are sent to the stimulation hardware generating the desired voltage pulse patterns for the electrodes.

This stimulator was explicitly designed to address complex sets of electrodes with independent stimulation parameters and timing

when connected to an HEC FES system. To validate this capability 12 channels were selected and set to biphasic cathodic-first stimulation, monophasic stimulation (cathodic only), or biphasic anodic-first stimulation. The electrodes were placed in groups for interleaved or synchronous stimulation and each group was assigned a different stimulation frequency. Each electrode was also assigned independent stimulation parameters (such as pulse width). A **single stimulation command**, containing all stimulation information, was sent from the integrated HEC FES system control module to the stimulator control software(Fig. 1).

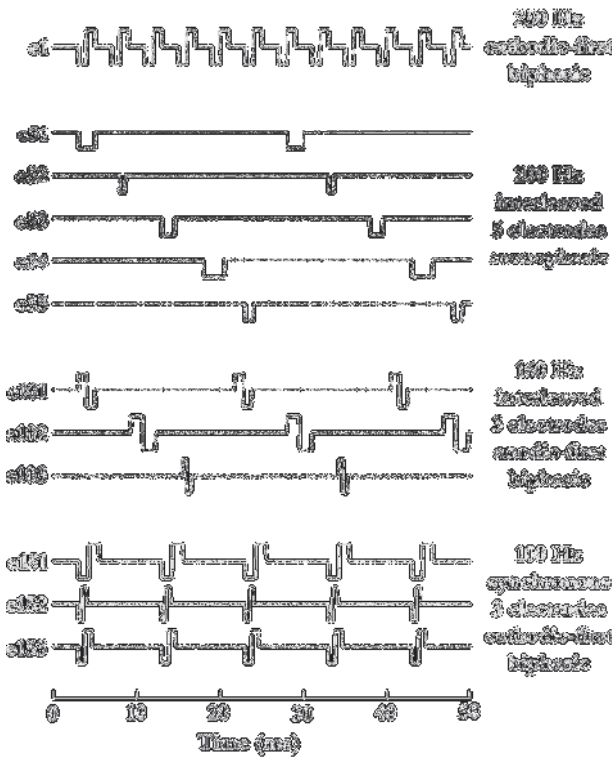


Figure 1. Simultaneous Multi-Electrode Stimulation Control. One multi-electrode command from High-Channel-Count Functional Electrical Stimulation (HEC FES) software was used to stimulate 12 electrodes simultaneously in a complex, user-defined manner.

Experiments were conducted on two adult male cats under guidelines of the University of Utah Animal Care and Use Committee. Detailed surgical procedures have been described previously [4]. In summary, the left femoral and sciatic nerves were exposed and two 10x10 Utah Slanted Electrode Arrays (USEA) were implanted. Fine-wire EMG electrodes were implanted into the femoris, gastrocnemius, soleus and tibialis anterior, and the medial and lateral portions of the quadricep muscles

The left ankle was instrumented with a torque load cell. Each of the 100 stimulation sites was mapped to determine the muscle activated by each electrode as determined by EMG, and the stimulation threshold for evoked torque using the integrated HEC FES system described elsewhere [5]. Then torque recruitment curves for all stimulation sites with an evoked torque threshold under 100 μs were collected using an automated stimulus-response mapping routine in the custom software referenced above. The torque load cell was then used to instrument the knee. Torque recruitment relationships were then determined as for the sciatic implant.

The supporting trough was then permitted to rotate, allowing the cat to assume a sitting posture. The feet were strapped to the table, and a counter weight was placed to offset approximately ¾ of the cat's weight. Ten electrodes capable of independently either evoking knee extension or ankle plantar flexion were selected. Stimulus intensity for each channel was set to a level that produced 15% of maximum torque. Pulse trains were applied to ankle plantar flexors while bearing ¼ of the animal's weight, beginning with one electrode and adding an additional electrode every 200 ms until all five electrodes were active, then subtracting electrodes in the reverse order at 200-ms intervals. Individual electrode stimulation parameters were adjusted to obtain graceful plantar flexion with a maximum joint angle of approximately 100 degrees. Similar trials were conducted on the knee extensors with a target joint angle of approximately 150 degrees.

Results

Stance-like behavior involving two joints was attempted by applying stimuli obtained individually for knee and ankle motion overlaid in various temporal sequences. Individual electrode stimulation parameters and timing were adjusted to produce graceful and natural motion. Fig. 2 shows selected frames from a video of a sit-to-stand-to-sit maneuver accomplished after choosing appropriate stimulation parameters. The full maneuver was accomplished over a 9.8 second period. Other maneuvers including a sit-stand-squat-stand-sit behavior have also been achieved with the stimulator.

Discussion

The ability of the stimulator described in this paper to independently control hundreds of stimulation sites facilitates neural research by allowing for multiple HEC neural implants to be collectively controlled by one FES system. This ease of use has been shown by using the stimulator in an integrated FES system to quickly characterize the stimulus-response characteristics of HEC neural interfaces [5]. This allows a researcher to

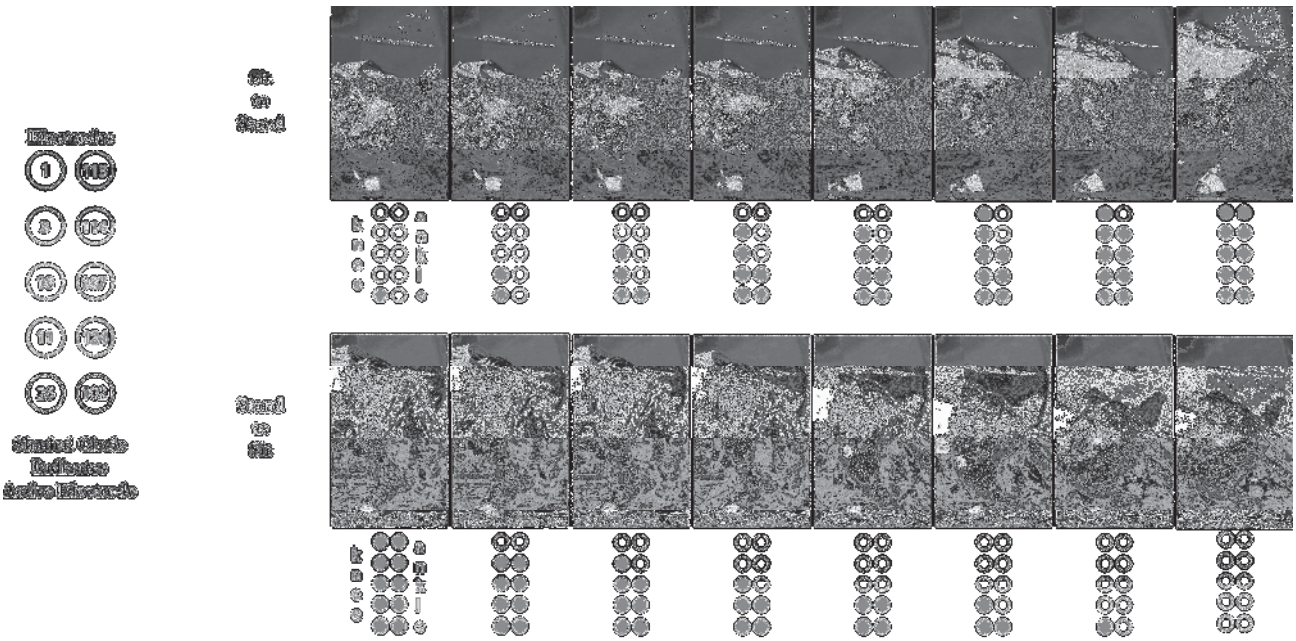


Figure 2.Hind Leg Stance in an Anesthetized Feline. Slow, graceful stance was achieved using graded force recruitment that was controlled by sequential activation and deactivation of different electrodes. Full maneuver lasted 9.8s: 4.3s for complete sit-to-stance, 1.5s for stance maintenance, and 4s for return to sitting position

quickly select individual stimulation sites for desired movements, and to investigate control strategies for graded fatigue-resistant motor restoration.

The circuit design of this stimulation system is useful for exploratory experiments using trans-cutaneous connectors to the neural interfaces. Researchers can easily explore various timing and rate parameters over many stimulation sites that could then be included in implantable high-electrode-count neural stimulators.

Conclusions

We have described an 1100-channel constant-voltage pulse-width modulated neural stimulator and its controlling software and hardware drivers. The stimulation system has been shown to have the ability to selectively activate large numbers of small sets of neurons, the control of cathodic, anodic and bias voltages, and independent stimulation circuitry for each channel. The system has the ability to evoke coordinated movements using multiple high-electrode-count (HEC) neural interfaces that are controlled by user defined temporal patterns. Future work on the stimulator will involve the development of more sophisticated stand-alone capabilities and a more dense data scheme for hardware control to increase the temporal resolution of the stimulator when coordinating many HEC interface devices.

References

[1]Troyk PR and Donaldson NN, *Implantable FES Stimulation Systems: What is Needed?* Neuromodulation, 2001. **4**(4): p. 196-204.

[2]Hu Z, Troyk PR, and Cogan SF, *A 96-channel neural stimulation system for driving AIROF microelectrodes.* Conf Proc IEEE Eng Med Biol Soc.6:4244-7,2004

[3]Yao Y, et al., *A self-testing multiplexed CMOS stimulating probe for a 1024-site neural prosthesis.* Transducers, Solid-State Sensors, Actuators and Microsystems, 12th International Conference on, 2003, 2003. **2**.

[4]Dowden, BR, et al., *Selective and Graded Recruitment of Cat Hamstring Muscles with Intrafasicular Stimulation.* IEEE Trans Neural Syst Rehabil Eng., 6:545-52, 2009.

[5]Wilder AM, et al., *Automated Stimulus-Response Mapping of High-Electrode-Count Neural Implants.* IEEE Trans Neural Syst Rehabil Eng., 5:504-11,2009

Acknowledgements

Supported by NIH, NINDS, R01-NS039677 and DARPA Revolutionizing Prosthetics program, contract N66001-06-C-8005.

Scott Hiatt
University of Utah
scott.hiatt@utah.edu

Sacro-lumbar Anterior Root Stimulator Implant for Exercising

Nonclercq A[1], Vanhoestenberghe A[1], Aqueveque P[1], Cirmirakis D[2], Donaldson, N[1]

[1] Implanted Devices Group – University College London, London, United Kingdom

[2] Electronics and Electrical Engineering – University College London, London, United Kingdom

Abstract

Functional Electrical Stimulation has been used since 1970s for providing patients with thoracic spinal-cord injury (SCI) with leg, urinary and sexual functions. After recognizing that people with SCI tend to suffer ill-health due to the secondary effects of inadequate exercise, much work has been done on using functional electrical stimulation (FES) for cycling and rowing using surface electrodes. However, applying the electrodes is tedious and few of those who start FES training continue. It is now timely to develop an implanted stimulator for these functions that will allow this to be done without taking so much of the users´ time to apply surface electrodes. The Implanted Devices Group (IDG), University College London, is currently developing a new Sacro-lumbar Anterior Root Stimulator Implant (SLARSI) system to improve quality of life of patients and reduce the cost of healthcare. This paper assesses the pros and cons of this new implant by comparing it with a previous lumbar anterior root stimulators implant (LARSI), also developed by the IDG.

***Keywords**: FES exercising, FES-cycling, LARSI, SARSI, urological functions, sexual functions.*

Introduction

People with spinal-cord injury (SCI) tend to suffer ill-health due to the secondary effects of inadequate exercise especially by the large muscles of the legs. Substituting the arms, such as in wheelchair sports, is liable to cause injury to joints of the shoulder and therefore is not ideal for long-term maintenance of fitness. Much work has been done on using functional electrical stimulation (FES) for cycling and rowing using surface electrodes. Cycling and rowing can be enjoyed as sports if sufficient training is maintained. Surface-electrode FES-cycling systems are now commercially-available and it is generally acceptable for patients to use them without supervision.

Games and races in sports halls may be exciting but to build up and maintain the muscles, FES exercise must be frequent (at least three times per week) which means that it probably must be done at home. However, applying the electrodes is tedious and few of those who start FES training continue. An implant that is always available, so that the patient only needs to transfer onto the exercise machine, might make FES exercise much more practicable.

In the 1990s, the Implanted Devices Group (IDG) trialled lumbar anterior root stimulator implants (LARSI) in two patients in the hope of providing a method for standing and stepping. However, after two years of practice, one of the two subjects implanted was only able to take 24 consecutive steps before needing to sit down, and her standing posture is still very unsatisfactory. Yet, she was able to cycle with the muscle combinations available [1]. She was therefore the first person to demonstrate FES cycling using nerve root stimulation (See Fig. 1) and has cycled over 1 km on several occasions [2].

Based on this experience, the IDG is now working on a Sacro-Lumbar Anterior Root Stimulator implant (SLARSI). The first aim of this implant is exercising. However, it also will allow bladder voiding and the recovery of some sexual functions by sacral anterior root stimulation.



Fig. 1: FES cycling.

This paper assesses the pros and cons of this new SLARSI by comparing it to the LARSI, previously developed by the IDG.

Comparing the SLARSI with previous LARSI

The LARSI system [1, 3] consists of an R.F. coupled multiplexed receiver implant with intradural book electrodes trapping the anterior spinal roots from L2 to S2 on both sides. The controller, worn externally, powers and controls the implant via a transdermal transmitter, which is placed immediately over the receiver implant when in use.

Compared to the LARSI, that was research based, the aim of the SLARSI is to provide the patients with a tool they can use daily to improve their quality of life and their health. The two systems differ in many ways, detailed in the following paragraphs.

Focus on rehabilitation

The LARSI system was originally intended for standing and stepping, but has failed to show satisfactory results for those aims (see Introduction). Cycling and rowing are more practical activities than walking, safer and without the strenuous effort of standing up and balancing. They are much simpler to control because the feet are fixed to pedals or foot-rests so the motion of the body is highly constrained.

The current project is therefore focussed on cycling and rowing, for exercising and thus long-term health, rather than walking. In this way, the implant system is designed to be integrated in a seamless manner to a recumbent tricycle or rower (e.g. through the use of a shaft encoder).

Functions

Besides exercising, patients who opt for SLARSI will also be able to empty their bladders by S3 stimulation and to regain some sexual functions by S2 stimulation (SARS technique). Those functions were not available using the LARSI.

However, patient suffering from detrusor overactivity will have to decide whether or not to undergo a rhizotomy. Some urologists consider that deafferentation should be avoided because it is destructive and irreversible so might preclude the patient from benefitting from future new neuroregenerative therapies.

If they do not want a deafferentation, and they are content to continue to empty their bladder by self-catheterisation, they would continue to use anticholinergics or Botox injections as before to prevent incontinence.

Electrode arrangement

The LARSI electrodes were configured as tripoles with connected anodes, as shown on Fig. 2a [4]. This electrode arrangement was attractive because only one wire is necessary for all anodes of a book. Three tripoles were used per book on a four wires cable. It was advantageous because all the wires need to pass through a *grommet* in the dura, where space is restricted.

Unfortunately, a high level of cross-talk was found in the implanted patients. To solve this problem, the electrode arrangement proposed in Fig. 2b is used in the SLARSI system. By using separate tripoles, the current is confined to the slot, hence stimulation should only occur under the active cathode.

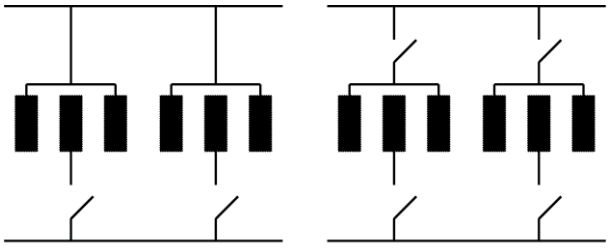


Fig. 2: Electrode arrangement.

Technology improvement

Since the LARSI implant was designed about twenty years ago, it did not benefit from modern technology. Improvements of the new SLARSI system include:

- bidirectional communication (to and from the implant) that will inform the user of the state of the implant, humidity level, electrode loads, etc.;
- a custom integrated circuit for the implant that will reduce the size and power consumption, while allowing independent stimulation of each slot;
- a larger range of current amplitude for the output stage;
- an integrated transmitter that will be smaller and more robust;
- a smaller external control box with a friendlier user interface, and a data logger that will be able to monitor the state of the implant, electrode loads and patient use.

This combination of technological advances will allow a state of the art implant uniquely adapted for nerve root stimulation.

Reliability and risk management

As far as possible, the SLARSI system design is similar to that of the Sacral Anterior Root Stimulator Implant (SARSI), which has been successfully used in many countries throughout the world [5], because this simplifies the process for getting permission to carry out experimental implantations. For the same reasons, the LARSI system was also based on SARSI.

More precisely, when possible, components and materials are the same. Furthermore, the surgical procedure will also be based on SARSI system, because it has proven to be very reliable, especially compared to FES implants with intramuscular electrodes. About 3000 SARSIs have been implanted, generally with good clinical outcomes [6].

Work achieved

The whole system is currently under development. The implant system bidirectional communication was successfully tested using two FPGA. The output stage was also successfully tested in an ASIC (Fig. 3). The final implant ASIC is now being designed, including both the communication and the new output stage architecture. The transmitter specification and architecture have both been completed, and the transmitter ASIC is also being designed. The control box is being implemented, including the user interface.

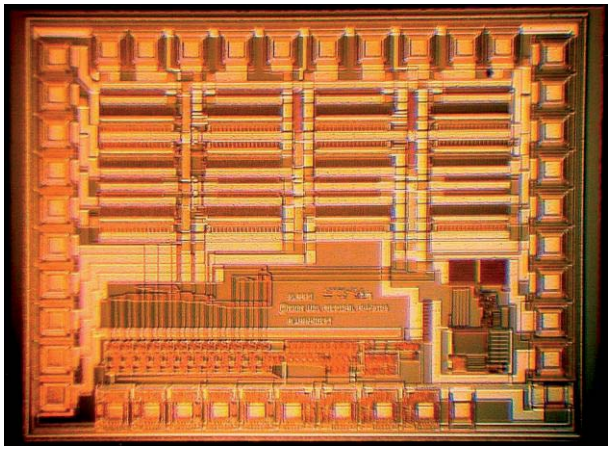


Fig. 3: Output stage ASIC.

Future work

Our first aim is to complete the development of the new SLARSI system and liaise with hospitals where the clinical teams are able to competently implant the system, measure the responses to stimulation and set up the stimulator program for the exercise that the patient will use.

The scientific question is whether the functional anatomy allows useful exercise when stimulating whole roots. If the conclusion is favourable, the method will be transferred to a company. This second step is difficult unless sales increase reasonably quickly after the investment needed to reach regulatory approval (CE Mark, etc).

If we succeed, patients with spinal cord injury will benefit from a commercial product that improves their quality of life while reducing the cost of healthcare. In the longer term, this research also opens new horizons in other related fields such as direct control of paralysed muscles by cortical neurons [7].

References

[1] Perkins TA, Donaldson N de N, Hatcher NAC, et al., “Control of leg powered paraplegic cycling using stimulation of the lumbo-sacral anterior spinal roots.” IEEE Trans Rehab., 10:158-164, 2002.

[2] Perkins TA, Donaldson N de N, Dunkerley AL, et al., “Development of paraplegic leg powered cycling with the Lumbo-sacral Anterior root Stimulator Implant,” in IFESS99: Proc. 4th Annual Conf. IFESS, Y. Handa, Ed., Sendai, Aug. 23–27, 1999, pp. 139–142.

[3] Donaldson N., Perkins T.A. & Worley A.C.M. (1997) "Lumbar root stimulation for restoring leg function. Methods: Stimulator and measurement of muscle actions." Artificial Organs, 21, 247-249.

[4] Donaldson N. de N., Rushton D.N., Perkins T.A., Wood D.E., Norton J. & Krabbendam A. (2003) “Recruitment by motor nerve root stimulators: significance for implant design” Med. Eng. Phys, 25 (7), 527-37.

[5] van Kerrebroeck PEV. “Worldwide experience with the Finetech–Brindley Sacral Anterior Root Stimulator.” Neurourol Urodyn 1993;12: 497–503.

[6] Brindley GS, The first 500 patients with sacral anterior root stimulator implants: general description. Paraplegia, 32:795-805, 1994.

[7] Moritz CT, Perlmutter SI, Fetz EE, “Direct control of paralysed muscles by cortical neurons”. Nature 456:639-42, 2008.

Acknowledgements

P. Aqueveque appreciates the support of postdoctoral project 3100136 of the Chilean Fund for Science and Technology development (FONDECYT).

Author’s Address

Antoine Nonclercq
Implanted Devices Group – Dep. Medical Physics
Malet Place Engineering Building, Gower Street
London WC1E 6BT, United Kingdom
Email: anoncler@medphys.ucl.ac.uk

Development of a Thin-Film Array for Cortical Stimulation

Townsend, Benjamin[1,3], Stitt, Iain[2], Engler, Gerhard[2], Engel, Andreas K.[2], Rubehn, Birthe[1,3], and Stieglitz, Thomas[1,3]

[1] Laboratory for Biomedical Microtechnology, Department of Microsystems Engineering – IMTEK, University of Freiburg, Freiburg, Germany

[2] Department of Neurophysiology and Pathophysiology, University Medical Center Hamburg-Eppendorf, Hamburg, Germany

[3] Bernstein Focus Neurotechnology – Freiburg/Tübingen, Freiburg, Germany

Abstract

Cortical stimulation provides a useful tool for investigating mechanisms of plasticity and functional connectivity within the brain, as well as offering the potential to facilitate learning and rehabilitation in patients. Here we describe use of a thin film electrode array for stimulation experiments in the visual system. In a preliminary attempt we electrically stimulated visual cortex while monitoring effects in the superior colliculus (SC). Visually activated SC neurons showed excitatory responses to stimulation in visual cortex demonstrating that thin-film electrocorticogram (ECoG) arrays can be readily modified for stimulation purposes. Ongoing experiments will probe these stimulation effects in more detail.

Introduction

Cortical electrical stimulation has emerged as a potential therapy to promote functional recovery of the brain following stroke [1], as well as enhancing motor learning and skill acquisition [2], potentially by reinforcing pre-existing/underlying cortical plasticity mechanisms [3]. Electrical stimulation can also be used to probe functional connectivity between cortical and subcortical brain structures [4]. Stimulation thus represents a useful tool for both clinical therapy and basic research.

In both these fields there is a need for small, flexible cortical stimulation devices which can be chronically implanted for long time periods. Thin-film MEMS (micro-electromechanical systems) technology has already been used to develop long-term implantable stimulation/recording electrodes for mapping somatotopy in rat motor cortex [5]. We aim to extend this approach to incorporate use of thin-film arrays for recording and stimulation across multiple cortical areas. As a preliminary step, the work outlined in this paper demonstrates stimulation of visual cortex with a thin-film electrocorticogram (ECoG) grid array, in order to influence spiking activity of visually-responsive neurons in the superior colliculus of an anaesthetized ferret.

Methods

ECoG array

A schematic of the electrode EcoG array for cortical stimulation is shown in figure 1. This basic array was originally designed for cortical recordings in the rat; in the current study it was used purely for stimulation. It was processed using cleanroom techniques, as described previously [6], and comprised 20 platinum electrodes (diameter 0.2mm, pitch 0.4mm) on a thin film polyimide U-Varnish S (UBE Tokyo Japan) substrate. Electrode sites were subsequently coated with platinum black by electrochemical deposition. The impedance magnitude of the Pt-black coated electrodes ranged from 3.44 kΩ to 4.16 kΩ at 1 kHz.

Conductor tracks (width 15µm, pitch 30µm) lead via a cable section to bonding pads, to which a custom-made screen printed ceramic adaptor was connected via microflex bonding. This adaptor was then soldered via insulated copper wires to a conventional connector (Farnell) allowing the electrode to be connected to a laboratory stimulator. Bonding pads, cables and connectors were coated with silicone rubber to protect them during experimental handling.

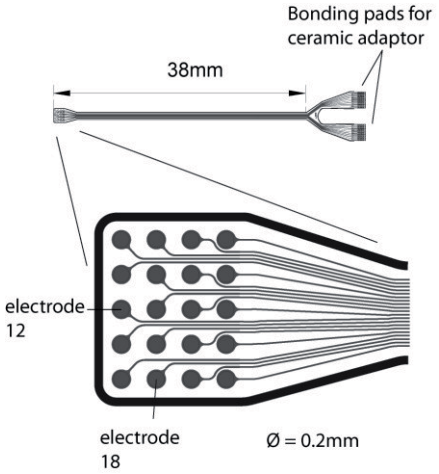


Fig.1 Schematic of thin-film array. Electrodes used for monopolar stimulation are highlighted.

Recording from superior colliculus

Testing of the suitability of the EcoG array for electrophysiological experiments was conducted in a single anaesthetized ferret. The animal was prepared for recording and visual stimulation as described previously [7]. Briefly, after being placed in a stereotaxic frame, the skull was removed over the approximate location of ferret parietal cortex in the right hemisphere, and the dura was resected to expose the underlying pia and cortical surface. Following this, a recording electrode (dual shank Michigan probe with 16 contacts per shank) was inserted through the pia and cortical tissue into the superior colliculus (SC) by means of a manipulator. Location of the electrodes within the SC was confirmed using stereotaxic coordinates and by testing the responses of single and multi-unit spikes to brief stroboscopic flashes of light presented to the contralateral eye. Signals were recorded at each probe contact via a Neuralynx Cheetah recording system (Neuralynx, MN, USA) and separated online into two components by band-pass filtering the data accordingly, 0.1-300Hz for local field potentials (LFPs) and 500-5000Hz for spike data. LFPs were then sampled at 2713 samples/sec and spikes at 32556 samples/sec; all data was recorded to disk for offline analysis. LFPs will be the subject of further analyses and are not dealt with further in the current report.

Stimulation via thin-film array

After positioning the recording electrode within SC, a second craniotomy and dura removal was made over visual cortex. The array for stimulation was then placed on the cortical surface in the approximate location of V1/extrastriate cortex according to stereotaxic coordinates (fig 2). Monopolar stimulation of the cortical surface was carried out through electrodes 12 and 18 of the array (against a ground wire inserted in the nose) using biphasic symmetric cathode-first current pulses with intensities ranging from 0.1 to 1mA, phase width 50ms. With such long, almost DC stimulation pulses the theoretical charge density at maximum current intensity of 1 mA would have been extremely high (150 mC / cm^2 per phase) exceeding the reversible limits for safe stimulation with platinum. Electrode 12 was subsequently destroyed after stimulating at this level. However, electrode 18 remained intact after stimulating at 0.8mA. Ongoing stimulation experiments will use significantly shorter pulse widths (e.g. 100 µs) and much lower current intensities in order to stay within safe limits for platinum electrodes (although see [2] for use of DC stimulation).

Stimulation pulses were delivered manually via a function generator connected to a stimulus isolator. Approximately 100 biphasic pulses were delivered with a frequency of 1-2Hz while recording from SC. Times of stimulation were recorded in parallel with neural data by means of TTL pulses. Offline, spikes were discriminated in Plexon Offline sorter. Despite the long stimulation period it was still possible to discriminate multi-unit spikes from stimulus artefact. Peri-stimulus time histograms (PSTHs) were compiled for SC units by binning each unit's spike times relative to the onset time of stimulation in the cortex, bin width 5ms.

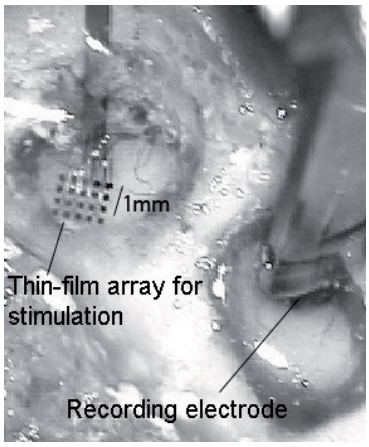


Fig.2. Photograph of exposed visual cortex with thin-film array in place

Results

With the stimulating array in place (fig 2), we recorded low amplitude, multi-unit spikes at one contact of the SC electrode. We analysed the effect of cortical stimulation on the spiking activity of these SC units via the PSTH. Increased or decreased spiking activity time-locked to the onset of stimulation

would reveal itself as a peak or trough in the histogram, respectively. Figure 3a shows a clear peak at a latency of 25-30ms in comparison to the mean spontaneous background activity of the unit from the pre-stimulus time window (horizontal dashed line). This can be interpreted as a brief period of increased spiking probability following stimulation at the cortical surface. The peak was relatively narrow in duration (1-2 bins, 5-10ms) and its magnitude increased as a function of stimulus current intensity (fig 3b) suggesting that spiking activity was facilitated as a result of stimulation and not due to other factors.

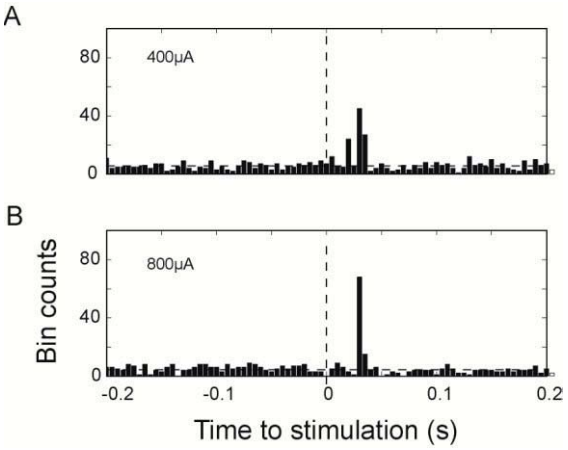


Fig 3. Peristimulus time histograms show excitatory effect on spontaneous superior colliculus discharge in response to cortical stimulation. Each plot compiled from approx. 120 stimuli. A and B: responses to 400 and 800uA stimulation current, respectively.

Discussion

The work presented here demonstrates putative effects in SC due to visual cortical stimulation. Multi unit spikes that responded to electrical stimulation at the cortical surface could also be activated by a brief flash of light, in line with previous work [8]. Response latencies to electrical stimulation, however, were approximately 30ms, which is longer than the short-latency effects (6-8ms) mediated by monosynaptic afferent projections from primary visual cortex to superficial layers of SC [8]. Longer latency responses could be mediated by oligosynaptic pathways involving additional cortical or subcortical structures (e.g. extrastriate cortex or lateral geniculate nucleus). The relatively imprecise nature of the stimulation location and parameters used in the present study most likely account for this indirect activation of SC neurons.

Conclusion

A thin-film polyimide-platinum ECoG electrode array was used for visual cortical stimulation. Ongoing work aims to yield focal stimulation via iridium oxide electrode coatings, narrow pulse-width stimulation protocols, and precise mapping of cortical areas using visually-evoked responses. Optimal alignment of stimulating and recording sites will allow examination of modulatory influences of cortical stimulation on plasticity.

References

[1] Plow EB, Carey JR, Nudo RJ, and Pascual-Leone A, "Invasive cortical stimulation to promote recovery of function after stroke: a critical appraisal," *Stroke*, vol. 40, no. 5, pp. 1926-1931, 2009.

[2] Reis J, Schambra HM, Cohen LG, Buch ER, Fritsch B, Zarahn E, Celnik PA, Krakauer JW, "Noninvasive cortical stimulation enhances motor skill acquisition over multiple days through an effect on consolidation," *PNAS*, vol. 106, no. 5, pp. 1590-1595, 2009.

[3] Nudo RJ, "Postinfarct cortical plasticity and behavioral recovery," *Stroke*, vol. 38, no. 2 Suppl, pp. 840-845, 2007.

[4] Holdefer RN, Miller LE, Chen LL, Houk JC, "Functional connectivity between cerebellum and primary motor cortex in the awake monkey," *J.Neurophysiol.*, vol. 84, no. 1, pp. 585-590, 2000.

[5] Molina-Luna K, Buitrago MM, Hertler B, Schubring M, Haiss F, Nisch W, Schulz JB, and Luft AR, "Cortical stimulation mapping using epidurally implanted thin-film microelectrode arrays" *J.Neurosci.Methods*, vol. 161, no. 1, pp. 118-125, 30-3-2007.

[6] Rubehn B, Bosman C, Oostenveld R, Fries P, and Stieglitz T, "A MEMS-based flexible multichannel ECoG-electrode array," *J.Neural Eng*, vol. 6, no. 3, pp. 036003, 2009.

[7] Manger PR, Engler G, Moll CK, and Engel AK, "The anterior ectosylvian visual area of the ferret: a homologue for an enigmatic visual cortical area of the cat?," *Eur.J.Neurosci.*, vol. 22, no. 3, pp. 706-714, 2005.

[8] Berson DM, "Convergence of retinal W-cell and corticotectal input to cells of the cat superior colliculus," *J.Neurophysiol.*, vol. 60, no. 6, pp. 1861-1873, 1988.

Acknowledgements

This work was supported by the German Research Foundation (GRK 1247/1 “CINACS”).

Author’s Address

Ben Townsend, Laboratory for Biomedical Microtechnology, Department of Microsystems Engineering – IMTEK, University of Freiburg, Germany. bt1000@imtek.de

An Energy-Efficient and Multiple-Waveform Stimuli Generator for Visual Cortex Microstimulation

Hasanuzzaman Md.[1], Sawan Mohamad[2], Raut Rabin[3]

[1,2] Polystim Neurotechnologies Laboratory, Polytechnique Montréal, Canada
[3] Department of Electrical and Computer Engineering, Concordia University, Montréal, Canada
[1]md.hasanuzzaman@polymtl.ca

Abstract

In this paper, we propose a multiple waveform energy-optimal stimuli dedicated to intracortical microstimulation. Therefore, we focused on designing improved exponential and quarter-sine waveforms generators with output current ranging from 0 to 300 μA. The proposed circuits deliver an exponentially rising current with maximum value of 200 μA with a dynamic range of 60 dB, and a quarter-sine pulse with maximum value of 300 μA. Both stimuli have been made biphasic using a H-Bridge output driver circuit. Minimizing the area (number of transistor counts), improving the dynamic range and the pulse duration of the generated output currents and saving the energy are also some other major concerns, we took into consideration.

Keywords: *Stimuli generator, rising exponential waveform, quarter-sine pulses.*

Introduction

In bio-medical instrumentation energy-efficiency is a prime factor for both the safety concern of human tissues and the minimum power dissipation of the whole circuit as well as in the intracortical sites. In [1], it has been proved that the rising exponential signal is the most energy-efficient waveform to safely stimulate the neural tissues. Similar to rising exponential signal, a quarter-sine pulse signal generates less energy compared with square and half-sine pulse signals [2]. The energies are compared by estimating the areas under the graphs of the signals for same peak amplitudes and over the same time durations. An energy-efficient signal pulse needs less battery power to produce it, leading to circuits that are more economic to implement when hundreds of channels are used for microstimulation purpose.

With the considerations of energy-efficiency and economics of the electronic circuitry in our minds, we have proposed a new quarter-sine waveform and an improved exponential waveform generator, to be used in the implantable stimulation module dedicated for visual cortex microstimulation, aimed for the 'Cortivision' project which is in progress in the Polystim Laboratory.

In the following section, we present the detailed circuit diagrams for the pulse generators together with the supporting circuitry, such as, the ramp voltage generator and output driver circuits. The theories and working principles for these circuits are included under the section on material and methods. The simulation result is presented in the results and discussion section, and finally, we conclude summarizing the achievements.

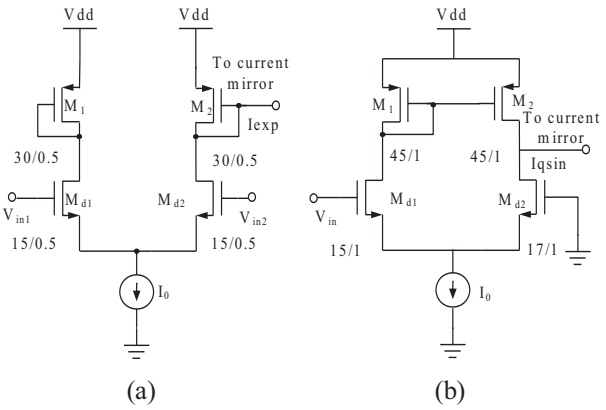


Fig. 1. Pulse generators: (a) Rising exponential and (b) Quarter-sine pulse (*All units are μm/μm)

Material and Methods

Proposed Exponential Pulse Generator:

Fig.1(a) shows the schematic diagram of exponential pulse generator, consists of a differential pair with two diode connected loads, a biasing current source, I_0 and a cascode current mirror. The bias voltage at V_{in1} was set to 0.9 V. A ramp voltage with a range from 0.5 to 0.9 V was generated using the ramp generator circuit designed in [2] and applied to the V_{in2} input of the circuit shown in Fig. 1(a). The biasing current source, I_0 was set to 2 μA to operate all of the transistors in weak inversion region. The drain to source current, I_{DS} of an N-MOS transistor operated in weak inversion region can be expressed as follows

$$I_{DS} = I_{D0}\frac{W}{L}\exp\frac{V_{GS}-V_{th}}{nV_T} \qquad (1)$$

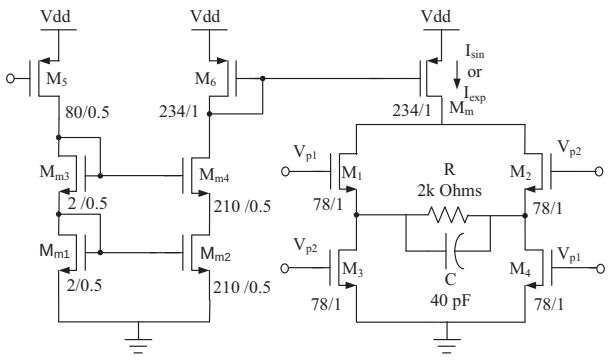


Fig. 2. (a) Cascode current mirror followed by (b) H-Bridge output driver circuit (*All units are μm/μm)

As shown in equation (1), by simply varying the gate-to-source voltage, V_{GS} from 0 to a value, which is less than the threshold voltage of N-MOS, V_{th}, which is 0.6 V in our case, we obtained an exponentially rising drain-to-source current. Afterwards, this current signal has been amplified to 200 μA using a cascode current mirror.

Proposed Quarter-Sine Pulse Generator:

If the differential pair transistors, M_{d1} and M_{d2} as shown in Fig 1(b), operate in subthreshold region, then assuming equal threshold voltage for M_{d1} and $M_{d2,}$ equation (1) can be re-arranged as

$$V_{GS1} = nV_T \ln(\frac{L_1}{W_1}\frac{I_{DS1}}{I_{D0}}) + V_{th} \quad (2)$$

$$V_{GS2} = nV_T \ln(\frac{L_2}{W_2}\frac{I_{DS2}}{I_{D0}}) + V_{th} \quad (3)$$

Again, we can write these following two equations for bias current, I_0 and the output current, I_{out}

$$I_0 = I_{DS1} + I_{DS2} \quad (4)$$

and

$$I_{out} = I_{DS1} - I_{DS2} \quad (5)$$

After manipulating equations (2), (3), (4) and (5) we obtain our desired equation for I_{out}, which is a hyperbolic tangent function, and can be approximated as a quarter-sine function for a certain range of V_{in} beyond which the generated signal does not resemble a quarter-sine pulse.

$$I_{out} = I_0 \tanh\frac{V_{in}}{nV_T} \quad (6)$$

In equations (2) and (3) we have assumed that both M_{d1} and M_{d2} have same dimensions.

The bias current I_0 for this circuit was set to 15 μA. The width of the transistor, M_{d2}, in Fig 1(b) is made slightly greater than that of M_{d1} in order to minimize the DC current, which was flowing through the output terminal even in the absence of input signal.

Ramp Voltage Generator:

We used the ramp voltage generator depicted in [2] to set the duration of quarter-sine and exponential pulse signals. The voltage ramp can be generated from the nanoscopic output current of this circuit realizing the following function of a capacitor.

$$\frac{dV}{dt} = \frac{I_{in}}{C} \quad (7)$$

To obtain the required pulse duration the capacitor, C, and the biasing current, I_{in} are made programmable with the range from 0.25 pF to 10 pF and from 5 nA to 1.5 μA respectively. The resulting slope range of voltage ramp is 539 V/s to $9x10^4$ V/s. To generate the quarter-sine and rising exponential pulse we increased V_{in} from 0 to 205 mV and from 500 mV to 900 mV respectively.

Biphasic Output Driver:

The biphasic output driver circuit, designed using an H-Bridge circuit as shown in Fig. 2(b), consists of four switching transistors, M_1 to M_4, one transistor, M_m for mirroring the current from cascode current mirror, one load resistor, R and a capacitor, C. Here, R represents the electrode-tissue interface impedance which can be as high as 100 kΩ [4]. A multichannel, high-density stainless steel-platinum microelectrode array designed by the Polystim Laboratory team [5] or irridium oxide microelectrode array with impedance of 50 kΩ from Blackrock Microsystems will be used for performing the in-vivo test. As the load current may drop for large value of electrode-tissue impedance, our next design goal is to increase the output impedance of the stimuli generator. For a maximum stimulation current of 150 μA, a voltage compliance of 15 volt is required across the microelectrode with an impedance of 100 kΩ and this on-chip technology is available in our laboratory [4]. Capacitors with values of 40 pF and 150 pF have been used for quarter-sine and rising exponential cases respectively for suppressing the clock feed-through effect during switching, and in our next design, this capacitor will be eliminated as it occupies large area.

Results and Discussion

All the circuits shown in Fig. 1 and Fig. 2 have been designed using CMOS 0.18 μm technology. The supply voltage was set to 1.8 V to minimize

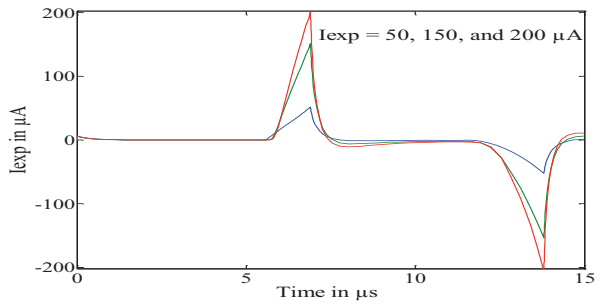


Fig. 3. Generated biphasic exponential signal

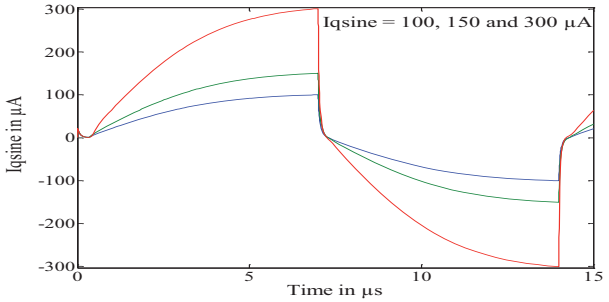


Fig. 4. Generated biphasic quarter-sine signal

TABLE I

PARAMETERS AND RESULTS COMPARISON

Case	[2]	This work
Process	0.18 µm	0.18 µm
Waveform	Half-sine, Exponential	Quarter-sine, Exponential
Maximum stimulation current	200 µA	300 µA
Dynamic range in dB	49.52 dB (Iexp = 150.27 µA)	60 dB (Iexp = 201.9 µA)
No. of transistor counts without output driver circuit (expon.)	-	9
No. of transistor counts without output driver circuit (sine)	14 (Half-sine)	8 (Quarter-sine)

the power consumption. The simulation results of the circuits shown in Fig. 1 and Fig. 2 are plotted in Fig. 3 and Fig. 4. The biphasic rising exponential current pulse for three different ranges, 50 µA, 150 µA and 200 µA is shown in Fig. 3. The dynamic range of exponentially rising signal of amplitude 200 µA is approximately 60 dB (not shown here), which is quite large. As shown in Fig. 3 the duration of the pulse is 8 µS, which can be programmed by varying the capacitor and the bias current in the ramp voltage generator circuit. In quarter-sine case, current pulse with the peak value higher than 300 µA was obtained. The simulation result for three different ranges of current, 100 µA, 150 µA and 300 µA has been plotted in Fig. 4.

A fair comparison between this work and [2] is shown in Table I and it is noted that, we have improved in some aspects such as dynamic range, maximum output current and number of transistor counts. Dynamic range of rising exponential current has been improved to 60 dB compared to 49.52 dB [2]. The output current range has been improved to 0 to 300 µA and the number of transistors without output driver circuit has been minimized to 9. An in-vivo test will be performed to ensure the efficacy of this stimuli generator in visual cortex microstimulation.

Conclusions

In this paper, we have proposed quarter-sine pulse and improved exponential pulse generators, which are highly flexible to use for microstimulation purpose. Due to the safety concern of intracortical tissues, optimal energy issues have been taken into consideration to design the circuits and consequently, CMOS 0.18 µm technology has been used to design the circuits. The amount of energy and power that can be saved has not been quantified yet and we look forward to investigate this issue afterwards.

References

[1] Robillard, J. Coulombe, P. Nadeau, and M. Sawan, "Neural stimulation safety and energy efficiency: Waveform analysis and validation," in Proc. 11th IFESS, Japan, 2006, pp. 94-96.

[2] Sebastien Ethier, Mohamad Sawan, and Mourad El-Gamal, "A novel energy-efficient stimuli generator for very-high impedance intracortical microstimulation," ISCAS 2010, May 2010.

[3] Lorant Andras Szolga, Leila Festila, Mihaela Cirlugea, "Four quadrant analog current mode modular multiplier designed with differential amplifiers," Acta Technica Napocensis, Electronics and Telecommunications, Vol. 49, No. 2, 2008.

[4] Sebastien Ethier, Mohamad Sawan, El Mostapha Aboulhamid, and Mourad El-Gamal, "A ±9 V fully integrated CMOS electrode driver for high-impedance microstimulation," 52nd IEEE Int. Midwest Symp. on Circuits. and Systems, 2009.

[5] Amer E. Ayoub, Benoit Gosselin, and Mohamad Sawan, "A microsystem integration platform dedicated to build multi-chip-neural interfaces," Proc. of the 29th Annual Int. Conf. of the IEEE EMBS, pp. 6604-6607, August 23-26, 2007.

Acknowledgments

The author would like to thank the NSERC and the Microsystems Strategic Alliance of Quebec (ReSMiQ) for providing the financial support, and technical facilities offered by CMC Microsystems.

Author's Address

[2] Polytechnique Montréal, Dept. of Electrical Eng. 2900 Edouard-Montpetit, P.O. Box 6079, Station Centre-ville, Montreal, QC, Canada, H3C 3A7
e-mail: mohamad.sawan@polymtl.ca

Therapeutic FES with distributed units

Jovičić N[1]

[1] Faculty of Electrical Engineering, University of Belgrade, Serbia

Abstract

We describe the hardware of a new wireless distributed functional electrical stimulation system. Battery powered peripheral nodes comprise stimulators and sensors and directly attach to the electrodes. The peripheral nodes are compact, small and optimized for low energy consumption. Central node implements bridge connection between the set of wireless peripheral nodes and the computer. Software running on a computer implements algorithm and enables real-time monitoring and on-the-fly changes of all stimulation parameters. The system is also self-standing, and operates without computer. The feature of the system is that the central node manages network traffic in order to minimize and equalize delays that are typical for distributed systems. Synchronized data are sent to computer with calculated overall delay which can be used to adapt main control algorithm in order to maintain stability. Once the algorithm is evaluated in laboratory environment, processing can be redistributed onto peripheral nodes enabling standalone application.

Keywords: *FES, distributed system, wireless, sensors and stimulator.*

Introduction

Functional electrical stimulation (FES) activates paralyzed or paretic muscles by stimulating motor and sensory nerves. The timely control and selective activation of sensory-motor systems provide function to persons after spinal cord or brain injury. Lately, it was suggested that the use of FES if integrated into an intensive exercise program contributes to the cortical plasticity; thereby, have therapeutic effects. In order to guaranty effective response and long-term stimulation effects, FES must adapt to individual needs and level of disability. The available FES systems with one stimulator and multiple electrodes and sensors are somewhat limited, especially for clinical applications. The idea of distributed electrical stimulation was introduced in the optimal way by the BION technology [1]. However, BION technology uses implants, and for relatively short therapies surface stimulation is advantageous. The current problems with the implantable devices are related to the efficiency of energy transmission [2], which likely can be resolved in the near future, but the obvious invasiveness compared to the use of surface systems remains. We suggest the use of distributed FES with surface electrodes [3]. A suitable architecture for the FES with distributed units is described by Andreu *et al.* [4].

We present here a new distributed system for surface FES based on IEEE 802.15.4 wireless communication. Main goals were hardware miniaturization, integration of sensors and stimulators and software interface development. Motivated by works in literature [5], we made adaptation on standard MAC protocol in order to lower effects of data delays.

Material and Methods

Architecture:

Architecture of the system is presented in Fig. 1. A set of battery powered peripheral nodes is placed on the body of the subject. Peripheral nodes establish communication with one central node through low power 2.4GHz wireless link.

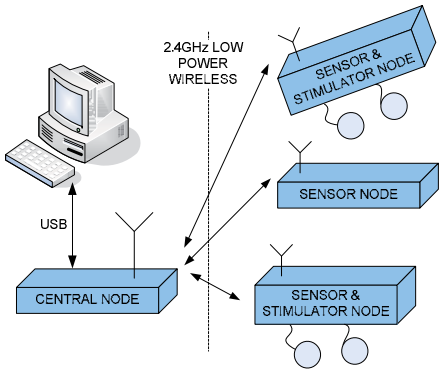


Fig. 1: Architecture of the system.

The central node is connected using USB interface to computer. Wireless communication is bidirectional with central node acting as a master, and peripheral nodes as slaves. Peripheral nodes include sensors and/or stimulator functionality. The central node manages network traffic and USB connection with computer. Main stimulation

algorithm runs on computer in open or closed loop configuration.

Hardware:

Central node has Texas Instruments CC2430 microcontroller, RF front end, and USB transceiver. As the size of the central node is not the limiting factor, external high gain antenna is used enabling good link quality and long distance operation. Central node is powered over USB connection, and the maximum current consumption is lower than 250mA.

Peripheral nodes (Fig. 2, left) have two or three printed circuit boards packed in a sandwich structure, depending whether they perform sensor and/or stimulation functionalities. Connection is made with multi-pin connector. Top board incorporates processor and RF front-end. Middle board incorporates sensors (3D accelerometers and 3D gyroscope) and bottom board is the stimulator. Each peripheral node is powered with Li-Ion 500 mAh battery mounted between bottom and middle boards.



Fig. 2: Photography of the peripheral node (left); and sketch of the positions of the nodes for muscles stimulation on the leg (right).

Processing and communication functionality is integrated in CC2430 system on chip (SoC). Microcontroller core and RF transceiver are connected through internal system bus. Due to this direct link between RF and processor part, there is almost no delay in packet data transfer. CC2430 also integrates eight channel 12-bit AD converter, SPI controller and several output compare units for PWM generation. Small PCB antenna is used due to need for miniaturization.

The sensor board contains digital 3D accelerometer and analogue 3D gyroscope forming miniature inertial measurement unit. The board also includes a circuitry for conditioning signals from the specially designed shoe insole with force sensing resistors (FSR).

Stimulation board has DC/DC step up converter that produces 85V DC voltage from single 3.7V Li-Ion battery. Electrodes are driven with two current-controlled output channels, with negative pulse compensation capability. Current amplitude is determined by 10 bit SPI DAC, and lies in range of [0, 70] mA. Duration of stimulation pulses is in the range of [10, 1000] μs with 10-bit resolution. Frequency and duty ratio of stimulation pulses are controlled by using the output compare units of microcontroller. Efficiency of the stimulator is about 40%, and maximum averaged output power is 0.7W. Full load output current diagrams for single channel are displayed in Fig. 3.

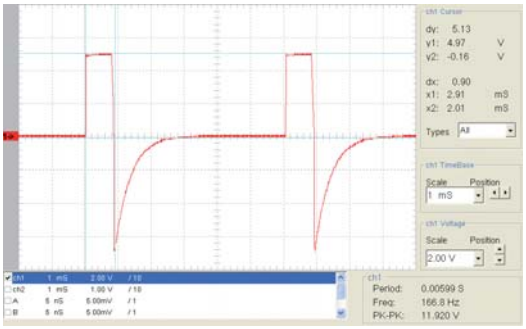


Fig. 3: Current diagrams measured at full load (scale: 1V~10mA).

In full configuration (all three boards), peripheral node dimensions are 70x25x30mm, and weight is ~50 grams. If the node used only as the sensory part of the system the dimensions are 70x25x15mm, weighing ~30 grams.

Networking:

Wireless communication is based on IEEE 802.15.4 standard. MAC layer is adapted to real-time demands of the system. Network has star topology, with central node as a master (network coordinator), and peripheral nodes as slaves. Every communication and action is strictly controlled by the central node. Due to the nature of wireless communication, there is always a possibility for packet losses and data delays. Since the system is distributed, these delays are not the same for each node. Central node implements delay equalizing algorithm. Main scheduling algorithm is round-robin with equal node priorities. If for some reason, significant delay or data loss occurs on one node, network traffic is rearranged, and that node receives high priority. The data from other nodes are delayed while the data from “silent” node are trying to be undertaken and sent to the central node. When the delay is equalized, all nodes receive same priorities again.

Firmware:

Central node runs algorithm for network scheduling and delay equalization. This is a demanding task, and needs a lot of memory and processing power. Microcontroller CC2430 is efficiently used. Peripheral nodes in this

configuration of the system do some basic signal processing (filtering) of sensor data, and execute online stimulation commands.

Software:

Synchronized data collected from peripheral nodes and delay information are sent over USB interface to computer. Network protocol and software driver achieve that main control application running on computer is not aware of distribution effects (different delays). Control algorithm can be calculated to operate with constant maximum delay or can adapt to dynamic changes of it. Dedicated software for data acquisition, stimulation running and monitoring is developed in LabWindows/CVI. We also developed plug-in for Simulink/Matlab. We consider that this distributed system with the central unit with graphical user interface enables therapist to online monitor sensor signals and program that is being executed and to set the parameters of stimulation pulses in order to match the needs of a specific patient.

Performance:

Tested experimental setup contains three nodes on each leg (Fig. 2, right). Achieved equivalent bandwidth of the system is 220kBit/s of raw data in ideal case with no data losses. Sampling frequency for sensors is 100Hz, and frequency of updating stimulation pattern is 50Hz. Range between central and peripheral nodes is up to 20m. Overall round trip time is about 20ms. Autonomy of the system for 20% stimulation cycle use is about 2 hours. We tested the walking controlled with the algorithm described in Kojović *et al.* [6], and found that the system is operating in real time and allows FES assisted walking of hemiplegic individual. In this configuration four muscle groups were activated based on the information from five sensors.

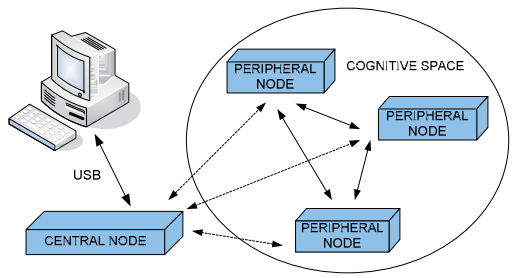


Fig. 4: Redistribution of control algorithm.

The extension of the system:

Once the algorithm is formed, executed and tested on computer in stationary laboratory environment, processing can be redistributed onto peripheral nodes. This leads to another approach presented in Fig. 4. Architecture and hardware remains the same, but with changed roles of nodes. Computer with central node becomes optional monitoring device. Each peripheral node receives part of control algorithm. Network traffic is adapted and one of peripheral nodes becomes coordinator. This redistribution enables system to be used standalone, that is, without computer.

The feature that is being evaluated is the integration of the processing hardware and software for recordings from stimulated and volitionally activated muscles (EMG) which will output the envelopes or other parameters that relate to the EMG with the intention to integrate this data into control. The recordings from the stimulated muscles incorporate the blanking of stimulation artifacts. The processing is necessary in order to reduce the amount of data that is being circulated within the distributed system.

This configuration is directly applicable for therapy of upper extremities, treatment of low-back pain and other applications.

References

[1] Gerald EL, Raymond AP, William HM et al. BION - system for distributed neural prosthetic interfaces. Medical Engineering & Physics 23: 9–18, 2001.

[2] Gudnason G, Nielsen JH, Bruun E, Haugland M. A distributed transducer system for functional electrical stimulation. The 8th IEEE International Conference on Electronics, Circuits and Systems, ICECS 2001, 2001.

[3] Poulton AS, Andrews BJ. A simple to program but sophisticated distributed control system for surface FES applications. 9th Annual Conference of the International FES Society - Bournemouth, UK, September 2004.

[4] Andreu D, Guiraud D, Souquet G. A distributed architecture for activating the peripheral nervous system. Journal of Neural engineering, 6, 2009.

[5] Su H, Zhang X. Battery-Dynamics Driven TDMA MAC Protocols for Wireless Body-Area Monitoring Networks in Healthcare Applications. IEEE Journal on selected areas in communications, vol 27, no. 4, may 2009.

[6] Kojovic J, Djuric-Jovicic M, Dosen S et al. Sensor-driven four-channel stimulation of paretic leg: functional electrical walking therapy. Journal of neuroscience methods 2009; 181(1):100-5. 2009.

Author's Address

Jovičić Nenad

Faculty of Electrical Engineering, University of Belgrade, Serbia

nenad@etf.rs

IMPLANTABLE PRESSURE SENSOR FOR DETECTING THE ONSET OF A BLADDER CONTRACTION – PRELIMINARY RESULTS

Melgaard J[1], Rijkhoff NJM[1]

[1] Center for Sensory-Motor Interaction (SMI), Aalborg University, Aalborg, Denmark

Abstract

In this study we examined the ability of an implantable pressure sensor to detect the onset of bladder contractions. Experiments were performed in 2 pigs, where a custom built pressure sensor was placed in the bladder wall, and a reference sensor was used to monitor intravesical pressure via a catheter. The implantable sensor was a small piezoresistive sensor encapsulated with silicone; it was lens shaped with a diameter of 13 mm and height of 1.5 mm. In the model, bladder contractions were generated by unilateral electrical stimulation of the pelvic nerve. Our data suggests that the implantable pressure sensor performs similar to the reference sensor regarding both sensitivity and ability to detect the onset of contractions. Because of the small amount of data, statistical comparisons have not been performed. A very slowly increasing offset (3 cmH_2O over 1 hour) is seen in the traces from the implantable sensor. This may be due to thermal drift or absorption of body fluids; further analyses are required to clarify this issue. This offset does not influence the performance of the sensor. In conclusion, the implantable pressure sensor performs similar to the reference sensor in detecting the onset of a bladder contraction.

***Keywords**: incontinence, urinary bladder, pressure sensor, closed loop control*

Introduction

Neurogenic bladder dysfunction is commonly seen with spinal cord injury (SCI), multiple sclerosis, Parkinson's disease and other neurological disorders. Such patients typically develop neurogenic detrusor overactivity (NDO), and in most cases also detrusor-sphincter-dyssynergia. While incontinence episodes caused by NDO are being perceived as detrimental to quality of life by patients, a more important clinical factor is the increased storage pressure, which can lead to vesicouretral reflux and renal damage [1]. Even if clinical relevance is set aside, studies show that bowel and bladder function, sexual function, hand function, and breathing are the functions prioritized the highest among SCI affected individuals [2].

It has been shown that involuntary bladder contractions can be suppressed by stimulation of pudendal nerve afferents [3], and that conditional genital nerve stimulation is at least as effective as continuous stimulation [4]. Using external equipment Hansen et al. showed that conditional stimulation could be performed automatically [5].

While continuous stimulation is capable of suppressing bladder contractions, there is no feedback about the amount of urine in the bladder. Using a conditional stimulation scheme, it can be observed that the involuntary bladder contractions start to occur when the bladder is relatively full. Thus, the first contraction can be used to provide the user with a warning signal, indicating that it would be a good idea to void when convenient. This allows for the patient to become fully continent.

Conditional stimulation requires a sensor capable of detecting the onset of a bladder contraction. Many types of sensors have been suggested; focus in this paper is on pressure sensors. Early attempts of using an implantable pressure sensor to detect bladder contractions can be ascribed to Brindley [6]. Later, chronic experiments were conducted in dogs [7] and goats [8]. These studies have been concerned with the issue of chronic applicability, but have not investigated the ability of such sensors to detect the onset of bladder contractions.

The aim of this work is to investigate the ability of a small silicone encapsulated pressure sensor to detect the onset of a bladder contraction.

Material and Methods

Animal Model

The study was performed on one female landrace pig weighing 30-40 kg. Anaesthesia was induced with a mixture of Zolitol and Rompun, and the pigs were subsequently intubated and anesthetised using isoflurane 1 % vol. Saline was administered intravenously at 330 ml/hour. Heart rate and oxy-

gen saturation were monitored, and the pig was placed on a heating blanket.

Surgical Procedure

With the pig in the prone position, a 2-lumen 8 Fr catheter was placed in the bladder. One lumen was connected to a pressure transducer (TruWave, Edwards Lifesciences; relative type transducer), the other lumen was used for emptying the bladder, and later for artificial filling.

The pelvic nerve was exposed by following a procedure described by Wen et al. [9]. An incision was made along the lateral border of the spine, and the gluteus muscle was detached from the sacral bone. A small part (elliptical, approx. 1 by 1.5 cm) of the piriformis muscle was removed to form a window, through which the pelvic nerve could be exposed. The nerve was positively identified by the bladder response to electrical stimulation with a hook electrode. Once the nerve was identified, a bipolar cuff electrode was implanted on the nerve, and sutured in place. The gluteus muscle and the skin were flipped back, and the incision was sutured to keep everything in place.

The pig was then placed in the supine position, and a low midline incision was made to expose the bladder. A small slit was made in the serous coat of the bladder using a scalpel. Using this as entry point, a small pouch was made in the bladder wall by blunt dissection. In this pouch a custom built pressure sensor was placed. The sensor is a small piezoresistive pressure sensor (absolute type transducer, die is 8 by 8 mm), encapsulated with silicone. The final assembly is lens shaped with a diameter of 13 mm and height of 1.5 mm.

Both the implanted sensor and the reference sensor were connected to an amplifier (Axon CyberAmp 380) and data acquisition system (NI USB-6009). The signals were amplified (500x for the implantable; 2000x for the reference sensor), lowpass filtered at 10 Hz, and sampled at 100 Hz. For offline viewing, an additional 2nd order Butterworth lowpass filter with a cutoff frequency of 0.5 Hz was applied.

The bladder was filled with 100 or 150 ml ~37°C water, and bladder contractions were generated by unilateral electrical stimulation of the pelvic nerve. Stimulation parameters were 30 pps, pulse width 150µs and stimulation current approx. 2.5 mA. Stimulation was on for 10 s, and there was at least 5 minutes between consecutive bladder contractions, to minimize fatigue.

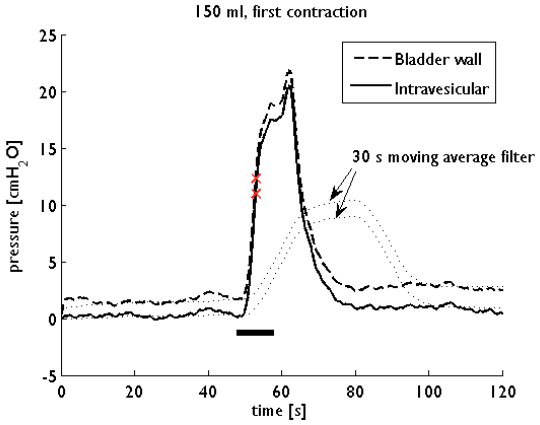


Fig. 1: A bladder contraction recorded during the second experiment. Morphologically the two traces are very similar; detection occurs at practically same time (see table 1). The black bar indicates stimulation of the pelvic nerve; thin dotted lines are the output from the 30 s moving average filter; crosses indicate the points where the onset of the contraction is detected.

Results

From pig 1, a total of 13 contractions were recorded; in pig 2, 6 contractions were recorded.

In pig 1 the sensor was placed on different positions and with the membrane facing both towards and away from the lumen of the bladder. No differences were observed between ipsilateral and contralateral placement of the sensor. With the membrane facing the lumen of the bladder, the two sensors measure almost identical pressures. When the membrane was turned away from the bladder lumen, a damped signal was observed on the implantable sensor.

In pig 2, the sensor was in the same place during all 6 contractions. Fig. 1 shows the pressure during a typical bladder contraction. The morphologies of the two traces are very similar, and the noise floor is of the same level. The pressure peak occurring about stimulation off was consistent across all contractions.

Table 1: Comparison of onset detection times between the two sensors. The two sensors can be seen to perform identically.

	Time of bladder onset [s]		
Cont. #	Ref.	Imp.	Delay
1 (150 ml)	5.16	5.10	-0.06
2 (150 ml)	4.69	4.69	0.00
3 (150 ml)	4.52	4.53	0.01
4 (100 ml)	5.22	5.18	-0.04
5 (100 ml)	5.02	4.94	-0.08
6 (100 ml)	5.88	5.57	-0.31

The onset of a bladder contraction is detected by a simple threshold algorithm. The threshold is defined as the output of a 30 s moving average filter plus 10 cmH_2O. When the pressure increases above this value, the onset is detected. Table 1 shows the time of detection from both the reference sensor and the implantable sensor, relative to stimulation onset.

Discussion and Conclusions

This work evaluated the ability of an implantable pressure sensor to detect the onset of bladder contraction.

In this regard, two factors are important. One is that the sensor shows adequate sensitivity (relative to the noise level) to resolve bladder contractions. The other is that there is no or little delay in the registration, compared to a standard reference pressure sensor monitoring the bladder pressure through a catheter.

Figure 1 shows the output from both sensors. With the amplification settings used (500x for the implantable sensor and 2000x for the reference sensor), the sensitivity is approximately the same for both sensors. Morphologically there is little difference between the two signals, indicating that there is neither damping nor delay introduced by the bladder wall or the sensor encapsulation.

In pig 2, the sensor was at the same location throughout the experiment. The offset between the two signals seen in figure 1, increased from about 2 cmH_2O in the first contraction, to 5 cmH_2O in the last contraction. This may be due to thermal drift, as the sensor was at room temperature before implantation, and the pig is assumed to be ~37°C. It could also be due to silicone swelling from absorption of body fluids, resulting in a small pressure being applied to the membrane.

Even with the simple contraction onset detection algorithm used, this offset did not influence the performance of the implantable sensor. This is because of the moving average filter used in the threshold; only relatively fast pressure changes are detected with this scheme. As long as the offset stabilizes at a level well below saturation, it does not influence the application.

In conclusion, the ability of the implantable sensor to detect the onset of bladder contractions is similar to that of the reference sensor.

References

[1] Lawrenson R, Wyndaele JJ, Vlachonikolis I, et al. Renal Failure in Patients with Neurogenic Lower Urinary Tract Dysfunction. Neuroepidemiol., 20: 138-143, 2001.

[2] Becker D, Sadowsky CL, McDonald JW. Restoring Function After Spinal Cord Injury. The Neurologist, 9:1-15, 2003.

[3] Vodusek DB, Light JK, Libby JM. Detrusor Inhibition Induced by Stimulation of Pudendal Nerve Afferents. Neurourol. Urodyn., 5: 381-389, 1986.

[4] Dalmose AL, Rijkhoff NJM, Kirkeby HJ, et al. Conditional Stimulation of the Dorsal Penile/Clitoral Nerve May Increase Cystometric Capacity in Patients With Spinal Cord Injury. Neurourol. Urodyn., 22:130-137, 2003.

[5] Hansen J, Media S, Nøhr M, et al. Treatment of Neurogenic Detrusor Overactivity in Spinal Cord Injured Patients by Conditional Electrical Stimulation. J. Urol., 173:2035-2039, 2005.

[6] Brindley GS. A substitute for hermeticity in implantable pressure sensors. J. Physiol. 272(1):7P-8P, 1977.

[7] Takayama K, Takei, M, Soejima T, et al. Continuous Monitoring of Bladder Pressure in Dogs in a Completely Physiological State. Brit. J. Urol., 60:428-432, 1987.

[8] Koldewijn EL, Van Kerrebroeck PEV, Schaafsma E, et al. Bladder Pressure Sensors in an Animal Model. J. Urol., 151:1379-1384, 1994.

[9] Wen JG, Jezernik, S, Chen Y, et al. Accessing Pelvic and Pudendal Nerve from a Simple Posterior Surgical Approach: An Experimental Bladder Control Study in Pigs. Asian J. Surg., 22(3):285-290, 1999.

Acknowledgements

This project was supported by the Danish National Advanced Technology Foundation. The authors wish to thank Dorthe Deding and Mathias Diernæs for their help with the surgical procedure.

Author's Address

Jacob Melgaard
SMI – Center for Sensory-Motor Interaction
Dept. Of Health Science and Technology
Aalborg University
Fredrik Bajers Vej 7D3
DK-9220 Aalborg, Denmark
jm@hst.aau.dk

Methods for *in vitro* study of electrical current and potentials distribution in layered biological tissue

Malešević N[1,2], Bijelić G[2]

[1] Faculty of Electrical Engineering, University of Belgrade, Serbia

[2] Fatronik, Serbia Ltd., Belgrade, Serbia

Abstract

In this work we present the improved method for studying of electrical current and potentials distribution in a layered biological tissue. The intimate contact between the electrode and outer skin layer often called electrode-skin interface is considered to be a principal barrier for electrical stimulus delivery and detection. The skin itself is composed of number of layers with different electrical properties as well the tissues beneath the skin and this heterogeneity and anisotropy are cause of current nonuniformities. Those effects are highly difficult to simulate by computer modelling techniques but can be measured in an in vitro study on human like tissue. We investigated how the electrical current distribution and potential field between transcutaneous electrodes are affected by properties of layered biological tissue. The measurements of electrical properties for different tissue layers were performed on pig abdomen in vitro used as a general model for layered biological tissue. We propose an improved experimental setup and method for such measurements. Our experimental findings provide insight into electrical properties of non excitable tissues and the effectiveness of related measurement method.

Keywords: *FES, multi-pad electrode, electrical current distribution*

Introduction

Biomedical events related to functional electrical stimulation applications are initiated by means of transcutaneous use of electrodes. Different types of electrodes used in the field of electrical stimulation are reviewed in [1], together with their properties. Recent investigation [2] has shown that inhomogeneity of the skin and electrode have a great influence on current density distribution. Different methods of electrode-skin interface modification and analysis are proposed in order to improve the distribution of current densities underneath the surface electrodes.

The difficulties in prediction of the electrical behavior of biological tissues such as skin, fat, muscle and nerve includes their heterogeneity and anisotropy. In addition the effects of electrode size, electrode separation and configuration are to be considered especially when using small pads within array electrode [3-6].

Array electrode, a device recently introduced to transcutaneous electrical stimulation field, are shown to be a promising concept in several applications [4, 5]. The array of electrodes enables selective activation of desired sensory or motor function with only minor activation of unwanted functions. Additionally array electrode device provides dynamic control of electrode position size and shape. The use of advanced stimulation array electrodes aims at reconstruction of functional movement such as grasping that will be very close to the one resulting from voluntary, physiological activation of muscles. In order to achieve this goal we are developing intelligent control system to interface the electrode function and desired movement properties. It appears that important confirmation of our advanced stimulation array electrode concept relies on detailed understanding of electrical stimulus interaction and distribution within excitable and non excitable biological tissue.

In this work we present the improved method for studying the electrical currents and potentials distribution in layered biological tissue when the array electrode is used for stimulation.

Material and Methods

Electric potentials inside flesh were measured using SBW (LMG Smith Brothers Limited) needle electrodes aligned in a matrix template, with 2.5 cm distance between neighboring measurement points, Fig.1. In present study 4x2 matrix of needle electrodes was incorporated. Electrical potentials on needle tips were acquired by NI USB-6212 A/D card at sampling rate of 20 KHz, and recorded using a program written in Matlab which collects

data from up to 16 analog input channels simultaneously.

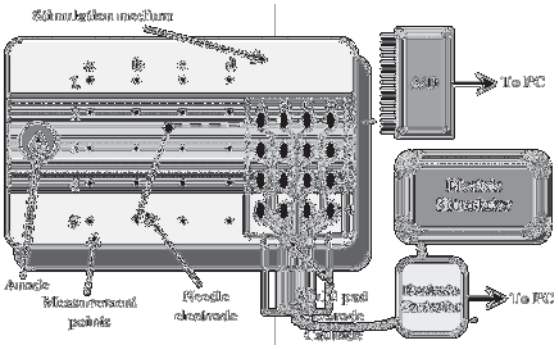


Fig. 1: Measurement system consists of measuring (needle) electrodes, acquisition system, testing (multi-pad) surface electrodes, stimulator, data processing and visualizing software and stimulation medium.

A custom made multi-pad electrode called INTEFES acted as a cathode. Electrode controller (PIC 18F4520) set a pad within multi-pad electrode to active state in a predefined manner; stimulation pulses were routed to every pad for the 400 ms. The anode was the Pals Platinum, 2x2 cm circular electrode.

For the electrical stimulation we used UNA-FET 4-channel stimulator [7]. The stimulator produced asymmetric, biphasic, current-controlled stimulation pulses. The pulse duration was 300 μs, amplitude 10 mA, with exponential charge compensation at stimulation frequency of 20 Hz.

A custom made program in Matlab was made to graphically illustrate electric potentials and current streamlines inside stimulation medium based on measured data.

Fresh pig abdomen was used for the experiments. The skin was washed with warm water and dried under nitrogen stream and two equal samples were sectioned. Both samples were stored for 24 hours at 5 °C to equilibrate. Hydration level and electrical properties equilibration was tested on each sample by means of impedance magnitude measurements using 100 Hz / 0.1 V stimuli.

Results and Discussion

The described set-up was utilized in evaluation of electrical field distribution during stimulation via multi-pad electrode. The experiment conducted comprised number of consecutive measurements of potentials at different depths at different distances between the stimulation and measurement electrodes. Measurement points chosen were distributed in 4x5 matrices (labeled from a-d and 1-5) with defined measurements point separation. Some of the results are summarized in Figures 2-4 for a2-d2 and a3-d3 lines at 2 cm depth.

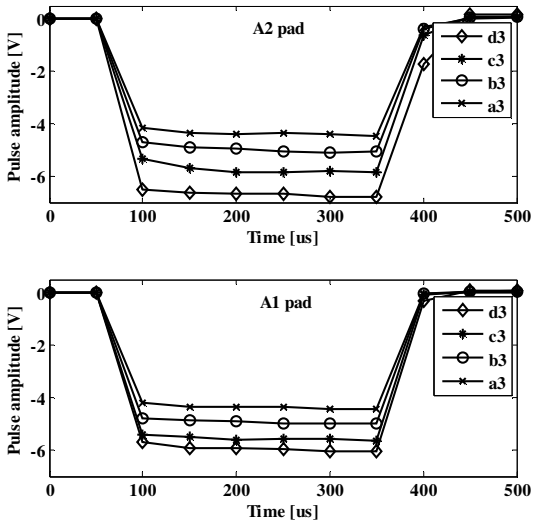


Fig. 2: Measured electric potential while stimulating with pads A2 and A1 at 2 cm depth.

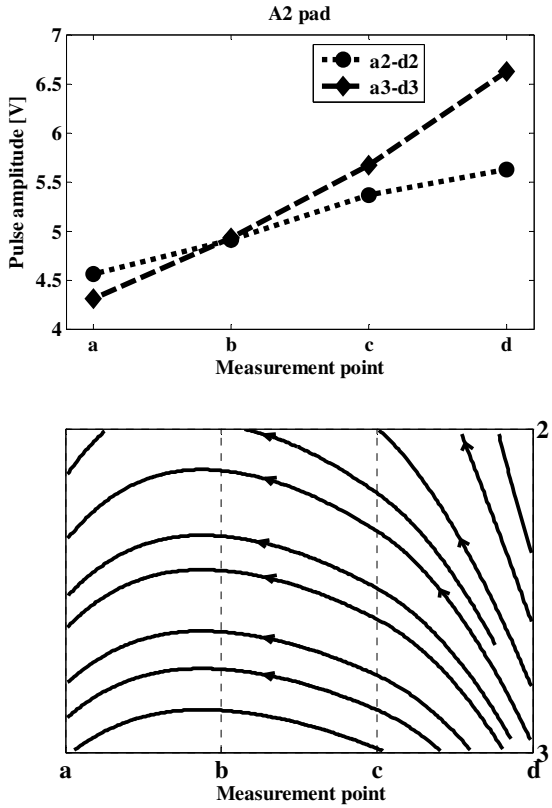


Fig. 3: Measured electric potential and calculated current streamlines while stimulating with pad A2, at 2 cm depth.

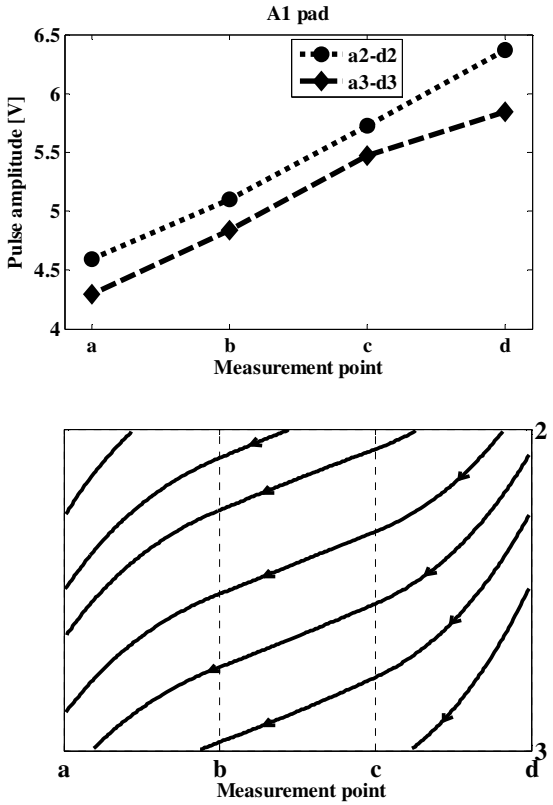


Fig. 3: Measured electric potential and calculated current streamlines while stimulating with pad A1, at 2 cm depth.

Calculated current streamlines roughly reflect trajectories predicted by computer modeling [3]. If extrapolated, calculated streamlines tend to converge towards area of nearby active field, which is desirable result of conducted measurement. When the active field is away from measurement points, e.g. D1-D2, streamlines are getting parallel because of homogenization of current density while passing through tissue.

Conclusions

The measurement system presented in this work is designed for investigation of electrical currents and potentials distributions in layered biological tissue.

The results shown demonstrate good qualitative correlation with computer modeling; however, large quantitative differences for potentials were observed in comparison with [3]. In our experiment gradient of measured potentials inside tissue was 3-4 times milder than suggested by computer modeling, implying that some of tissue properties were omitted by the model but included in the *in vitro* study.

The investigation of the effects of array electrode stimulation showed that we can define the size and configuration of the pads within multi-pad electrode, engaged in order to produce the desired pattern of electrical current streamlines inside biological layered tissue sample. This is of major importance for selective activation in multi-channel applications that are envisioned for therapy of both lower and upper extremities.

In order to investigate the evaluation method and measurement system presented in this work and its applicability we started *in vivo* experiments in animals. Those experiments consider the functional output (muscle contractions), but also the direct response to stimulation by recording the M wave.

References

[1] Popović D, Sinkjaer T. Control of Movement for the Physically Disabled. London: Springer-Verlag, 2000.

[2] Keller T, Kuhn A. Electrodes for transcutaneous (surface) electrical stimulation. Journal of Automatic Control, 18(2):35-45, 2008.

[3] Livshitz ML, Mizrahi J, Einziger DP. Interaction of Array of Finite Electrodes with Layered Biological Tissue: Effect of Electrode Size and Configuration. IEEE Transactions on Neural Systems and Rehabilitation Engineering. 9(4): 355-361, 2001.

[4] Popović-Bijelić A, Bijelić G, Jorgovanović N, Bojanić D, Popović MB, Popović DB,. Schwirtlich . Multi-Field Surface Electrode for Selective Electrical Stimulation. Artificial Organs, 29(6):448-452, 2005.

[5]Kuhn A, T Keller, Micera S, Morari M. Array electrode design for transcutaneous electrical stimulation: A simulation study. Medical Engineering & Physics, 31: 945–951, 2009.

[6] Kuhn A, T Keller, Lawrence M, Morari M. A model for transcutaneous current stimulation: simulations and experiments. Med Biol Eng Comput, 47: 279–289, 2009.

[7] UNA-FET. http://www.unasistemi.com/

Acknowledgements

This work was supported by Ministry of Science and Technological Development of Republic of Serbia (ET 11019).

Author's Address

Name: Malešević Nebojša, PhD student

Affiliations: Faculty of Electrical Engineering, Bulevar kralja Aleksandra 73, Belgrade, Serbia; Fatronik Serbia, Vladetina 13, Belgrade, Serbia
e-mail: nebojsa.malesevic@etf.bg.ac.rs
Homepage: bmit.etf.rs

Iterative learning control for FES of the ankle

Nguyen R[1], Micera S[1], Morari M[1]

[1] Automatic Control Laboratory, ETH Zurich, Zurich, Switzerland

Abstract

Existing methods for the control of the ankle joint during gait training are limited by poor performance or extensive tuning or training. Iterative learning control (ILC) has been effective in the control of functional electrical stimulation (FES) during repetitive tasks of the upper limbs. In this study, ILC was used to control the ankle joint via surface electrodes that stimulated the tibialis anterior and triceps surae muscles. The control objective was to track a repeating reference trajectory of the ankle obtained from normal walking. The controller was tested with 11 unimpaired individuals who were seated on a table with feet hanging over the edge. During a first experiment, individuals were asked to relax their legs and cease volitional effort. The controller provided good reference tracking and the root mean square error converged monotonically within 10 strides to approximately 2.5°. During a second experiment, in addition to FES, individuals were asked to actively participate with voluntary activity to track the reference trajectory. The controller reduced FES assistance in the presence of the new voluntary activity. Good performance was achieved using the proposed controller, which will be used with the robotic gait trainer Lokomat to provide better gait training.

Keywords: *FES, ILC, Lokomat.*

Introduction

Two emerging technologies to restore normal gait in individuals with gait impairments are functional electrical stimulation (FES) and robotic gait training. Although FES has been shown to improve rehabilitation outcomes, it has been limited by the lack of control strategies that result in normal kinematic walking patterns [1]. On the other hand, robotic gait training provides good kinematics by providing passive movements of the limbs. However, passive movements alone are not desirable as a rehabilitation strategy. Combining both technologies promises to provide better rehabilitation as one technology's disadvantage is compensated by the other's advantage.

The eventual goal of the work presented here is to combine FES with the Lokomat [2], a robotic gait trainer, to provide more complete gait training. The feasibility of such a combination has been shown, for example, by Dohring and Daly [3]. The main focus of our work is to develop control strategies that can adapt to individual patients and incorporate voluntary abilities whenever available. We focus in this paper on initial work on the control of the ankle joint using FES alone. Such control is useful to replace the passive foot lifters within the Lokomat.

Although open loop control of FES for gait training is possible, high levels of performance are desired for rehabilitation. Such levels could be obtained by more complex control architectures [4,5], but may require extensive tuning or training. Avoiding these limitations while still achieving good performance has been possible using iterative learning control (ILC) in repetitive tasks for the upper limbs [6,7]. ILC takes advantage of repetition to automatically adjust to individual physiologies and thus is well suited for the task of repetitive gait training.

Material and Methods

Apparatus

Two channels of an FES stimulator (Compex Motion, Compex SA, Switzerland) were used to induce muscular contractions of the tibialis anterior and triceps surae muscles through transcutaneous electrodes of size 5 cm by 10 cm and 5 cm by 5 cm (Compex Medical SA, Switzerland). Asymmetric biphasic pulses of width 400 μs were delivered at 40 Hz. Current amplitude was controlled by ILC, which was implemented using custom software (Labview, National Instruments Corporation, USA). Measurements of the ankle angle were received from a strain gauge goniometer (SG 110, Biometrics Ltd., UK).

Controller

The control objective was to have the ankle angle track a repeating reference trajectory. Thus one cycle of this trajectory will be referred to as a stride.

Using ILC, the input profile was updated as:

$$u_{i+1}(n) = LP * [u_i(n) + c_{LG} \cdot e_i(n+k)]$$

where the subscripts indicate the stride index, n the sample index within a stride, k the constant sample offset, u the stimulation current input, LP the low pass filter, c_{LG} the constant learning gain, and e the error between the actual and reference ankle

trajectory. During the entire first stride, the input was set to zero so that the controller would comfortably increase stimulation gradually.

Since there was a delay from the time the input u was applied to the time this input had an effect on the error e, a constant sample offset k was required to take this into account. The lowpass filter LP acted to prevent high frequency components of the stimulation that could cause discomfort. For all individuals and experiments, the same empirically derived controller parameters were used.

A stride time of 2 s was chosen because it was close to stride times that were typically used in the Lokomat for rehabilitation. Also, a sampling frequency of 40 Hz was used since the stimulation was delivered at that frequency.

Protocol

Experiments were performed with 11 individuals with mean age 21 years (SD 2 years) with no gait impairments. The goniometer was attached to a bare foot and calibrated such that the ankle angle was 0° during upright standing, positive during dorsiflexion, and negative during plantarflexion. Individuals sat upright on the edge of a table with the lower leg hanging perpendicular to the table. Two electrode pairs, one for the tibialis anterior and the other for the triceps surae, were placed on the shank such that inversion/eversion was minimized during stimulation. The reference trajectory was obtained from the normal walking of one individual, averaged over all strides.

During the first experiment, the controller was set to track the reference trajectory for 30 strides and individuals were asked to completely relax their ankles. This was verified by turning off the controller at the end without indication and observing that the foot had dropped.

During the second experiment, the individuals were asked to relax their ankles for the first 20 strides and then to participate activity to track the reference trajectory shown on a monitor for the next 20 strides. To aid tracking, the monitor displayed both the reference and actual trajectories as functions of time. Voluntary tracking was practiced by individuals before the experiment until consistent performance was achieved.

Results

Trajectory Tracking without Volitional Effort

Fig. 1 shows typical results from one individual without volitional effort over the last 10 strides of the experiment when the error had converged, that is the error was found to be consistent from stride to stride. Because the foot was hanging in the air, triceps surae stimulation was needed for only a short period of time during fast plantarflexion.

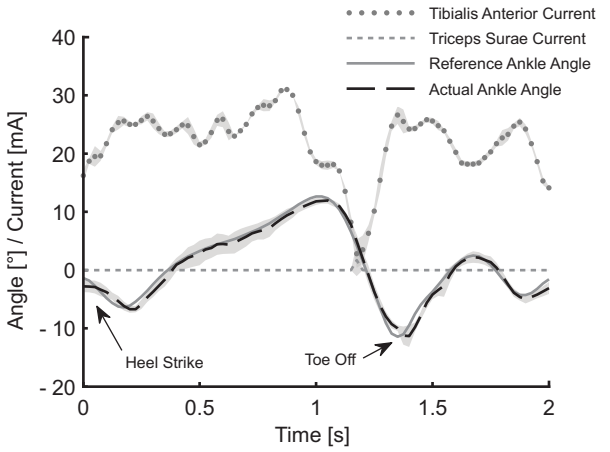


Fig. 1: Mean stimulation currents with actual and reference ankle trajectories over the last ten strides of one individual with no volitional effort. The shaded areas indicate the bounds of one standard deviation.

The root mean square (RMS) error was determined for each stride of each individual and averaged over all individuals. The progression of this error with stride number is shown in Fig. 2. The results show a good learning transient with monotonically decreasing RMS error between stride 1 and stride 10 before settling at an RMS error of approximately 2.5°.

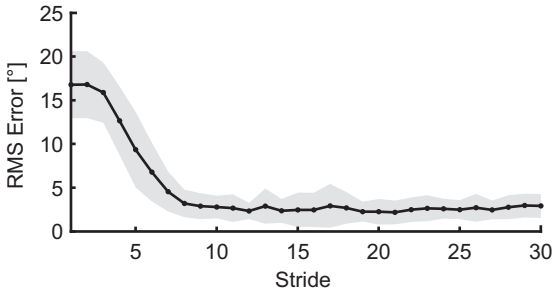


Fig. 2: Mean RMS error of all individuals with no volitional effort. The shaded areas indicate the bounds of one standard deviation.

Trajectory Tracking with Active Participation

The progression of the mean RMS error across all individuals during active participation is shown in Fig. 3. As expected, the learning transient for the first half is similar to the previous experiment with no volitional effort.

Once active participation began, the amount of stimulation decreased. However, an unexpected result was that trajectory tracking performance worsened under such voluntary activity.

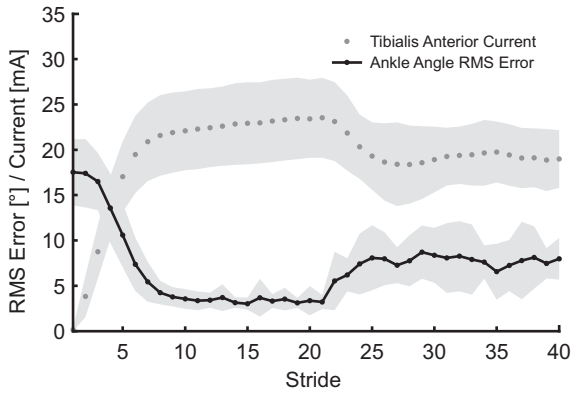


Fig. 3: Mean RMS ankle angle error and tibialis anterior stimulation current of all individuals with no voluntary effort during the first 20 strides and voluntary effort during the next 20 strides. The shaded areas indicate the bounds of one standard deviation.

Discussion and Conclusions

Trajectory Tracking

The results show good trajectory tracking performance using the proposed ILC. Moreover, the error decreased monotonically before settling at a low value within only 10 strides, a behaviour that is not guaranteed for all ILC [8]. The results were obtained using the same set of control parameters for all individuals, despite differences in physiology, which is particularly important when applied to individuals with gait impairments.

The experiment with active participation demonstrated that assistance, in the form of stimulation current, was reduced when voluntary effort was present. The controller acted by supplementing voluntary movements only when needed. Such assist-as-needed behaviour is desirable because it has been shown to be an effective rehabilitation paradigm [9].

Limitations

Although good performance was obtained, modifications will likely be needed before successful implementation of the ILC to individuals with gait impairments in the Lokomat. For example, the implicit assumption of repetitive voluntary activity may not be valid. Indeed, even with unimpaired individuals in this study, non-repetitive activity caused increased RMS error. To compensate for such non-repetitive disturbances, a feedback component should be added.

Strictly speaking, ILC is only applicable when a task of finite interval is repeated with resetting between intervals. Because resetting does not occur during normal walking, repetitive control (RC) [10] may be more appropriate for gait training. RC assumes a repeating trajectory but does not assume resetting between intervals.

Conclusions

ILC provides good ankle trajectory tracking that quickly adjusts stimulation to take into account individual abilities and limitations without the use of a priori models or training experiments. Thus, ILC promises to be an effective way to control FES within the Lokomat for gait rehabilitation.

References

[1] Peckham HP and Knutson JS. Functional Electrical Stimulation For Neuromuscular Applications. Annu Rev Biomed Eng, 7: 327-360, 2005.

[2] Colombo G, Wirz M, Dietz V. Driven gait orthosis for improvement of locomotor training in paraplegic patients. Spinal Cord, 39: 252-255, 2001.

[3] Dohring ME and Daly JJ. Automatic Synchronization of Functional Electrical Stimulation and Robotic Assisted Treadmill Training. IEEE Trans Neural Syst Rehabil Eng, 16: 310-313, 2008.

[4] Fuhrs T, Quintern J, Riener R, et al. Walking with WALK! IEEE Eng Med Biol Mag, 27: 38-48, 2008.

[5] Kojović J, Djurić-Jovičić M, Došen S, et al. Sensor-driven four-channel stimulation of paretic leg: Functional electrical walking therapy. J Neurosci Methods, 181: 100-105, 2009.

[6] Freeman CT, Hughes A-M, Burridge JH, et al. Iterative learning control of FES applied to the upper extremity for rehabilitation. Control Eng Pract, 17: 368-381, 2009.

[7] Dou H, Tan KK, Lee TH, et al. Iterative learning feedback control of human limbs via functional electrical stimulation. Control Eng Pract, 7: 315-325, 1999.

[8] Bristow DA, Tharayil M, Alleyne AG. A survey of iterative learning control. IEEE Contr Syst Mag, 26: 96-114, 2006.

[9] Cai LL, Fong AJ, Otoshi CK, et al. Implications of Assist-As-Needed Robotic Step Training after a Complete Spinal Cord Injury on Intrinsic Strategies of Motor Learning. J Neurosci, 26: 10564-10568, 2006.

[10] Longman RW. Iterative learning control and repetitive control for engineering practice. Int J Control, 73: 930-954.

Acknowledgements

We wish to thank Felix Jonasch for his assistance in development and data collection, Hocoma AG for their support in this project, and the individuals who participated in this study.

Author's Address

Robert Nguyen
Automatic Control Laboratory, ETH Zurich
nguyen@control.ee.ethz.ch
www.control.ee.ethz.ch

Blink prosthesis for facial paralysis patients

McDonnall D[1], Gossman MD[2], Guillory KS[1]

[1] Ripple LLC, Salt Lake City, USA

[2] University of Louisville, Louisville, USA

Abstract

Six subjects with profound facial paralysis were tested to determine the feasibility of restoring functional blink via electrical stimulation of the orbicularis oculi muscle (OOM) without also evoking painful sensations. Stimulation of the paretic eyelid was triggered by EMG detection of blink in contralateral healthy OOM to deliver charge during inhibition of the levator palpebrae antagonist. Transcutaneous and percutaneous stimulation electrode placements were tested during multiple stimulation trials in subjects. Stimulation was delivered via two constant voltage computer controlled channels. Sensory activation thresholds were approximately an order of magnitude lower for percutaneous stimulation (0.4 V) vs. transcutaneous stimulation (3 V). Exploration of multiple possible stimulation paradigms yielded a means by which sufficient muscle activation could be recruited to evoke complete eyelid closure without producing prohibitively painful sensation. Stimulation efficacy across subjects correlated with degree of patient neuromuscular recovery following initial paresis.

Keywords: *neuroprosthesis, FES, eye blink, facial paralysis*

Introduction

Patients with facial nerve damage suffer substantial disfigurement and dysfunction due to the loss of ability to convey facial expression and produce eye blink. The loss of function of the orbicularis oculi muscle (OOM), which produces eye blink, also makes patients highly susceptible to related eye pain, eye infection, and, in many cases, loss of the affected eye. We are developing an implantable blink prosthesis to electrically activate the paretic OOM to restore blink in patients with facial paralysis. Patients with seventh nerve trauma do not necessarily lose sensation in the face because sensory nerves that innervate the eyelid are located in the fifth cranial nerve. Thus, electrical stimulation in this area can produce a painful sensation that is prohibitive to its use as a therapeutic approach. To date all experimentation of electrically evoked blink has been performed in animals, and the question of inadvertent painful stimulation has not been addressed in the literature. The goal of this study is to determine if it is possible to electrically evoke blink in patients with facial paralysis without also eliciting a painful sensation.

Methods

Subject selection

In the course of this pilot clinical study we recruited six patients for participation in stimulation experiments under approval from the University of Louisville Institutional Review Board. These patients included five women and one man ranging in ages from 41 to 62 whose facial paralysis was the result of complications ranging from long-term Bell's palsy and tumor resections, which took place between six months and fifteen years ago.

Experimental design

Several stimulation paradigms were tested during independent sessions to assess the feasibility of electrically evoking blink. Each experimental session with all patients consisted of the same steps: parametric assessment of stimulation thresholds, baseline spontaneous blink measurement, and stimulation triggered by contralateral blink. Only the specific stimulation parameters were changed during subsequent experimental sessions.

Assesment of stimulation thresholds

To assess the senstitivity of patients, stimulation paradigms were tested to determine if a motor response could be elicited within a comfortable range of stimulation intensities. Patients were instructed to rate discomfort on a scale of 1 to 5, with 1 representing a small, barely perceptible sensation and 5 representing a sensation that is not painful, but at the upper limit of what would be comfortable for extended periods. Stimulation pulse amplitude (STM100C, BIOPAC Systems, Inc., Goleta, CA) was increased slowly as patients

reported increased sensation perception until either an evoked blink was produced or patients reported level 5 discomfort. If patients reported level 5 discomfort before blink could be evoked, higher levels of stimulation intensity were not tested.

Baseline spontaneous blink measurement

All patients tested were capable of some degree of closure during spontaneous blink; however, none of the patients included in the study could produce complete eyelid closure during spontaneous blink. It was necessary to record the degree of closure each patient could produce to assess how much additional eyelid closure was evoked by electrical stimulation.

Ten spontaneous blinks were recorded for each subject to determine the degree of closure subjects were capable of producing with the paretic eyelid. Patients were instructed to watch a computer screen playing a video placed at eye level six feet away. A high-speed video camera was placed directly above the video screen to capture eyelid motion. Spontaneous eye blink was recorded with a high-speed video camera (EPIX, Inc., Buffalo Grove, IL) at 500 frames per second (fps). The camera was triggered to record spontaneous blink for one second when triggered from an EMG signal collected (EMC100C, BIOPAC Systems, Inc., Goleta, CA) from the contralateral healthy OOM. In order to record pre-blink eyelid position, imaging software continually updated collected images at 500 fps in a buffer until the triggering pulse signaled the video card to include 30% of pre-triggered images in the one-second recording. Eyelid motion was tracked frame-by-frame in post-hoc analysis.

Stimulation triggered by contralateral blink

The normal waking condition, with the eyelids open, is accomplished by tonic contraction of the levator palpebrae (LP) muscle and a lack of activity within the OOM. During spontaneous blink these patterns of activity reverse, such that the LP relaxes just prior to the initiation of the OOM contraction at the onset of blink and resumes contraction following OOM relaxation at the completion of a blink. Thus it is believed a stimulated OOM response evoked during spontaneous blink would produce a greater degree of closure when LP is inhibited than during non-triggered stimulation. Once tolerable stimulation parameters were determined, stimulation was triggered by EMG detection of contralateral blink to evoke a synchronous contraction. The degree of eyelid closure during triggered spontaneous blink, quantified by off-line analysis of high-speed video recordings, was compared with baseline closure data to determine effect of stimulation.

Results

Initial surface pulse stimulation

Biphasic pulses (5 ms per phase in 60 ms pulses trains at 50 Hz) were delivered at subthreshold voltages using a pair of ball electrodes 2 mm in diameter spaced approximately 5 mm apart 2 mm above the lid, and pulse amplitudes were increased while within tolerable patient discomfort levels. All patients experienced sensory activation at relatively low stimulation levels. Data averaged across five facial paralysis patients resulted in sensory stimulation thresholds at 3 ± 0.7 V (mean±SEM). Stimulation amplitudes were further increased to evoke a motor response; however, in all patients a level 5 discomfort sensation was reported (13 ± 0.5 V) before an evoked blink response was elicited.

Stimulation was repeated at maximum tolerable discomfort levels triggered by the contralateral blink response; however, no evoked motion beyond recorded baseline activity was detected during LP inhibition.

Previous studies investigating evoked blink were all performed in animal models, thus the observation that this commonly used stimulation protocol produced a **prohibitively painful sensation at stimulation levels below motor activation thresholds** was a new finding. Stimulation at amplitudes exceeding the proscribed patient maximum discomfort level were not investigated to determine motor thresholds, despite patients' stated willingness to continue. A blink prosthesis which delivers a painful stimulation each time a patient blinks has little clinical relevance.

Multichannel percutaneous stimulation

Given the painful response evoked by stimulation in our initial experiments, we explored additional stimulation paradigms designed to selectively recruit a motor response independent of nociceptor activation. It was hypothesized that surface stimulation produced a prohibitively painful sensation because the ball electrodes were closer to dermal pain receptors than underlying OOM fibers. Implanted percutaneous stimulation electrodes would deliver charge directly to the paretic OOM. We used 30 gauge needles to insert platinum microwires (100 μm diameter) approximately 1 mm into the upper paretic eyelid. The Teflon-coated wires were deinsulated 500 μm at the tip, threaded through needles, and the deinsulated portion was advanced past the needle cannula and

bent to create a barb to keep electrodes in place during stimulation. Four microwires were implanted 2 mm above the lid margin at approximately 4 mm spacing across the upper eyelid. Stimulation was distributed across an additional pair of electrodes to activate a larger population of OOM fibers. Multichannel stimulation has been shown [1] to evoke a motor response in paretic dog eyelids using pulse amplitudes lower than those used to evoke contractions using a single stimulation channel.

Sensory thresholds for this interleaved percutaneous stimulation paradigm were almost an order of magnitude lower (0.4 ± 0.1 V) than the transcutaneous single pair paradigm. In four of the five patients tested, a motor response was detected prior to reaching discomfort level 5. At the upper limit of comfortable stimulation, the OOM between mid-iris and the medial canthus was deflected downward, producing significantly ($p<0.05$, *student's paired T-test*) more eyelid closure than patients were capable of during spontaneous blink. However, this increased closure was not sufficient to completely close the palpebral fissure in any of the patients.

Although even a modest increase in eyelid closure may have some therapeutic benefit in preventing ocular complications in facial paralysis patients, multichannel percutaneous stimulation did not evoke functional blink. Additional stimulation paradigms needed to be tested to demonstrate feasibility.

Interferential stimulation

Given the apparent inability of stimulation paradigms shown in previous animal studies to evoke pain-free blink, additional stimulation paradigms were tested. Interferential stimulation is commonly used in rehabilitation surface stimulation applications to transcutaneously evoke muscle contractions without producing a painful sensation [2]. In this experiment, we applied stimulation with two channels across eight electrodes – one channel was stimulated at 2000 Hz and the other at 2028 Hz to produce an interferential stimulation frequency of approximately 30 Hz.

Interferential stimulation evoked a motor response in all three patients tested below the maximal discomfort threshold (two patients declined to participate in the final phase of the study). Furthermore, in two of these three patients, a complete functional blink was evoked below the maximal discomfort threshold. Patients described the sensation of interferential stimulation as "an involuntary twitch" in contrast with the previously tested stimulation paradigms, which were described as "sharp" and "biting." A substantial increase in evoked motion was elicited within the range of tolerable sensation.

Discussion

It is likely that interferential stimulation may have been more effective at evoking a pain-free blink because stimulation was more broadly distributed across the paretic OOM. It has been shown [3] that muscle fibers within OOM do not extend across the length of the eyelid. Instead, muscle fibers are 7-8 mm in length and are distributed radially around the palpebral fissure. Effective stimulation of the OOM must activate muscle fibers across the entire width of the eyelid. We are developing an implantable array to insert into the palpebral portion of the upper lid with electrodes positioned to specifically target muscle fibers responsible for spontaneous blink.

References

[1] Somia NN, Zonneviljlle ED, Stremel RW , et al. Multi-channel orbicularis oculi stimulation to restore eye blink function in facial paralysis. Microsurgery, 21(6): 264-270, 2001.

[2] Ward AR, Lucas-Toumbourou S. Lowering of sensory, motor and pain-tolerance thresholds with burst duration using kilohertz-frequency alternating current electric stimulation. Arch Phys Med Rehab, 88(8): 1036-1041, 2007.

[3] Lander T, Wirtschafter JD, McLoon LK. Orbicularis oculi muscle fibers are relatively short and heterogeneous in length. Invet Ophthalmol Vis Sci, 37(9): 1732-1739, 1996.

Acknowledgements

The authors would like to thank Robert Askin and Jessica Roby for assisting in data collection. This work was completed with support from the National Eye Institute (R44EY017247).

Author's Address

Daniel McDonnall, Ph.D.
Ripple LLC
danny@rppl.com
www.rppl.com

Effects of the number of pulses on evoked sensations in pairwise electrocutaneous stimulation

Geng B[1], Yoshida K[1, 2], Jensen W[1]

[1] Center for Sensor-Motor Interaction, Aalborg University, Aalborg, Denmark

[2] Biomedical Engineering Department, Indiana University-Purdue University Indianapolis, Indianapolis, USA

Abstract

This study aimed to investigate the effect of the location and the number of stimulation pulses on evoked sensations in pairwise electrocutaneous stimulation. Five electrodes were placed around the forearm of 16 healthy human subjects. Fixed amplitude, biphasic stimuli with five different pulse numbers (n = 1, 2, 5, 10, 20) were applied to three pairs of electrode sites. Evoked sensations were evaluated by using a computerized questionnaire to qualify and quantify the evoked sensation. We found that the sensations elicited with stimulating electrodes close to the median nerve were less pin-prick like. A larger number of pulses introduced a blunt sensation, than those evoked with fewer pulses. The strength of tactile sensations was positively related to the number of pulses. These findings provide further understanding of the effect of stimulation parameters on evoked sensations, and will assist to the design of efficient and user-acceptable sensory feedback scheme.

Keywords: *Electrocutaneous stimulation, sensory feedback, psychophysical test.*

Introduction

Electrocutaneous stimulation has shown to be a promising means to provide or enhance sensory feedback, mainly due to its non-invasiveness and capability of producing a sensation whose frequency and intensity can be reliably controlled [1]. A number of successful applications of electrocutaneous stimulation have been reported to improve sensory feedback in limb prostheses [2-4].

Apart from the application in sensory feedback for limb prostheses, there is evidence showing that sensory feedback can be used to reduce phantom limb pain (PLP) and chronic limb pain. For example, a regimen of surface stimulation in combination with a sensory discrimination task was able to reduce PLP in five amputee patients [5]. They were asked to discriminate different locations and frequencies of stimuli applied to the stump. After two weeks of training, the PLP was found to be relieved. In addition, a recent study demonstrated that tactile discrimination, other than stimulation alone can relieve pain in patients with complex regional pain syndrome (CRPS) [6].

In both applications, however, an effective stimulation paradigm may largely depend on the stimulation parameters chosen for sensory modulation. It is thus important to find out how the stimulation input affects the sensory output. The objective of this study was to investigate the effect of location and the number of pulses in a stimulus on evoked sensations. Pulse trains of five pulse numbers × three pairs of electrode sites were applied to the forearm skin. The sensations perceived by the subjects were evaluated by performing psychophysical tests.

Material and Methods

Subjects

16 healthy subjects (8 male and 8 female, aged 22-36, mean 28.3 years) participated in the experiment, which was approved by the Danish Local Ethics Committee (ref no.: N-20090009).

Electrode placement

Five Ambu Neuroline 700 surface electrodes were placed around the left forearm. The five electrode sites will be referred to as: S1, S2, S3, S4 and S5. They were positioned according to the following rules: 1) S1 over the median nerve, 2) S2 laterally adjacent to S1, 3) S3-5 equally spaced between S2 and S1. The schematic of the electrode placement is shown in fig.1.

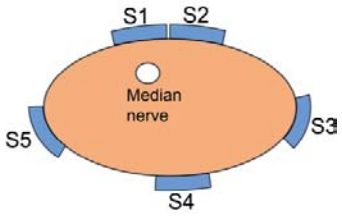


Fig. 1: The cross-section view of the electrode locations on the left forearm (view from the distal side).

Stimulation protocol

Symmetric, biphasic, rectangular 400 μs pulses were applied. The current amplitude was fixed to the level at which non-painful, but clearly local sensations were evoked when stimulation applied to S1. The amplitude level was approximately three times of the perception threshold.

Pulse trains (pulse number n = 1, 2, 5, 10, and 20) were simultaneously applied to selected pairs of electrodes: S1&S2, S1&S4 and S3&S5. In total, 48 trials for each pulse number, and 80 trials for each pair of electrode sites have been evaluated.

Sensation evaluation

The sensations were evaluated from four aspects: modality, location, quality, and strength. A customized psychophysical questionnaire was designed to perform the evaluation. Pre-defined answers were provided for the subject to describe the sensation just perceived. The subjects were instructed in the definition of the answers before the experiments. The words that best describe the sensation should be chosen. The strength of the sensation was rated by a Visual Analogue Scale (VAS, 10 cm).

The pre-defined answers are a set of standard words describing a sensation. The selection of the pre-defined answer words was based on relevant literature and our pilot experiments.

The questionnaire was displayed on a computer screen. The subject's task was to concentrate on perceiving the stimulus. When a stimulus was delivered, the subject answered the questionnaire and submitted the answers via the computer interface. The next stimulus was then delivered automatically after approximately 5 s. During the experiment, the stimulus information was blind to the subject.

Data Analysis

The data collected from the measurement of the modality, location and quality is binary data. Therefore, the Cochran's Q test was used to test if the number of pulses had an effect on the modality of the evoked sensations. The VAS data is essentially a type of ranking data. The Friedman test was used to evaluate the effect of the number of pulses on the strength of the sensations. The significance level was chosen to be 0.05.

Results

Fig.2 shows a heat map of the results. The colors encode the number of subjects reporting the same sensation. A warmer color (i.e., red) represents that more subjects reported the answer, and a cooler color (i.e., blue) indicates fewer subjects. Each block corresponds to one pair of electrodes, including the measurement (x-axis) under five different pulse numbers (n = 1, 2, 5, 10, and 20; y-axis, right).

The highlighted areas marked with the number '1' in Fig. 2 shows that touch, pinprick and movement were the three most frequently reported sensation types. Among the three pairs of electrode sites, the stimulation at S1&S2 appeared to produce less pin-prick like sensations than S1&S4 and S3&S5. The higher the number of pulses was, the more pin-prick sensations were reported. Similarly, a larger number of pulses produced more sensations of movement. The highlighted area marked with the number '2' in Fig 2, indicated that, a larger number of pulses was more likely induce sensations in an area spreading from the electrode sites, instead of a local (i.e., right under the electrodes) and referred (i.e., discrete) areas. A spreading sensation was more easily occurred at S1&S2 than at S1&S4 and S3&S5.

The subjects were inclined to choose words 'mild' or 'intense', 'sharp' or 'blunt', rather than 'comfortable' or 'uncomfortable' to describe the quality of the sensations they perceived. A larger number of pulses appeared to produce more 'intense' and 'blunt' sensations, which can be observed in the highlighted area 3 in Fig 2.

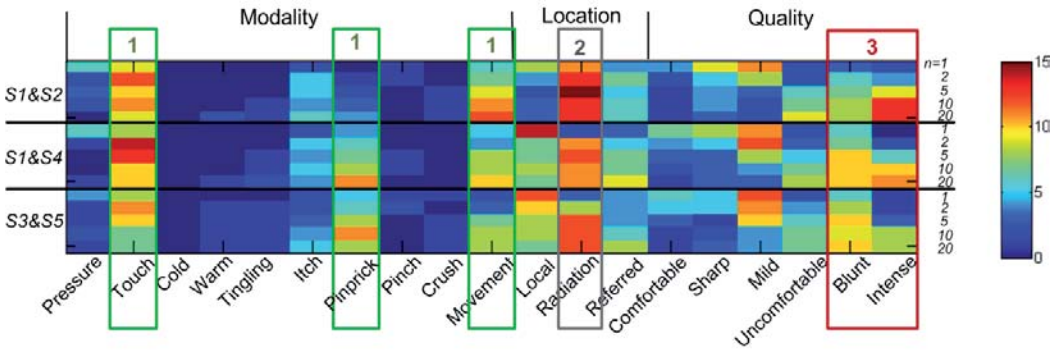


Fig.2. Heat map of the data of sensation modality, location and quality collected from 16 subjects.

Since tactile sensation is particularly useful in most sensory feedback applications [1], we analyzed the data of tactile sensation in further detail. Fig. 3 shows the proportions of subjects that reported tactile sensations (i.e. touch or pressure) in the three electrode combinations. It can be observed that fewer subjects perceived tactile sensations at the S3&S5 than S1&S4 and S1&S2. Additionally, it appeared that more subjects perceived tactile sensation when the pulse number was fewer than 10, regardless of the electrode combination. A Cochran's Q test was used to test if there was a significant difference in the five proportions in the case of three electrode combinations, respectively. The results indicated a significant difference (p = 0.003) at S1&S4, but no significant differences were found at S1&S2 and S3&S5.

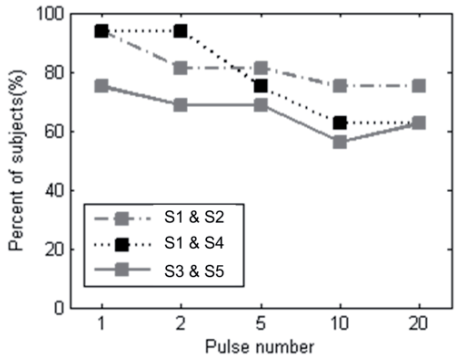


Fig. 3: Proportions of the subjects that reported tactile sensation when the stimulation was applied to S1&S2, S1&S4, and S3&S5, respectively.

Fig. 4 shows the mean and standard deviations of the VAS scores for the five types of perceived sensations at the S1&S2. With growing number of pulses, an increase in the strength of perceived sensations can be clearly observed. A Friedman test was then performed and the results indicated a significant difference ($p < 0.01$) in the strength of tactile sensation among the five different pulse numbers. There is also significant difference in the case of stimulation at S1&S4 ($p < 0.01$) and S3&S5 ($p < 0.01$).

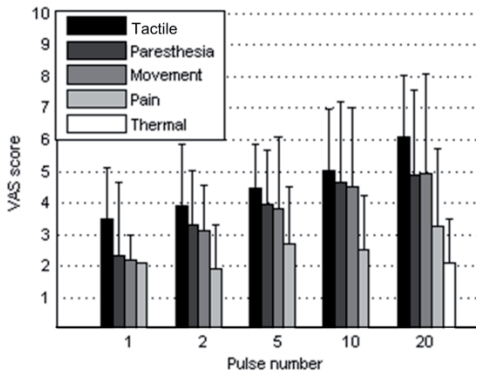


Fig. 4: Means and standard deviations of the VAS score for five sensation modalities with stimulations applied to S1&S2.

Discussion and conclusions

In the present work, we evaluated the effect of the number of pulses and the stimulating location on the evoked sensations in pairwise electrical surface stimulation in the human forearm. We found that touch, pinprick, and movement were the three sensation modalities. A larger pulse number more likely induced sensations distributed in a spreading area. Less pin-prick like sensation was elicited when the electrodes were placed close to the median nerve. Based on the analysis of the tactile sensation, the pulse number seemed to have more impact on the strength, than the type of evoked sensations. Our finding suggests that appropriate selection of the number of pulses is important to artificially induce stable sensations in an electrical-stimulation based sensory feedback system.

References

[1]Szeto AY, Saunders FA. Electrocutaneous stimulation for sensory communication in neurorehabilitation engineering. *IEEE tran. Biomed. Eng.,* **29**: 300-8, 1982.

[2] Beeker TW, During J, Den Hertog A. Technical note: Artificial touch in a hand prosthesis. *Med. & Biol. Eng. & Comput.*, **5:** 47-9, 1967.

[3] Schmidl H. The importance of information feedback in prostheses for the upper limbs. *Prosthetics and Orthotics International*, **1:** 21-4, 1977.

[4] Shannon GF. A myoelectrically-controlled prosthesis with sensory feedback. *Med. & Biol. Eng. & Comput.*, **17:** 73-80, 1979.

[5] Flor H, Dencke C, Schaefer M, et al. Effect of sensory discrimination training on cortical reorganization and phantom limb pain. *Lancet*, **357**: 1763-4, 2001.

[6] Moseley GL, Zalucki NM, Wiech K. Tactile discrimination, but not tactile stimulation alone, reduces chronic limb pain. *Pain*, **137**: 600-8, 2008.

Acknowledgements

This work was funded by the EU TIME project (CP-FP-INFSO 224012/TIME).

Author's Address

Bo Geng and Winnie Jensen
Center for Sensor-Motor Interaction
Aalborg University, Fredrik Bajersvej 7D-3,
9220 Aalborg, Denmark
bogeng@hst.aau.dk, wj@hst.aau.dk

Ken Yoshida
Biomedical Engineering Department
Indiana University-Purdue University Indianapolis
723 West Michigan Street SL-220F
Indianapolis, IN 46202, U.S.A.
yoshidak@iupui.edu

Development of a Wearable Sensory Prosthetic Device for Patients with Peripheral Neural Disturbances

Mabuchi K[1], Niiro H[2], Kunimoto M[3], Suzuki T[1], Ishikawa M[1], Shimojo M[2]

[1] Graduate school of Information Science and Technology, The University of Tokyo, Tokyo, Japan

[2] Faculty of Electro-communications, The University of Electro-communications, Chofu, Japan

[3] Saiseikai Yokohamashi Tobu Hospital, Yokohama, Japan

Abstract

This paper presents a prototype of a wearable sensory prosthetic system with which patients suffering from peripheral sensory disturbances and lost sensory function of the extremities will be able to feel somatic sensations as if they were touching an object with their healthy hand. Test results indicate that the system will be able to compensate or even enhance the sensory function that has been lost due to peripheral neuropathy.

The system consists of flexible fingerstalls and a palm patch equipped with pressure sensors and percutaneous micro-electrical stimulation to sensory nerve fibers of the peripheral nerve was used in order to evoke pressure sensation to the subject.

The results show that the system works satisfactorily, with subjects able to feel the pressure sensation resulting from the pressure applied to the pressure sensor of the fingerstall.

There was also a good correlation between the pressure applied to the pressure sensor system and the subjective intensities of the evoked pressure sensations.

Keywords: *sensory prosthetics, microstimulation, artificial somatic sensation*

Introduction

For people whose peripheral nerve functions have been lost or disturbed due to injury or diseases, it is very important to substitute for their lost neural functions in some way.

Functional electrical stimulation (FES) has been widely studied as a way to substitute for motor functions, but it has not been thoroughly examined for the substitution of sensory functions.

In this study, we developed a prototype of a sensory prosthetic system for patients who have lost the sensory function of the extremities due to peripheral nerve injury or peripheral neuropathy.

The system is composed of a fingerstalls and a palm patch equipped with pressure sensors. The sensors detect mechanical stimuli, which are transferred stimuli to the subject by means of a microstimulation method so that the subject experiences the stimuli as the corresponding somatic sensations [1].

In trials, the system worked satisfactorily and there was a good correlation between the pressure applied to the pressure sensors and the subjective intensities of the evoked pressure sensations.

Material and Methods

One healthy male subject participated in the experiment. Experimental arrangement is shown in Fig.1. The system consists of the two subsystems, one for sensing mechanical stimuli and the other for stimulating sensory nerve fiber.

Microstimulation Method

The microneurographic technique involves the percutaneous and direct insertion of a tungsten microelectrode into a peripheral nerve so that the signal from the nerve fiber attached to the tip of the electrode can be measured and so that a microstimulation can be given to the nerve fiber.

There are mainly four kinds of mechanosensitive receptors on the skin: Merkel discs, Ruffini endings, Meissner corpuscles, and Vater-Pacini corpuscles [2]. The response of these receptors is classified into four patterns: slowly adapting I (Merkel), slowly adapting II (Ruffini), rapidly adapting type (RA: Meissner), and Pacinian type (PA: Vater-Pacini).

Ochoa et al have reported that a pressure sensation is evoked by stimulating an SA-I mechanoreceptor unit and that the magnitude of the evoked sensation is influenced by the

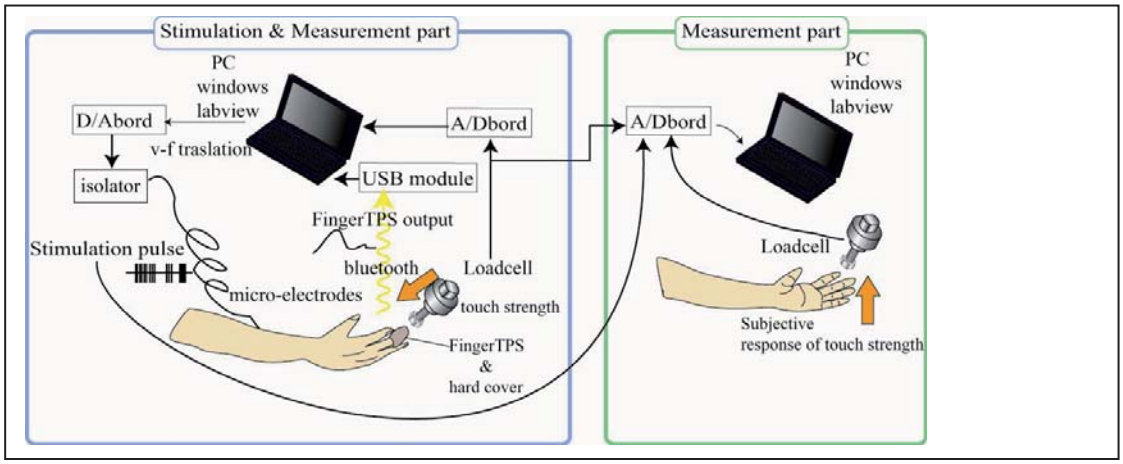


Fig.1 Experimental arrangement

frequency of the stimulus but not by the amplitude of the stimulus [3].

First, we inserted a microneurographic electrode into the median nerve of the subject and fixed the electrode where the nerve signals from a single SA-I mechanoreceptor unit can be measured. We then switched the electrical circuit to stimulation mode and gave electrical stimulation to the nerve fiber using the same microelectrode.

As a single electrical input pulse for the stimulation, we used a biphasic square-wave pulse for 250 micro-seconds. The amplitude of the electrical stimulation (electrical current) was fixed at around 1.2 times the level of the threshold value (the current at which the subject first felt a sensation when the frequency was fixed at 50 Hz). The amplitude was then gradually raised from 0.

System for Sensing Mechanical Stimuli

A commercially available pressure sensing system (Finger TPS system) was used in this study. The sensor probe has a flexible fingerstall shape and is equipped with a pressure sensor of the electrostatic volume (Fig.2).

The subject first put a hard plastic fingerstall on the finger and then put the Finger TPS system on the fingerstall.



Fig.2 Sensor probes of the Finger TPS system

With this arrangement, the hard fingerstall protects the skin from mechanical stimuli, so that the mechanical stimuli given to the finger do not affect the mechanoreceptors of the skin and the subject can feel only the pressure sensation evoked by the microstimulation of the SA-I sensory nerve fiber.

When pressure stimuli were given to the subject's finger covered with the sensor probe, the intensity of the pressure detected by the Finger TPS system was transferred to a personal computer, and the value of repetition frequency of the electrical stimulation was determined and output to the microstimulation system.

(The pressure stimuli were given using a bar-shaped force sensor and the pressure applied to the Finger TPS system was measured by the sensor.)

The repetition frequency of the output electrical pulse train was determined in accordance with the strength of the pressure by the following equation.

$$f = 50 \times P$$

where f is repetition frequency of the electrical pulse train used for stimulation (Hz) and P is the pressure measured by the Finger TPS system (N).

Evaluation of the Intensity of the Evoked Pressure Sensation

The intensity of the pressure sensation that was evoked by the microstimulation of the SA-I sensory nerve fiber and subjectively perceived by the subject was evaluated as follows.

When the pressure sensation was evoked to the subject by the microstimulation of the SA-I sensory nerve fiber, the subject indicated the intensities of the evoked pressure sensation by pushing a bar-shaped force sensor (load cell) with the contralateral hand so that the pressure he felt from the bar became the same intensity as that evoked by the electrical stimulation of the sensory

nerve fiber. We defined the intensity of the evoked pressure sensation as the pressure value he indicated with the load cell.

Results and Discussion

Stimuli (pressure) were successfully conveyed to the subjects via the developed system, which produced the same somatic sensation (pressure sensation) as the original stimuli, and did so with the corresponding magnitude.

Figure 3 shows an example of the results. The upper graph shows the changes with respect to time in the force with which the Finger TPS sensor system is pressed (green line), force measured by the Finger TPS sensor system (red line), and the intensities of the subjective pressure sensation that the subject expressed by pushing a load cell using the contra-lateral hand in the manner written in the "method" item (blue line). The middle figure shows changes with respect to time in the repetition frequency of the electrical stimulation to the sensory nerve. In this case, as the frequency for electrical stimulation was determined as 50 times the value of pressure detected by the finger TPS system, the shape of the waveform basically becomes similar to the red line (of the upper graph). The lower graph shows the train of the electrical pulses used to stimulate the nerve fiber of interest.

As can be seen in the upper figure, the changes in the pressure sensation generated by the electrical stimulation of the SA-I sensory unit in accordance with the pressure value measured by the Finger TPS system and the changes in the pressure applied to the Finger TPS system showed a very similar tendency. The correlation coefficient between these two factors was 0.91, indicating that the system transfers mechanical stimuli to the subject so that the subject can experiences the stimuli as the corresponding somatic sensations and can do so with the same intensity.

The correlation coefficient between the pressure applied to the Finger TPS system and the value of the pressure measured by it was 0.97, showing that the Finger TPS system can measure the applied pressure with high reliability.

These results indicate that the system will be able to not only compensate the sensory function that has been lost due to peripheral neuropathy but also even enhance the natural sensory functions of the living body when high-performance sensors are adopted for the system.

Conclusion

In this study, we developed a prototype of a sensory prosthetic system capable of substituting for sensory functions that have been lost due to injury or diseases of peripheral nerve system.

In trials, stimuli were successfully conveyed to the subjects via the system, and the system produced the same somatic sensation as the original stimuli, with the corresponding magnitude. The results indicate the possibility that the system could substitute for sensory functions that has been lost in people with peripheral neural disorders.

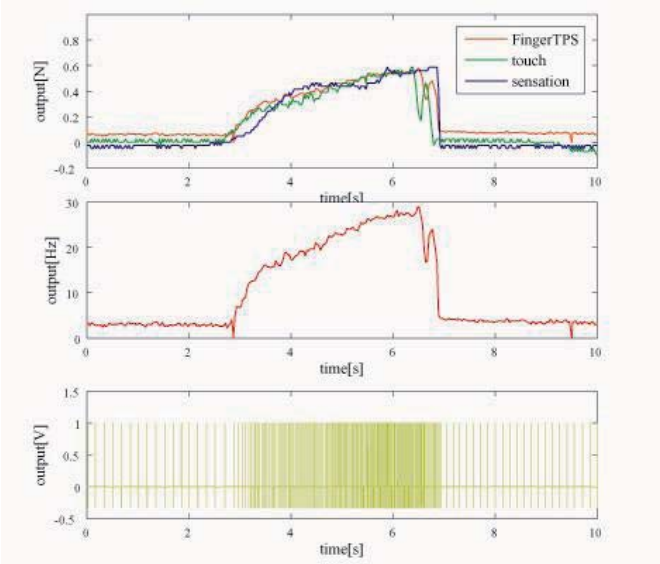


Fig.3 An example of the results. (please refer the text.)

References

[1] Suzuki T, Mabuchi K, Nishimura H, Saito T, Kakuta N, Kunimoto M, Shimojo M. The Relationship between Stimulation Signals and Subjective Intensities and Areas. Proc. Int. Conf. of the IEEE EMBS: 459, 1999

[2] Bear M. F., Connors B. W., Paradiso M. A.. Neuro-science - Exploring the Brain (3rd edition). Lippincott Williams & Wilkins, Baltimore:388-393, 2007

[3] Ochoa J, Torebjörk E. Sensations evoked by intraneural microstimulation of single mechanoreceptor units innervating the human hand. J. Physiol., 432: 633-654, 1983

Acknowledgements

This study was supported partly by Health Labour Science's Research Grant H20-nano-003 from the Ministry of Health, Labour and Welfare of Japan and a Grant-in-Aid for Scientific Research (A) 20246045 from the Ministry of Education, Culture, Sports, Science and Technology of Japan.

Author's Address

Name: Kunihiko Mabuchi
Affiliation: Graduate school of Information Science and Technology, The University of Tokyo
7-3-1, Hongo, Bunkyo-ku, Tokyo, 113-8656, Japan
e-Mail: Kunihiko_Mabuchi@ipc.i.u-tokyo.ac.jp
Homepage: http://www.mels.ipc.i.u-tokyo.ac.jp/

Cortically controlled functional electrical stimulation: a neuroprosthesis for grasp function

Ethier C[1], Oby ER[1], Bauman MJ[1], Miller LE[1]

[1] Northwestern University, Chicago, United-States

Abstract

We have developed a neuroprosthesis that allows a monkey subject to pick up and move objects despite a peripheral nerve block causing complete paralysis of the flexor muscles below the elbow. The restored voluntary control was achieved using signals recorded from approximately 100 neurons in the primary motor cortex to control real-time electrical stimulation that generated contractions of the paralyzed muscles. After nerve block, the monkey was able to use the neuroprosthesis to perform a functional grasping task with a success rate approaching his normal performance. The monkey was essentially unable to complete this task without its assistance. Such a system could provide natural control of arm and hand movements to human spinal cord injured patients, through normal cognitive processes, and greatly enhance the patient's independence and overall well being.

Keywords: *neuroprosthesis, brain-machine interface, functional electrical stimulation, spinal cord injury, EMG prediction, Motor Cortex*

Introduction

Patients with spinal cord injury lack the connections between their brain and spinal cord that are essential for voluntary movement. Functional electrical stimulation (FES) systems have proven to be effective in allowing patients with tetraplegia to regain the control of hand movements [1,2,3]. In typical FES systems, the patient controls grasp through residual proximal limb movements that trigger pre-programmed stimulation causing the paralyzed muscles to contract.

We have instead, developed an FES system that is controlled by recordings made from tiny electrodes permanently implanted in the brain of a monkey. Our neuroprosthesis successfully restored the monkey's ability to pick up and move objects despite complete paralysis of its hand and forearm flexor muscles. We simulated the paralysis due to C5-C6 spinal cord injury by injecting a local anaesthetic to block the nerves at the elbow [4], then used recordings from approximately 100 neurons in the motor cortex to predict the intended activity of several of the paralyzed muscles [5]. The intensity of muscle stimulation was determined by these predictions, essentially bypassing the blocked nerves and restoring voluntary control of the paralyzed muscles.

Related results were reported by another group that operantly conditioned monkeys to modulate the activity of individual neurons, whose discharge was made to control the activity of one or two muscles [6]. Our results represent a major step forward, and serve as an important proof of concept that an FES neuroprosthesis could provide natural control over the arm and hand through normal cognitive processes, and greatly enhance a patient's independence and overall well being.

Material and Methods

Experimental subject and task

Experiments were conducted with a 9 kg male Macaca mulatta monkey trained to perform a ball grasp task. The monkey was allowed 5 seconds from the time he made initial contact with the ball, to grasp it and place it into the top of the tube in Fig. 1. All procedures were approved by the Institutional Animal Care and Use Committee of Northwestern University.

EMG prediction and nerve block

We implemented FES-controlled grasping during 20 experimental sessions across 7 weeks, using roughly 100 single and multi-unit neural signals recorded from a 100-electrode array (Blackrock Microsystems Inc., Utah) implanted within the hand area of M1. EMG activity was acquired using electrodes implanted in the ulnar and radial heads of flexor digitorum profundus, two locations in flexor digitorum superficialis, and in flexor carpi radialis. The same electrodes were used for stimulation.

At the beginning of each week, we computed nonlinear, Weiner cascade decoders [5,7]. These decoders consisted of multiple-input impulse response functions between the full set of neural inputs and each recorded muscle. This dynamic, linear output was transformed by a 2nd

order static nonlinearity. In each subsequent experimental session throughout the week, we injected 2% Lidocaine and 1:100k Epinephrine into subdermal ports leading to cuffs on the ulnar and median nerves [4].

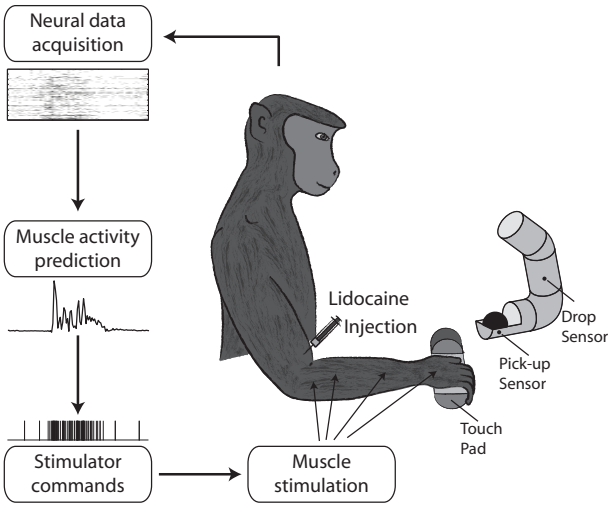


Fig. 1: Brain-controlled FES. While the monkey's forearm and hand is temporarily paralyzed by a peripheral nerve block, a Brain Machine Interface (BMI) controls the FES that restores the monkey's ability to perform a functional grasping task. The monkey places its hand on a touch pad and waits for a go tone to initiate a trial. The ball grasp device is equipped with a pick up sensor and a ball drop sensor which are activated when the monkey initially touches the ball and drops it into the tube, respectively.

Brain-controlled FES

All muscles were stimulated at a single, fixed rate of either 25 or 30 Hz, which achieved nearly fused contractions. The EMG predictions were transformed into stimulus pulse widths by mapping the EMG noise floor to the stimulus force threshold, and the maximum predicted EMG to the maximum pulse width (200 μs). The current was chosen to yield a useful force range, typically 2-8 mA. With the onset of fatigue caused by electrical stimulation, we typically increased both the global stimulus frequency and the stimulus currents by as much as 50%.

On a random 15% of trials, the stimulators were turned off to assess the functional improvement afforded by the FES. We evaluated the effectiveness of the nerve blocks at frequent intervals throughout the experiment by briefly stopping the FES and recording EMG activity and neural discharge as the monkey attempted the task. We used the ratio between the predicted and actual EMG as a measure of nerve block effectiveness.

Results

Fig. 2 illustrates a representative experimental session which begun by Lidocaine injection to block the median and ulnar nerves just proximal to the elbow. After 15 minutes, the nerve block was essentially complete, as determined by the loss of flexor muscle EMG activity (black circles, Fig. 2b) and the onset of profound motor deficits.

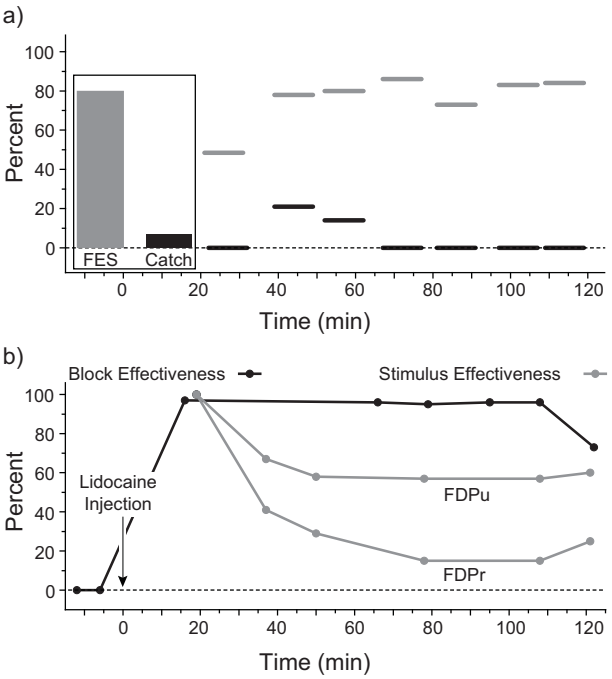


Fig. 2: Summary of grasp task performance during median and ulnar nerve block. (a) Success rate for the seven experimental data sets for both FES trials (grey) and randomly inserted catch trials without stimulation (black). The monkey was essentially unable to pick up the ball during the catch trials, completing only 4 of 57 attempts. (b) Both nerve block and stimulus effectiveness for were tested at frequent intervals during the experiment.

The remainder of each session consisted of a series of 10 minute blocks in which the monkey attempted to complete the grasp task either with or without FES assistance (Fig. 2, top panel). The average success rate in this session with FES assistance was 80%. While the movements were not entirely normal, they did not differ so completely as to be obvious to casual observation. In stark contrast, the catch trial success rate in this session was only 7%.

Across all experimental sessions, the monkey achieved an overall success rate seven times higher with FES than without it, a difference that was significant at $p \sim 0$ (two-sample test for equality of proportions), although it remained somewhat below the monkey's normal 100% success rate (Fig. 3a). In addition, the cortically-controlled FES system significantly improved the speed at which

the monkey successfully completed trials (Fig. 3b, $p<0.0001$, two-tailed Mann Whitney test). The vast majority of catch trials ended unsuccessfully with a 5 second time out. The mean catch trial time represents only the occasional success, achieved mostly through an alternate, "scooping" motor strategy.

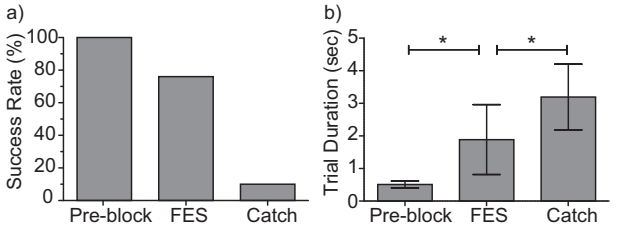


Fig. 3: Summary of the results of 20 FES sessions. (a) Success rates for normal, FES, and catch trial conditions comprising nearly 6000 trials. The monkey completed 77% of the trials with FES but only 11% without FES. (b) The speed at which the successful trials were completed was significantly different for all three conditions ($p<0.0001$, two-tailed Mann Whitney test).

Discussion

Existing FES systems for grasp have been used to restore limited hand use to hundreds of patients. This study serves as an important proof of concept that an FES prosthesis controlled by neural input may achieve even more impressive improvements in the activities of daily living by providing more natural, voluntary control of muscle activation. Furthermore, this technology may offer hope even to patients with injuries at higher cervical levels who have greater needs for replaced function with less available control.

Among the factors that compromised performance, one of the most important is muscle fatigue, a concern in all FES applications, as electrical stimulation does not cause the normal motor unit recruitment order [8,9]. In an effort to counteract this effect, we typically increased either the stimulus current or frequency. This appeared to be sufficient in our experiments for the monkey to maintain his performance. In a clinical application, fatigue may be somewhat less extreme, as chronically stimulated muscles develop some level of fatigue resistance [10,11].

References

[1] Keith, M. W. *et al.* Implantable functional neuromuscular stimulation in the tetraplegic hand. *J Hand Surg [Am]* 14, 524-530, 1989.

[2] Peckham, P. H. *et al.* Efficacy of an implanted neuroprosthesis for restoring hand grasp in tetraplegia: a multicenter study. *Arch. Phys. Med. Rehabil.* 82, 1380-1388, 2001.

[3] Popovic, M. R., Popovic, D. B. & Keller, T. Neuroprostheses for grasping. *Neurol Res* 24, 443-452 (2002).

[4] Pohlmeyer, E. A., Jordan, L. R., Kim, P. & Miller, L. E. A fully implanted drug delivery system for peripheral nerve blocks in behaving animals. *Journal of neuroscience methods* 182, 165-172, 2009.

[5] Pohlmeyer, E. A., Solla, S. A., Perreault, E. J. & Miller, L. E. Prediction of upper limb muscle activity from motor cortical discharge during reaching. *Journal of neural engineering* 4, 369-379, 2007.

[6] Moritz, C. T., Perlmutter, S. I. & Fetz, E. E. Direct control of paralysed muscles by cortical neurons. *Nature* 456, 639-642, 2008.

[7] Anderson, K. D. Targeting recovery: priorities of the spinal cord-injured population. *Journal of neurotrauma* 21, 1371-1383, 2004.

[8] Gregory, C. M. & Bickel, C. S. Recruitment patterns in human skeletal muscle during electrical stimulation. *Phys Ther* 85, 358-364, 2005.

[9] Knaflitz, M., Merletti, R. & De Luca, C. J. Inference of motor unit recruitment order in voluntary and electrically elicited contractions. *J Appl Physiol* 68, 1657-1667, 1990.

[10] Peckham, P. H., Mortimer, J. T. & Marsolais, E. B. Alteration in the force and fatigability of skeletal muscle in quadriplegic humans following exercise induced by chronic electrical stimulation. *Clin Orthop Relat Res*, 326-333, 1976.

[11] Kernell, D., Donselaar, Y. & Eerbeek, O. Effects of physiological amounts of high- and low-rate chronic stimulation on fast-twitch muscle of the cat hindlimb. II. Endurance-related properties. *Journal of neurophysiology* 58, 614-627, 1987.

Acknowledgements

This work was supported in part by grant #NS053603 from the National Institute of Neurological Disorders and Stroke to L.E. Miller and post-doctoral fellowship from the Fonds de la Recherche en Santé du Québec to C. Ethier. We also wish to acknowledge the surgical assistance of Drs. Jason Ko and Sonya Paisley Agnew, Division of Plastic and Reconstructive Surgery, Northwestern University Feinberg School of Medicine.

Author's Address

Christian Ethier, Northwestern University
c-ethier@northwestern.edu
Lee E. Miller, Northwestern University
lm@northwestern.edu

Dependence of implantation angle of the transverse, intrafascicular electrode (TIME) on selective activation of pig forelimb muscles

Kundu A[1], Jensen W[1], Kurstjens M[1], Stieglitz T[3], Boretius T[3], Yoshida K[1,2]

[1] Center for Sensor-Motor Interaction, Dept. Health Science and Technology, Aalborg University, Denmark

[2] Biomedical Engineering Dept., Indiana University-Purdue University Indianapolis, Indianapolis, USA

[3] Laboratory for Biomedical Microtechnology, Albert-Ludwigs University, Freiburg, Germany

Abstract

The aim of the present study is to investigate the stimulation selectivity of the transverse intrafascicular multichannel electrode (TIME). The TIME is a multichannel neural prosthetic interface being developed to deliver relatively high stimulation selectivity for use in applications, such as the control of multiple-degree prosthetic devices or for eliciting sensory feedback. The electrodes were implanted in the median nerve in the upper left limb of one landrace pig at four different implantation angles (45°, 90°, 135° and 180°) with respect to the cross section of the nerve. Monopolar, 100µs long, rectangular pulses (pulse amplitude 40- 800 µA, steps of 40µA) were sequentially delivered to each of the 12 contact sites on the electrode structure to evoke muscle activation in the upper limb. The recruitment of seven muscles in upper limb was quantified as a function of stimulation. The preliminary results indicated that the selectivity of muscle activation and recruitment was dependent on the implantation angle.

Keywords: *neural interface, selective activation, intrafascicular, phantom limb pain*

Introduction

Amputation of a limb involves truncation of all afferent and efferent nerves that innervated the amputated limb. Consequent retrograde changes may impact both the peripheral nervous system and the central nervous system [1]. These changes often result in a sensation that the missing body part is still present (i.e. phantom limb awareness) and kinaesthetically perceived (i.e. phantom limb sensation). In 50-80% of all amputees, phantom limb pain (PLP) develops [2]. Today, it is not completely understood why the pain occurs, and there are no fully effective treatment.

Several studies have demonstrated that by providing appropriate sensory feedback signals to the amputee subject can assist to alleviate PLP. For example, the intensive use of myoelectric prosthesis [3], or daily training sessions involving discrimination between different surface electrical stimuli [4] applied to the stump experienced significant reduction of PLP. Intrafascicular, electrical stimulation of severed nerves proved to be capable of eliciting tactile or proprioceptive sensations by implanted LIFE electrodes in human subjects [5]. Rossini et al. also demonstrated that training for control of a robotic hand (with a limited amount of sensory feedback) significantly reduced PLP in a human amputee volunteer implanted with four LIFE electrodes [6]. The reduction in PLP lasted several weeks after the LIFE electrodes were removed and changes in sensorimotor cortex topography were shown [6].

The present work is part of an ongoing EU project 'TIME', where we hypothesize that given selective activation a sufficient number of nerve fibres, a neural interface may be able to artificially evoke sensations and eventually allieve PLP. A new generation of transverse, intrafascicular electrodes (TIME) has been developed for this purpose (see [7] for a review of development and use of the intrafascicular electrodes). The main objective of the present study was to investigate the degree of stimulation selectivity of the TIME electrodes in an animal model with nerve size similar to humans. We further investigated the morphological structure of the porcine median nerve to determine the number of fascicles in/around the implant site.

Material and Methods

Animal preparation

All experimental procedures were approved by the animal experiment inspectorate under the Danish Ministry of Justice. 7 female, Yorkshire landrace pig (<50 kg) were included in the present work. These preliminary results are from analysis of one animal (selectivity) and 6 animals (histology). The

animals were placed under general anaesthesia (ventilated at 15 breaths/min, 50-50% air/oxygen, 1-1.2 % Isoflurane), received 0.9% saline to prevent dehydration and pancuronium bromide/fentanyl (Esmeron® 10mg/ml and "Hameln" 50 µg/ml) as analgesia. The animals were placed in a supine position, and access to the median nerve in the upper limb was created through the axilla. Heart rate and oxygen saturation were monitored throughout the experiment.

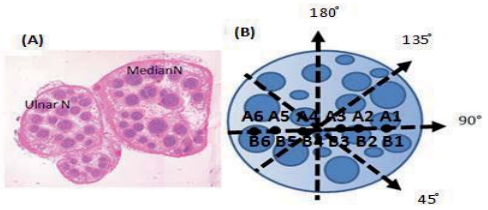


Fig 1. A) H&E stain of the median and ulnar nerves approx. 2-3 cm above the elbow joint, where the electrodes were implanted. B) Schematic drawing of electrode implantation angles of the TIME electrodes in the median nerve.

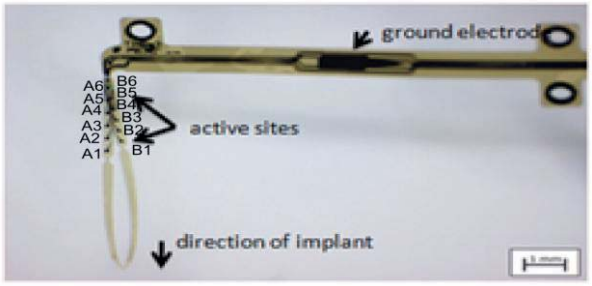


Fig 2. Transverse-intrafascicular, multi-channel electrode (TIME) with 12 active sites to be placed inside the median nerve. The broader, horizontal part of the polyimide substrate serves as insertion stop and stays outside the nerve.

The transverse, intrafascicular electrodes (TIME) were implanted in the median nerve approximately 2-3 cm above the elbow joint at implantation angles of 45°, 90°, 135° and 180° (see Fig. 1b). The TIME electrodes were manufactured at IMTEK (see Fig 2.; see [8] for detailed description). The electrode has 12 equidistant active sites with a pitch of 440 µm, with 6 contacts placed on either side of the polymide loop structure. They are referred as A1, A2, A3, A4, A5, A6 and B1, B2, B3, B4, B5, B6.

To evaluate the selective activation of individual fascicles in the median nerve, we recorded EMG responses from seven forearm muscles using bipolar patch electrodes placed at three extensor muscles (biceps brachii [M1], extensor carpi radialis [M2], extensor carpi ulnaris [M7]), three flexor muscles (flexor carpi radialis [M3], flexor digitalis superficialis [M4], flexor carpi ulnaris [M5]) and the muscle interosseus medius [M6]. We applied cathodic monopolar, rectangular constant-current pulses between the individual contacts and an external ground placed within the animal using a Multichannel Systems STG2008 stimulator. Stimuli were 100µs with amplitudes 40µA to 800µA, and presented at 2Hz. 5 pulses were repeated at each current level.

At the end of the experiment, the animal was euthanized with an overdose of sodium pentobarbital. To evaluate the morphology of the pig nerve, a nerve section were harvested immediately after euthanasia at the level of the implant and prepared for histological analysis. The specimens were placed on a metal plate, fixated with tissue glue (CryoJane) to maintain orientation of the specimen during freezing in liquid nitrogen. 5 µm frozen transverse sections of the nerve were taken and subsequently stained using H&E (see Fig. 1A).

Data analysis

Muscle activation was quatified by measuring the amplitude of the EMG amplitude. EMG signals were band-pass filtered (100 Hz - 2 kHz) and its RMS value was calculated in the period 2 – 12 ms time interval after stimulation. These values were normalized to the maximum RMS for each muscle (including data from stimulating contacts at all four implant directions) to generate recruitment curves (Fig. 3). Stimulation selectivity was then evaluated for each contact at the maximum current 800 µ A (Fig. 4), where we expect the worst-case selectivity performance.

To evaluate the morphological structure of the median nerve, the number of fascicles and fascicle diameter/area were determined at three levels of the nerve; ~3-4 cm above, at, and ~3-4cm below the level of the implant site. Digital photomicrographs were taken and analyzed using Axio Vision (Axio Vs40 v. 4.6.30, Carl Zeiss Imaging solutions GmbH, Germany).

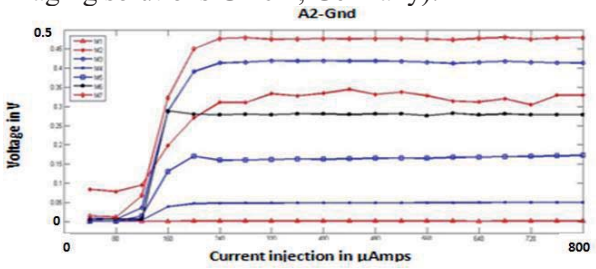


Fig 3. The generated muscle recuitment curves. X-axis represents the 20 simulation levels (40 µA to 800 µA), and the y-axis reflects the corresponding EMG activity for each of the 7 muscles.

Table 1. Results of histological evaluation from 6 nerves (left and right forelimb). All numbers are given as mean ± std. (*) indicates that 4 nerve speciments were included in the analysis

	Proximal to implant site	At implant site	Distal to implant site
Fascicle diameter [mm]	0.27 ± 0.083	0.23 ± 0.086	0.24 ± 0.093
Fascicle count	29 ± 5	36 ± 4	33 ± 8
Whole nerve diameter [mm]	No data	2.9 ± 0.4mm (*)	2.2 ± 0.6mm (*)

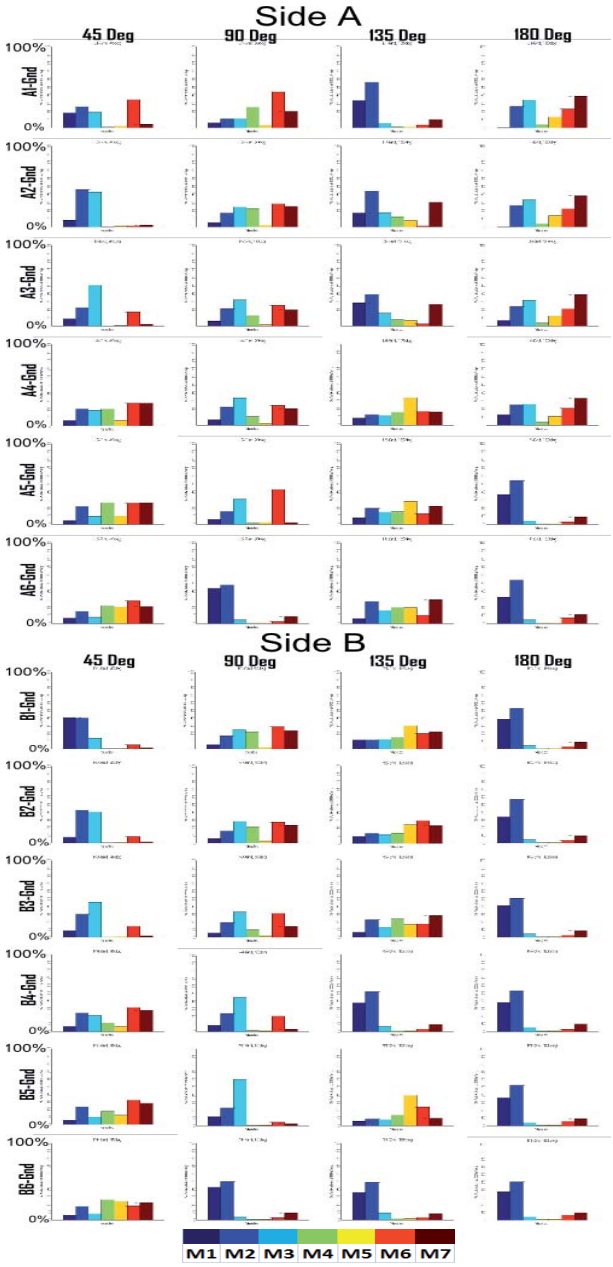


Fig 4. Comparison of the activation of selected muscles at saturation as a function of electrode contact and implant angle. Upper panel: results from stimulating 6 contacts on the side A of the electrode. Lower panel: results from stimulating the six contacts on side B .

Results

The cursory selectivity analysis (Fig. 4) indicate that there was strong possibility of activating extensor muscles (M1, M2 and M 7) when implantation is made at 180°. On the other hand, mostly the flexor muscles (M3, M4 and M5) and muscle interosseus medius (M6) were activated when the electrode was implanted at 90°. Implantation at 45° and 135° activated all seven muscles in the majority of the cases. Different orientation angles resulted in different activation characteristics.

The histological evaluation from 6 pig forelimb nerves (both left and right arm) are shown in Table 1. The median nerve contained the highest number of fascicles at the implant sited just above the elbow joint. The fascicle diameters were similar at all three levels.

Discussion and conclusions

Our objective was to investigate the stimulation selectivity of the TIME electrode within an animal model with nerve size similar to humans. These preliminary results show the importance of implantation angle on the selectivity and reachability of muscle activation. This parameter may be an important factor for optimization, where there is a trade off of reachability with selectivity. The morphological analysis revealed up to 40 fascicles at the level of implantation. Although further investigation is needed to optomize how many of these fascicles can be reached versus the number of electrode structures and contacts used, the transversely implant intrafascicular electrode may be an important step towards reaching this compromise.

Acknowledgements

This work was funded by the EU TIME project (CP-FP-INFSO 224012/TIME). Authors would like to thank O. Sørensen, T. Madsen, J. Sørensen and B. Jensen (Dept. Pathology, Aarhus University Hospital-Aalborg) for assistance in the animal experiments and preparation of nerves for histological evaluation.

Author's Address

Kundu A, Center for Sensor-Motor Interaction, Department of Health Science and Technology, Aalborg University, Fredrik Bajersvej 7D-3, 9220 Aalborg, Denmark, akundu@hst.aau.dk

References

[1] X. Navarro, M. Vivó and A. Valero-Cabré, "Neural plasticity after peripheral nerve injury and regeneration," Prog.Neurobiol., vol. 82, pp. 163-201, 2007.

[2] P.L. Ephraim, S.T. Wegener, E.J. MacKenzie, T.R. Dillingham and L.E. Pezzin, "Phantom pain, residual limb pain, and back pain in amputees: results of a national survey," Arch.Phys.Med.Rehabil., vol. 86, pp. 1910-1919, 2005.

[3] M. Lotze, W. Grodd, N. Birbaumer, M. Erb, E. Huse and H. Flor, "Does use of myoelectric prosthesis reduce cortical reorganization and phantom limb pain?" Nat.Neurosci., vol. 2, pp. 501-502, 1999.

[4] H. Flor, C. Dencke, M. Schaefer and S.M. Grusser, "Effect of sensory discrimination traning on cortical reorganization and phantom limb pain," Lancet, vol. 357, pp. 1763-1764, 2001.

[5] G.S. Dhillon and K. Horch, "Direc neural sensory feedback and control of prosthetic arm," IEEE Trans Neural Syst Rehabil Eng, vol. 13, pp. 468-472, 2005.

[6] P.M. Rossini, "Double nerve intraneural interface implant on a human amputee for robotic hand control," Accepted for Publication in Clinical Neurophysiology, 2010.

[7] K. Yoshida, D. Farina, M. Akay and W. Jensen, "Multichannel Intraneural and Intramuscular Techniques for Multiunit Recording and Use in Active Prostheses," Proc IEEE, vol. 98, pp. 432-449, 2010.

[8] T. Boretius, J. Badia, A. Pascual-Font, D. Andreu, C. Azevedo-Coste, J. Divoux, T. Stieglitz, X. Navarro and K. Yoshida, "Transverse Intrafascicular Multichannel Electrode (TIME) an Interface to Peripheral Nerves: Preliminary In-vivo Results in Rats," Proceedings of the 14th IFESS Conference, Seoul, South Korea, pp. 37-39, 2009.

High Performance Motion Control by Neuro-Muscular Electrical Stimulation applied to the Upper-Limb

Klauer C.[1], Schauer T.[1], Raisch J.[1,2]

[1]Control Systems Group, Technische Universität Berlin, Germany

[2]Systems and Control Theory Group, Max Planck Institute for Dynamics of Complex Technical Systems, Magdeburg, Germany

Abstract

For the development of an upper-limb neuro-prosthesis in the project MUNDUS an approach for high performance control of artificially induced arm movements is proposed. By neuro-muscular electrical stimulation of antagonistic muscles pairs acting on the shoulder and elbow joints arm movements can be generated. Because of strong system nonlinearities a linearising controller is applied at first, which at the same time decouples the multi-input/multi-output (MIMO) system. On top of this controller two independent cascaded control structures with three levels are implemented to separately control the corresponding joint angles by modulating the stimulation intensities of the antagonistic muscle pairs. An acceleration controller at the lowest cascade level counteracts high frequency disturbances which can occur due to imperfect model inversion and decoupling. Velocity and position control form the outer loops of the cascaded control structures. Whenever identical movements have to be repeatedly generated a fourth cascade level with iterative learning control is used to minimise the tracking errors from trial to trial. The control design was verified through numerical simulations at first. Furthermore, the feasibility of such a control approach was demonstrated by elbow-joint control in a healthy subject.

Keywords*: neuro muscular electrical stimulation, position control, acceleration control, iterative learning control*

Introduction

Induction of movements through electrical stimulation is a long proven concept in persons with upper neuro motor lesion. Feedback control methods enable the realisation of complex desired movement trajectories and therefore are a prerequisite for neuro-prosthesis development.

This article shows first results of the project MUNDUS aiming at the development of a neuroprosthesis for daily upper-limb support. The final neuroprosthesis will involve a lightweight exoskeleton to compensate gravitational forces acting on the arm.

The main difficulties for a highly accurate control system are uncertain muscular properties. The nonlinear recruitment curve of a muscle forms for a pair of antagonistic muscle a dead-zone. Parameters of this static input nonlinearity are difficult to identify and therefore represent uncertain parameters for the controller design. While gravitation compensation is active only small muscular forces are necessary to move the upper limb. Thus operation close to the dead-zone will occur which dramatically can limit the control performance unless special measurements are taken. This work investigates the use of cascade control with a very fast inner loop based on acceleration control to reject disturbances caused by imperfect cancellation of the dead-zone.

Methods

Experimental Setup

Simplified, a human arm (elbow and shoulder joint) has four mechanical degrees of freedom for movements. To validate the proposed control concept the number of degrees of freedom was initially restricted to two. Using a simple seesaw,

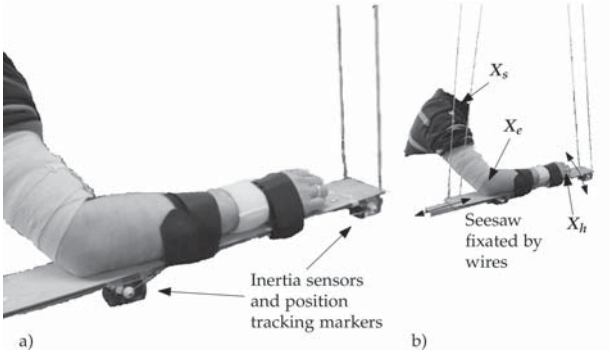


Fig. 1: Experimental setup showing gravitational force compensation and sensors.

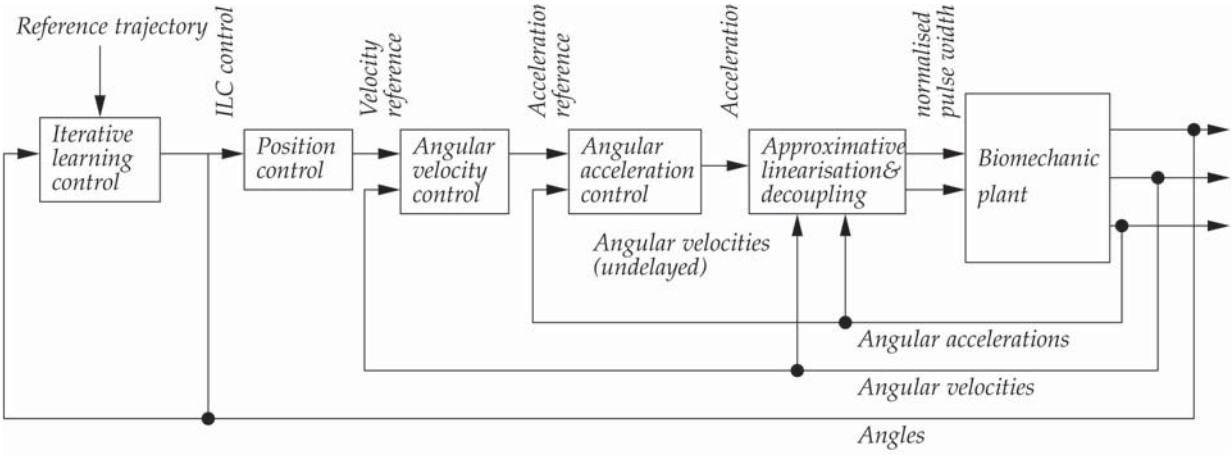


Fig. 2: Overview of the used cascaded control system.

as shown in Fig 1., the forearm is forced to almost remain in a defined horizontal plane. Hence, only a rotation around the shoulder (quantified by the shoulder angle) and an elbow flexion / extension (quantified by the elbow angle) are left. Moreover, gravitational force compensation was achieved by this fixation as the final exoskeleton was not available at this time. Electrical stimulation is applied to the muscle pairs acting on the shoulder and elbow joint.

Sensors and Stimulation Device

For feedback position control real-time estimates of the shoulder as well as the elbow angle are needed. For angular position measurement an ultrasound marker tracking system is used, which gives the coordinates of three markers placed at characteristic points X_s , X_e , X_h (see Fig. 1). In a next step, these positions are converted to the angles. Two inertial sensors give extra information that can be used to calculate angular accelerations and velocities through sensor fusion. This way, there is the full information describing arm motion available. For stimulation a commercial device is used which is controlled from a PC.

Human Arm Model

For controller design a nonlinear dynamic model of the human arm is set up. There are two main parts involved: At first there is a Hill-type muscle model [1] model fitted to all involved muscles. The second part describes the dynamical behaviour of the arm mechanics that contains friction, arm mass etc. and represents the coupled equations of motion.

Cascaded Feedback Control

All measured signals (accelerations, velocities and positions) have their dominant frequency components in different bands: Acceleration signals tend to include higher spectral components while position signals consist of the lowest frequency parts. Last but not least velocities are somewhere in between.

The idea is to use all information available for feedback control in order to achieve the best possible control performance. This is done through a cascaded structure shown in Fig. 2. At the lowest level a nonlinear linearising controller is applied to the system for the decoupling and linearisation. In all higher cascade levels control of each joint is done separately by two SISO paths respectively. The acceleration controller compensates high frequency disturbances which may result from an imperfect decoupling and linearisation. Details on this controller are shown later on. In the next cascade stage, a velocity feedback loop is used to compensate for middle frequency band disturbances and at the next higher cascade level the low frequency position control is performed.

When identical movements have to be repeated several times, e.g. during eating, there is another level at which iterative learning control [2] is be employed for further optimisation of movement accuracy.

Acceleration Feedback Controller

Using acceleration feedback for position control may seem to be uncommon but – if it is done correctly – high performance disturbance rejection becomes possible. As already said, muscular control is taking place within the highly nonlinear and uncertain area of the muscle recruitment curve. Thus there are many unwanted effects that occur in practice which would significantly reduce control performance. For compensation of such disturbances a fast reacting low level closed-loop is necessary which is realised by acceleration feedback control.

The controller involves two degrees of freedom: A feedforward path where the nominal plant is inverted and a feedback loop that compensates the re-

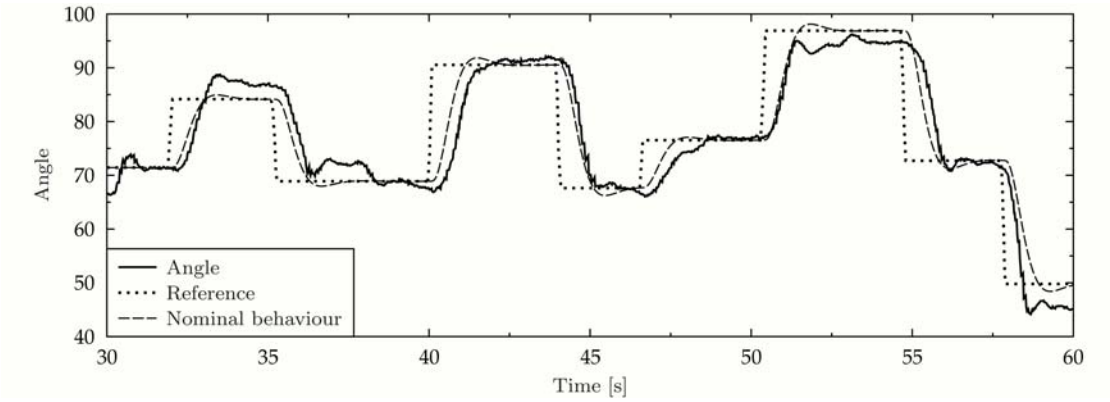


Fig. 3: Experimental result of an elbow-joint angle control test.

maining disturbances resulting from the non-ideal muscular action. The controller operates at 300 Hz - the rate at which acceleration is measured – for optimal use of sensory information. Rate reduction is necessary since the stimulator is running at 50 Hz. Stability analysis for such systems is possible through multi-rate signal processing theory.

Iterative Learning Control

For repeated movements – as they occur when patients are eating for example - ILC is additionally used to further improve control accuracy. ILC is an adaptive feedforward control technique. The input reference trajectory to the angle controller is optimised from cycle to cycle based on the movement error in order to drive the tracking error (to be precise its Euclidean norm) towards zero. This operation is performed offline between the cycles allowing the use of acausal filtering (smoothing) techniques.

Results

Fig. 3 shows the results of an elbow-joint angle tracking test with a neurologically intact subject. During this test, the ILC was not active and the angle reference trajectory was given directly to the position feedback controller. Additionally, a simulation result with active ILC control for combined elbow and shoulder movements is presented in Fig. 4. Circular movements of the distal end of the forearm had to be performed within three seconds per turn while the arm was nearly extended. This makes this task quite difficult because small angular derivations result in a large position failure. The first five trials are reported in Fig. 4.

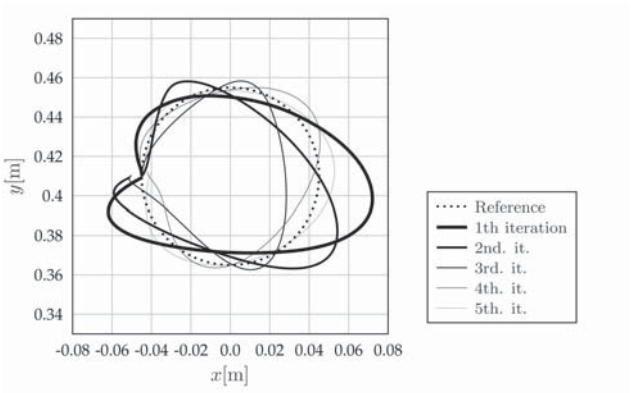


Fig. 4: Experimental result of several circular movement trials under ILC

Discussion

The position controller is shown to be quite fast (rise time less than 0.5 s) while the observed angular motion is very close to the nominal behaviour. Looking at the ILC test, the first iteration shows some deviations, that are significantly reduced in the following trials.

Conclusions

Since the experimental results agree well to the expected ones the applied control structure is proven to be feasible for human arm position control. Especially the acceleration controller enables high tracking performance. MIMO control experiments will be carried out in future with patients who also tolerate a stimulation at the shoulder. Furthermore, ILC turned out to be a suitable method for reducing any remaining performance lacks whenever performing cyclic movements. The control system may be extended to more degrees of freedom after an exoskeleton for gravity compensation will be available within the MUNDUS project.

Acknowledgements

The research leading to these results has received funding from the European Community's Seventh Framework Programme under grant agreement no. 248326 within the project MUNDUS.

References

[1] A. V Hill. First and last experiments in muscle mechanics. Cambridge UP, 1970

[2] D. A. Bristow, M. Tharayil, and A. G. Alleyne. A survey of iterative learning control. IEEE Control Systems Magazine, 26(3):96–114, 2006

Reduction of the Onset Response in High Frequency Nerve Block with Frequency and Amplitude Transitioned Waveforms

Bhadra N[1], Gerges M[2], Foldes E A[1], Ackermann D M[1], Bhadra N[23], Kilgore K L[123].

[1] Case Western Reserve University, Cleveland,USA.

[2]MetroHealth Medical Center, Cleveland,USA.

[3]Louis Stokes VA Medical Center, Cleveland,USA.

Abstract

High frequency alternating currents (HFAC)produce a reversible and rapid peripheral nerve conduction block. The delivery of HFAC is characterized by a transient, but intense, period of neural firing at the onset of current delivery called the "onset response". The onset response is minimized for higher frequencies and higher amplitudes. However, these parameters require a large amount of current to maintain the block. In this in-vivo study on whole mammalian peripheral nerves, we demonstrate a method to minimize the onset response by initiating the block using a waveform with a high frequency and large amplitude, and then transitioning to a low frequency and low amplitude waveform, which reduces the magnitude of current required to maintain the conduction block. In five of six animals it was possible to transition from a 30 kHz to a 10 kHz waveform, at block threshold, without inducing any transient neural firing. The minimum transition time was 0.03 sec. The results of this study show that this method is feasible for achieving a nerve block with minimal onset responses and current amplitude requirements.

***Keywords**: High frequency nerve block, functional electrical stimulation, onset response, in-vivo model.*

Introduction

The delivery of high frequency alternating currents (HFAC) has proven to be a reversible and rapid method of blocking peripheral nerve conduction [1-5]. HFAC in the frequency range of 1 – 40 kHz [5,7] and amplitudes between 1-10 V, delivered through a cuff electrode in direct contact with a peripheral nerve, reversibly blocks the propagation of action potentials [5]. This block is established in less than 100 ms [6] and is completely reversible when the HFAC is turned off, as the nerve returns to full conductivity within approximately one second [3,5]. The fast onset of the conduction block and the quick reversibility makes HFAC block appealing for potential clinical uses.

One undesirable aspect of HFAC nerve block is the initial volley of action potentials when the HFAC is first turned on, termed the "onset response". The onset response has been demonstrated in many animal studies [2-5,7], and in computer simulations [8,9]. HFAC block requires amplitudes above a minimum "block threshold" in order to completely block a peripheral nerve. The motor "block threshold" is defined as the lowest amplitude at which all motor axons in the nerve are blocked, and the block threshold increases monotonically for increasing frequencies [5,7,8]. There is a trade off between minimizing the onset response and minimizing the voltage/current required to block. Specifically, the onset response is minimized with high amplitude and high frequency, whereas the voltage/current is minimized at the lower frequencies where block thresholds are lower. As a result, it is desirable to consider utilizing a waveform that minimizes the onset response by initiating the block with a high frequency and large amplitude and then transitioning to a low frequency, low amplitude waveform in order to reduce the voltage/current required to maintain block.

The goal of this study was to evaluate whether the transition in frequency and amplitude during HFAC block could be accomplished without inducing any additional nerve activity beyond the onset response. We hypothesized that a smooth simultaneous transition of both frequency and amplitude could be accomplished without activating the nerve if the transition period was sufficiently long. Furthermore, we hypothesized that less activity would be induced by a transition from a high amplitude to a low amplitude than vice versa. This type of amplitude transition would be naturally coupled with the frequency transition from high to low, since block thresholds also decrease as the HFAC frequency is lowered [5].

Material and Methods

Frequency and amplitude transitions were evaluated in 6 adult Sprague-Dawley rats under institutional approval. The animals were anesthetized with intraperitoneal Nembutal (pentobarbital sodium). The surgical procedure has been described previously [5,10]. The sciatic nerve was carefully exposed through a postero-lateral incision and the sural and common peroneal nerves were cut. The gastrocnemius-soleus muscle complex was exposed and its insertion into the calcaneus was severed. The calcaneal tendon was attached to a force transducer that was pre-tensioned with approximately 1-2 Newtons.

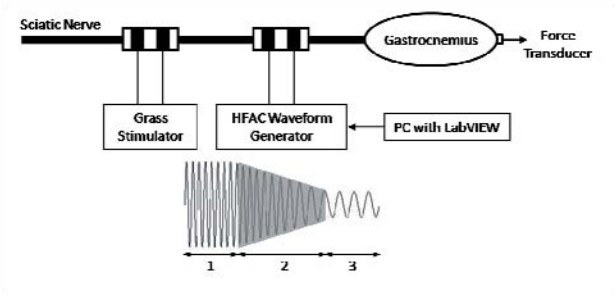


Figure 1: Showing the experimental setup with the waveform transition shape on the bottom. The HFAC starts at 30 kHz high amplitude and transitions to 10 kHz low amplitude.

Two bipolar platinum cuff electrodes were positioned along the sciatic nerve as illustrated in Figure 1. The proximal electrode was used to deliver suprathreshold monophasic square pulses from an isolated current source (Grass S88 Stimulator, Grass Technologies, West Warwick, RI, USA) at a rate of 1 Hz. The distal electrode was used to deliver the HFAC waveform, which was generated by an arbitrary waveform generator (Wavetek 395, now Willtek Communications GmbH, Ismaning, Germany). Labview software (National Instruments, Austin, Texas, USA) was used to control the Wavetek output to simultaneously sweep the frequency and ramp the amplitude as illustrated in Figure 1.

The HFAC waveform used in each trial consisted of three phases. First, the HFAC waveform was turned on at 30 kHz at 10 Vpp. The frequency and amplitude were held constant during this first phase. The second phase consisted of the frequency and amplitude transition with the frequency sweeping from 30 kHz to 10 kHz at a constant linear rate and the amplitude ramping linearly to its final value. The duration of the second phase was termed the transition time. The third phase began at the end of the transition time, once the frequency and amplitude reached their final values. During this third phase, the frequency was maintained at 10 kHz and the amplitude was held at an amplitude just above the 10 kHz block threshold (measured experimentally in each animal). Four different transition times were tested during each experiment in a randomized order and ranged between 0.03 seconds to 60 seconds. Of the 6 animals in the randomized series, transition times of 0.03, 0.1, 1, and 10 seconds were tested in 3 animals; 0.1, 1, 10, and 20 seconds were tested in 2 animals; and 1, 10, 30, and 60 seconds were tested in 1 animal. The peak muscle force (N) and the force-time integral (N.s), of the transition activity were the output measures of the experiments.

Results

The experiments demonstrated that the onset response for a HFAC initiated at 30 kHz was much smaller than one at 10 kHz (Figure 2, top two traces). Waveform transitions that were not optimized led to a large burst of transition activity (Figure 2, bottom trace).

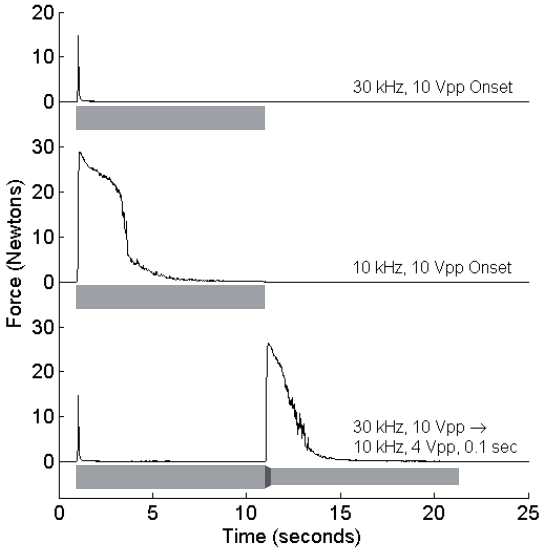


Figure 2: 30 kHz onset (top), 10 kHz onset (middle). A waveform transition at 0.1 s leads to a large burst of transition activity. The light gray bars show the timing of the HAFC and the dark area the transition zone.

Optimal transitions allowed the HFAC to be initiated at 30 kHz (with a small onset) and then transitioned to 10 kHz without any transition activity. The critical condition was the transition time of the frequency/amplitude sweep. Figure 3 demonstrates that there is a minimum transition time at which there is no transition activity. Transition times shorter than this lead to activity while longer times show no activity.

In 5 of 6 animals, successful transition times were obtained, ranging between 0.03 s to 20s. In one animal, the transition even at 60 s was unsuccessful in totally eliminating transition

activity, though here too the activity was reduced with the longer transition times.

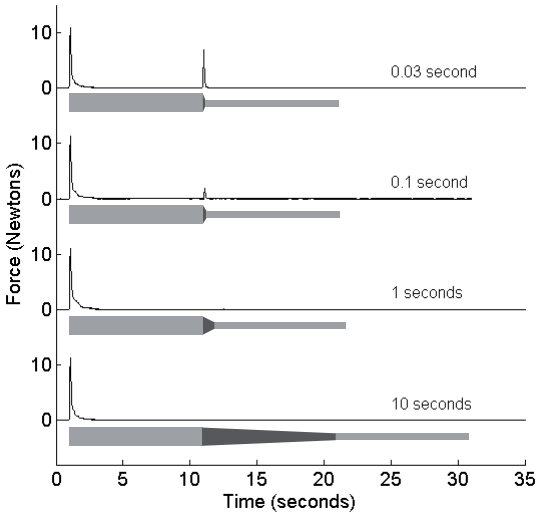


Figure 3: Example in one animal of successful transitions at 1 s and 10 s. Transition regions are shown in the dark gray bars.

Discussion

This set of experiments demonstrates that it is possible to start the HFAC block at a high frequency where the onset response is minimized. Subsequently, the frequency can be transitioned to a lower frequency and nerve block maintained at lower amplitudes. This technique has possible clinical implications in targeting HFAC nerve block in motor conditions, for example muscle spasms in spinal cord injury.

References

[1] Tanner JA, "Reversible blocking of nerve conduction by alternating-current excitation," Nature (London), vol. 195, p. 712, 1962.

[2] Woo MY and Campbell B, "Asynchronous Firing and Block of Peripheral Nerve Conduction by 20 kC Alternating Current," Bull Los Angel Neuro Soc, vol. 29, p. 87, 1964.

[3] Bowman B and McNeal D, "Response of Single Alpha Motorneurons to High-Frequency Pulse Trains," Appl. Neurophysiol., vol. 49, pp. 121-138, 1986.

[4] Kilgore KL and Bhadra N, "Nerve conduction block utilizing high-frequency alternating current," Medical and Biological Engineering and Computing, vol. 42, pp. 394-406, 2004.

[5] Bhadra N and Kilgore KL, "High-frequency electrical conduction block of mammalian peripheral motor nerve," Muscle and Nerve, vol. 32, p. 782, 2005.

[6] Foldes EA, et al., "Counted Cycles Method to Quantify the Onset Activity in High-Frequency Peripheral Nerve Block," Conference proceedings: Annual International Conference of the IEEE Engineering in Medicine and Biology Society., vol. Accepted, 2009.

[7] Bhadra N, et al., "High frequency electrical conduction block of the pudendal nerve," Journal of Neural Engineering, vol. 3, p. 180, 2006.

[8] Bhadra N, et al., "Simulation of high-frequency sinusoidal electrical block of mammalian myelinated axons," J Comput Neurosci, vol. 22, pp. 313-326, 2007.

[9] Williamson RP and Andrews BJ, "Localized electrical nerve blocking," IEEE Transactions on Biomedical Engineering, vol. 52, p. 362, 2005

[10] Ackermann DM, et al., "Effect of Bipolar Cuff Electrode Design on Block Thresholds in High Frequency Electrical Neural Conduction Block," IEEE Transactions on Neural Systems and Rehabilitation Engineering, vol. 17, pp. 469-477, 2009.

Acknowledgements

This work was supported by the National Institute of Biomedical Imaging and Bioengineering Grant No. R01-EB-002091 and through the American Recovery and Reinvestment Act Summer Supplement through NIBIB.

Author's Address

Dr. Niloy Bhadra, MD, PhD.
Case Western Reserve University, Hamman 601, MetroHealth Medical Center, Cleveland, Ohio, USA, 44109.

Email: nxb26@case.edu

Optimization of a Tremor-Reduction Algorithm for Asynchronous Stimulation of Independent Motor-unit Groups

Wilder A. M.[1], Normann R. A.[2] Clark G. A.[2]

[1] University of Utah, School of Computing, Salt Lake City, Utah, United States

[2]University of Utah, Bioengineering Department, Salt Lake City, Utah, United States

Abstract

Rapid muscle fatigue, a major concern for many clinical FES applications, can be mitigated with the use of multi-electrode stimulation protocols. Determining proper parameters for such protocols, however, is often challenging. Here we analyze and optimize a previously reported algorithm designed to iteratively reduce tremor in muscle contractions elicited by asynchronous stimulation of independent motor-unit groups (ASIM). The algorithm was optimized for speed of convergence and steady-state tremor level. Three independent algorithm parameters, response-filter-bandwidth, error-sampling-delay and phasing-adjustment-gain, were examined. Behavior of the algorithm for various parameter values was simulated. The muscle response after each iteration of the algorithm was modeled by linearly summing pre-recorded responses to single electrode stimulation trains, shifted by the corresponding electrode phasings. For each algorithm parameter, the value producing the best performance is reported. Optimal parameter selection reduced convergence time by a factor of 3 and improved steady-state tremor reduction by approximately 17%.

***Keywords**: ASIM, IIFMS, tremor, multi-electrode sstimulation, interleaved, fatigue, USEA.*

Introduction

Asynchronous stimulation of independent motor-unit groups (ASIM) is a promising approach to fatigue-resistant motor function restoration [1, 2]. However, the increased complexity of stimulus parameter selection inherent in ASIM (as compared to single-electrode stimulation) makes it challenging to employ in clinical settings. For example, a major problem associated with ASIM is that without proper parameter selection, muscle contractions can display high levels of tremor, even when the composite stimulation rate (i.e. across all electrodes) would yield a fused tetanus if applied to a single-electrode [3]. To address this problem several groups have investigated means of automating ASIM parameter selection and control [3, 4]. One group [4] has devised an iterative stimulus phasing adjustment algorithm (ISPAA) for reducing tremor in isometric contractions. This algorithm represents significant progress towards making ASIM clinically practical. As presented, however, the specific steps of the algorithm were not entirely clear. Additionally, its performance and optimality were poorly characterized.

Correspondingly, the research presented here focuses on enhancing the value of the existing ISPAA by producing an explicit, parameterized implementation of the algorithm, testing the performance of the implementation under various conditions, and optimizing the three parameters associated with our implementation: response-filter-bandwidth, error-sampling-delay, and response-adjustment-gain. To accomplish these goals we utilized a novel ASIM response prediction technique [3] which enables us to simulate a sequence of ISPAA iterations of arbitrary length, and measure its performance for various parameter values.

Testing the behavior of this concrete ISPAA implementation under various conditions, and optimizing parameter selection to improve its performance will, we hope, increase its utility and effectiveness in the clinical FES arena.

Material and Methods

In-vivo Motor Responses:

This research employed *in-vivo* muscle response data recorded during a previous series of neuromotor physiology experiments. In those experiments muscle responses were collected from two isolated plantar flexor (Soleus, Media and Lateral Gastrocnemius, and Plantaris) preparations in cat, described in detail in [3]. To summarize, muscle contractions were evoked via constant-pulse-width, constant-frequency stimulation trains delivered on individual electrodes within a Utah slanted electrode array (USEA) implanted in the sciatic nerve. Response waveforms were measured by a single-axis force transducer attached to the Achilles tendon and recorded by a commercial data acquisition system.

Muscle Response Modeling:

ASIM trains used in this study were composed of phase-shifted single-electrode trains with known responses (i.e. as mentioned in the previous step). The predicted muscle response to an ASIM train was computed by shifting the single-electrode train responses an amount corresponding to the inter-

electrode phasings specified in the ASIM train and then summing the shifted waveforms.

Tremor Reduction Algorithm:

We implemented the ISPAA as follows (Figure 1).

1) Start with a period-long segment of the ASIM response waveform corresponding to the most recently completed stimulation cycle.
2) Bandpass filter the segment from frequency band f_{low} to f_{high}, where $f_{low} = f_{constituent}\ x(1-\alpha)$ and $f_{high} = f_{constituent}\ x(1+\alpha)$. (Note: We used a 3rd order Butterworth applied in both directions for zero phase distortion).
3) Remove any remaining DC offset.
4) Normalize the adjusted segment to the mean of the original segment. The resultant waveform is the error signal.
5) Sample the error signal at t_{delay} ms after each electrode stimulus.
6) Multiply all of these error-sample values by some gain g.
7) Multiply each inter-electrode phasing by the corresponding, adjusted error value.
8) REPEAT 1-8 after the next stimulation cycle.

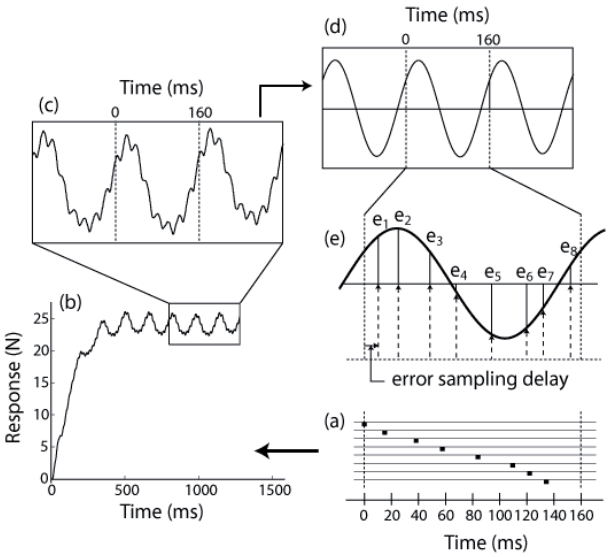


Figure 1: Diagram of the ISPAA. a) The stimulus phasing, within one ASIM cycle, for each electrode. b) The predicted ASIM response. c) The last 3 periods of the response. d) The filtered, demeaned and normalized response segment. e) The error signals to be used for updating the phasings.

Simulating Algorithm Behavior:

Behavior of the algorithm over multiple iterations was simulated using the response modeling technique listed above. Each simulation started with an ASIM train with evenly distributed electrode phasings. The predicted response was computed, and the phasing adjustment algorithm was executed. This sequence was continued until the change in response tremor from one iteration to the next converged to below a pre-determined threshold. If convergence was not reached within 200 iterations the simulations was terminated.

Optimizing Algorithm Performance:

Algorithm performance was measured in two dimensions: iterations to convergence, and tremor in steady-state response. The effect of each parameter on performance was evaluated by simulating algorithm behavior for various values of the parameter while holding the other two parameters constant. Effects of each parameter were evaluated for multiple electrode set sizes (4, 5, 6) and many unique sets of single electrode responses (n = 19,320).

Results

Simulation results show that the algorithm, as we have implemented it, does reduce response tremor (Figure 2). Additionally, results demonstrate that, over a wide range of parameter values, the algorithm converges (Figure 3). Optimal values, with respect to both steady-state tremor and speed of convergence, for the three ISPAA parameters are as follows: 1) Optimal response filter band is 80%-120% of constituent stimulation frequency. 2) Optimal error-sampling-delay is 15 ms. 3) Optimal phase-adjustment-gain is 0.5.

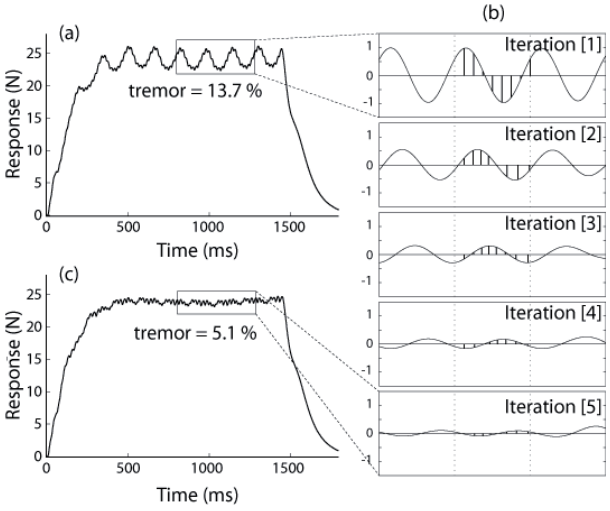


Figure 2: Five example iterations of the phasing-adjustment algorithm. (a) Predicted response to the ASIM train with evenly-distributed electrode phasings. Tremor for this train is 13.7%. (b) Change in error signal over 5 iterations of the algorithm. (c) Predicted response to ASIM train with optimized electrode phasings. Tremor for this train is 5.1%.

Discussion

The results presented here, specifically those displayed in Figure 3, demonstrate that there is significant potential for optimizing the ISPAA

algorithm as originally presented in [4]. Overall, convergence speed seemed to be the performance metric most affected by changes in algorithm parameter values. For example, changing the phasing adjustment gain from 1.0 to 0.4 decreases the average number of cycles to convergence from approximately 13 to 4. For ASIM cycle times of 100 ms (10 Hz constituent frequency) this would yield a reduction in convergence time from 1300 ms to 400 ms—valuable from both a controls perspective and that of improving the clinical FES patient's subjective experience.

Steady-state tremor was also affected by modulation of algorithm parameters (though the effects were not as large as those for convergence). Delaying the error sample time by 15 ms improves the steady-state tremor by approximately 17% as compared with a delay of 0 ms (apparently used in the algorithm as originally presented in [4]).

These results are encouraging; however, additional work is needed to confirm these findings *in-vivo*.

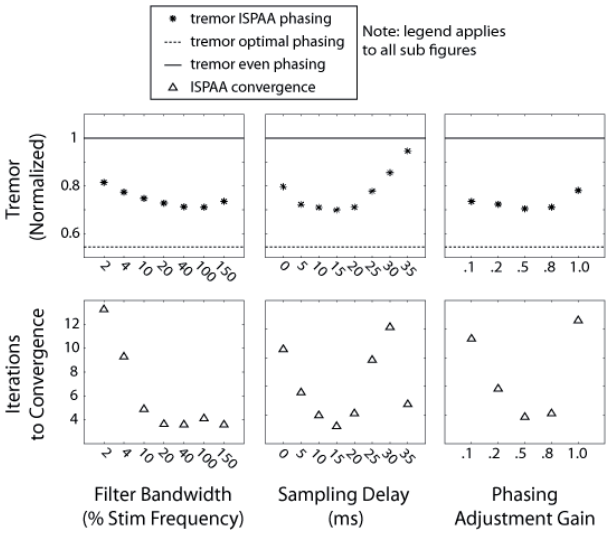


Figure 3: Performance of the ISPAA algorithm for various parameter values. Top row shows algorithm performance in terms of steady-state response tremor (i.e. after algorithm convergence) normalized to tremor at start of algorithm. Dashed line shows tremor for optimal phasings (as determined by a technique described in [3]). Bottom row: algorithm performance in terms of iterations to convergence. Left column: change in algorithm performance for various filter bandwidths. Middle column: algorithm performance for various error sampling delays. Right column: algorithm performance for various phasing adjustment gains.

Another point to consider is the validity of the simple, linear-summation model used to predict ASIM responses. Although this technique is not exact, it has been shown to be quite accurate for isometric contractions [3, 5] which are the very sort targeted by this relatively slow, iterative approach to stimulation control.

Ultimately we feel that the specific optimizations presented here, and more generally, the use of ASIM response modeling, for purposes of parameter optimization, represent a valuable contribution to the nascent field of asynchronous multi-electrode FES.

References

[1] K. Yoshida and K. Horch, "Reduced fatigue in electrically stimulated muscle using dual channel intrafascicular electrodes with interleaved stimulation," *Annals of Biomedical Engineering,* vol. 21, pp. 709-714, 1993.

[2] D. McDonnall, G. A. Clark, and R. A. Normann, "Interleaved, multisite electrical stimulation of cat sciatic nerve produces fatigue-resistant, ripple-free motor responses," *IEEE Transactions on Neural Systems and Rehabilitation Engineering,* vol. 12, pp. 208-215, 2004.

[3] A. M. Wilder, R. A. Normann, and G. A. Clark, "Automated Parameter Selection for Smooth Isometric Force Recruitment with Asynchronous Multi-Electrode Stimulation," *Journal of Applied Physiology,* in review.

[4] A. K. Wise, D. L. Morgan, J. E. Gregory, and U. Proske, "Fatigue in mammalian skeletal muscle stimulated under computer control," *Journal of Applied Physiology,* vol. 90, pp. 189-197, 2001.

[5] T. G. Sandercock, "Nonlinear summation of force in cat soleus muscle results primarily from stretch of the common-elastic elements," *Journal of Applied Physiology,* vol. 89, pp. 2206-2214, 2000.

Acknowledgements

These studies were funded in part by NIH, NINDS, R01 NS039677-06, and DARPA contract N66001-06-C-8005.

Author's Address

Gregory A. Clark
University of Utah, Department of Bioengineering
greg.clark@utah.edu

INCLUDING NON-IDEAL BEHAVIOUR IN SIMULATIONS OF FUNCTIONAL ELECTRICAL STIMULATION APPLICATIONS

Lynch CL[1,2], Graham GM, and Popovic MR[1,2]

[1] Institute of Biomaterials and Biomedical Engineering, University of Toronto, Toronto, Canada

[2] Toronto Rehabilitation Institute, Toronto, Canada

Abstract

Simulations of FES systems are usually based on the typical or ideal stimulated muscle response, which may result in an overly optimistic prediction of the FES system's performance in real-world applications. We have developed a Simulink block that allows actual non-ideal behaviour of electrically stimulated muscles to be incorporated into existing FES simulations. This block is based on data collected from complete SCI subjects, and it modifies the nominal stimulated muscle response to reflect undesirable behaviour seen in real-world FES applications, including spasms, tremors, and fatigue. The severity of each type of undesirable behaviour can be specified by the user. In this paper, we discuss the design of the block, and also present an example of how the block can be used to more accurately assess the probable real-world performance of FES systems prior to testing with SCI subjects.

***Keywords**: functional electrical stimulation, spinal cord injury, stimulated muscle response, model, simulation*

Introduction

Functional electrical stimulation (FES) can be used to restore or replace lost motor function in individuals who have spinal cord injuries (SCI). Each new FES application must be thoroughly tested with SCI individuals. However, it is time-consuming and expensive to recruit suitable subjects, re-condition the subjects' muscles using electrical stimulation, and then conduct exhaustive testing to verify the performance of a particular FES system.

For these reasons, it is common to refine the design of a FES system in simulation prior to the testing phase. Such simulations are usually based on models of the typical or ideal stimulated muscle response, which may result in an overly optimistic assessment of the FES system's likely performance in the real world. Stimulated muscle contractions in individuals with SCI are subject to fatigue, muscle spasms, and tremors due to incomplete tetanus, in addition to other undesirable effects. It is necessary to account for these non-idealities in an accurate simulation of the real-world performance of a FES system.

We created a Simulink block (The Mathworks, Natick, USA) that represents the range of spasm, tremor, and fatigue behaviour that stimulated muscles exhibit in the real world. This block uses data collected from complete SCI subjects, and modifies the nominal stimulated muscle response to reflect the undesirable behaviour seen in the real world. This "non-idealities block" can be incorporated into existing FES simulations in Simulink to analyze the performance of FES systems in the presence of undesirable behaviour.

This paper presents our pilot work on this project. We discuss the design of the block, and also present an example of how the non-idealities block can be used to assess the likely real-world performance of a FES system.

Material and Methods

Data Analysis

We developed the non-idealities block using previously collected data from subjects with complete SCI. The experiments were approved by the local research ethics board, and all subjects provided informed consent.

We extracted the muscle spasm and tremor data from experiments done with a single complete SCI subject. The subject's muscles were re-conditioned using electrical stimulation prior to data collection. The subject was seated with the shank free to swing during the data collection experiments. We transcutaneously stimulated the subject's quadriceps muscle group with a Compex Motion stimulator (Compex SA, Switzerland) using a bipolar, biphasic square wave pulse train with pulse width 250 μs and frequency 40 Hz. The stimulation amplitude was randomized for each trial between 0 mA and a pre-set maximum amplitude. We sampled the resulting knee angle at 100 Hz for 5 seconds after the onset of stimulation, by which time the knee angle had reached its steady state behaviour in each trial. We passed

each trial through a de-noising filter. After identifying those trials that exhibited muscle spasms or tremors, we extracted only the spasm or tremor behaviour from the affected trials. The resulting spasm waveforms are zero except where the spasms are present, and the tremor waveforms are centred about zero. We also assigned each spasm and tremor waveform a classification of mild, moderate, or severe with respect to its particular type of undesirable behaviour.

We extracted the fatigue waveforms from data from a separate experiment done with seven complete SCI subjects. The experimental setup was similar to that of the experiment described above, except this experiment concerned isometric contractions of the quadriceps muscles. The stimulation amplitude was determined individually for each subject to produce maximal force, and the isometric force was sampled at 100 Hz during 2 minutes of maximal electrically stimulated contractions [1]. We used a polynomial fit to approximate each force curve, and then scaled each curve from 1 to 0 to generate a fatigue waveform, with 1 corresponding to no fatigue and 0 corresponding to no measurable response to stimulation. We then classified each fatigue waveform as mild, moderate, or severe.

Construction of Non-idealities Block

The output of the non-idealities block can be described by

$$v(t) = (\tau(t) + s(t) + m(t)) \cdot fat(t)$$

where $\tau(t)$ is the nominal response of the stimulated muscle, $v(t)$ is the modified, realistic stimulated muscle response, and $s(t)$, $m(t)$ and $fat(t)$ are instances of the spasm, tremor, and fatigue waveforms, respectively. We implemented the block using a MatLab S-function, which defines a custom Simulink block. The user can vary the severity of the fatigue, spasm, and tremor waveforms that are included in a particular instance of the block. The actual waveform that is used for each facet of the block (spasm, tremor, and fatigue) is selected randomly from the group of waveforms having the desired classification (mild, moderate, or severe) each time the simulation is run.

Example of Block Implementation

We implemented the non-idealities block in a FES simulation to show how this block can be used to examine the potential real-world behaviour of a FES system. The example is a simulation of proportional-integral-derviative (PID) control of knee angle, based on the model of stimulated knee response described by Ferrarin and Pedotti [2]. Knee extension is provided by stimulated quadriceps contractions, and knee flexion is provided by gravity. Fig. 1 shows a block diagram of this simulation. We recorded unit step response metrics [3] for the nominal case and using the non-idealities block with different parameter values.

Results

Fig. 2 shows how the non-idealities block modifies the nominal stimulated muscle response. The dotted line corresponds to the simulated nominal knee torque produced at the maximum stimulation amplitude in the open-loop. The solid line corresponds to the modified torque produced by the non-idealities block with mild spasms, mild tremors, and mild fatigue. Fig. 3 shows the response of the knee angle control example to a 60 degree unit step trajectory (controller parameters: Kp = 175, Ki = 250, Kd = 325). The dotted line corresponds to the step response without the non-idealities block. The solid line corresponds to the same response with the non-idealities block (mild spasms, tremors, and fatigue).

Table 1 shows selected unit step response metrics for the knee control example. The results for the moderate and severe cases of spasms, tremors, and fatigue were similar to but more pronounced than those shown in Table 1.

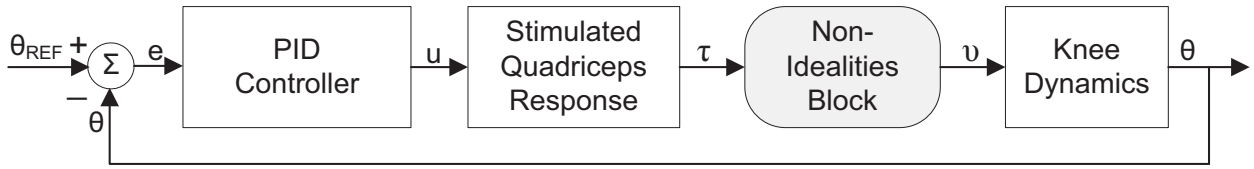


Fig. 1: Block diagram of simulation of PID control of electrically stimulated knee angle θ.

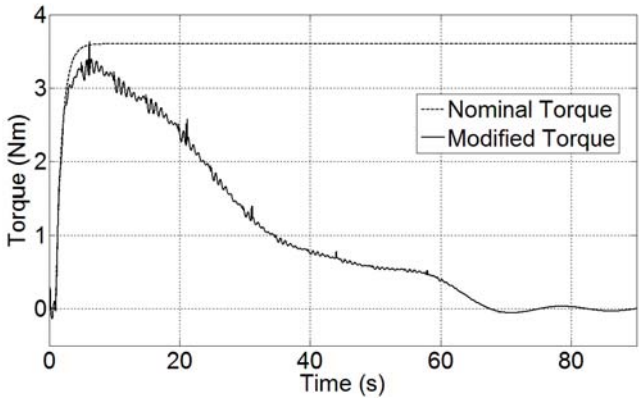


Fig. 2: Nominal knee torque at maximum stimulation, and modified torque generated by non-idealities block for mild spasms, tremors, and fatigue.

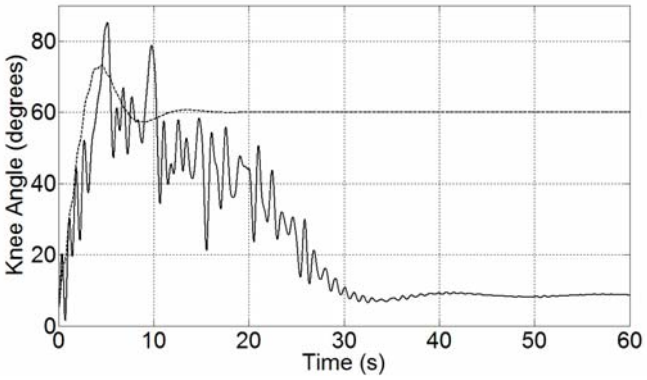


Fig. 3: Response of knee control example to 60 degree unit step trajectory. Dotted line is without non-idealities block. Solid line is with non-idealities block (mild spasms, tremors, and fatigue).

Table 1: Unit step response metrics for knee angle control example.

Case	10%-90% Rise Time (s)	Over-shoot (%)	RMS Error (deg)
Nominal	2.21	22.10	5.01
Mild Fatigue Only	2.24	21.00	41.77
Mild Spasm Only	2.14	22.14	5.06
Mild Tremor Only	3.53	45.65	11.73
Mild Fatigue, Spasm, and Tremor	3.51	42.15	46.54

Discussion

The modified torque produced by the non-idealities block is clearly different from the nominal torque. The spasms did not significantly degrade the performance of the control system, but fatigue and tremors both had a large effect on control performance. All combinations of undesirable behaviour resulted in poorer performance than the corresponding undesirable behaviours in isolation.

The non-idealities block represents a worst-case scenario with no muscle recovery. In reality, control performance will likely be modestly better than is indicated by the simulated results, since some recovery will occur during periods of no stimulation. Also, we use fatigue data collected from isometric contractions of untrained quadriceps muscles. Isotonic contractions in trained muscles may result in different fatigue profiles than those used in the non-idealities block. The data were collected from a limited number of subjects, and therefore do not reflect all of the undesirable behaviour that can occur with real-world FES use.

Conclusions

We have developed a Simulink block that introduces realistic undesirable behaviour into simulations of the performance FES systems. This non-idealities block is based upon actual stimulated muscle responses of subjects with complete SCI, and allows researchers to assess the likely real-world performance of FES systems before testing with SCI subjects, thereby saving time and expense.

In the future, we plan to expand this work by including additional stimulated response data from SCI subjects. We also plan to make the MatLab code for this project freely available on our website for use by others in the FES field.

References

[1] Graham GM, Thrasher TA, Popovic MR. The effect of random modulation of functional electrical stimulation parameters on muscle fatigue. *IEEE Trans Neural Syst Rehabil Eng*, 14:38-45, 2006.

[2] Ferrarin M, Pedotti A. The relationship between electrical stimulus and joint torque: A dynamic model. *IEEE Trans Rehabil Eng*, 8:342-352, 2000.

[3] Vegte JVD. *Feedback Control Systems*, 3rd ed. Upper Saddle River, NJ, USA: Prentice Hall, 1994.

Acknowledgements

We would like to thank the Natural Sciences and Engineering Research Council of Canada (#249669), Canadian Institute of Health Research (FRN-97952 and FNR-94018), Toronto Rehabilitation Institute, and Ontario Ministry of Health and Long-Term Care for financial support.

Author's Address

Cheryl Lynch
IBBME, University of Toronto, Toronto, Canada
and Toronto Rehab, Toronto, Canada
clynch@ieee.org, http://www.toronto-fes.ca

Influence of back muscle strength on Vertebral Stress -Formation of Trunk Musculoskeletal Model-

Hatakeyama K[1], Matsunaga T[1], Ishikawa Y[2],Ohtaka K[3], Sato M[1], Chida S[1], Watanabe M[1], Misawa A[2], Sasaki K[2], Tomite T[2], Yoshikawa T[2], Daisuke K[2], Iwami T[3], Shimada Y[2], Iizuka K[4]

[1] Akita University Hospital, Akita, Japan.

[2] Department of Neuro and Locomotor Science, Division of Orthopedic Surgery, Akita University School of Medicine, Akita, Japan.

[3] Department of Mechanical Engineering, Faculty of Engineering and Resource Science, Akita University, Akita, Japan.

[4] BIOTEC, Ltd.

Abstract

<Porpose> to design a musculoskeletal spine model with which we can perform Functional Electrical Stimulation (FES) effectively as well as the simulation of spinal motion and analysis of stress distribution to the vertebra. <Methods> A 28 years old healthy male was scanned with CT. After obtaining the CT data, we made three-dimensional model of spine, rib cage and pelvis by using 3D design software "EICAS". We used a 3D motion analysis system, VICON MX to estimate the muscular strength in the standing position from the comfigured musculoskeletal model, and measured the static standing posture. Measurement conditions included relaxed posture with weakened erector spinal muscles, upright posture and mild f1exion. Then, we input the estimated position of coordinate into the musculoskeletal model to estimate the muscular strength and the joint angle of each muscle. We a1so used this data analyze the stress with Visual Nastran 4D. <Results> Flexion moment in each facet joint showed the highest rate in the mild forward f1exion, decreased in the relaxed posture, ref1ecting the mobility of spine. Specifically, the flexion moment decreased around Level T8, located near the top vertebra in the relaxed posture. The stress analysis showed that stress increased in the mild forward flexion and the relaxed posture. <Discussions> When the muscular strength of the erector spinal muscles decreased, stress to a ligament and a vertebra was strengthened to increase the vertebral stress.

Keywords: *Trunk Musculoskeletal Model, Back extensor muscle, Vertebral stress*

Introduction

The average Japanese life expectancy is increasing from year to year, and Japanese men and women already have one of the highest life expectancy rates in the world. In line with the increase of an ageing population, people suffering from osteoporosis and spinal deformity are increasing as well. Trunk extensor muscle strength is very important to support spinal stability for sitting or standing. The effectiveness of functional electrical stimulation (FES) or therapeutic electrical stimulation (TES) of trunk extensor muscle has been reported by some literatures [1-3]. The spinal deformity is caused by multiple vertebral fractures, and compression of supported muscles, such as the erector spinal muscles. With the spinal simulation model, it was reported that muscle weakness of the erector spinal muscles, enhances the kyphosis to allow the increase of vertebral stress [4]. However, in order to examine the vertebral stress in detail, an estimate of the muscular strength is needed with a musculoskeletal model based on the measured posture and movement, and the stress analyzed.

A significant development, in the form of a motion analysis system in recent years allowed the assessment and analysis of the movement in detail. An estimation of moving muscular strength is available, and is applied to extremital joints. However, there are few reports regarding a musculoskeletal model of a trunk , and insufficient reviews. This is because there are a large number of facet joints and muscles. The movement range of facet joints differs from case to case, and there are too many factors including; abdominal pressure, influence of ligaments and the physiological cross

section of muscles. The purpose of this study was to design a musculo-skeletal dynamic spine model with which we can perform Functional Electrical Stimulation (FES) effectively as well as the simulation of spinal motion and analysis of stress distribution to the vertebra.

Material and Methods

Design of skeletal model

A 28 years old healthy male was scanned with CT. After obtaining the CT data, we made three-dimensional model of spine, rib cage and pelvis by using 3D design software ”EICAS” (Fig.1). This model could be worked under 3D analysis software “Visual Nastran 4D”. The vertebrae could be meshed to analyse the stress distribution (Fig 1). Meshing could be done to some vertebrae as far as the capacity of computer processing allows.

Design of muscle model

We designed muscle component that had a contractile element. Our model included M. erector spinae (M. iliocostalis, M. longissimus and M. spinalis). M, semispinalis, M. multifidus, M. rotators, M. interspinales, M. quadratus lumborum, M. rectus abdominis, M. psoas major, and M. psoas minor. We attached these muscles to the skeletal model on 3D analysis software “Visual Nastran 4D” (Fig 2). Each muscle was represented as an “actuator” which was attached between two bones to transmit a muscle contraction. Abdominal pressure was set up as an external force because it cannot be reproduced in the model. The movement range of each facet joint was estimated from X rays and this was included in the musculoskeletal model.

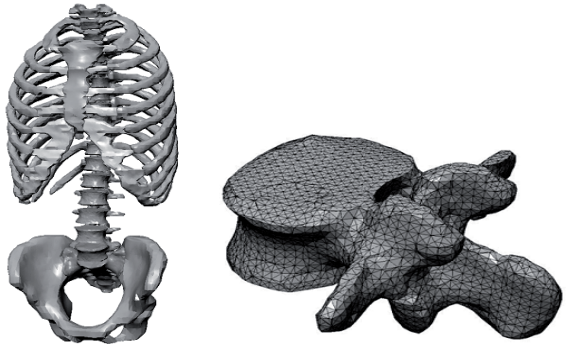


Fig 1. Three-dimensional spine model with the rib cage and pelvis, and vertebra with mesh.

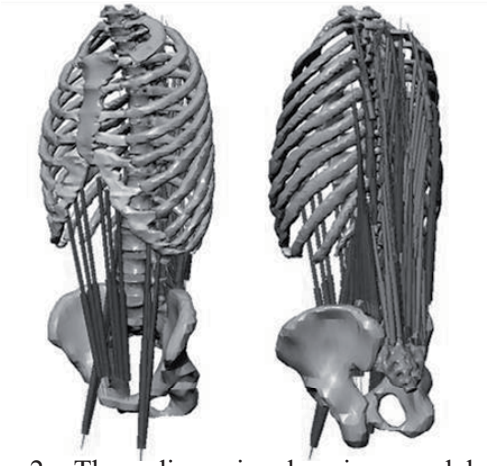


Fig 2. Three-dimensional spine model with muscle.

Motion analysis

We used a 3D motion analysis system, VICON MX to estimate the muscular strength in the standing position from the comfigured musculoskeletal model, and measured the static standing posture. Measurement conditions included relaxed posture with weakened erector spinal muscles, upright posture and mild forward f1exion. We estimated the position of coordinate of each marker by 72 ref1ective markers on the surface of the body (Fig 3). Then, we input the estimated position of coordinate into the musculoskeletal model to estimate the muscular strength and the joint angle of each muscle. This data was also used to analyze the stress with the Visual Nastran 4D.

Result

The muscular strength could be estimated through the musculoskeletal model that was made. Flexion moment in each facet joint showed the highest rate in the mild forward flexion and decreased in the relaxed posture, reflecting the mobility of the spine. Specifically, the flexion moment decreased around Level T8, located near the top vertebra in the relaxed posture. The

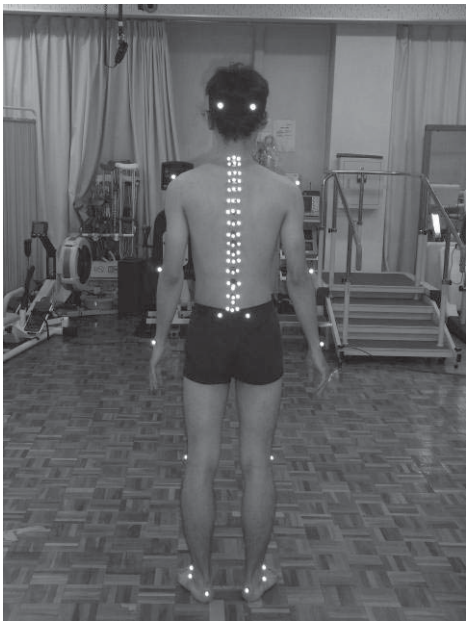
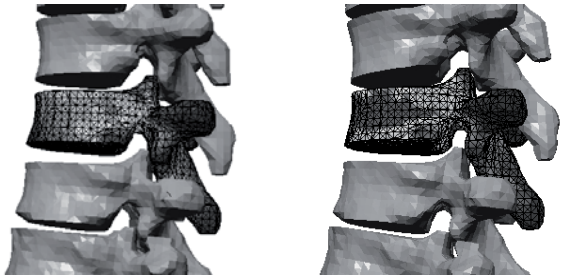


Fig 3. Motion analysis for standing position using 72 ref1ective markers on the surface of the body.



The upright posture The relaxed posture

Fig 4. The stress analysis in the upright posture and relaxed posture. The stress analysis showed that anterior border of the vertebra in the relaxed posture.

muscular strength in the upright posture was similar to the advanced research. The stress analysis showed that stress increased in the mild forward flexion and the relaxed posture (Fig 4). The stress analysis showed that anterior border of the vertebra in the relaxed posture.

Discussion and Conclusions

There were many influences on the spinal alignment. Of these influences, muscular force affected the spinal alignment to a large extent. In this study, the musculoskeletal model could be formed, and an estimate of the moment and muscular strength in each facet joint could be found. When the muscular strength of the erector spinal muscles decreased, stress to a ligament and a vertebra was strengthened to increase the vertebral stress. In the case of the flexed posture with a base of osteoporosis and a pressured fracture, further weakening of the muscle was assumed to strengthen the stress on the vertebra. The pressured fracture based on osteoporosis easily occurred with the increase of vertebral stress, and the sequential flexed posture was closely related to QOL. It is important to work with drug therapy as well as to consider the approach to decrease the stress to the vertebra by proceeding with therapeutic exercises. Moreover our model has ability to inbestigate not only spine motion but also the vertebra stress with FES or TES for back muscle weakness. This study enabled us to examine influences of the muscle force and posture that are bases of stress reduction. We need to measure the patients with roundback posture, examine the stress to the vertebra, and the effect of TES on the back muscle in the future.

References

[1] S. N. Kukke and R. J. Triolo. The effects of trunk stimulation on bimanual seated workspace. *IEEE Trans Neural Syst Rehabil Eng,* vol. 12, 177-85, 2004.

[2] S. Nandurkar*, et al.* Percutaneous implantation of iliopsoas for functional neuromuscular stimulation. *Clin Orthop Relat Res,* 210-7, 2001.

[3] R. J. Triolo*, et al.* Implanted Functional Neuromuscular Stimulation systems for individuals with cervical spinal cord injuries: clinical case reports. *Arch Phys Med Rehabil,* vol. 77, 1119-28, 1996.

[4] Y. Ishikawa, *et al.* Model simulation for restoration of trunk in complete paraplegia by functional electrical stimulation. *10th Annual Conference of the International FES Society,* 403-405, 2005.

Author's Address

Kazutoshi HATAKEYAMA

Akita University hospital

hata@hos.akita-u.ac.jp

Motion analysis of low-intensity back muscle exercise using a three-dimensional musculoskeletal model

Yoshikawa T[1], Matsunaga T[2], Hongo M[1], Tomite T[1], Sasaki K[1], Kudo D[1]

Sato M[2], Chida S[2], Hatakeyama K[2], Iwami T[3], Shimada Y[1]

[1] Department of Orthopedic Surgery, Akita University Graduate School of Medicine, Akita, Japan

[2] Department of Rehabilitation Medicine, Akita University Hospital, Akita, Japan

[3] Faculty of Engineering and Resource Science, Akita University, Akita, Japan

Abstract

Low-intensity back muscle exercise is that the subject is placed in a slight trunk flexion in which they assumed a prone position with a cushion under his trunk and perform intermediate extension. This exercise was proved the safety and effectiveness in elderly individuals in previous studies. In order to conduct safe and effective low-intensity back muscle exercise used electrical stimulation in patients with mild hemiplegia to improve quality of life, we developed a three-dimensional musculoskeletal model and used this model to analyse muscle strength and verify effective positions during low-intensity back muscle exercise with normal subjects. Subjects were 10 healthy adults (8 men, 2 women; mean age, 24.5 years). They placed in a slight trunk flexion position in which they assumed a prone position with a cushion under their trunk. They carried out the low-intensity back muscle exercise with the three each position of the cushion (i.e., their chest, abdomen, pelvis). Paraspinal muscle activation during low-intensity back muscle exercise is sufficient compared with that during maximum extension. And when the cushion was placed under the abdomen is the most safe and effective. Motion analysis of low-intensity back muscle exercise using a three-dimensional musculoskeletal model anabled estimation of the optimal exercise level and position. In future studies, we plan to incorporate electrical stimulation into this model.

***Keywords**: three-dimensional musculoskeletal model, low-intensity back muscle exercise,*

Introduction

We have clinically demonstrated, in previous studies, the safety and effectiveness of low-intensity back muscle exercise in elderly individuals.(Hongo et al. Osteoporos Int, 2007) Low-intensity back muscle exercise is that the subject is placed in a slight trunk flexion in which they assumed a prone position with a cushion under his trunk and perform intermediate extension. And We have tried to exercise this method in mild hemiplegic patients with electrical stimulation in order to improve quality of life. But the safety and efficacy on this approach in mild hemiplegic patients with electrical stimulation have not proved. Therefore using three-dimensional musculoskeletal model we will try to analyze the spine motions in mild hemiplegic patients when the subjects do low-intensity back muscle exercise with electrical stimulation. As a first step, we developed a three-dimensional musculoskeletal model of normal subjects and used this model to estimate muscle strength and verify effective positions during low-load back muscle exercise.



Fig. 1 : low-intensity back muscle exercise

Methods

Subjects were 10 healthy adults (8 men, 2 women; mean age, 24.5 years). Each subject was placed in a slight trunk flexion position in which they assumed a prone position with a cushion under their trunk. Subsequently, the subjects were asked to perform intermediate extension and maximum extension from this assumed position. These trunk extension motions were measured using a force plate and three-dimensional motion analysis device, while paraspinal electromyography was simultaneously performed at the third and eighth thoracic vertebrae and the third lumbar vertebra. Changes in the trunk extension motions corresponding to different cushion locations (i.e., under the chest, abdomen, and pelvis) were

analyzed and verified using a three-dimensional musculoskeletal model. As a result, the muscle activation was calculated for each operation. By comparing the muscle activation at each position, we examined whether any position is the most safe and effective.

Results

When the cushion was placed under the abdomen, paraspinal muscle activation during intermediate extension was somewhat lower than during maximum extension, but still sufficient. With the cushion placed under the chest, muscle activation around the lower vertebrae was lower compared to when the cushion was placed under the abdomen and pelvis, for both intermediate and maximum extension. Muscle activation was the greatest when the cushion was placed under the pelvis, but this position was unstable due to the knees being lifted from the floor,etc.

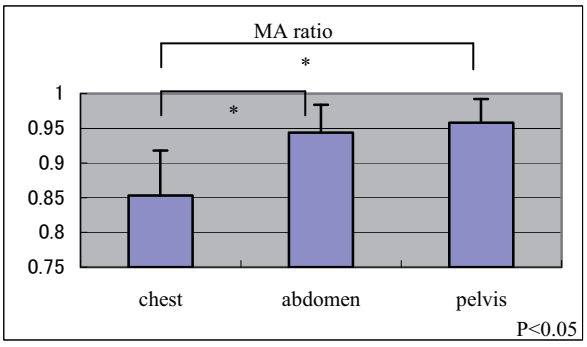


Fig.2 The ratio of muscle activation at each cushion's position (MA ratio=intermediate extension MA / maximum extension MA)

Discussion

In the analysis of 3D motion analysis model created by this, when the cushion was placed under the abdomen was considered to be most useful in three positions in terms of safety and efficacy. When the cushion was placed under the Chest is safe, but paraspinal muscle activity is insufficient compared to the abdomen position. And With the cushion placed under the pelvic is unstable and dangerous.

Conclusion

Motion analysis of low-intensity back muscle exercise using a three-dimensional musculoskeletal model enabled estimation of the optimal exercise level and position, which is considered useful for performing safe and effective exercise therapy. In future studies, we plan to incorporate electrical stimulation into this model.

References

(1) Briggs AM, Dieen HV Thracic Kyposis Affects Spinal Loads and Trunk Muscle Force. Physical Therapy 2007; 87: 595-607

(2) Hongo M, Itoi E Effect of low-intensity back exercise on quality of life and back extensor strength in patients with osteoporosis. Osteoporosis International 2007; 18:1389-1395

Author's Address

Takayuki Yoshikawa

Department of Orthopedic Surgery, Akita University Graduate School of Medicine, Akita, Japan

taka4445@doc.med.akita-u.ac.jp

A Review on Functional Electrical Stimulation in China

Zhang Dingguo

State Key Laboratory of Mechanical System and Vibration, Shanghai Jiao Tong University, Shanghai, China

Email: dgzhang@sjtu.edu.cn

Abstract

In this paper, we make a survey on research of functional electrical stimulation (FES) in China including mainland, Taiwan and Hong Kong based on the statistics of literatures. The related Chinese academic journals are provided, and the database used is given. FES research began in China in 1980's. The history is reviewed and the primary works are introduced. The literatures surveyed include papers, theses and patents. Our review shows the publications and communities of FES research increase dramatically during recent years. We find the majority of FES research in China focuses on clinical evaluation, and the study on FES technology representing the level of FES is limited. Some typical works on FES system and technology are presented. The current situation is optimistic, and it has a promising prospect. In addition, we expect the traditional Chinese medical technique, acupuncture, may bring new power into FES technology in future.

Keywords: *FES, Rehabilitation, Review, BCI, Acupuncture*

Introduction

It is well known that the term of functional electrical stimulation (FES) firstly appeared to treat footdrop in sixties last century, while FES research in China just began in early eighties. There is a 20-year delay compared with the international development. In this paper, we study the situation of FES research in China. Please note FES is used in a narrowed sense here, i.e. the stimulation related to muscles, which is also named as functional neuromuscular stimulation (FNS) or neuromuscular electrical stimulation (NMES).

The Chinese version of this paper is published in *Chinese Journal of Rehabilitation Theory and Practice.*

History and Current Situation

In order to have an overview of FES history in China, we make a statistic study on the native published literature since 1980 containing journal/conference papers, master/PhD theses, patents and other related documents. The data are from the authoritative "China Knowledge Resource Integrated (CNKI) Database". We use the searching mode that FES appears in "full text", and the number of literature is altogether 1,984 up to April 3, 2010. In this mode, we can achieve a comprehensive result, but some unrelated papers may be wrongly included. We can also search FES in "keywords", while the number of literature is only 395. Obviously, many important literatures are omitted in this mode.

Most of the papers are published in the following major Chinese academic journals: *Chinese Journal of Physical Medicine and Rehabilitation (1979), Chinese Journal of Biomedical Engineering (1982), Chinese Journal of Rehabilitation (1986), Chinese Journal of Rehabilitation Medicine (1986), Chinese Journal of Rehabilitation Theory and Practice (1995)*, *and Chinese Journal of Clinical Rehabilitative Tissue Engineering Research (1996)*. Please note the year of start publication is given in the brackets.

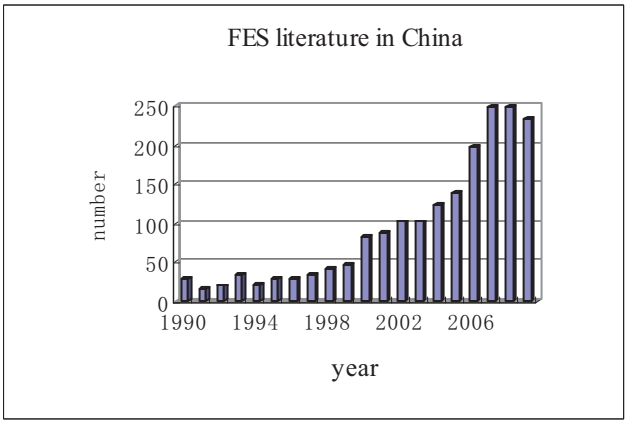


Fig.1. Number of FES literatures between 1990 and 2009 in academic database (CNKI) of China. (Data of Hong Kong and Tai Wan are not included.)

Fig.1 shows the number of literature related to FES

in China since 1990. The increasing tendency is obvious especially during recent years. After 2003, the number is over 100 stably.

The first academic literature of FES appeared in a Chinese journal in 1983, but it is not an original work. It is written by Edel et al., and translated into Chinese by Gu XC [1]. The first native research achievement was reported by Zheng DG [2], where a stimulator called "FES-1" was developed jointly by Shanghai No.2 Medical College, Shanghai No.21 Radio Factory and Zhejiang Xiangshan Instrument Factory.

The earliest research of FES was launched by group of Dai KR, who is currently an academician of the Chinese Academy of Sciences. In their work, the rehabilitation and therapy performance of FES on 277 patients was evaluated [3]. The self-designed stimulators called "MFNS-6" and "MCC-1" were used. The paralyzed patients included traumatic injury (188 subjects), cerebral palsy (9 subjects), cerebrovascular disorder or stroke (47 subjects), acute anterior poliomyelitis (21 subjects), and others (12 subjects). The shortest course of disease has 40 days, while the longest course of disease has 36 years. According to our knowledge, it is rare to study the rehabilitation performance of FES in such a wide range all over the world. In the corresponding time, the invasive FES research was launched by the group of Jiang DZ, while their work is much closer to the category of neural stimulation, e.g selectivity [5]. Their typical work provided the bladder control technique via FES, and experimental work was conducted on animals (dog) [4]. The basic theory is to selectively stimulate the sacral nerve to control the coordinated contraction of sphincter and detrusor, and thus accomplish the urinary function for paraplegia.

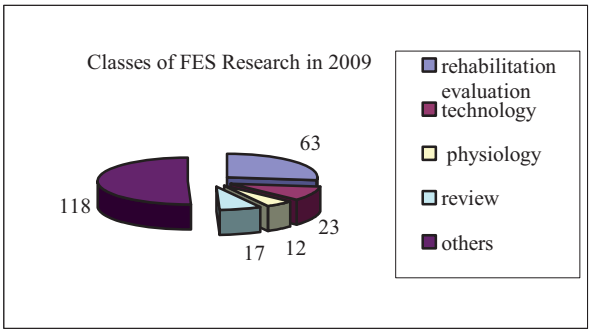


Fig.2. Classes of FES literatures in 2009 based on academic database (CNKI) of China. (Data of Hong Kong and Tai Wan are not included.)

Most FES research in China focuses on therapy in rehabilitative perspective, i.e. FES rehabilitation evaluation for stroke, paraplegia, spasticity, and muscle atrophy etc. The research on FES technology in engineering perspective seems not much. A case study of survey is performed on the FES literatures in 2009 as shown in Fig.2. The total number is 233 by searching mode of "full text", while only about 115 literatures exactly match the term of FES. The others contain artificial cochlear, visual prosthesis, electrical acupuncture and some literatures wrongly searched. Among the 115 literatures, there are roughly four classes: rehabilitation evaluation of FES, FES technology, physiology of FES, and review. The number of literature is 63, 23, 12, and 17 respectively. We find FES technology occupies only about 20% of the 115 literatures, nearly the highest proportion among all the previous years. As FES technology is the key factor to promote FES application in reality, and we expect the focus can be moved to FES technology gradually in China.

We also make a survey on the patents about FES particularly, which indicates the potential of transforming FES research into commercial market. The number of patents is about 20, and all the patents are publicized in recent 3 years. It means FES research in China just begins to step into marketing, while the potential is huge.

Typical Works

Regarding FES technology, we introduce some typical works in China. Bi S and Dou HY et al. investigated the iterative learning algorithm for FES control respectively, which aims to realize the cyclic movements of lower limbs [6, 7]. Jiang HY et al. conducted a series of study on FES cycling under the help of Hunt KJ of Glasgow University [8-10]. Their work is mainly about FES control algorithms, such as robust PID control [8] and fuzzy parameter self-tuning PID control [9]. Ming D et al. designed a force measurement system for FES walking [11, 12]. The walker tipping index was used to analyze and process gait stability in FES-assisted paraplegic walking.

At present, brain-computer interface (BCI) technology is progressing with rapid expansion, which offers a good opportunity for FES, because BCI could be an ideal control source. Some groups in China have already begun the research on BCI controlled FES [13, 14]. Our group is also focusing on this research topic now [15]. The basic theory is that FES can be triggered by EEG signals related to the imaginary movement (e.g mu rhythm). The main task is to predict the intention from EEG using some methods of feature extraction and pattern recognition.

In recent years, some oversea Chinese scholars studying FES have returned to China, such as Lan N [16], He JP [17], Zhang DG [18], and Sha N [19, 20]. The first three persons once studied FES control, neuro-musculo-skeletal modelling and simulation. The last one targeted the design of FES surface electrode. However, most of their achievements were accomplished abroad.

Different from mainland, it is not easy for us to access the local academic databases of Hong Kong and Tai Wan, which are not included in CNKI database. Therefore, it is hard to get a comprehensive review on FES research in these two areas.

According to our knowledge, the FES research level in Hong Kong and Tai Wan is higher than that in mainland. Tong KY began his research on FES technology in late nineties last century [21], and established the FES research centre in Hong Kong Polytechnic University [22]. He has cooperation with groups of Gao SK of Tsinghua University and Zheng XX of Zhejiang University respectively. There are also some excellent works done in Tai Wan as follows. Chang GC et al. used neural network method to control keen joint movement with FES [23]. Chen JJ et al. developed a FES cycling system using fuzzy logic control [24]. Chen CC et al. adopted EMG as feedback to design FES cycling system [25]. Chen SC et al. developed a kind of versatile FES system [26]. Chen YL et al. developed a FES system for gait training [27].

Conclusion and Prospect

In this paper, FES research in China was surveyed. The current situation is optimistic although FES has a short history in China.

An interesting traditional medical technology caught our interest in China, which is acupuncture, the most popular Chinese medicine. We found that acupuncture combined with electrical stimulation is widely used in practice in China. Even a tiny private Chinese clinic may have this technology. We search for "acupuncture + electrical stimulation" by mode of "full text" in CNKI database. There are about 10,363 related literatures. It is an amazing number, and the research strength is much stronger than that of FES in China. Acupuncture targets to stimulate "Xue Wei" (acupoints) of the "Jing Luo" (meridians and collaterals) in human body, which has some complex relationship with nervous system. We think electrical acupuncture stimulation and FES should share some common ground. We are considering expanding FES research by "borrowing" the power from acupuncture research in China. It may be a win-win plan.

References

[C]=[Chinese Language]

[1] Gu XC, Possibility of adopting electrotherapeutics in rehabilitation for cerebral palsy and spasticity caused by cerebrovascular disease [C]. *Foreign Medical Science: Physical Medicine and Rehabilitation*, 1:30-32, 1983. / Edel E et.al, [Germany] *Z Physiother* 33:321, 1981.

[2] Zheng DG, Gospel for the paraplegia [C]. *Zhejiang Briefing of Science and Technology*. 3:17, 1984.

[3] Dai KR, Wu RS, Tang RG, Fan JX et al. Preliminary evaluation of FES rehabilitation on paralyzed patients [C]. *Chinese Journal of Rehabilitation* 1:72-75, 1984.

[4] Zhang TS, Jiang DZ, Dang JG and Liu WS, Investigation of applying neural electrical stimulation into the bladder control of paraplegia [C]. *Chinese Journal of Rehabilitation* 3:106-110, 1986.

[5] Tai CF and Jiang DZ, Selective stimulation of smaller fibers in a compound nerve trunk with single cathode by rectangular current pulses. *IEEE Trans. Biomed. Eng*. 41:286-291, 1994.

[6] Bi S, Yan DL, Wang FG, Dou HF and Zhou ZY, Application of P type iterative learning control in functional neuromuscular stimulation feedback control for upper limbs [C]. *Chinese Journal of Rehabilitation Medicine*, 15(1): 37-39, 2000.

[7] Dou HF, Tan KK, Lee TH, and Zhou ZY, Iterative learning feedback control of human limbs via functional electrical stimulation. *Control Engineering Practice*, 7:315-325, 1999.

[8] Jiang HY, Geng JH, Ao HR, Hu XL, and Hunt KJ, FES cycling robust PID control strategies and simulation [C]. *Chinese Journal or Biomedical Engineering*, 24:217-221, 2005.

[9] Jiang HY, Ma CB, Lu NL, Wei W, and Liao ZW, Application of fuzzy parameter self-tuning PID control in FES cycling system [C]. *Chinese Journal of Rehabilitation Medicine*, 21:538-540, 2006.

[10] Jiang HY, Wei W, and Ma CB, Research on the stimulation pattern which is based on FES cycling train [C]. *Chinese Journal of Rehabilitation Medicine*, 22:147-150, 2007.

[11] Ming D, Wan BK, Hu Y and Liang RZ, A new assessment method for FES-assisted paraplegic walking stability based on WRI graph [C]. *Chinese Journal or Biomedical Engineering*, 24: 118-121, 2005.

[12] Ming D, Bai Y, Liu X, Qi H, Cheng L, et al. A gait stability investigation into FES-assisted paraplegic walking based on the walker tipping index. *Journal of Neural Engineering*, vol.6, 2009: 066007.

[13] Zhou P, Cao HB, Xiong Y, Ge JY, Zhang S and Wang MS, Design of intelligent rehabilitation system based on brain-computer interface [C]. *Computer Engineering and Application*, 43 (26):1-4, 2007.

[14] Meng F, Tong KY, Chan ST, Wong WW, Liu KH, Tang KW, Gao XR, and Gao SK. BCI-FES training system design and implementation for rehabilitation of stroke patients. *IEEE IJCNN Conference*, pp.4103-4106, 2008.

[15] Zhang DG, Liu GQ, Huang G, Liu JR and Zhu XY. A hybrid FES rehabilitation system based on CPG and BCI technology for locomotion: A preliminary study. *Lecture Notes in Computer Science*, 5928:1073–1084, 2009.

[16] Lan N, Crago PE, and Chizeck HJ. Control of end-point forces of a multijoint limb by functional neuromuscular stimulation. *IEEE Trans. Biomed. Eng.*, 38(10):953-965, 1991.

[17] He JP, Levine WS and Loeb GE, Feedback gains for correcting small perturbation of a standing posture. *IEEE Trans. Automatic Control*, 36(3):322-332, 1991.

[18] Zhang DG and Zhu KY. Modeling biological motor control for human locomotion with functional electrical stimulation. *Biological Cybernetics*, 96:79-97, 2007.

[19] Sha N, Howard D, Heller BW, Barker AT, Wang Y, Kenney L. The effect of the impedance of a thin hydrogel electrode on sensation during functional electrical stimulation. *Medical Engineering and Physics*, 30(6):739-746, 2008.

[20] Sha N, Kenney L, Heller BW, Barker AT, Howard D, Moatamedi M. A finite element model to identify electrode influence on current distribution in the skin. *Artificial Organ*, 32:639-643, 2008.

[21] Tong KY and Granat MH. Virtual artificial sensor technique for functional electrical stimulation. *Medical Engineering and Physics.* 20(6):458-68, 1998.

[22] Webpage of FES in Hong Kong Polytechnic University:http://www.polyu.edu.hk/rec/fes/indexc.html

[23] Chang GC, Lu JJ, Liao GD, Lai SJ, Cheng CK, Kuo TS. A neural-control system for the knee joint position control with quadriceps stimulation. *IEEE Trans. Rehab. Eng.*, 5(1):2-11, 1997.

[24] Chen JJ, Yu NY, Huang DG, Ann BT, Chang GC. Applying fuzzy logic to control cycling movement induced by functional electrical stimulation. *IEEE Trans. Rehabilitation Engineering*, 5(2):158-169, 1997.

[25] Chen CC, He ZC, and Hsueh YH. An EMG feedback control functional electrical stimulation cycling system. *Journal of Signal Processing Systems*. DOI 10.1007/s11265-009-0425-5, 2009.

[26] Chen SC, Luh JJ, Chen YL, Liu CL, Yu CH, et al. Development and application of a versatile FES System. *Journal of Medical and Biomedical Engineering*, 24(1): 37-43, 2004.

[27] Chen YL, Li YC, Kuo TS, and Lai JS. The development of a closed-loop controlled functional electrical stimulation (FES) in gait training. *Journal of Medical Engineering & Technology*. 25:41-48, 2004.

Acknowledgements

This work is supported by the Project-sponsored by SRF for ROCS, SEM, and SJTU Interdisciplinary Fund in Medicine & Engineering (YG2009MS45).

Author's Address

Name: Zhang Dingguo
Affiliation: Institute of Robotics, Shanghai Jiao Tong University, Shanghai, 200240, China
Email: dgzhang@sjtu.edu.cn
Homepage:
http://www.biorob.sjtu.edu.cn/dgzhang.htm

Cortical change and functional recovery of upper limb by therapeutic electrical stimulation with chronic hemiplegic patient: a case report

Sasaki K[1], Matsunaga T[2],Misawa A[1],Tomite T[1] Yoshikawa T[1],Kudo D[1],

Chida S[2], Sato M[2], Hatakeyama K[2],and Shimada Y[1]

[1] Department of Orthopedic Surgery, Akita University Graduate School of Medicine, 1-1-1 Hondo, Akita 010-8543, Japan

[2] Department of Rehabilitation Medicine, Akita University Hospital , 1-1-1 Hondo, Akita 010-8543, Japan

Abstract

Objective: *to investigate the effect of electrical stimulation on functional recovery of the upper limb and cortical activation in chronic hemiplegia.*

Methods: *Therapeutic electrical treatment (TES) for affected upper extremity was applied once a week for six months. Brunnstorm stage, modified Ashworth scale and ROM of affected side were compared pre and post treatment as a functional survey item. Functional MRI was performed pre and post treatment.*

Results: *The function of affected hand was improved after six months TES. In functional MRI, bilateral SMC and PMC, SMA which are skirt SMC were activated. This activation was intensified after the electric stimulation of the first time. In addition, the change was occurred after first TES exercise. In this research, it is suggested that 6 months TES treatment produce functional recovery for hemiplegic upper limb and change of cortical activation.*

Conclusions: *Electrical stimulation may have the facilitator potential for central nerve systems. There is a possibility that the regeneration of cortex was occurred by TES exercise.*

Keywords: *electrical stimulation, functional MRI ,motor recovery*

Introduction

Electrical stimulation is one of the therapeutic strategies that are applied to improve impaired upper limb function. Recently there have been some many reports that described cortical reconstruction had occurred along with improvement of upper limb. On the other hand, there are few paper reported the effect of intervention with electrical stimulation.

The purpose of this study is (1) to evaluate the functional recovery of affected upper limb and cortical plasticity, (2) to assess whether electrical stimulation gives an immediate effect for the brain activation.

Material and Methods

Patient

Patient was 72-year-old man, who had left-side chronic hemiplegia, participated in this study. He had reached a plateau of neurologic recovery.

Training

Patient received TES with NESS H200™ (Bioness Inc, USA) which consisted of orthosis with five surface electrodes and controller.

Patient was fitted with the device that was adjusted to elicit full finger extension and flexion. TES treatment was performed for fifteen minutes once a week during 6 months. The training mode was exercise mode which repeated open and grasp.

Outcome Measures

Hand function was evaluated using Brunnstorm stage, modified Ashworth scale, ROM of upper limb. We recorded that outcome measures pre-treatment and post-treatment 1months, 3 and 6 months.

Functional MRI (fMRI) was performed as an evaluation of the brain plasticity three times, pre-treatment and after patient received the TES at first time and 6 months.

The fMRI data were analyzed with SPM-2 software running under MATLAB.

Results

Brunnstrom stage was stage4 in the hand and stage4 in the arm, modified Asworth scale was grade1+ before treatment. After 6 months treatment, Brunnstrom stage of the finger improved to stage 5 despite that of arm remained stage 4. The spasticity was retrograded, while the change was slight.

The ROM was significantly expanded 20～30 degree on an average after TES rehabilitation .Especially automatic extension became 20 degrees from -20 degree.

Functional MRI images showed that the changes of the cortical activation. Activity was accepted in bilateral cerebral hemisphere by the grasp movement of the paralysis hand before the TES treatment and the brain cortex which is not only sensorimotor cortex (SMC) but also supplementary motor area(SMA),premotor cortex(PMC) had activated. After first TES training, these activations became intensive and the area grew wider. The activation varied from SMC, SMA, PMC of contralateral cortex to the ipsilateral cortex in fMRI after TES training for six months.

Discussion

Six months of TES treatment caused improvement upper limb joint active ROM. Furthermore, the spasticity becomes milder than before treatment. This change occurred after treatment from one week, and it was maintained afterwards for a training period. We reported excellent results of the functional electric stimulation with implantation electrode[1]. And the improvement of the upper limb function could get by the treatment with orthoses-stimulation system which used the surface electrode.

Recently, in the process of the functional restoration of the paralyzed limbs, activation of SMC PMA, ipsilateral cerebellum and bilateral SMA were reported .In this case, bilateral SMC and PMC,SMA which are skirt SMC were activated. This is similar to a past report, and it is considered that activation of large lesion except SMC is associated by remarkable action of motor-related cortex, the motor network of broad bilateral cortex was active for expression of the paralysis limb movement.[2]

This activation was intensified after the electric stimulation of the first time. This result suggested that electrical stimulation has facilitatory for central nerve systems.

The activation of the ipsilateral SMC disappeared after TES for six months, and activation of the contralateral SMC came to resist adversely. Hwa Kyung Shin et al reported such a change of fMRI and they describe that the cortical change was accompanied by the functional recovery of the affected hand.

It means regeneration of cortex was occurred by TES exercise. In addition, the change was occurred after first TES exercise.

Conclusions

In this research, it is suggested that 6 months TES treatment produce functional recovery for hemiplegic upper limb and change of cortical activation.

References

(1) Matsunaga T, Shimada Y et al: Clinical experience of functional electrical stimulation(FES) for restoration of tetraplegic hand function. Akita J. Med; 34 ;137-144

(2) Hwa Kyung Shin, Sang Hyun Cho, et al: Cortical effect and functional recovery by the electmyograrhy-triggered neuromuscular stimulation in chronic stroke patients. Neuroscience Letters;442;174-179(2008)

Author's Address

Kana Sasaki

Department of Orthopedic Surgery, Akita University Graduate School of Medicine

ksasaki@doc.med.akita-u.ac.jp

Therapeutic Electrical Stimulation through Surface Electrodes for Hemiplegic Shoulder Subluxation – Comparative study of the low-frequency stimulation method and the Russian method

Kudo D[1], Matsunaga T[2], Tomite T[1], Sasaki K[1], Yoshikawa T[1]

Sato M[2], Chida S[2], Hatakeyama K[2], Shimada Y[1]

[1] Department of Orthopedic Surgery, Akita University Graduate School of Medicine, 1-1-1 Hodo, Akita 010-8543, Japan

[2] Department of Rehabilitation Medicine, Akita University Hospital, 1-1-1 Hodo, Akita 010-8543, Japan

Abstract

There are reports that therapeutic electrical stimulation (TES) is useful for treating shoulder subluxation secondary to hemiplegia.TES through surface electrodes has conventionally been performed by using a low-frequency stimulation method by which stimulation is delivered with monophasic rectangular waves having frequencies of about 3 Hz to 100 Hz. In this study, we performed TES by the Russian method, by which the bursts of mid-frequency waves having carrier frequencies of around 2500 Hz occur with low-frequency rectangular waves. The subject was a 64-year-old man with hemiplegic shoulder subluxation. A treatment frequency of 20 Hz was used and the stimulus intensity was kept constant under the conditions in which the subluxation was reduced to the same position as on the healthy side. The voltage, current, and workload on the muscle per Hz were measured. In the low-frequency stimulation method,the stimulating conditions were a voltage of 40 V, current of 57 mA, and a workload on the muscle per Hz of 0.0008 W ,and the corresponding values for the Russian method were 50 V, 25 mA, and 0.001 W. The Russian method provides a greater workload on the muscles at a lower current than the low-frequency stimulation method, and it is useful when performing TES through surface electrodes.

***Keywords**: shoulder subluxation, low-frequency stimulation, Russian method, mid-frequency stimulation*

Introduction

Hemiplegic shoulder subluxation is reported that it occurs 15% to 81% in the patients with stroke, and it causes shoulder girdle pain, brachial plexus injury, rotator cuff tear, and inflammation of articular capsule. Several treatments, the brace to support shoulder, operations like biceps tenodesis or arthrodesis, and therapeutic electrical stimulation (TES) for hemiplegic shoulder, are reported. There are reports that therapeutic electrical stimulation (TES) is useful as a means of treating shoulder subluxation secondary to hemiplegia. TES through surface electrodes has conventionally been performed by using a low-frequency stimulation method by which stimulation is delivered with monophasic rectangular waves having frequencies of about 3 Hz to 100 Hz. (Figure 1). But skin pain was sometimes probrems when TES was performed. Recently, because of development of medical engineering, we performed TES by the Russian method, by which the bursts of mid-frequency waves having carrier frequencies of around 2500 Hz occur with low-frequency rectangular waves (Figure 2), and compared the results with those obtained by the conventional low-frequency stimulation method.

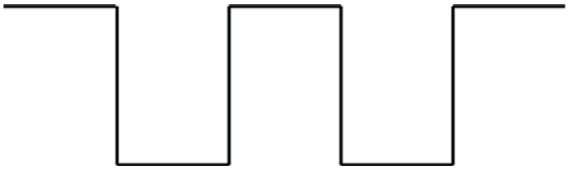


Fig. 1: A low-frequency stimulation method

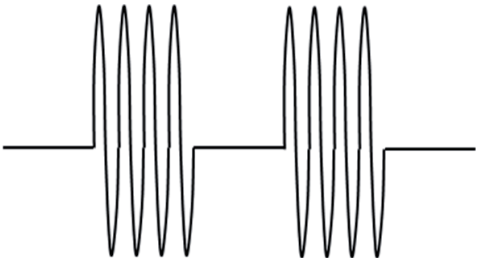


Fig. 2: A mid-frequency stimulation method

(Russian method)

Methods

Subjects

The subject was a 64-year-old man with left hemiplegia after the operation of brain abscess. Three years after the onset of the hemiplegia, his upper limb was evaluated as Brunnstrom stage I,

and anteroposterior radiograph of the shoulder showed subluxation with an acromio-humeral interval of approximately 25 mm. (Figure 3)

Measurement

The surface electrodes were positioned so that the posterior fibers of the deltoid and supraspinatus muscle would contract, and a treatment frequency of 20 Hz was used as the stimulation condition for both the low-frequency stimulation method and the Russian method. The stimulus intensity was kept constant under the conditions in which the subluxation was reduced to the same position as on the healthy side under the fluoroscopic observation (Figure 4). The voltage, current, and workload on the muscle per Hz were simultaneously measured, and the measurements were compared when the low-frequency stimulation method and the Russian method were used.



Fig. 3



Fig. 4

The 64-year-old man with shoulder subluxation was treated by the low-frequency stimulation method and the Russian method.

Results

The stimulation conditions under which the head of the humerus in the subluxated shoulder was reduced to the same position as on the unaffected side were a voltage of 40 V, current of 57 mA, and a workload on the muscle per Hz of 0.0008 W for the low-frequency stimulation method, and the corresponding values for the Russian method were 50 V, 25 mA, and 0.001 W.

Discussion

Baker and Paker reported that the effect of TES through surface electrodes with stimulation of 6 weeks for hemiplegic shoulder subluxation, which improved shoulder subluxation. Takahashi et al reported TES through percutaneus embedded electrodes, which embedded into the muscles around the shoulder, was effective for shoulder subluxation. Kobayashi et al also reported that improvement of shoulder subluxation and active abduction of the shoulder joint after TES through surface electrodes performed 6 weeks. Thus, several researchers reported usefulness of TES. In this study, the Russian method was greater in terms of workload on the muscles at a lower current and less skin pain when TES performed than the low-frequency stimulation method. In the future, we need to evaluate more cases and the long term effect of the Russian method.

Conclusion

The Russian method provides a greater workload on the muscles at a lower current than the low-frequency stimulation method; therefore, we believe it is more useful when performing TES through surface electrodes.

References

1) Baker LL, Parker K. Neuromuscular electrical stimulation of the muscles surrounding the shoulder. Phys Ther. 66(12):1930-7, 1986.

2) Kobayashi H, Onishi H, Ihashi K, Yagi R, Handa Y. Reduction in subluxation and improved muscle function of the hemiplegic shoulder joint after therapeutic electrical stimulation. J Electromyogr Kinesiol. 9(5):327-36, 1999.

Author's Address

Daisuke Kudo

Department of Orthopedic Surgery, Akita University Graduate School of Medicine, Akita, Japan

dkudo@doc.med.akita-u.ac.jp

Improving the Hemiplegic Hand Function by FES using Direct Myoelectric Control

Thorsen R[1], Cortesi M [2], Jonsdottir J [2], Carpinella I[1], Morelli D[2], Casiraghi A[2], Converti RM[2] , Ferrarin M[1]

[1] Biomedical Technology Department - Fond. Don Carlo Gnocchi Onlus, Milan, Italy

[2] Rehabilitation Unit, Milano - Fond. Don Carlo Gnocchi Onlus, Milan, Italy

Abstract

The feasibility and effectiveness of myoelectrically controlled functional electrical stimulation (MeCFES) as a tool in rehabilitation of stroke victims was assessed by a case control pilot study enrolling 20 patients. All subjects had a hemiparetic hand with impaired volitional opening, and thus difficulty in grasping objects. The hypothesis was that MeCFES could facilitate hand opening and thus assist the physiotherapist in working specifically on training functional hand movements. Myoelectric activity from wrist and finger extensors was proportionally controlling homologous stimulation on wrist and finger extensors in the study group and a placebo stimulation was applied to the control group. The setting was the standard physiotherapy consisting in 25 sessions of 45 minutes treatment. The protocol requested at least 3 sessions a week. The Action Research Arm Test (ARAT) and questionnaires were applied pre and post treatment to evaluate treatment effect.

Using MeCFES resulted in a significiantly ($p<0.02$) better ARAT score among the 11 patients (5 treatment & 6 controls) compliant with the protocol, whereas patients receiving less than 3 treatments a week (n=6) did not demonstrate relevant improvement.

***Keywords**: Myoelectrically controlled FES, Stroke, Rehabilitation, Hand function, Action Research Arm Test*

Introduction

Some cases of cerebrovascular accidents result in a severe paresis of the distal part of the upper limb presenting a closed hand, which the patient is unable to open volitionally. When the patient attempts hand opening the result may be counterproductive because the effort may result in further activation of the flexors. The physiotherast have few means of turn these attempts into a sensible reaching movements. Functional electrical therapy, where paretic muscle groups of the hand are stimulated in a synchronized sequence to assist the subject in performing functional movements, has shown to be a valid method for increasing functional recovery of the hand [1]. Though hand opening is absent, the myoelectric signal from the wrist and finger extensors may be present and can be utilized for FES control of the same muscles. The study of Francisco et. al. [2] indicated that the myoelectric signal as a FES trigger (as opposed to e.g. a mechanical trigger) may have the additional effect of providing the user with feedback about the onset of muscular activity. Clinical experience has taught us that also the cessation of muscle contraction may be impaired after CVA. Therefore a logical consequence seems to let the muscle be in direct control of the stimulation, in order to follow onset and cessation as well as intensity of volitional contraction of the controlling muscles; the wrist and finger extensors [3].

Material and Methods

In-patients were successively enrolled in this subject-and-rater blinded randomised case-control study. Baseline and final evaluations were made to quantify the motor recovery. Compliant patients received at least 3 treatments a week of either MeCFES or sham stimulation. Both treatments were incorporated in the standard physiotherapy setting of 45 minutes with standardized exercises. First 5 minutes of each session were dedicated to stretching and mounting of the systems, followed by 20 minutes of reaching and grasping exercises with MeCFES/sham stimulation. In the last 20 minutes the exercises were repeated without device to promote a carry over effect.

The MeCFES was recording the myoelectric activity from the 2/3 proximal part of the forearm at the level of innervation zones of ECR, ECU and EDL. Stimulation was applied as appropriate to

either wrist extensors or finger extensors. Stimulation was proportional to the filtered value of the myoelectric signal subtracted by an offset. An upper limit of stimulation (typically around 20mA) was imposed to avoid flexion reflex activation and/or inadvertent stimulation of flexor muscles due to spill over of current. The offset served to avoid that quiescent muscle activity and noise activates the stimulation prematurely. The gain was imposed by trial and error as a compromise of being high enough to ensure that the patient could activate the full range of stimulation but also sufficiently low to avoid instability of the intrinsic feedback loop caused by stimulation responses and artefacts.

The action research arm test (ARAT) [4] was employed to measure the functional change as the main outcome. Assessment of the patients perceived improvement was assessed by the questionnaires, Disabilities of the Arm Hand and Shoulder (DASH) [5] and the Individually Prioritized Problem Assessment (IPPA) [6].

A 5-point improvement on the ARAT is often regarded as clinically relevant for the improvement of the hand function [7]. The one tailed Mann-Whitney U-test (MWU) was applied. The main hypothesis was that MeCFES could improve ARAT score from before to after treatment in compliant patients with respect to the same physiotherapy utilizing sham stimulation.

Results

A total of 20 patients were enrolled in the study, see table 1. Due to secondary complications of the stroke 3 patients dropped out of the study before final evaluation could be made. Further 6 patients did not adhere to the study design prescribing at least 3 treatments a week and will be treated as non complaints when differentiating the analysis in analysis-per-protocol and intent-to-treat.

All but two compliant patients recovered some arm function as gaining a higher ARAT score, whereas the non-compliant group had no significant improvement. The compliant MeCFES group (A) had a significant and clinically important (more than 5 points) increase in ARAT score with a median of 10 whereas the compliant control group (B) presented less improvement with a median of 2 points. Thus the MeCFES helped to recover significantly (p=0.014) more of the hand function with respect to the control group (see fig 1.).

The non compliant patients did not demonstrate any significant improvement.

ID	SEX	TSS (yrs)	Group	Sess /Week	ARAT pre	ARAT post	ARAT change
1	**M**	**0.38**	**A**	**3.2**	**9**	**16**	**7**
2	**M**	**0.26**	**A**	**4.4**	**1**	**25**	**24**
3	**M**	**6.43**	**A**	**3.1**	**5**	**37**	**32**
4	**M**	**0.72**	**A**	**4.2**	**10**	**16**	**6**
5	**F**	**0.69**	**A**	**3.7**	**10**	**20**	**10**
6	**M**	**0.29**	**B**	**4.6**	**32**	**47**	**15**
7	**F**	**3.94**	**B**	**4.7**	**46**	**43**	**-3**
8	**M**	**0.44**	**B**	**4.6**	**1**	**2**	**1**
9	**F**	**0.90**	**B**	**3.2**	**39**	**42**	**3**
10	**F**	**7.45**	**B**	**5.0**	**36**	**36**	**0**
11	**M**	**0.58**	**B**	**4.0**	**31**	**36**	**5**
12	M	1.85	A	1.1	25	24	-1
13	F	3.02	A	1.7	10	13	3
14	M	4.83	A	2.4	38	38	0
15	M	0.67	A	1.8	3	3	0
16	M	0.68	A	2.5	5	5	0
17	M	3.08	B	1.3	5	11	6
18	F	0.31	B		6		DO
19	M	6.58	B		9		DO
20	F	0.70	B		10		DO

Table 1 List of patients (compliant subjects in boldface) with time since stroke (TSS), treatment group (A=MeCFES, B=Control), mean treatment sessions per week, the ARAT score at baseline (pre) and after 25 treatments (post) together with the calculated improvement (change). Subjects #12 to 17 were not compliant to protocol by treatment frequency and subjects #18 to #20 dropped out (DO) of the study due to relapse.

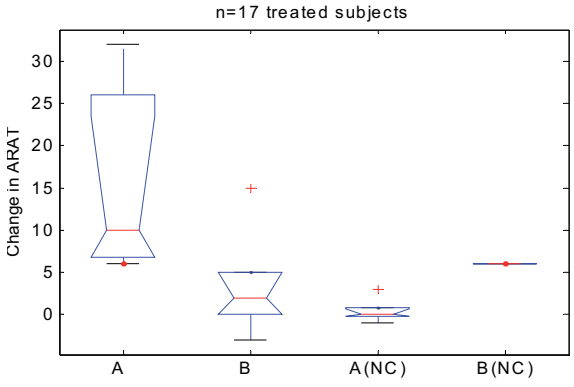


Fig.1: Change in ARAT from the baseline for compliant and non compliant (NC) patients. All five patients in the compliant MeCFES group (A) showed at least 6 points improvement.

The IPPA score was significantly higher (p=0.048) for the compliant MeCFES group. This means that they perceived an improvement of their self prioritised activities of daily living.

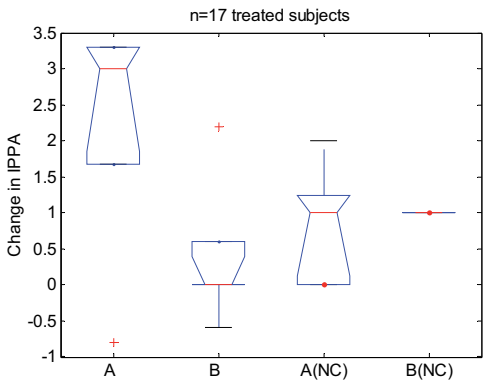


Fig.2: Change in IPPA. Only for the compliant subjects there is a significant difference.

The outcome of the DASH did not differ significantly between groups. There was an overall tendency of and improvement in all groups.

Discussion

Using the MeCFES as a tool to initiate muscle activity in paretic muscles appears to be powerful in that it can help the physiotherapist to break the barrier of 'the patient giving up on the limb'. An immediate increase in hand opening was noticed within the first week of treatment, allowing the therapist to start immediately to work with functional movements. From a clinical point of view it has been seen that hand opening alone does not necessary imply better hand function and without a good proximal function this treatment does not provide value for the patient. This may also explain lack of compliance to protocol by some of the patients. From a research standpoint it is valuable to apply the technique to only one muscle group to answer the fundamental question of feasibility. To answer the clinical need the technique must however be expanded to incorporate treatment of the entire upper limb and ontgoing research is investigating the application of multiple channels to the shoulder and upper arm as well. Using the MeCFES requires specific instrumentation and knowledge by the physiotherapist. An understanding of the inner workings of the device is needed to be able to successfully apply the instrument. In some cases difficulties can arise in finding the right electrode configuration and thus be too time consuming to be clinically practical. Some patients may not be responding due to several factors, such as dry skin (thus extreme electrode impedance), spasticity, sensitivity or total lack of volitionally controlled muscle contraction.

Conclusions

The results indicates that MeCFES can be a clinically important tool in physiotherapy using functional training of the hemiparetic hand. Increase in hand function is supported by subjective judgment by the patients. Since proximal function is crucial to the overall limb function the application of this technique, multiple muscles of the upper limb must be investigated in future research.

References

[1] Popovic M, Popovic BD, et. al. Clinical Evaluation of Functional Electrical Therapy in Acute Hemiplegic Subjects. J Reh Res and Dev 2003; Vol. 40 No 5, 2003, pp. 443-53.

[2] Francisco G, Chae J, et.al. Electromyogram-triggered neuromuscular stimulation for improving the arm function of acute stroke survivors: a randomized pilot study. Arch Phys Med Rehabil. Vol. 79 No. 5, 1998, pp.570-575

[3] Thorsen R, Cortesi M, et al. A Pilot Study on the Therapeutic Effect of MeCFES Assisted Figer Extension on the Hand of Hemiparetic Subjects - Preliminary Data. Biomedizinische Technik, Freiburg, Germany 2008;53,Supplement 1,:pp 71-3.

[4] Van der Lee JH, De Groot V, et.al. The intra- and inter-rater reliability of the Action Research Arm Test: a practical test of upper extremity function in patients with stroke, Arch Phys Med Rehabil, Vol 82, 2001, pp. 14-19

[5] Hudak PL, Amadio PC et al. Development of an upper extremity outcome measure: the DASH (disabilities of the arm, shoulder and hand) [corrected]. The Upper Extremity Collaborative Group (UECG). Am J Ind Med. 1996 Vol. 29 No. 6, 1996, pp. 602-8.

[6] Wessels R., de Witte L. et al. IPPA, a user-centered approach to assess effectiveness of assistive technology provision. Technology and Disability, Vol 13, 2000, 105-115.

[7] Burns A, Burridge J, et al. Does the use of a constraint mitten to encourage use of the hemiplegic upper limb improve arm function in adults with subacute stroke? Clin Rehabil, 21:895-904, 2007

Acknowledgements

This work has been supported by the Italian Ministry of Health (Ricerca Corrente IRCCS).

Author's Address

Rune Thorsen,
Fond. Don Carlo Gnocchi Onlus, via Capecelatro, 66 - 20148 Milano Italy
rthorsen@dongnocchi.it

EMG-triggered Neuromuscular Electrical Stimulation Combined with Motor Point Block to Improve on Hand Function in Hemiplegic Patients with Severe Spasticity

LEE YH[1], *LEE JH[1,2], Yoo EY[3], Park SH[3], Choi IS[1], Kim YH[4]

[1] Department of Rehabilitation Medicine, Yonsei University Wonju College of Medicine, Wonju, Republic of Korea

[2] Department of Rehabilitation Therapy, The Graduate School, Yonsei University, Wonju, Republic of Korea

[3] Department of Occupational Therapy, College of Health Science, Yonsei University, Wonju, Republic of Korea

[4] Department of Biomedical Engineering, Institute, Yonsei University , Wonju, Republic of Korea

Abstract

This study investigated the effects of EMG-triggered neuromuscular electrical stimulation (NMES) combined with motor point block to improve the hand function in chronic hemiplegic patients with severe spasticity in hand. The subjects were five patients who had hemiplegic hand with more than MAS scale III spasticity. EMG-triggered NMES was applied to wrist and finger extensor for 1hour a day, 5 days a week, for 4 weeks after motor point blocks at the spastic finger and wrist flexor muscles. The muscle activities of the extensor carpi radialis longus and extensor digitorum communis, active range of motion of wrist and finger extension, Modified Ashworth Scale, Fugl-meyer assessment and Box and Block test were examined before and after intervention. The result of study was that Active range of motion, Modified Ashworth Scale, and Fugl-meyer assessment showed significant immediate improvement. EMG-triggered NMES combined with motor point block improved on hand function in hemiplegic patients with severe spasticity.

Keywords: *stroke,spasticity, EMG-triggered neuromuscular electrical stimulation, motor point block*

Introduction

Hemiparesis is the most common deficit after a stroke, affecting 80% of subjects acutely and 40% chronically.[1] A common course of hemiparetic recovery reveals the development of uncontrolled flexion synergy. Abnormal synergies constitute a significant impairment that needs to be addressed by rehabilitation.[2]

The emerging behavioral therapies for recovery of upper–limb function include neuromuscular electrical stimulation, robot-aided sensory motor stimulation, real-time auditory feedback, and repetitive bilateral arm training with rhythmic auditory cuing.[3]

Constraint-induced movement therapy (CIMT) has attracted great attention because of its efficacy and sound physiologic principle. Eligible patients for CIMT must meet a minimum motor criterion including a certain degree of extension in wrist and finger. However a large number of stroke patients with severe spasticity are ineligible for CIMT. [4]

Cauraugh et al. and Chae et al. reported that electromyography(EMG)-triggered neuromuscular electrical stimulation (NMES) treatment was useful for rehabilitating wrist and finger extension movements of hemiparetic individuals. However, for hemiplegic patients with severe flexor muscle spasticity in an upper extremity, Electrical stimulation therapy alone does not produce satisfactory improvement of hand function. Because muscle spasticity often disturbs extensor muscle activity, it is important to reduce finger and wrist flexor spasticity to improve hemiparetic hand function. [5]

Kong et al. reported that motor point block with alcohol provide good relief of flexor spasticity in hemiplegic individuals.[6]

The rationale for using both modalities is to reduce the neurogenic component of finger and wrist flexors spasticity by means of motor point block with the FES as an adjunct therapy to improve hand function. [5]

The specific objective of this study was to investigate the effect of EMG-triggered NMES in combination with motor point block to improve the hand function in hemiplegic patients with severe spasticity.

Material and Method

Subjects

Five hemorrhagic or non-hemorrhagic stroke patients (three males, two females) with severe spasticity were recruited for this study. The mean age of the stroke patients was 50.3 (SD 19.5), the mean duration since the onset was 30.5 (SD 17.6) months. The subject selection criteria was duration of 12 months or longer since the stroke onset, spasticity of paretic finger and wrist flexors measured with Modified Ashworth Scale (MAS) greater than or equal to G3, power of paretic finger and wrist extensors measured with Manual Muscle Test (MMT) greater than or equal to poor grade, no sensory loss and contracture of paretic upper extremity, no history of relapse stroke and other neurologic disease, a score of at least 24 on the Korean Mini-mental State Examination (Kang et al. 1997), and no contraindication of electrical stimulation. All recruited subjects met these criteria.

Intervention

Motor point block

The muscles selected for neurolysis include the Flexor Carpi Radialis, Palmaris Longus, Flexor Carpi Ulnaris, Flexor Digitorum Superficialis, Flexor Digitorum Profundus and Flexor Pollicis Longus. Approximately 10~20cc injection of 50% dehydrated ethyl alcohol in water was given to subjects at each motor point. The actual number of muscles neurolysed varied among individuals. All blocks were performed under the guidance of a neuromuscular stimulator with 22-gauge sterile needle, administered by a physiatrist. [6]

EMG-triggered NMES

EMG-triggered NMES was applied to wrist and finger extensor for 1 hour a day, 5 days a week, for 4 weeks after motor point blocks at the spastic finger and wrist flexor muscles. The trigger level was set at 75% of the maximum EMG response of target muscles. The electrical stimulation was carried out under the supervision of occupational therapist using a stimulator unit (Myomed 932, Enraf-Nonius B.V., Netherlands) with biphasic symmetric pulses (35 Hz, single pulse width 200 μs, 10 s ON, approximately 20 s OFF, time delay: 3s ra ramp up, 2 s ramp down, 15-30 mA intensity). [7] The acquisition of EMG signal and stimulation were performed using the same 4 X 3 cm surface electrodes(Nicolet Biomedical, USA).

Outcome Measures

Subjects completed a pretest and a posttest after 4 weeks of intervention. Outcome measures consist of four clinical tests, muscle activities of the extensor carpi radialis longus (ECRL), and extensor digitorum communis (EDC). MAS, active Range of Motion (AROM), Fugl-Meyer assessment (FM) (Sanford et al., 1993) and Box & Block test(BBT)(Mathiowetz et al., 1985), were used to assess arm function. Muscle activities changes at posttest and pretest were tested to the root mean square of EMG wave in ECRL and ECD maximum voluntary contraction.

Statistical Analysis

SPSS (version 12.0) was used for nonparametric Wilcoxon matched-paired singed-ranks test. The significance level was set at $p<0.05$.

Results

Modified Asworth Scale (MAS)

All patients had severe spasticity of paretic finger and wrist flexors measured with MAS greater than or equal to G3. Comparison of pretest MAS of wrist flexor with that achieved after 4weeks of EMG-triggered NMES showed a significant decrease from 4.8 ± 0.4 to 3.4 ± 0.8($p< .042$;Fig. 1). And MAS of finger flexor was also significantly decreased from 4.6 ± 0.5 to 3.6 ± 0.5($p< .042$; Fig. 1).



Fig. 1: Modified asworth scale. Comparison of pretest MAS of wrist flexor and finger flexor with posttest MAS. MAS scale of pretest was significantly decrease after 0wks of treatment in wrist flexor and finger flexor. (P<.042)

Active Range of Motion (AROM)

All patients showed improvement in the active ROM of wrist and Finger (MP, PIP) joints compared to the pretest, which was statistically significant ($p = .042$; table 2).

Fugl-Meyer assessment

The Fugl-Meyer score of before and after the intervention was shown in Table 2 All patients improved in Fugl-Meyer assessment scores(p= .042).

Box and Block test

All five subjects could not move any block during the pretest. Although three subjects could move some blocks during the posttest, that change was not statistically significant.

	Pretest	Postest	z	p
Wrist AROM	16.0(10.8)	47.6(6.4)	-2.032	.042
MP AROM	10.0(12.2)	22.2(11.2)	-2.032	.042
PIP AROM	4.0 (4.1)	23.6(11.3)	-2.032	.042
FM	24.4(12.4)	30.2(12.5)	-2.032	.042
ECR RMS	35.6(11.2)	58.2(25.7)	-1.483	.138
EDC RMS	29.4 (7.6)	53.0(33.6)	-1.753	.080
BBT	0 (0)	1.8(2.0)	-1.633	.102

Table. 2: Comparison of clinical results and muscle activity between pretest and posttest. MP: metacarpophalangeal joint, PIP: proximal interphalangeal joint, FM: Fugl-Meyer assessment, ECR RMS: root mean square of the extensor carpi radialis longus, EDC RMS: root mean square of extensor digitorum communis, BBT: Box and Block test

Muscle Activity

Improvement on the RMS value of the ECRL and EDC during maximum voluntary contraction, was shown in four out of five subjects, which was not a significant change (Table 2).

Discussion and Conclusions

This study showed that EMG-NMES combined with motor point block could improve hand function in hemiplegic patients with severe spasticity. And result suggest that two subjects were able to meet CIMT criteria, which were 10 degrees of volitional extension of the wrist, 10 degrees of volitional abduction of the thumb, and 10 degrees volitional extension of two other digits in 3minutes. It seems that combined use of EMG-triggered NMES with chemical neurolysis could make hemiplegic hand with severe spasticity possible to be treated by another technique, such as CIMT, which was not indicated before treatment.

This study, however has few limitations. Only five subjects were enrolled for this study, and the ENG-FES training period 4 weeks of was not long enough to track changes in subjects. Further study that incorporates more subjects and randomized controlled design for generalization of the study`s results is need.

References

[1] Gresham GE, Duncan PW, Stason WB, et al: Post-Stroke Rehabilitation. Rockville, U. S. Department of Health and Human Services, Public Health Service, Agency for Health Care Policy and Research, 1995.

[2] Kamper DG, and Rymer Wz. Impairment of voluntary control of finger motion following stroke: Role of inappropriate muscle coactivation. Muscle Nerve, 24(5):673-681, 2001.

[3] Oujamaa L, Relave I, Froger J, et al. Rehabilitation of arm function after stroke: Literature review. Ann Phys Rehabil Med, 52: 269–293, 2009.

[4] Levy CE, Giuffrida C, Richards L, et al. Botulium toxin A, Evidence-based exercise therapy, and constraint induced movement therapy for upper limb hemiparesis attributable to stroke. Arch Phys Med Rehabil, 86: 696-706, 2007.

[5] Hara Y, Ogawa S. and Muraoka Y. Hybrid power-assisted fuctional electrical stimulation to improve hemiparetic upper-extremity function. Arch Phys Med Rehabil, 85: 977-985, 2006.

[6] Kong KH, and Chua KSG. Intramuscular neurolysis with alcohol to treat post-stroke Finger flexor spasticity. Clinical Rehabilitation, 16: 378-381, 2002.

[7] Friederrike L, Sabine H, Jurgen K, et al. Efficacy og EMG-triggered electrical arm stimulation in chronic hemi paretic stroke patients. Restorative Neurology and Neuroscience, 27 :189-197, 2009.

Acknowledgements

This research was financially supported by the Ministry of Education, Science Technology (MEST) and Korea Industrial Technology Foundation (KOTEF) through the Human Resource Training Project for Regional Innovation

Author's Address

Jong Hoon, Lee
Department of Rehabilitation Therapy, The Graduate School, Yonsei University, Wonju, Republic of Korea
petty-97@hanmail.net

Effect of combined peripheral motor electrical stimulation and anodal transcranial direct current stimulation(tDCS) in stroke patients

*Ko AR[1], Lee YH[1], Son J[2], Kim YH[2]

[1] Department of Rehabilitation, Yonsei University Wonju College of Medicine, Wonju, Republic of Korea

[2] Department of Biomedical Engineering, Institute, Yonsei University , Wonju , Republic of Korea

Abstract

The purpose of this study was to test the hypothesis that combining peripheral motor stimulation to the paretic hand with anodal transcranial direct current stimulation (tDCS) to the ipsilesional primary motor cortex (M1) would facilitate beneficial effects of motor training more than each intervention alone in six stroke patients that completed a randomized crossover designed study. In separate sessions, we investigated the short-term effects of single applications of no stimulation(S0), tDCS(S1), peripheral motor electrical stimulation(S2), and tDCS+ peripheral motor electrical stimulation(S3) that were done before training the patients on the ability to perform finger motor sequences with the paretic hand. The mean time of key presses decreased significantly in S3(20.44%) compared to S0(6.92%), S1(7.39%)and S2(1.00%). These results indicate that combining the effects of these interventions can potentiate relearning of motor skills to a level unattained by either of the interventions alone.

***Keywords**: Stroke, Transcranial direct current stimulation, EMG-triggered NMES, Finger sequence task*

Introduction

Despite the best rehabilitation efforts, stroke survivors are often left with significant and permanent residual motor impairments. Yet recovery of motor function following a stroke is known to be enhanced with motor training aimed at reducing impairments and relearning motor skills. New techniques, still under evaluation, are becoming the practical applications for the concept of post-stroke brain plasticity. Noninvasive brain stimulation (NBS) modulates motor cortical function and can enhance cortical plasticity. One of these interventions, tDCS, is capable of modulating the excitability of targeted brain regions by altering neuronal membrane potentials based on the polarity of the current transmitted through the scalp via sponge electrodes. Anodal stimulation increases cortical excitability in the stimulated brain tissue while cathodal stimulation decreases it. tDCS has enormous clinical potential for use in stroke recovery because of its ease of use, its non-invasiveness, its safety, its sham mode and the possibility to combine it with other methods [1]. The recent studies have shown that the effects of non-invasive brain stimulation on stroke recovery might be enhanced by combining it with peripheral stimulation using neuromuscular facilitation techniques. Hesse et al. [2] showed that the combination of tDCS of the motor cortex with robot-assisted arm training is effective in improving motor function in patients with subcortical stroke lesion. This study applied the peripheral motor electrical stimulation (EMG-triggered NMES) that is more practical than robot-assisted training in terms of clinical application. We compare the effects of non-invasive central nervous system stimulation with techniques of peripheral electrical stimulation, in order to provide new insights for future developments.

Material and Methods

Participants

Six stroke patients participated in this study (Table1).

Table 1. Patient Charateristics

Age, y (sex)	POD, mo[a]	Lesion site	MMSE[b]	FMS(%)[c]	MAS[d]
50(F)	8	Rt. s-ICH[d]	28	92.4	1
49(M)	5	Rt. s-ICH[e]	29	43.9	2
72(M)	2	Rt. Subcortical infarction	23	24.2	1+
43(M)	13	Lt. s-ICH	30	96.9	0
66(M)	11	Rt. ICH	25	90.9	1
62(M)	83	Rt. ICH	30	66.6	1

[a]Postonset duration , month
[b] Mini Mental State Examination-korean
[c]Fugle-Meyer Scale,
percent scores for the paretic upper extremity
[e]Subcortical intracranial hemorrhage
[d]Modified Ashworth Scale

The inclusion criteria were: (1) unilateral lesion in brain image, and (2) ability to perform the finger sequence task independently. The exclusion criteria included: (1) an intracranial metallic

implant, (2) existence of cerebellar or brain stem lesion, and (3) serious cognitive deficits (MMSE<23/30 points). The experimental protocol was approved by the institutional Review Board of the Yonsei university Wonju College of Medicine.

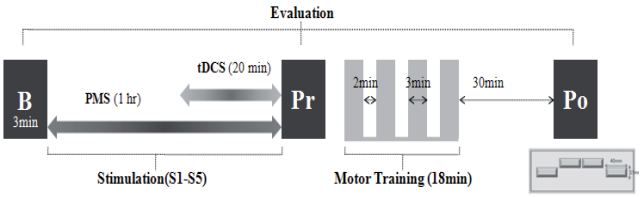
Experimental design

Subjects trained finger sequence task three times per week for 30 minutes to exclude learning effect, and participated in 4 experimental sessions separated by 6.6±0.54 days (Table 2). Different forms of stimulation were applied in different sessions. The order of the sessions was randomized. Each experimental session started with baseline determination of motor performance followed by the type of stimulation of corresponding day, and motor practice. Post assessments were then done 30 minutes after the end of training (Fig. 1) [3].

Table 2. Experimental sessions

Session	Stimulation	Time(min)
S0	No stimulation	0
S1	tDCS	20
S2	Peripheral motor stimulation	60
S3	tDCS + Peripheral motor stimulation	60

Fig .1 Experimental design



Stimulation types

Transcranial direct current stimulation (tDCS)

tDCS was applied with the anode positioned over the ipsilesional M1 and the cathode over the contralateral supraorbital region for 20 minutes (2 mA). Anodal tDCS (Phoresor II Auto, Iomed, Inc., Salt Lake City, UT) was delivered through a 4×6 sponge electrode (Daeyang medical co., ltd, Korea) placed on the patient's scalp while sitting. The anode was placed on the C3 and C4 of the International ten-twenty electrode system and the cathode was placed over the contralateral supraorbital area.

Peripheral motor stimulation

In this study Patients received EMG-triggered NMES treatment on the EDC, with the Myomed 932(Enraf-Nonius, Netherlands) as one channel EMG and electrical stimulator. The acquisition of EMG signal and stimulation were performed using the same 4x3 surface electrode (Nicolet Biomedical, USA). At first, subjects were instructed to initiate wrist/finger extension so that a target threshold level of EMG activity was voluntarily achieved, which triggered the neuromuscular electrical stimulation to assist the muscles to reach a full range of motion. (2s ramp up, 5s asymmetrical biphasic current at 25 Hz, pulse width 200μs, 2s ramp down, 20-30 mA). The target threshold stimulation level was set on 75% of MVC(maximum voluntary contraction). The 20-second rest period was set between contractions to minimize local muscle fatigue [4].

Finger Evaluation Tool

The indexes of evaluating subjects' finger performance ability are score and the response time of the subjects as they respond to a certain target number on the screen. The evaluation system consists of two parts; (1) Sensing and Transmission, and (2) Reception and Processing. In Sensing and Transmission part, a microcontroller (ATmega128, Atmel, USA) and four membrane buttons, which is 40×15 mm each, were used to decide which finger responds to a target number. The decided number was then transmitted to personal computer (second part) using RS232 communication. We developed the software for 'Reception and Processing', named "Finger Evaluation Tool ver. 1.7" using C# language to display a target number and perform post processing such as score, response time, and so on. This software allows various conditions such as sequence of target numbers, total evaluation time, and impaired hand side. After evaluation, the stored data were exported to ASCII file.

Motor practice

Subjects were instructed to press each key on a special keyboard containing only 4 keys using the 2nd, 3rd, 4th, or 5th digit of the paretic hand. The following 4 finger sequences were used in random order across subjects for the 4 training sessions: 2 to 5 to 3 to 4 to 2, 4 to 3 to 5 to 2 to 4, 3 to 2 to 4 to 5 to 3, 5 to 2 to 4 to 3 to 5. Subjects were instructed to repeat the 5 elements sequence for a period of 3 minutes, which constituted 1 block. A computer was used to display the sequences to the patient and to record the time and accuracy of each key press. Subsequently, they practiced 4 blocks of 3 minutes each, separated by 2 minutes rest periods for a total of 18 minutes (Fig. 1).

Finger performance test

Motor performance was tested at baseline, after each form of stimulation (pre) and after motor

training (post) (Fig. 1). In each of these tests, patients performed 1 block of 3 minutes, similar to those implemented in the practice period. We defined the primary outcome measure as the mean time of key presses per 90 seconds. We excluded the initial 30 seconds during which patients often warmed up after each resting interval, and the last 60 seconds because some patients showed slowing and reported fatigue at that stage.

Results

At baseline, the mean time of key presses was comparable in the 4 sessions. All interventions resulted in comparable performance improvement at post assessment. The mean time of key presses increased significantly at Pre assessment (after electrical stimulation) of S1, but decreased significantly at following Post assessment (after finger motor training) (Fig. 2)

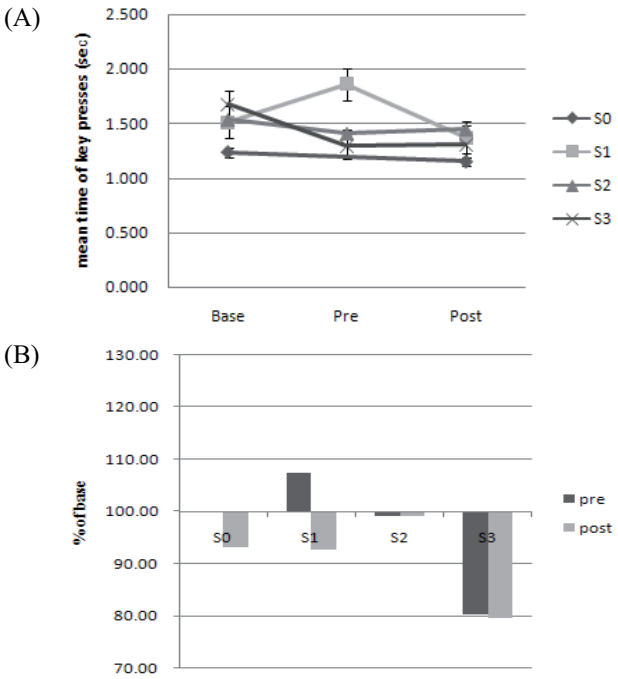


Fig. 2 Effects of different technique on finger performance. Mean time of key presses : (A), Percent of pre- and post- response time (% of base) : (B). Finger performance ability improved significantly in S3 compared to S0, S1 and S2.

The mean time of key press improved significantly in S3 compared to S0 (Wilcoxon test, $p = 0.028$), S1 (Wilcoxon test, $p = 0.046$) and S2 (Wilcoxon test, $p = 0.046$).

Discussion

Our results show that anodal tDCS of affected hemisphere results in decreased paretic finger performance. These effects are probably located intracortically; the excitability of the cortico-spinal tract remains unchanged [5]. Also, recent studies have revealed the importance of homeostatic plasticity, that the existence of a homeostatic mechanism in the human motor cortex stabilizes corticospinal excitability. Therefore, we need peripheral strategy such as robotic assist therapy and EMG-triggered NMES that would influence neuroplasticity. EMG-triggered NMES is more practical than robotic assist therapy because it is smaller, less expensive and easier to use. It also proves advantageous for various degrees of motor impairments in that it can be used in home settings by the patients due to its convenience.

Conclusions

These findings indicate that combining peripheral motor stimulation with anodal brain polarization before physical practice could represent a better adjuvant than application of each intervention alone in neurorehabilitation. These results suggest that this interventional strategy in combination with customary rehabilitative treatments may play an adjuvant role in neurorehabilitation.

References

[1] Schlaug G, Renga V, Nair, D. Transcranial direct current stimulation in stroke recovery. Arch Neurol, 65: 1571-6, 2008.

[2] Hesse S, Werner C, Schonhardt E. M, Bardeleben A, el al. Combined transcranial direct current stimulation and robot-assisted arm training in subacute stroke patients: a pilot study. Restor Neurol Neurosci, 25:9-15, 2007.

[3] Celnik P, Paik NJ, Vandermeeren Y, et al. Effects of combined peripheral nerve stimulation and brain polarization on performance of a motor sequence task after chronic stroke. Stroke, 40 : 1764-71, 2009.

[4] Shin HK, Cho SH, Jeon HS, et al. Cortical effect and functional recovery by the electromyography-triggered neuromuscular stimulation in chronic stroke patients. Neurosci Lett, 442 : 174-9, 2008.

[5] Nitsche MA, Seeber. A, Frommann K, et al. Modulating parameters of excitability during and after transcranial direct current stimulation of the human motor cortex. J Physiol, 568 : 291-303, 2005.

Acknowledgments

This research was financially supported by the Ministry of Education, Science Technology (MEST) and Korea Industrial Technology Foundation (KOTEF) through the Human Resource Training Project for Regional Innovation

Author's Address

ARa Ko
Department of Rehabilitation, Yonsei University Wonju College of Medicine, Wonju, Republic of Korea
goara@yonsei.ac.kr

Neuroprosthesis for finger rehabilitation and independent user application: Testing with one patient

Oskarsdottir A[1], Sigthorsson H[1], Svanbjornsdottir D[1], Helgason T[12]

[1] Reykjavik University, Reykjavik, Iceland

[2] Landspitali University Hospital, Reykjavik, Iceland

Abstract

In this work a prototype of a neuroprosthesis is developed in order to enable spinal cord injured (SCI) people, with injury at cervical vertebrae level, to increase finger mobility and activity with the use of functional electrical stimulation (FES). The new neuroprosthesis is developed with the main objective to make the patient's application of the device independent of any external help. He has to be able to put the neuroprosthesis on himself, control the equipment and take it off at the end of session. The neuroprosthesis has been used to stimulate atrophied muscles.

Results show that a patient with SCI at level C6-C7 is able to fulfill the following three steps. First, opening the prosthesis and fasten it on the right arm. Second, activating the stimulator connected to the prosthesis and deactivating it at the end of session and third, taking the prosthesis off. He can use the prosthesis independently and apply it for muscles exercise. Results also show increased movement in fingers and increase muscle strength after twelve month application of the neuroprosthesis.

***Keywords**: Neuroprosthesis, FES, SCI, Rehabilitation, Independency.*

Introduction

In this work a prototype of a neuroprosthesis is developed in order to enable spinal cord injured (SCI) people, with injury at cervical vertebrae level, to increase finger mobility and activity with the use of functional electrical stimulation (FES). FES is a method to activate paralyzed muscle with the purpose of generating or improving lost muscle control. For patients with SCI between levels C4-C8 FES can be used to improve grasp capabilities, by reducing the rate of muscle atrophy, and to strengthen muscles which might result in regain of some lost hand functions [1].

In the frame of this work research has been done on the application of electrode matrix to control electrode current through a forearm to elicit finger movements and to locate optimal stimulation sites for specific hand functions of SCI patient [2]. A map has been made of optimal electrode places for one patient and a list of feasible finger movements he can manage in his present condition of muscles and joints. Results indicate that even if some finger movements are possible, muscle force is small in magnitude and needs to be enhanced considerably for muscle movements to be usable in every day live.

The new arm neuroprosthesis is developed with the main objective to make the patient's application of the device independent of any external help. He has to be able to put the neuroprosthesis on himself, control the equipment and take it off at the end of session. Existing commercially available prosthesis presume that the user either is able to use the other hand and fingers for putting the prosthesis on or a helping person is at site. Optimal electrode placements [2] are used when choosing electrodes positions inside the new prosthesis. The prosthesis is developed for patients with SCI between levels C4-C8 but has up to now been used with one patient for training and testing.

Material and Methods

Subject

In development of the neuroprosthesis one patient participated in the testing. He is a male of age 48 and has been SCI at level C6-C7 for seven years, since 2003. He has voluntary shoulder and elbow control as well as wrist extension and flexion. He has minimum voluntary finger movements, is not able to grasp and release everyday objects, but can manage to hook for example a cup on his thumb and use his stiffened fingers to some extent. This is done without activating the finger muscles. Finger extensors for ring and little finger (digit 4 and 5) on the right arm were considered denervated but they seem to be reinnervated at least partly by the time of this work. They can therefore be stimulated with shorter pulses than 1 ms. The patient has not undergone a tendon transfer or other surgical

procedures that might be an alternative to gain finger function.

Neuroprosthesis prototype

The neuroprosthesis prototype is made out of soft cast. It consists of three parts, one covers finger extension, another covers finger flexion and thumb flexion, and the third part covers thumb extension. A Velcro used to close the neuroprosthesis around the user's arm, see fig. 1 and 2. At the end of every Velcro is a loop which the user hooks on his contra lateral thumb to fasten or release the prosthesis on his arm. By putting the prosthesis on the user lays his arm on the flexor part of the prosthesis and then turns over the other parts with his free hand. The prosthesis is tight and well fixed on the arm which gives the user a secure feeling. Electrodes are positioned inside prosthesis at specific location found in former research work [2]. Every location is related to a specific muscle group. Stimulation at these locations increase the muscle mass and elicit the following movements: finger flexion, finger extension, thumb flexion and thumb extension. Attached to the neuroprosthesis is a control unit which determines the current distribution. The control unit has four switches, each to activate one specific finger movement. The prosthesis is connected to a stimulator, Actigrip CS®[1], which can be controlled by the user. Stimulation parameters were pre fixed and programmed into the stimulator. Frequency was set to 25 Hz, pulse duration 250 µs and the pulse is asymmetric charge compensated. The pulse intensity was mostly between 10-40 mA. Stimulation took place 4x a week on the average on the right arm.



Fig. 1: The figure shows the neuroprosthesis prototype on the users arm. The three parts and the gap between them can be readily seen. Also the Velcro´s with rubber loops are evident.

Testing

The neuroprosthesis was tested with one subject mentioned above. The test consisted of three steps done daily during exercise period. First, opening the prosthesis and fasten it on the right arm. Second, activating the stimulator connected to the prosthesis, testing the movements and deactivating it at the end of session and third, taking the prosthesis off and putting it into a carrying case. This was done in the patient's home and at his holiday location for extended time periods (40 and 4 weeks respectively).

The neuroprosthesis has been used to stimulate atrophied muscles. Finger movement range and force is monitored and changes in muscle volume and density are measured with the aid of spiral CT.

Results

The results are given in the following three points:

1. Given a firm underground for the prosthesis, a table or similar, the patient is able to open the prosthesis with his passive fingers and using shoulder, elbow and wrist movements. He uses both hands. The stimulated hand is used to fix the position of the prosthesis and the contra lateral hand to open the prosthesis. See fig 2. The result of the test is that these movements and closing the prosthesis with the contra lateral thumb, as described earlier, are done fast and securely without any hesitation each time.

2. The most difficult step for the patient was to connect the prosthesis cable (one connector) with our experimental stimulator (Actigrip). This includes pushing the connector and holding the stimulator at the same time. The result is the same when pulling. Pushing the buttons on the device was on the other hand an easy task done with the lateral side of a passive digit five.

3. Taking the prosthesis of the arm the above movements are done in reversed order. Herby the movements are considerably slowed down when self adhering electrodes are used. After one hour training session they stick firmly on the skin and go off slowly as the upper part of the prosthesis is pulled off. The same happens when the hand is taken out of the flexion part of the prosthesis. That movement takes some time and has to be done with care not to hurt the skin.

The results are in summary that a patient with SCI at level C6-C7 is able to fulfill the following three steps. First, opening the prosthesis and fasten it on the right arm. Second, activating the stimulator connected to the prosthesis and deactivating it at the end of session and third, taking the prosthesis off. He can use the prosthesis independently and apply it for muscles exercise.

[1] Actigrip CS®, Neurodan A/S, Aalborg, DK.

A significant increased finger movement and muscle force are detected after twelve month application of the neuroprosthesis. Measurements with CT-scans indicate muscle density increase but volume has not yet been evaluated.



Fig. 2: The left image shows the user putting the neuroprosthesis on his right arm. The right image shows the user adjusting the Velcro to close the prosthesis around the arm.

Discussion

It is a huge increase of independence and hence life quality when people with SCI at cervical level can use their arms and fingers to do everyday work. People with this type of injury can voluntary move their shoulder and elbow joints and many attempts have been made to activate fingers and even wrist with technical aids. The sophisticated system Free Hand System developed in Cleveland Ohio was implanted in more than two hundred patients' worldwide in the late nineties[3]. Its approach was to have the stimulating electrodes and a part of the system implanted. On one side this means a relatively extensive operation with all risks of such an invasion and complicated stimulating system. On the other side the gain were manly two movements, a finger grip and a grasp [1,3]. It is a great advantage if the same degree of independency for the patient and the same movements can be reached without invasive means and with much simpler technique. This is the goal of the work described here. Up to now a prototype of an arm neuroprosthesis with integrated electrodes has been developed. It can be used independently by the SCI patient for muscle training. He does not need the help of other people when applying the equipment. The search for the right stimulation site for the electrodes has been simplified by using electrode matrixes instead of single electrodes [2]. It also enables a more complex current paths through the arm and hence the activation of the intended muscles. But the movements, a finger grip and a hand grasp have yet not been reached. In order to reach this at least a control electronic for the stimulating current through the electrode matrix has still to be realized and the muscles have to be trained further.

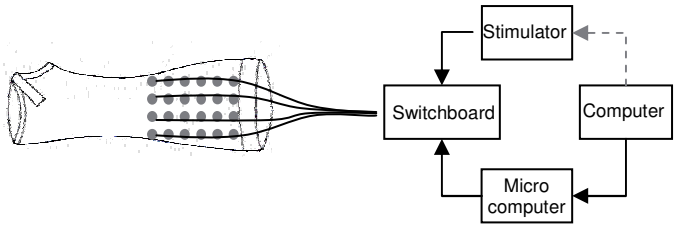


Fig. 3: The image shows the neuroprosthesis system. A prototype of an arm neuroprosthesis has been developed and a switchboard. The micro computer based stimulus control unit is in process and system software .

Conclusions

Results indicate that muscle exercise using FES and the use of the neuroprosthesis, for the independence of a SCI person, is an eligible chose to enhance lost finger movement. If this is confirmed by further work it will be feasible to use arm neuroprosthesis for the rehabilitation of finger movements.

References

[1] O'Dwyer SB, O'Keeffe DT, Coote S, Lyons GM. An electrode configuration technique using electrode matrix arrangement for FES-based upper arm rehabilitation systems. Medical Engineering & Physics, 28:166-176, 2006.

[2] Oskarsdottir A, Helgason T. Application of electrode matrix to locate stimulation sites for hand functions of SCI patients. World Congress on Medical Physics and Biomedical Engineering, 25/9: 377-380, 2009.

[3] Ragnarsson KT. Functional electrical stimulation after spinal corf injury: current use, therapeutic effects and future directions. Spinal Cord, 46:255-274, 2008.

Acknowledgements

The project is done in collaboration of Department for Biomedical Engineering Reykjavik University, Rehabilitation Centre of Landspitali University Hospital and Department for Research and Development of Landspitali University Hospital. The projects are funded by Reykjavik University, Landspitali – University Hospital, The Icelandic Centre for Research (RANNIS) and The Icelandic Student Innovation Fund. The authors thank them for their support.

Author's Address

Name: Arna Óskarsdóttir.
Affiliation: Reykjavik University
eMail: arnao05@ru.is
homepage: ru.is

Repetitive Exercises using Electrical Stimulation and a Robot Arm for Upper Extremities: a pilot study

Chida S[1], Matsunaga T[1], Sato M[1], Hatakeyama K[1], Tomite T[2], Sasaki K [2], Yoshikawa T [2], Kudo D [2], Iwami T[3], Kosaka T[3], Shimada Y[2]

[1] Department of Rehabilitation Medicine, Akita University Hospital, Akita, Japan

[2] Department of Orthopedic Surgery, Akita University Graduate School of Medicine, Akita, Japan

[3] Faculty of Engineering and Resource Science, Akita University, Akita, Japan

Abstract

We verified the feasibility of repetitive motions of the robot arm by muscle contractions of normal upper extremities using electrical stimulation. The subjects were 5 normal males. They tried to push and return the robot arm in a repetitive manner using muscle contraction only by the electrical stimulation without voluntary efforts. The repetitive movements included a pattern to alternately stimulate the anterior and posterior fibers of the deltoid, and a pattern to stimulate only one side, such as the anterior fibers of the deltoid for the pushing movement while using gravity and inertia for the returning movement. We examined the anteroposterior travel distance of the robot arm and the force this applied to the robot arm. All subjects were able to carry out 2 types of repetitive motions. The average anteroposterior travel distances showed no significant difference. The average anteroposterior force also showed no statistical significant difference, and allowed the one-sided stimulation to move in the same way as the alternate stimulation. In this verification, there is a big possibility to allow various exercises of motions for the treatment of hemiplegic upper extremity by combining electrical stimulations and robot technology.

Keywords*: repetitive exercise, electrical stimulation, robot arm*

Introduction

Recently, there have been many reports on effectiveness of the intensive therapeutic method for cerebral stroke hemiplegic upper extremity [1-10]. However, the methods were intended for the treatment of a comparatively mild paralysis [1-5]. The exercises using robot technology can treat patients with severe paralysis, but they were limited to the passive training [6, 7, 10]. There is a possibility that repetitive motion exercises consisting of the electrical stimulation and the robot technology creates new therapeutic methods for hemiplegic upper extremity which is poor in voluntary movement. This approach will have the advantage of the best recovery, compared to traditional exercises. The purpose of this study is to verify the feasibility of repetitive motions of the robot arm by muscle contractions of normal upper extremities using electrical stimulation, and to examine its applicability to hemiplegic upper extremities.

Methods

Subjects

The study included 5 normal male subjects who were informed of the purpose and method, and who had agreed to the experiment. Their average age was 22 years (range, 22 - 23).

Repetitive Exercise

As an electrical stimulator, we used Pulse-Cure-Pro (KR-7, OG Giken Co. Ltd.). The stimulus wave was a negative rectangular wave, with 300 μsec of pulse width and 50 Hz of stimulus frequency, and the range of stimulus intensity was to the extent that it gave enough muscle contraction to move the robot arm, but no pain to the muscle. We used a surface electrode with a length of 6 cm and positioned it to simulate the anterior fibers and the posterior fibers of the deltoid. The robot arm was a general purpose arm (PA-10A-ARM, Mitsubishi Heavy Industries, Ltd.) (Fig. 1). We mounted a 6-axis force/torque sensor (IFS-67M25A15-14, NITTA Corp.) at the base of the terminal device of the robot arm to allow the impedance control and the measurement of the force applied to the robot arm.

The subjects sat upright on a chair with the shoulder joint at a basic position and the elbow joint flexed at a 90 degree angle with their hands fixed to the robot arm, as a starting position. The repetitive motion specified in this research was to push the robot arm from the starting position, and then return to this same position; by the subject using muscle contraction only brought about by electrical stimulation without voluntary efforts.

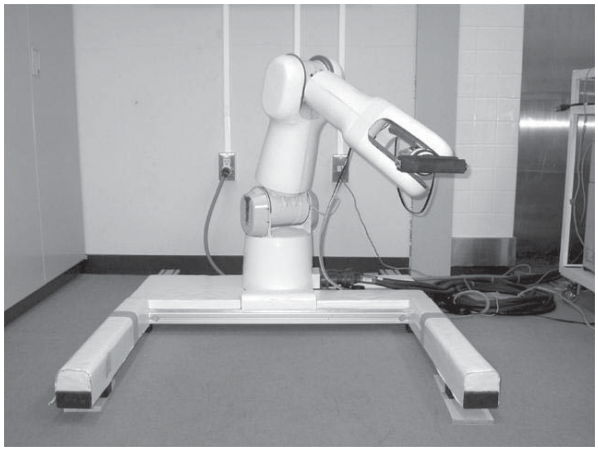


Fig. 1: PA-10A-ARM, a 7-Axis general purpose Robot Arm (Mitsubishi Heavy Industries Ltd.).

Measurement

In the experiment, we preset the movement of the robot, so that it moves parallel to the floor, back and forth, and limited it within the mechanical resistance, which does not bother the subject's movement. The repetitive movements included a pattern to alternately stimulate the anterior fibers and the posterior fibers of the deltoid every 5 seconds. Then the pattern was changed to stimulate only the anterior fibers of the deltoid for the pushing movement, while using gravity and inertia for the returning movement. We examined the feasibility of two repetitive motions with only electrical stimulation, and anteroposterior distance travelled by the robot arm and anteroposterior force applied to the robot arm.

Results

Five subjects were able to carry out 2 types of repetitive motions. The stimulate force applied to both the anterior fibers and the posterior fibers of the deltoid were in the range of 32V to 44V, which did not cause any pain (Fig. 2, 3). The average anteroposterior distances travelled by the robot arm

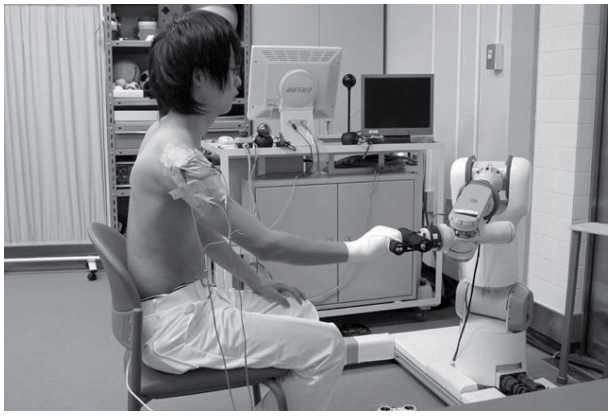


Fig. 2: A repetitive motions of the robot arm by muscle contractions using electrical stimulation.

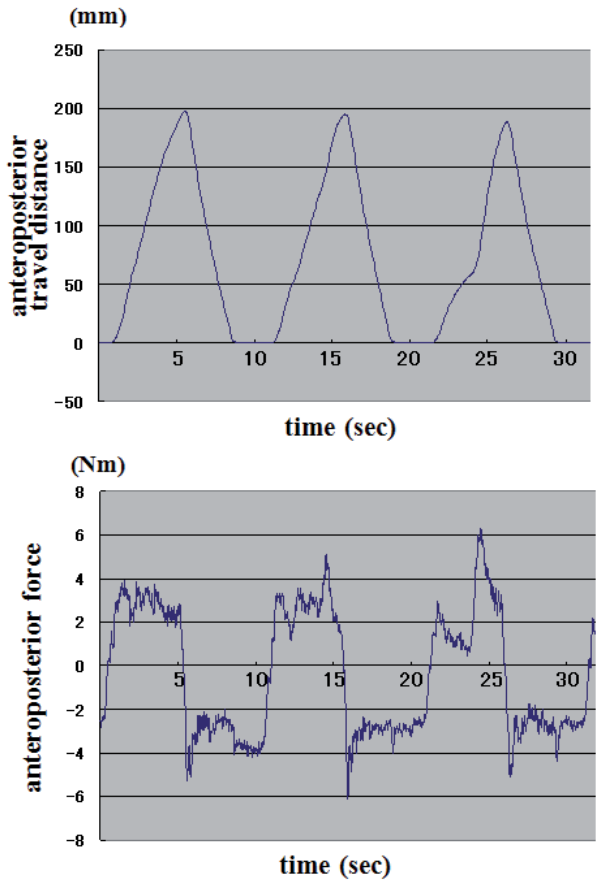


Fig. 3: An example of the anteroposterior travel distance and the force (+ anterior, - posterior) applied to the robot arm in the alternate stimulation.

were 231 mm in the alternate stimulation, and 201 mm in the one-sided stimulation, showing no significant difference. The average anteroposterior force applied to the robot arm showed 2.9Nm for the forward direction and 1.7Nm for the backward direction using the alternate stimulation, and 2.6 Nm for the forward direction and 1.0 Nm for the backward direction using the one-sided stimulation. It also showed no statistical significant difference, and allowed the one-sided stimulation to move in the same way as the alternate stimulation.

Discussion

Conventional therapeutic methods for the patients with severe hemiplegic upper extremities have been limited to passive exercises. It is important for the patients to accumulate the physical experiences by using their own muscle contraction, through electrical stimulation, for the best recovery. Also, we are able to set the range and direction of exercise, and assistance and resistance with the robot arm, according to the needs of the individual patient. Even if the patients have no voluntary movement or a weak reaction to the electrical stimulation, the full support of the hemiplegic upper extremities against gravity by the robot arm

could make the exercise feasible [7, 9, 10]. There is large opportunity to allow various exercises for the treatment of the patients' upper extremities by combining electrical stimulation and robot technology. It was confirmed that muscle contraction by the electric stimulation allowed repetitive motions to move the robot arm, and was assumed applicable for hemiplegic upper extremities. However, there is a limitation in terms of the results were obtained from young healthy subjects and cannot be generalized to a disabled, elderly population and especially in patients with severe paralysis for a prolonged period.

Consequently, we are required to examine which muscle to stimulate, the optimal stimulation method, and direction and volume of exercise through simulation. Brain-machine interface is ideal as a trigger of electrical stimulation, but for the time being, we need a switch operation or a system to connect the exercise of the paralyzed limb by detecting the movement of the non-paralyzed limb.

Conclusion

The combination of electrical stimulations with a robot would allow the patients to have diverse physical exercises for treatment of hemiplegic upper extremities.

References

[1] Taub E, Uswatte G. A new approach to treatment and measurement in physical rehabilitation: constraint-induced (CI) movement therapy. In: Frank R, Elliott T, eds. Handbook of Rehabilitation Psychology. Washington, DC: American Psychological Association; 2000.

[2] Dromerick AW, Edwards DF, Hahn M. Does the Application of Constraint-Induced Movement Therapy During Acute Rehabilitation Reduce Arm Impairment After Ischemic Stroke? Stroke, 31: 2984-2988, 2000.

[3] Page SJ, Levine P, Back From the Brink: Electromyography-Triggered Stimulation Combined With Modified Constraint-Induced Movement Therapy in Chronic Stroke. Arch Phys Med Rehabil, 87: 27-31, 2006

[4] Knutson JS, Harley MY, Hisel TZ, et al. Improving Hand Function in Stroke Survivors: A Pilot Study of Contralaterally Controlled Functional Electric Stimulation in Chronic Hemiplegia. Arch Phys Med Rehabil, 88: 513-520, 2007.

[5] Broeren J, Rydmark M, Sunnerhagen KS. Virtual Reality and Haptics as a Training Device for Movement Rehabilitation After Stroke: A Single-Case Study. Arch Phys Med Rehabil, 85: 1247-1250, 2004.

[6] Hesse S, MD, Schulte-Tigges G, Konrad M, et al. Robot-Assisted Arm Trainer for the Passive and Active Practice of Bilateral Forearm and Wrist Movements in Hemiparetic Subjects. Arch Phys Med Rehabil, 84: 915-920, 2003.

[7] Susan EF, Hermano IK, Joel S, et al. Robotic Therapy for Chronic Motor Impairments After Stroke: Follow-Up Results. Arch Phys Med Rehabil, 85: 1106-1111, 2004.

[8] Prange GB, Jannink MJ, Groothuis-Oudshoorn CG, et al. Systematic review of the effect of robot-aided therapy on recovery of the hemiplegic arm after stroke. J Rehabil Res Dev, 43: 171-184, 2006.

[9] Brewer BR, McDowell SK, Worthen-Chaudhari LC. Poststroke upper extremity rehabilitation: A review of robotic system and clinical results. Top Stroke Rehabil, 14: 22-44, 2007.

[10] Masiero S, Celia A, Rosati G, et al. Robotic-Assisted Rehabilitation of the Upper Limb After Acute Stroke. Arch Phys Med Rehabil, 88: 142-149, 2007.

Author's Address

Satoaki chida

Department of Rehabilitation Medicine, Akita University Hospital
satoaki@hos.akita-u.ac.jp

FES-ASSISTED CYCLING TRAINING CAN IMPROVE CYCLING PERFORMANCE, CARDIORESPIRATORY FITNESS, STRENGTH, GAIT AND FUNCTIONAL ACTIVITY FOLLOWING AN 8-WEEK, HOME-BASED TRAINING PROGRAM – A CASE REPORT

Lee SCK[1,2,3], Harrington AT[2], McRae CGA[3], Kachmar AN[1]

[1]Physical Therapy Department, University of Delaware, Newark, DE, USA, 19716
[2]Interdisciplinary Program in Biomechanics and Movement Science, University of Delaware, Newark, DE, USA, 19716
[3]Research Department, Shriners Hospitals for Children, Philadelphia, PA, USA, 19140

Abstract

Individuals with spastic cerebral palsy (CP) are often unable to participate in traditional forms of exercise because of impairments such as muscle weakness, abnormal muscle tone and poor motor control. The purpose of this case study was to determine the efficacy of using a home based, closed-loop controlled, functional electrical stimulation (FES)-assisted recumbent cycling system to exercise train an adolescent with CP.

An 18-year old male with spastic diplegic CP (GMFC System Level II) having no previous cycling experience completed 8-weeks of FES-assisted cycling training, 3 times per week, for 30 minutes of cycling per session. Computerized closed-loop control modulated the stimulation intensity to assist the individual maintain exercise power targets. Outcomes included cycling and cardiovascular performance measures lower extremity strength, gait, and activity measures.

Following training, the subject demonstrated improved cycling performance and improvements in cardiorespiratory measures (peak VO_2 and O_2 pulse). Strength improved in all muscle groups tested. Walking velocity increased and the week averaged number of steps taken per day increased.

This case demonstrates that FES-assisted cycling technology can be successfully applied in a home-based setting to produce improvements in cycling performance, cardiorespiratory fitness, strength, gait and functional activity.

***Keywords**: cerebral palsy, FES, recumbent cycling, exercise, strength, fitness*

Introduction

Cerebral Palsy (CP) is a non-progressive disorder caused by a lesion of the fetal or infant brain that results in muscle weakness, spasticity and other motor impairments. These impairments often lead to decreased independence and a lack of physical activity in children with CP. Furthermore, individuals with CP tend to peak in their functional ambulatory ability prior to adolescence and then decline into adulthood. One major cause of decline in function is the disparity that occurs when muscle strength gains are not commensurate to gains in body size or weight. Finally, weakness is often exacerbated by the surgical procedures and other procedures such as serial casting and Botulinum toxin injections used to correct adverse orthopedic adaptations or to mitigate abnormal muscle tone. Thus, as children with CP mature, they have marked difficulties in maintaining fitness and functional ability.

Many children with CP also have difficulties in exercising at intensities necessary to achieve cardiorepiratory and musculoskeletal training effects. Thus, additional means may be necessary to improve exercise output. The use of functional electrical stimulation (FES) during cycling to elicit appropriately timed muscle contractions has been successful in improving fitness, bone mineral density, and muscle mass in individuals with paralyzed muscle due to spinal cord injuries (SCI) [1]. This project uses FES-assisted cycling for an individual with CP to improve cardiorespiratory fitness and muscle strength.

The purpose of this case study was to determine the efficacy of using a home based, closed-loop controlled, FES-assisted recumbent cycling system to exercise train an adolescent with CP.

Methods

Participant:

An 18-year old male with spastic diplegic CP (GMFC System Level II) having no previous

cycling experience completed the FES-assisted training program.

FES Exercise Training:

The participant completed 8-weeks of FES-assisted cycling training, 3 times per week, for 30 minutes of cycling per session. During training sessions, FES was applied to the bilateral quadriceps muscles at the appropriate angles to assist crank rotation. Computerized closed-loop control modulated the stimulation intensity to assist the individual maintain exercise power targets [2]. The stimulation intensity ramped up if the individual required FES-assistance to achieve the prescribed power output and conversely, maintained and declined when the target output was sustained. A simple video game provided feedback of cycling performance.

FES Exercise Testing:

Baseline, mid-, and post-training data were collected. Outcomes included cycling and cardiovascular performance measures during constant and graded (incremental) load volitional metabolic cycling tests and lower extremity strength (maximum volitional isometric contractions-MVICs), gait, and activity measures.

Results

Following 8-weeks of FES-assisted cycling, the subject demonstrated improved cycling performance. Mean and peak power output increased by 21% and 17.5%, respectively. Cardiorespiratory measures of peak VO_2 and O_2 pulse increased by 10.5% and 14.8%, respectively. Strength improved in all muscle groups tested with an average 26%, 11.5%, 7.7%, 16.5%, and 20.2% increase in MVIC for the hip extensors, hip flexors, quadriceps, hamstrings and plantarflexors, respectively. Walking velocity increased by 16.8% with respective step length and single support increases of 7% and 4%. The week averaged number of steps taken per day increased by 45% (from 8917 to 12964) following the training intervention.

Discussion

Because of volitional contributions or resistance to movement, FES-assisted exercise is fundamentally different than that used for individuals with complete paralysis in which FES controls all muscle activity and movement. This case demonstrates that FES-assisted cycling technology can be successfully applied in a home-based setting to produce improvements in cycling performance, cardiorespiratory fitness, strength, gait and functional activity.

Conclusions

We have demonstrated the feasibility FES-exercise to enhance function in an adolescent with motor impairments, in particular with CP. Future work will include larger studies and those that examine the effects of FES-assisted cycling vs. volitional effort only**.**

References

[1] Johnston TE, Smith BT, Oladeji O, Betz RR, Lauer RT. J Spinal Cord Med 2008; 31(2):215-21.

[2] McRae CGA, Johnston TE, Lauer RT, Tokay AM, Lee SCK, Hunt KJ. Cycling for Children with Neuromuscular Impairments Using Electrical Stimulation - Development of Tricycle Based Systems, Med.Eng. Phys. 2009, 31(6), 650-9

Acknowledgements

Shriners Hospital for Children Grant #9159 to S.C.K. Lee; Foundation for Physical Therapy PODS II grant to A. Tokay Harrington

Author's Address

Samuel C.K. Lee, PhD, PT
301 McKinly Laboratory
Department of Physical Therapy
University of Delaware
USA, Newark, DE 19716
slee@udel.edu

Bi-Moment Chair for the Measurement of Joint Moments

de Jager K[1], Donaldson NdeN[1], Newham DJ[1]

[1] University College London, London, UK

[2] Kings College London, London, UK

Abstract

FES cycling for paraplegics is known to have low efficiency and power output. The reason for this is not currently understood, but is believed to partly be biomechanical in nature. It may be possible to improve the biomechanics by selectively stimulating the muscles in the quadriceps so that maximum knee extension can be achieved, with minimum hip flexion. To this end a bi-moment chair was developed to simultaneously measure knee and hip joint moments associated with various electrode positions. However, the results obtained were not as expected. This lead to an error analysis of the chair in which random and systematic errors were identified, and their influence on the resultant joint moments measured. Alternative causes for the unexpected results can now be considered, as the possibility of measurement error has been eliminated.

Keywords: *FES cycling, SCI, bi-moment chair, joint moments, knee extension, hip flexion, error analysis.*

Introduction

FES cycling for Spinal Cord Injured (SCI) people has been studied for many years [1, 2]. However, the power output and metabolic efficiency of SCI cyclists remains considerably lower than that of Able Bodied (AB) cyclists [3], even after a long period of muscle training [4]. Three hypotheses for the low efficiency have been suggested [3]:

1. Inefficiency due to electrical stimulation.
2. Inherent SCI factors, e.g. abnormal muscles.
3. Biomechanics of FES cycling.

The influence of the first two hypotheses on metabolic efficiency were investigated by performing electrical stimulation (ES) on AB subjects [3,5,6]. These studies showed that AB cyclists have poorer efficiency than normal during FES cycling but nonetheless high efficiencies were found for AB subjects during stimulated concentric contractions of quadriceps [3]. This would imply that the low FES cycling efficiency is somehow related to the motion of the cycling action and not purely attributable to ES. Currently all four component muscles of the quadriceps are stimulated. This causes activation of Rectus femoris, which produces an unwanted hip flexion when leg extension is required, which we hypothesise reduces the net power generated [1].

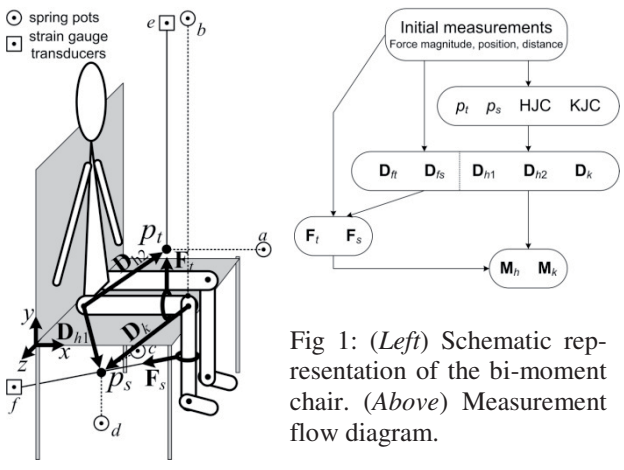


Fig 1: (*Left*) Schematic representation of the bi-moment chair. (*Above*) Measurement flow diagram.

By selectively stimulating the quadriceps, it is hoped to minimise the hip flexion while still maintaining maximum knee extension. The testing of this hypothesis required a means to measure moments about both the knee and hip joint simultaneously. To this end a *bi-moment chair* was developed, as shown in Fig. 1, whereby the joint moments of a seated subject could be measured with various electrode positions. Confidence in measurements taken with the chair was built by performing an error analysis and validation on the bi-moment chair.

Methods

Bi-moment chair design

The bi-moment chair has a number of position sensors (spring pots [7]), and force sensors (strain gauge transducers). The measurements taken by these sensors were used to calculate the joint moments, as laid out in the flow diagram of Fig. 1.

The positions of the Hip (HJC) and Knee (KJC) Joint Centres and the sensors were measured relative to a reference frame, positioned along the coordinate axis indicated in Fig. 1. The initial distance between the position sensors and the points in space they are used to track (points p_t, p_s and a point above the KJC), were recorded. The sensors could then monitor changes in the location of these

points, which were used to determine the orientation of the direction and force vectors. These locations were found by using the position sensor measurements to set up two and three-dimensional distance equations that were simultaneously solved [7, 8]. The force sensors were used to measure the magnitude of forces $\mathbf{F}_t$ and $\mathbf{F}_s$, which, combined with the direction vector measurements were used to calculate the moments about the knee and hip joints, as in equation 1.

$$\begin{aligned} \mathbf{M}_k &= -\mathbf{D}_k \times \mathbf{F}_s \\ \mathbf{M}_h &= -(\mathbf{D}_{h1} \times \mathbf{F}_s + \mathbf{D}_{h2} \times \mathbf{F}_t) \end{aligned} \quad (1)$$

Measurement errors can be separated into two main categories, random and systematic [9]. The influence, that both of these errors would have on the calculated moments, was investigated.

Error analysis

The random errors were quantified for the sensor measurements, as well as the initial position and distance measurements, by estimating the standard deviation, σ, from the spread of repeated measurements [9]:

1. For the position sensors, sp_1 through sp_4, changes in string length were recorded for measurements taken around an arbitrary point.
2. Calibration measurements were taken for the force sensors, using a series of consecutively heavier weights. The standard deviation seen in the corresponding voltage measurement was found after using least squares to fit a line to each repeated measurement.

A Codamotion system was used to monitor movement in the HJC and KJC, thereby estimating the uncertainty in their respective positions. The bi-moment chair makes the assumption that the HJC is stationary throughout an entire test, while movement of the KJC is monitored in the *x*- and *y*-directions, by sp_2. Any movement in the *z*-direction is considered negligible.

Validation

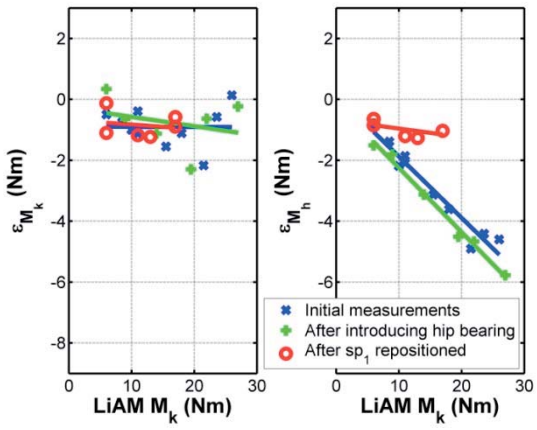
The random error analysis did not help to identify the presence of systematic errors. These errors were isolated using a spring-loaded dummy-leg, LiAM (Limb for the Application of Moments), to generate moments of known magnitude about pin joint models of the hip and knee joints. These results also served to validate the moments measured by the chair in the presence of the combined effect of all the random errors.

Results

Joint moment data was recorded with a subject in the chair to help understand measurement errors.

Table 1: Percentage error in $\mathbf{M}_h$ and $\mathbf{M}_k$ due to a measurement change of one standard deviation.

Error parameter		σ	% Error	
			$\mathbf{M}_h$	$\mathbf{M}_k$
sp_1 (Fig.1 label *a*)		0.28 [mm]	0.7	-
sp_2 (*b*)		0.51 [mm]	-	0.2
sp_3 (*c*)		0.53 [mm]	-	-
sp_4 (*d*)		1.4 [mm]	1.1	1
SG_t (*e*)		0.0037·mass-0.004 [V]	3.0	2.1
SG_s (*f*)		0.0011·mass + 0.0015 [V]	3.0	2.1
Distance measurements		2.2 [mm]	-	0.8
Position measurements	x	1.3 [mm]	3.5	-
	y	11 [mm]	8.5	7.7
	z	1.8 [mm]	-	-
HJC	x	3.5 [mm]	1.8	-
	y	2.4 [mm]	1.7	-
	z	1.6 [mm]	-	-
KJC	x	3.2 [mm]	-	-
	y	4.8 [mm]	-	1.6
	z	6.8 [mm]	-	-



(a) (b)

Fig 2: Difference measured in moments between the bi-moment chair and LiAM for (a) the knee moment and (b) the hip moment.

These measurements were modified by one standard deviation, the moments recalculated and the percentage difference in the joint moments, as compared with the original dataset, found. (Table)

These results indicate to which errors the joint moments were particularly sensitive and provided an estimation of the size of the error. Percentage errors, less than 0.2%, were considered negligible. From the table we can see that the moments are particularly sensitive to errors in the position measurements. Consequently, care should be taken when recording the initial positions. Furthermore, as we are only interested in knee moments that occur in the sagittal plane, any movement of the KJC in the *z*-direction, is seen to have no influence on $\mathbf{M}_k$ and can thus be considered negligible. KJC movements in the *y*-direction will be less than that estimated in the table, as sp_2 measures deflection

of the KJC along this axis, which the Codamotion results did not take into account.

Fig. 2 shows the difference between $\mathbf{M}_k$ and $\mathbf{M}_h$ measured by the chair, and those generated by LiAM. Good agreement was consistently seen in the $\mathbf{M}_k$ measurements. However, initially there was a large disagreement in the hip joint moments. The pin joint at the hip was replaced with a bearing to try to reduce the error. However, in so doing, the spread of the measurements was reduced, but not the overall error. A systematic error was found that was dependent on the position of sp_1. By moving this spring pot, to the location shown in Fig. 1, the sensitivity and error were drastically reduced.

Discussion

Once confidence had been gained in the measurements made by the bi-moment chair, it was used to perform a preliminary test using three different electrode positions:

1. Standard (current practice) - One pair of electrodes placed diagonally over the thigh and designed to stimulate all component muscles.
2. Rectus - One pair of electrodes placed on the midline of the anterior thigh.
3. Vastii (medialis and lateralis) - Two pairs of electrodes, attached to independent stimulation channels, placed over these muscles.

The results, as shown in Fig. 3, did not show the expected reduction in the hip flexion moment, when comparing the Vastii and Standard setups. The reason for this is currently unknown and being investigated. However, due to the extensive error analysis and validation already carried out, it was possible to rule out measurement error.

Conclusions

A bi-moment chair was developed that allowed us to measure joint moments about the hip and knee joints, simultaneously. This will be used in a study to investigate the selective stimulation of the quadriceps, with an aim to improving the performance of FES cycling. Before the chair could be used in such a study it was necessary to validate the measurements taken by the chair. This was accomplished by taking a series of measurements to ascertain the magnitude of the random errors present in the system, as well as by using the specially designed LiAM, to identify systematic errors and to evaluate the combined effect of all the random errors. Preliminary results have been measured with the chair, looking at the selective stimulation of quadriceps muscles. However, the unexpected results need further investigation as to whether there is a physiological explanation.

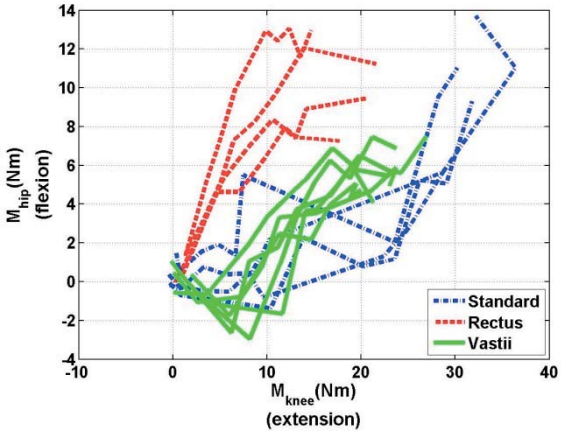


Fig 3: Joint moments measured for a subject using three different electrode positions.

References

[1] Szecsi J, Krause P, Krafczyk S, Brandt T and Straube A. *Functional ouput improvement in FES cycling by means of forced smooth pedalling.* Medicine & Science in Sports & Exercise, 39(5):764-780, 2007.

[2] Perkins TA, Donaldson NdeN, Fitzwater R, Phillips GF and Wood DE. *Leg powered paraplegic cycling system using surface functional electrical stimulation.* Proceedings of the 7th International Workshop on FES, (Vienna, Austria), 1:36-39, 2001.

[3] Duffell L, Donaldson NdeN, and Newham D. *Why is the metabolic efficiency of FES cycling low?* IEEE Neural Systems and Rehabilitation Engineering, 17(3):263-269, 2009.

[4] Duffell LD, Donaldson NdeN, Perkins TA, Rushton DN, Hunt KJ, Kakebeeke TH and Newham DJ. Long-term intensive electrically stimulated cycling by spinal cord-injured people: Effect on muscle properties and their relation to power output. Muscle & Nerve, 38(4):1304-1311, 2008.

[5] Hunt K, Saunders B, Perret C, Berry H, Allan D, Donaldson N and Kakebeeke T. *Energetics of paraplegic cycling: a new theoretical framework and efficiency characterisation for untrained subjects.* European Journal of Applied Physiology, 101:277-285, 2007.

[6] Kjær M, Perko G, Sechler NH, Boushel R, Beyer N, Pollack S, Horn A, Fernandes A, Mohr T, Lewis SF and Galbo H. *Cardiovascular and ventilatory responses to electrically induced cycling with complete epidural anaesthesia in humans.* Acta Physiologica Scandinavica, 151(2):199-207, 1994.

[7] Yu CH. New Method for Restoring Standing to Paraplegics: Control of Leg Muscle Stimulation by the Handle Support Reactions. PhD thesis, University College London, 1999.

[8] Hsiao H and Keyserling WM. *A three-dimensional ultrasonic system for posture measurement.* Ergonomics, 33:1089-1114, 1990.

[9] Taylor JR. An Introduction to Error Analysis: The Study of Uncertainties in Physical Measurements. University Science Books, U.S., 1982.

Author's Address

Kylie de Jager
Implanted Devices Group, University College London.
k.dejager@medphys.ucl.ac.uk
http://www.ucl.ac.uk/medphys/

Combined video game and neuromuscular stimulation based training

Sayenko DG[1], Milosevic M[1,2], Robinson MF[1], Masani K[1], McConville KMV[1,2,3], Popovic MR[1,3]

[1] Rehabilitation Engineering Laboratory, Toronto Rehabilitation Institute, Toronto, Canada

[2] Electrical and Computer Engineering, Ryerson University, Toronto, Canada

[3] Institute of Biomaterials and Biomedical Engineering, University of Toronto, Toronto, Canada

Abstract

A video game-based training system was designed to integrate neuromuscular electrical stimulation (NMES) and visual feedback as a means to improve strength and endurance of the lower leg muscles, and increase the range of motion (ROM) in the ankle joints. The system allowed the participants to perform isotonic concentric and isometric contractions in both plantarflexors and dorsiflexors using NMES. The contractions were performed against exterior resistance, and the angle of the ankle joints was used as the control input to the video game. To test the feasibility of the proposed system, an individual with chronic complete spinal cord injury (SCI), participated in the study. The system provided a progressive overload for the trained muscles. The results show that the training resulted in a significant improvement of the strength and endurance of the paralyzed lower leg muscles, and in an increased ROM of the ankle joints. The participant indicated that he enjoyed the video game-based training. Video game-based training programs might be effective in motivating participants to train more frequently and adhere to otherwise tedious training protocols. It is expected that such training will not only improve the properties of their muscles, but also decrease the severity and frequency of secondary complications that result from SCI.

Keywords: *active gaming, muscle atrophy, muscle training, neuromuscular electrical stimulation, spinal cord injury, visual feedback*

Introduction

Neuromuscular electrical stimulation (NMES) training can counteract musculoskeletal atrophy in individuals with spinal cord injury (SCI), and thus, decrease the likelihood of secondary complications and ultimately reduce costs associated with caregiving [1]. It has been demonstrated that training with isotonic contractions result in a smaller risk of bone fracture [2] and increased blood circulation [3, 4], in comparison with isometric contractions. Furthermore, it has been emphasized that the amount of stress delivered to paralyzed muscle tissue should meet a threshold consistent with overload and/or endurance training principles to make the training effective [5, 6].

We proposed a video game-based training system that is designed to integrate NMES and visual feedback therapy as a means to improve strength and endurance of the lower leg muscles, as well as the range of motion in the ankle joints. The purpose of the present study was to evaluate the concept of the new training system using the following criteria: (1) the NMES training protocol must include isotonic contractions against exterior resistance; (2) the system must include an entertaining component which should be tied to the exercise challenge and guide the user through the protocol; and (3) the system must be easy to control and operate and require minimal supervision of medical or technical staff.

Material and Methods

Dynamic ankle joint training device

During the training, the participant was seated on a padded bench with a backrest support (Fig. 1a). The foot platform was attached to the main shaft, which was inserted into the side bearings. The inverted pendulum was used to provide resistance during the training exercise. The range of angular displacements of the foot platform was mechanically restricted within the range of 30° plantarflexion and 20° dorsiflexion. The Reaction Torque Sensor (TS11-200, Durham Instruments, Germany) with a capacity of 200 Nm was mounted to the main shaft to measure the torque produced during the exercise. Tilt of the foot platform was registered by a differential capacitance Micro-Electro-Mechanical System 3-axial accelerometer (KXM52-1050, Kionix Inc., USA). Signals were sampled using a 12-bit resolution data acquisition system (USB-6008, National Instruments, USA). Real-time data acquisition, processing, visualization, and storage were performed using the LabVIEW 8.5 software package (National Instruments, USA). The calculated tilt was used as the real-time input to control the video game.

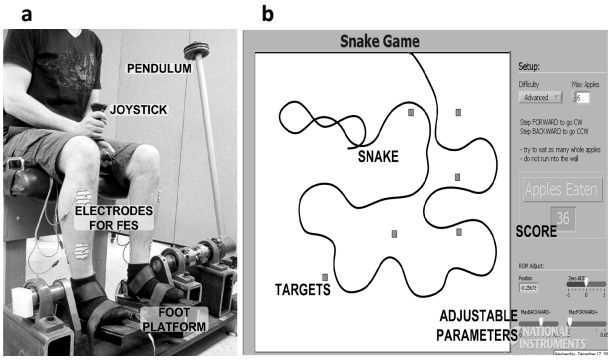


Figure 1. (a) Foot platform with the inverted pendulum locked in place on the end of the main shaft; (b) Interface of game-based exercise.

Neuromuscular electrical stimulation

A programmable 4-channel neuromuscular electrical stimulator (Compex Motion, Compex SA, Switzerland) was used to deliver transcutaneous NMES to the ankle joint muscles. The stimulation current had a rectangular, biphasic, monopolar pulse waveform with a pulse duration of 300 μs, and the stimulation was delivered with a frequency of 40 Hz [7]. The stimulation intensity was controlled by the participant in response to the video game scenario using an analog joystick controller. A forward inclination of the joystick, which was connected to the electrical stimulator through an analog input port, resulted in stimulation of plantarflexors (PF), whereas a backward inclination resulted in stimulation of dorsiflexors (DF).

Game-based exercise

The goal of the game was to navigate a moving "snake" around the screen in an attempt to hit randomly appearing targets (Fig. 1b). The turning radius of the "snake" was controlled by the position of the ankle joints detected by the tilt sensor. With the joints in neutral position, the "snake" moved in a straight line; in order to produce clockwise or counterclockwise turns of the "snake", the participant had to elicit plantarflexions or dorsiflexions, respectively. Visual feedback was provided by a large LCD monitor placed at eye level about 1.5 meters in front of the participant. To motivate the participant to improve his performance, a score representing the number of collected targets was displayed. With an increased number of collected targets the "snake" increased its length.

Outcome measurements

The following parameters were recorded during the 1st, 25th, and 48th training sessions: (a) the NMES intensity, (b) the overall torque, and (c) the angular displacement of the foot platform (corresponding to ankle joint position).

Participant

The male participant was 57 years old and has sustained chronic SCI (T3-T4) four years prior to taking part in this study. The participant's lesion completeness was classified as AIS A (i.e., American Spinal Injury Association Impairment Scale classification A). His personal treatment goals were to prevent secondary complications associated with impaired blood circulation and bone demineralization, and to improve his muscle mass. The participant gave written informed consent to the experimental procedure, which was approved by the local institutional ethics committee in accordance with the declaration of Helsinki on the use of human subjects in experiments.

Data processing and analysis

To analyze the data, we divided the acquired data into intervals of 3 min each. A two-way ANOVA with repeated measures ($\alpha = 0.05$) along with a subsequent Tukey post-hoc test was applied to identify significant differences in recorded parameters throughout each training session and in comparison with the 1st training session. Results of the pooled data are presented as mean values and standard deviations (SD).

Outcome measurements

The following parameters were recorded during the 1st, 25th, and 48th training sessions: (a) the NMES intensity, (b) the overall torque representing resultant torque exerted by the stimulated muscles and passive torque produced by the training device, and (c) the angular displacement of the foot platform (corresponding to ankle joint position). All data were sampled at 500 Hz. The signals were low-pass filtered using a fourth-order, zero phase-lag Butterworth filter with the cut-off frequency of 5 Hz.

Results

During the game-based exercise, the weight on the pendulum that the participant controlled via NMES was 3 kg. Fig. 2 depicts the change of the intensity (Fig. 2a) of NMES for each muscle group, the peak torque (Fig. 2b), and the angular displacement of the foot platform (Fig. 2c) over time during 1st, 25th, and 48th training sessions.

The participant reported that he enjoyed the video game-based training. He stated that the video game was challenging to play, but could be easily adjusted to meet the needs of the participant.

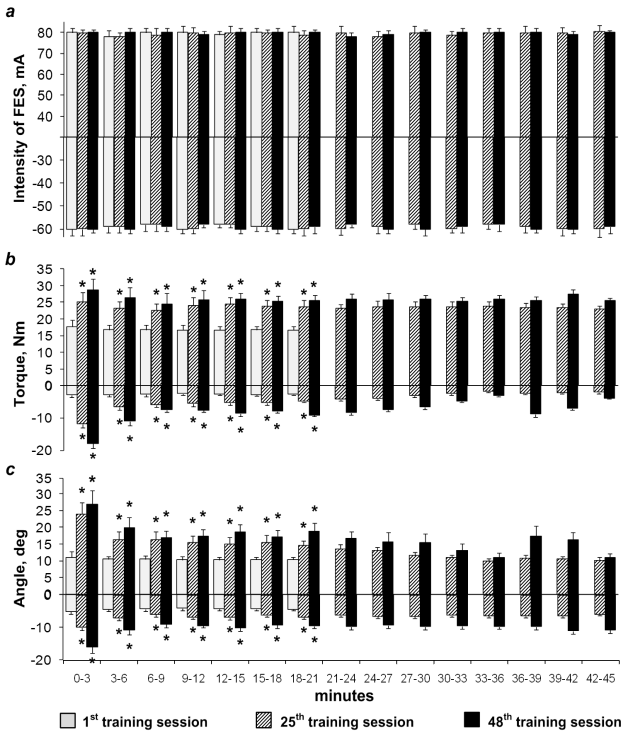


Figure 2. Pooled data showing the parameters recorded during the training session: (a) intensity of NMES cycles for each muscle group, (b) torque, and (c) angular displacement of the foot platform over time during 1st, 25th, and 48th training sessions. Positive values represent parameters during plantarflexion; negative values represent parameters during dorsiflexion.

Discussion

We developed a new training system that integrates NMES and visual feedback. We demonstrated that the protocol used in this study yielded significant training effects on the strength and endurance of the paralyzed lower leg muscles, and improved the ROM in the ankle joints. Additionally, the duration of the training sessions significantly increased indicating the improvement in the endurance. Though the current training protocol's settings stayed unchanged throughout the training period, the exercise challenge provided an overload for the muscles during the training. The key observation resulting from this study was that the interactive gaming NMES intervention can motivate a person with chronic SCI to perform muscle training exercises. Characteristics of the system would allow individuals with even less preserved motor function to participate in this training program. The system setup and applied protocol required minimal supervision from a medical or research staff: once the game parameters, range of motion, and the level of resistance were set, the participant was able to perform the training without any further assistance.

Conclusions

The proposed video game-based training that integrates NMES and visual feedback successfully motivated the participant, and resulted in significant training effects on the strength and endurance of the paralyzed lower leg muscles, and improved the range of motion in the ankle joints. The system provided a progressive overload for the trained muscles, which is a prerequisite for successful muscle training. Video game-based training programs must be effective in motivating participants to train more frequently and adhere to otherwise tedious training protocols. It is expected that such training will not only improve the properties of their muscles, but also decrease the severity and frequency of secondary complications that result from SCI.

References

[1] Ragnarsson KT: Functional electrical stimulation after spinal cord injury: current use, therapeutic effects and future directions. Spinal Cord 46:255-274, 2008

[2] Belanger M, Stein RB, Wheeler GD, et al: Electrical stimulation: can it increase muscle strength and reverse osteopenia in spinal cord injured individuals? Arch Phys Med Rehabil 81:1090-1098, 2000

[3] Crameri RM, Cooper P, Sinclair PJ, et al: Effect of load during electrical stimulation training in spinal cord injury. Muscle Nerve 29:104-111, 2004

[4] Petrofsky JS, Stacy R, Laymon M: The relationship between exercise work intervals and duration of exercise on lower extremity training induced by electrical stimulation in humans with spinal cord injuries. Eur J Appl Physiol 82:504-509, 2000

[5] Shields RK, Dudley-Javoroski S: Musculoskeletal plasticity after acute spinal cord injury: effects of long-term neuromuscular electrical stimulation training. J Neurophysiol 95:2380-2390, 2006

[6] Enoka RM: Neuromechanics of human movement. Champaign, IL, Human Kinetics, 2002

[7] Thrasher TA, Flett HM, Popovic MR: Gait training regimen for incomplete spinal cord injury using functional electrical stimulation. Spinal Cord 44:357-361, 2006

Acknowledgements

We would like to thank the Canadian Paraplegic Association of Ontario, Toronto Rehabilitation Institute, and Ontario Ministry of Health and Long-Term Care for financial support.

Author's Address

Dimitry G. Sayenko
Rehabilitation Engineering Laboratory, Toronto Rehabilitation Institute, Toronto, Canada
dimitry.sayenko@utoronto.ca
www.toronto-fes.ca

A Comparative Study on Electrical Stimulation and Magnetic Stimulation as for the Muscle Contractility and the Pain Perception

Song T[1], Khang G[2] , Hwang SH[2], Lee BS[3], Jung DW[3], Kim DG[3], Park DS[3], Ryu JC[4], Kang SJ[4]

[1] Faculty of Biomedical Engineering/Jungwon University, Goesan-gun, Chungbuk, Korea

[2] Department of Biomedical Engineering/Kyung Hee University, Yongin-si, Gyeonggi-do, Korea

[3]National Rehabilitation Hospital and Research Institute, Seoul, Korea

[4]Korea Orthopedic & Rehabilitation Engineering Center, Inchoen, Korea

Abstract

This research was designed to investigate the difference between electrical stimulation (ES) and magnetic stimulation (MS) by measuring or estimating the fatigue resistance, the pain perception (Borg Scale), the skin flare, the blood pressure and the heart rate before and after the stimulation. Seven paraplegic patients and 4 healthy subjects participated in the experiment, where intermittent ES and MS was applied to the quadriceps for 20 minutes with the duty cycle at 50% (3s on/3s off). The statistical analysis employed the two-sample t-test. The result showed no statistically-significant difference in the measured values, implying that ES and MS cause no difference in the locomotion mobility and the pain perception when they generate the same amount of muscle torque.

***Keywords**: functional electrical stimulation (FES), magnetic stimulation (MS), fatigue index, pain*

Introduction

Functional electrical stimulation (FES) has been widely applied to mobility recovery for the paraplegic and the restrengthening program of paralyzed muscles since it was used for preventing foot-drop of the stroke patients in 1961 by Liberson et al. [1]. Magnetic stimulation (MS), on the other hand, also began to draw attraction with a clinical evaluation reported in 1987 [2], mostly because of the fact that the users do not need to don/doff the electrodes.

Many researches have been performed to assist the paraplegic in walking by applying MS directly to the motor cortex and the paralyzed muscle for the past 20 years [3-5]. Polkey and his colleagues [6] reported that MS could be clinically useful without causing pain. Szecsi and his colleagues [7][8] compared MS with electrical stimulation (ES), reporting that MS induced higher muscle torque with less pain than ES. A contradicting result was also obtained by Verges et al. [9] that the two stimulation methods showed almost the same muscle force and the M-wave shape.

This study was designed to compare the effects of MS with those of ES by investigating the muscle fatigue, pain, skin flare, blood pressure (BP) and heart rate (HR) before and after the stimulation.

Material and Methods

Subject

Seven paraplegic patients and 4 healthy subjects participated in this study. The patients were selected among the inpatients of the National Rehabilitation Hospital, Seoul, Korea, and the rehabilitation medicine team did medical examinations, such as the bone density examination, computerized tomography of the lower extremities, etc., to avoid any contraindication of FES. The healthy subjects were selected among the employees in the National Rehabilitation Hospital, determined to have no medical problems by the physical and mental examinations.

The subject was seated on a chair, developed by our research team, with the trunk at the upright position, and the knee angle was fixed at 135°. The fully extended position corresponds to 180°. A load cell (SBA-100L, CAS, Co., Seoul, Korea) was used for measuring the force acting on the ankle when the knee extensor was stimulated.

Experiment Protocol

The stimulation intensity applied to the quadriceps was determined such that the resulting knee extensor torque did not make a difference for each subject. 3s on/3s off intermittent ES and MS were applied to train the quadriceps for 20 minutes, respectively, and the knee extensor torque was measured after the stimulation. BP and HR were also measured before and after the stimulation, and the pain perception was estimated by employing

the Borg Scale (1-5). The skin flare was examined at the end of each stimulation session.

ES and MS were applied to the quadriceps of each leg once a day, and the stimulation type was switched the next day (at the next stimulation session). That is, if ES was applied to the right leg and MS to the left leg, then MS was applied to the right leg and ES to the left leg at the next stimulation session. The resting period between two stimulation sessions was set at not less than 24 hours to avoid any effect from the previous stimulation.

Muscle Stimulation and Torque Measurement

For electrical stimulation, one surface (reference) electrode (5×9cm, Axelgaard, Fallbrook, CA, USA) was attached slightly proximal to the patella of each subject, and the other surface (stimulating) electrode was positioned at the motor point of the quadriceps. For magnetic stimulation, the magnetic coil of the magnetic stimulator (BioCon-1000pro™, Mcube Technology Co., Seoul, Korea) was positioned at the motor point of the quadriceps. Electrical and magnetic stimulation was applied to both legs of the subjects with the frequency fixed at 20Hz.

Data Collection

The blood pressure, the heart rate, the Borg scale, and the skin flare were measured or examined. Also, the fatigue indices (defined below) after intermittent stimulation for 60 seconds (FI 60s) and 120 seconds (FI 120s) were measured for each subject. The t-tests were done to each of the measurement groups, and the t-tests were done to the blood pressure and the heart rate before and after the stimulation with the level of significance at 0.05. In all torque measurements, the torque was normalized with respect to the initial (peak) value. Note that a low fatigue index indicates high fatigue resistance.

$$\text{FI 60s} \triangleq \frac{\text{initial torque - torque after 60s}}{\text{initial torque}} \times 100(\%)$$

$$\text{FI 120s} \triangleq \frac{\text{initial torque - torque after 120s}}{\text{initial torque}} \times 100(\%)$$

Results

Table 1 shows the two fatigue indices, FI 60s and FI 120s. The average FI 60s of the healthy subjects under ES and MS was 16.29% and 21.70%, respectively, indicating that ES caused less fatigue than MS by approximately 5.4% to healthy subjects, but no statistical significance was noticed (p=0.4463). Little difference was found for FI 120s for healthy subjects (p=0.9099).

On the Contrary, The average of FI 60s of the paraplegic patients was 22.64% and 19.24% under ES and MS, respectively, indicating that MS caused less fatigue, but we again found no statistical significance (p=0.4149). In case of the 120s stimulation, MS resulted in the lower fatigue index with no statistical significance as well (p=0.1896).

Table 1: Fatigue Index (%)

Subject	Fatigue Index	ES (mean±SD)	MS (mean±SD)	p-value
Healthy	FI 60s	16.29±12.84	21.70±9.69	0.4463
	FI 120s	33.28±6.03	33.90±9.62	0.9099
Patients	FI 60s	22.64±11.28	19.24±9.60	0.4149
	FI 120s	34.64±11.92	28.18±12.48	0.1896

We investigated the pain caused by ES and MS to all subjects, and the Borg Scale results are shown in Table 2. The higher Borg Scale point means the more serious pain. The average Borg Scale point under ES was 2.38 point and 2.15 point for the healthy subjects and the paraplegic patients, respectively, which implies that ES gave the healthy subjects more serious pain than the paraplegic patients although the difference was not statistically significant (p=0.2702). The average Borg Scale point under MS was 2.88 point and 2.00 point for the healthy subjects and the paraplegic patients, respectively, which again means that the healthy subjects felt more serious pain under MS than the paraplegic patients. This result was statistically significant contrary to ES (p=0.0103).

Comparing the pain perceived by the healthy subjects resulted in 2.38 point and 2.88 point under ES and MS, respectively, without statistical significance (p=0.1728). In case of the paraplegic patients, we found no statistical significance, either (p=0.4285).

Table 2: Pain (Borg Scale)

Stimulation	Healthy (mean±SD)	Patient (mean±SD)	p-value
ES	2.38±0.52	2.15±0.38	0.2702
MS	2.88±0.83	2.00±0.58	0.0103

The experiment did not induce a statistically-significant difference in BP and HR before and after the stimulation. During the whole experiment we noticed no skin flare regardless of the stimulation type.

Discussion

In most of the published researches, the fatigue resistance under external stimulation was estimated by applying continuous pulse trains and comparing the muscle torques generated at the beginning and

after 30 seconds of the stimulation. When ES was used, however, for recovering mobility to the paraplegic patient and/or restrengthening the paralyzed muscle, intermittent stimulation has been usually employed and the fatigue effect of intermittent stimulation is generally not the same as that of continuous stimulation. Consequently, now that this research was performed with intermittent stimulation, our results would, we believe, be of help to practical clinical applications. It should be also noticed that we selected the fatigue index calculated after 60 seconds of stimulation because the duty cycle in this study was 50%.

We adjusted the stimulation intensity applied to each subject in such a way that both stimulation (ES and MS) generated the same amount of the initial knee extensor torque. The reason was because we could naturally assume that when two stimulation types generate the same muscle torque, the lower fatigue index (i.e. the higher fatigue resistance) indicates the better locomotion mobility with the more muscle fibers activated at the measurement time instance.

We found a difference in the fatigue resistance between ES and MS, but no statistical significance. It can be agreed that MS may be able to generate the larger initial torque than ES as reported in Szecsi et al. [7][8], we cannot state, i.e. there is no statistical significance, that MS leads us to the better locomotion mobility than ES when the initial torque is adjusted at the same value.

The statistical analysis showed no significant difference in the pain perception in terms of the subject group and the stimulation type as well. This result contradicts those by Szecsi et al. [7][8] and Polkey et al. [6] reporting that MS causes no or little pain compared to ES. We found, as for the average values, that the healthy subjects felt the more serious pain under MS than under ES.

We found no difference in BP and HR before and after the stimulation. Now that the quadriceps was the only muscle we stimulated, it can be suggested that ES and MS of the lower extremities muscles do not affect the cardiovascular system of the subject.

Conclusions

The statistical analysis led us to a conclusion that MS may not be advantageous over ES from the viewpoint of the muscle contractility and vice versa, and that MS may not cause less pain than ES either. Also, stimulation of the lower extremities muscles only may not affect the cardiovascular system.

References

[1] Liberson WT, Holmguest HJ, Scott D, and Dow A. Functional electrotherapy: stimulation of the peroneal nerve synchronized with the swing phase of the gait in hemiparaplegic patients. Arch Phys Med Rehab, 42:101-105, 1961.

[2] Barker AT, Freeston IL, Jalinous R, and Jarratt JA. Magnetic stimulation of the human brain and peripheral nervous system: an introduction and the results of an initial clinical evaluation. Neurosurgery, 20:100-109, 1987.

[3] Capaday C, Lavoie BA, Barbeau H, Schneider C, and Bonnard M. Studies on the corticospinal control of human walking. I. Responses to focal transcranial magnetic stimulation of the motor cortex. J Neurophysiol, 81:129-39, 1999.

[4] Petersen N, Christensen, LO, and Nielsen, J. The effect of transcranial magnetic stimulation on the soleus H reflex during human walking. J Physiol, 513:599-610, 1998.

[5] Christensen LO, Andersen JB, Sinkjaer T, and Nielsen J. Transcranial magnetic stimulation and stretch reflexes in the tibialis anterior muscle during human walking. J Physiol, 531:545-557, 2001.

[6] Polkey MI, Kyroussis D, Hamnegard CH, Mills GH, Green M, and Moxham J. Quadriceps strength and fatigue assessed by magnetic stimulation of the femoral nerve in man. Muscle & Nerve, 19:549-555, 1996.

[7] Szecsi J, Schiller M, Straube A, and Gerling D. A comparison of functional electrical and magnetic stimulation for propelled cycling of paretic patients. Arch Phys Med Rehab, 90:564-570, 2009.

[8] Szecsi J, Gotz S, Pollmann W, and Straube A. Force-pain relationship in functional magnetic and electrical stimulation of subjects with paresis and preserved sensation. Clin Neurophysiol, In press, 2010.

[9] Verges S, Maffiuletti NA, Kerherve H, Decorte N, Wuyam B, and Millet GY. Comparison of electrical and magnetic stimulations to assess quadriceps muscle function. J Appl Physiol, 106:701-710, 2009.

Acknowledgements

This research was supported by Korea Institute of Industrial Technology Evaluation and Planning under the Core Technology Research for Silver Medical Devices Project (ITEP-10029934)

This research was supported by the MKE(The Ministry of Knowledge Economy), Korea, under the ISTK(Korea Research Council for Industrial Science & Technology) support program supervised by the 2010 Cooperative research projects

Author's Address

Song, Tongjin
Faculty of Biomedical Engineering/Jungwon University
tongjinsong@hanmail.net

Gait cycle detection using 3-axes linear accelerometers & gyroscopes in hemiplegic patients.

Tomite T*, Shimada Y*, Matsunaga T**, Sasaki K*, Yoshikawa T*, Kudo D*, Sato M**, Chida S**, Hatakeyama K**, Iwami T***, Kizawa S****, Iizuka K*****
*Department of Orthopedic Surgery, Akita University Graduate School of Medicine,
1-1-1 Hondo, Akita, 010-8543 JAPAN
**Rehabilitation Division, Akita University Hospital
***Department of Mechanical Engineering, Akita University Faculty of Engineering and resource Science
****Department of Mechanical Engineering, Akita National College of Technology
*****BIOTEC, Ltd

Abstract

Objective: To evaluate the ability of gait cycle detection using 3-axes linear accelerometers and gyroscopes in hemiplegic patients. ***Materials & Methods:*** 27 hemiplegic patients (18male, 9female) participated in this study. 3-axes accelerometers & gyroscopes fixed were placed around the knee. And a heel sensor was placed on the sole as a control signal. Patients were asked to walk 30m on flat and straight floor at their normal self selected pace. We compared the heel sensor signals with 3-axes accelerometers & gyroscopes signals by using Neural Network Learning. ***Result:*** The total number of steps were 1231. The total number of errors were 27 (2.1%). 17 patients didn't have any errors and 10 patients had 27 errors. ***Conclusion:*** 3-axes accelerometers & gyroscopes could detect the gait cycle in hemiplegic patients.

1 Introduction

Functional electrical stimulation (FES) has been used for the correction of dropped foot after the occurrence of an upper motor neuron disease, such as a stroke.

There are some FES devices to correct drop foot using a heel sensor for the hemiplegic patients. Usually, Japanese sit on a tatami floor without shoes, so the current FES devices which use a heel sensor placed in the shoe sole are difficult to use in Japanese-style rooms. To apply a FES system effectively in Japan, a gait cycle detection system which can accurately detect the gait cycle without a heel sensor is needed for the Japanese hemiplegic patient. Recently, some researchers have reported gait cycle detection using accelerometers instead of heel sensors and succeeded in gait cycle detection (2,3). In these reports, accelerometers were placed on the foot, thigh, lower limb and trunk, and 2-axes accelerometers were used.

We placed accelerometers and gyroscopes around the knee. By placing accelerometers and gyroscopes around the knee, we will be able to detect gait cycle and stimulate the peroneal nerve at the same time and same place. And with 3-axes accelerometers and gyroscopes, we expect we will be able to detect the gait cycle more correctly rather than using 2-axes accelerometers gait detectors.

2 Materials & Methods

27 hemiplegic patients (18males, 9females) participated in this study. They were chronic stroke patients (more than 6 months have passed since the onset), and could walk by themselves using walking assistant tools and AFO. The average age was 66 years old (range, 41-84 years). We classified them into the Brunnstrom Stage. The number of each stages were Stage 3:6, Stage 4:6, Stage 5:12, Stage 6:3.

They were asked to walk 30m at their normal self selected pace. And they were permitted to use tools to assist walking and AFO.

3-axes accelerometers (Hitachi Metals H48D, 4.8×4.8×1.5mm) & gyroscopes (Murata ENC-03R, 4.0×8.0×2.0mm) were fixed on one base (2.0×1.4cm) and were placed around the knee . Heel sensors were placed on the sole as a control signal (Click BP, Tokyo Sensor Co., 35×17×4mm). We asked patients to walk (first walk) and collected data by using a data logger (Hioki 8430 Memory Hilogger) (Fig. 1). The data was transferred to a computer for processing using Neural Network Learning (MATLAB Neural Network Toolbox). To use Neural Network learning can make detecting gait cycle by using only 3-axes accelerometers and gyroscopes possible. After studying data, we asked patients to walk (second walk) and collected data again.

The data obtained from the second walk was compared with the data obtained from the heel sensor. So, we converted the data into a graph and counted the number of errors. If the graph signal of Neural Network Learning was different from the graph signal of the heel sensor, this was counted as an error.

3 Results

We compared the graph of the accelerometers and gyroscopes with the graph of the heel sensor. Typical graph examples are shown in Fig. 2-1 and 2-2 (Example 1 is a good pattern and example 2 is a failure (appearing errors) pattern).

The total number of calculated steps were 1231. The total number of errors were 27 (2.1% of total steps). 17 patients didn't have any errors and 10 patients had 27 errors. According to the Brunnstrom Stage, the number of steps in each stage were Stage 3:253, Stage 4:276, Stage 5:561, Stage 6: 141. The number of errors were Stage 3:9 (3.6%), Stage 4:8 (2.9%), Stage 5:10 (1.8%), Stage 6:0 (0%) (Fig. 3). There weren't significant differences among these groups.

4 Discussion

Heel sensors have always been used to detect the gait cycle. Shimada et al. reported that FES system using heel sensor and percutaneous intramuscular electrodes improved walking speed and step cadence in hemiplegic patients. But, there are some faults with the heel sensor. There is a need for greater durability in the heel sensor and the long electric wire which connects the heel sensor to the stimulator. And the long electric wire is cosmetically unappealing. The heel sensor isn't suitable for the Japanese life style where one needs to take off their shoes (1).

Recent studies have reported that gait cycle detection which use other methods instead of heel sensors.Jasiewicz et al. reported the gait cycle detection using tilt sensors placed on the knee and the foot, and using accelerometers placed on the foot in able-bodied and spinal-cord injured individuals (2). Mansfield et al. reported the gait cycle detection using accelerometers placed on the trunk in able-bodies individuals (3). They reported 2-axes accelerometers were a valid sensor for the hemiplegic patient gait detection.

There have been few studies using 3-axes accelerometers and gyroscopes in hemiplegic patients. In this study, we could detect gait cycle of the hemiplegic patients using 3-axes accelerometers & gyroscopes placed around the knee in spite of the level of paralysis. We expect that we can develop a new FES system by using 3-axes accelerometers & gyroscopes and apply it to other motion analyses.

5 Conclusions

3-axes accelerometers & gyroscopes could detect the gait cycle in hemiplegic patients.

Legend of figures

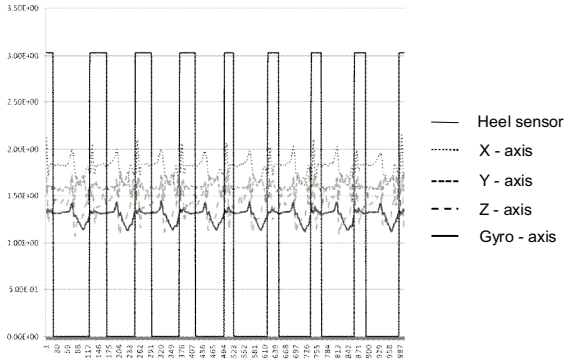


Fig.1: The data before doing Neural Network Learning (first walk data).

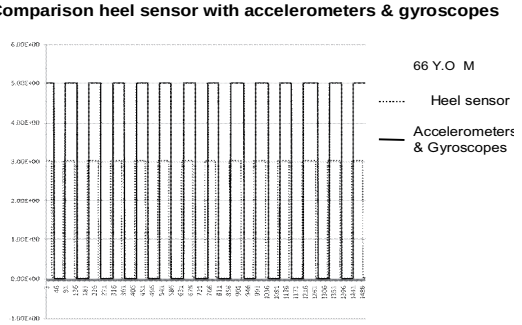


Fig.2-1: The solid line graph shows heel sensor signals. And the dotted line graph shows accelerometers and gyroscopes signals. We can see that the graph obtained from accelerometers follows the graph obtained from heel sensor.

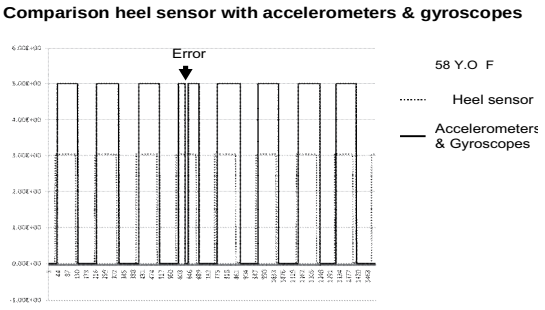


Fig. 2-2: The arrow in this graph shows errors. The solid line graph shows heel sensor signals. And the dotted line graph shows accelerometers and gyroscopes signals. We can see a different signal in the heel sensor graph from the accelerometers and gyroscopes graph.

Brunnstrom Stage	3	4	5	6
The number of patients	6	6	12	3
Total steps	253	276	561	141
Error steps	9	8	10	0

Fig. 3: Steps according to Brunnstrom Stage.

References

(1). Yoichi Shimada, Toshiki Matsunaga, Akiko Misawa, Shigeru Ando, Eiji Itoi, Natsuo Konishi: Clinical Application of Peroneal Nerve Stimulator System Using Percutaneous Intramuscular Electrodes for Correction of Foot Drop in Hemiplegic Patients. Neuromodulation Vol 9: 2006: 320-327.

(2). Jan M. Jasiewicz, John H.J Allum, James W. Middleton, Andrew Barriskill, Peter Condie, Brendan Purcell, Raymond Che Tin Li: Gait event detection using linear accelerometers or angular velocity transducers in able-bodied and spinal-cord injured individuals. Gait and Posture 24: 2006: 502-509.

(3). Avril Mansfield, Gerard M. Lyons: The use of accelerometry to detect heel contact events for use as a sensor in FES assisted walking. Medical Engineering and Physics 25: 2003: 879-885.

Author's Address

Takenori Tomite
Department of Orthopedic Surgery, Akita University Graduate School of Medicine,
1-1-1 Hondo, Akita, 010-8543 JAPAN
E-mail:tomite@doc.med.akita-u.ac.jp

Movement of Ankle Plantar flexor and Subjective Pain by Monophasic Electrical Stimulation

Suzuki T[1], Watanabe T[2], Saura R[3], Uchiyama H[4]

[1] Department of Mechanical Engineering, Maizuru National College of Technology, Maizuru, Kyoto, Japan

[2] Department of Biomedical Engineering, Tohoku University, Sendai, Miyagi, Japan

[3] Department of Rehabilitation Medicine, Osaka Medical College, Takatsuki, Osaka, Japan

[4] Department of Mechanical Engineering, Kansai University, Suita, Osaka, Japan

Abstract

The aim of this study was the investigation of the dynamical movement of the ankle plantarflexor and subjective pain by electrical stiumulation, which are considered as key points to improve the walking performance effectively, and to make users more comfortable. These results apply for developing assisting walking devices for elderly people and improving the performance of FES walking system for hemiplegia patients. From results, the rapid movement of ankleflexor without load can be obtained at higher frequency 30Hz above and longer pulse width W>0.6ms, but the subjective pain is high the region on the rapid ankleflexor movement. The subjective pain under level 6 is tolerable. The stimulating frequency around 30Hz and pulse width around 0.6ms is considered as one of good condition for well ankle plantar movement and less subjective pain.

Keywords: *ankle plantar flexor, subjective pain, monophasic electrical stimulation*

1. Introduction

Increased gait variability by slow walking speed predicts future fall risks. Slow walking in elderly people [1] and stroke patients [2] is well known. Slow walkers such as elderly people and stroke patient have a possibility of hip fracture caused by side fall, because the body in side fall is difficult to be supported by hands, so the hip crashes to the ground in many cases. The slow walking is one of causes of side fall is reported. [3] So walking speed has a important role to keep the stability of walking because the kinetic energy to the front, which reduces side movements, increases along with the walking speed.

Ankle plantar flexor by gastrocnemius and soleus muscle is very important to increase walking speed. Weakness of ankle plantar flexor should be considered as one factor of slow walking in elderly [4] and stroke patients. [2, 5] Also the results of dynamic simulation of normal walking shows that the ankle plantar flexor by gastrocnemius and soleus well contribute to increase forward progression of the trunk. [6] The FES walking system for hemiplegia patients focused on preventing the foot-drop by stimulating Dorsiflexor muscles in swing period. A Recent study to aim at improving the FES walking system delivered to the ankle plantarflexor and dorsiflexors [7] shows that the average contribution of the paretic leg increases 33.1% from 28.8% without FES, but there is no difference between dorsiflexors with plantarflexor and dorsiflexors only, though the ankle plantarflexor is important for walking.

The aim of this study was the investigation of the dynamical movement of the ankle plantarflexor and subjective pain by electrical stiumulation, which are considered as key points to improve the walking performance effectively, and to make users more comfortable. These results apply for developing assisting walking devices for elderly people and improving the performance of FES walking system for hemiplegia patients.

2. Methods

Experiment

The experimental device is shown by the Figure 1.

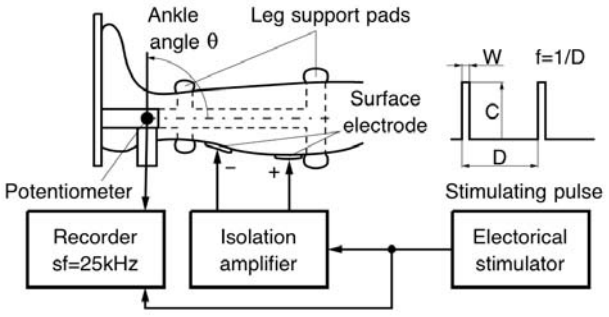


Fig.1 Experimental device

The device was designed for measuring the angle of ankle movement. The potentiometer dynamically detected the angle of subject's ankle. The recording of ankle measurement, whose sampling frequency was 100Hz, was started by a trigger of electrical stimulation of ankle plantarflexor muscles via self-glued surface electrode. The size of the surface electrode for both anode and cathode electrodes are 50mm by 80mm. The cathode electrode is adhered on the top belly mid of both the medial and lateral gastrocemius muscles. The anode electrode was on the bottom end of gastrocemius muscles. The monophasic and rectangular pulse wave in electrical stimulation was employed for this experiments, because the stimulation with monophasic and rectangular shape are the most effective from experimental results.[8] The pulse generated by the stimulator is amplified by the isolation amplifier. The bottom plate under a feet was designed much lighter weight than a feet weight, so we assumed the effect of rotating inertia of the device can be neglected. The subjects in experiments were lie on the right side to prevent from the mass effect of the plate by gravity.

Procedure

The pulse interval D and width W were randomly chosen from 0.1ms to 1.2ms at W and from 20ms, 33ms and 50ms at D; The frequency were 50Hz, 30Hz and 20Hz respectively. The current C of the pulse was fixed at 20mA. The subjective pain in each trial was assessed by Revised Face Pain Scale (FPS-R) [9]. The right leg in all subject were tested. In advance, the comfortable ankle positions were determined at each subject lying on the right side with relax. Each trials start at the predetermined ankle position by a trigger, which also start electrical stimulation and recording. The stimulations continue 2s, then the hearings of the subjective pain were done.

Methodology for analyzing data

The dynamic ankle movements were assumed as the step response of 1st system with lag by Eq. (1).

$$G(s)=\frac{Ke^{-Ls}}{Ts+1}, \quad \theta(t)=K(1-e^{-\frac{t-L}{T}}) \qquad (1)$$

The important parameters of Eq.(1) are gain K, time constant T and lag time L.

Table 1 Subject specification

Subject	A	B	C
Age	42	20	20
Height [cm]	175	172	161
Weight [kg]	65	66	55

Subject

Three healthy subjects joined this study. The description of subjects are on Table 1. The subjects were well informed this study and made consents before experiments.

3. Results and Discussions

Typical dynamic movement of ankle at f=30Hz and W=0.8ms on subject A shows in the Figure 2. The voluntary ankle movement delayed against FES ankle movement, because the voluntary movements were measured under the procedure including visual feedback. The most of ankle responses showed likely responses given by Eq. (1). The results of gain K, delay time L and time constant T shows in the Figure 3-1, 3-2 and 3-2 respectively. No ankle movement at W=0.1ms is observed on all subjects. The gain K by Figure 2 rose with the increase of pulse width W until W=0.6ms. But, the gain K almost be constant over W=0.6ms. The increasing stimulating frequency f contributed slight increase of the K, but there were no clear differences between 30Hz and 40Hz. The likelihood of the gain K was the same on all subject, but the absolute value of the K in subject C was twice larger than the K of other subject. Also the voluntary movement of the K at each subject were taken various value. The lag time L by Figure 3-2 shows similar tendency on all subjects. In the range of W<0.7ms, the L increased against the decrease of the W. the L at W>0.8ms on all subjects took the constant value around 0.055s. Higher frequency, especially 40Hz posed small L value. The time constants T at all subjects were constant value on the range of W>0.6ms. The T of subject C was twice larger than the T of other subjects. Small time constant shows rapid movement, so subject C's movement were slower than other subjects. But the voluntary value of the T at all subject were the same. From the analysis with Eq. (1) shows the similar tendency in all subject on stimulating pulse frequency f and width W, but the absolute values are different. The reason is expected that there are the difference on the growth of the ankle plantarflexor muscle in each subject.

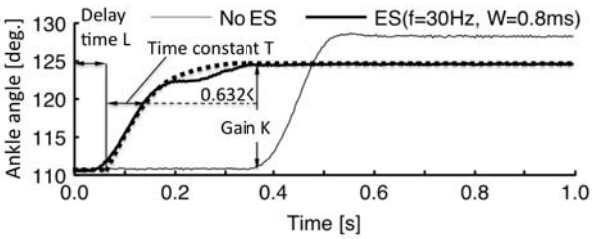


Fig. 2 Time responces without and with ES

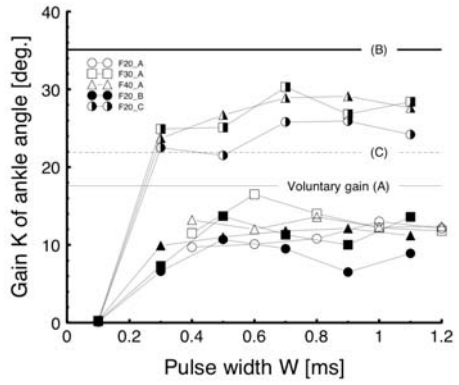


Fig. 3-1 Gain K of ankle angle

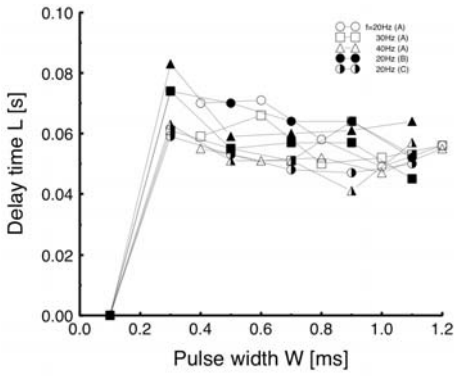


Fig. 3-2 Delay time of ankle movement

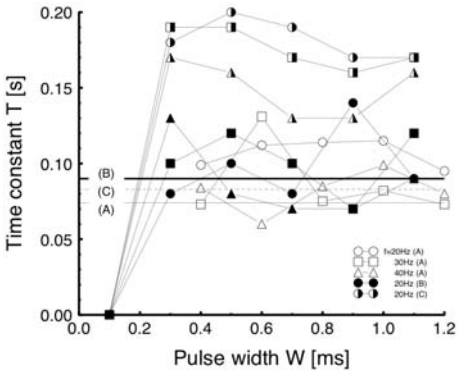


Fig. 3-3 Time constant T of ankle movement

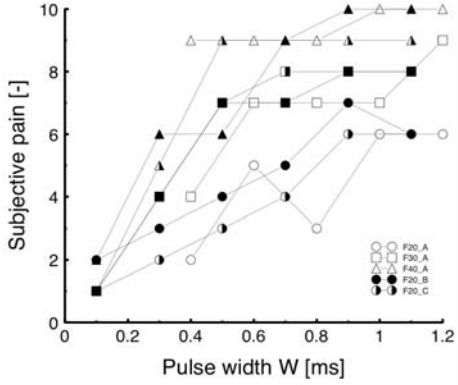


Fig. 3-4 Subjective pain by FPR-S

The subjective pain shows in the Figure 3-4. The pain rose in all subject against the increase of the W. The increase of the frequency f caused the increase of the pain. From the hearing, the tolerable subjective pain were estimated under 6 level by FPS-R. The movements of ankle plantarflexor at f=40Hz and W>0.6ms were good, but the subjective pain were not tolerable.

4. Conclusions

The rapid movement of ankleflexor without load can be obtained at higher frequency 30Hz above and longer pulse width W>0.6ms, but the subjective pain is high the region on the rapid ankleflexor movement. The subjective pain under level 6 is tolerable. The stimulating frequency around 30Hz and pulse width around 0.6ms is considered as one of good condition for well ankle plantar movement and less subjective pain.

References

[1] Kang HG, Dingwell JB, Effect of walking speed, strength and range of motion on gait stability in healthy older adults, J Biomech, vol.41:2899-2905, 2008

[2] Jonkers I, Delp S, Patten C, Capacity to increase walking speed is limited by impaired hip and ankle power generation in lower functioning persons post-stroke, Gait Posture, vol. 29:129-137, 2009

[3] Smeesters C, Hayes WC, Disturbance type and gait speed affect fall direction and impact location, J Biomech, vol. 34:309-317, 2001

[4] Nadeau S, Gravel D, Arsenault AB, et al. Plantarflextor weakness as a limiting factor of gait speed in stroke subjects and the compensating role of hip flextors, Clin Biomech(Bristol, Avon), vol. 14:125-135, 1999

[5] Kerrigan DC, Todd MK, et al. Biomechanical gait alterations independent of speed in the healthy elderly: evidence for specific limiting impairments, Arch Phys Med Rehabil, vol.79:317-322, 2001

[6] Neptune RR, Kautz SA, Zajac FE. Contribution of the individual ankle plantar flextors to support, forward progression and swing initiation during walking, J Biomech, vol:34:1387-1389, 2001

[7] Kesar T, Perumal R, Resman SD, et al. Functional Electrical Stimulation of Ankle Plantarflextor and Dorsiflextor Muscles - Effect on Poststroke Gait, Stroke, vol. 40:3821-3827, 2009

[8] Merrill DR, Bikson M, Jefferys JGR, Electrical stimulation of excitable tissue: desgin of efficacious and safe protocols, J Neurosci Methods, vol. 141:171-198, 2005

[9] von Baeyer et al, The Faces Pain Scale - Revised (FPS-R) around the world, Canadian Pain Society, Toronto. Pain Research and Management, vol.8 (Supp. B):57B, 2003

Acknowledgements

This project is supported by Japan Science and Technology Agency, grant for finding seeds 10-091, FY2009

The dynamics of cortical reorganization associated with voluntary and peripheral electrical stimulus

Nielsen SDI[1], Grey MJ[1,3] ,Sinkjær T[1,2], do Nascimento OF[1]

[1] Center for Sensory-Motor Interaction (SMI), Department of Health Science and Technology (HST), Aalborg University (AAU), Denmark
2 Danish National Research Foundation, Copenhagen, Denmark
3 Departments of Neuroscience and Pharmacology & Exercise and Sport Sciences, University of Copenhagen, Denmark

Abstract

Therapeutic application of functional electrical stimulation (FES) has shown promising clinical results in the rehabilitation of post-stroke hemiplegia, but little is known about how this therapy affects the central nervous system. In a previous fMRI study, we have shown that variations in the hand grasp function cause different patterns of brain activity. These variations were voluntary grasp (VOL), passive grasp elicited by electrical stimulation (FES) and voluntary grasp assisted by electrical stimulation (FESVOL). Considering that the fMRI technique provides high spatial, but low temporal resolution, and it does not allow inferring about the nature of the brain activation (i.e. excitatory or inhibitory), the objective of the present study was to determine if the effects we observed in the previous fMRI study were indeed excitatory as we postulated. We assessed cortical function, using multichannel surface EEG, with analysis of alpha oscillatory activity. The power spectra of EEG signal decreased in the alpha band bilaterally with movement initiation over the motor and parietal areas under FESVOL condition. One interpretation of this result is that different task-related afferent inputs produced a state of activation/deactivation of neural networks in different cortical areas, which was reflected in the modulation of alpha rhythm.

Keywords*: peripheral electrical stimulation, voluntary movement, alpha rhythm, beta rhythm.*

Introduction

In a previous study [1], we used fMRI to investigate brain activity evoked with four hand grasp tasks involving voluntary motor activation (VOL), in combination with functional electrical stimulation (FES), a technique involving patterned electrical stimulation of finger flexor/extensor muscles to effect movement. We observed bilateral cerebellar activity when the voluntary activity was combined with FES (FESVOL). In addition, differences in activation were observed bilaterally in secondary somatosensory (SII) areas when the FES-assisted hand grasp task was contrasted with voluntary grasp alone.

With classical fMRI methods it is not possible to differentiate between increases and decreases in neuronal firing and, therefore, it is not possible to know if the contrasts represent net excitatory vs. inhibitory effects. The polarity and amplitude of the potentials observed with EEG, in contrast, are directly related to the modality (excitatory or inhibitory) and intensity of the neural population at the cortical level.

The objective of the present study was to determine if the effects we observed in the previous fMRI study were indeed excitatory as we postulated. We assessed cortical function, using multichannel surface EEG, with analysis of alpha oscillatory activity associated with three grasp tasks: VOL, FES and FESVOL. We hypothesized that the processing of VOL, FES and FESVOL peripheral inputs would be reflected differently in the modulation of cortical alpha oscillatory activity.

Based on the fact that the strength of alpha rhythm inversely correlates with the fMRI signal strength in cortical areas [2], we hypothesized that FESVOL input would show a bilateral decrease in the strength of alpha band over the cortical areas. Specifically, based on our previous findings with fMRI technique, we hypothesized a decrease over parietal areas.

Material and Methods

EEG recordings were performed with a 32-channel digital EEG amplifier while the subjects performed three different motor tasks (VOL, FES and FESVOL) in addition to a resting task where they were asked to remain still (REST). The VOL, FES and FESVOL tasks involved repetitive extension movement of the fingers of the right hand: 1) VOL,

in which the subject voluntary opened and closed the hand; 2) FES, in which the open/close hand movement was elicited by patterned electrical stimulation of the finger extensor muscles with no voluntary contribution to the movement; and 3) FESVOL, in which the open/close hand movement was performed as described under the FES condition with the addition of voluntary activation.
Patterned neuromuscular electrical stimulation was used to effect finger flexion movements in the FES and FESVOL trials. The stimuli were delivered at 50 Hz with 200 μs pulses, and controlled by a commercial FES stimulator. The stimulation pattern was triggered by a push-button switch held in the left hand. Each button press initiated a stimulation pattern that produced a 1.5 s finger extension. While the magnitude of stimulation varied from one subject to another, the range of stimulation current intensity ranged from 10-15 mA.
Averaged EEG waveforms were band-pass filtered to compute the energy in the alpha (8–12 Hz) band for three different intervals: 1) preparation (from -2 to -1 s before movement onset), 2) execution (between movement onset and 1 s before it) and 3) control (between movement onset and 1 s after it).
A one-way repeated-measures analysis of variance (ANOVA) was used to assess task-related power changes in the alpha band. Significant differences between individual conditions were identified by the Student Newman-Keuls test for multiple comparisons. The outcomes were declared significant at $p < 0.05$.

Results

Task-related power decrease in alpha band

Alpha energy level decreased at all electrode locations when evaluating preparation with the control phase of the movement.
In the VOL and FES conditions, there was a significant alpha energy decrease between preparation and control over the central and parietal areas bilaterally (C3, Cz, C4, P3, Pz and P4 electrodes). For the FESVOL condition, a significant bilateral energy decrease in the alpha band was observed over the central (motor) and parietal areas between the preparation and control phases (C3, Cz, C4, P3, Pz, P4 electrodes), see Figure 1B.

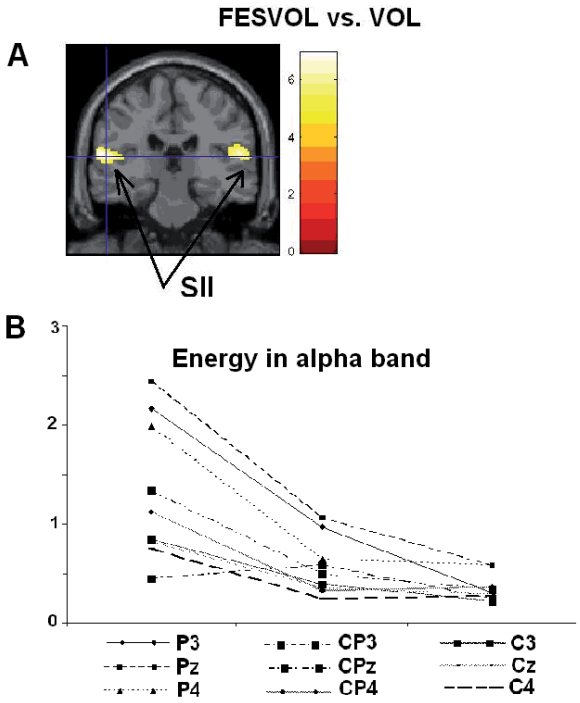


Fig. 1: (A) Neural activation for FESVOL vs. VOL (bilateral secondary SII) [3] (B) Energy levels in the alpha band at different electrode locations as a function of movement phase in the FESVOL experimental condition.

Discussion

Task-related power decrease in the alpha band

Power decreases in the alpha band extends bilaterally with movement initiation over the motor and parietal areas (Figure 1B). This is consistent with data from [4] and [5] that studied EEG changes in healthy volunteers during wrist movements induced either by FES or during active and passive movements. They suggested that sensorymotor processing during FES involves some of the processes that are also involved in voluntary hand movements. This is an important observation with clinical significance for rehabilitation.
[6] reported that with increasing finger movement task complexity, the power in the alpha band decreased bilaterally in centroparietal regions. They suggested that with increasing movement complexity, a neuronal circuitry responsible for the generation of alpha band activity in both hemispheres is activated including bilateral primary sensorimotor areas, parietal cortex and SMA. This is in agreement with our EEG findings and also our fMRI findings that showed activity in bilateral parietal areas.
Alpha band decrease during the motor task indicates enabled information processing through

hand area networks. The alpha band decrease may reflect a mechanism responsible for selective attention to a motor subsystem. This effect of selective attention can be accentuated when other cortical areas not directly involved in the specific motor task (e.g. parietal areas) are `inhibited' [7].
The strength of alpha rhythm inversely correlates with the fMRI signal strength in cortical areas. laufs found a robust pattern of negative correlations between blood oxygen level dependent (BOLD) signal change in association with alpha power in the frontal and parietal cortices. [8] also observed BOLD signal changes in parts of the frontal and occipital lobes to correlate negatively with alpha power. A decrease in the power of sensorimotor rhythms could be correlated with an activated cortical network, servicing planning and execution, while an increase in power could reflect deactivation.
In our previous fMRI study [1], the only areas where the FESVOL condition showed significantly more activity than the VOL condition, when correcting for multiple comparisons, were the bilateral secondary somatosensory areas, see figure 1A. The prominent decrease in alpha band over parietal areas could therefore reflect excitatory activity.

Conclusions

Neuromuscular stimulation combined with voluntary activation (FESVOL) produces a decrease in the power spectra of EEG signal in the alpha band bilaterally over the motor and parietal areas. The EEG analysis is complementing our previous fMRI results confirming the excitatory effect postulated previously by the fMRI study**.**
This study should be understood as contribution to the actual effort of the researchers in the rehabilitation field. Future studies should investigate whether patients with altered strengths of afferent input show similar patterns.

References

[1] S. D. I. Nielsen, M. S. Christensen, R. J. Vingborg, T. Sinkjaer, A. Roepstorff and M. J. Grey, "Interaction of electrical stimulation and voluntary hand movement in SII and the cerebellum during simulated therapeutic Functional Electrical Stimulation," *Human Brain Mapping,* under revision, 2010.
[2] H. Laufs, A. Kleinschmidt, A. Beyerle, E. Eger, A. Salek-Haddadi, C. Preibisch and K. Krakow, "EEG-correlated fMRI of human alpha activity," *NeuroImage,* pp. 1463-1476, 2003.
[3] S. D. I. Nielsen, R. J. Vingborg, T. Sinkjaer, A. Roepstorff and M. J. Grey, "Changes in cortical activity during functional electrical therapy assessed by functional magnetic resonance imaging.," in Washington, DC, USA, 2005, nov 11-16, .
[4] G. Pfurtscheller, C. Neuper and G. Krausz, "Functional dissociation of lower and upper mu rhythms in relation to voluntary limb movement." *Clin Neurophysiol,* pp. 1873-1879, 2000.
[5] G. R. Muller, C. Neuper, R. Rupp, C. Keinrath, H. J. Gerner and G. Pfurtscheller, "Event-related beta EEG changes during wrist movements induced by functional electrical stimulation of forearm muscles in man," *Neuroscience Letters,* pp. 143-147, 2000.
[6] P. Manganotti, C. Gerloff, C. Toro, H. Katsuta, N. Sadato, P. Zhuang, L. Leocani and M. Hallett, "Task-related coherence and task-related spectral power changes during sequential finger movements. " *Electroenceph Clin Neurophysiol,* vol. 109, pp. 50-62, 1998.
[7] G. Pfurtscheller, "Event-related synchronization (ERS): an electrophysiological correlate of cortical areas at rest." *Electroenceph. Chn. Neurophysiol.,* pp. 62-69, 1992.
[8] R. I. Goldman, J. M. Stern, J. J. Engel and M. Cohen, "Simultaneous EEG and fMRI of the alpha rhythm." *NeuroReport,* pp. 2487-2492, 2002.

Acknowledgements

Funding support received from NOVI Ejendomsfond, the Spar Nord Foundation and the Obel Family Foundation.

Author's Address
Simona Denisia Iftime Nielsen
Center for Sensory-Motor Interaction (SMI), Department of Health Science and Technology (HST), Aalborg University (AAU), Denmark
simden@smi.auc.dk

A biofeedback treatment based on FES to recover the medial hamstring use in stroke patients suffering of stiff legged gait

Ferrante S[1], Ambrosini E[1], Ravelli P[1], Ferrigno G[1], Molteni F[2], Pedrocchi A[1]

[1] NearLab, Bioengineering Department, Politecnico di Milano, Milan, Italy

[2] "Villa Beretta", Unità Operativa Complessa di Medicina Riabilitativa, Ospedale Valduce di Como

Abstract

It is widespread among hemiparetic patients an impairment of the medial hamstrings, which compromises knee flexion during gait. This disability is usually known as stiff-legged gait. A biofeedback treatment focalized on the recovery of the hamstrings action during the pulling phase of a cycling task was proposed. The patient was asked to pedal voluntarily, concentrating the maximum effort in the knee flexion of the paretic leg. At each revolution, the work produced in this phase was visually displayed to the patient. If the work was under a certain threshold, FES was provided to "remember" the subject the correct activation timing of the interested muscle. One hemiparetic patient, who suffered from stiff-legged gait, was involved in the treatment. After one session lasting 12 minutes, the patient improved the ability to activate the hamstrings during cycling. Longer treatments on more patients are needed to confirm the results. Furthermore, gait analysis before and after treatment may be an interesting tool to assess any progress in walking performance. The proposed treatment could become an attractive option in the recovery and strengthening of the medial hamstrings, combining the role of FES in improving motor relearning and the one of biofeedback in maximizing patient involvement.

Keywords*: hemiparesis, biofeedback treatment, functional electrical stimulation, cycling*

Introduction

Stiff or straight legged gait is a common disability in stroke patients that interferes with normal limb advancement. A treatment able to effectively strengthen and recover the use of the medial hamstring muscles during knee flexion has not yet been found. Recently, it was demonstrated that functional electrical stimulation (FES) could help in strengthening muscles and relearning the patient the correct muscular activation timing needed during a complex movement [1, 2].

The focus of most FES training paradigms has been on the direct motor consequences of stimulation elicited by the activation of efferent motor neurons and/or selected muscles. It is envisaged that through the appropriate placement and tuning of the stimulation, adaptive behavioral patterns can be regularly elicited and maintained [3]. Stimulation, of course, also engages sensory fibers that relay signals to the spinal cord. This afferent input can, depending upon its nature and strength, activate spinal circuits that induce, modulate or even inhibit the performance of the target response. Surprisingly, little is known about how spinal circuitry impacts the consequences of FES. Recently, evidences based on animal models suggest that spinal neurons can foster adaptive behaviour in an FES paradigm [4]. This study outlines that the recovery may be facilitated by (1) linking stimulation to a specific functional response, and (2) allowing the 'spinal cord' to minimize exposure to FES.

Starting from this concept and the hypothesis that an active participation of the patient increases efficacy of the treatment, we developed a biofeedback (BF) protocol aimed at recovering the use of the flexor muscles of the knee during cycling. The cycling task was chosen because it represents a functional, safe and widely accessible mode of exercise that has a kinematic pattern very similar to the one of walking. During the proposed BF protocol a combination of a visual feedback and sensorial feedback are fed to the patient. The visual feedback shows the force produced in each revolution during the knee flexion by the paretic leg while the sensory feedback is provided by FES when the force produced is not enough in order to "remember" the patient the correct activation timing.

Material and Methods

Experimental Setup

The experimental setup, reported in Fig.1, includes a current–controlled 8-channel stimulator and a motorized cycle-ergometer equipped by sensors able to measure the torques at the left and right crank. These signals are transmitted from the ergometer to a desktop PC (PC master) able to

compute the work produced in each revolution by the hamstring of the paretic leg during the knee flexion (W_{ham}).

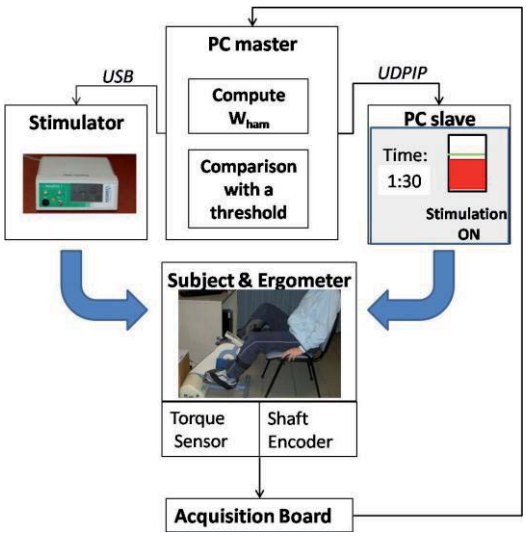


Fig. 1 Experimental Setup

Then, W_{ham} is transmitted via UDPIP to a PC slave which provides a visual display to the patient.
When W_{ham} is lower than a selected threshold, the PC master send the stimulation to the hamstring of the paretic leg.

Treatment protocol

The BF treatment was designed to last three times a week for two weeks. Each trial lasts 12 minutes: (1) 1 minute of passive cycling; (2) 1½ minute of voluntary cycling; (3) 7 minutes of BF protocol; (4) 1½ minute of voluntary cycling; (5) 1 minute of passive cycling.

During the BF protocol, the subject is asked to focus on the knee flexion during cycling. When the work produced by the paretic leg, displayed through the graphical interface (Fig. 1, PC slave) does not exceed the threshold, the stimulation is sent during the angular range corresponding to the knee flexion in the following revolution. The threshold is set according to the patient skill.

Results

As an example, we report the results of a case study on one hemiparetic patient performing one single treatment trial.

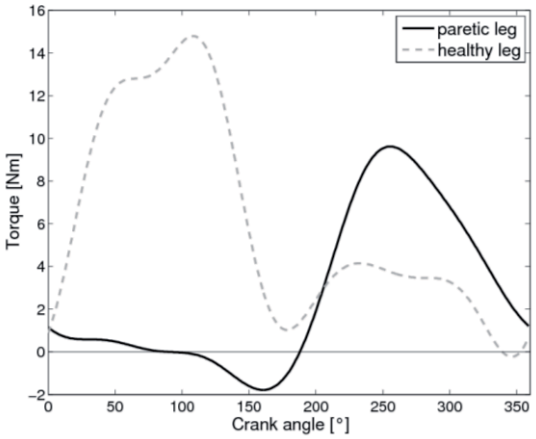


Fig 2: Mean active torque profiles during voluntary cycling before the BF protocol. 0° corresponds to the maximum flexion of the healthy hip.

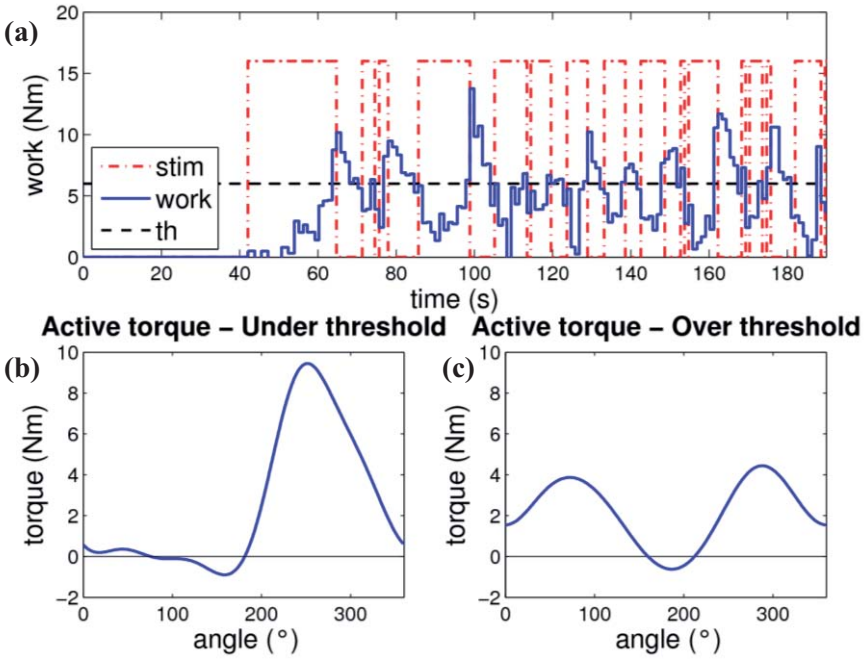


Fig 3: BF protocol results: panel (a) depicts the fluctuation of W_{ham} produced by the patient in each revolution (solid line) compared to the work threshold (dashed line), and the stimulation on-off signal (dash-dot line). Panels (b) and (c) show the active torque produced by the paretic leg when W_{ham} is under threshold and W_{ham} over threshold, respectively.

Fig. 2 depicts the mean active torque profiles, i.e., the difference between the torques produced voluntarily and the ones obtained during passive cycling, computed before the BF protocol averaging 40 s of voluntary cycling. The torque generated by the healthy limb (dashed line) is characterized by two peaks: the first one represents the contribution during knee extension, while the second one is due to the hamstrings pulling action. It is noteworthy that the paretic leg profile (solid line) shows only one peak around 250° corresponding to the quadriceps pushing action (note that the paretic profile is shifted by 180° with respect to the healthy one). Therefore, a treatment focused on the recovery of the hamstrings action was proposed.

Fig. 3 shows the performance of the patient during the BF protocol. Panel (a) illustrates the fluctuation around threshold (dashed line) of W_{ham}. When the work is under threshold, the stimulation is on, as shown by the dash-dot line. On the contrary, the stimulation is off when the work is over threshold. Panels (b) and (c) report the active torque profiles produced by the paretic limb, corresponding to two representative revolutions of these two opposite situations. In panel (b) it is noticeable the absence of the peak due to the pulling action, while in panel (c) both the peaks are visible.

Finally, Fig. 4 depicts the mean active torque profiles generated by the both the legs averaging 40 s of voluntary pedalling after the BF protocol. It may be noticed that the profile of the paretic leg recovered a peak corresponding to the hamstrings action.

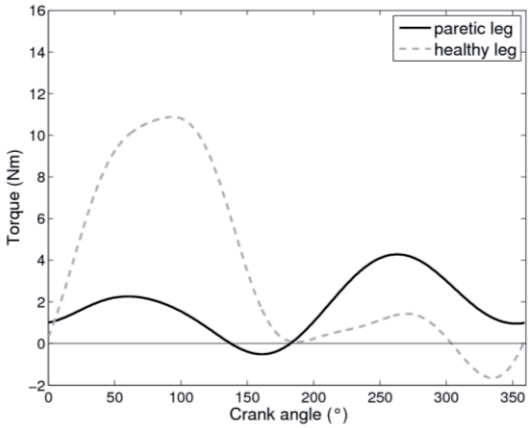


Fig 4: Man active torque profiles obtained during the voluntary cycling phase after the BF protocol.

Discussion

The work introduces a case study on one hemiparetic patient suffering from stiff-legged gait. The patient has been involved in a BF treatment aimed at the recovery and strengthening of the medial hamstrings. The BF consisted of a visual signal, which displayed the torque produced by the paretic hamstrings during a cycling task, and of a sensorial signal provided by FES. After one session, lasting 12 minutes, the patient increased the hamstring strength and started to use it systematically during voluntary cycling.

The treatment effectiveness could be based on the sum of two crucial factors: the afferent signal, provided by FES to the central nervous system, which may improve motor relearning and plasticity, and the patient involvement, which is maximized by the visual feedback displayed during the exercise.

More patients treated over different sessions should be involved in a pilot study to confirm the results here obtained. Besides, it may be worth performing quantitative gait analysis before and after the longer treatments in order to compare kinematic and electromyography patterns during gait and assess the efficacy of the therapy in improving gait performance. Indeed, the recovery of walking ability is the final aim af any rehabilitative treatments which involve the lower limb of hemiparetic patients.

Conclusions

The proposed treatment seems to be an interesting option for the focalized recovery of the medial hamstrings, whose impairment widely concerns the paretic leg of patients after stroke. Trials on an increased number of hemiparetic patients are necessary to assess the real effectiveness of the proposed treatment. Moreover, further investigations are required to proof and quantify its efficacy in reducing physical exertion and improving gait pattern in patients walking with a stiff-legged gait on the affected side.

References

[1] Ferrante S., Pedrocchi A., Molteni F. et al. Cycling induced by functional electrical stimulation improves the muscular strength and the motor control of individuals with post-acute stroke. , Eur J Phys Rehabil Med, 44(2):159-67, 2008

[2] De Conti C, Gualdi S, Salghetti A, et al., FES cycling in children affected by cerebral palsy: a pilot study, Proc. of the 14th IFESS Conference, Seoul, pp. 81-83, 2009.

[3] Sheffler LR, Chae J, Neuromuscular electrical stimulation in neurorehabilitation, Muscle & Nerve, 35: 562–590, 2007

[4] Hook MA and Grau JW, An animal model of functional electrical stimulation: evidence that the central nervous system modulates the consequences of training, Spinal Cord, 45: 702-12, 2007

Author's Address

simona.ferrante@polimi.it

Reducing the upper body effort during FES-assisted arm-supported standing up in paraplegic patients

Seyedi A, Erfanian A

Neuromuscular Control Systems Lab., Iran Neural Technology Centre, Dept. of Biomed. Eng.,
Iran University of Science and Technology, Tehran, Iran

Abstract

In this work, the effects of the artificial ankle joint stiffness on the performance of sit-to-stand movement and upper body effort have been assessed during FES-assisted arm-supported standing up in paraplegic patients. An ankle-foot orthosis (AFO) was developed with the plantar-assisting spring. By changing the spring, the rigidity of the AFO could be adjusted. Experimental results on two complete paraplegic subjects indicated that by suitable selection of the stiffness in the plantar flexion direction, the paraplegic patient could stand up comfortably with less upper body effort. The results showed that the peak arm force was reduced from 67.2% to 44.3% of the body weight in subject RR and from 77.7% to 47.9% in subject MS.

Keywords: *Sit-to-stand, paraplegic, upper body effort, Functional Electrical Stimulation.*

Introduction

Sit-To-Stand (STS) maneuver is one of the repetitive movements in daily life and it is also a prerequisite for standing, walking, and reaching distant objects. It has been demonstrated that using Functional Electrical Stimulation (FES) on paraplegic's lower extremities they can complete the STS task [1]. One of the main issues in STS movement in paraplegic patients using FES is the amount of upper body effort during the task [2]. The long term effects of repetitive high transient loading of the arm during activities such as transfers and wheeling have been implicated in the high incidence of overuse syndromes in the spinal injured population [3]. Therefore it is essential to find a solution to minimize the patient's upper extremity efforts during movement.

Many STS aspects in healthy subjects and some issues in able-bodied young and elderly have been analyzed during past studies [4]-[8]. However, few studies exist on the FES-assisted STS movement in paraplegic subjects [9], [10]. Donaldson and Yu [9] measured the handle forces and the posture during open-loop FES-assisted standing up of two paraplegic subjects. The tests show that they use a strategy called *quick knee-locking* in which the hip extension occurs after the knees are locked and while a flexion deficit is being applied at the knees. The results shows that most of the forces needed to lift up the body in an upward position are provided by upper extremities. Bahrami et al. [10] analyzed the biomechanical aspects of STS transfer in healthy subjects with/without arm-support and in paraplegic patients with/without FES and suggested that some significant differences exist between the strategy used by the paraplegic patients to stand up and the strategies used by the healthy adults rising with arm-support.

In all FES-assisted arm-supported standing up [9], [10], only the knee joint or both the knee and hip joints were actively contributed to the STS movement by stimulating the quadriceps and gluteal muscles. Previous studies on STS movement in healthy subjects reveal that during seat off to standing posture the plantar flexion muscles are active and an extension torque is generated in the ankle joint [7], [8].

The aim of current study is to investigate the effect of ankle joint stiffness on the upper body efforts during FES-assisted standing up in paraplegic subjects.

Material and Methods

The experiments were conducted on two thoracic-level complete spinal cord injury subjects in different days. The paraplegic subjects were active participants in a rehabilitation research program involving daily electrically stimulated exercise of their lower limbs (either seated or during standing and walking) using ParaWalk neuroprosthesis [11]. The hip, knee, and ankle joint angles were measured by using the motion tracker system MTx (Xsens Technologies, B.V.) which is a small and accurate 3-DOF Orientation Tracker. A Kistler

piezoelectric force plate type 9286AA (Winterthur, Switzerland) was used to measure the 3D ground reaction forces (GRF) under both feet (with an accuracy of ±0.5% of the full scale) and the corresponding CoP. The vertical forces on the arm support frame were measured by two Load cells (LRF350, Futek Advanced Sensor Technology, Inc, USA) mounted underneath the both walker handles (Fig. 1). An ankle-foot orthosis (AFO) was developed with the plantar-assisting spring. By changing the spring, the rigidity of the AFO could be adjusted.

The experiments were performed while the paraplegic subjects were seated in their wheelchair. Both feet were placed symmetrically and parallel to each other on a force plate. For rising, stimulation is voluntarily triggered by the patient wearing AFO, and the body is lifted upward from the initial to the extended upright position by the help of stimulating the quadriceps and gluteal muscles using an eight-channel computer-based FNS system [12] and arm support.

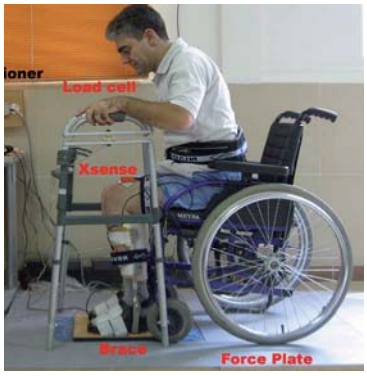


Fig. 1: Experimental Setup

Results

Fig. 2 shows the hip, knee, and ankle joint angles, hand and ground reaction forces, for different values of the stiffness controlling the plantar flexion for two paraplegic subjects. It is observed that the peak hand reaction forces (PHF's) are 48% (60%) and 52% (58%) of the body weight in subject RR (MS) when the stiffness values are 22.14 Nm/rad and 10.53 Nm/rad, respectively. The PHF's are 73% and 72% of the body weight with no spring in subjects MS and RR, respectively.

Fig. 3 shows the average of the hand reaction forces with different values of stiffness. Totally, 172 experimental trails were conducted on two subjects in different days. The results indicate that the mean hand reaction force is reduced form 48.2% of the body weight to 32.9% by applying 22.14 Nm/rad mechanical stiffness on the ankle joint in subject RR, and from 53.2% to 30.8% by applying 10.53 Nm/rad stiffness in subject MS.

Discussion and Conclusions

In this work, we investigate the effect of the ankle joint stiffness on the upper body efforts during FES-assisted standing up in paraplegic subjects. The results indicate that applying artificial stiffness in the plantar flexion direction could significantly reduce the upper body effort in paraplegic patients standing up using FES.

References

[1] Kralj A. and Bajd T., Functional Electrical Stimulation: Standing and Walking After Spinal Cord Injury. *Boca Raton, FL: CRC Press*, 1989.

[2] Kamnik R., Bajd T., and Kralj A., Functional electrical stimulation and arm supported sit-to-stand transfer after paraplegia: a study of kinetic parameters. *Artif. Org.*, vol. 23, pp. 413–417, 1999.

[3] Bayley J. S., Cochran T. P., and Sledge C. B., The weight-bearing shoulder: The impingement syndrome in paraplegics. *J. Bone Joint Surg.,* vol. 69-A, pp. 676–678, 1987

[4] Papa E., Cappozzo A., Sit-To-Stand motor strategies investigated in able-bodied young and elderly subject. *Journal of Biomechanics* vol. 33, pp. 1113-1122, 2000.

[5] Hutchinson E. B., Riely P. O. and Krebs D. E., A dynamic analysis of the joint force and torques during rising from a chair. *IEEE Trans. Rehab.* vol. 2, pp. 49-56, 1994.

[6] Hughes M. A., Weiner D. K., Schenkman M. L., Chair rise strategies in the elderly. *Clin. Biomech.,* vol. 9, pp. 187- 192, 1994.

[7] Roebroeck M., et al., Biomechanics and muscular activity during sit-to-stand transfer. *J. Clin. Biomech.* vol. 9, pp. 235-244, 1994.

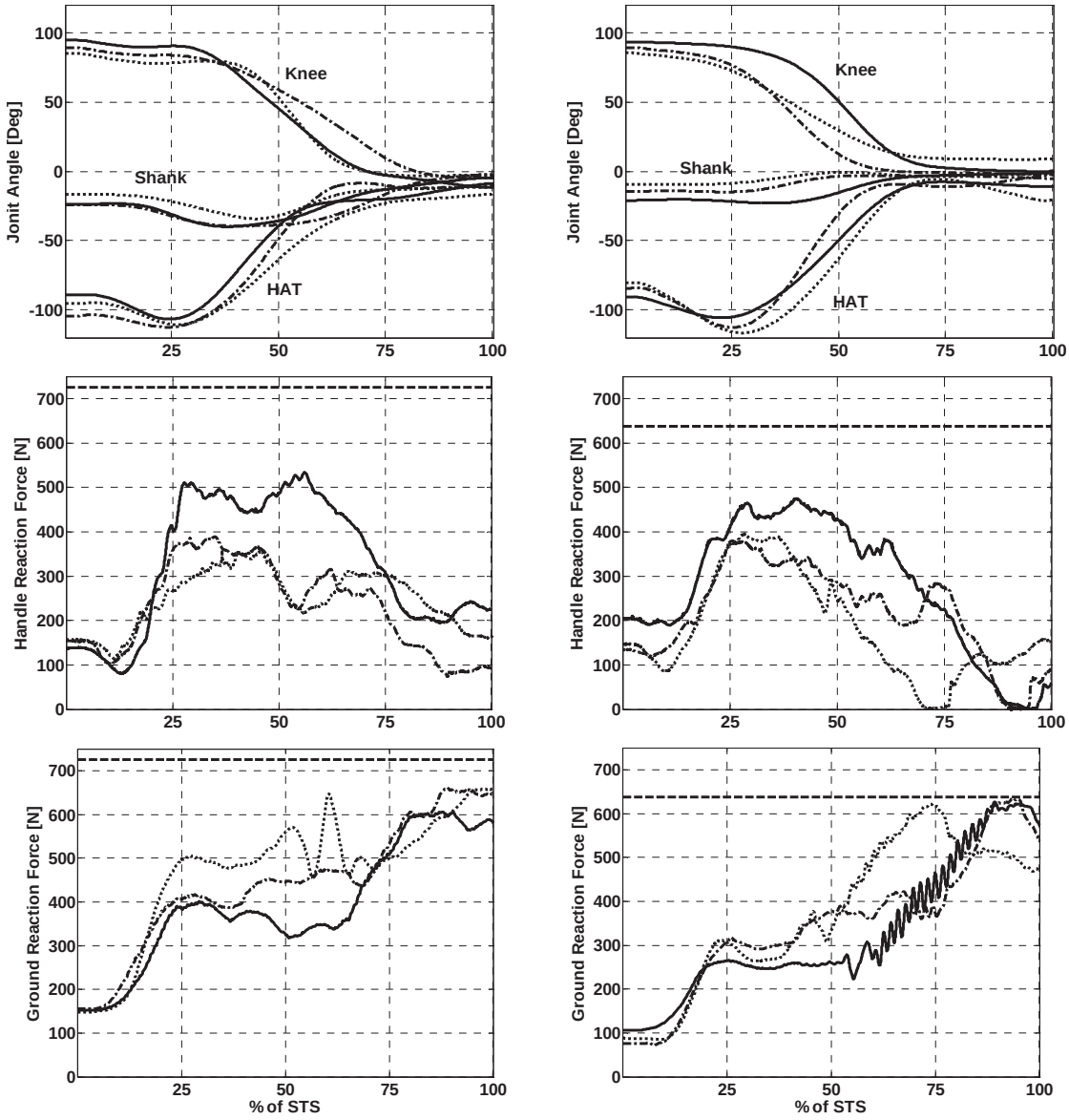
[8] Doorenbosch CA, et al., Two strategies of transferring from sit-to-stand: the activation of monoarticular and biarticular muscles. *J Biomech*, vol. 27, pp. 299-307 1994.

[9] Donaldson N. and Yu C., A strategy used by paraplegics to stand up using FES. *IEEE Trans. Rehab*. Vol. 6, pp. 162-167, 1998.

[10] Bahrami F., et al., Biomechanical analysis of sit-to-stand transfer in healthy and paraplegic subjects. *Clinical Biomechanics*, vol. 15 pp. 123-133, 2000.

[11] Erfanian A, Kobravi H.R., Zohorian O. and Emani F., A portable programmable transcutaneous neuroprosthesis with built-in self-test capability for training and mobility in paraplegic subjects. *in Proc. 11th Conf. Int. Functional Electrical Stimulation Society 2006.*

[12] Kobravi H.-R. and Erfanian A., A transcutaneous computer-based closed-loop motor neuroprosthesis for real-time movement control *in Proc.* 9th *Annual Conf. Int. Functional Electrical Stimulation Society 2004*.



(a) (b)

Fig. 2: Joint angles, hand and ground reaction forces with different values of stiffness in the ankle joint for two paraplegic subjects RR (a) and MS (b): no spring (solid line), 10.53 Nm/rad (dashed line), and 22.14 Nm/rad (dotted line).

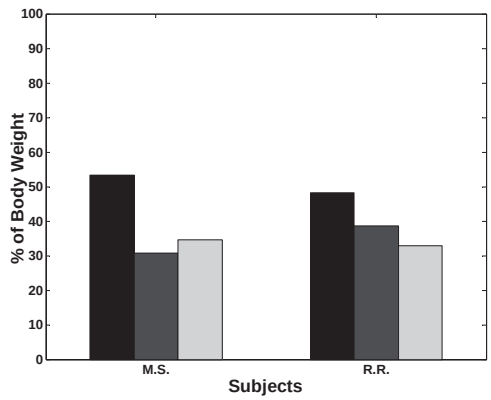


Fig. 3: Average of the hand reaction forces with different values of stiffness: no spring (black), 10.53 Nm/rad (dark gray), and 22.14 Nm/rad (light gray).

Acknowledgements

This work was supported by Iran Neural Technology Centre, Iran University of Science and Technology.

Author's Address

Seyedi A., Erfanian A.
Dept. of Biomedical Engineering,
Faculty of Electrical Engineering,
Iran University of Science and Technology,
Iran Neural Technology Centre,
Tehran, Iran.
erfanian@iust.ac.ir
aseyedi@ee.iust.ac.ir

Use of ultrasound current source density imaging (UCSDI) to monitor electrical stimulation of denervated muscles and fiber activity, some theoretical considerations

Gudjonsdottir B[1,2], Gargiulo, P[1,2], Helgason Th[1,2]

[1] Landspitali University Hospital, Reykjavik, Iceland

[2] Reykjavik University, Reykjavik, Iceland

Abstract

In order to have an effective therapy of denervated muscle and ensure that whole muscles are stimulated a monitoring method is needed. Up to now the method has been to put the finger on the muscles tendon, for example the patella tendon, to detect whether the muscle is contracting or not. The information from this is limited. To ensure a balanced therapy we suggest a method to monitor the electrical stimulation therapy. The application of an ultrasound wave modulates the tissue resistance to the stimulating current and produces a voltage signal that can be detected by surface electrodes. This is known as the electro acoustic effect (AE). Using it to map the distribution of an electrical current in a conductive volume is known as Ultrasound Current Source Density Imaging(UCSDI). In this work we use the mathematical description of the effect to estimate whether the method can be used to map the distribution of a stimulating electrical current and even for mapping the electrical activity of the muscle fibres of muscles in the thigh. The results indicate sufficient signal strength using stimulation current for signal generation.

Keywords: Denervated muscle, electrical stimulation therapy, ultrasound density imaging, therapy monitoring.

Introduction

A fundamental difference of neuromuscular electrical stimulation and electrical stimulation of denverated muscle is the location of the action potential's creation. In the former case the action potential is created on a nerve fiber. It propagates down to the muscle, crosses the neuromuscular junction by all muscle fibers in one motor unit and from there along the fibers. The result is fiber contraction. If on the other hand, the muscle is denervated there is no nerve fiber to propagate the action potential. In this case the muscle fibers have to be stimulated directly. And since in a skeletal muscle the potential is not transmitted from one muscle fiber to another each and every fiber has to be stimulated. This means that the stimulating electrical current has to reach each fiber in intensity high enough to depolarize the fiber membrane crossing the threshold potential. To realize this in thigh muscles with electrodes on the surface of the skin is a difficult task that has not been solved satisfactory. The current state of the art is to use high stimulating current [1].In this way many fibers are reached but the energy of a stimulating pulse used for denervated muscle is about thousand fold that for an innervated muscle [1]. The possible current intensity is though limited by the danger of damaging the tissue around the electrodes. In order to have an effective treatment of denervated muscle and ensure that whole muscles are stimulated a monitoring method is needed. It is a prerequisite tool for designing effective electrode systems. Up to now the muscle contraction monitoring method has been to put the finger on the muscles tendon, for example the patella tendon, to detect the contraction. The information from this is limited. If the muscle is a bipennad muscle or if the tendon has more than one muscle connected to it the information is only whether there was a contraction or not, but what muscle or part of muscle is still unknown. The result can be a very unbalanced therapy leading to an overgrowth of one muscle or muscle part whereas other muscle or muscle parts are still degenerating. To ensure a balanced therapy we suggest a method to monitor the electrical stimulation therapy. It is based on the fact that a pressure wave modulates the electrical conductivity of the tissue. The application of an ultrasound wave therefore modulates the resistance to the stimulating current and produces a voltage signal that can be detected by surface electrodes. This is known as the electro acoustic effect (AE). Using it to map the distribution of an electrical current in a conductive volume is known as Ultrasound Current Source Density Imaging

The aim of the current work is to estimate the possibilities of using UCSDI for A: mapping of

electrical stimulating current and B: mapping of electrical activity of denervated muscle.

Material and Methods

Denervated degenerated muscle

Conus cauda lesion causes paralysis accompanied by loss of muscle tone and absence of muscle reflexes in the lowest part of the spinal column after degeneration of the motorneuron. Patients suffering from conus cauda lesions have therefore denervated degenerated thigh muscles. Today the only possible therapy for these individuals to regain muscle size and to some extent its former strength is to use electrical stimulation therapy.

AE effect

An ultrasound wave spreading in a conducting medium produces periodical change in pressure and temperature which locally modifies the conductivity of the medium:

$$\frac{\Delta\sigma}{\sigma_0} = -K_I \Delta P \qquad (1)$$

where K_I (MPa^{-1}) is the interaction coefficient of the medium, σ (S/m) is the conductivity, Δσ the conductivity change and ΔP (Pa) the pressure change [2-4].

AE signal

By applying external current to the conductive medium along with the ultrasound wave an interaction signal is produced due to the changes in conductivity. This is called the acousto-electric signal (AE). As the acoustic wave travels through the conductive medium an AE signal will be produced at the location of the wave. The signal strength will have the highest intensity where the multiplication of ΔP and I has the highest value. By focusing the acoustic wave to a focus point the location of the AE signal genesis can be determined. A focus point of a typical ultrasound transducer is about 5x4 mm. A method to measure the AE signal and localize it on the boundary of a conducting medium has been developed [5-7], based on the lead field theory originally developed for electro cardiology [8]. [5] derived the AE signal equation for focused ultrasound, which relates the conductivity change seen by an arbitrary electrode recording system due to a spatially distributed pressure field at time t:

$$V = \iiint (\boldsymbol{J}^L \bullet \boldsymbol{J}^I)(\sigma_0 - K_I \sigma_0 \Delta P)\, dx\, dy\, dz \qquad (2)$$

where $\mathbf{J}^L$ is the lead field of the recording electrodes, $\mathbf{J}^I$ is the distributed current source and V is the voltage detected by the recording electrodes. This way we can record an AE signal on the surface by moving the ultrasound probe in small steps and record an AE signal each time, forming a spatial map of an electric current distribution. The frequency of the recorded signal is the same as of the ultrasound wave. This property makes it easy to filter the AE signal from the detected voltage. By expanding equation 2 we get the detected voltage,V, between 2 recording electrodes as the sum of 2 signals, V^{LF} and V^{AE}:

$$V = \underbrace{\iiint (\boldsymbol{J}^L \bullet \boldsymbol{J}^I)\sigma_0 dxdydz}_{\hat{V^{LF}}} + \underbrace{\iiint (\boldsymbol{J}^L \bullet \boldsymbol{J}^I)\,(-K_I \sigma_0 \Delta P) dxdydz}_{\hat{V^{AE}}} \qquad (3)$$

where the first term represents the low frequency of the injected current and the second term represents the high frequency of the AE signal.

Signal strength estimation in the thigh

The amplitude of the measured AE signal is proportional to the pressure and the current. The size of the conducting volume and distribution of the current density also affect the strength of the signal.

We can estimate the magnitude of the AE signal using another version of equation 2, derived by [3]:

$$V(t) = K_I I R_0 P(t) \qquad (4)$$

where R_0 is the resistance experienced by the electrodes. Using stimulating current on the scale of 10^{-1} A, a pressure wave on the scale of MPa and the K_I is 10^{-9} MPa^{-1} we get a signal with the size of 10^{-4} V closest to the current injecting electrodes where the current density is the highest.

[6] and [9] have shown that AE signal can also be detected at physiologically relevant current densities less than 10 mA/cm^2. With a focal pressure of 2 MPa the signal sensitivity of the used recording system was 0,7 μV/(mA/cm^2).

Using a simple cylindrical model of a cross section of a thigh (r = 8 cm), where a denervated muscle also of cylindrical form (r = 1 cm) is surrounded by fat tissue, we can estimate the current density in the thigh when stimulating with two electrodes on the surface, 5 cm apart. A simple equivalent electrical circuit model are two parallel resistors (fig. 1). The resistivity, ρ, is 0,15-0,5 Ωcm for fat depending on the water content and 0,012-0,018 Ωcm for muscle tissue[10]. Using 250 mA as the injecting current and a current division for two parallel resistors, the current density for fat is 1,1-2,0 mA/cm^2 and 17-46 mA/cm^2 for the muscle.The corresponding values for injecting or stimulating

current of 30 mA are 0,13-0,24 mA/cm^2 for fat and 2,0-5,5 mA/cm^2 for muscle.

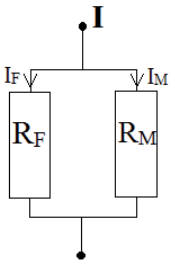


Fig. 1: Circuit model of the thigh. R_F is the resistor for the fat and R_M for muscle. The current, I, is the stimulating current injected to the thigh from the surface electrodes.

Results

The following table summarizes the results.

Table 1: Injected current of 250 and 30 mA

I (mA)	R_F	R_M	I_M (mA)	J_M (mA/cm^2)
250	25,8	19,1	144	46
	7,74	28,7	53	17
30	25,8	19,1	17	5,5
	7,74	28,7	6,4	2,0

Comparing these current density values to the values used in [9] the AE signal to be expected in the muscle is in the range of 1-4 μV for 30 mA injecting current and 12-32 μV for 250 mA. These signals have the same frequency as the ultrasound wave and can easily be filtered from other signals. The results imply that it´s possible to calculate the stimulating current strength on locations in the denervated muscle and hence evaluate the probability of success of muscle fiber stimulation.

Discussion

The advantages of using ultrasound current source density imaging are that it´s non-invasive, mapping of current distribution in the denervated muscle seems to be possible and by that we can estimate if the patient is corresponding to the electrical stimulation treatment. The method is also practicable in clinical settings needing only a ultrasound device a one channel EMG device along with an electrical stimulator used for the stimulation therapy. Uncertain is the signal quality in the presence of high stimulating current. This and other uncertainties have to be addressed in an experimental setup. Detecting the physiological current from the active fiber after electrical stimulation is not disturbed in the same way as it occurs with some delay and hence the effects from the stimulation current have vanished.

Conclusions

Results suggest that ultrasound current source density imaging can be used to map stimulation current distribution in denervated thigh muscle. Hence it seems to be a promising method to monitor electrical stimulation of denervated muscles. Possibly, detection of the AE signal when the current source is of physiological origin can be reached.

References

[1] Kern H, Hofer C, Mödlin M, Forstner C, et al. Functional Electrical Stimulation (FES) of Long-Term Denervated Muscles in Humans: Clinical Observation and Laboratory Findings. Basic Appl Myol 12 (6): 291-299, 2002.

[2] Jossinet J, Lavandier B, Cathignol D. The phemenology of acousto-electric interactions signals in aqueous solution of the electrolytes. Ultrsonics, 36: 607-613, 1998.

[3] Lavandier B, Jossinet J, Cathignol D. Experimental measurement of the acousto-electric interaction signal in saline solution. Ultrasonics, 38: 929-936, 2000.

[4] Lavandier B, Jossinet J, Cathignol D. Quantitative assessment of ultrasound-induced resistance change in saline solution. Med. Biol. Eng. Comput., 38: 150-155, 2000.

[5] Olafsson R, Witte RS, O'Donnell M. Measurement of a 2D electric dipole field using the acousto-electric effect. Proc. Of SPIE, 6513, 2007

[6] Olafsson R, Witte RS, Huang SW, et al. Ultrasound current source density imaging. IEEE Transactions on biomedical engineering, 55(7), 2008.

[7] Olafsson R, Witte RS, Jia C, et al. Cardiac activation mapping using ultrasound current source density imaging (UCSDI). IEEE Transactions on ultrasonics, ferroelectrics, and frequency control, 56(3), 2009.

[8] Malmivuo J, Plonsey R. Bioelectromagnetism: principles and applications of bioelectric and biomagnetic fields.Oxford University press, 1995.

[9] Witte R, Olafsson R, Huang SW. Imaging current flow in lobster nerve cord using the acoustoelectric effect. Applied Physics Letters, 90: 163902, 2007.

[10] Grimnes S, Martines T. Kirurgisk Diatermi. Medisinisk-teknisk avdelings forlag, Medinnova Rikshospitalet 2001.

Acknowledgements

This project has been granted by the Landspitali Research Fund and the Icelandic Student Innovation Fund.

Author's Address

B.Gudjonsdottir
Landspitali University Hospital
bjorgg@ru.is
Armuli 1a, 108 Reykjavik, Iceland

Joint reaction force of lower extremities during rowing in non-disabled individuals

Matsunaga T[1], Shimada Y[2], Sato M[1], Chida S[1], Hatakeyama K[1], Watanabe M[1],
Takeshima M[2], Sasaki K[2], Tomite T[2], Yoshikawa T[2], Kudo D[2], Iwami T[3], Iizuka K[4]
[1] Department of Rehabilitation Medicine, Akita University Hospital, Akita, Japan
[2] Department of Orthopedic Surgery, Akita University Graduate School of Medicine
[3] Department of Mechanical Engineering, Akita University Faculty of Engineering and Resource Science

Abstract

Objective; *to identify the joint reaction forces of the lower extremities required to perform FES-rowing through the biomechanical analysis.* ***Methods;*** *Twenty non-disabled volunteers participated in this study. The subjects were instructed to perform rowing without electrical stimulation of the lower extremities at a pace of 23 cycles / min. The changes in joint reaction force of the hip, knee, and ankle during rowing were calculated using a musculoskeletal model.* ***Results;*** *Mean maximum joint reaction force of hop, knee and ankle were 990 ± 490 N (Mean ± SD), 470 ± 220 N and 420 ± 160 N, respectively.* ***Conclusions;*** *It was suggested that joint reaction force of lower extremities during rowing was lower than during walking and FES has the potential to be applied in the low-load and safe exercise for the paraplegics.*

Keywords*: FES rowing, spinal cord injury, paraplegia*

Introduction

In paraplegic individuals after spinal cord injury, the onset of metabolic syndrome and increased cardiovascular diseases have been reported as the long-term health management problems due to a decreased amount of activity, and the importance of fitness exercise has been recognized [1].

FES rowing is a full-body exercise in which the lower extremities are moved by electric stimulation and the upper extremities are moved voluntarily by paraplegic patients. This exercise is recognized as a superior endurance training program for both the cardiovascular and musculoskeletal systems. Wheeler and colleagues reported that FES rowing is safe in patients with spinal cord injury and was capable of reducing the risks associated with cardiovascular diseases [2].

The objective of the present study was to identify the joint load of the lower extremities required to perform FES rowing for non-paraplegic volunteers through the kinematic study.

.

Material and Methods

Subjects

Twelve non-disabled adult males (age range 18 to 30 years; mean, 23 years) volunteered for this study. The mean height of the subjects was 172.6cm. The mean weight was 67.1kg. The subjects had no previous disease or injuries to their musculoskeletal systems. All subjects provided informed consent to participate in this study.

The device and rowing

The Akita FES-rowing machine for the exercise of paraplegics was used in this study [3]. The inclination angle of the seat rail of the rowing machine from the ground was set at 4 degrees.

The subjects were instructed to perform rowing without electrical stimulation of the lower extremities at a pace of 23cycles/min.

Motion analysis

Using 6-axial tension transducer (IFS-105M50A220, Nitta Co. Ltd., Japan) attached to the footrest where both feet were fixed; measurements of reaction force were made at a sampling frequency of 60 Hz. Retro reflective markers were attached to the subject's body. Kinematic data were collected with 7 cameras using the VICON 370 system (Vicon Motion Systems Ltd., Oxford, U.K.). During rowing, electromyography data were collected from 3 muscles (gastrocnemius, rectus femoris, and vastus medialis).

Evaluations

The changes in joint reaction force of the hip, knee, and ankle during rowing were calculated using a musculoskeletal model. In this study, the

optimization problem for estimating muscle tension for the calculation of joint reaction forces was resolved by the linear matrix inequality (LMI) problem related to muscle tension.

Results

During rowing, mean maximum joint reaction force of hop, knee and ankle were 990 ± 490 N (Mean ± SD), 470 ± 220 N and 420 ± 160 N, respectively. Fig. 1 shows the profile of joint reaction force of the hip, knee and ankle joint during one rowing cycle.

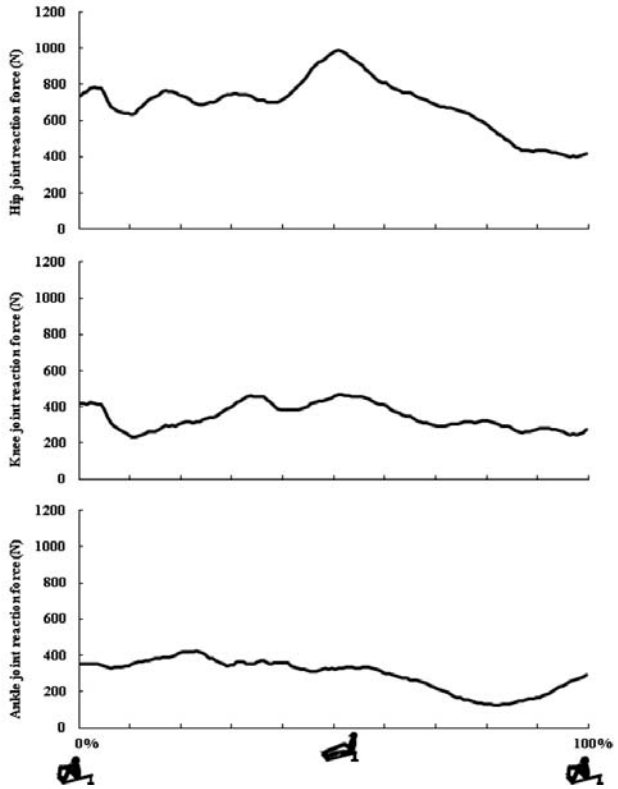


Fig.1. Joint reaction force during rowing. The horizontal axis normalized to 100% of the rowing cycle.

Discussion

To develop effective and safe rehabilitation programs in FES rowing, the biomechanical analysis of the lower extremity during rowing is important. In the past study, the optimization problem for estimating muscle tension for the calculation of joint reaction forces was resolved by the conventional estimation methods with measured myoelectric data. In this study, the optimization problem for estimating muscle tension for the calculation was resolved by the LMI problem related to muscle tension.

The maximum joint reaction forces in the hip, knee, and ankle were about 990, 470, and 420 N. When comparing these results to the values in the walking [4], the overall values are small. In the present study, subjects were instructed to perform the motions separately, and the maximum reaction force measured from the foot was 50-100 N. In previous studies, in which rowing was performed with a competitive attitude, the maximum reaction force measured from the foot was 400-500 N. From this perspective, the value of the reaction force in the present study is about 1/4 to 1/5 of previous studies, and so a simple calculation of the joint reaction force is estimated to be about 1/4 to 1/5 that in previous studies. Through this calculation, the joint reaction forces are nearly equal, and so the results have validity.

Conclusions

From this study, it was suggested that joint reaction force of lower extremities during rowing was lower than during walking and FES has the potential to be applied in the low-load and safe exercise for the paraplegics. Further study is necessary to develop of FES rowing exercise.

References

[1] Davis EA, Hamzaid NA, Fornusek C. Cardiorespiratory, metabolic, and biomechanical responses during functional electrical stimulation leg exercise: health and fitness benefits. Artifical Organs, 32 (8), 625-629, 2008.

[2] Wheeler GD, Andrews BJ, Lederer R, et al. Functional electric stimulation-assisted rowing: increasing cardiovascular fitness through functional electric stimulation rowing training in persons with spinal cord injury. Arch Phys Med Rehabil, 83, 1093 – 1099, 2002.

[3] Shimada Y, Sato M, Miyawaki K, et al. The Akita functional electrical-assisted rowing machine for rehabilitation exercise. Akita J Med, 33, 105-111, 2006.

[4] Thambyah A, Pereira BP, Wyss U. Estimation of bone-on-bone contact forces in the tibiofemoral joint during walking. The Knee, 12, 383-388, 2005.

Author's Address

Toshiki Matsunaga, MD
Department of Rehabilitation Medicine, Akita University Hospital, 1-1-1 Hodo, Akita 010-8543, JAPAN
eMail: tmatsunaga@hos.akita-u.ac.jp

Author Index

Abdul Malik, Noreha 93
Ackermann, Michael 321
Agnew, Sonya P. 312
Alesch, F 223
Allan, David 55, 244
Alon, Gad 127
Alvarado Pacheco, Laura Elena .. 233
Ambrosini, Emilia 115, 378
Aoyagi, Yoichiro 52
Aqueveque, Pablo 37, 282
Arnold, Dirk 145, 148
Azevedo-Coste, Christine 105

Bakhshaie, Behamin 190
Baselli, Giuseppe 217
Bauman, Matthew J. 312
Beesau, Christophe 173
Beghi, Ettore 188
Bhadra, Narendra 321
Bhadra, Niloy 321
Bijak, Manfred 80, 215, 262
Bijelić, Goran 297
Binda, Luca 188
Binder-Macleod, Stuart 206
Bonmassar, Giorgio 68
Boretius, Tim 28, 315
Botter, Alberto 87
Burridge, Jane 16

Cadetti, Lucia 173
Cahuzac, Bertrand 173
Çaldıran, Ozan 71
Carpinella, Ilaria 343
Carraro, Ugo 164, 227
Casellato, Claudia 217
Casiraghi, Anna 343
Caulfield, Brian 212
Chappell, Paul 93
Chiaramonte, Sara 188
Chida, Satoaki 330, 333, 339, 341, 355, 369
Choi, Ik Sun 346
Chong, Su Ling 233, 239
Cikajlo, Imre 181
Cirmirakis, Dominik 37, 282
Ciupa, Radu V. 215
Clark, Gregory 324
Converti, Rosa Maria 343
Converti, Roza 188
Cortesi, Marco 343
Craven, B.Cathy 184
Craven, Colm 244
Crowe, Louis 212
Curtis, Cara A. 239

Dörge, Thomas 133, 142
Dalla Costa, Davide 188
Dandrea, Giovanni 173
Danner, Simon 268
Davis, Glen 247
Davis, Glen M 242
de Jager, Kylie 360
Deliagina, Tatiana 255
Demosthenous, Andreas 31, 34, 74
Dibb, Bridget 16
Dietl, Hans 133
Dimitrijevic, Milan 256, 259, 268
Djilas, Milan 173
Djurić-Jovičić, Milica 203
do Nascimento, Omar Feix 375
Donaldson, Nick 25, 31, 34, 37, 74, 96, 282, 360
Donovan-Hall, Maggie 16
Dosen, Strahinja 190

Ellis-Hill, Caroline 16
Engel, Andreas K 285
Engler, Gerhard 285
Erfanian, Abbas 236, 381
Erfurth, A 223
Estigoni, Eduardo 247
Ethier, Christian 312
Everaert, Dirk G. 230

Faenger, Bernd 145, 148
Farina, Dario 99
Ferrante, Simona 115, 217, 378
Ferrarin, Maurizio 188, 343
Ferrigno, Giancarlo 217, 378
Fischer, Martin 148
Fjeldborg, Lars Christian 154
Foldes, Emily 321
Fornusek, Che 242, 247
Francis, Colin 40
Frattini, Tiziano 217
Freeman, Daniel 68
Fridgeirsson, Egill 164
Fried, Shelley 68
Fries, Pascal 43
Fukushima, Keisuke 124
Furlan, Julio 184

Götz, Stefan 209
Gail, Alexander 133
Gale, John 68
Gallego, Juan Alvaro 108
Gandolla, Marta 217
Gargiulo, Paolo 164, 384
Geng, Bo 306
Gerges, Meana 321
Glindemann, Heiko 133
Gollee, Henrik 55, 58, 244
Gon, Khang 366
Gossman, M. Douglas 303
Graham, Geoff 327
Grassme, Roland 148
Grey, Michael James 375
Gudjonsdottir, Bjorg 384
Guillory, K. Shane 303
Gullapalli, Rao 127

Hakansson, Nils 206
Haller, Michael 80
Hanc, Cristina 215
Hankin, David 139
Harreby, Kristian Rauhe 77
Harrington, Ann 358
Hasanuzzaman, Md. 288
Hatakeyama, Kazutoshi 330, 333, 339, 341, 355, 369
Hayashibe, Mitsuhiro 105
Helgason, Thordur 164, 352, 384
Henderson, Graham 58
Hernandez Arieta, Alejandro 71
Hiatt, Scott 279
Higginson, Jill 206
Hochmair, Erwin 23
Hofer, Christian 80
Hoffer, Joaquin Andres 40
Hoffmann, Klaus-Peter 133
Hofstoetter, Ursula 256, 259, 268
Holinski, Brad J. 230
Hongo, Michio 333
Huebner, Agnes 145
Hwang, Sun Hee 366

Iftime Nielsen, Simona Denisia ... 375
Iizuka, Kiyomi 330
Ishikawa, Masatoshi 309
Ishikawa, Yoshinori 330
Iwami, Takehiro ... 330, 333, 355, 369

Jankovic, Milica M. 200
Jensen, Winnie 136, 154, 306, 315
Jezernik, Saso 173
Jiang, Dai 74
Jonsdottir, Johanna 343
Jovicic, Nenad 291
Jung, Da-Woon 366

Kainz, W 223
Kamavuako, Ernest Nlandu 99
Kanai, Hiroshi 102
Kang, Sung Jae 366
Kapadia, Naaz 184
Kern, Helmut 80, 227
Kesar, Trisha 206
Kiehn Kristensen, Grethe 190
Kilgore, Kevin 321
Kim, Dong-Gu 366
Kim, Young Ho 346, 349
Klauer, Christian 318
Kneisz, Lukas 215
Ko, A 349
Kojovic, Jovana 200
Kollmann, Christian 215
Kolomiets, Bohdan 173
Kosaka, Tomoya 355

Koutsou, Aikaterini 108
Krajnik, Janez 197
Krenn, Matthias 80, 215
Krohova, Jana 190
Kudo, Daisuke 330, 333, 339, 341, 355, 369
Kuhn, Andreas 173
Kundu, Aritra 315
Kunimoto, Masanari 309
Kuno, Hiroaki 52
Kurstjens, Mathijs 136, 315

Ladmiral, Robin 173
Lee, Bum-Suk 366
Lee, Jong Hoon 346
Lee, Samuel 358
Lee, Young Hee 346, 349
Lewis, Chris 43
Lewis, Sören 133
Liu, Xiao 31, 34
Lockhart, Joseph 139
Lowery, Madeleine 212
Luo, Runhan 96
Lynch, Cheryl 118, 327

Mabuchi, Kunihiko 309
Maciejasz, Paweł 142
Malesevic, Nebojsa 65
Malešević, Nebojša 297
Manola, L 223
Marcol, Wiesław 142
Martegani, Alberto 217
Masani, Kei 118, 363
Matjačić, Zlatko 181
Matsunaga, Toshiki 330, 333, 339, 341, 355, 369, 387
Mayr, Winfried .. 3, 80, 215, 256, 259, 268, 271
Mazurek, Kevin 230
Mazzocchio, Riccardo 115
McConville, Kristina 363
McDonnall, Daniel 303
McGillivray, Colleen 184
Mclachlan, Angus 55
Mclean, Alan 55
McRae, Calum 358
Melgaard, Jacob 294
Merletti, Roberto 87
Merrill, Daniel 139
Meyyappan, Ramasamy 40
Micera, Silvestro 300
Miljkovic, Nadica 200
Miller, Lee E. 312
Milosevic, Matija 363
Milovanović, Ivana 203
Minassian, Karen 256, 259, 268
Minetto, Marco Alessandro 87
Minogue, Conor 212
Misawa, Akiko 330, 339
Miura, Naoto 102
Molteni, Franco 217, 378
Morari, Manfred 300
Morelli, Daniela 343
Moreno, Juan Camilo 108
Mushahwar, Vivian K. . 230, 233, 239

Nahrstaedt, Holger 49, 115
Nekoular, Vahab 236
Newham, Di 360
Nguyen, Robert 300
Nielsen, TN 151
Niiro, Hirotaka 309
Nolette, Marc-Andre 40
Nonclercq, Antoine 37, 282
Normann, Richard 324
Norton, Jonathan 96

Oblak, Jakob 181
Oby, Emily R. 312
Occhi, Eugenio 188
Ogilvie, Robert J. 233
Ohtaka, Kohei 330
Oskarsdottir, Arna 352
Ottesen, Kasper Juhl Graesboell 154

Paredes, Liliana 167, 170
Park, Dae-Sung 366
Park, Soo Hyun 346
Paśniczek, Roman 142
Pečlin, Polona 197
Pedrocchi, Alessandra .. 115, 217, 378
Perkins, Tim 74
Petrovic, Igor 65
Pfeifer, Serge 71

Picaud, Serge 173
Pizzolato, Marco 190
Plenk, Hanns Jr 11
Pons, Jose Luis 108
Popović, Mirjana 190
Popovic, Dejan B. 200
Popovic, Lana 65
Popovic, Milos 118, 184, 327, 363
Popovic, Mirjana 65
Purcell, Mariel 244

Qiao, Shaoyu 161

Rafolt, Dietmar 215
Raisch, Jörg 318
Rattay, Frank 167, 170, 256, 259, 268
Raut, Rabin 288
Ravelli, Paola 378
Redaelli, Tiziana 188
Reisman, Darcy 206
Reynisson, Pall Jens 164
Riener, Robert 71
Rijkhoff, Nico 294
Robinson, Mark 363
Rocon, Eduardo 108
Rothwell, John 267
Roys, Steven 127
Rozman, Janez 197
Rubehn, Birthe 43, 285
Rushton, David 16
Russold, Michael Friedrich 133
Ryu, Jei Cheong 366

Sablayrolles, Bertrand 105
Saeidi, Nooshin 31
Sahel, Jose 173
Sandoval, Rodrigo 40
Sasaki, Kana 330, 333, 339, 341, 355, 369
Sato, Mineyoshi 330, 333, 339, 341, 355, 369
Saunders, James 40
Saura, Ryuichi 372
Sawan, Mohamad 288
Sayenko, Dimitry 363
Schauer, Thomas 49, 115, 318
Scholle, Hans-Christoph 145, 148
Schuettler, Martin 28, 31
Schumann, Nikolaus-Peter 148
Seidl, Rainer O. 49
Seru, Surbhi 40
Sevcencu, Cristian 77, 151
Seyedi, Ali 381
Shiba, Naoto 121
Shimada, Yhoichi 355
Shimada, Yoichi 330, 333, 339, 341, 369
Shimojo, Makoto 309
Sinkjaer, Thomas 375
Smith, Richard 247
Smondrk, Maros 190
Son, Jongsang 349
Song, Tongjin 366
Stein, Richard B. 230
Stieglitz, Thomas 28, 43, 285, 315
Stitt, Iain 285
Straube, Andreas 209
Struijk, Johannes Jan 77, 151
Suzuki, Takafumi 309
Suzuki, Tatsuto 372
Szecsi, Johann 209

Tagawa, Yoshihiko 121
Tan, John 118
Tang, Jessica 40
Tanner, Almira 40
Tansey, Keith 259
Taylor, Paul 13, 93
Tedesco Triccas, Lisa 16
Thorsen, Rune 188, 343
Tomite, Takenori 330, 333, 339, 341, 355, 369
Townsend, Benjamin 285
Tran, Bao 40
Troyk, Phil 139
Tsubahara, Akio 52

Uchiyama, Hironobu 372
Unger, Ewald 80

Vallery, Heike 71
Vanhoestenberghe, Anne 25, 31, 34, 37, 282
Vette, Albert 118

Vognsen Nielsen, Michael 154
Vossius, Gerhard 5
Vrbova, Gerta 275

Wang, Helen 40
Watanabe, Motoyuki 330
Watanabe, Takashi 102, 124, 372
Watanabe, Takuya 121
Weir, Richard 139
Wenger, Cornelia 167, 170
Westendorff, Stephanie 133
Wilder, Andrew 324
Wood, Duncan 93

Yamamoto, Naosuke 52
Yamamoto, Toshiyasu 52
Yoo, Eun Young 346
Yoshida, Ken 161, 306, 315
Yoshikawa, Takayuki ... 330, 333, 339, 341, 355, 369

Zadravec, Matjaž 181
Zariffa, Jose 118
Zhang, Dingguo 335
Zhang, Qin 105
Zivanovic, Vera 184

Sponsors and Exhibitors (in alphabetic order):



Edited by:
Paul S. Malchesky, D. Eng.
http://www.wiley.com/bw/journal.asp?ref=0160-564X



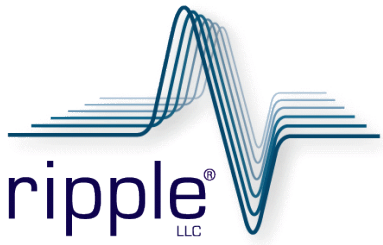
Dr. Schuhfried
Medizintechnik GmbH
Van Swieten-Gasse 10
A-1090 Wien
Austria



Matzka Rehatechnik GmbH
Gentzgasse 166
1180 Wien
Austria



Otto Bock Healthcare Products GmbH
Kaiserstraße 39
1070 Wien, Austria



Ripple, LLC
2015 South 1100 East
Salt Lake City, UT 84106
USA

librix.eu
The best solution for your printing
wherever you are!